Peter S. Conti
Daniel K. Cham
Editors

PET–CT

A Case-Based Approach

Springer

PET-CT

Peter S. Conti, MD, PhD, FACNP, FACR
Professor of Radiology, Clinical Pharmacy & Biomedical Engineering, Director, PET Imaging Science Center, University of Southern California, Los Angeles, California

Daniel K. Cham, MD, MS
Clinical Research Fellow, PET Imaging Science Center, University of Southern California, Los Angeles, California

Editors

PET-CT

A Case-Based Approach

With 472 Illustrations, 107 in Full Color

With a Foreword by Henry N. Wagner, Jr., MD

Springer

Peter S. Conti, MD, PhD, FACNP, FACR
Professor of Radiology
Clinical Pharmacy & Biomedical Engineering
Director, PET Imaging Science Center
University of Southern California
Los Angeles, CA 90033
USA

Daniel K. Cham, MD, MS
Clinical Research Fellow
PET Imaging Science Center
University of Southern California
Los Angeles, CA 90033
USA

Library of Congress Cataloging-in-Publication Data
Conti, Peter S.
PET-CT : a case based approach / Peter S. Conti, Daniel K. Cham.
p. ; cm.
Includes bibliographical references and index.
ISBN 0-387-20858-5 (hc : alk paper)
1. Tomography, Emission—Case studies. I. Title: Positron emission tomography-computed tomography. II. Cham, Daniel K. III. Title.
[DNLM: 1. Tomography, Emission-Computed. WN 206 C762p 2004]
RC78.7.T62C665 2004
616.07′575—dc22 2004050430

ISBN 0-387-20858-5 Printed on acid-free paper.

Printed in Singapore. (BS/KYO)

9 8 7 6 5 4 3 2 1 SPIN 10939284

springeronline.com

To our patients.

__PSC

To my wife, Yenty, for her unconditional love and untiring efforts to help me achieve both my personal and professional goals;
To my father, James Cham, Margaret, Grace, Frank, and his wife, Sylvia for their spiritual support;
and
In loving memory of my mother, May Cham, who lost her battle with cancer.

*__DKC

To our friends and colleagues whose understanding and support have been invaluable in the preparation of this book.

__PSC, DKC

Foreword

Few advances in medicine have had more of an impact on modern health care than the invention of PET-CT studies of FDG in the living human body and experimental animals. Biochemistry has been superimposed on anatomy, which is a giant leap forward. The expertise required for the interpretation of CT must now be combined with the expert interpretation of the biochemical information of the FDG study. The idea that the interpretation of the images simply requires the superimposition of the two image modalities is simple is clearly not true. What is needed is a clear understanding of the sites of metabolic activity revealed by FDG studies in normal persons, and its variability from person to person. For example, FDG accumulates in various structures in the head and neck, and in the ovaries and uterus of normal women during certain phases of the menstrual cycle.

The case method of teaching has stood the test of time for more than a hundred years and is still valid as new modalities are developed and introduced into medical practice. The authors, both of whom have considerable experience in the performance and interpretation of PET-CT studies with FDG, have made an important contribution that will be of great value to nuclear medicine physicians, radiologists, oncologists, and other physicians with the responsibility of caring for patients with cancer.

Capabilities and limitations are discussed in the context of specific problems and patients. Most types of cancer are illustrated, with attention paid to the specific problems of each type. Technical artifacts are identified. F-18 fluoride, which is useful in delineating the normal skeleton, as well as lesions of the skeleton, is included, although the major emphasis is on FDG.

The book meets an immediate need of radiologists, nuclear physicians and oncologists, and will surely lead to great improvement in the care of patients. "Molecular imaging" added to the framework of CT revelations of anatomy is an idea whose time has come.

Henry N. Wagner, Jr., MD
Professor of Environmental Health Sciences
The Johns Hopkins Bloomberg School of Public Health

Preface

PET-CT: A Case-Based Approach provides practical clinical examples of studies performed with FDG on a state-of-the-art dedicated PET-CT device. Detailed histories and correlative imaging findings are given in each case to demonstrate the level of detail required for image interpretation and the capabilities of this instrumentation. Impressions are followed by relevant discussion points and insightful "pearls and pitfalls," all designed to provide novice as well as experienced readers a brief but concise summary of the advantages and limitations of using this technology in the clinical setting. Images are presented in PET only, CT only and fused format to highlight the advantages of this hybrid technology in displaying the spectrum of normal and pathological findings in the cases selected. Chapter 1 covers the fundamentals of PET-CT imaging with FDG including normal physiology, normal variants and technical artifacts. Chapters 2 to 12 and 15 to 26 cover a spectrum of clinical applications in oncology including common indications in lung and colorectal cancer, as well as less common cancers, such as germ cell tumors and nerve sheath tumors. The use of PET-CT in unknown primary malignancies is also covered in Chapter 15. In addition to brain tumors, Chapter 4 covers general neurological applications such as epilepsy. Cardiac and infectious disease applications are covered in Chapters 13 and 14. Finally Chapter 27 covers PET-CT applications using F-18 fluoride for bone scans. The book has two appendices. The first is a brief review of reimbursement policies; the second focuses on instrumentation.

This book is ideal for nuclear medicine practitioners, radiologists, and residents, as well as referring clinicians interested in learning more about how this new medical imaging technology can be applied in their patient populations.

Peter S. Conti, MD, PhD, FACNP, FACR
Daniel K. Cham, MD, MS

Acknowledgments

We wish to acknowledge the dedicated work of the faculty of the USC Department of Radiology for their assistance in case selection and discussions in the preparation of this book. In particular, we wish to thank Robert Henderson, Hossein Jadvar, Heidi Wassef, Lalitha Ramanna, and John Go. We also wish to thank Oscar Streeter of the Department of Radiation Oncology for his contributions. We would like to thank the USC PET technologists, Peter Shomphe and Priscilla Contreras, for their technical assistance in acquiring and processing the images shown in this book. Special thanks goes to Jennifer Keppler and James Bading of the USC PET Center for their technical input, advice and criticisms. We also wish to thank Grace W. Cham for contributing constructive suggestions and comments. Finally, we wish to thank all the USC PET Fellows who over the years have contributed to the teaching file established at the USC PET Center, and have provided a source of inspiration for the entire faculty.

Peter S. Conti, MD, PhD, FACNP, FACR
Daniel K. Cham, MD, MS

Contents

Contributors

James Bading, PhD
Associate Professor of Research, Department of Radiology, University of Southern California, Los Angeles, CA 90033 USA

Shahram Bouyadlou, MD
Resident, Division of Nuclear Medicine, Department of Radiology, University of Southern California, Los Angeles, CA 90033 USA

Daniel K. Cham, MD, MS
Clinical Research Fellow, PET Imaging Science Center, University of Southern California, Los Angeles, CA 90033 USA

Peter S. Conti, MD, PhD
Professor of Radiology, Clinical Pharmacy & Biomedical Engineering, Director, PET Imaging Science Center, University of Southern California, Los Angeles, CA 90033 USA

Anabella S. Din, MD
Clinical Research Fellow, PET Imaging Science Center, University of Southern California, Los Angeles, CA 90033 USA

Sherief Gamie, MD, MS
Resident, Division of Nuclear Medicine, Department of Radiology, University of Southern California, Los Angeles, CA 90033 USA

John L. Go, MD
Assistant Professor of Clinical Radiology, Chief, Division of Head and Neck Radiology, University of Southern California, Los Angeles, CA 90033 USA

Robert W. Henderson, MD
Associate Professor of Clinical Radiology, Director, Division of Nuclear Medicine, University of Southern California, Los Angeles, CA 90033 USA

Hossein Jadvar, MD, PhD
Associate Professor of Radiology and Biomedical Engineering, Division of Nuclear Medicine, University of Southern California; and Visiting Associate in Bioengineering, Division of Engineering and Applied Science, California Institute of Technology, Los Angeles, CA 90033 USA

Jennifer S. Keppler, CNMT, MBA
Clinical Instructor of Radiology, Research Administrator, University Advanced Bio-Imaging Associates, University of Southern California, Los Angeles, CA 90033 USA

Lalitha Ramanna, MD
Associate Professor of Clinical Radiology, Residency Program Director, Division of Nuclear Medicine, University of Southern California, Los Angeles, CA 90033 USA

Peter Shomphe, CNMT, ARRT
Chief Technologist, PET Imaging Science Center, University of Southern California, Los Angeles, CA 90033 USA

Heidi R. Wassef, MD
Assistant Professor of Clinical Radiology, Division of Nuclear Medicine, University of Southern California, Los Angeles, CA 90033 USA

Part I The Fundamentals

1 Normal Physiology and Variants: A Primer

Daniel K. Cham and Peter S. Conti

1.1 Normal Physiology

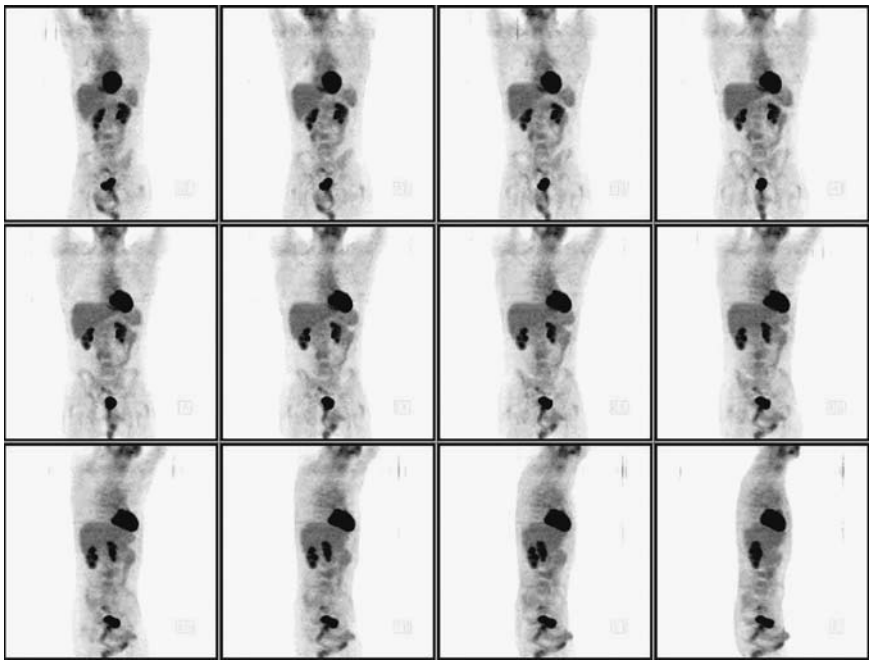

Figure 1.1.1. Normal PET study. In the interpretation of PET, a good understanding of the normal physiology is important. From right-to-left, the rotating images are a useful way to survey lesions prior to reading the planar images on PET-CT. Because FDG is cleared primarily through the renal system, the renal calices, ureters, and bladder are seen. There is mild generalized uptake in the liver, bone marrow, and spleen. Normal variant uptake in the heart and bowel can be seen. To better visualize the chest for abnormality, the patient should fast prior to the scan to minimize myocardial uptake. The brain (not shown here) is also a site of high FDG uptake due to marked glucose utilization, particularly in gray matter.

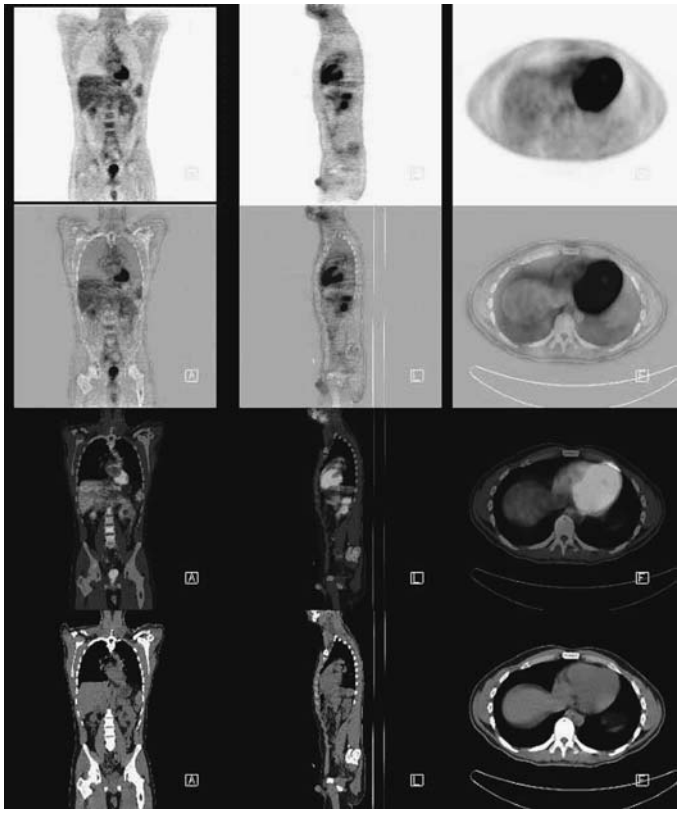

Figure 1.1.1A. This study is divided into 4 rows. The top row is 100% PET. The second row is 75% PET-based and 25% CT. The third row is 50% PET and 50% CT. The bottom row is 100% CT. There are three columns; coronal, sagittal, and transaxial, left to right.

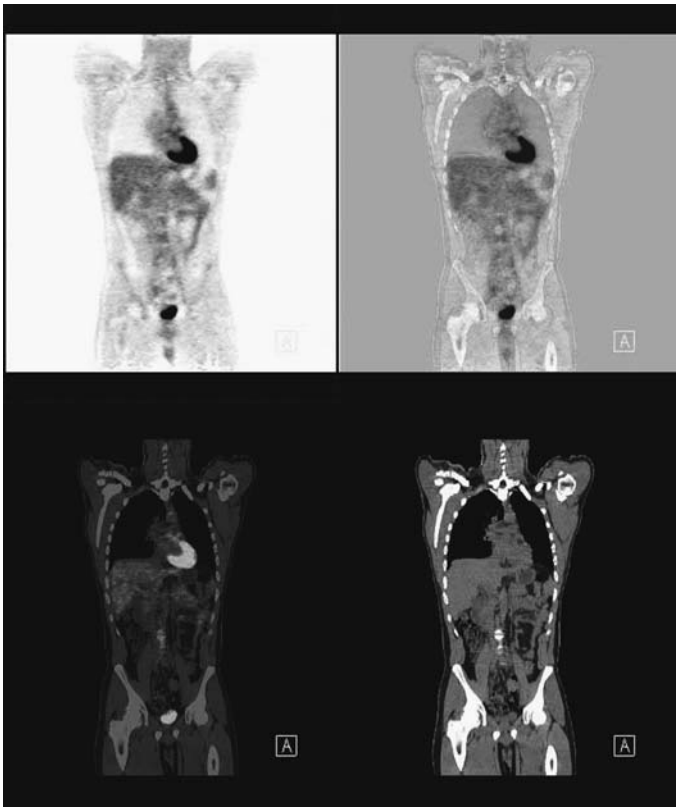

Figure 1.1.1B. In general, standard body PET scan starts from the skull base to the upper thighs. Depending on the patient's medical history (for example, a history of melanoma), the scans will include the extremities and head/neck region. A brain scan may also be included if clinically indicated.

FIGURE 1.1.1C. A: liver, B: heart; C: bladder; D: bone marrow.

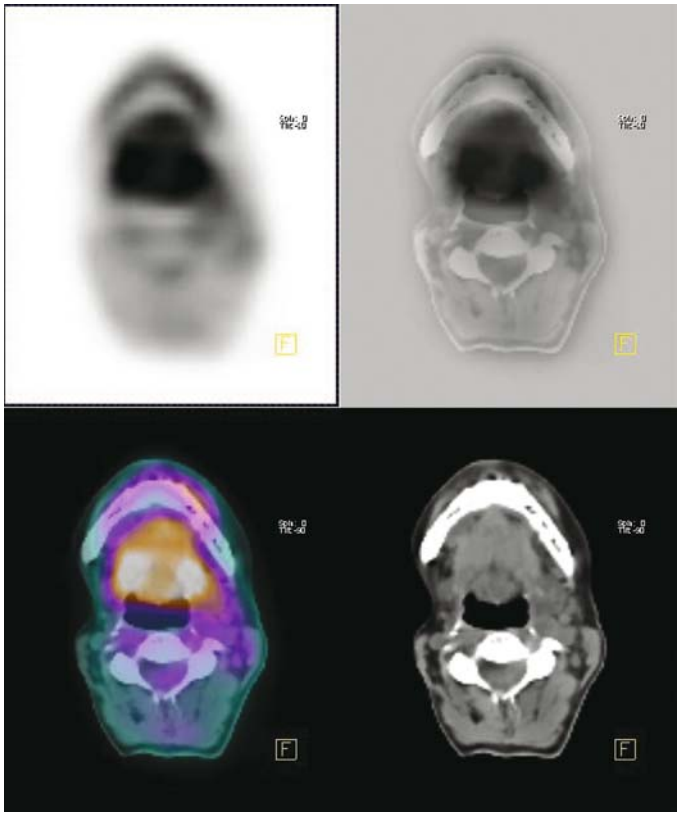

FIGURE 1.2.1. Tongue activity. Patient was talking during the 4-min uptake phase that followed injection of the tracer.

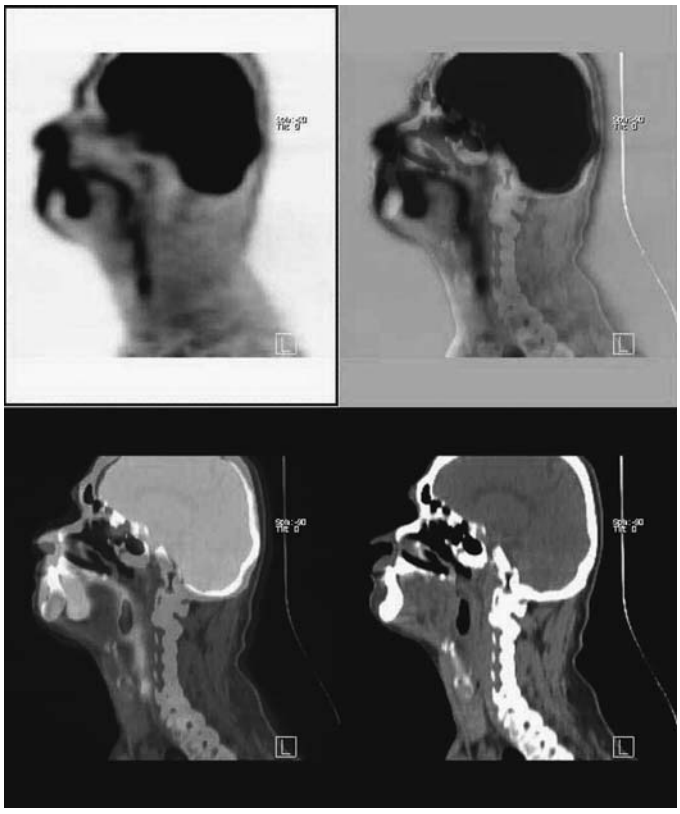

FIGURE 1.3.1. Physiological pharyngeal activity. After excluding pathology, physiological uptake can be seen with excessive talking and swallowing during the uptake phase.

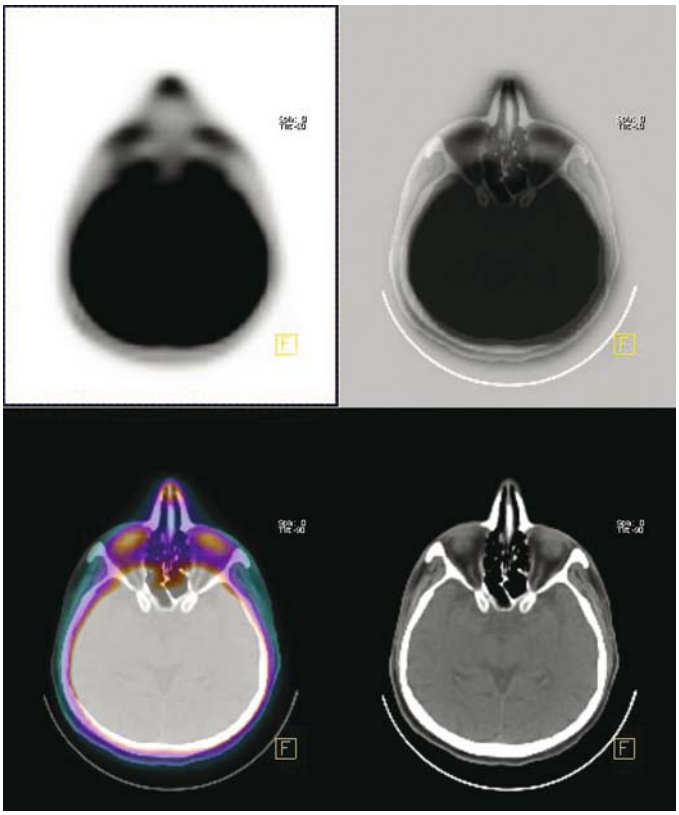

FIGURE 1.4.1. Extraoccular activity in muscles. Quiet rest with eyes closed is optimal during the uptake phase.

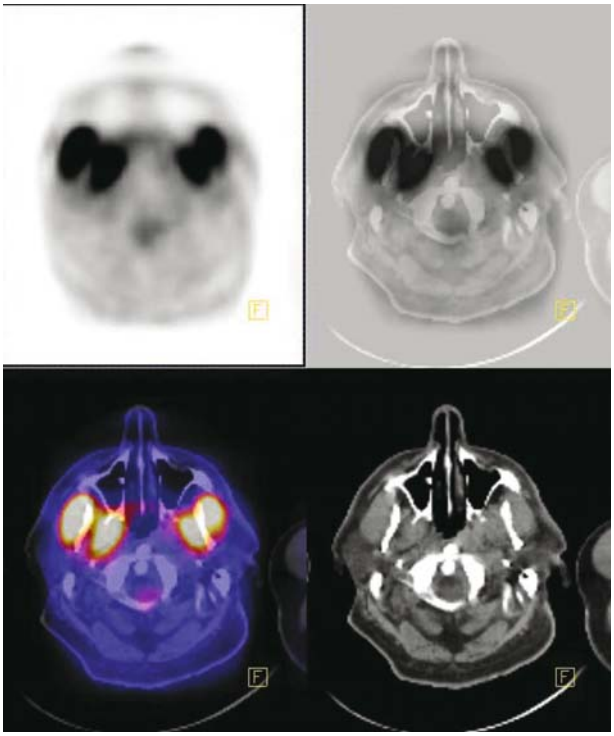

FIGURE 1.5.1. Masseter and pterygoid muscle activity. The patient was chewing gum prior to imaging consistent with mastication activity.

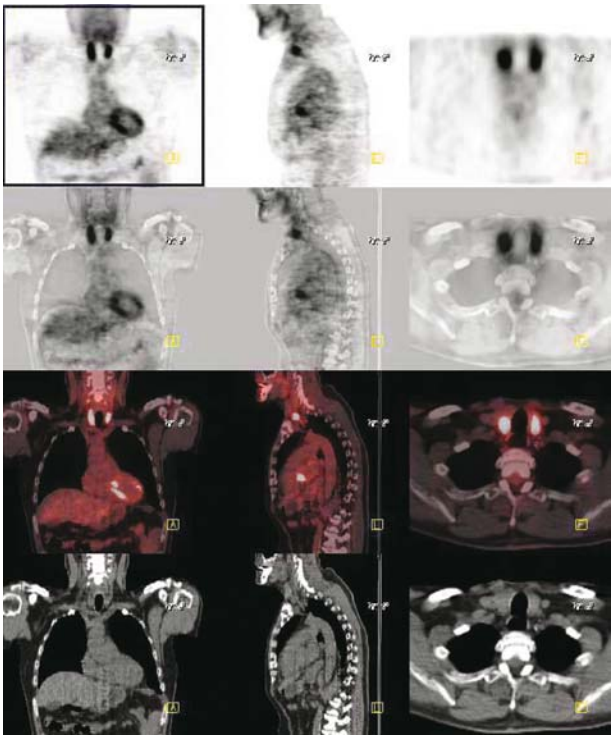

FIGURE 1.6.1. Thyroid activity. Consider the symmetry of the uptake. This is a normal physiologic tracer distribution. Approximately one third of the euthyroid patients can exhibit this bilateral uptake. Thyroiditis, such as Hashimoto's thyroiditis, can display similar activity, but is usually more intense. Asymmetric uptake may represent either thyroid goiter or thyroid cancer.

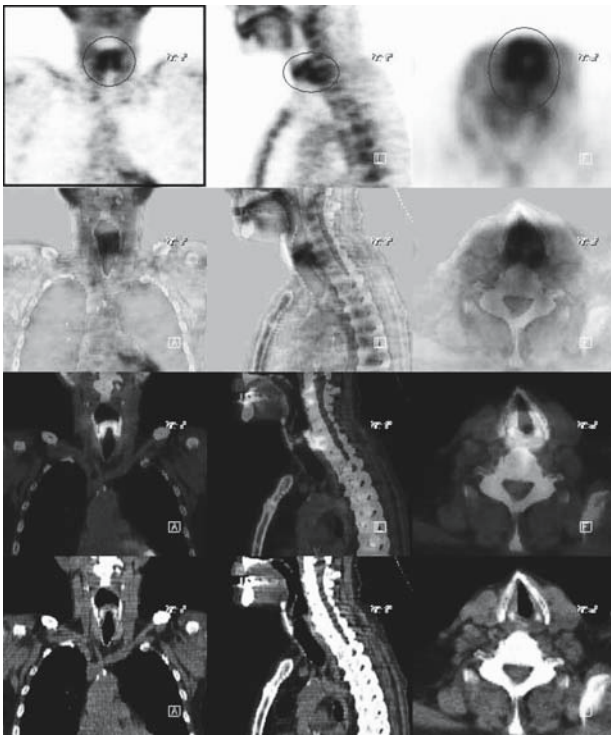

FIGURE 1.7.1. Vocal cord activity. The patient was talking during injection of the radiotracer.

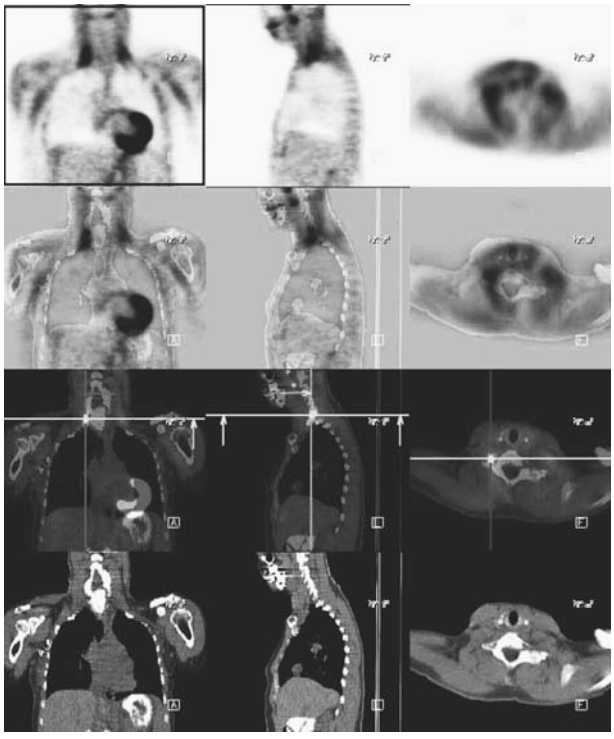

FIGURE 1.8.1. Neck muscle. Physiological muscle and fat uptake can make identification of pathology difficult. PET-CT allows differentiation of physiological muscle uptake from sites of fat uptake of FDG.

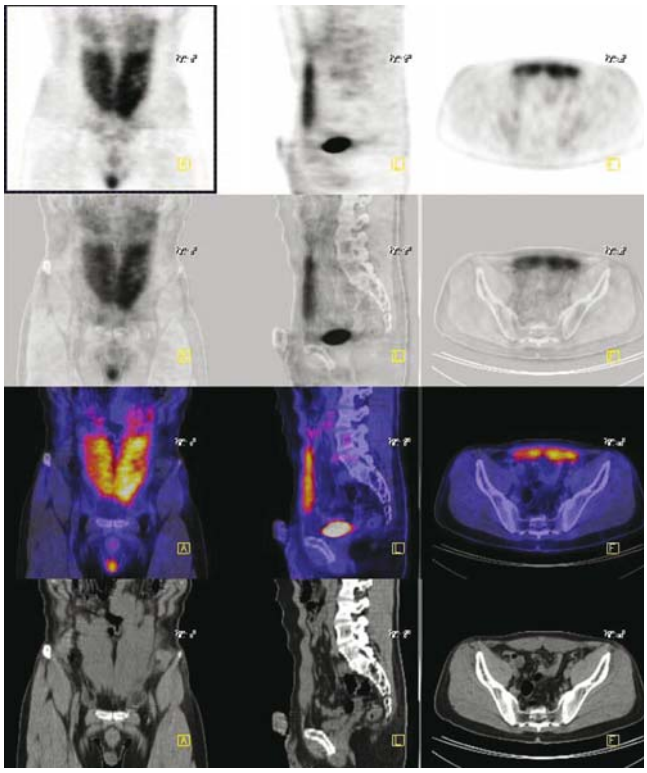

FIGURE 1.9.1. Abdominal rectus muscle. This patient has recently been doing push-ups for weeks before the scanning.

FIGURE 1.10.1. Generalized muscular activity. This is a young patient, who received no valium prior to the scan. Muscle relaxant (diazepam 5 mg–10 mg po, 30 min before FDG injection) may be used to suppress physiological muscle uptake.

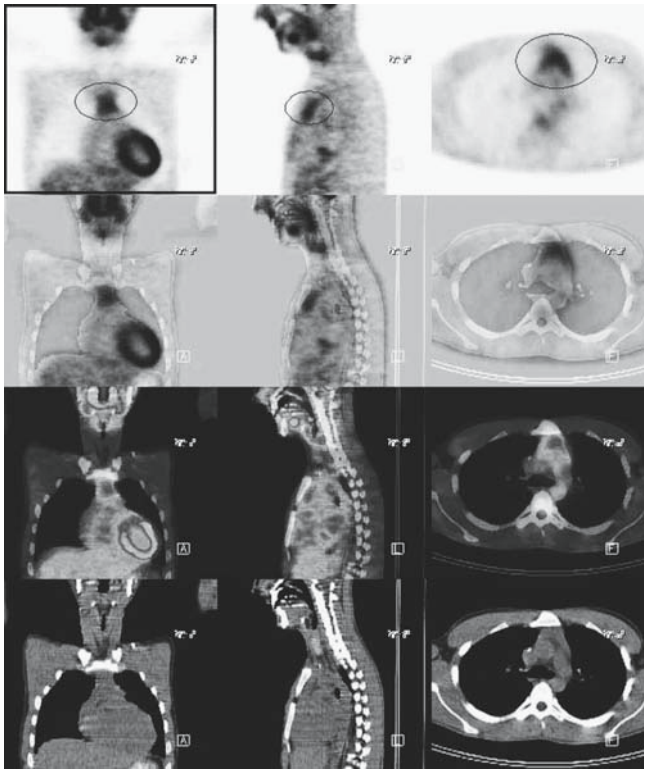

FIGURE 1.11.1. Thymic activity. Most commonly appears in the pediatric population and is normally seen at low levels. Post chemotherapy patients (usually those treated for Hodgkin's disease) may occasionally display marked uptake in the thymus resulting from "thymic rebound hyperplasia."

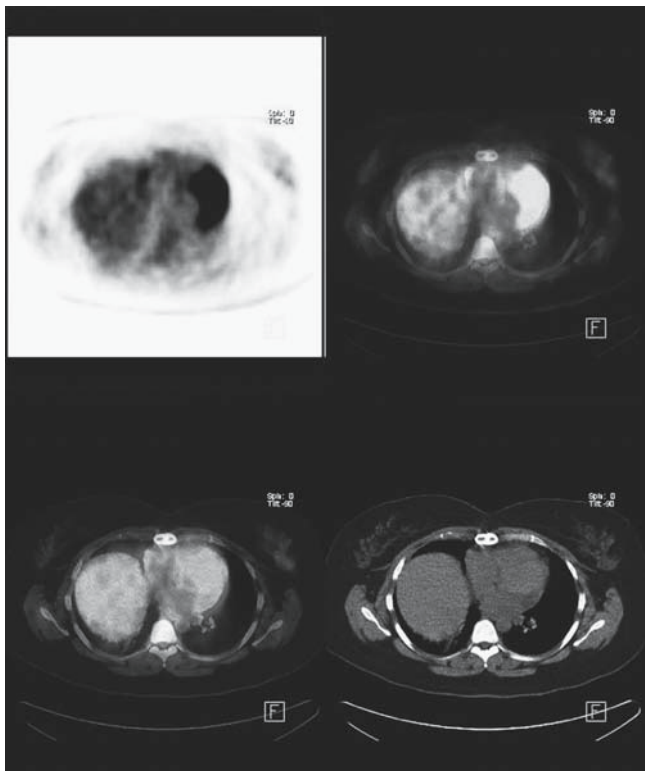

FIGURE 1.12.1. Physiological breast activity.

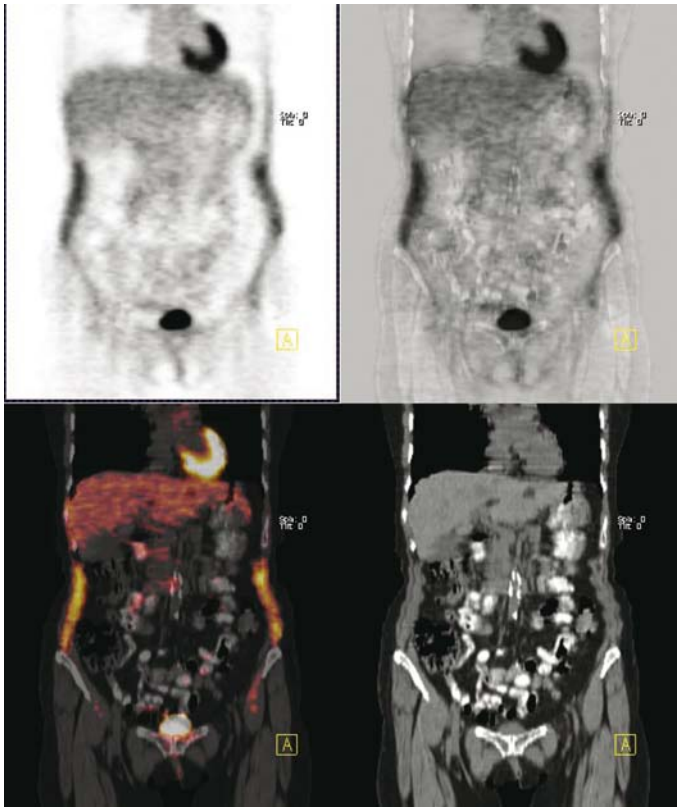

FIGURE 1.13.1. Thoracoabdominal wall musculature. Exercise prior to the study or motion during the study can lead to muscle uptake on the FDG scan.

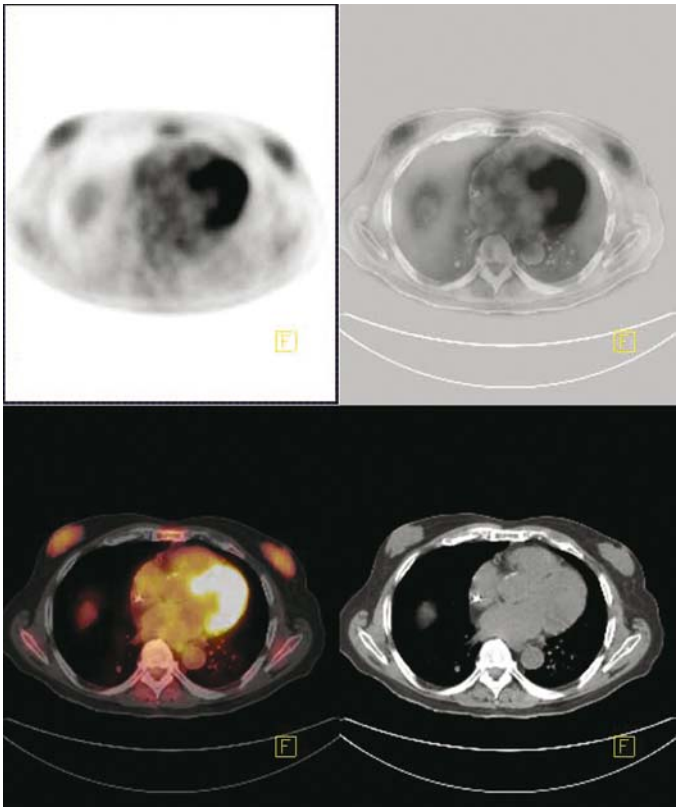

FIGURE 1.14.1. Gynecomastia. Enlargement of the male mammary glands.

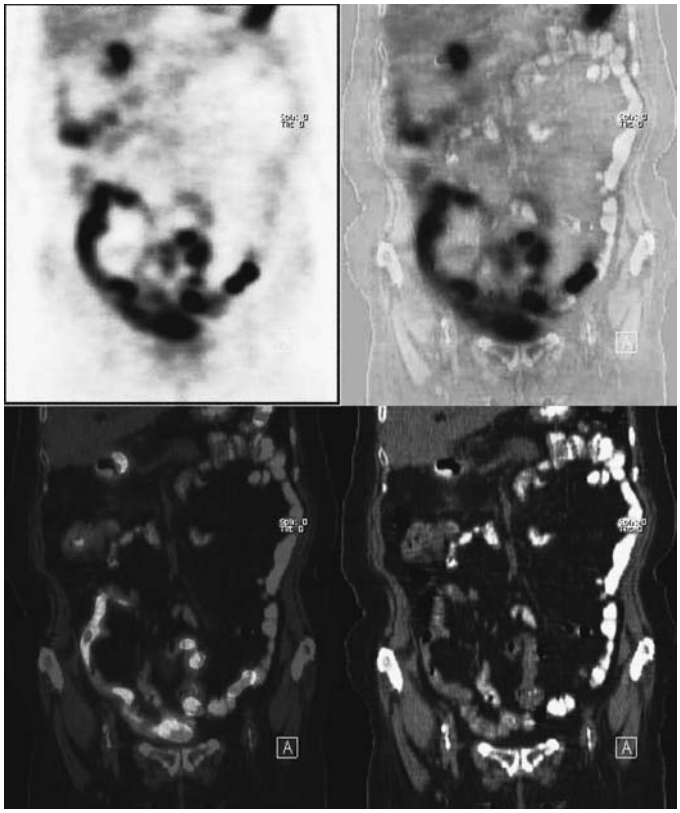

FIGURE 1.15.1. Bowel activity. Intense, but physiologic, colon activity.

1.2 Nononcologic Pathology

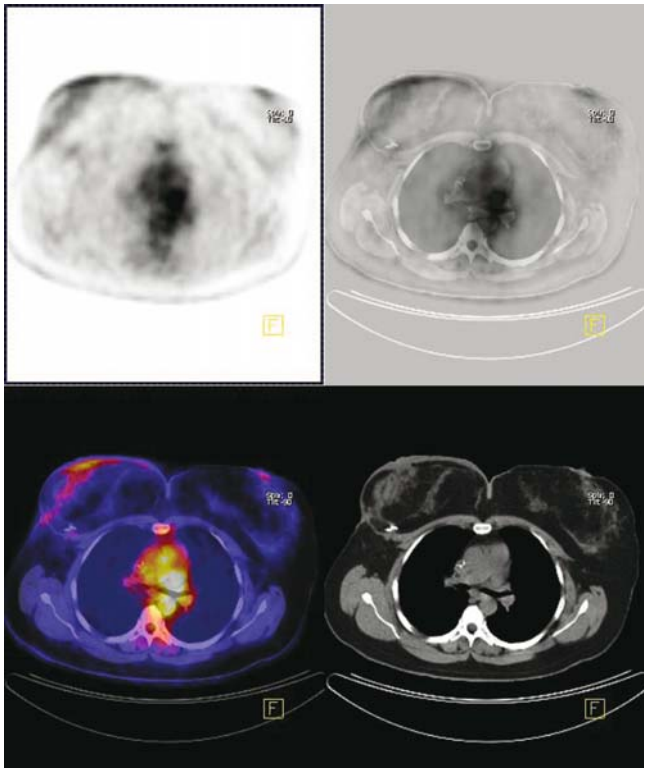

Figure 1.2.1. Acute mastitis. This is a childbearing patient. Diffuse elevated activity in the breast is highly suggestive of inflammation.

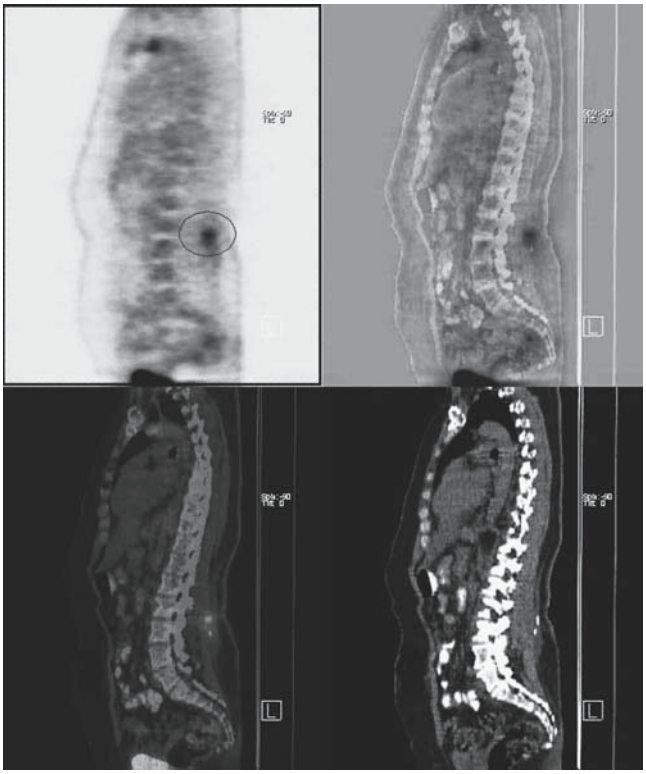

Figure 1.2.2. Lumbar puncture. The patient has a history of recent lumbar puncture.

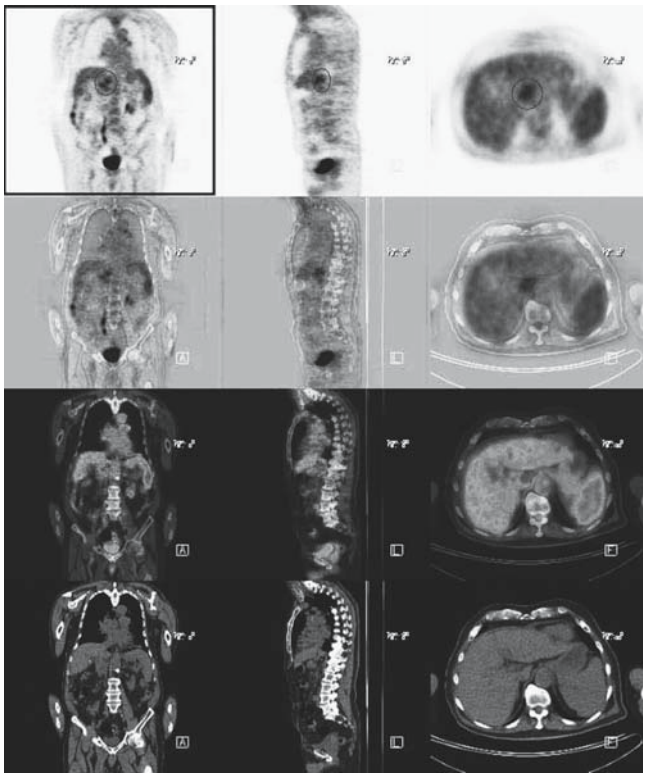

Figure 1.2.3. Duodenal activity. This patient has a history of peptic ulcer disease.

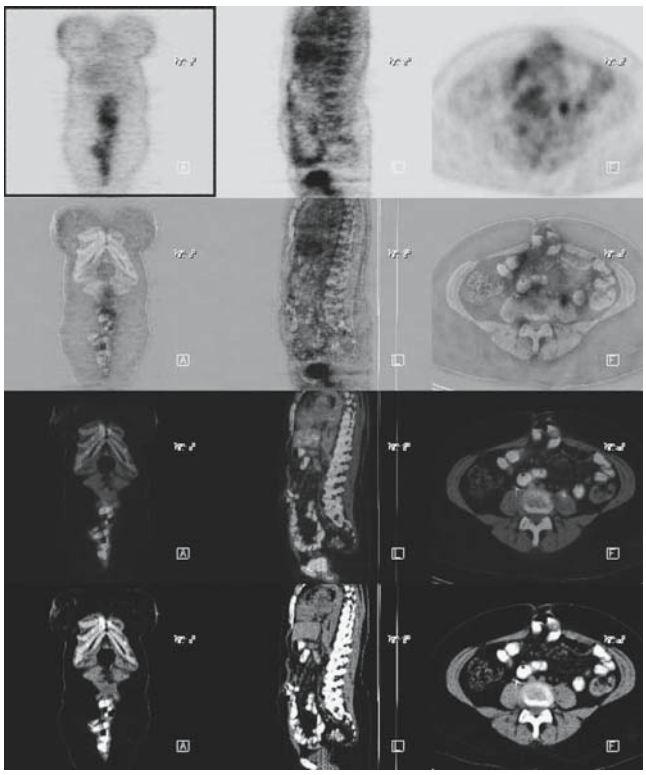

Figure 1.2.4. Ventral hernia. Bowel uptake.

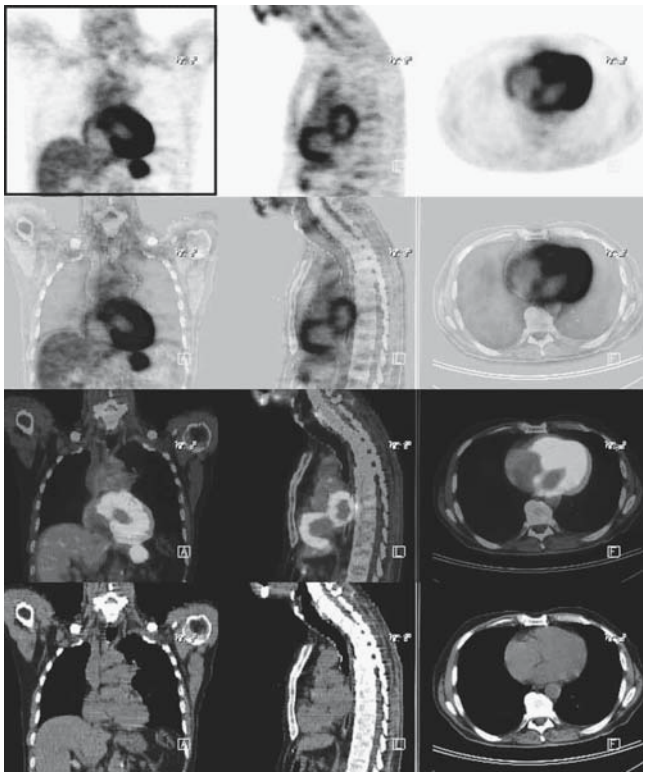

FIGURE 1.2.5. Cardiac hypertrophy. Cardiac hypertrophy with multichamber visualization. Stomach activity is seen as a ring of activity below the heart.

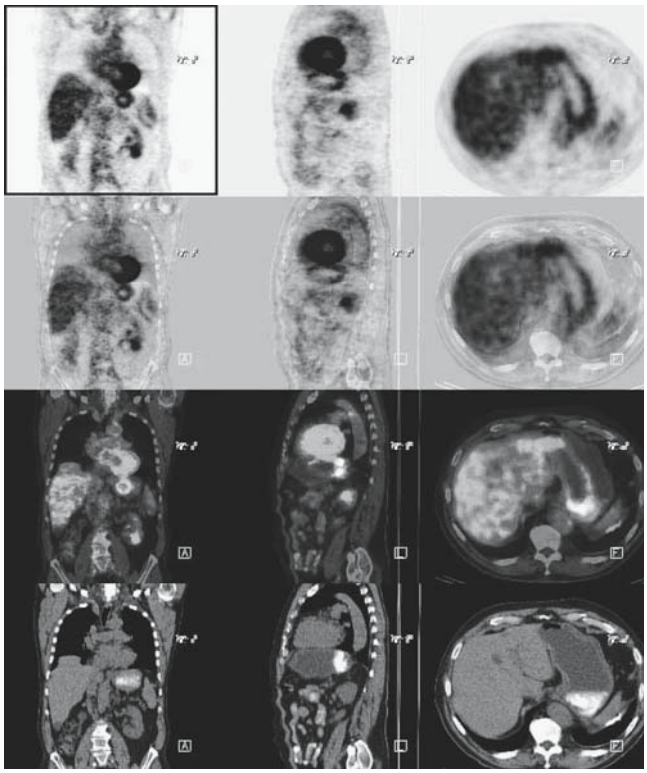

FIGURE 1.2.6. Gastric wall activity. Proximal stomach activity is seen in 10% to 15% of patients.

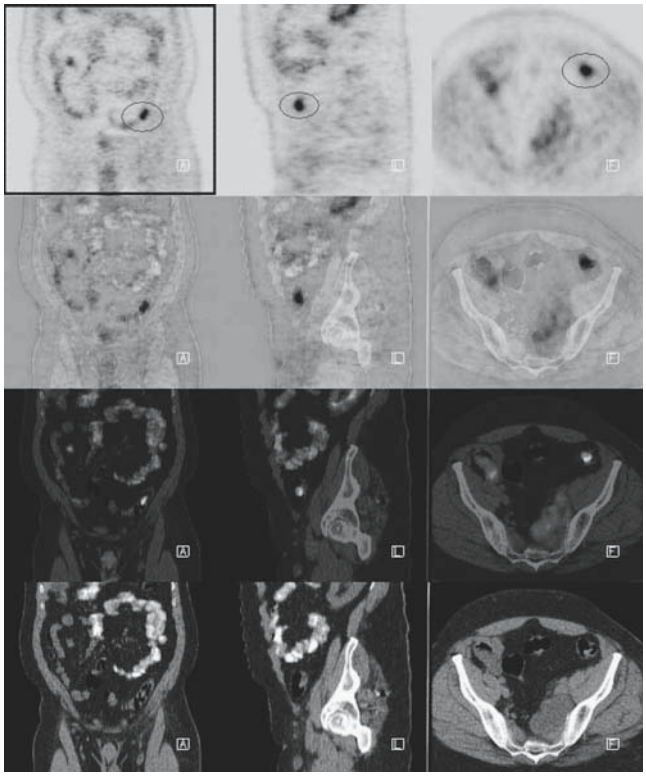

FIGURE 1.2.7. Colonic polyp. Colonic adenomas and polyps may demonstrate increased glucose metabolism.

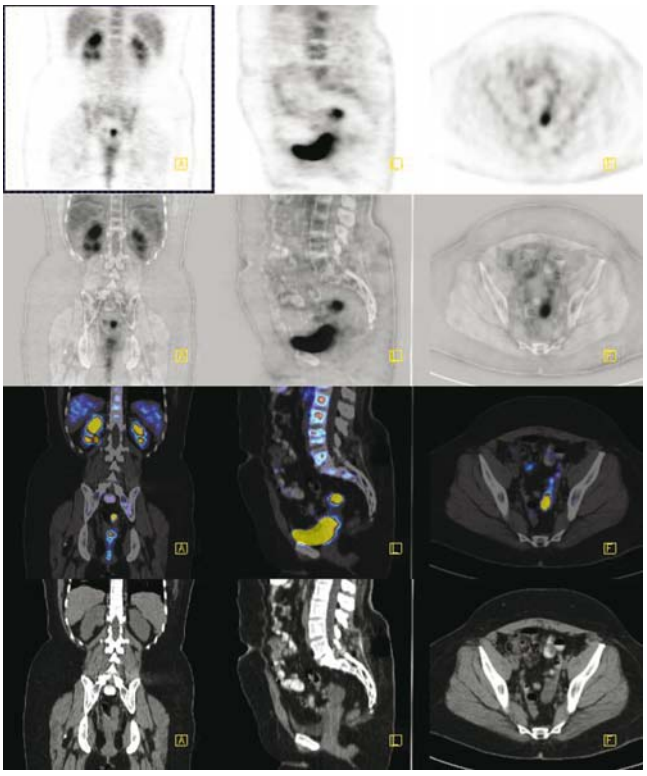

FIGURE 1.2.8. Corpus luteum. Adnexal uptake representing a corpus luteum. Uterine cavity uptake can also be found in menstruating patients.

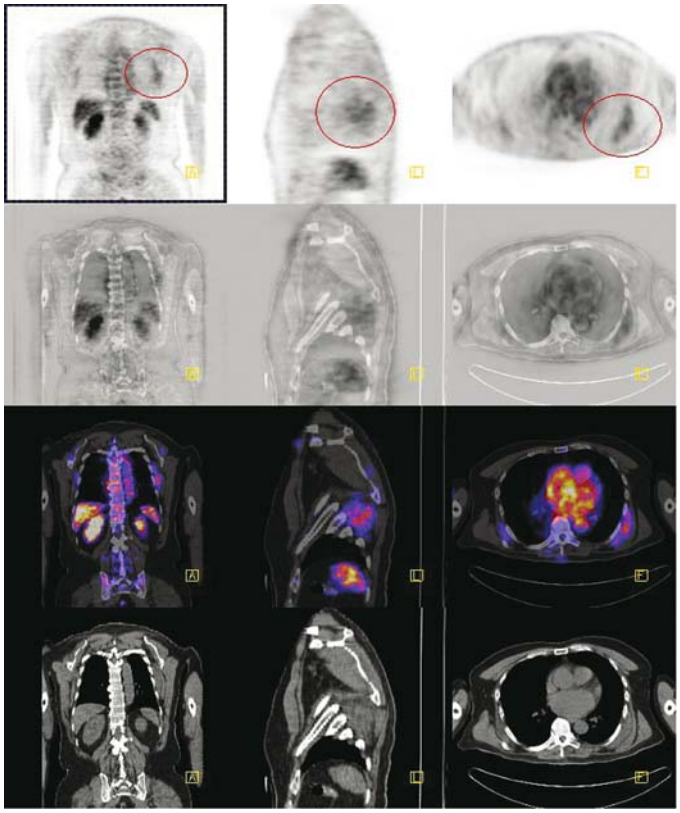

FIGURE 1.2.9. Elastofibroma dorsi. This can be confused with physiological muscle uptake.

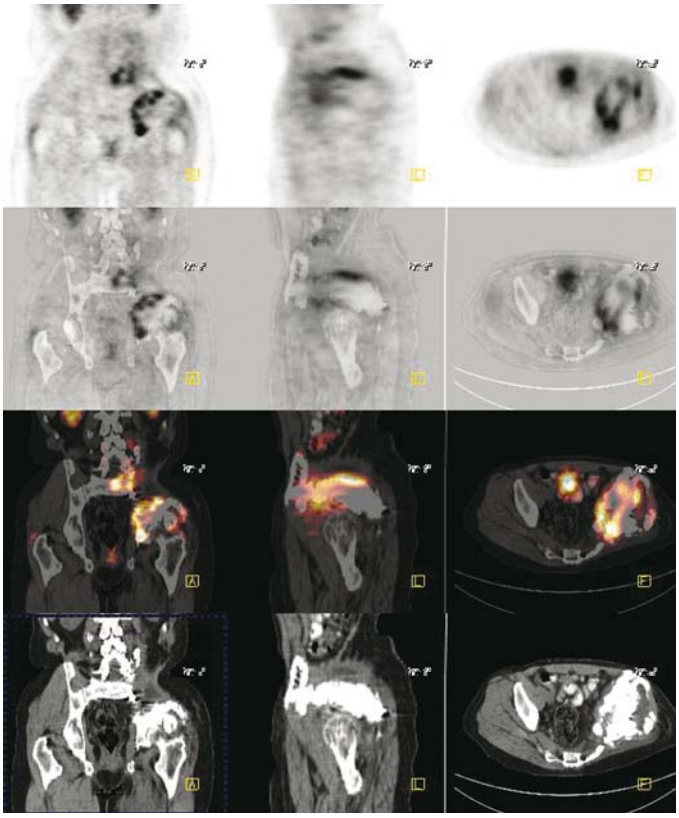

FIGURE 1.2.10. Myositis ossificans. Inflammatory changes in soft tissue account for increased uptake in myositis ossificans.

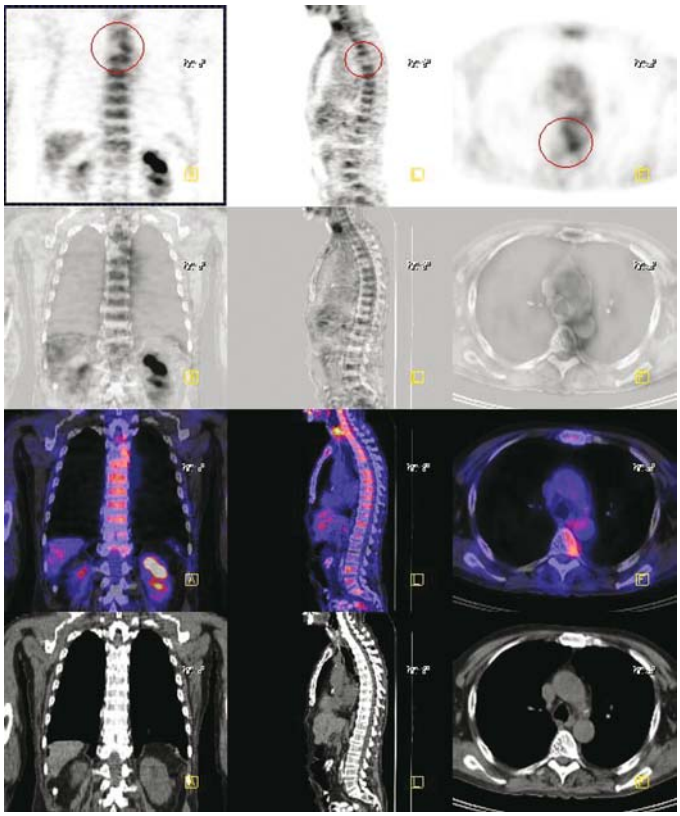

FIGURE 1.2.11. Hemangioma. A vertebral hemangioma may appear photopenic on 18-FDG PET, but is more recognizable on CT.

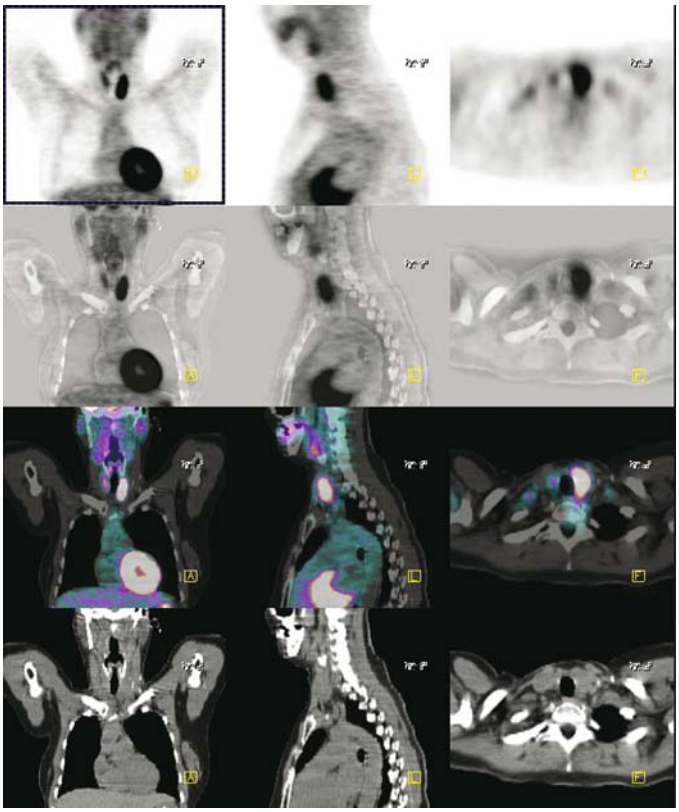

FIGURE 1.2.12. Goiter. Both benign and malignant thyroid pathology may demonstrate elevated FDG uptake.

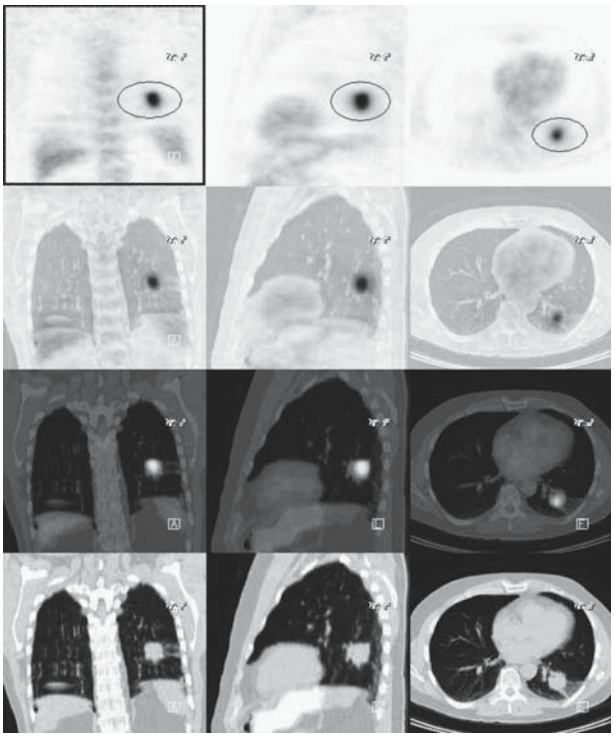

FIGURE 1.2.13. Histoplasmosis. One limitation of PET is that active infectious granulomatous disease in the lung can exhibit high FDG uptake. Certain fungal infections are more common in certain geographic areas. In St. Louis, for example, cystomyocosis is more prevalent. In California and Arizona, it is coccidioidomycosis. In the rest of the world, tuberculosis is more common.

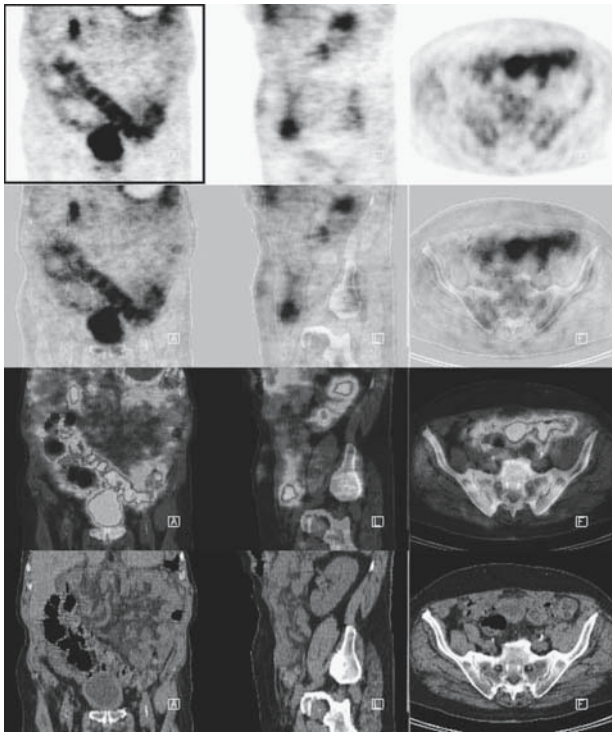

FIGURE 1.2.14. Inflammatory bowel disease. Elevated uptake can be seen in Crohn's disease and other forms of inflammatory bowel disease. It may be difficult to differentiate this from normal physiological bowel uptake in the absence of clinical symptoms.

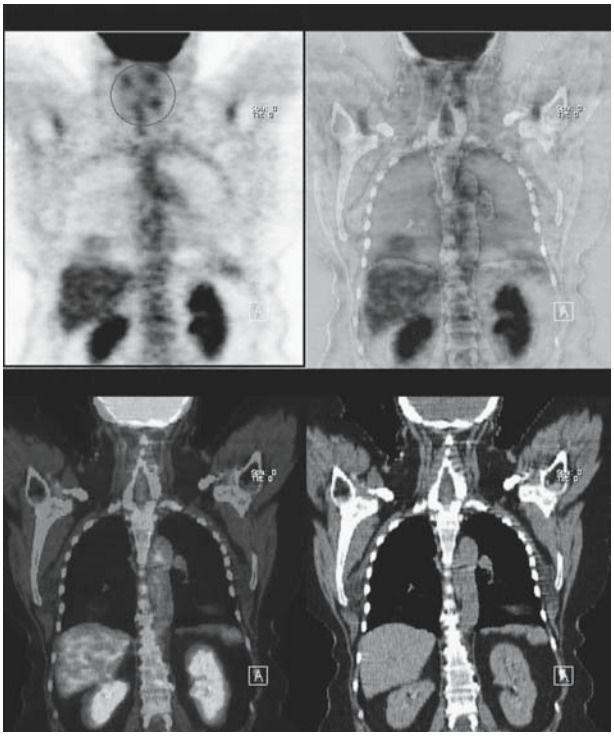

FIGURE 1.2.15. Nerve root neuritis. Focal neuritis can display elevated FDG uptake.

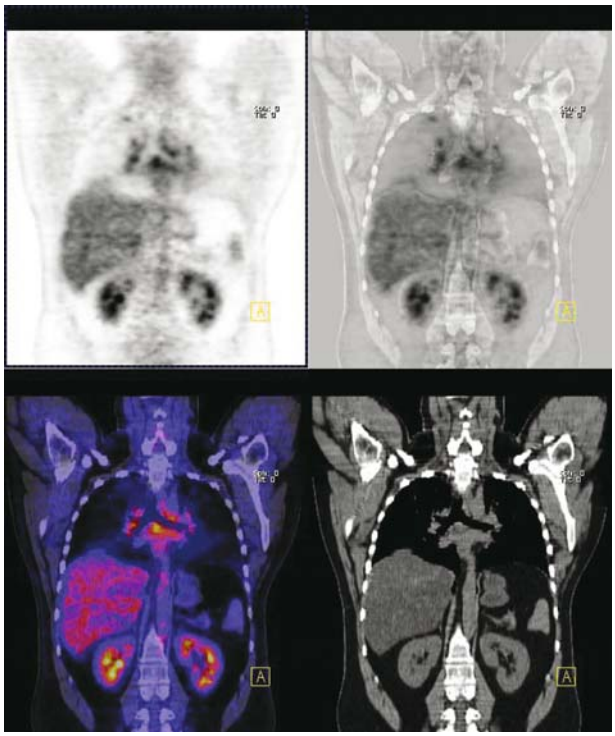

FIGURE 1.2.16. Sarcoidosis. These correspond to ill-defined irregular areas of subtle central pulmonary nodular densities on CT.

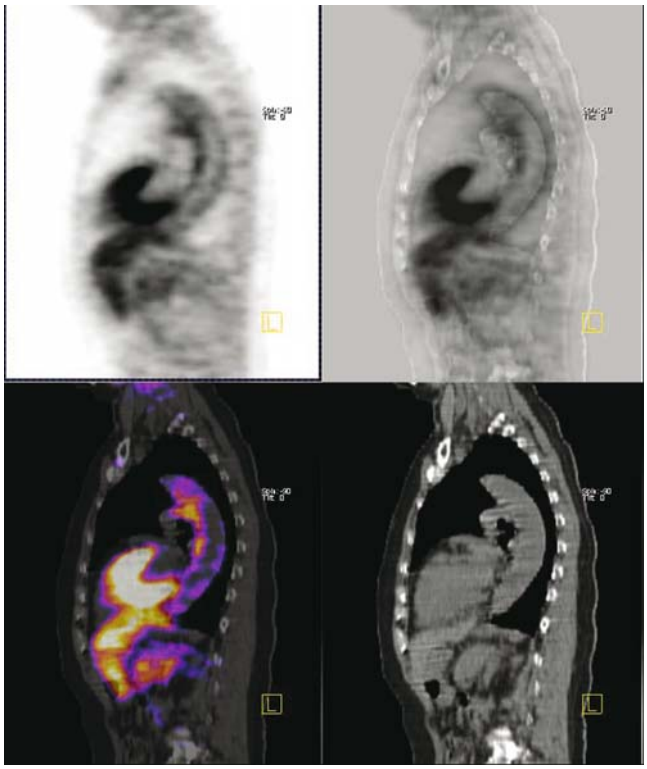

FIGURE 1.2.17. Aortitis (sagittal view). Inflammatory disease of major vessels can be associated with elevated FDG and may herald the presence of vulnerable plaque. Association with calcifications on CT is variable.

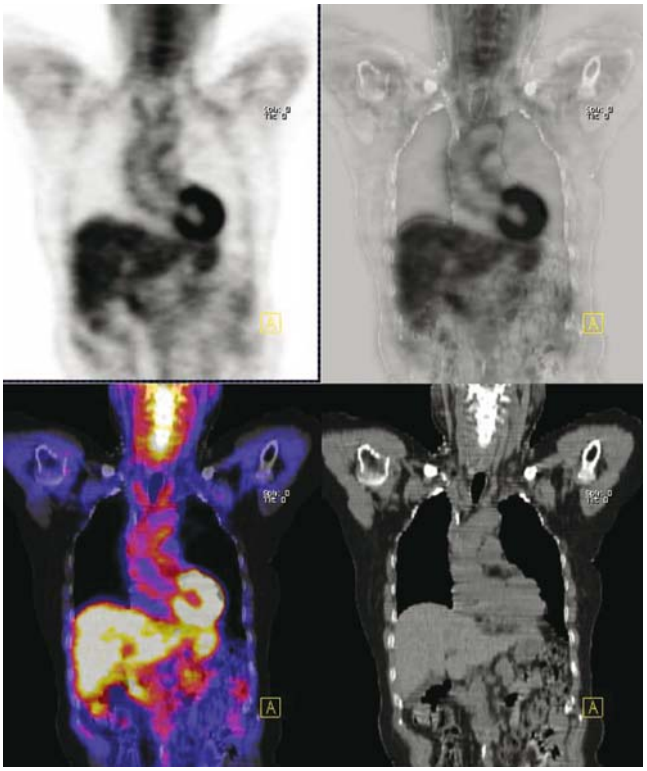

FIGURE 1.2.18. Aortitis (coronal view). Inflammation of the intima of the thoracic and abdominal aorta may be seen as a tube-like structure representing aortitis and possible vulnerable plaque.

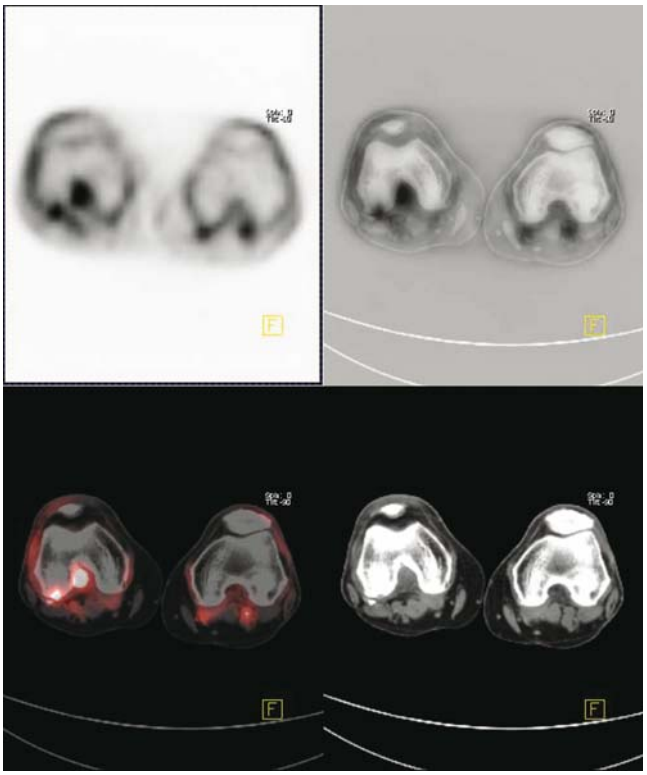

FIGURE 1.2.19. Subacute avulsion fracture. Focal defect in the posterior portion of the lateral right femoral condyle and an adjacent bone fragment posterior and lateral to it compatible with post-traumatic osteochondral defect with secondary local synovitis.

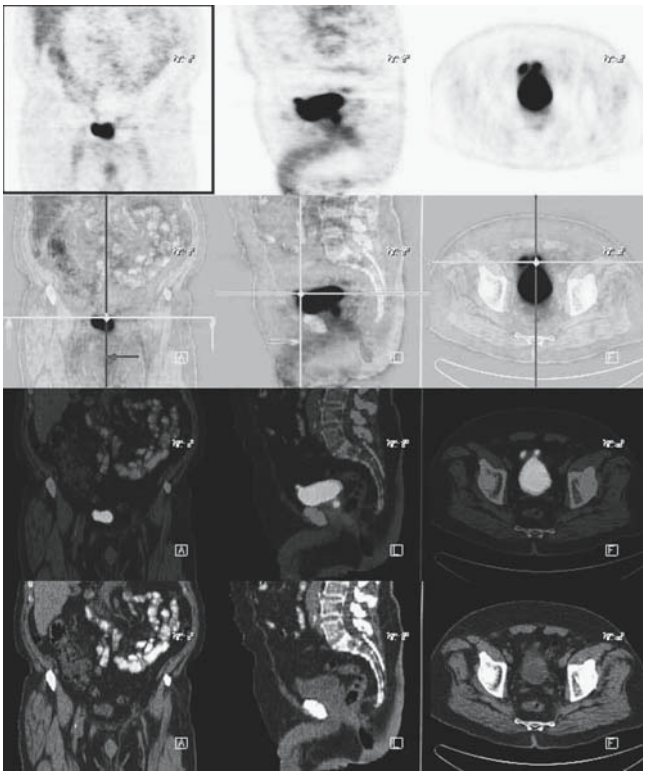

FIGURE 1.2.20. Bladder diverticulum. Anterolateral bladder diverticulum and a midline urachal diverticulum. Status post TURP.

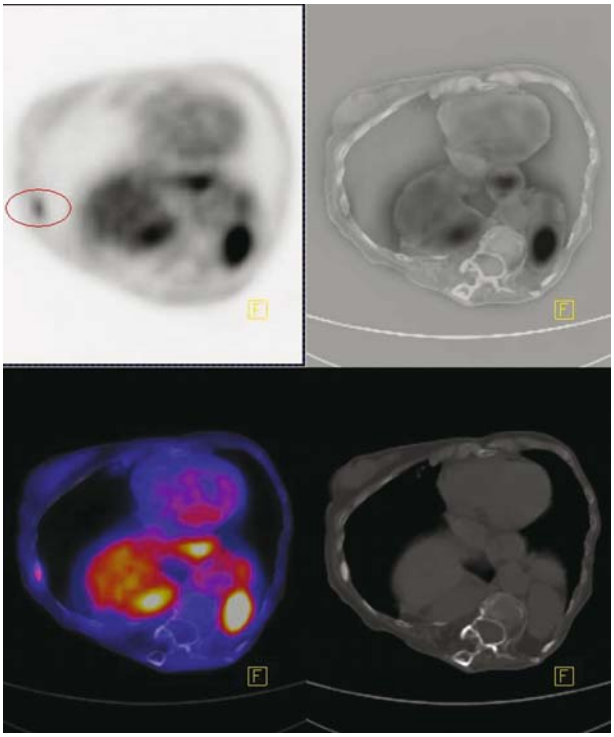

FIGURE 1.2.21. Callus. Rib callus seen on CT with elevated FDG uptake. This can be misinterpreted as a metastatic deposit.

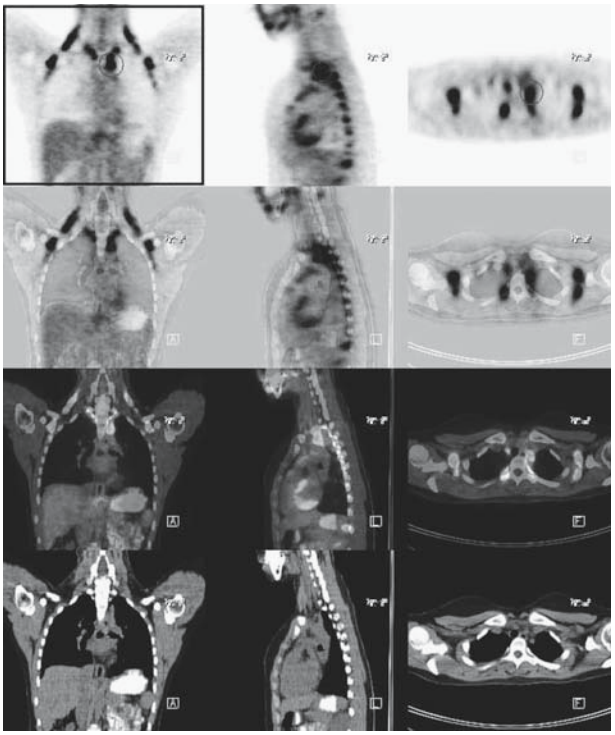

FIGURE 1.2.22. Fat mobilization. Brown fat as well as muscle can be associated with elevated FDG uptake. CT allows correct assignment of FDG activity to fat as opposed to muscle.

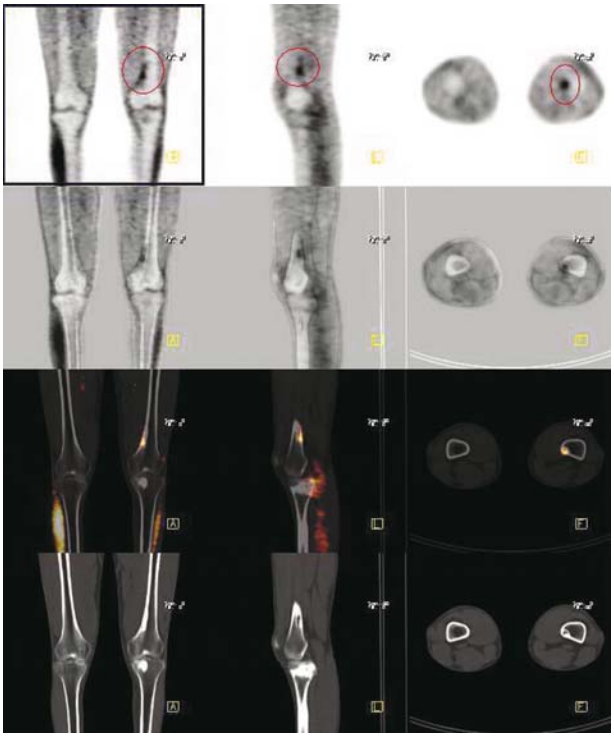

FIGURE 1.2.23. Fibroma. Certain benign lesions may display FDG uptake. This one demonstrates a well-circumscribed peripheral intraosseous lesion on CT with elevated FDG uptake.

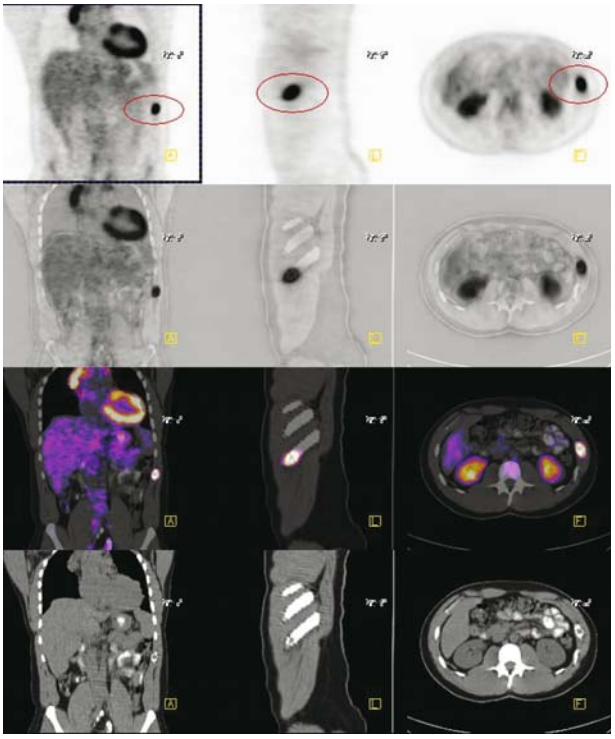

FIGURE 1.2.24. Fibrous dysplasia. Expansile rib lesion on CT with elevated FDG uptake. This can be difficult to discern from metastatic disease in the absence of correlative anatomic imaging and clinical history.

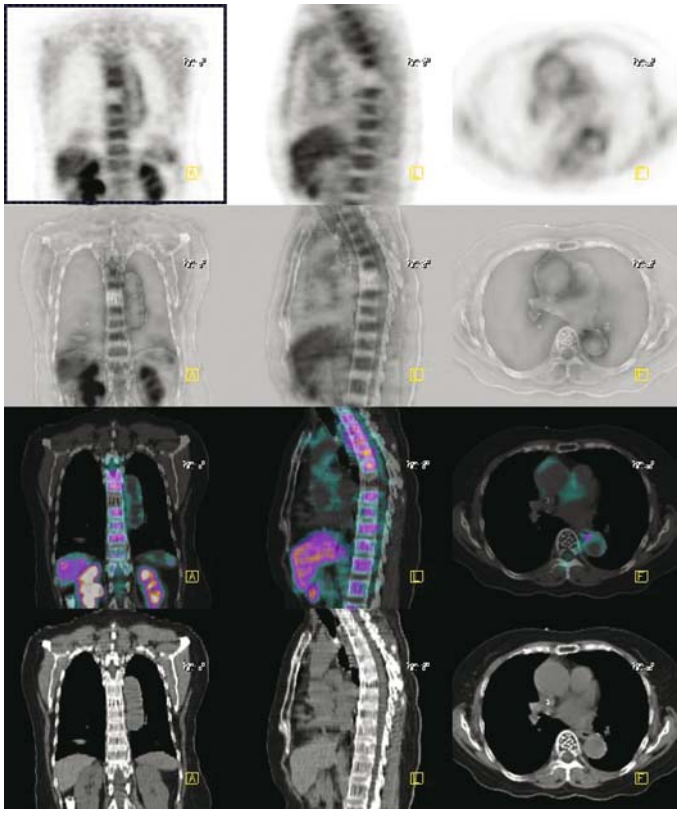

FIGURE 1.2.25. Hemangioma. In general, these lesions display low FDG uptake.

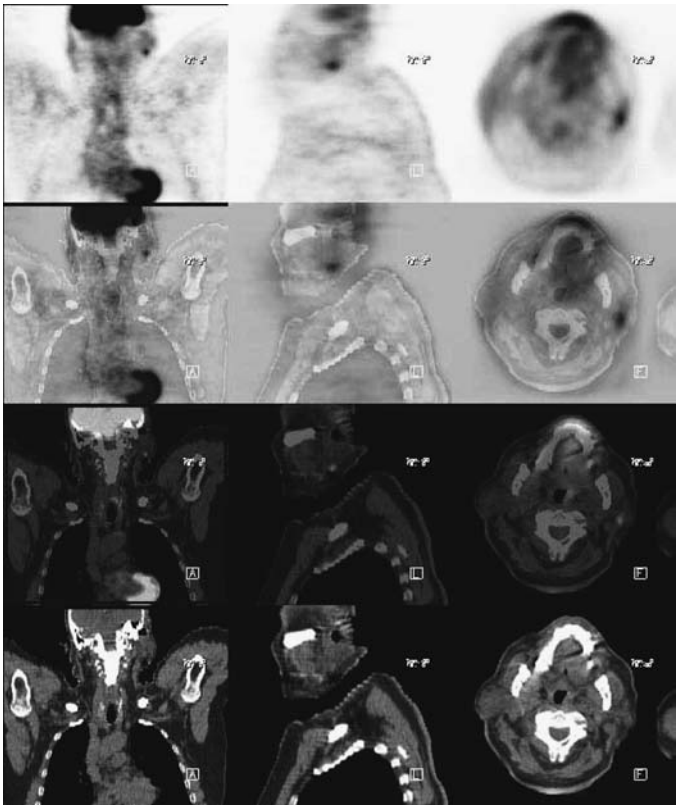

FIGURE 1.2.26. Pleomorphic adenoma. Benign lesions such as adenomas can display elevated FDG uptake.

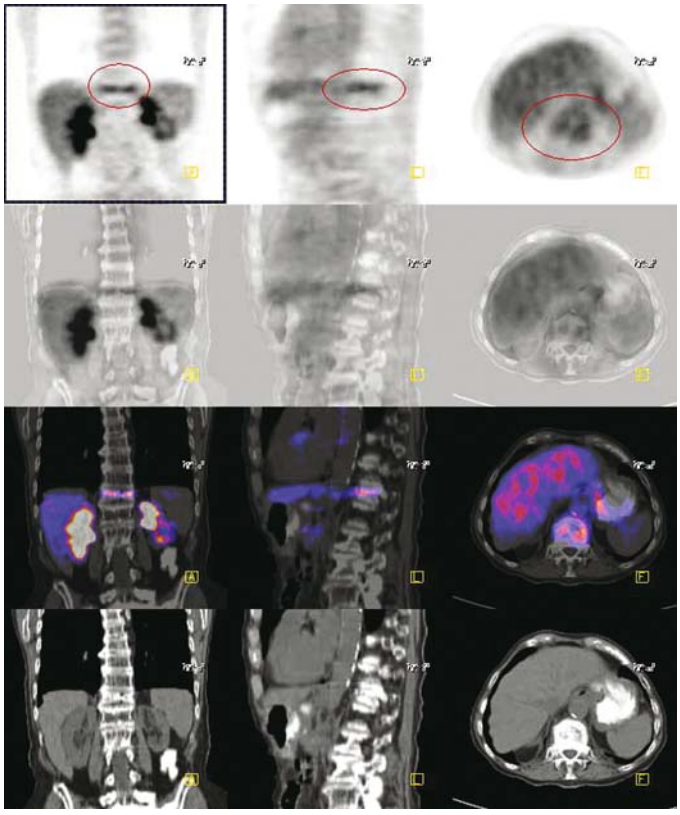

FIGURE 1.2.27. Insufficiency fracture. Acute fractures and insufficiency factors have been associated with elevated FDG uptake.

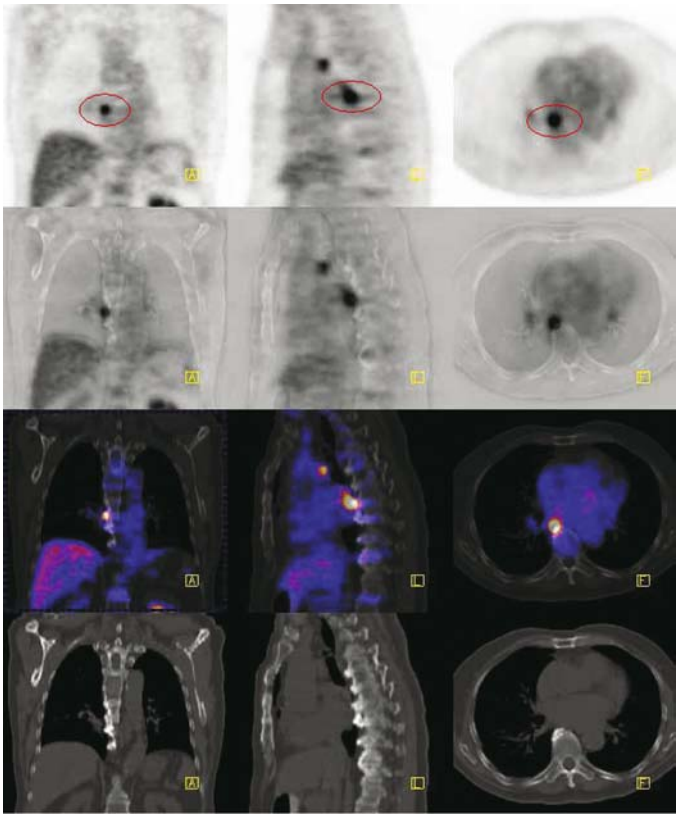

FIGURE 1.2.28. Bone spur formation. Surrounding soft tissue inflammation is the likely cause of FDG uptake.

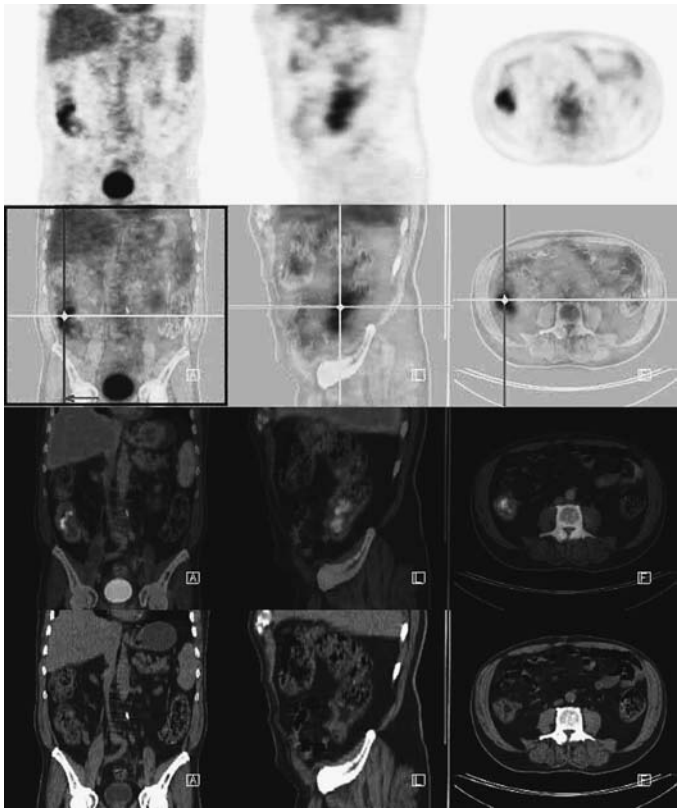

FIGURE 1.2.29. C. difficile. Infection as well as inflammatory disease can be associated with FDG uptake.

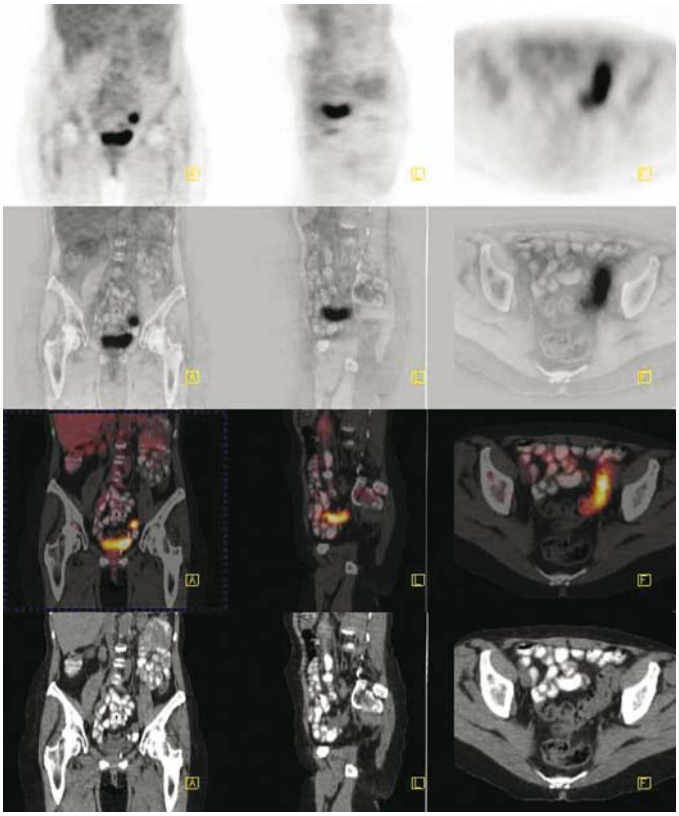

FIGURE 1.2.30. Diverticulosis. Diverticulosis, or more commonly diverticulitis, can display elevated FDG uptake.

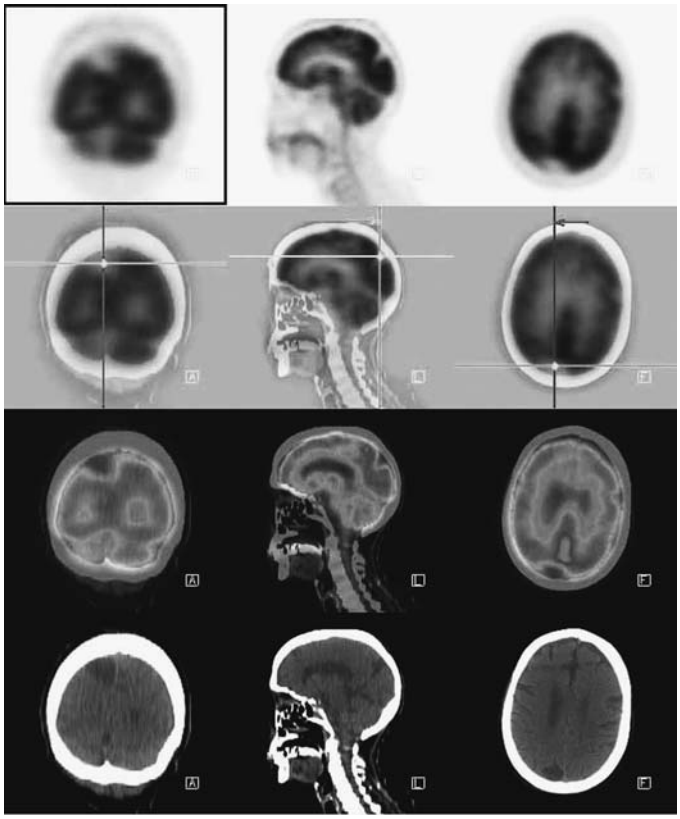

FIGURE 1.2.31. Stroke. Focal wedge-shaped hypometabolism is suggestive of vascular insult in the brain.

FIGURE 1.2.32. Cystic fibrosis. Disseminated muscular uptake of FDG.

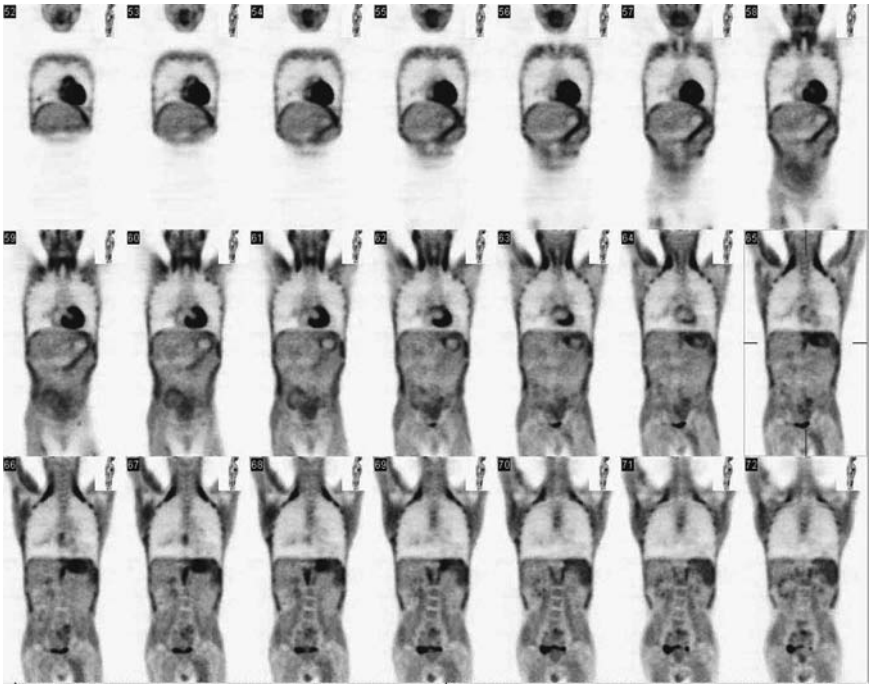

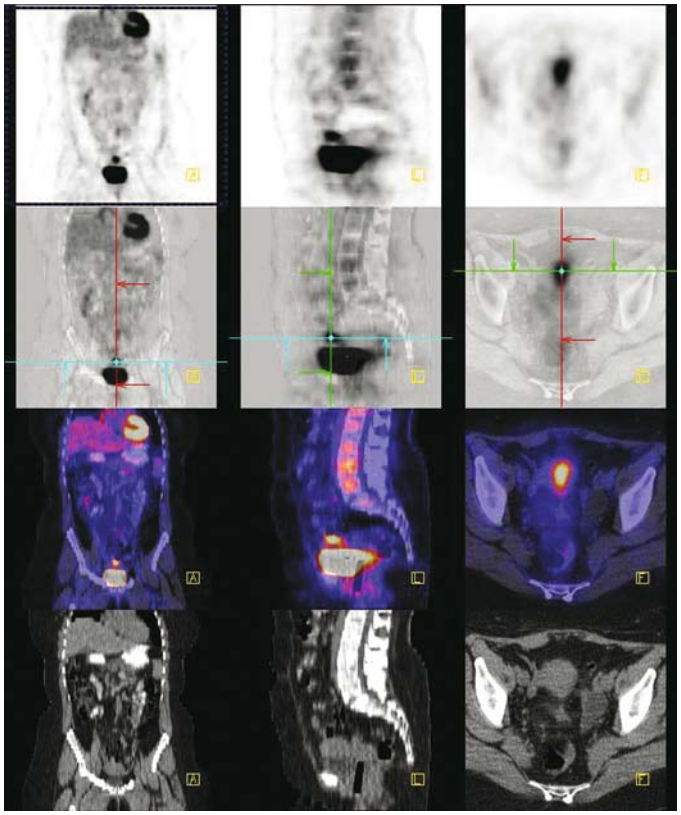

FIGURE 1.2.33. Menstruation. Active menstruation in a young female patient during imaging, with elevated activity in the uterus.

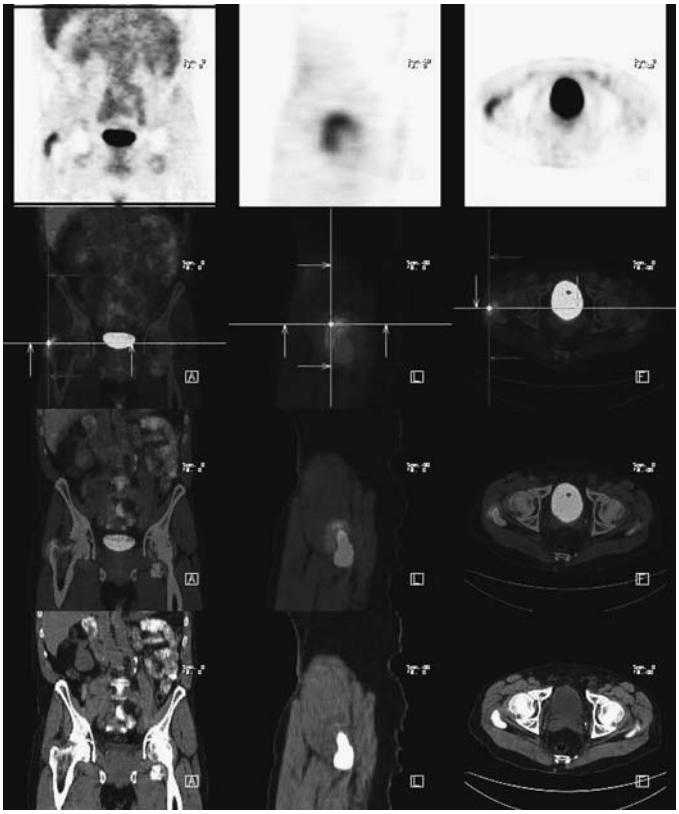

FIGURE 1.2.34. Bursitis. Mild tracer activity in the right hip region is consistent with trochanteric bursitis.

1.3 Posttherapeutic Changes

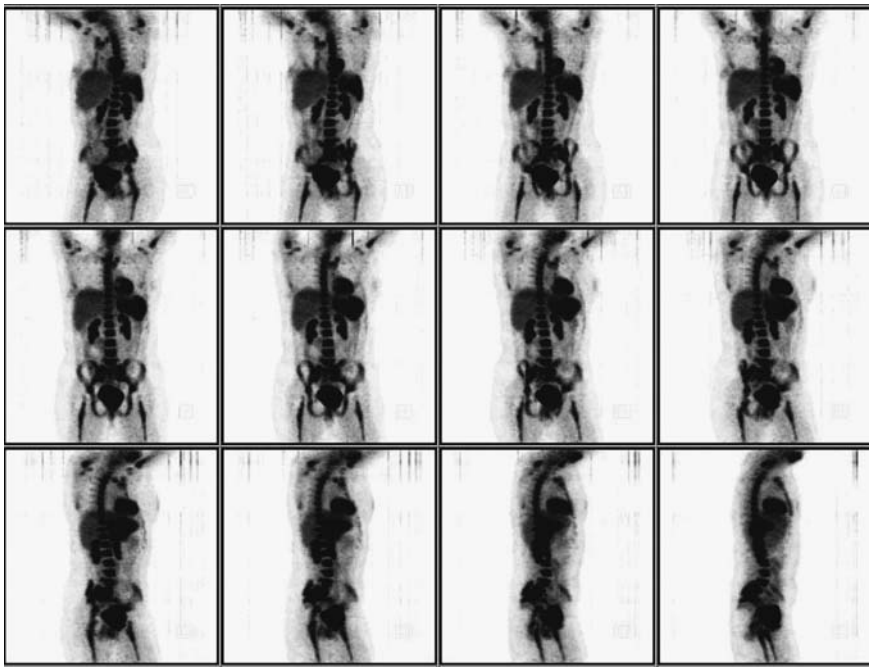

Figure 1.3.1. Bone marrow flare. From right to left, the rotating images demonstrate diffuse generalized uptake involving the axial and appendicular skeleton consistent with recent chemotherapy response. Postcytokine therapy (including GCSF, or granulocyte colony stimulating factor) patients usually display prominent marrow and splenic hyperplasia.

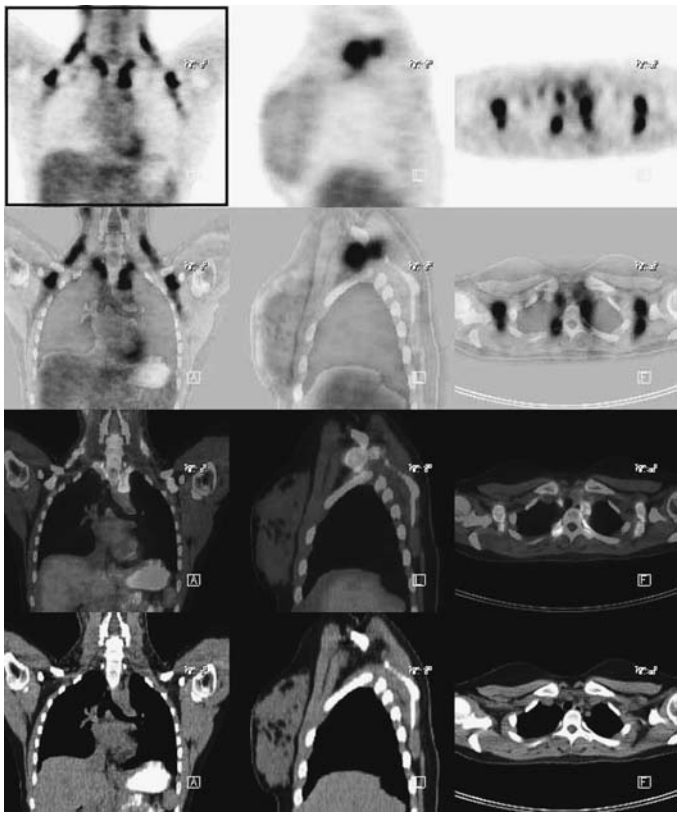

Figure 1.3.2. Fat mobilization. The patient was treated with chemotherapy recently. The previous baseline study was unremarkable for fat or muscular activity.

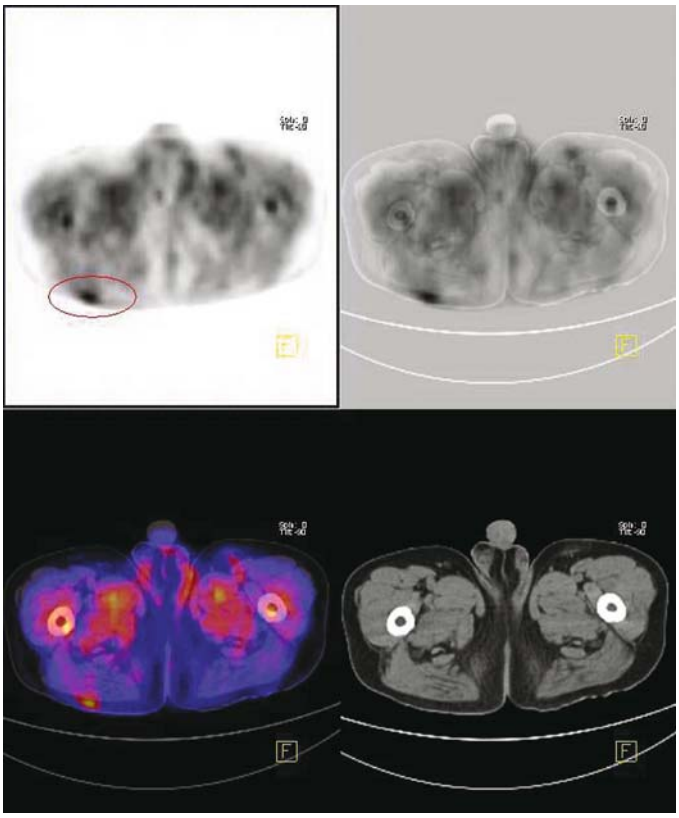

Figure 1.3.3. Injection site activity. There was a recent injection in the buttock resulting in local inflammation.

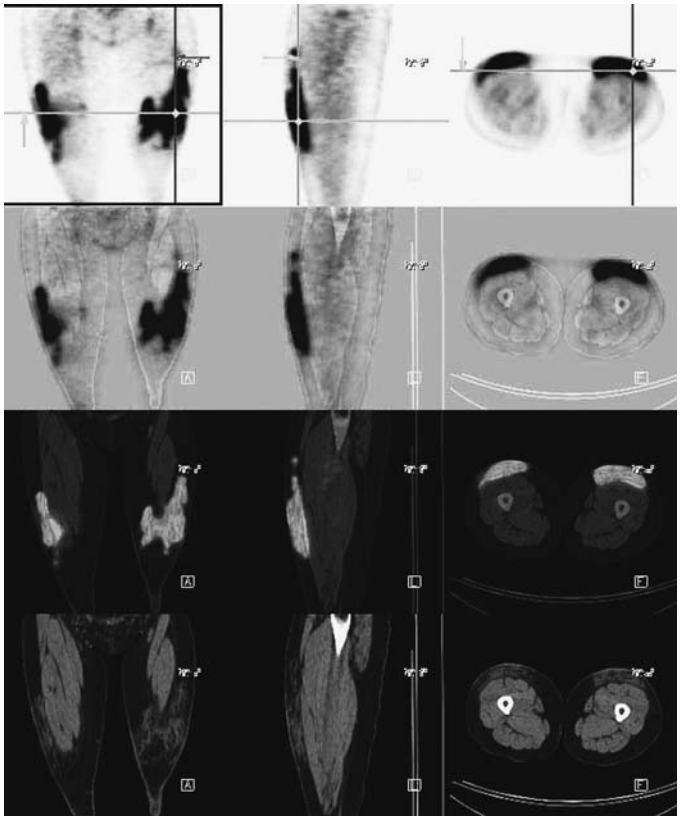

FIGURE 1.3.4. Immunotherapy. The changes in the fat correlate with this history of immunotherapy injections in the thighs.

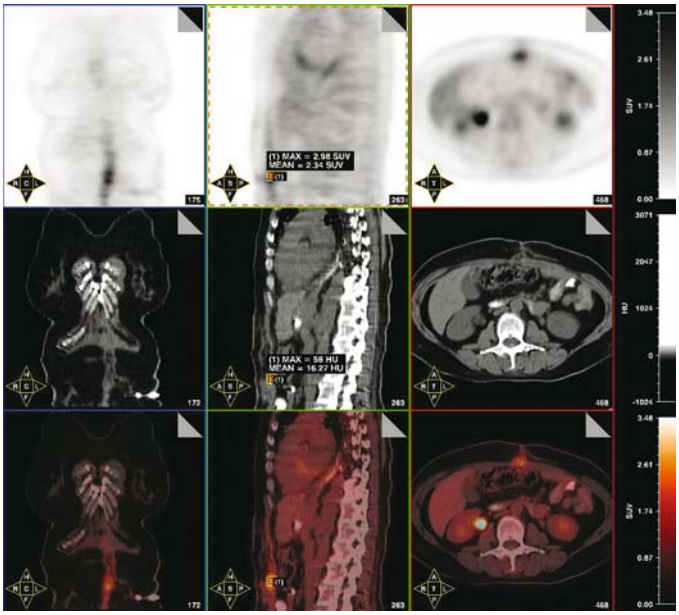

FIGURE 1.3.5. Abdominal incision. Postsurgical changes such as midline incisional inflammation usually resolve in 2–4 weeks.

1.4 Foreign Body Artifact

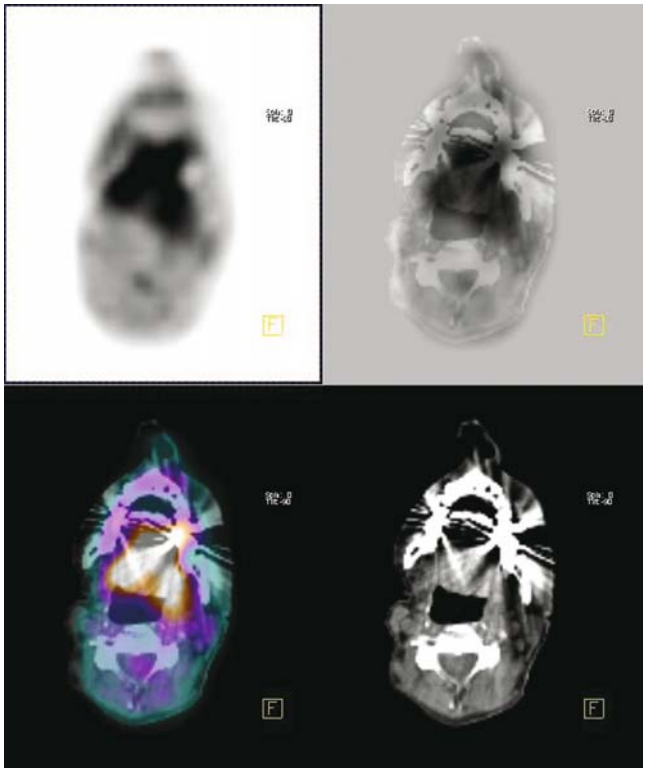

Figure 1.4.1. Dental artifact. Metal artifacts are known to cause artificial uptake. If it corresponds to CT findings and the patient has no known head or neck cancer, abnormality in this region is unlikely.

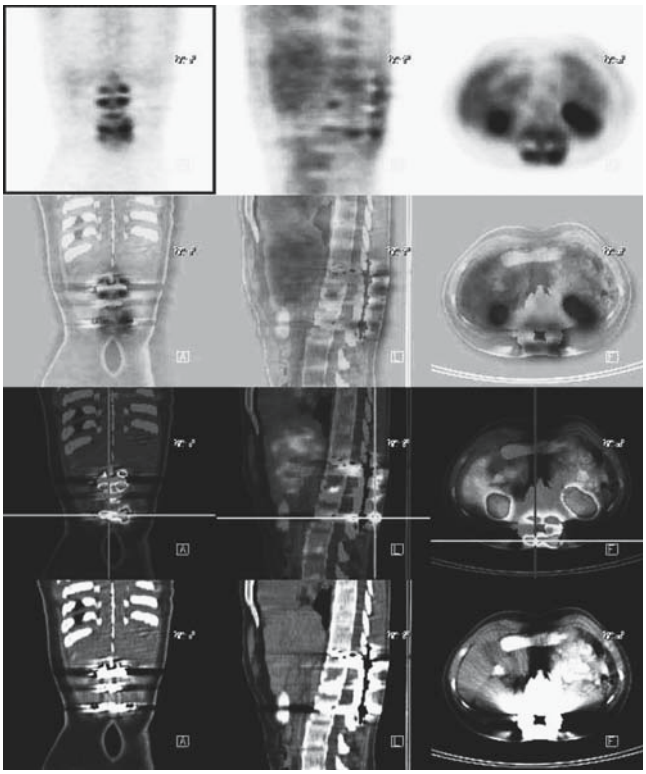

Figure 1.4.2. Spinal fusion. Metal artifacts are known to cause artificial uptake.

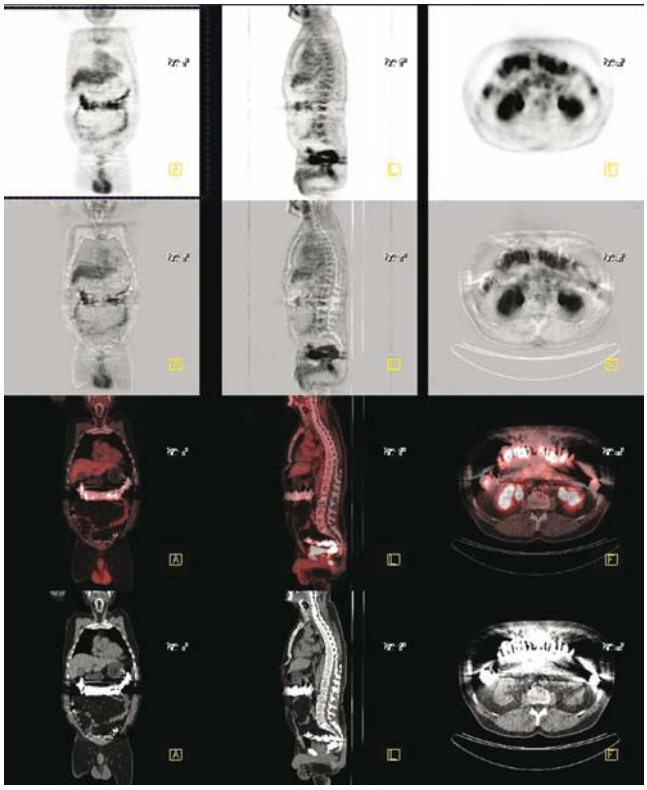

Figure 1.4.3. Barium enema. Scattered diffuse uptake in the bowel of this patient with barium edema prior to imaging is not unusual. It has been reported that if water-soluble enema is initially used instead of the conventional oil enema, bowel uptake will be reduced.

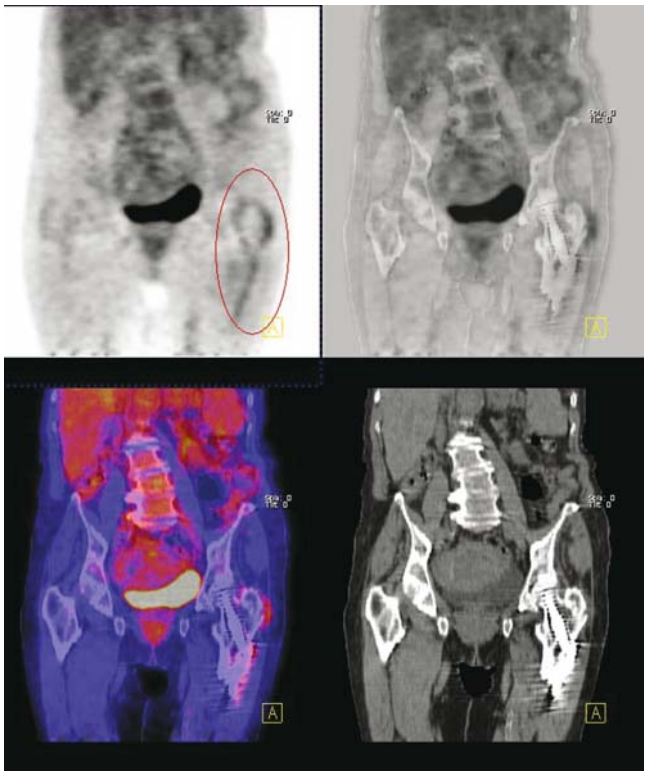

FIGURE 1.4.4. Prosthetic hip. Diffuse generalized uptake around the hip suggests chronic inflammatory changes.

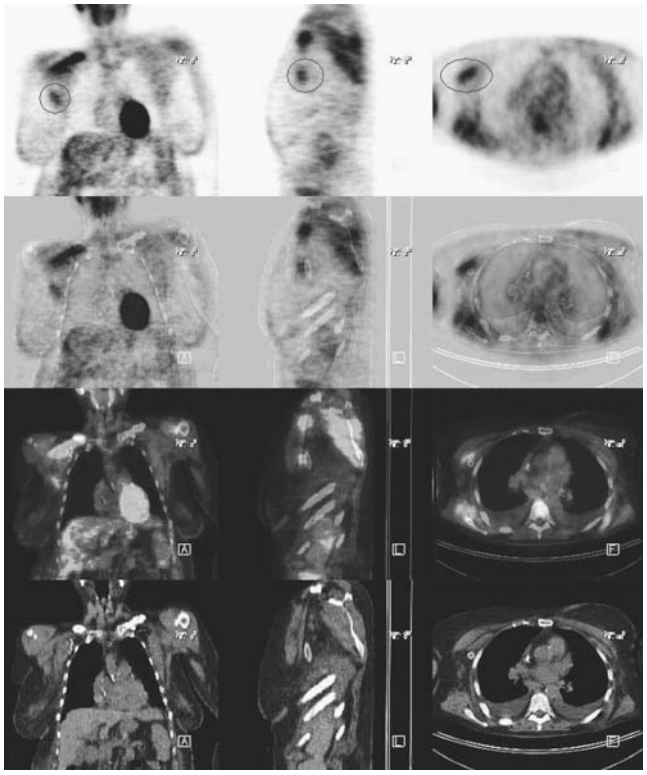

FIGURE 1.4.5. Bypass graft. The activity around the graft is compatible with recent surgery.

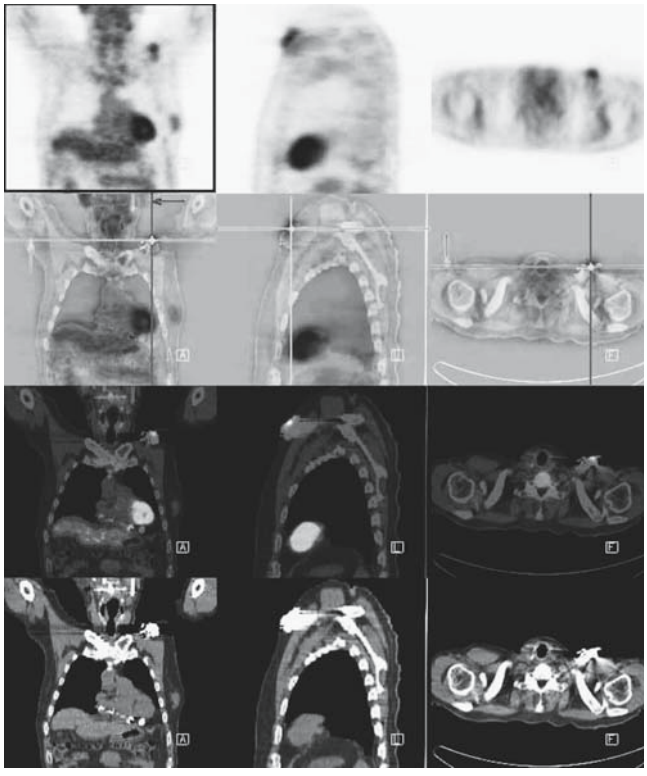

FIGURE 1.4.6. Pacemaker. Inflammation in soft tissue surrounding a pacemaker.

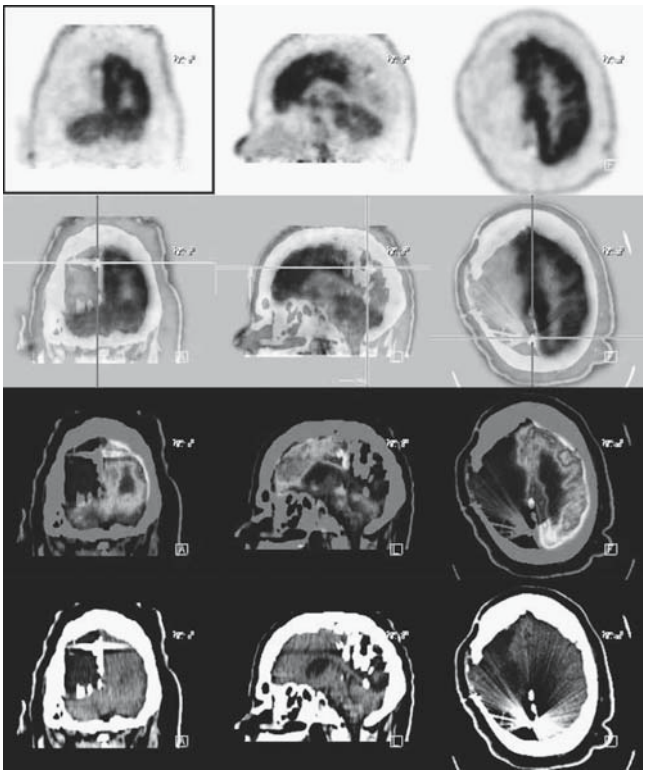

FIGURE 1.4.7. Gunshot wound. This patient has a history of high-velocity penetrating self-inflicted trauma to the head resulting in partial resection of the brain parenchyma and shrapnel residuals embedded in the skull.

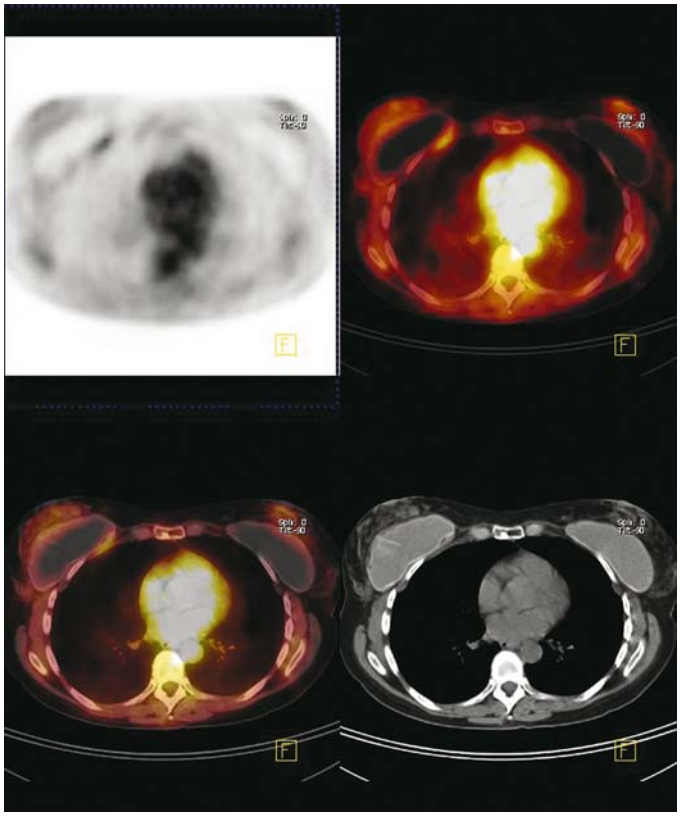

FIGURE 1.4.8. Breast prostheses. The photopenia in the breasts is compatible with breast prostheses.

1.5 Technical Artifacts

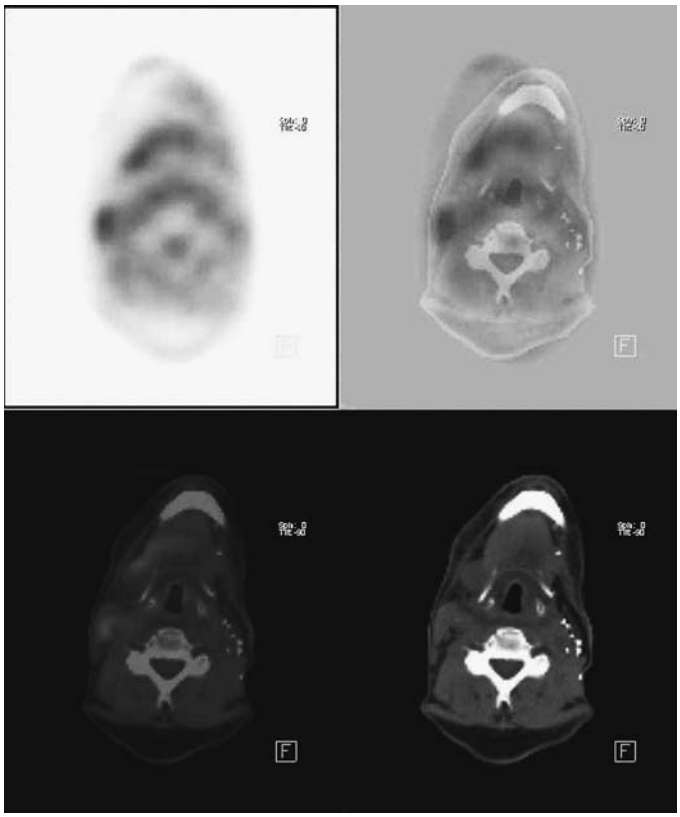

Figure 1.5.1. Horizontal (motion) artifact. The patient's head was moving in the middle of the study.

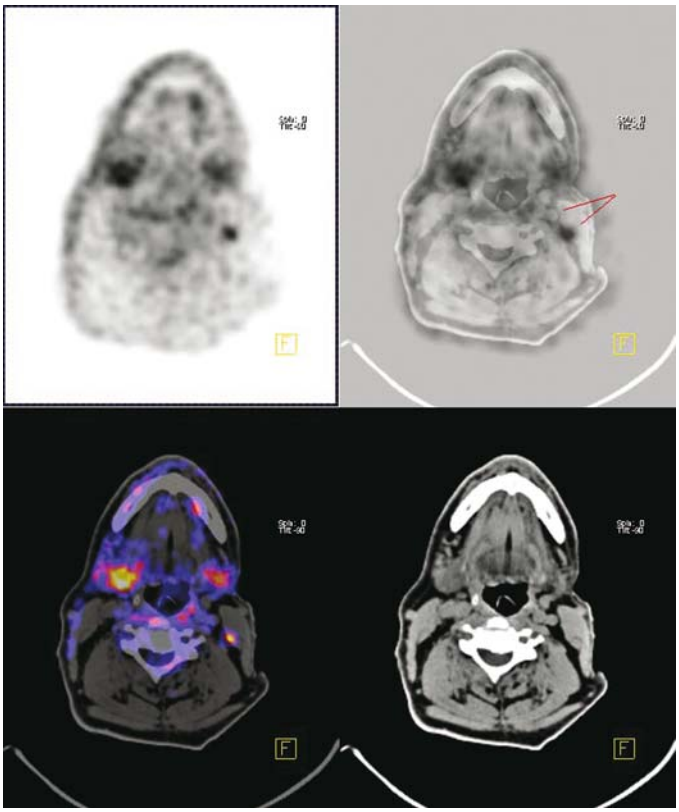

Figure 1.5.2. Vertical artifact. The cervical node activity on the left is several slices away from the node on CT.

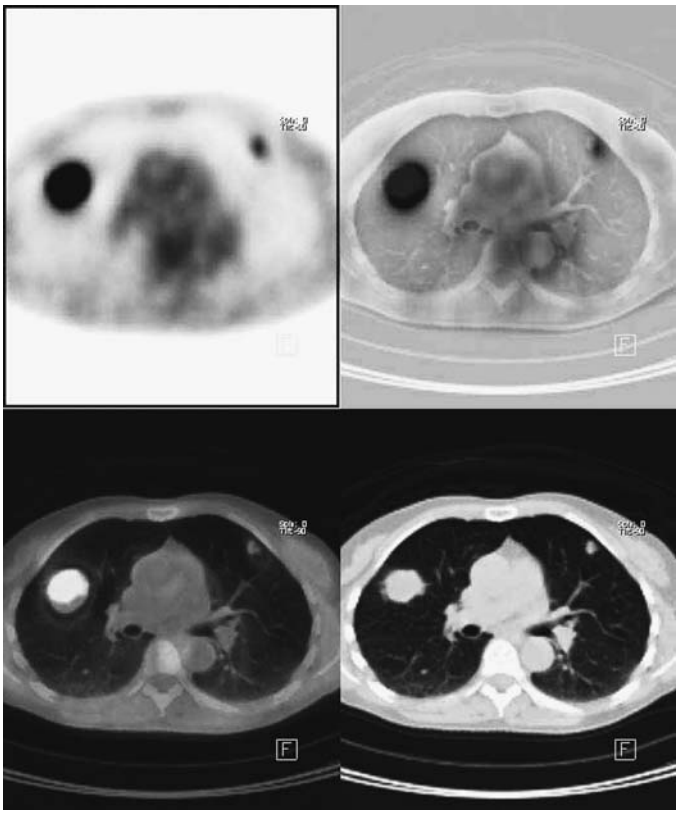

Figure 1.5.3. Diaphragmatic artifact (transaxial). The degree of lesion motion is location dependent within the lung. Lower lung lesions can move considerably more than the apical lesion. Respiration can produce a blurred lesion and will increase the lesion size. This will invariably decrease the activity concentration per pixel within the lesion and causes an underestimation of SUV.

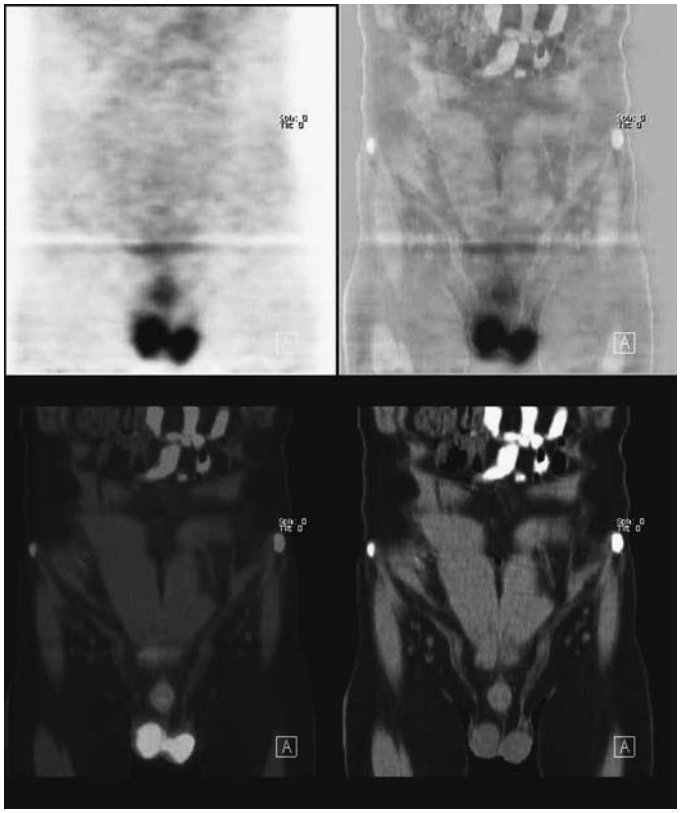

FIGURE 1.5.4. Streak artifact. Reconstruction artifact.

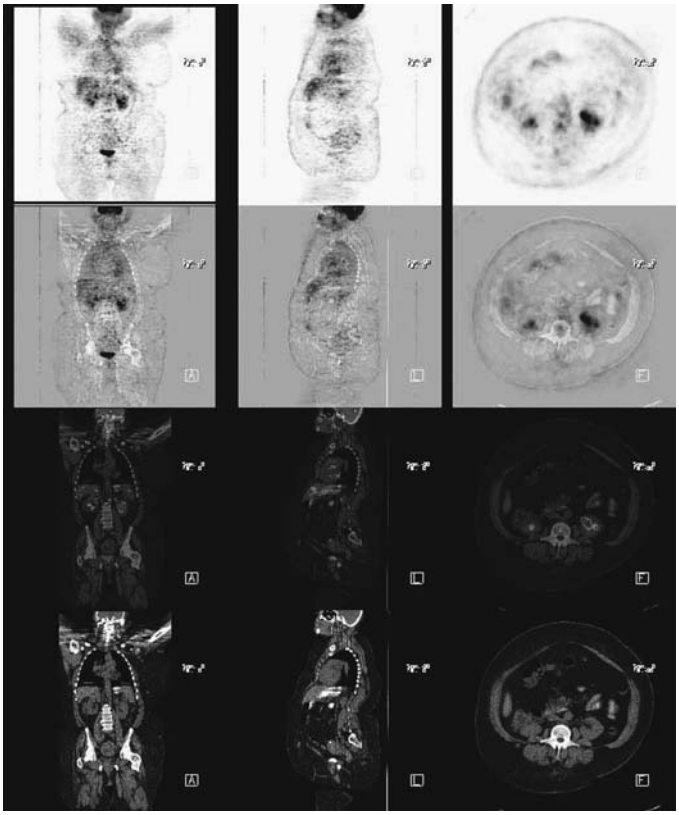

FIGURE 1.5.5. Poor counts. This is a heavy-set patient where a higher dose of FDG or longer emission scan times are necessary in order to produce an ideal study.

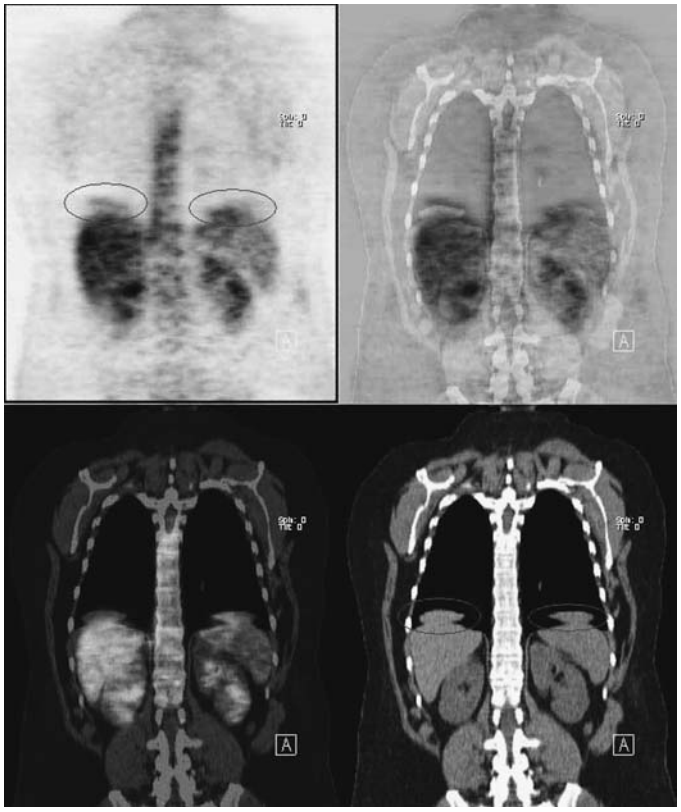

FIGURE 1.5.6. Diaphragmatic artifact (coronal). Respiratory motion causing artifact.

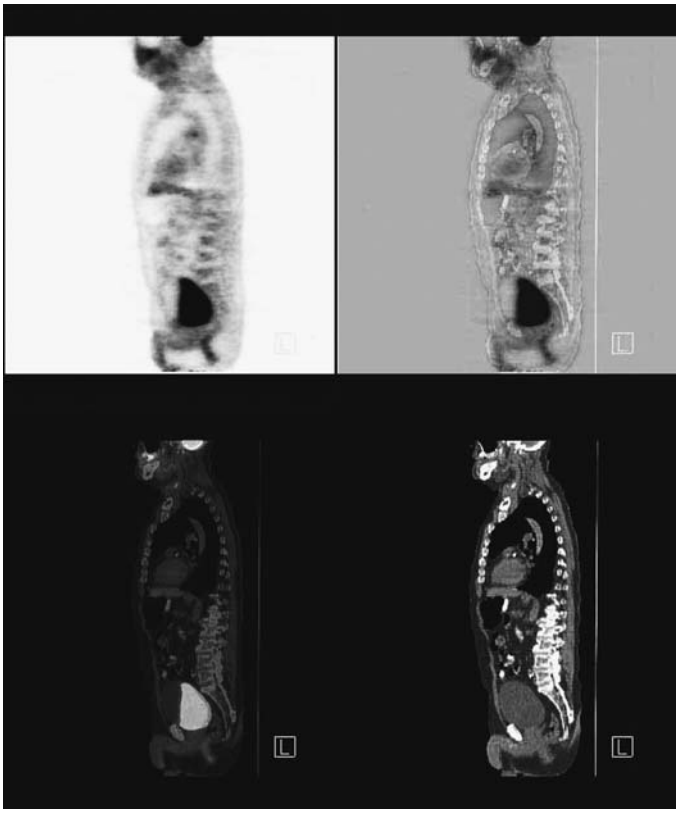

FIGURE 1.5.7. FDG-density phenomenon. The urine containing FDG appears to be denser than the urine without FDG.

Part II Clinical Cases

2 Adrenal Cancer

Heidi R. Wassef

Case 2.1

History

72-year-old male with previous resection of right adrenal carcinoma, who is being evaluated for recurrent disease.

Findings

There is a large right posterior lobe liver mass (*Figures 2.1.1 and 2.1.2*) measuring 10 cm × 9 cm. Above it, there is a satellite mass of 4.4 cm diameter in the dome of the right lobe of the liver. The left lobe appears uninvolved. The mass extends into the retroperitoneum with intrinsic involvement of the uppermost portion of the right kidney. There appears to be extension into the right renal vein with the mass also adjacent to the right lateral margin of the inferior vena cava. The entire complex is intensely hypermetabolic, consistent with recurrent adrenal carcinoma. No distant metastatic disease is apparent. Incidental notation is made of thoracolumbar scoliosis with asymmetrical disc disease.

Impression

Large intensely hypermetabolic recurrence of right adrenal carcinoma with a 10 × 9 cm mass involving the right lobe of the liver and a satellite mass extending into the dome of the right lobe. There is extension into the upper right kidney and apparent involvement of the right renal vein. The mass extends to the right lateral margin of the inferior vena cava. No distant metastatic disease is evident.

Pearls and Pitfalls

- *PET/CT is an effective tool for determining the extent of tumor recurrence.*[1–3]
- *The sensitivity for adrenal cancer approaches 100% with 94% specificity, and 96% accuracy.*[1–3]

Discussion

The incidence of **adrenal carcinoma** is 1 in 700,000 in the adult population. Most are identified as large, 5 cm or greater, in diameter. The majority (50% to 80%) of the cases

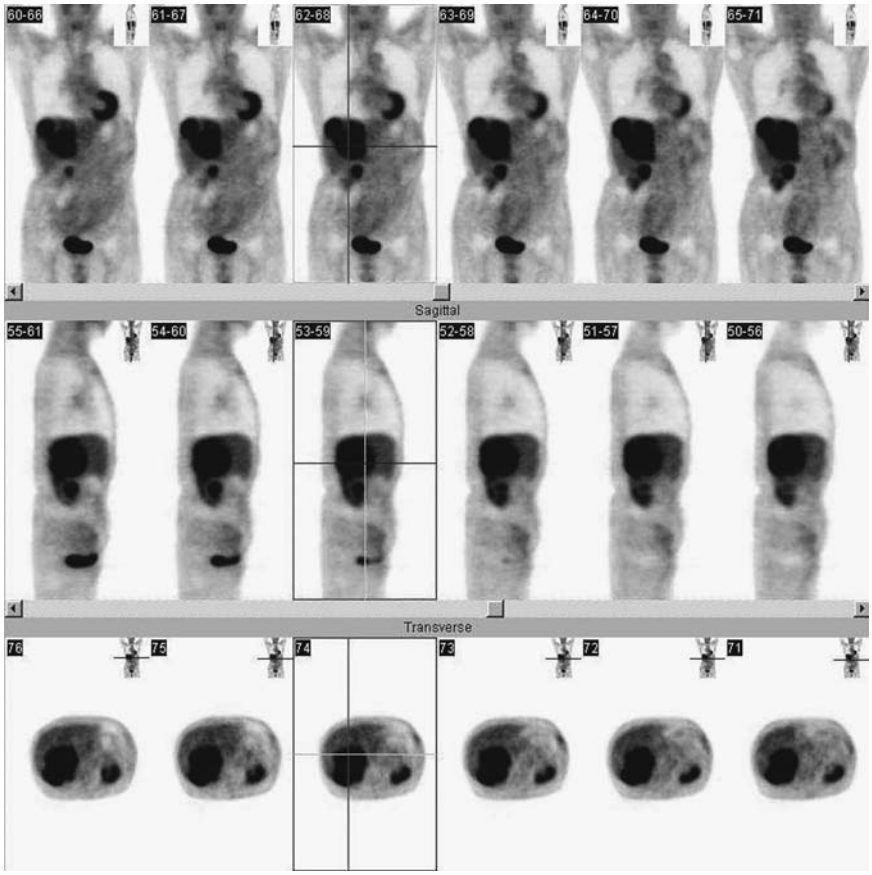

FIGURE 2.1.1.

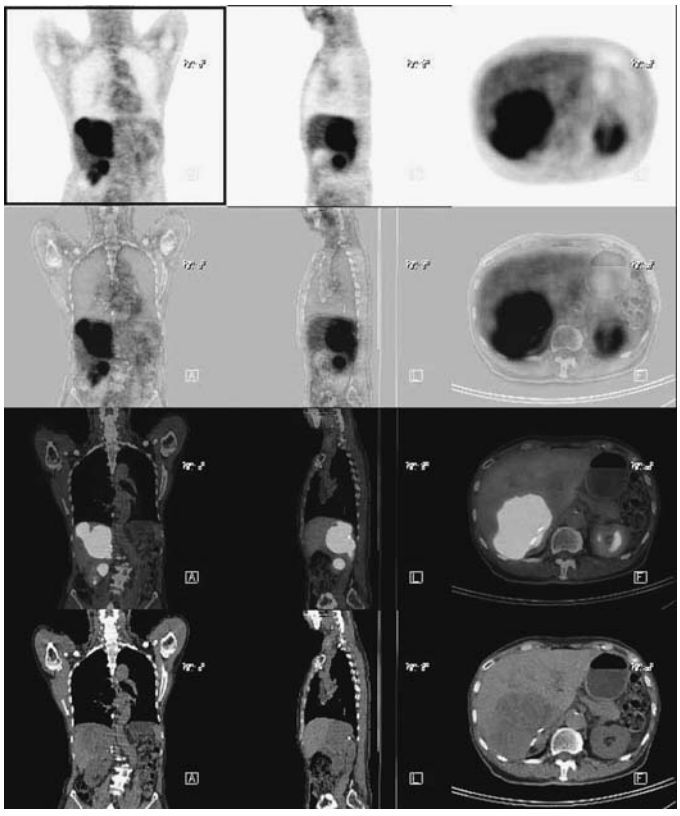

FIGURE 2.1.2.

are functional tumors. Most patients have a clinical presentation of Cushing's syndrome. This cancer peak is in the fourth and fifth decades of life. CT is an excellent tool for the diagnosis of an abdominal mass, with 30% of the patients presenting with calcification. Exophytic renal masses and exophytic pancreatic tail masses are common false-positives on CT. MR can demonstrate the mass as low signal intensity on T1-weighted images and higher intensity on T2-weighted images. However, large adrenal adenomas can be falsely identified as adrenal cortical carcinomas. Ultrasonography can demonstrate the mass with heterogeneity and cystic components suggestive of hemorrhage and necrosis. MIBG (radiolabeled metaiodobenzylguanidine) scintigraphy can differentiate neuroblastomas and pheochromocytomas from adrenocortical cancer. Angiography can be helpful differentiating the tumors from hypernephromas based on vascular characteristics.

3 Germ Cell Tumors: Choricocarcinoma and Testicular Cancer

Anabella S. Din and Peter S. Conti

Case 3.1A

History

25-year-old male with a history of testicular cancer status post left orchiectomy. His beta-HCG was 8.9 and AFP was 114. His most recent CT demonstrated several lesions involving the back, mediastinum, abdomen, and the left neck. The patient is being staged with PET-CT.

Findings

There is bilateral neck adenopathy particularly more in the left base than right (*Figures 3.1A.1 and 3.1A.1A*). The cervical area of the neck is involved including the right paratonsillar area. The superior mediastinum is more active on the left than right. Additional sites of activity involving the paratracheal, pericarinal, right hilum, and subcarinal nodal zones are seen. There is disease in the right paravertebral space within the chest extending to the right crus of the diaphragm. Inferiorly, adenopathy is seen in a para-aortic distribution below the crus of the diaphragm down to and involving the proximal iliac bifurcation. Mesenteric adenopathy is also evident. There are 2 to 3 sites of nodal activity seen adjacent to the lateral aspect of the left psoas muscle (*Figure 3.1A.2*). The left inguinal region also contains sites of active disease, along with soft tissue around the left pelvic bone anteriorly.

Impression

Multiple sites of metastatic disease.

Pearls and Pitfalls

- *CT can understage 50% of the patients.*[4,5,8]
- *10% to 25% of the patients with normal CT scans will have occult retroperitoneal lymph node metastases.*[4,5,8]
- *PET was associated with a positive predictive value of 100% and a negative predictive value of 97%.*[1,4,5,8]
- *40% of the patients with normalized tumor markers will have residual tumor lesions in nonseminoma germ cell tumors (NSGCT).*[1,4,5,8]

FIGURE 3.1A.1.

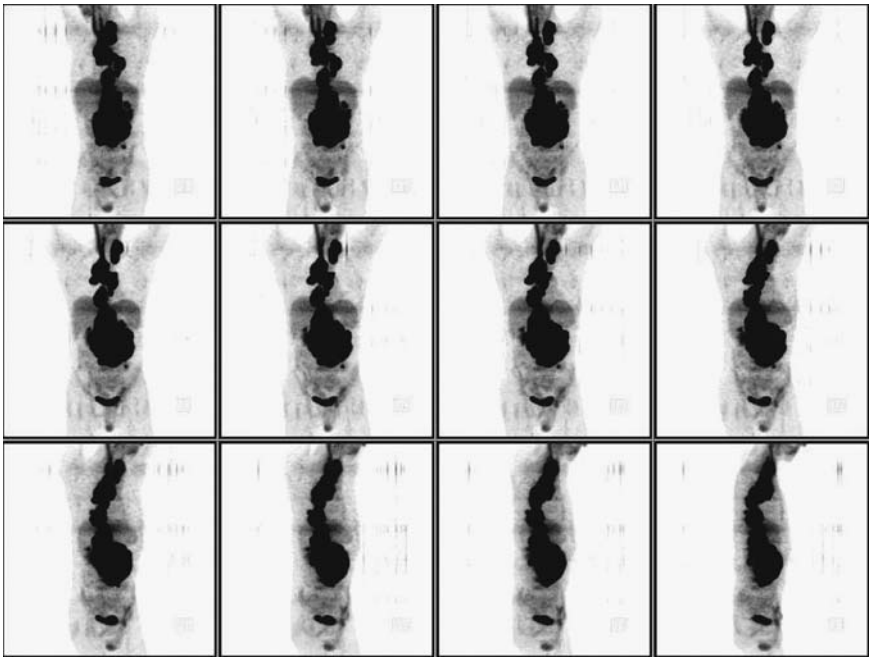

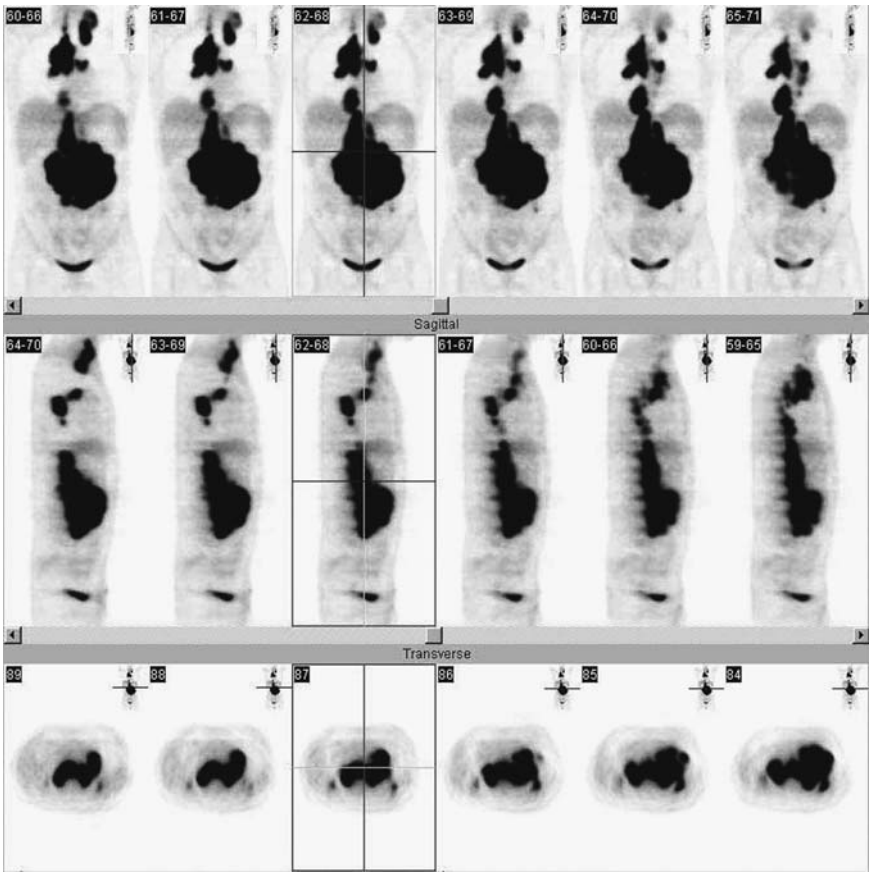

FIGURE 3.1A.1A.

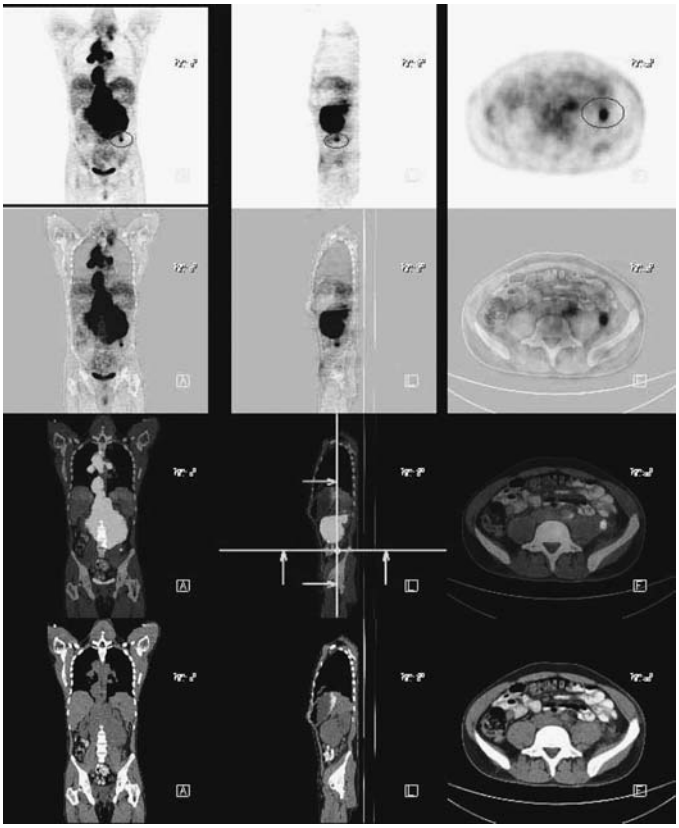

FIGURE 3.1A.2.

Discussion

Germ cell tumors represent 1% of all male malignancies and most commonly occur in patients in the age range of 10 to 35. Seminoma accounts for 40% of all germ cell tumors and nonseminoma germ cell tumors (NSGCT) account for 60%. A history of cryptorchidism is a risk factor. Seventy percent of testicular cancer clinical presentations include testicular swelling. Pain occurs in 18% to 46% of the cases. Ultrasonography is the initial imaging of choice.

Tumor markers can be helpful for monitoring disease process and response to therapy. HCG has a 5% to 40% sensitivity for seminoma and 50% to 60% for NSGCT. AFP is most commonly seen in yolk sac tumors and has 85% sensitivity for NSGCT. LDH isoenzyme-1 marker is used to assess treatment response and prognosis.

Radical inguinal orchiectomy is the standard for surgical resection and pathologic diagnosis. Treatment for seminoma is irradiation, and for nonseminomatous germ cell tumor is retroperitoneal lymph node dissection. Cisplatin-based combination chemotherapy is used in advanced seminoma.

Case 3.1B

History

25-year-old patient who has a history of testicular cancer status post left orchiectomy. His previous PET revealed multiple sites of hypermetabolism consistent with metastatic disease. He received chemotherapy several months ago, and is now being evaluated for treatment response.

Findings

There is a focus of activity in the right retrocrual area at the level of the tip of the right kidney medially correspond to a node on CT. Additional activity is seen in the left inguinal region (*Figure 3.1B.1*) compatible with persistence of disease. There is ill-defined activity in the midabdomen adjacent to the bowel loops suspicious for residual disease. The bone marrow activity is consistent with chemotherapy response. The small uptake in the right axilla (*Figure 3.1B.2*) is the result of injection extravasation. The paraspinal activity (*Figure 3.1B.3*) is physiologic.

Impression

Dramatic interval improvement since the prior study with minimum hypermetabolism consistent with residual disease as outlined above.

Pearls and Pitfalls

- *PET has a higher diagnostic accuracy for testicular cancer than CT for both staging and restaging; it is also helpful in the assessment of a residual mass visualized on CT following chemotherapy*.[5,8]

Discussion

PET FDG can be used to detect nonseminomatous germ cell tumors in the retroperitoneum better than CT. It can also detect the presence of mature teratoma in residual retroperitoneal masses better than CT.

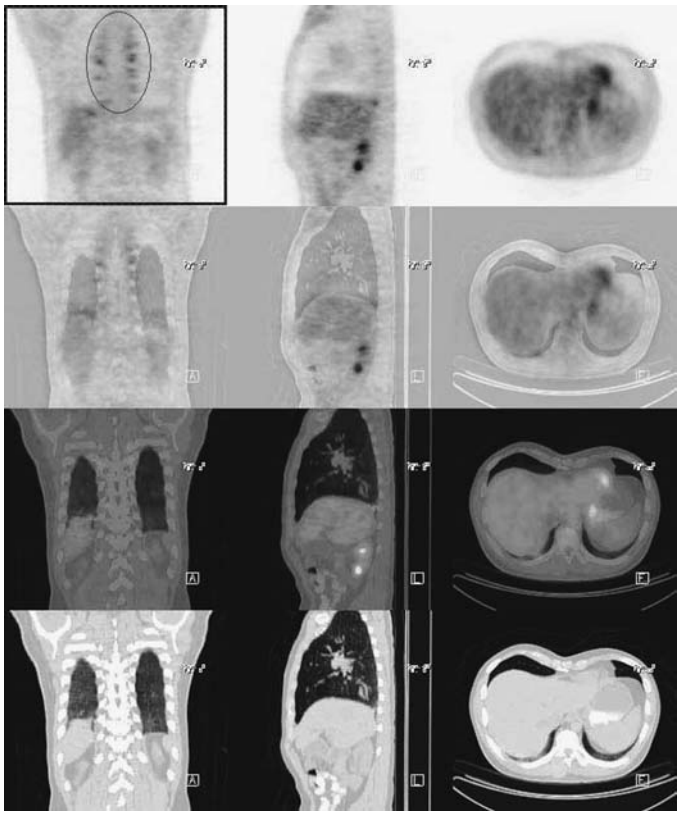

FIGURE 3.1B.1.

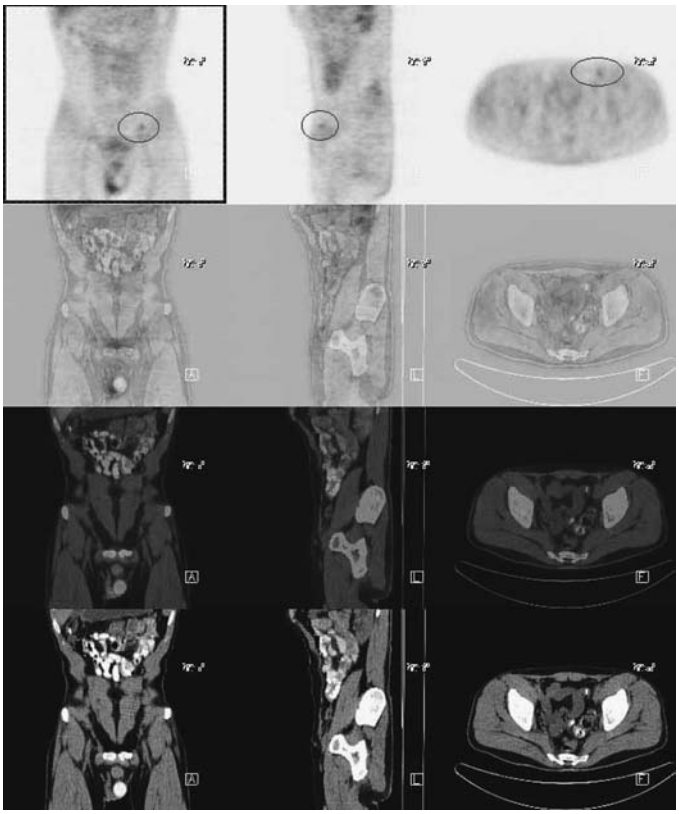

FIGURE 3.1B.2.

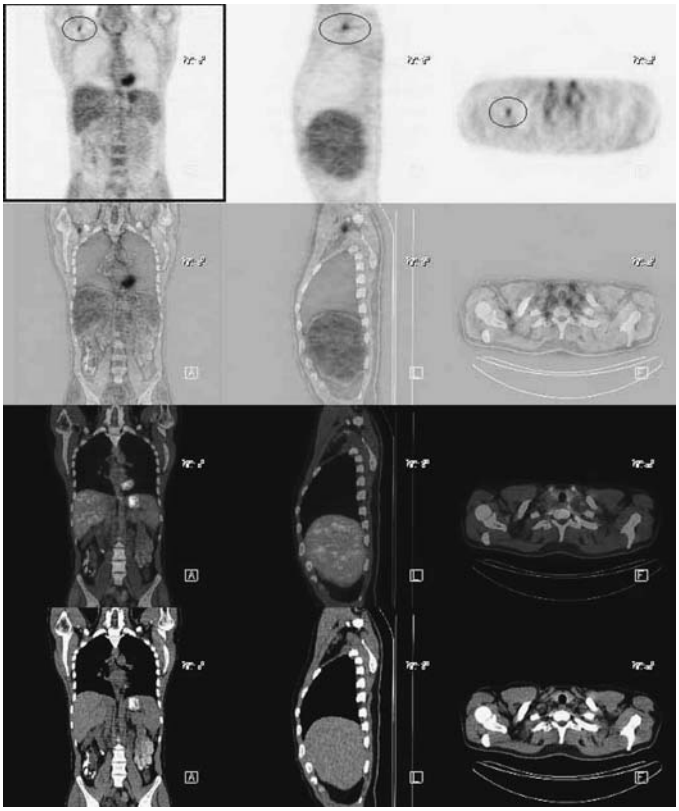

FIGURE 3.1B.3.

Case 3.1C

History

25-year-old male who has a history of testicular cancer status post left orchiectomy. A prior PET scan showed extensive metastatic disease above and below the diaphragm. A follow-up PET scan, post therapy, showed significant improvement with minimal findings in the abdomen suspicious for some residual disease. He was treated further with chemotherapy. The current PET scan is being done to assess treatment response.

Findings

In the neck and chest, there is symmetrical hypermetabolic activity in the region of the thyroid consistent with physiologic finding (*Figure 3.1C.1*). No hypermetabolic foci are seen in the lung to indicate metastatic disease. In the abdomen, no evidence for hypermetabolic activity is seen in the lymph node basin. Distribution of tracer in the liver is normal. There is photopenic area in the left scrotum consistent with a prosthesis.

Impression

No evidence for metastatic disease based on the PET scan pattern consistent with good response to therapy.

FIGURE 3.1C.1.

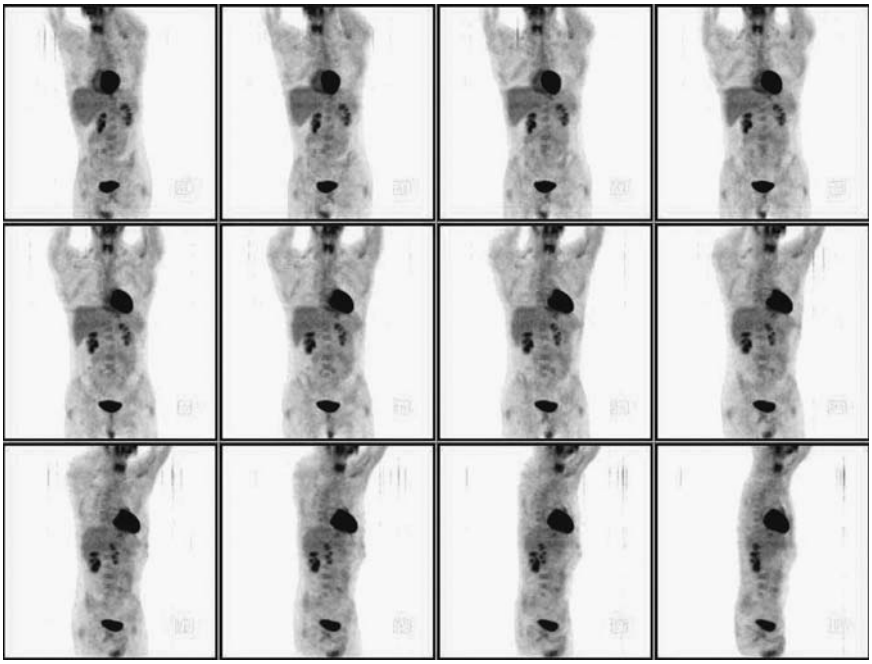

Case 3.2A

History

26-year-old male who has a history of testicular cancer status post orchiectomy and chemotherapy. He was later further treated with radiation therapy. The patient is being evaluated for residual disease.

Findings

There is a large and extremely hypermetabolic confluent mass in the region of the right hilum that dominates the appearance of CT-PET scintigraphy (*Figure 3.2A.1*). In addition, there are discrete nodal lesions found in the region of the right middle lung (*Figure 3.2A.2*) and the peritracheal regions (*Figure 3.2A.3*) bilaterally. Two other lesions are found in the left upper (*Figure 3.2A.4*) and left lower lung (*Figure 3.2A.5*) laterally. The right lower lung lesion is also hypermetabolic. No other lesions in the groin and abdomen are noted.

Impression

Abnormal whole body 18-FDG PET scintigraphy consistent with multiple sites of metastatic disease as discussed above.

Pearls and Pitfalls

- *A positive PET scan has a 91% positive predictive value.*[2,4,5]

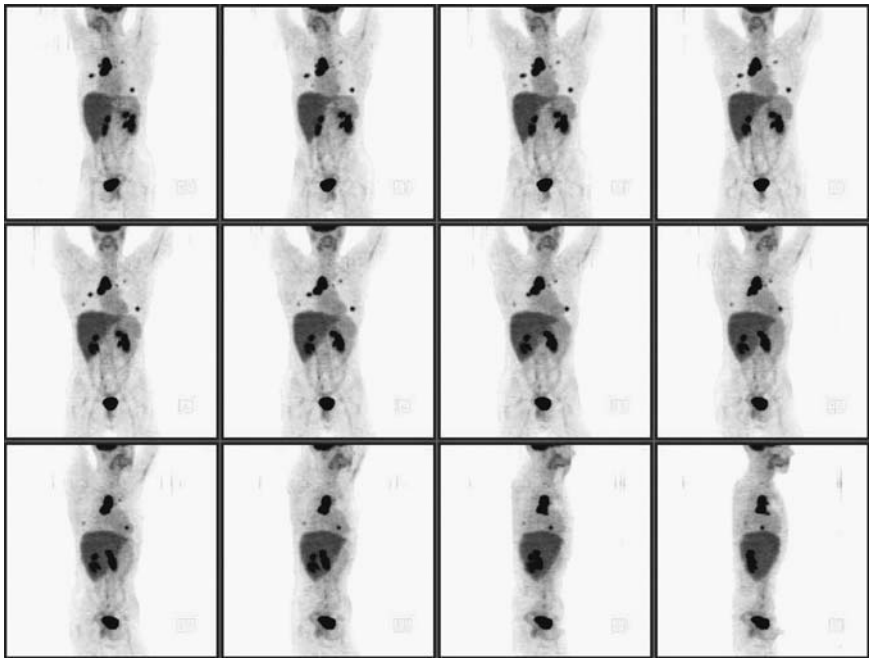

FIGURE 3.2A.1.

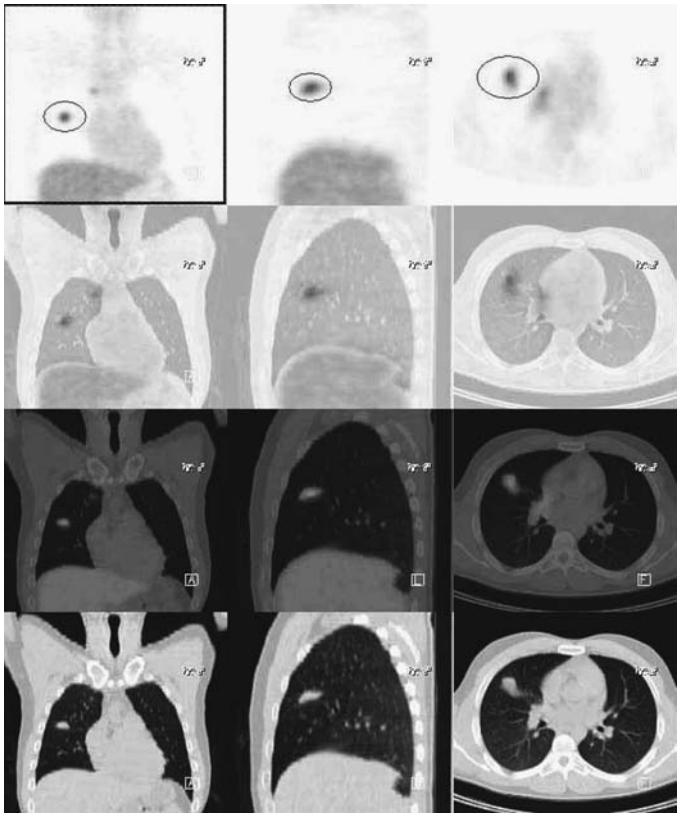

FIGURE 3.2A.2.

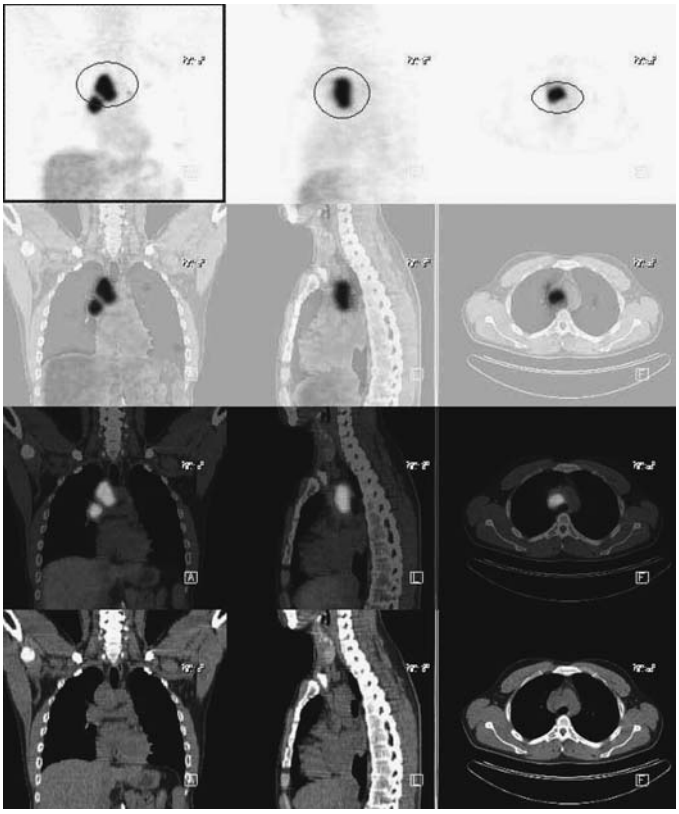

FIGURE 3.2A.3.

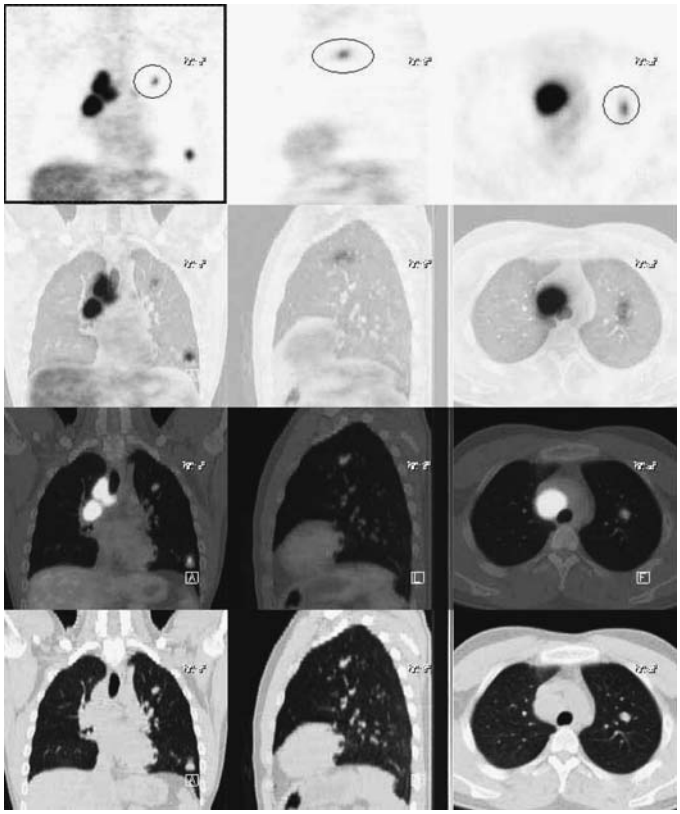

FIGURE 3.2A.4.

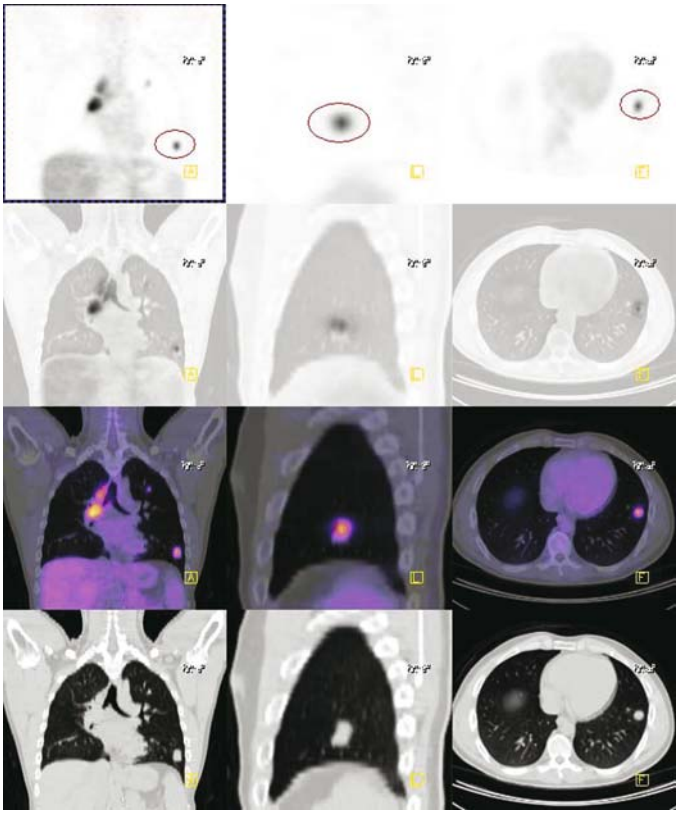

FIGURE 3.2A.5.

Case 3.2B

History

27-year-old male with a history of metastatic testicular carcinoma. The prior PET scan showed extensive recurrent disease. The patient received additional chemotherapy and is being evaluated for treatment response.

Findings

The prior exam had been positive for bulk mediastinal disease as well as pulmonary metastasis. Since that time, there has been a complete regression of disease, both by 18-FDG PET scintigraphy and by the accompanying CT. No mediastinal mass, pulmonary nodule or hypermetabolic focus in the chest is evident (*Figure 3.2B.1*). The abdomen exam also remains negative for metastatic disease. There is intense submandibular gland activity (*Figure 3.2B.2*) which may represent treatment-related salivary stasis.

Impression

Interval regression to free of evident disease since the prior exam, judging from 18-FDG PET scintigraphy and the accompanying CT.

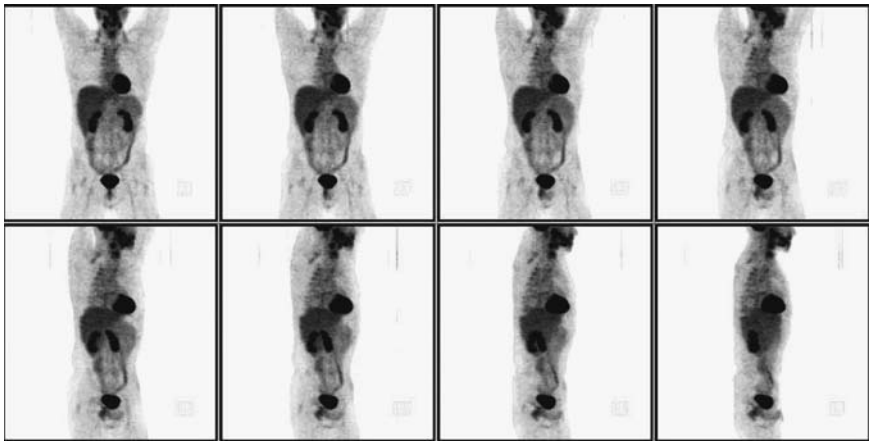

FIGURE 3.2B.1.

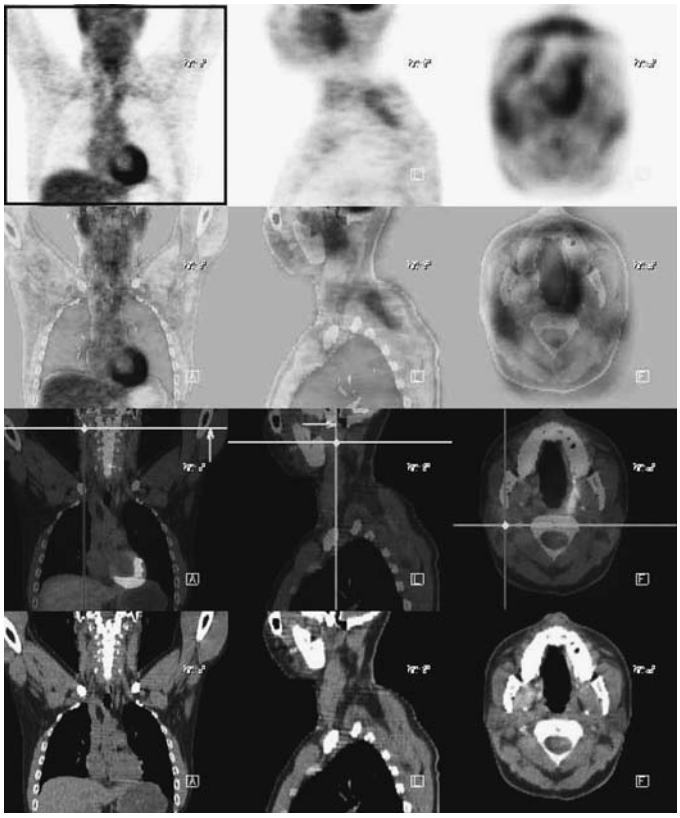

FIGURE 3.2B.2.

Pearls and Pitfalls

- *PET has the potential to image all stages of testicular cancer.*[2,4,8]
- *FDG PET has a sensitivity of 59% and a specificity of 92% in the evaluation of residual masses for viable tumor.*[2,8,9]

Case 3.3

History

55-year-old male with a history of testicular carcinoma ten years ago, status post left orchiectomy. There is a history of pelvic bone resection and of left groin lymph node

dissection. There is a history of right groin recurrence status post resection and chemotherapy. The current examination is compared with the most recent PET examination and is being done to assess treatment response.

Findings

As with the prior examination, there is pathologic activity related to the left anterior ilium (*Figures 3.3.1 and 3.3.2*). The activity previously had been more diffusely hypermetabolic. It is now less hypermetabolic and more patchy. It corresponds to a mixed lytic sclerotic expansile lesion of the left anterior acetabulum (*Figure 3.3.2A*), with calcific soft tissue extension into the iliopsoas musculature, as well as a smaller extension into the gluteal musculature. These soft tissue extensions have faint calcification and a thin sclerotic rim. The interval change probably reflects interval therapy with ossification of tumor. In the left lower pelvis, there is focal hypermetabolism in the soft tissue along the posterior aspect of the posterior column of the left acetabulum. There is also both abnormal hypermetabolic activity in the anterior pillar of the left acetabulum, as well as extension into the obturator internis. This soft tissue extension is also undergoing calcification. The degree of hypermetabolism in the acetabular area and the extent appear somewhat increased, versus the prior exam. Additionally, there are three pulmonary nodular densities visible on the current examination. One is a small nodule in the posterior segment of the right upper lobe (*Figure 3.3.3*). The second is a nodule located in the lung just posterior to the head of the left clavicle. The third and largest and most hypermetabolic nodule is anterior to the right hilum (*Figure 3.3.4*). This appears larger and more active than it had on the prior exam. There is focal activity which is fairly hypermetabolic in the area of the hepatic flexure. There is fairly prominent activity in the remainder of the hepatic flexure (*Figure 3.3.5*) and in the proximal transverse colon (*Figure 3.3.6*), and this one is suspected to be unusually intense physiologic colon activity, rather than peritoneal metastasis. There is intense activity in the urine in the right pelvic ileal conduit (*Figure 3.3.7*) and extending into the ostomy.

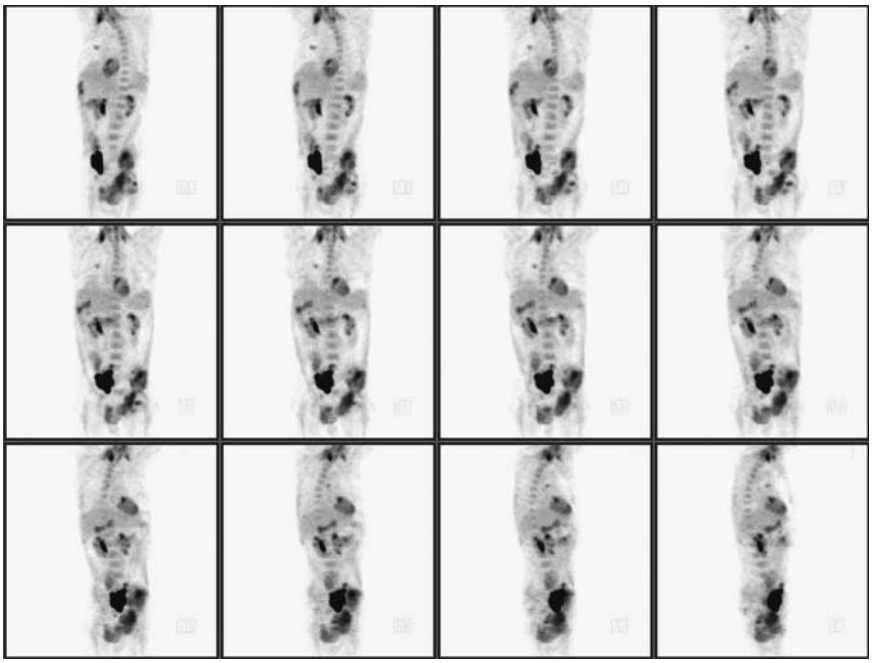

FIGURE 3.3.1.

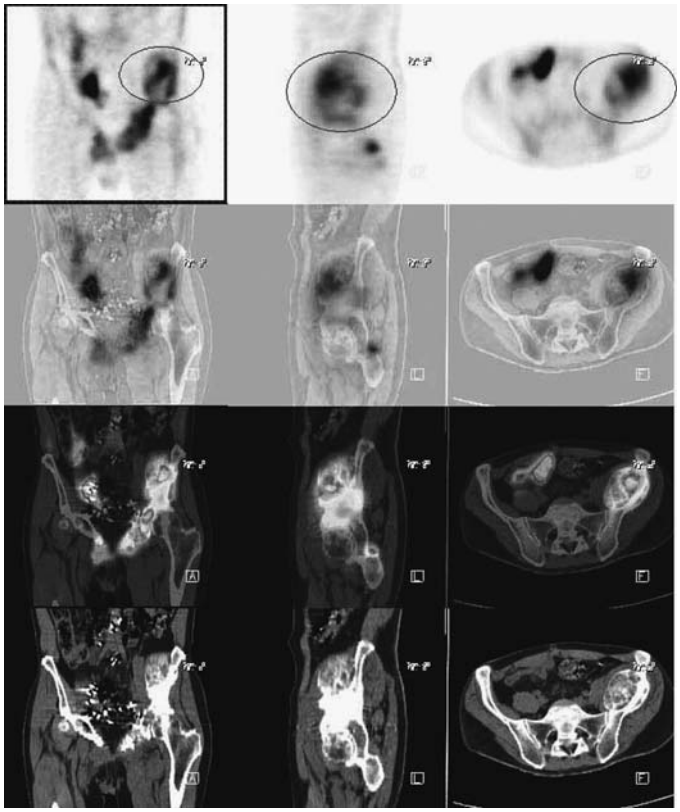

FIGURE 3.3.2.

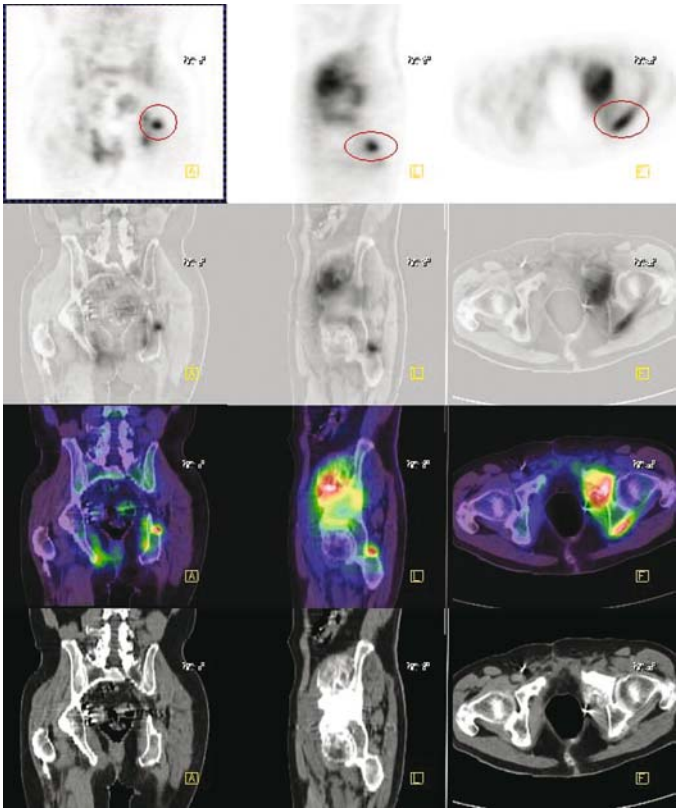

FIGURE 3.3.2A.

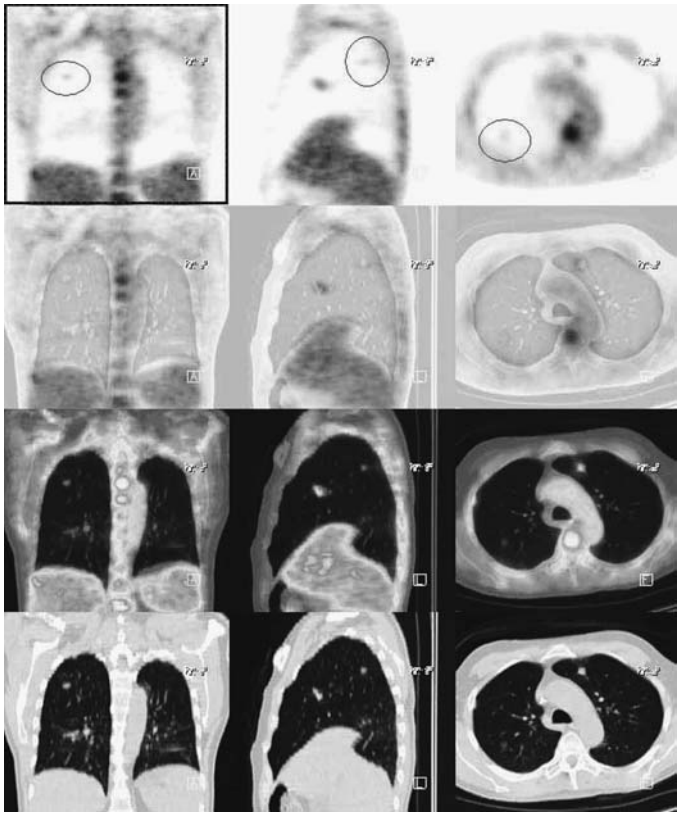

FIGURE 3.3.3.

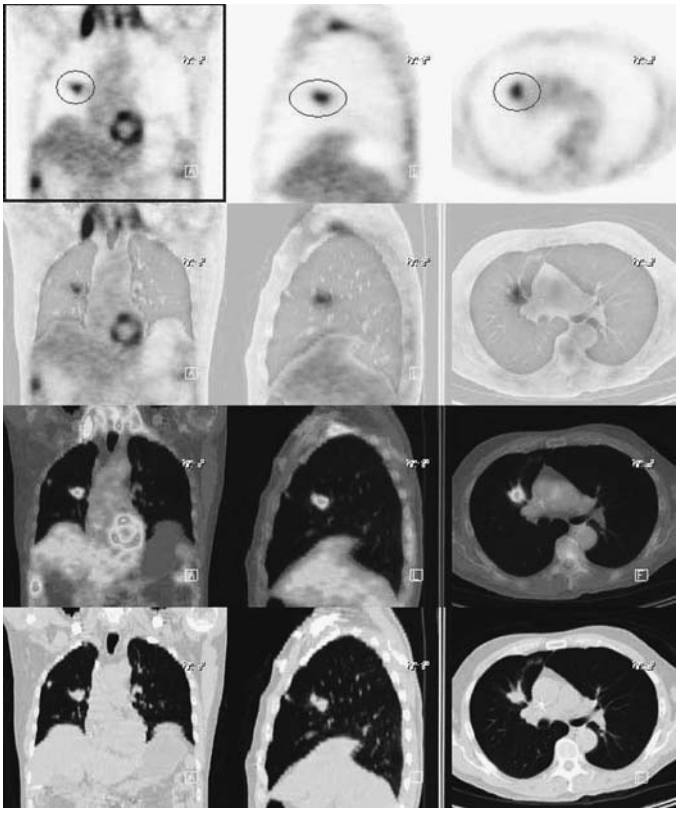

FIGURE 3.3.4.

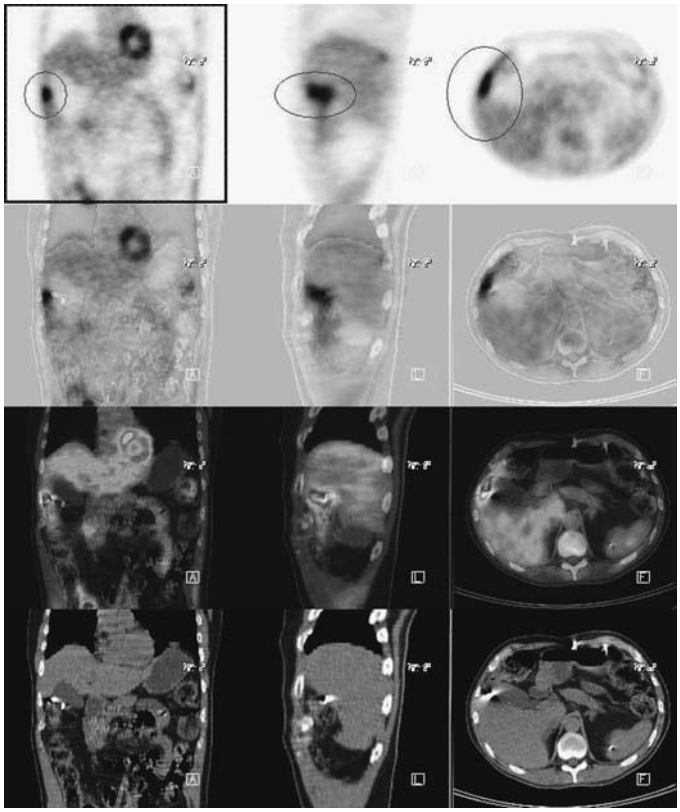

FIGURE 3.3.5.

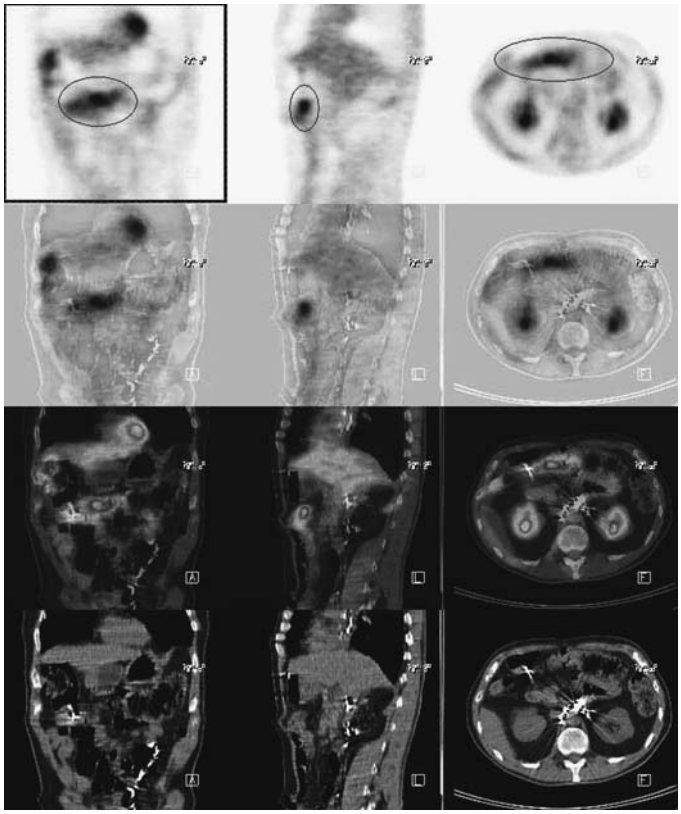

FIGURE 3.3.6.

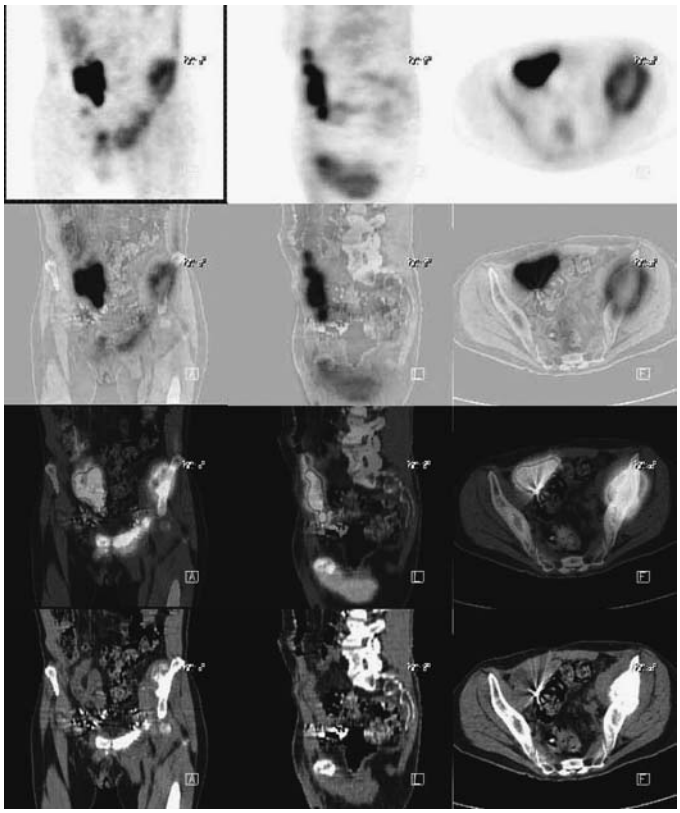

FIGURE 3.3.7.

Impression

1. Pulmonary metastas with definite increase in the size and activity of the most conspicuous nodule that is anterior to the right hilum.
2. The iliac wing disease has decreased in relative metabolic activity and become patchy. The CT findings are showing relatively mature calcification of the soft tissue components, which is presumed treatment related. The left acetabular activity appears similar, with sclerotic bone involvement and extension into the obturator internis musculature and along the posterior pillar of the acetabulum, with bone involvement of the anterior pillar, appearing increased in relative activity vs. prior. This soft tissue component is also undergoing ossification which is presumed treatment related.

Pearls and Pitfalls

- *C-11 methionine may be useful in the diagnosis of malignant testicular tumor, demonstrating 100% sensitivity, 91% specificity, and 93% accuracy.*[6,7]
- *PET has a positive correlation with histologic confirmation of persistent malignancy.*[1,5,8]

Discussion

Prognosis depends on the histology and extent of the tumor. The 5-year survival rate is more than 95% for seminomas and nonseminomas localized to the testis or low-volume metastases in the retroperitoneum. With extensive retroperitoneal metastases or pulmonary or other visceral metastases survival is poorer and varies with site, volume, and histology of the metastases.

Case 3.4

History

34-year-old female who has a history of metastatic choriocarcinoma. The baseline PET scan was negative. The second PET scintigraphy was negative except that the CT showed two small right-sided pulmonary nodules, one in the upper and one in the lower lobe. The diagnosis of recurrence was confirmed with nodulectomy and right thoracotomy. She is now being reevaluated because of rising HCG.

Findings

There is a small modestly hypermetabolic focus in the right apex (*Figures 3.4.1 and 3.4.2*). This corresponds to a costovertebral junction and is probably related to the thoracic surgery. There is a similar hypermetabolic focus at the surgical osteotomy site, lower down, where there was a transverse thoracotomy (*Figure 3.4.3*) indicated by mild residual hypermetabolism from vascular scar. The largest density in the right lung is seen on chest CT as 2.7 cm in dimension and is negative by 18-FDG PET scintigraphy, consistent with postsurgical rounded atelectasis. There is a 1.2 cm right apical pulmonary nodule which is obviously hypermetabolic on 18-FDG PET scintigraphy, consistent with a metastatic deposit (*Figure 3.4.4*). The two peripheral pleural-based nodules have much less but discernible hypermetabolism. The apparent lesser hypermetabolism probably relates more to the greater respiratory excursion of the lower

FIGURE 3.4.1.

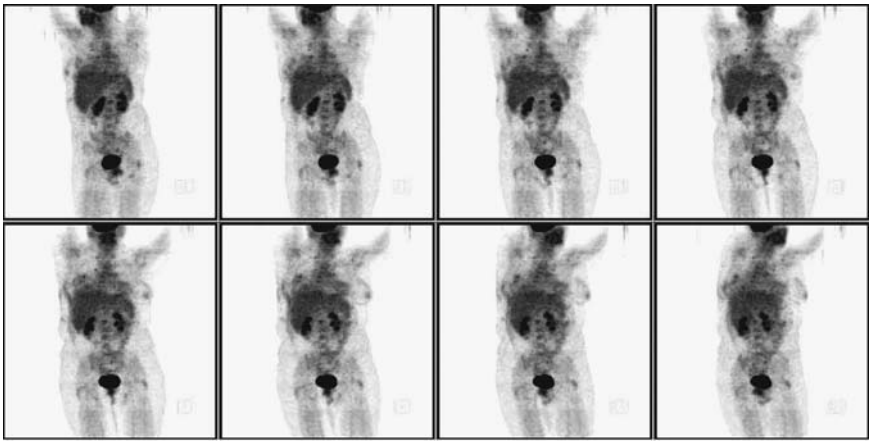

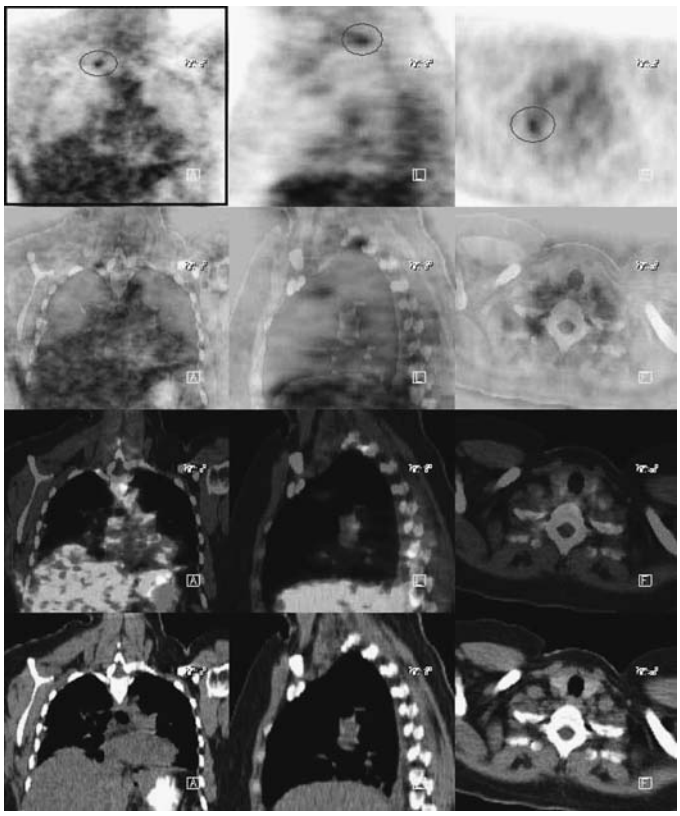

FIGURE 3.4.2.

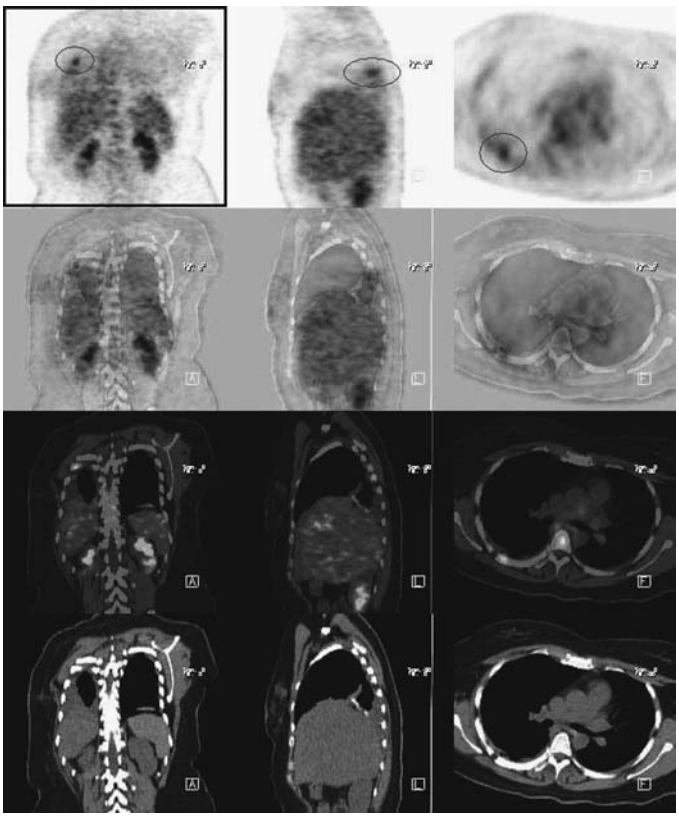

FIGURE 3.4.3.

lobe compared to the pulmonary apex, rather than a difference in histology or activity of disease.

Impression

1. Recurrent pulmonary metastatic choriocarcinoma with a single nodule in the right apex and two peripheral pleural-based lesions at the left base. There are a few tiny peripheral nodular densities at the left base which are below 18-FDG PET scintigraphy resolution.

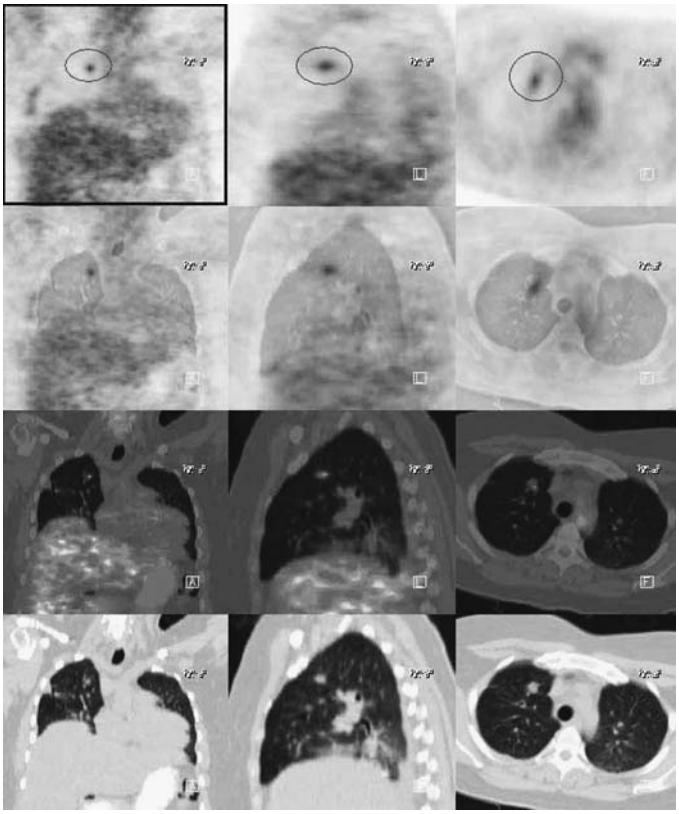

FIGURE 3.4.4.

2. Findings attributed to postthoracotomy status, including osteotomy of a lower posterior rib, mild hypermetabolism of the soft tissues at the transverse thoracotomy site, and postoperative rounded atelectasis and pleural thickening which lack hypermetabolism and are consistent with postsurgical change.

Pearls and Pitfalls

- *PET imaging can localize tumor lesions in patients with elevated b-HCG and negative findings on anatomical imaging.*[3,10,11]

Discussion

The incidence of choriocarcinoma is 1 out of 40,000 pregnancies in the United States. Incomplete abortions, hydatidiform mole, low socioeconomic status, low protein diet and folic acid insufficiency are risk factors. Continuous vaginal bleeding is a common finding. Test revealed continued b-HCG elevation postpartum. The treatment is chemotherapy with and without radiation. Ninety percent of all females with malignant, nonmetastatic disease are cured. For metastatic disease involvement, there is an 87% chance of remission. Choriocarcinoma may recur within 3 years.

4 Brain

Sherief Gamie and Peter S. Conti

Case 4.1

History

75-year-old female with left temporal glioblastoma, status postsurgery and radiation. She is now being evaluated because of involvement of the scalp and suspected intracranial recurrence.

Findings

The CT shows calcification and edema in the left temporal lobe subjacent to the craniotomy defect. The PET scintigraphy shows a discrete spherical area of intense hypermetabolism immediately subjacent to and centered at the temporal calvarial craniotomy defect (*Figures 4.1.1A and 4.1.1B*). The remainder of the calcification and edema is negative by PET with a decrease in relative metabolism, secondary to radiation.

Impression

Recurrent glioblastoma centered at and subjacent to the left temporal craniotomy defect. There is surrounding non-hypermetabolic calcification and edema.

Pearls and Pitfalls

- *The one-year survival rate for patients with high-grade glioma who are responsive vs. non-responsive to therapy is 75% and 29%, respectively.*[1,3,12]
- *FDG PET has a sensitivity of 81% to 86% and specificity of 50% to 94% in differentiating a recurrent tumor from radiation changes.*[5,6]
- *PET is useful for grading primary brain tumor, assessing tumor recurrence, and aiding in prognostic stratification of tumor grade.*[1,3,5]
- *Visual comparison between opposing brain parenchyma is more sensitive than quantitative comparison.*[1,3,12]

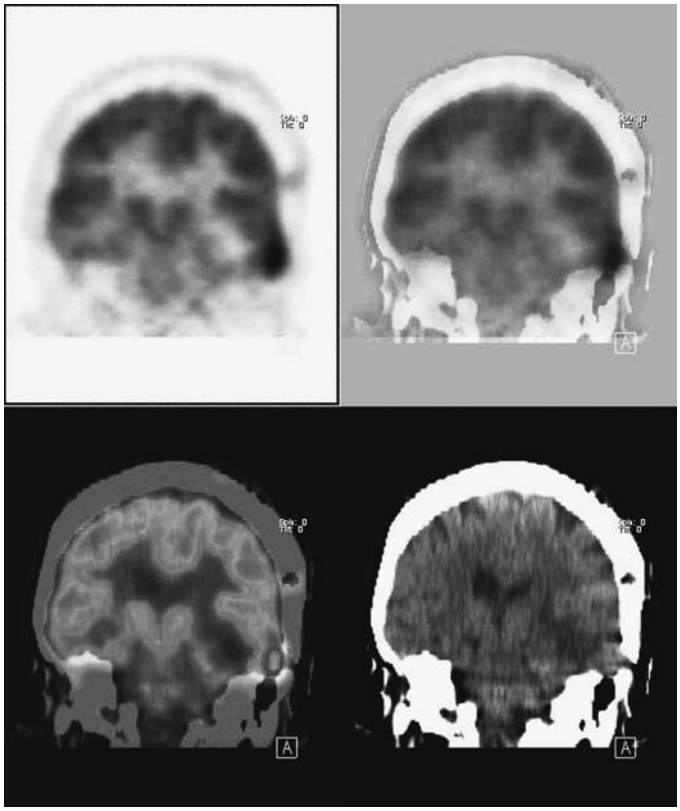

FIGURE 4.1.1A.

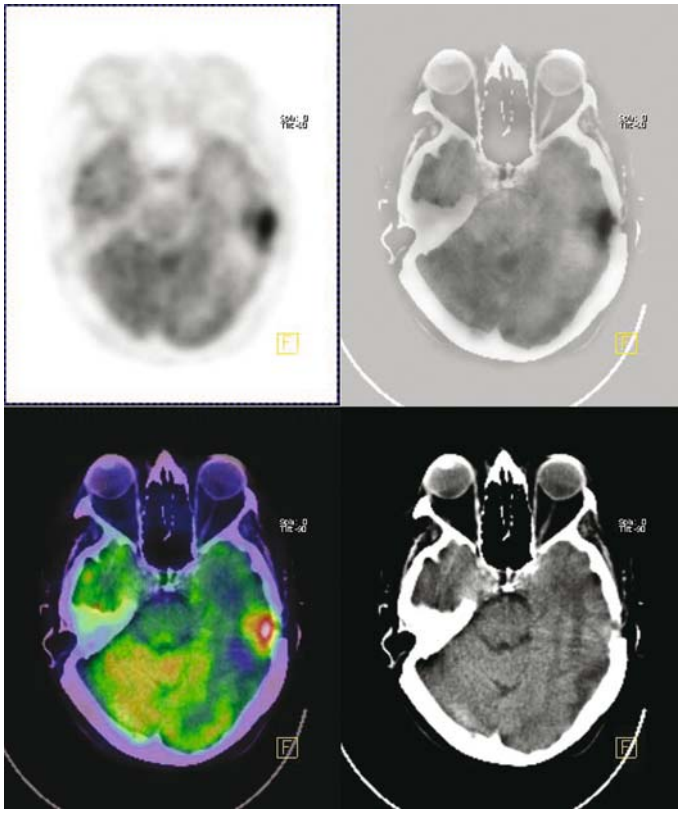

FIGURE 4.1.1B.

Discussion

Primary CNS tumors constitute 1% to 2% of all malignancies with more than half (55%) being malignant. Gliomas are the most common. High-grade glioma, Grade III and IV histologically, are more FDG-avid than low-grade (Grade I and II) tumors.

CT and MR are nonspecific at the surgical site. The contrast enhancement is commonly seen within days after surgery and will persist for several months. PET therefore is more accurate than contrast CT or MRI for detection of recurrent disease.

The differentiation of radiation injury from recurrent tumor is a common indication for PET imaging. Radiation necrosis will enhance for months with conventional CT/MR imaging. It is commonly associated with cerebral edema, mass effect, and blood brain barrier disruption.

PET has its limitations. False-negatives can occur with low volume malignancy below the threshold for detection and in situations where small hypermetabolic tumor may be indistinguishable from surrounding gray matter uptake of radiotracer. False-positives can occur <3 months postradiation, particularly with gamma knife therapy, seizure activity, and the presence of abscess.

Case 4.2

History

73-year-old male who has a history of brain mass and pulmonary carcinoid. A recent CT revealed a 2.5 cm left inferior hilar nodule and lymphadenopathy involving the right paratracheal region and aorticopulmonary window.

Findings

The photopenia in the left frontoparietal region (*Figure 4.2.1*) correlating with a densely calcified 3.3 cm extra-axial mass on CT (*Figure 4.2.2*) is consistent with a meningioma. The 2.5 cm left infrahilar lesion is mildly hypermetabolic. An adjacent linear opacity, possibly atelectasis extends inferolaterally to the pleural surface. Bilateral dependent atelectasis is seen posteriorly and there is minimal left apical scarring. Calcified precarinal, right hilar, right paratracheal lymph nodes due to old granulomatous disease are mildly hypermetabolic. The stomach activity is physiologic. There is intense hypermetabolism in the posterior wall of the lower rectum associated with wall thickening on CT.

Impression

1. Mild hypermetabolism in the 2.5 cm left infrahilar nodule, carcinoid by biopsy.
2. No evidence of metastasis.
3. Rectal wall thickening and hypermetabolism; advise colonoscopy.
4. Incidental left frontoparietal meningioma.

Pearls and Pitfalls

- *10% to 15% of all meningiomas are malignant meningiomas which require a more aggressive therapy. FDG uptake is generally low in meningioma, but can be elevated in the malignant subtype.*[1,3,12]

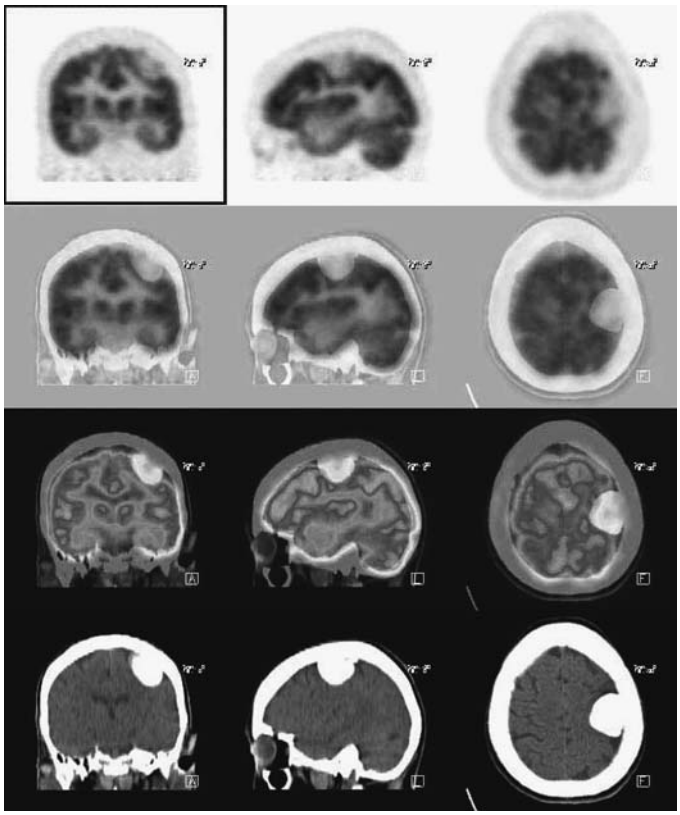

FIGURE 4.2.1.

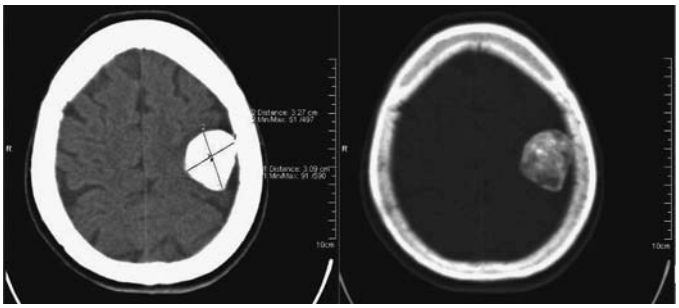

FIGURE 4.2.2.

- *The recurrence rate of meningiomas after a total excision is as high as 25%.*[1,3,12]
- *Pulmonary carcinoid tumors generally have a low FDG uptake. The 5-year survival rate is 83.2%.*[1,3,12]

Discussion

Meningiomas are intracranial tumors that are usually benign and slow growing. Total excision is usually the treatment of choice in those requiring treatment. However, adjuvant radiation therapy may reduce the risk of recurrence. PET can be used to identify suspected tumor but uptake is generally low, leading to difficulty differentiating this disease from benign pathology.

Case 4.3

History

81-year-old male who has a history of angiosarcoma of the forehead. The study is being done to evaluate for extent of disease.

Findings

On CT, there is soft tissue fullness anterior to the frontal calvarium corresponding to the metabolic focus on PET consistent with the known angiosarcoma (*Figure 4.3.1*). The small compressive ametabolic left sided intracranial mass on PET corresponds to a CT lesion consistent with a chronic subdural hematoma. The sulci are prominent, and there is ventriculomegaly, consistent with brain parenchymal atrophy.

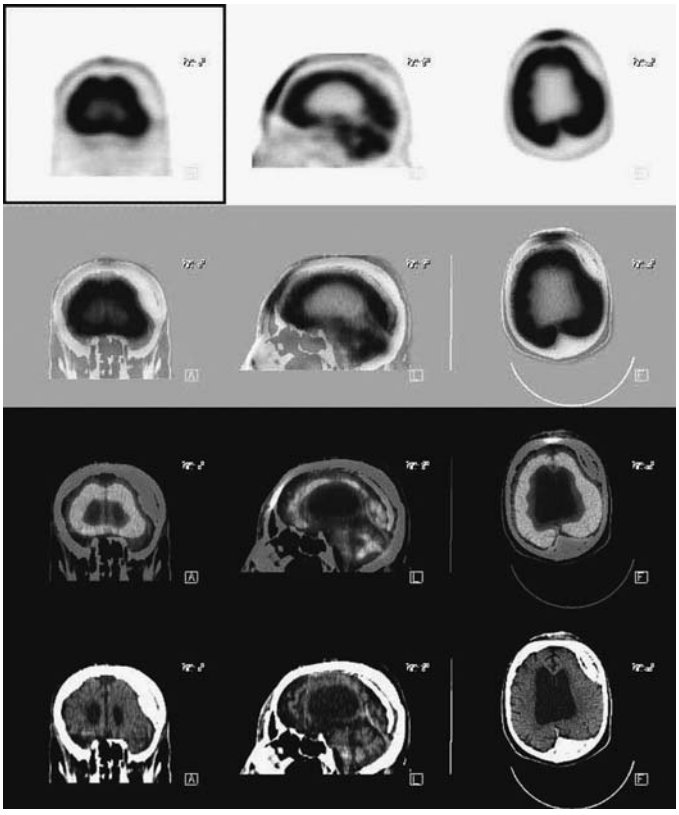

FIGURE 4.3.1.

Impression

1. Evidence for angiosarcoma anterior to the frontal skull; no evidence of metastatic disease.
2. Evidence for old subdural hematoma in the left frontal region.
3. Prominent sulci with ventriculomegaly consistent with brain atrophy.

Pearls and Pitfalls

- *A major limitation with PET imaging is the high cortical metabolic activity in the gray matter. This can potentially obscure tumors, especially those with similar FDG uptake in comparison to the surrounding parenchyma that demonstrates low metabolic activity. Similar problems may occur when evaluating low grade or benign lesions in the white matter.*[1,3,12]
- *Intense focal inflammation may lead to a false-positive result.*[1,3,12]

Discussion

Angiosarcomas are a group of rare, high-grade neoplasms derived from vascular endothelial cells. They account for 1% of all soft tissue sarcomas. Approximately 50% occur in the head and neck, but they account for less than 0.1% of head and neck malignancies. The cutaneous form tends to occur most often in the elderly population.

As in brain tumors and lymphoma, FDG PET can be helpful in grading subtypes of sarcomas, but can be problematic differentially low-grade from benign soft tissue masses.

Case 4.4

History

38-year-old female with multiple brain lesions. The study is being done to identify a primary extracranial neoplasm.

Findings

On the PET scan of the brain, there are multiple intensely hypermetabolic intracranial foci (*Figure 4.4.1*). There is a large bilobular deep left frontal lobe mass extending down into and nearly filling the left middle fossa (*Figure 4.4.2*). There is a small midline focus just above the clivus (*Figure 4.4.3*). There is an intermediate sized deep hypermetabolic white matter lesion in the left centrum semiovale. There is also a small lesion in the posterior lateral ventricle, with some associated dilatation seen on CT of the temporal horn posterior to it. There is focal hypermetabolic soft tissue medial to the right mandibular ramus near the angle of the jaw and anterior to the upper portion of the right submandibular gland. Two small nodules, 6 mm and 8 mm, are seen as pleural-based nodules at the dome of the right diaphragm. These are not calcified, but are not metabolically active. There is incidental notation of minor maxillary sinus disease.

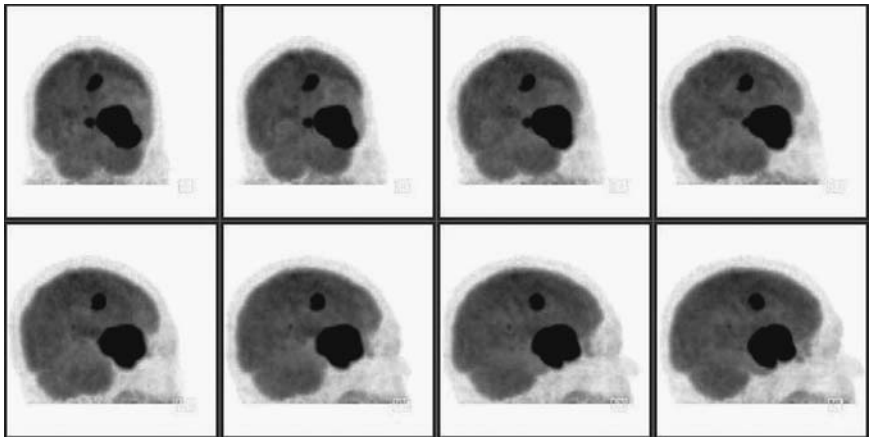

FIGURE 4.4.1.

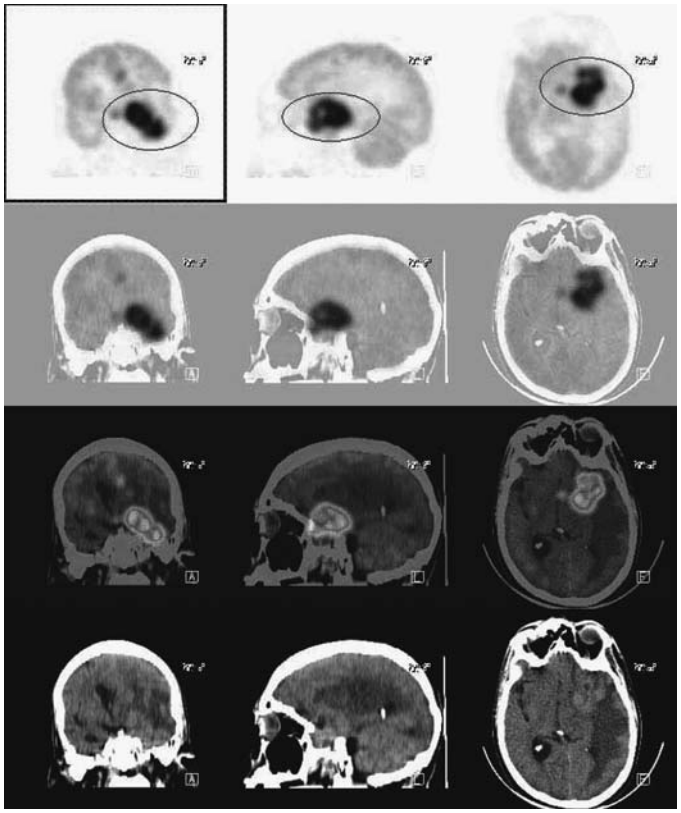

FIGURE 4.4.2.

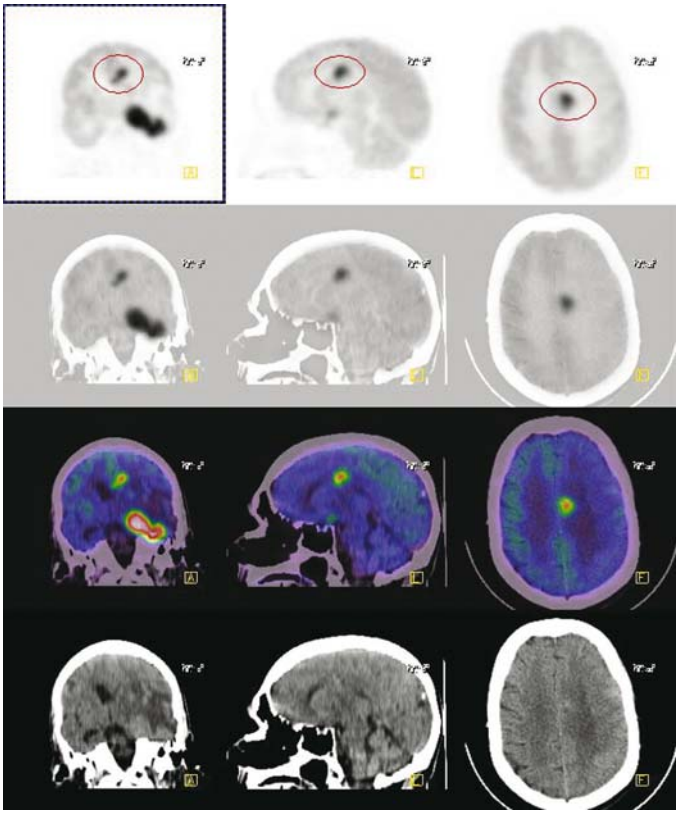

FIGURE 4.4.3.

Impression

1. Multiple intensely hypermetabolic intracranial foci, likely malignant neoplasia and likely metastatic, based on multiplicity.
2. There is a likely primary tumor site localized to the floor of the mouth on the right.
3. Multiple pleural based nodules not likely representing malignancy.

Pearls and Pitfalls

- *Brain metastases are 10 times more common than primary brain tumor, and can usually be visualized on PET scintigraphy. Difficulty can occur when lesions are small*

(<0.5 cm) and close to the gray-white junction, or when predominant cyst formation or necrosis is present, with limited volume of detectable viable tumor.[1,3,12]

- *The common primary tumors to consider that are FDG avid include lung, breast, and melanoma.*[1,3,12]

Discussion

The most common brain tumor in adults is the metastatic brain tumor that accounts for 50% of brain malignancy in adults. More than 50% of the metastases are from lung or breast carcinoma. PET whole body imaging can be used to survey the body for an occult primary tumor.

Case 4.5

History

46-year-old male who has a history of brain tumor diagnosed six months ago status post resection. The CT at that time demonstrated a contrast-enhancing suprasellar mass consistent with postsurgical changes. He now presents with left eye blindness. The current study is being done to evaluate for tumor recurrence vs. therapy changes.

Findings

There is a left sided suprasellar mass that is hypermetabolic compatible with recurrent malignancy (*Figure 4.5.1*). No other abnormality is observed.

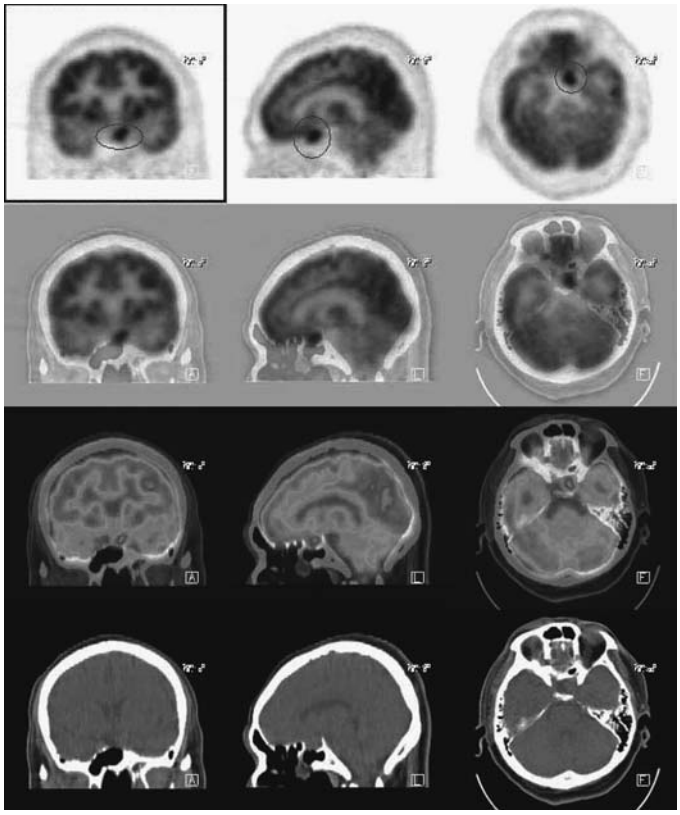

FIGURE 4.5.1.

Impression

Hypermetabolism of the contrast enhancing left sided suprasellar mass consistent with recurrent tumor.

Pearls and Pitfalls

- *PET can monitor postsurgical changes, radiation-induced necrosis, and recurrent tumor.*[2,5,11]

Discussion

Differentiation of radiation necrosis and posttreatment changes from recurrent brain tumor can be difficult with anatomic-based imaging, even with serial examinations and contrast enhancement. Progressive radiation necrosis and recurrent tumor can enhance, cause mass effect, and induce clinical symptoms. PET scintigraphy is helpful in differentiating these entities, leading to more appropriate management decisions.

Case 4.6A

History

21-year-old male who presented with seizure and was subsequently shown to have a 3 cm × 4 cm × 3.5 cm mass in the left parietal white matter. A recent MRI showed a left parietal area centered at the level of the upper portion of the posterior left lateral ventricle. The PET exam is being done to evaluate for malignancy and tumor grade.

Findings

The left parietal mass has increased in size significantly from the prior MRI exam. This area shows very faint metabolic activity which is barely discernibly greater than white matter and much less than gray matter (*Figure 4.6A.1*). No significant mass effect or edema is noted.

Impression

Low metabolism in the left parietal white matter tumor, definitely but only slightly greater than adjacent white matter, with very little mass effect on the adjacent parietal cortex consistent with a low-grade primary brain tumor.

Pearls and Pitfalls

- *F-18 fluoro-deoxyglucose and C-11 methionine are the most common tracers used for primary brain tumor PET imaging.*[2,4,7,8,11]
- *Ictal seizure focus activity can be hypermetabolic on FDG PET and, if in close proximity to the tumor bed, can be confused with a locally recurrent high-grade tumor. In a brain tumor patient presenting with seizures, the remaining portion of the brain should be thoroughly evaluated for remote sites of seizure foci.*[10]

FIGURE 4.6A.1.

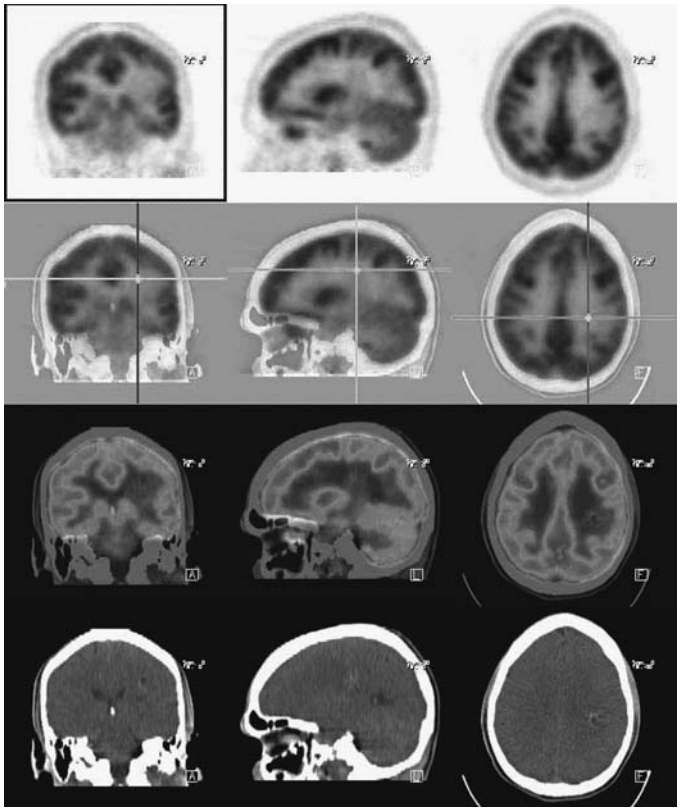

- *Low-grade brain tumors generally display low FDG uptake; upon dedifferentiating, FDG uptake can be seen to increase.*[1,9,12]
- *Patients treated with surgical resection of the seizure focus have a success rate of 65% to 85%.*[1,9,12]
- *10% to 20% of the partial complex seizure patients are unresponsive to anticonvulsant therapy.*[10]

Discussion

Anatomical imaging and clinical history are highly critical in narrowing the differential diagnosis in a patient with low uptake in a brain lesion. These including low-grade brain tumor, interictal epilepsy, and benign lesions such as meningioma and cyst.

In patients with intractable seizure, phenobarbital, phenytoin, carbamazepine, ethosuximide, valproate, and benzodiazepines are the most common drugs used. The epileptogenic focus is often localized to the temporal lobe. Patients with side effects from antiepileptic medications such as marrow suppression are candidates for surgical management.

PET can identify 60% to 70% of the epileptogenic foci and is superior to MRI for this purpose. The test is especially effective during the interictal phase where cerebral blood flow (CBF) and glucose utilization are at their lowest. If injected during a seizure, PET may show increased FDG activity.

Case 4.6B

History

21-year-old male who has a history of brain tumor presumably glioma. An earlier PET scan revealed minimal hypermetabolism in the left parietal lobe white matter suspicious for tumor. He was subsequently treated with cyberknife. Radiation therapy ended a few months ago. Evaluation for recurrence is requested.

Findings

There is a markedly hypermetabolic mass (*Figure 4.6B.1*) with central photopenia appearing in the left parietal lobe corresponding to the lesion on CT with surrounding edema. The tumor is compressing the deep gray matter and creating a mass effect on the left thalamus and caudate/putamen with decreased metabolic activity in those structures. There is gyral/sulcal pattern effacement of the left parietal cortex. No significant crossed cerebellar diaschisis is noted.

Impression

Recurrent high-grade tumor involving the left parietal lobe appearing since the prior PET examination, now with mass effect evident.

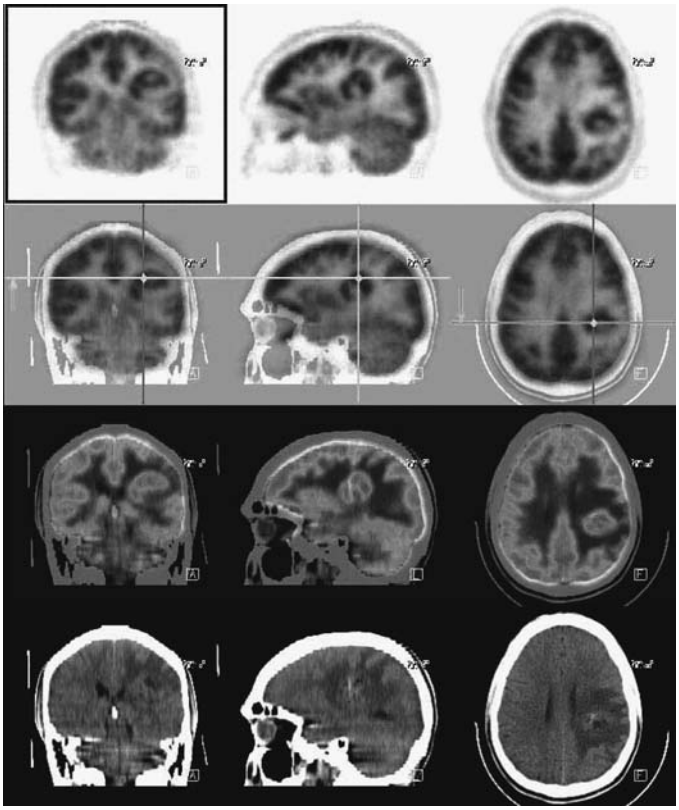

FIGURE 4.6B.1.

Pearls and Pitfalls

- *In recurrent glioma, 18-FDG is an independent predictor of outcome. In high-grade recurrence, those patients with intense tumor activity have lower 1-year survival rate (29%) than those patients with modest tumor activity (78%).*[1,9,12]
- *Gamma knife treatment can cause a thin, ring-like pattern of FDG uptake in the tumor bed that persists for up to one year. This usually represents inflammatory changes associated with therapy. Bulky or nodular uptake within this time-line or beyond is highly suggestive of tumor recurrence. Conventional radiotherapy associated changes usually subside within 2 to 3 months.*[5,8,11]

Discussion

When evaluated beyond 6 months following radiation therapy, FDG uptake in the region of the previously treated location usually suggests recurrent tumor.

Quantitative PET using cerebral metabolic rate for glucose (CMR-Glu) can be helpful in determining prognosis for survival outcome. Higher values suggest poor outcome. In patients with CMR-Glu <1.4, the median survival is 19 months vs. in patients with CMR-Glu >1.4, the median survival is only 5 months.

C-11 methionine is superior to FDG in that it has better background to target ratio which equates with better detection for smaller lesions. As in FDG studies, false-positive results can be seen with abscess and acute hematoma.

Case 4.7

History

62-year-old female who has a history of glioma status post chemotherapy. The previous PET scan one month after chemotherapy was unremarkable. Evaluation is being done for recurrence.

Findings

There is generalized left hypometabolism in the anterior temporal lobe, parietal lobe, and frontal lobe. The left deep gray matter structures including the caudate putamen (*Figure 4.7.1*) and thalamus (*Figure 4.7.2*) are also involved. These findings are minimally more prominent since the prior study, and likely represent progressive edema and post therapy changes. Additional edema has now resulted in mild midline shift. There is again noted splaying of the left temporal lobe gyri. There is mild cerebellar diaschisis on the right which is unchanged from prior study. On the contralateral side, there is prominence of the motor cortex with sparing of occipital lobe and basal ganglia noted suspicious for an underlying diagnosis of Alzheimer's disease (*Figure 4.7.3*). No evidence for high-grade tumor recurrence is seen.

Impression

1. Generalized hypometabolism in the temporal lobe, parietal lobe, and frontal lobe on the left with significant involvement in the caudate putamen and thalamus compatible with progressive edema and post therapy changes.
2. Prominent motor strip and sparing of the occipital lobe and basal ganglia suspicious for underlying Alzheimer's disease.

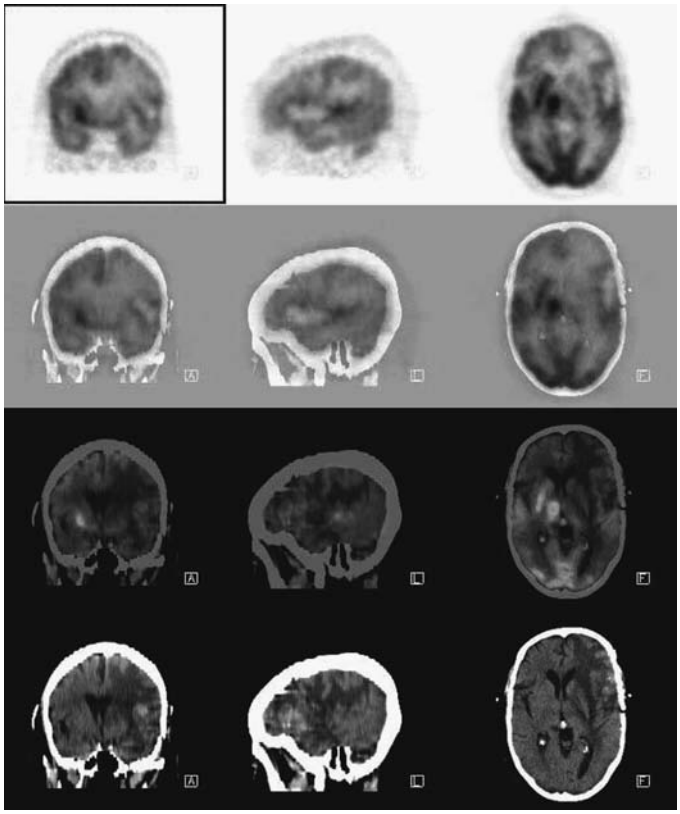

FIGURE 4.7.1.

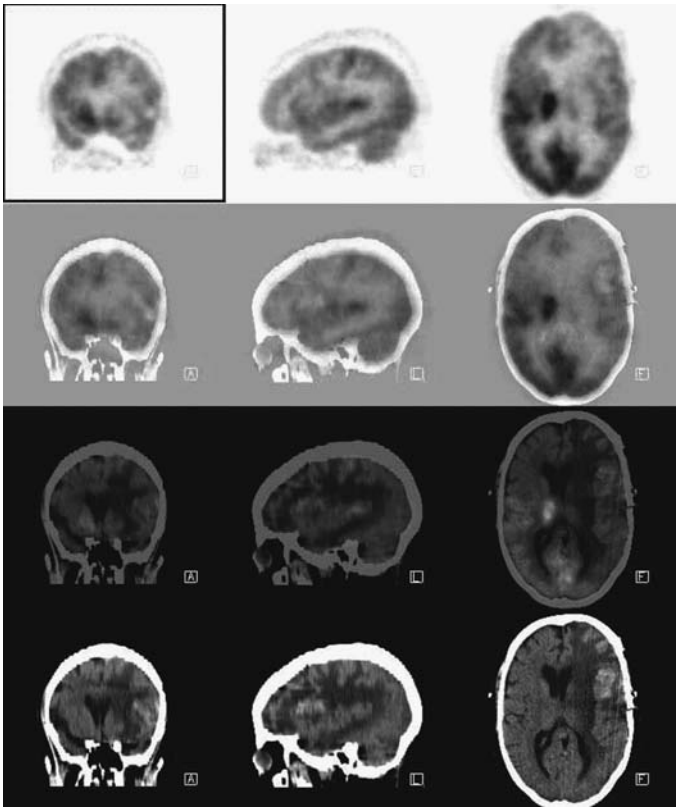

FIGURE 4.7.2.

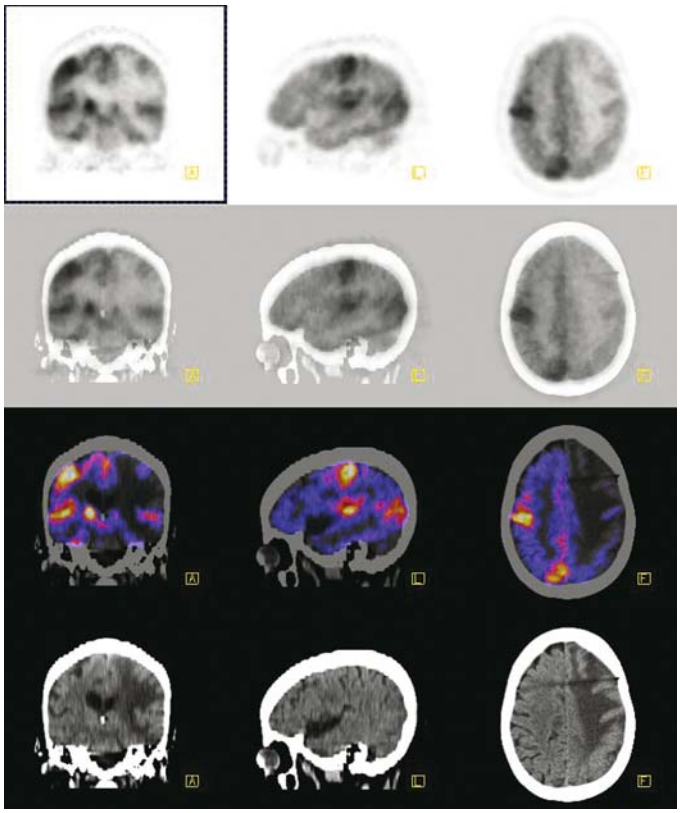

FIGURE 4.7.3.

Pearls and Pitfalls

- *8% of people over 65 years of age are believed to be at risk for development of Alzheimer's disease.*[9]
- *PET can identify people with Alzheimer's disease 2 to 3 years prior to any clinical manifestation.*[9]
- *The sensitivity of PET is 92% to 96%, specificity 63% to 71%, and accuracy 82% to 87% in the diagnosis of dementia of the Alzheimer type.*[9]

Discussion

Biparietotemporal hypometabolism is the typical pattern for Alzheimer's disease. When seen in the presence of sparing of the motor sensory cortex, deep gray matter and occipital lobes, FDG PET can be diagnostic.

Radiation therapy generally causes a decrease in FDG metabolism in the irradiated portion of the brain in the remote setting. Likewise edema can yield regions of hypometabolism.

The degree of crossed cerebellar diaschisis is sometimes helpful in determining disease status with greater diaschisis seen with progressive disease either related to tumor or edema.

Case 4.8

History

53-year-old female who has a history of progressive multiple sclerosis currently on a T-cell therapy protocol who presents with worsening headache for 2 months. Evaluation for malignancy is requested.

Findings

There is a large photopenic mass with peripheral mild hypermetabolism in the right frontal lobe compressing the adjacent structures (*Figure 4.8.1*). Surrounding hypome-

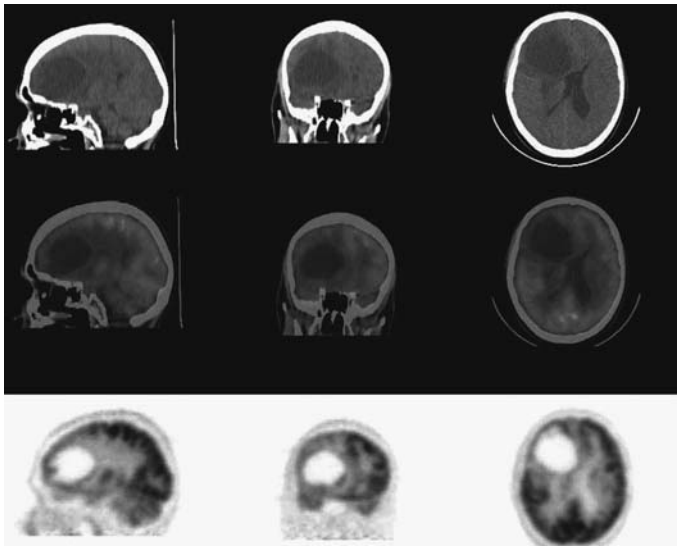

FIGURE 4.8.1.

tabolism is likely the result of edema. Anteriorly to this mass, there is an infolding of uptake attributed to a region of normal gray matter. The diminished uptake in the cerebellar contralaterally is suggestive of crossed cerebellar diaschisis. No high-grade tumor is evident.

Impression

Photopenic mass lacking FDG uptake in the right frontal lobe is compatible with progressive multiple sclerosis rather than high-grade malignancy.

Pearls and Pitfalls

- *PET is a potentially useful tool for distinguishing benign processes from malignant diseases.*[1,3,12]

Discussion

Multiple sclerosis is an autoimmune disease characterized by demyelination in the central nervous system. Fifty percent of affected patients will eventually require ambulatory assistance and 43% will have cognitive impairment. Caucasian, female, and early adulthood are all risk factors. MRS is useful for the diagnosis of demyelinating disease, monitoring its progression, and evaluating the response to treatment. CT is used to exclude other causes for neurologic impairment. PET can help to differentiate multiple sclerosis from malignant glioma based on the degree of uptake.

5 Breast Cancer

Hossein Jadvar

Case 5.1A

History

52-year-old female with a complex history. She has known right breast cancer (poorly differentiated ductal breast carcinoma). She had stem cell transplantation three years prior to the current study, and recently she had a right cervical lymph node biopsy which showed squamous cell carcinoma. There is also a remote history of resected fibrous histiocytoma from the facial area.

Findings

There is a chain of multiple hypermetabolic right jugular nodes (*Figures 5.1A.1 and 5.1A.2*) totaling five or six from the angle of the jaw to the base of the neck (*Figure 5.1A.3*). There is a right supraclavicular lymph node below this. There are two hypermetabolic right axillary nodes (*Figure 5.1A.4*). In the chest, there is a hypermetabolic left AP window lymph node as well as a right paratracheal hypermetabolic node (*Figure 5.1A.5*). In the abdomen, there is a single focus representing an adrenal lesion (*Figure 5.1A.6*). Although the adrenal gland is only minimally nodular, the hypermetabolic pattern is highly suspicious for metastatic disease. Incidental notation is made of asymmetrical breast tissue and some mild increase in cutaneous activity of the right breast. Also incidentally noted is a 4 mm nodule in the anterior segment of the left lower lobe. This solitary small nodule is indeterminate in character by CT criteria but is not hypermetabolic on the PET study. A small peripheral ground glass density is noted in the anterior segment of the right upper lobe. This raises some concern for pulmonary embolism.

There is a hypodensity at the right hilum, a hypodensity within the descending right pulmonary artery, and a hypodensity (relative to unenhanced blood) in the right atrium. These findings are highly suspicious of embolic disease of cardiac origin.

Impression

1. Contiguous nodular hypermetabolic lymphadenopathy in the jugular chain from the angle of the right jaw to the base of the right neck compatible with metastatic disease.
2. There are metastases in the right axillary, right paratracheal, and left AP window nodes.
3. In the abdomen, there is a left adrenal metastasis.

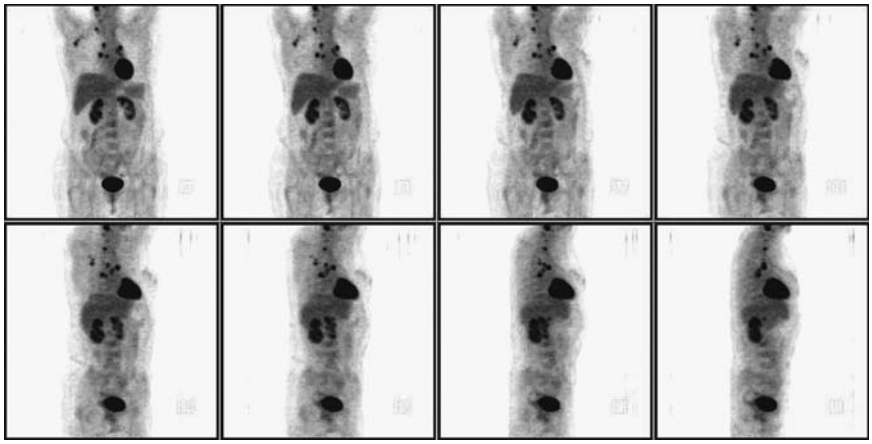

FIGURE 5.1A.1.

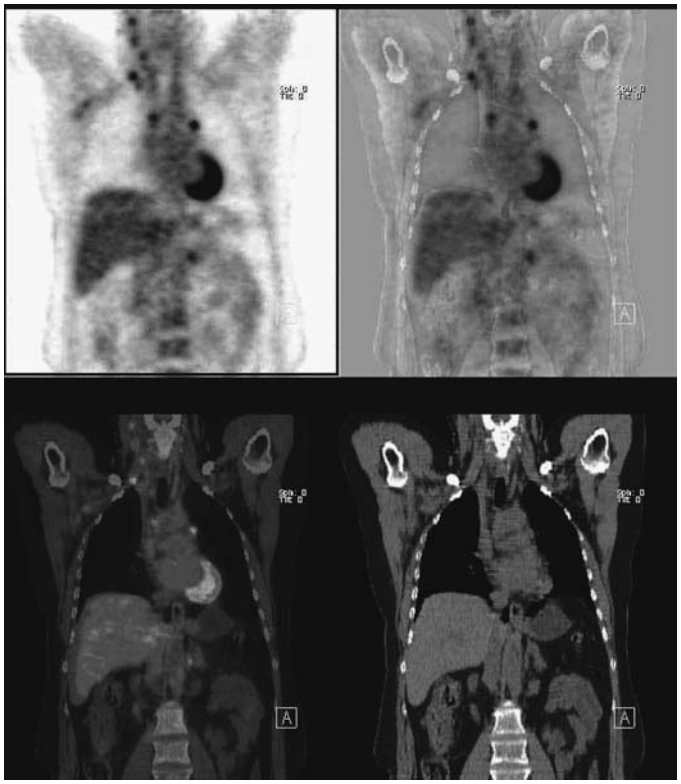

FIGURE 5.1A.2.

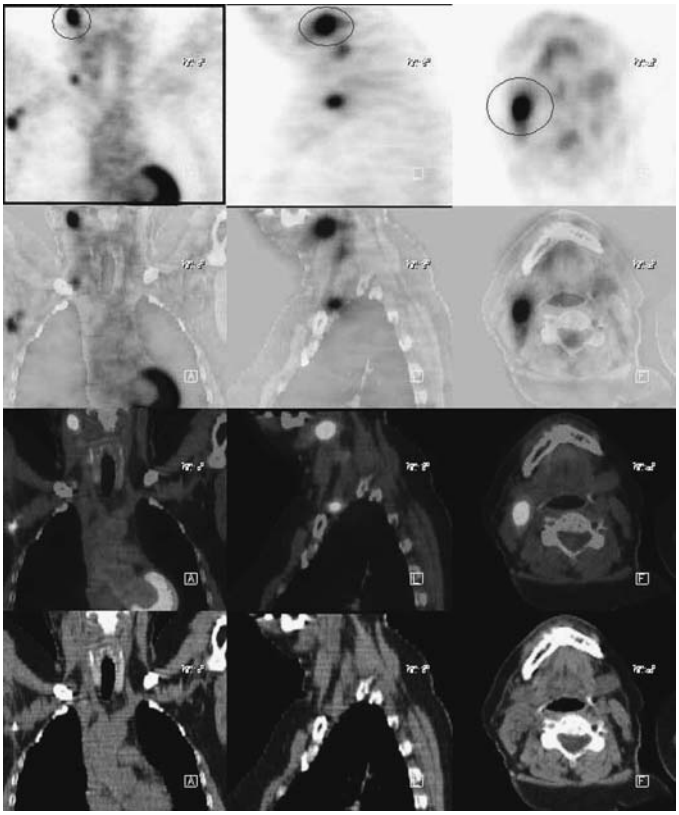

FIGURE 5.1A.3.

4. There is a combination of findings suspect for pulmonary embolism of cardiac origin as detailed above.

Pearls and Pitfalls

- *In general, there is higher FDG accumulation in focal nodular neoplasm than infiltrative diffuse neoplasm because of difference in density of viable cells.*[2,7,18]
- *It is difficult to differentiate carcinoma in situ from normal breast tissue since it exhibits low FDG uptake as a result of a low tumor cell volume and an infiltrative nature.*[2,7,18]

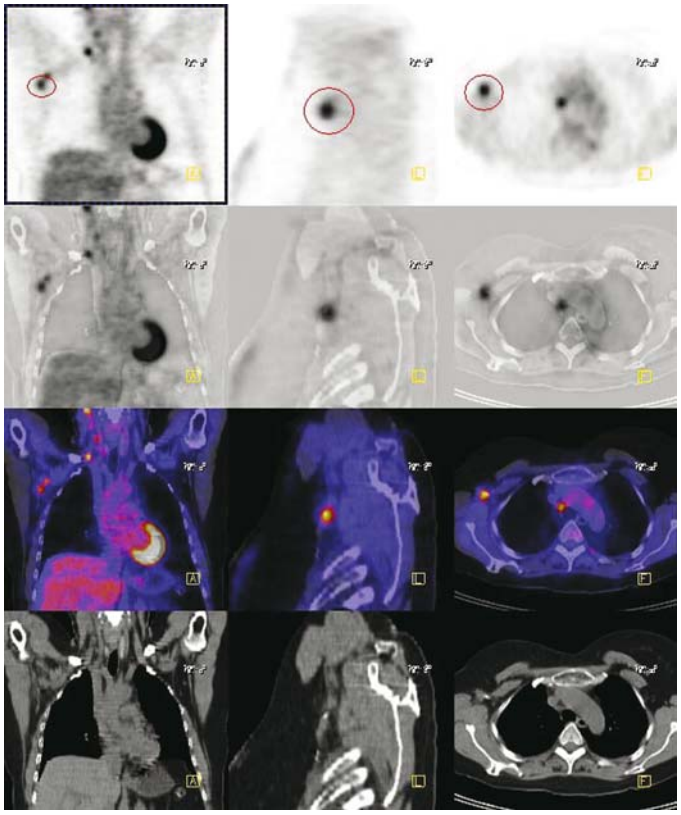

FIGURE 5.1A.4.

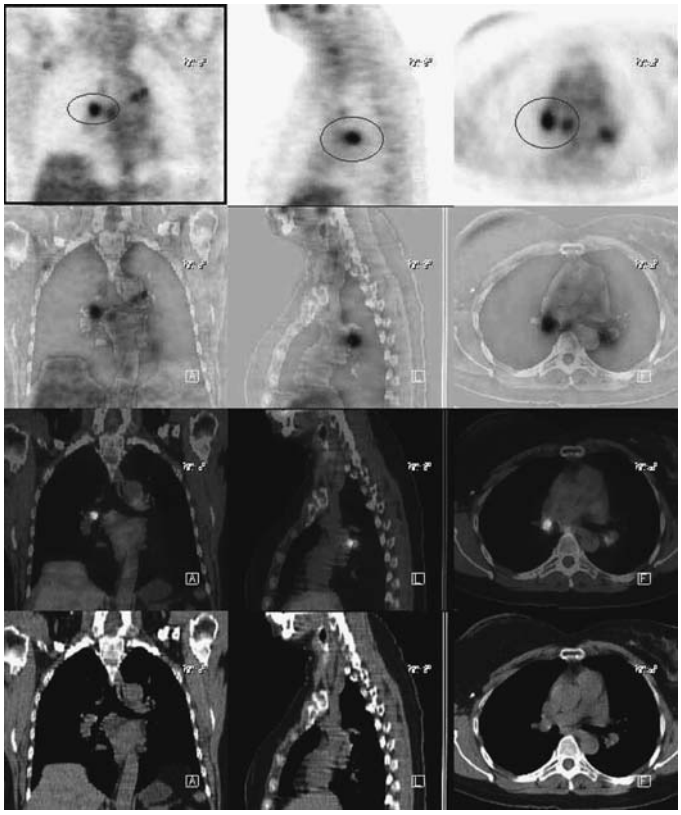

FIGURE 5.1A.5.

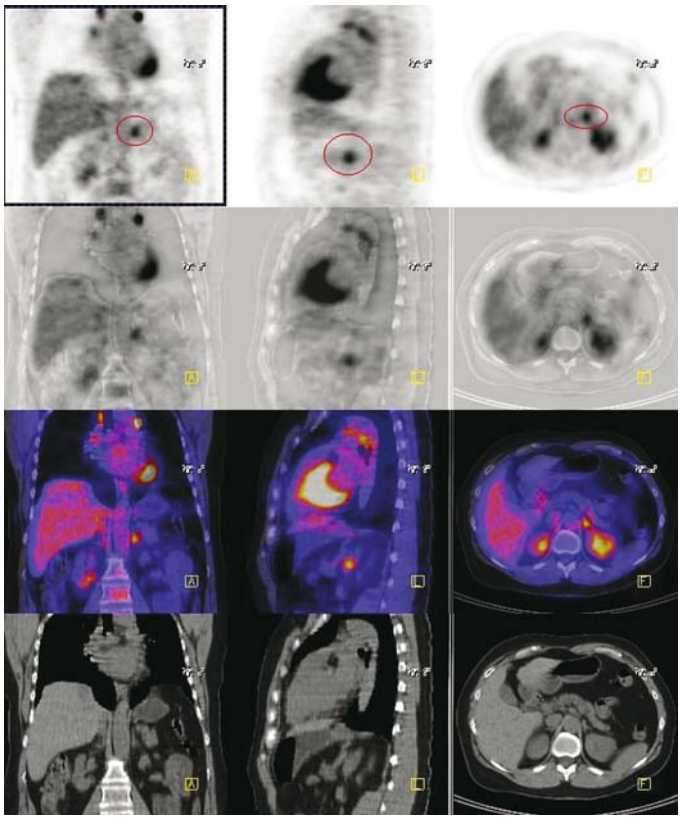

FIGURE 5.1A.6.

- *65% of invasive lobular carcinomas of the breast go undetected due to the inherent characteristics of low metabolic activity and low tumor cell density.*[2,7,18]

Discussion

Invasive ductal carcinoma has a higher FDG uptake than invasive lobular carcinoma. There is a direct correlation in the degree of tumor proliferation and tumor dedifferentiation with the degree of FDG accumulation, although this relationship does not always hold across all cancer types.

Case 5.1B

History

53-year-old female who has a remote history of breast cancer and history fibrous histiocytoma. A recent PET (*Figure 5.1A.1*) study revealed hypermetabolism involving the right neck, right axillary, and left adrenal gland. She was treated with chemotherapy for 14 days with Taxotere and Xeloda. A recent CT demonstrated unchanged lymphadenopathy involving the cervical nodes and para-aortic nodes. The low-density focus in the right lobe of the liver was unchanged. The patient is being evaluated for treatment response.

Findings

There is activity seen involving the bone marrow likely related to hyperplasia from chemotherapy (*Figure 5.1B.1*).

Lymphadenopathy as described on the previous PET is not metabolically active.

Impression

Interval resolution of metastatic disease activity consistent with good response to prior therapy.

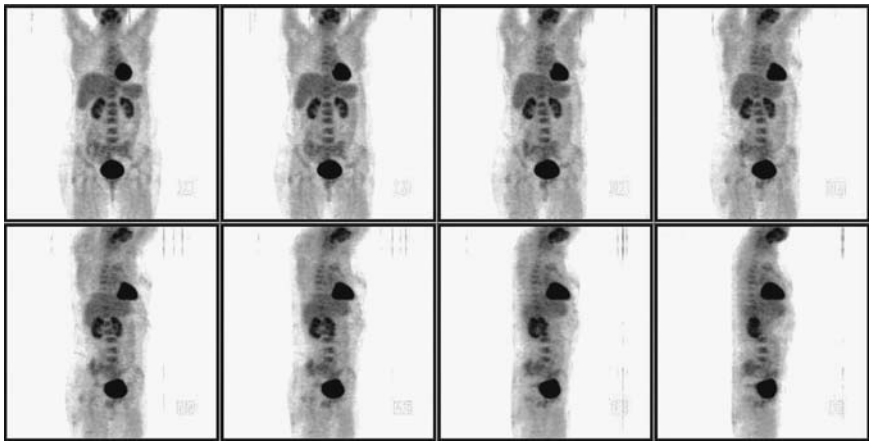

FIGURE 5.1B.1.

Pearls and Pitfalls

- *Various thresholds have been applied to assess tumor response. One study used a decrease in tumor glucose uptake ratio of 20% from the pre-treatment value to identify responders; whereas another study used a decrease in the tumor glucose uptake ratio below 55% of the baseline scan.*[4,9]
- *Although anatomical findings may persist on CT, absence of metabolically active lesions on PET can be used to assess the degree of response to treatment.*[10,12,13,16]

Discussion

PET imaging is an effective method to visualize the effectiveness of induction therapy. The sensitivity of PET increases the discrimination of tumor recurrence from post-therapeutic changes with the ability to survey the entire body. It can differentiate responders from nonresponders as early as following one cycle of chemotherapy.

Case 5.2

History

57-year-old female who has a history of left breast cancer diagnosed ten years prior to the current study. She was treated subsequently with chemotherapy and immunotherapy. A recent PET seen one year ago revealed hypermetabolism involving the right pleura and left midlung. No further treatment was given. The patient is being seen for restaging.

Findings

There is hypermetabolism involving the right iliac crest (*Figures 5.2.1 and 5.2.2*), right first rib, and left sternal border (*Figure 5.2.3*). Additional uptake is seen in the anterior rib at the level of the right midchest (*Figure 5.2.4*). There is significant activity in the proximal right femur and the region surrounding the left hip (*Figure 5.2.5*) with superior and inferior acetabulum involvement. Uptake in the sacral base at the level of the SI joint on the left is also noted. The soft tissue lesion has resolved since the last examination.

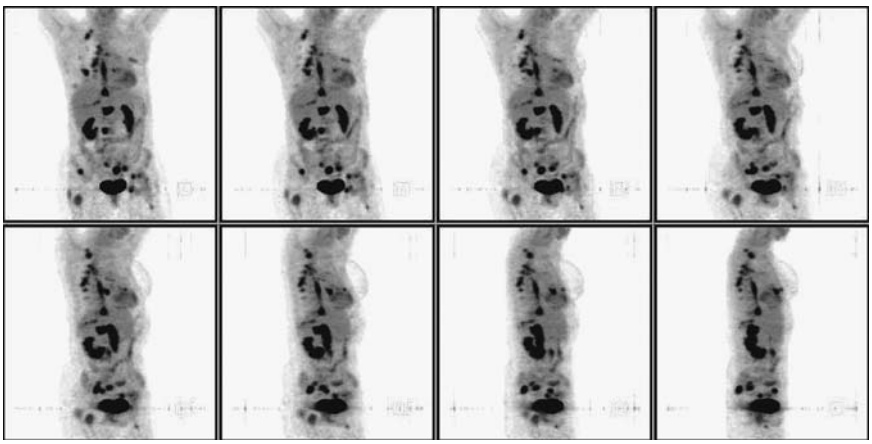

FIGURE 5.2.1.

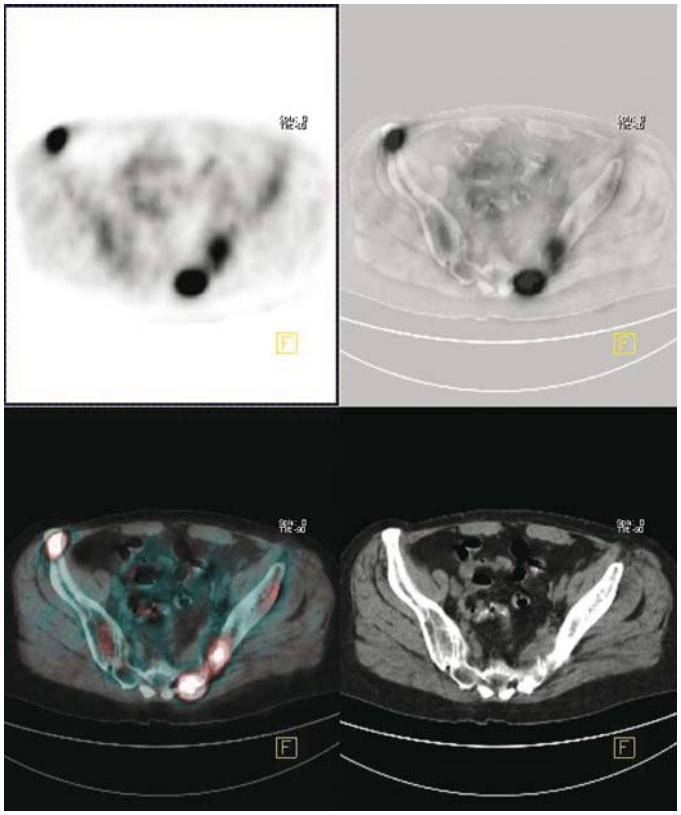

FIGURE 5.2.2.

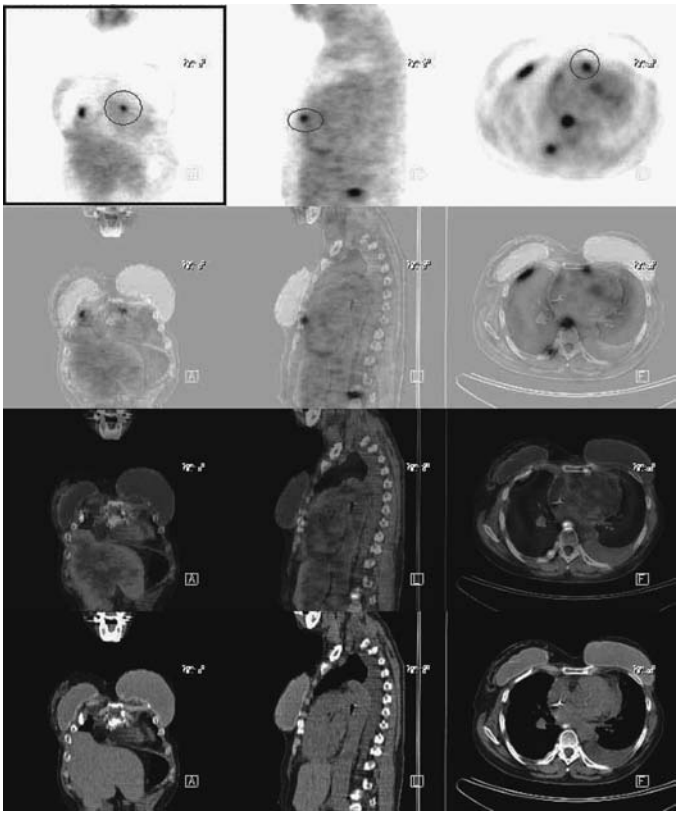

FIGURE 5.2.3.

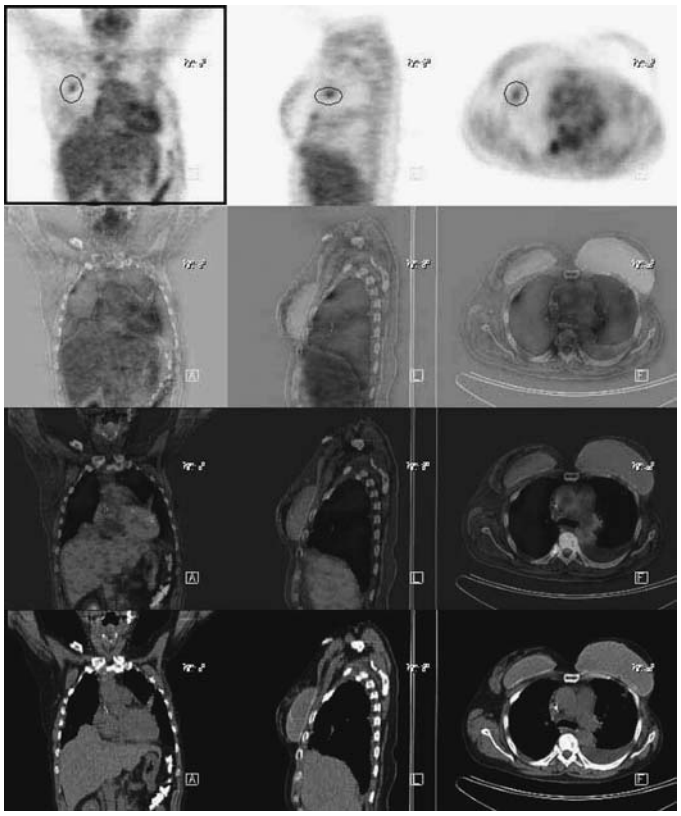

FIGURE 5.2.4.

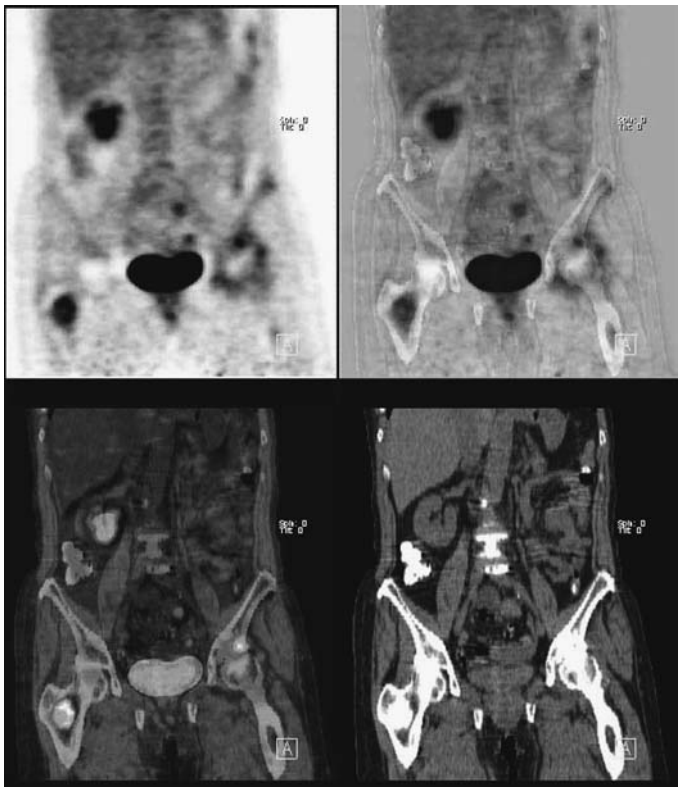

FIGURE 5.2.5.

Impression

Disease progression in bone since the last examination, with resolution of previously noted soft tissue disease.

Pearls and Pitfalls

- *8% of the breast cancer patients present with bony metastases.*[5,6,7,8,11]

Discussion

FDG imaging and bone scintigraphy are useful tools in the determination of bone metastases. FDG is sensitive for lytic lesions since the glycolytic rate in lytic metastases is higher. Bone scintigraphy including F-18 fluoride PET scanning, is more sensitive for osteoblastic lesions. Aggressive therapy is often necessary in patients with pure lytic bone lesions than in patients with sclerotic or mixed metastases since they carry a poorer prognosis.

Case 5.3

History

48-year-old female with reported small right axillary mass on ultrasound. She is status post prophylactic bilateral mastectomies for breast cancer. Her most recent CT demonstrated enlarged pretracheal and bilateral internal mammary lymph nodes. Evaluation for malignancy is requested.

Findings

There are two relatively symmetric moderately FDG-avid lesions in the bilateral high retrosternal areas (*Figures 5.3.1 and 5.3.2*) measuring at 2.0 cm × 1.5 cm (right) and 1.35 cm × 2.0 cm (left) (*Figure 5.3.3*) on CT. Another mildly hypermetabolic lesion is seen in the right paratracheal area which measures 1.14 cm × 0.9 cm. All these nodal lesions are at the level of the AP window and are consistent with metastatic disease. The photopenia in the breasts is compatible with breast prostheses. There is moderate hypermetabolism around the right breast prosthesis (*Figure 5.3.4*) with intense tracer localization inferolaterally, which on CT localizes to a rib or the adjacent chest wall soft tissue. Additionally, there is an irregular opacity in the posterior aspect of the left lower lobe (*Figure 5.3.5*) that demonstrates moderate hypermetabolism on PET. This may correspond to the suspicious finding on an earlier CT. The activity in the thyroid, stomach and colon is physiologic in nature. There is some urinary stasis seen in the renal collecting systems.

Impression

1. Abnormal hypermetabolism involving the bilateral high internal mammary and right paratracheal lymph nodes at the level of the AP window, consistent with metastatic disease.

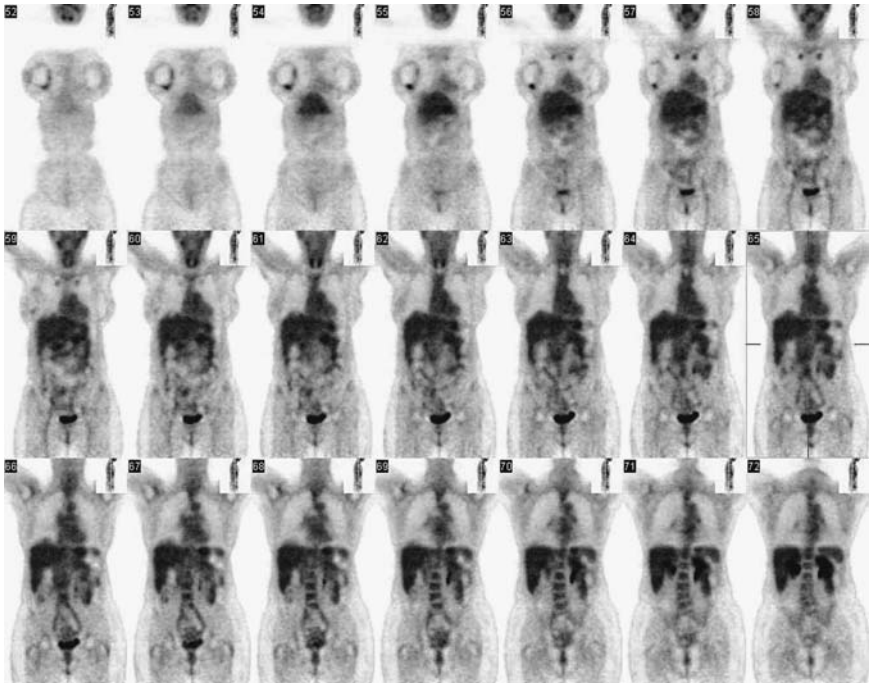

FIGURE 5.3.1.

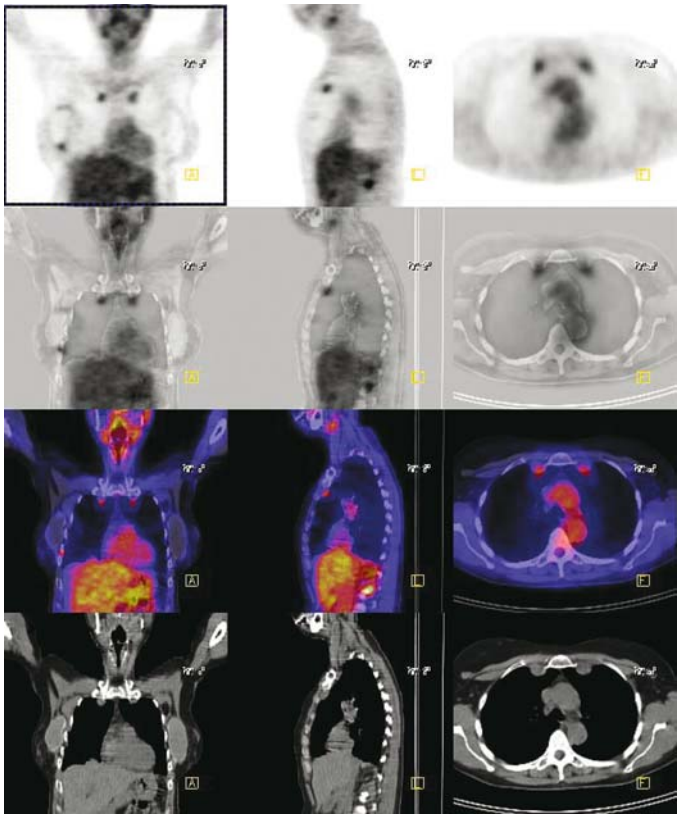

FIGURE 5.3.2.

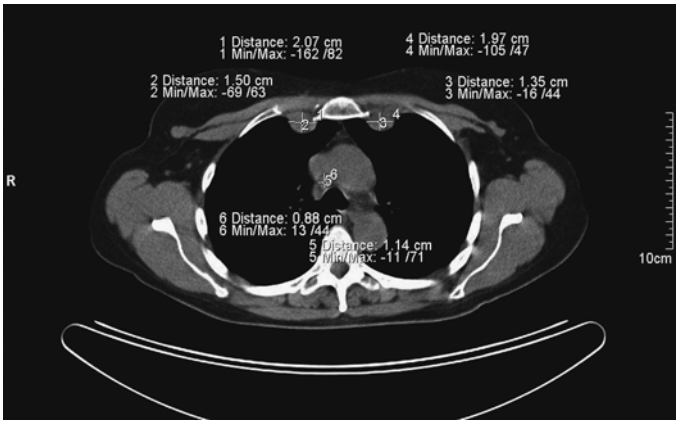

FIGURE 5.3.3.

2. Relatively diffuse hypermetabolism around the right breast prosthesis which is more intense inferolaterally. This most likely represents localized inflammatory changes associated with fibrosis surrounding the implant.
3. Pleural-based moderately hypermetabolic irregular lesion in the posterior left lower lobe, suspicious for a metastatic deposit.

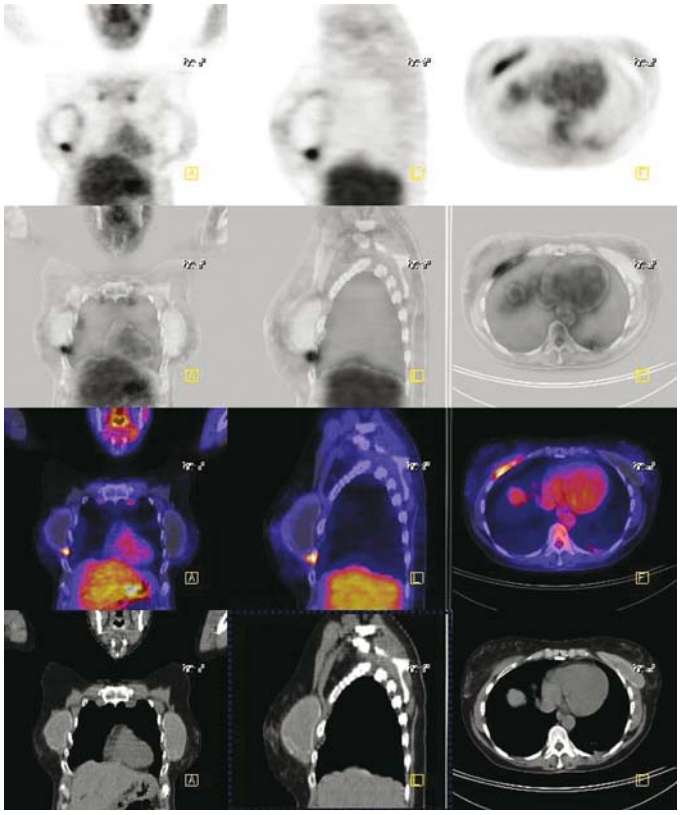

FIGURE 5.3.4.

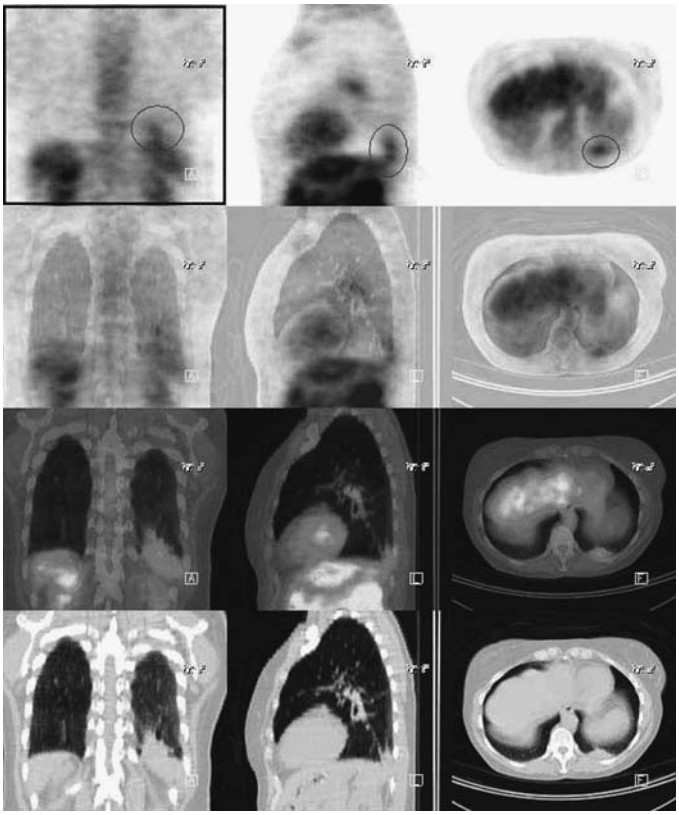

FIGURE 5.3.5.

Pearls and Pitfalls

- *The sensitivity for malignancy in a focal breast lesion is 64% to 96% and specificity 75% to 100%.*[1,3,7,14,18]
- *In the differentiation of benign from malignant breast diseases, PET has a sensitivity and specificity of 88% and 79% respectively.*[1,3,7,14,18]

Discussion

PET is more sensitive (85%) vs. CT (54%) in the identification of unsuspected metastases involving the internal mammary nodes and mediastinum. Presence of a positive internal mammary node is associated with a poorer long-term prognosis. Additional aggressive chemotherapy or radiation are necessary in the management of these patients.

Case 5.4

History

56-year-old female who has a history of breast cancer diagnosed 5 years prior to the current study, and status post left lumpectomy. She was then treated with radiotherapy and chemotherapy. Her most recent CT demonstrates multiple nodules in the upper and lower lungs bilaterally. The patient is being seen to evaluate for recurrence.

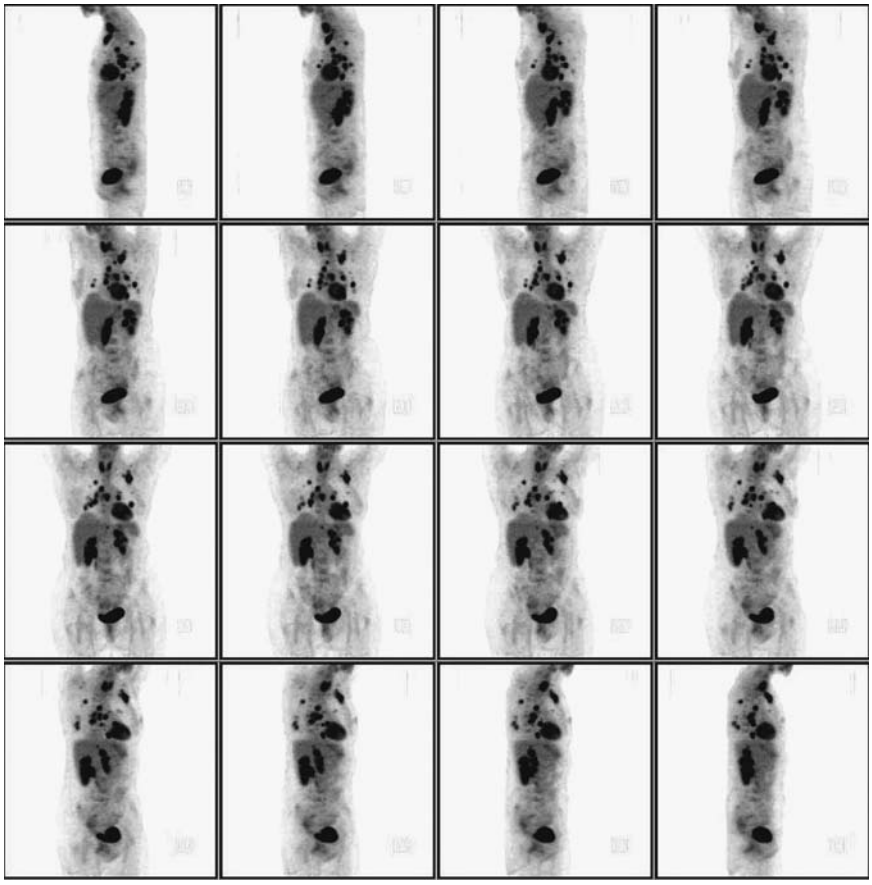

FIGURE 5.4.1.

Findings

There is an extensive adenopathy overlying the left chest wall with additional nodes extending to the high axilla (*Figures 5.4.1 and 5.4.2*). Multiple sites of FDG-avid uptake in the bihilar areas, and right paratracheal (*Figure 5.4.3*) nodal basin are also seen. There is hypermetabolism within the T-10 vertebral body at the level of the diaphragm. A right posterolateral rib lesion is present at the mid to lower thoracic level. There is a solitary metastatic lesion in the superior medial aspect of the right iliac bone (*Figure 5.4.4*) lateral to the SI joint. No evidence for hepatic involvement is seen.

Impression

Multiple sites of hypermetabolism involving the left axilla, left chest wall, mediastinum, ribs, pelvis, and spine consistent with metastatic disease.

Pearls and Pitfalls

- *PET is superior to CT in detecting nodal involvement.*[7,16]
- *The sensitivity of PET for detection of local-regional nodal metastasis is between 50% and 100% while the specificity for axillary nodal metastases ranges between 86% and 92%. The lower sensitivity for axillary nodal metastases is attributed to undetected micrometastases.*[15,17,18]

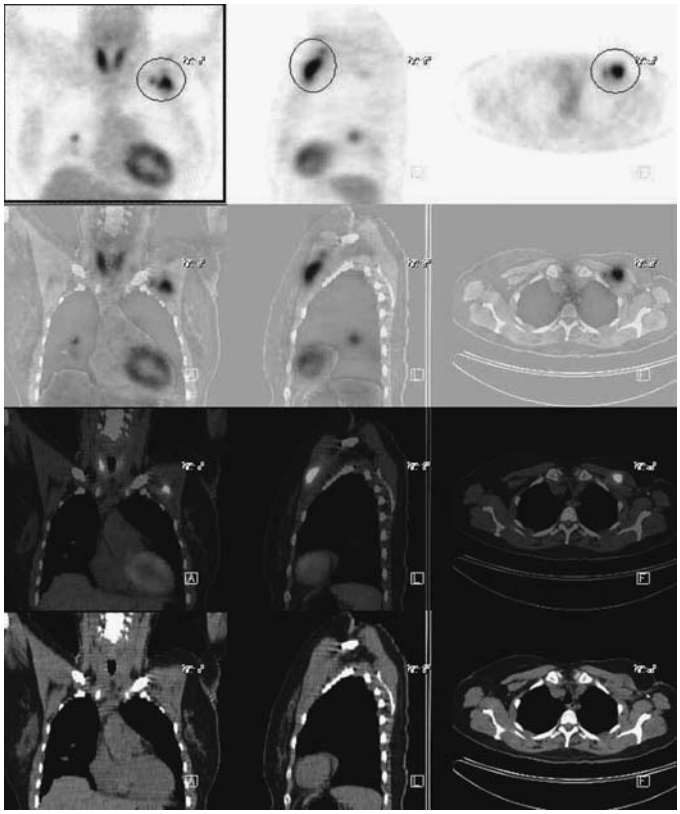

FIGURE 5.4.2.

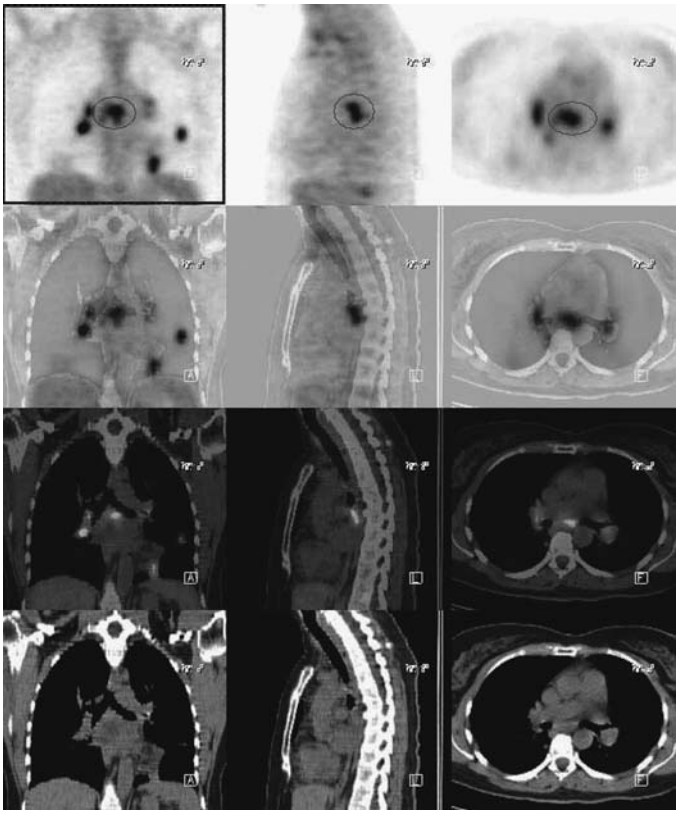

FIGURE 5.4.3.

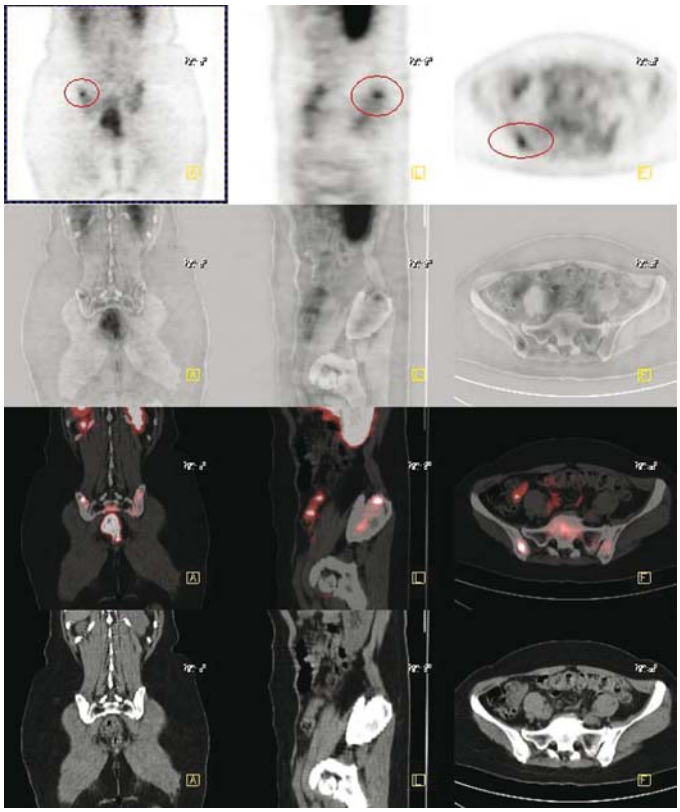

FIGURE 5.4.4.

- *7% to 30% of the breast cancer patients initially treated for cure represent with local or regional recurrent disease.*[7,9,11]

Discussion

Most common sites of locoregional recurrence include the breast, the skin of the breast, chest wall, and local nodal basins after surgical resection and radiation. Positive margins at surgery, age less than 40 years, and tumor with extensive intraductal component are a few of the risk factors for locoregional recurrence. The most common sites of locoregional recurrences are the supraclavicular nodes, the chest wall, and axillary nodes. Patients with four or more positive axillary nodes, tumor diameter over 4 cm and extranodal extension greater than 2 mm are all major risk factors for local recurrence and have a poor survival rate.

Case 5.5

History

36-year-old female who has newly diagnosed right breast cancer by biopsy with clinically positive neck and right axilla adenopathy. The patient is being evaluated to stage disease.

Findings

There is an intensely hypermetabolic mass in the central part of the right breast (*Figures 5.5.1 and 5.5.2*). A smaller satellite lesion is seen lateral to this lesion. A second large bilobed hypermetabolic mass (*Figure 5.5.3*) is present in the upper medial aspect of the right breast again with a smaller satellite lesion seen laterally. A small right hilar node (*Figure 5.5.4*) is present, but is too small to characterize as definite for malignancy. There is additional focus of hypermetabolism involving a right internal mammary node (*Figure 5.5.5*) and right periclavicular nodes. There is an axillary lesion on the right chest wall (*Figure 5.5.6*), which corresponds to a soft tissue mass seen on CT. The mild uptake in the shoulders is symmetrical and is likely related to inflammatory joint disease.

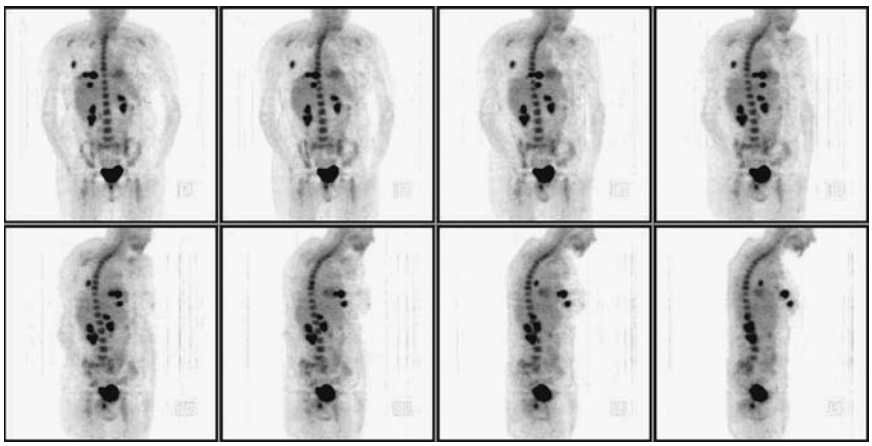

FIGURE 5.5.1.

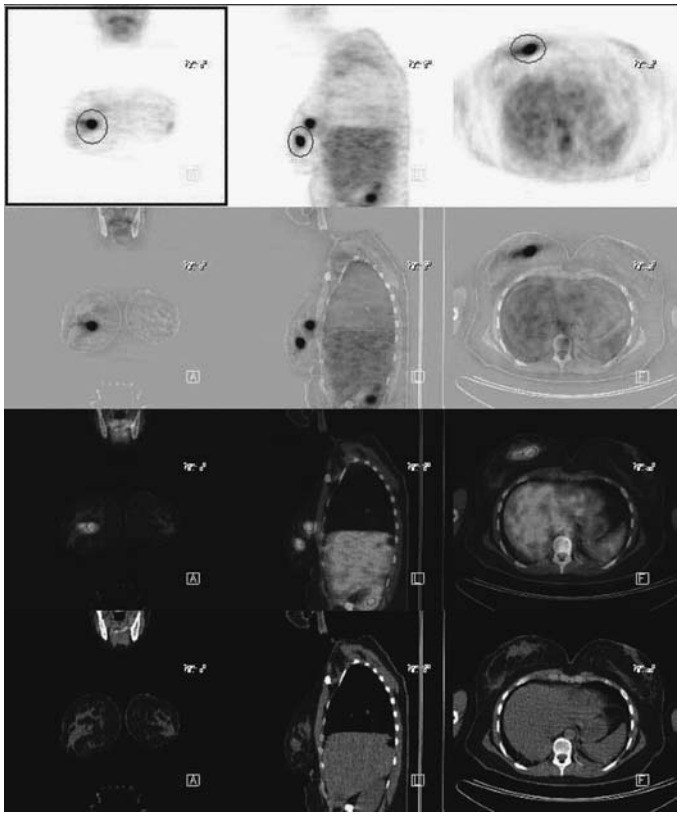

FIGURE 5.5.2.

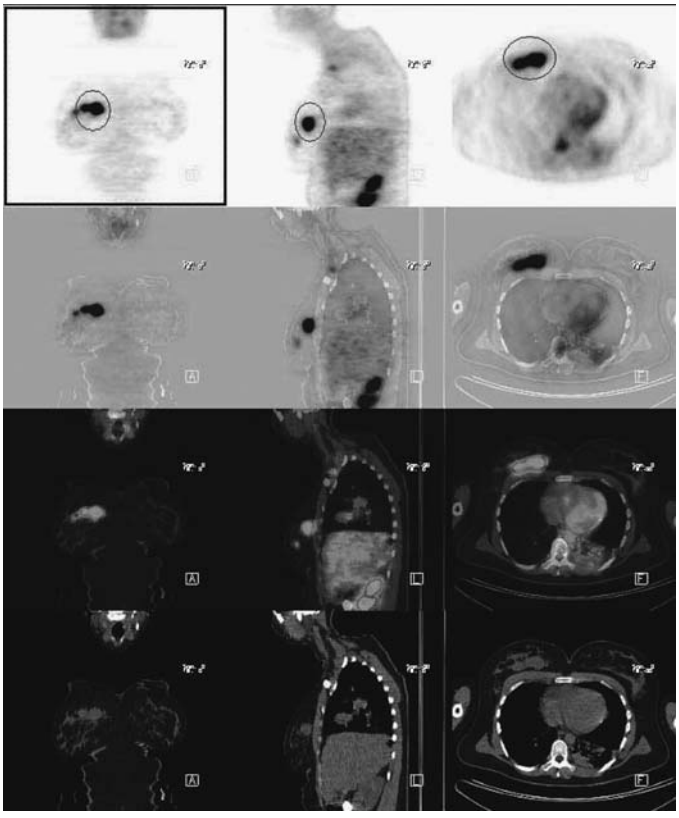

FIGURE 5.5.3.

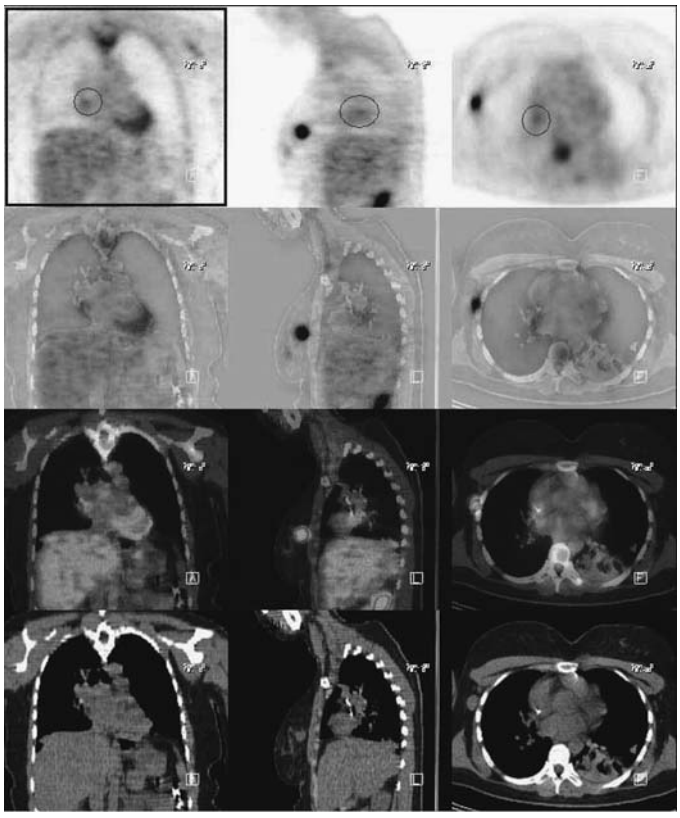

FIGURE 5.5.4.

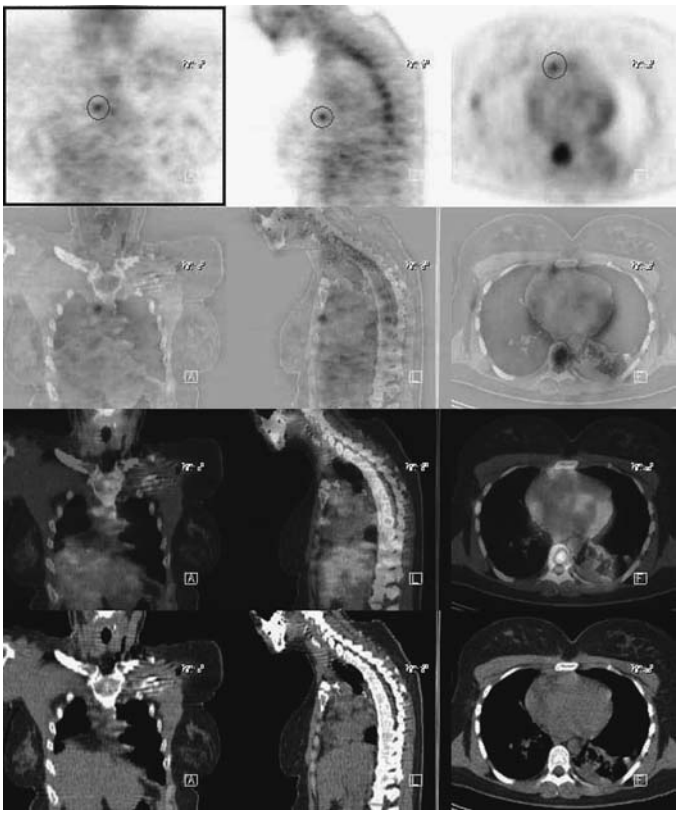

FIGURE 5.5.5.

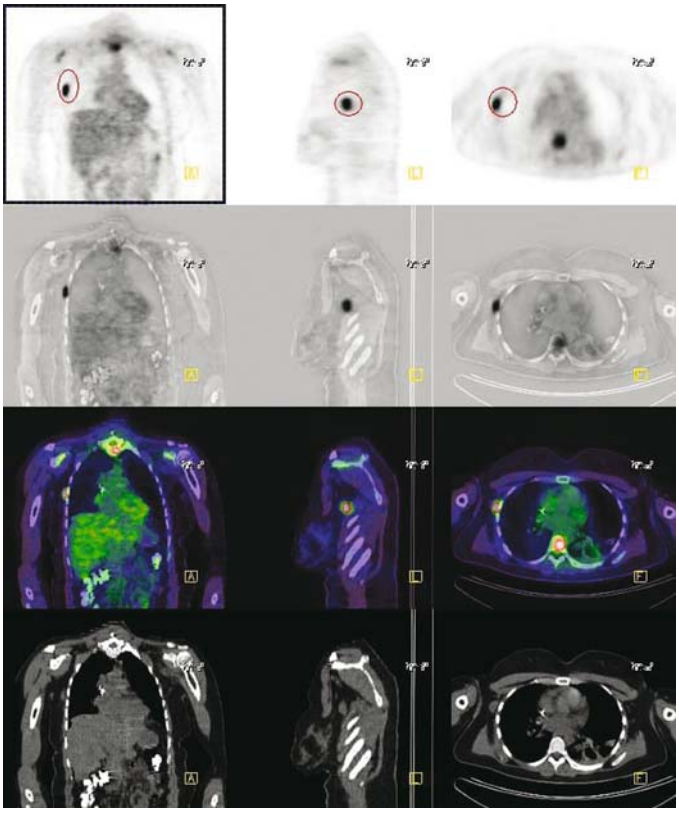

FIGURE 5.5.6.

Impression

PET evidence for advanced stage breast cancer with bulky primary disease in the right breast.

Pearls and Pitfalls

- *In contrast to mammography, PET is not affected by the breast tissue density.*[7,13,16]

Discussion

PET is four times more accurate than CT in isolating malignant breast lesions. There is a poorer prognosis when PET findings remain positive after the completion of therapy. Locally advanced breast disease including a tumor >5 cm, chest wall or skin involvement, and fixed lymph node metastases will indicate a poor response to neo-adjuvant chemotherapy.

6 Gynecologic Malignancies: Cervical, Uterine, and Vulvar Cancer

Hossein Jadvar

Case 6.1

History

32-year-old female who has a history of cervical cancer with a positive pelvic lymph node dissection two years following her original diagnosis. At the time of the dissection her CT demonstrated lymphadenopathy involving the periaorta, left external iliac, and left renal region. The patient is undergoing PET-CT to determine residual disease prior to initiation of chemotherapy.

Findings

There is mild hypermetabolism in the left external iliac node chain and para-aortic nodes (*Figures 6.1.1 and 6.1.2*) at the bifurcation of the iliac vessels representing malignancy. A band of activity is present in the left lower abdomen (*Figure 6.1.3*) consistent with recent surgery. Multiple surgical clips are seen in the pelvis compatible with prior tumor removal and lymph node dissection. There is focal uptake possibly involving the nerve root of the right upper thoracic spine at the T-5 level (*Figure 6.1.4*) likely inflammatory in nature. A UPJ obstruction with evidence of right-sided renal caliectasis is noted. The liver, chest, and mediastinum are clear from visible abnormality.

Impression

1. The left iliac and para-aortic adenopathy compatible with the presence of malignancy.
2. Right renal caliectasis with UPJ obstruction.

Pearls and Pitfalls

- *The sensitivity and specificity of PET for early recurrent cervical cancer is 90% and 76% respectively.*[4,5]
- *30% of the cervical cancers in treated patients will recur after treatment.*[4,5]
- *11% of the patients definitively treated with cervical cancer who are clinically asymptomatic are identified afterwards with recurrence using PET.*[4,5]

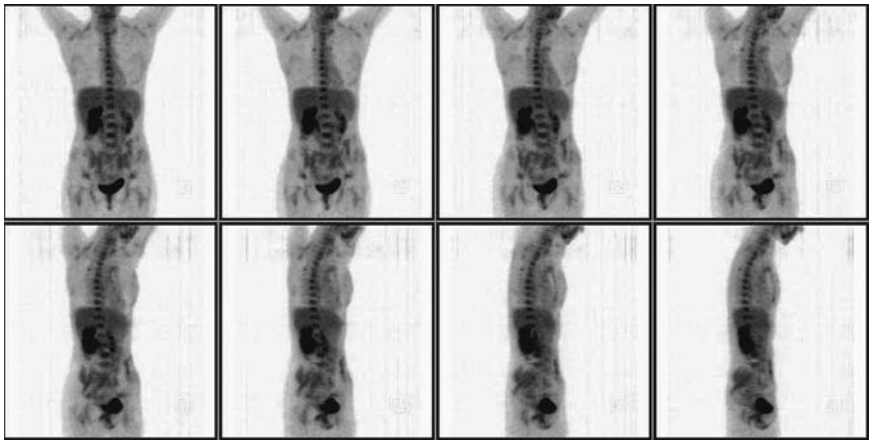

FIGURE 6.1.1.

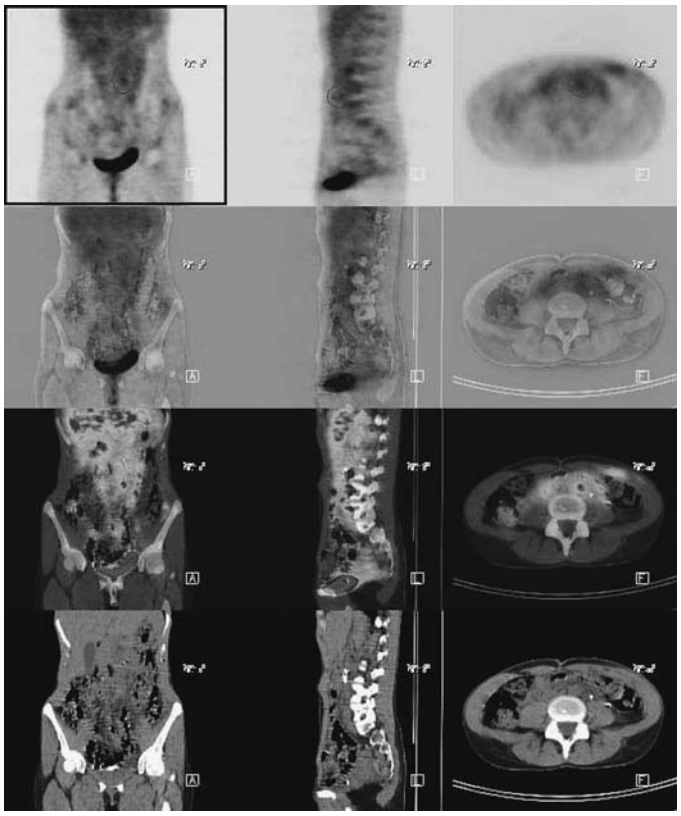

FIGURE 6.1.2.

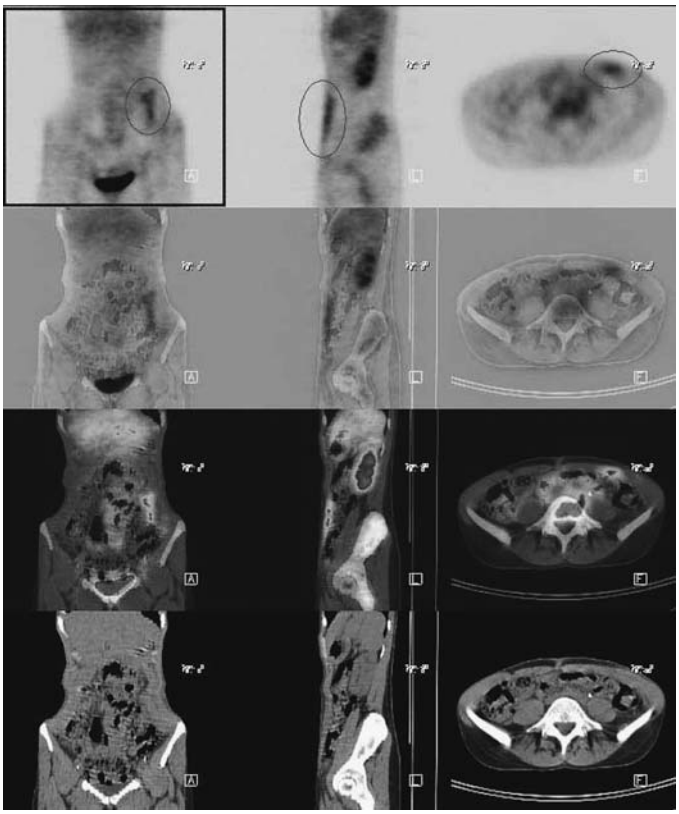

FIGURE 6.1.3.

Discussion

Squamous cell carcinoma is the most frequent **cervical cancer** with 85% to 90% being invasive. The most common risk factor is a history of sexually transmitted disease including gonorrhea, syphilis, herpes simplex, and Trichomonas or Chlamydia. In the United States, most cases found are carcinoma in situ or as premalignant disease.

MRI is considered the method of choice in the staging of primary tumor since it can evaluate tumor depth and stromal invasion. However, it lacks the ability to accurately diagnose nodal involvement. For this reason, PET is used to assess nodal malignancy

FIGURE 6.1.4.

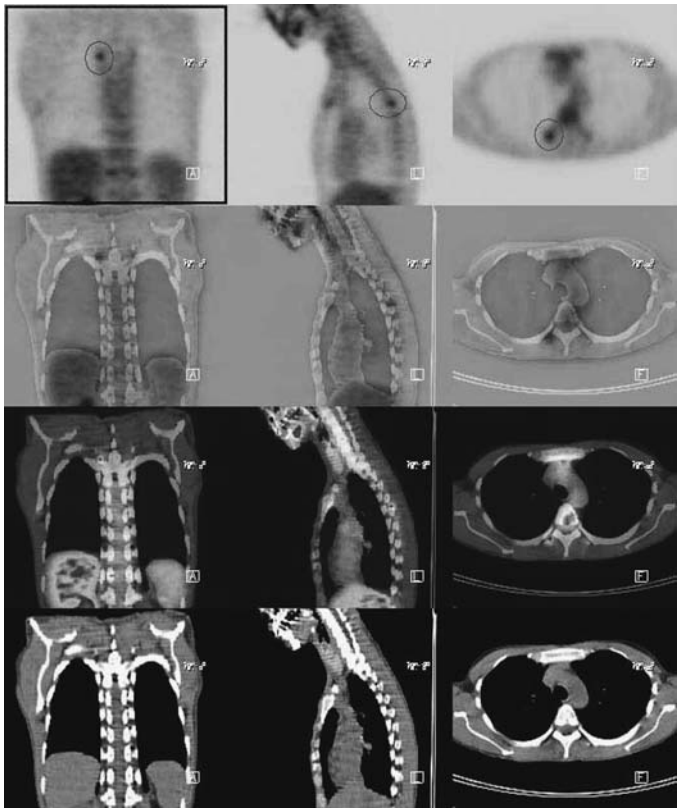

as well as regional and distant metastatic disease. PET has a 91% positive predictive value for pelvic and para-aortic lymphadenopathy.

The standard management of patients with early cervical carcinoma (stages IA-IIA) in surgical removal of the cervix. The extent of resection of surrounding tissue depends on the size of the lesion and depth of invasion. A recent GOG trial demonstrated the benefit of the addition of cisplatin chemotherapy to pelvic radiation followed by extrafascial hysterectomy in this group of patients. Therefore, many experts feel that patients with stage IB2 and bulky IIA cervical cancer should be treated initially with chemoradiation followed by adjuvant extrafascial hysterectomy.

Case 6.2

History

69-year-old female who has a history of cervical cancer treated 25 years ago with radiation therapy. She recently had a left neck and abdominal lymph node dissection, positive for tumor. She recently received chemotherapy and radiation to the neck and abdomen. The current PET-CT is being done to evaluate for residual disease.

Findings

The dominant feature of the exam is the mass between the urinary bladder and the rectum, which was also reported on a recent CT as being 6.5 cm × 4 cm × 5 cm. As with that exam, the uterus appears in situ. The described mass has feces-like central contents, with a peripheral hypermetabolic rim. The hypermetabolism extends into the uterus (*Figure 6.2.1*). It also extends to the anterior aspect of the rectum and to the

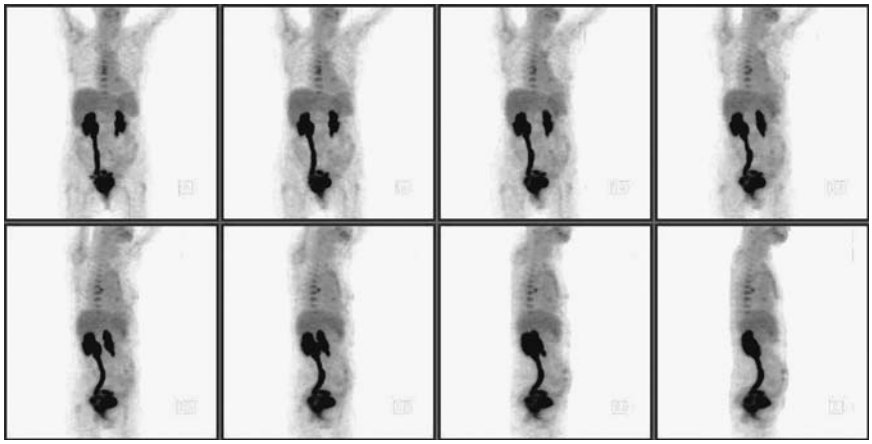

FIGURE 6.2.1.

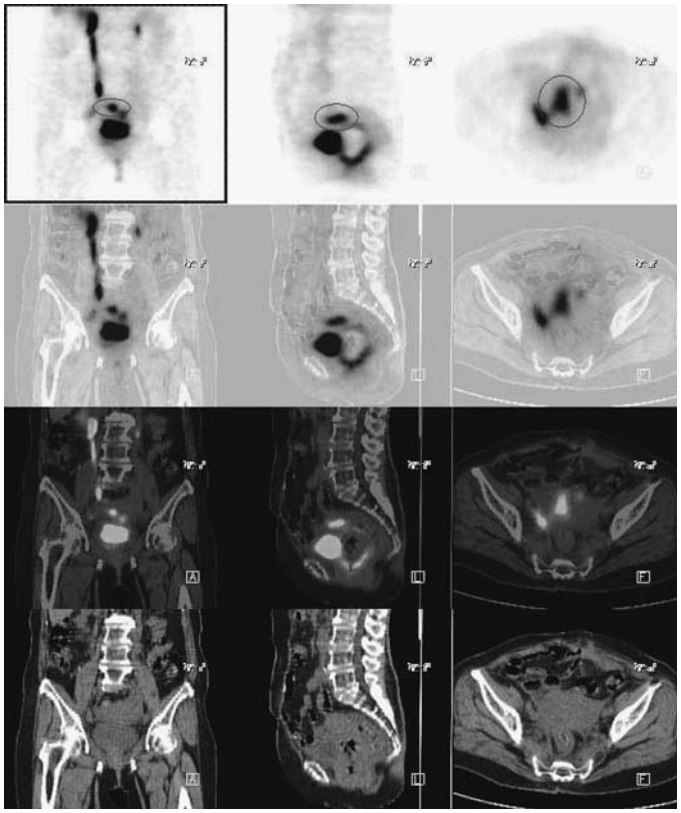

FIGURE 6.2.2.

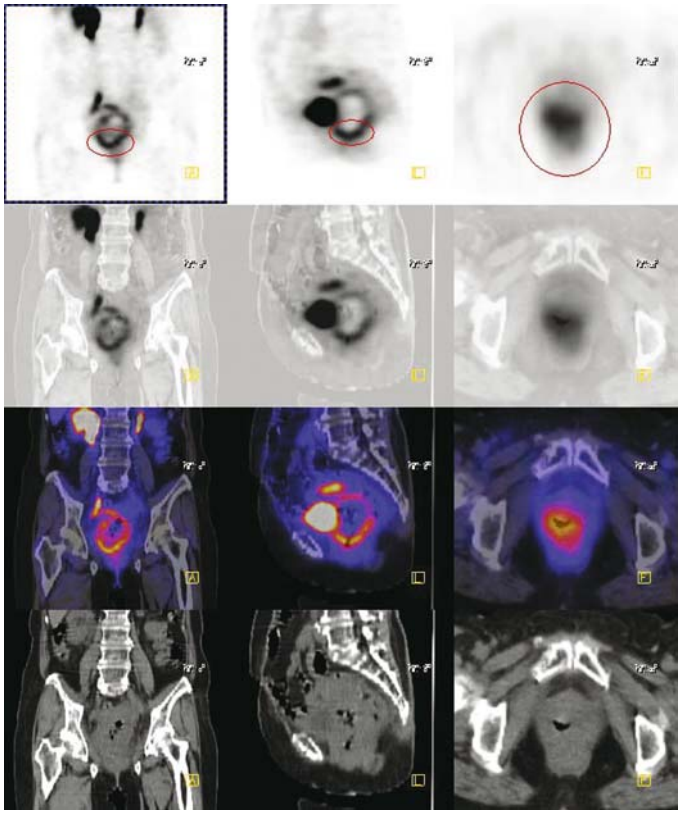

FIGURE 6.2.3.

posterior aspect of the urinary bladder. The mass elevates and compresses the ureters with bilateral ureteral stasis (*Figures 6.2.2 and 6.2.3*). The feces-like contents of the mass could represent inspissation of secretions in a vaginal recurrence with osteal obstruction vs. fistula to bowel. This mass is likely to represent a vaginal recurrence with osteal obstruction and extension into the endometrial cavity by the recurrent tumor. Additionally, there is a single intrathoracic hypermetabolic focus (*Figure 6.2.4*) in the middle/posterior mediastinum, between the horizontal course of the right pulmonary artery and the esophagus. This small lymph node is intensely hypermetabolic and consistent with metastatic disease.

FIGURE 6.2.4.

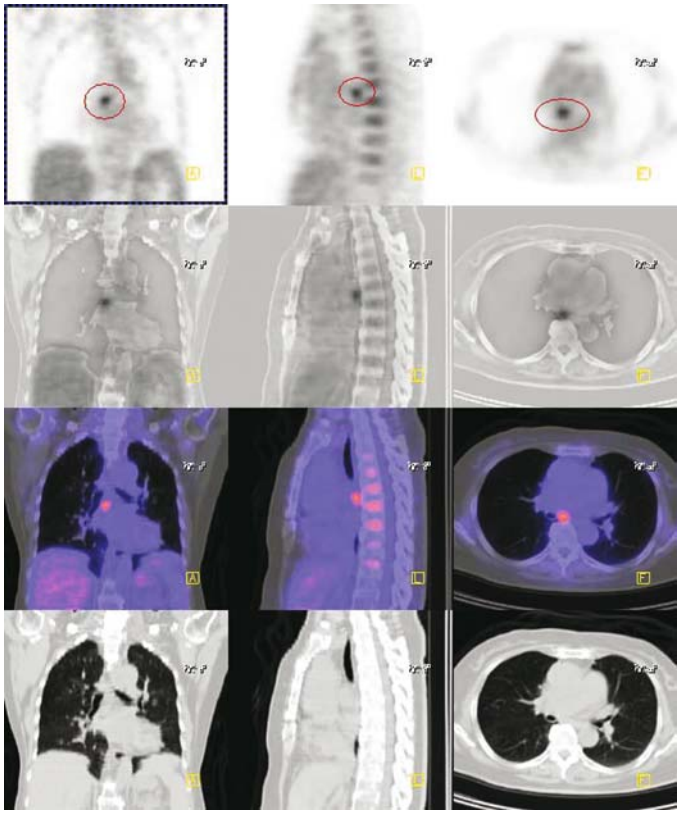

Impression

1. The reported mass between the rectum and the urinary bladder is probably a distended involved vagina with central inspissated secretions related to osteal obstruction.
2. There is extension of tumor into the endometrial cavity of the in situ uterus. The mass elevates and compresses the ureters with bilateral stasis. There is extension to the anterior wall of the rectum and to the posterior urinary bladder.
3. There is a metastatic deposit to the chest in the middle/posterior mediastinum, normal sized, but representing an involved lymph node in that location.

Pearls and Pitfalls

- *Most cervical cancers recur within two years after therapy with the peak period for recurrence at 9 to 12 months.*[4,5]
- *A repeat PET scan is recommended at least 1 year after treatment for all patients with advanced disease.*[4,5]

Discussion

The role of curative surgery diminishes once cervical cancer has spread beyond the confines of the cervical and vaginal fornices. Intracavitary radiation for central pelvic disease and external-beam radiation therapy for lateral parametrial and pelvic nodal disease are typically combined to encompass the known patterns of disease spread with an appropriate radiation dose while sparing the bladder and rectum from receiving full

doses. The addition of intracavitary radiation to external-beam radiation is associated with improved pelvic control and survival over external radiation alone, as the combination can achieve high central doses of radiation.

At present, the use of adjuvant pelvic radiotherapy should be considered for patients with negative nodes who are at risk for pelvic failure, and remains the standard postoperative treatment for patients with positive lymph nodes. Treatment consists of external pelvic radiation (45 Gy–50 Gy), with specific sites boosted with further external-beam or intracavitary radiation as needed.

Various combination chemotherapy regimes have been evaluated, and high response rates (>50%) were noted even in patients who had received prior radiation therapy. The past few years have provided what may be the most important breakthrough in cervical cancer treatment in 50 years. Five separate studies that compared combinations of cisplatin-containing chemotherapy with concurrent RT have demonstrated a consistent advantage to the chemotherapy-RT combination.

Case 6.3

History

50-year-old female who has a history of cervical cancer ten years ago now with a biopsy-proven pulmonary nodule malignancy. PET-CT is being done to evaluate extent of metastatic diseases.

Findings

There is an intensely hypermetabolic lesion corresponding to a 1.8 × 2.3 cm noncalcified soft tissue nodule in the right anterior lung (*Figures 6.3.1 and 6.3.2*) adjacent to the cardiac border. A noncalcified hypermetabolic nodule is also seen in the right upper lobe at the level of the carina (*Figure 6.3.3*) roughly 1.0 cm in size. The pulmonary nodule in the right lower lobe adjacent to the diaphragmatic surface is also hypermetabolic measured at 1.0 cm. There is an apparent bronchiectatic lesion (*Figure 6.3.4*) seen in the left lower lobe with mild hypermetabolism. The few nonenlarged bilateral axillary lymph nodes are metabolically inactive and considered benign. The mild increased distal esophageal activity is likely related to esophagitis (*Figure 6.3.5*). The bilateral lower neck base (*Figure 6.3.6*) increased tracer uptake is compatible with activity involving the fat and muscle extending to the supraclavicular areas and the thoracic inlet. Moderate physiologic paraspinal muscle activity is also noted.

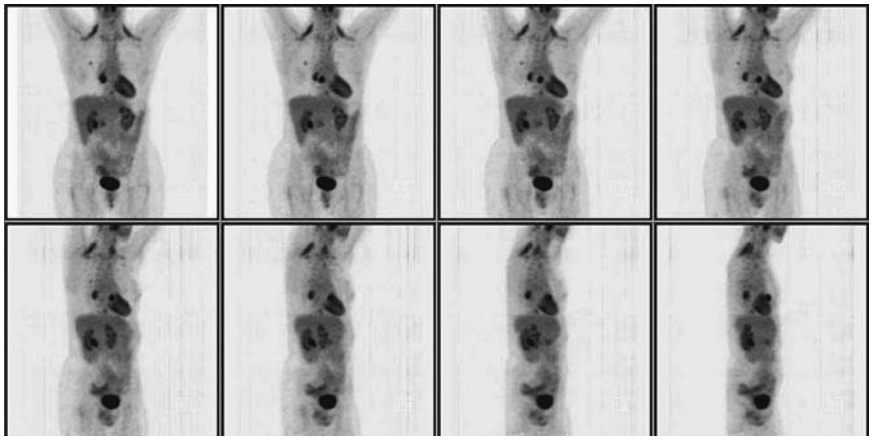

FIGURE 6.3.1.

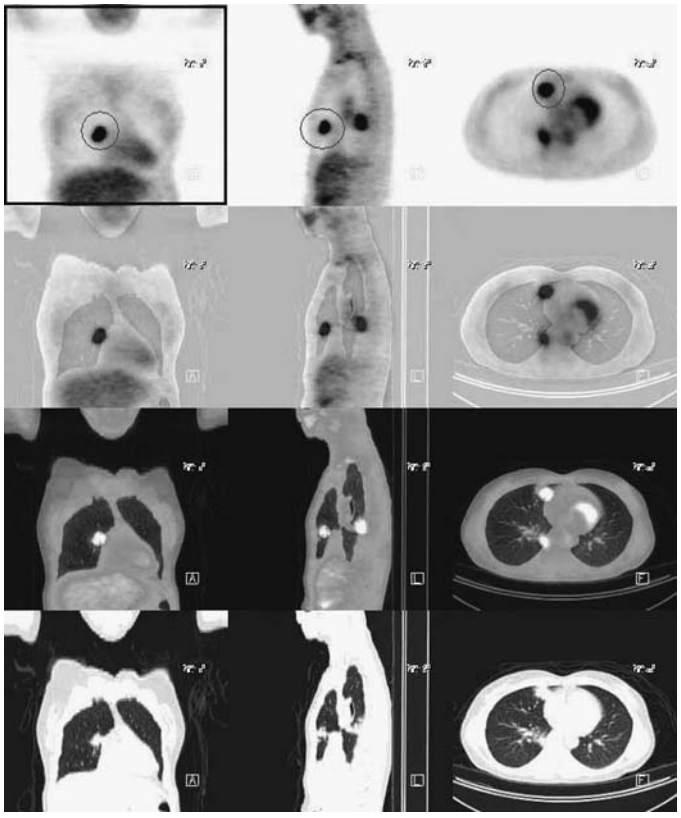

FIGURE 6.3.2.

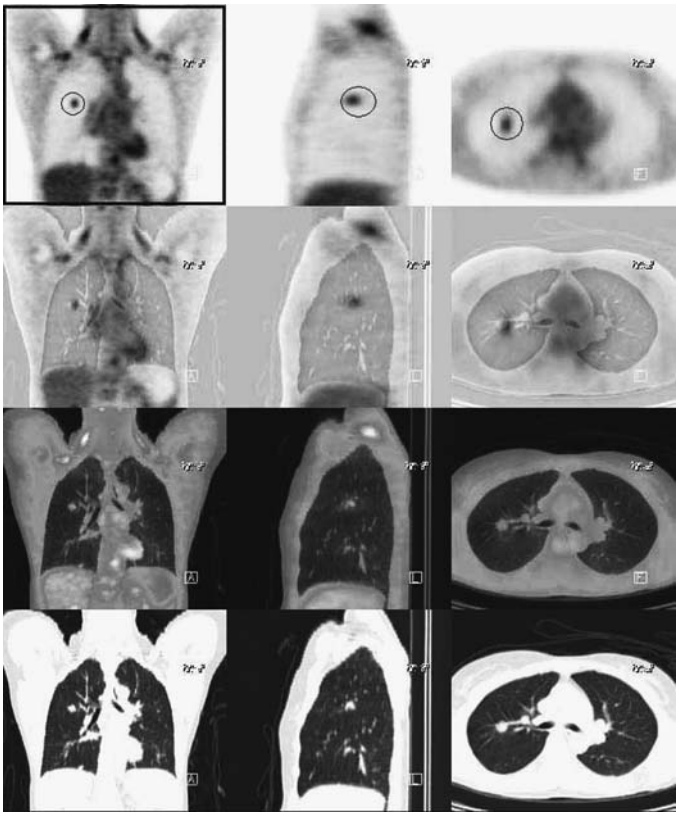

FIGURE 6.3.3.

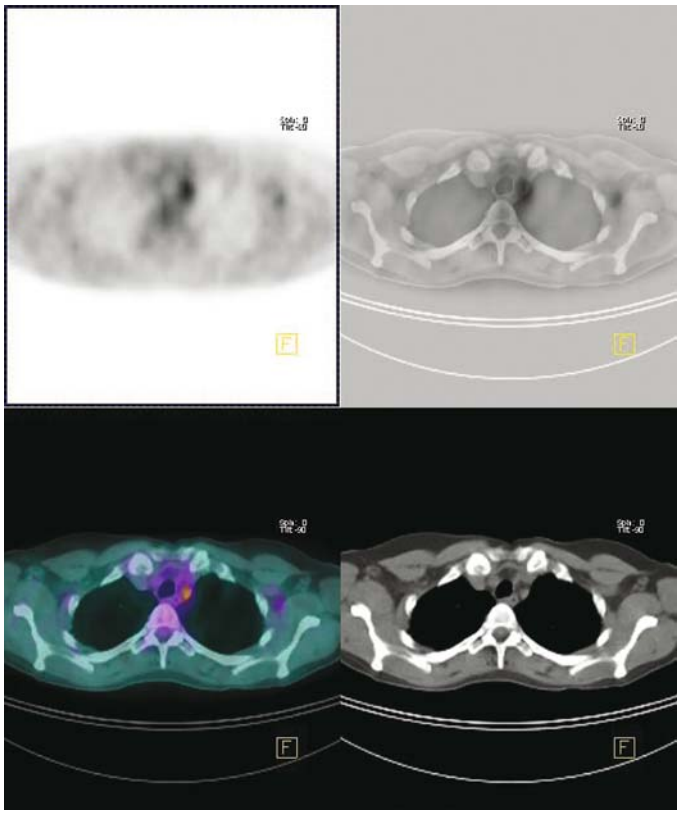

FIGURE 6.3.4.

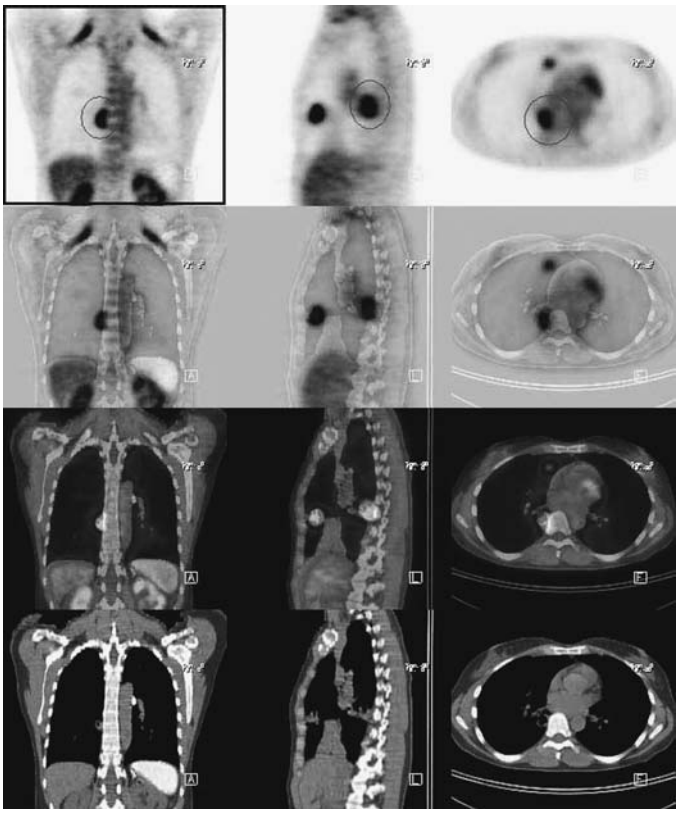

FIGURE 6.3.5.

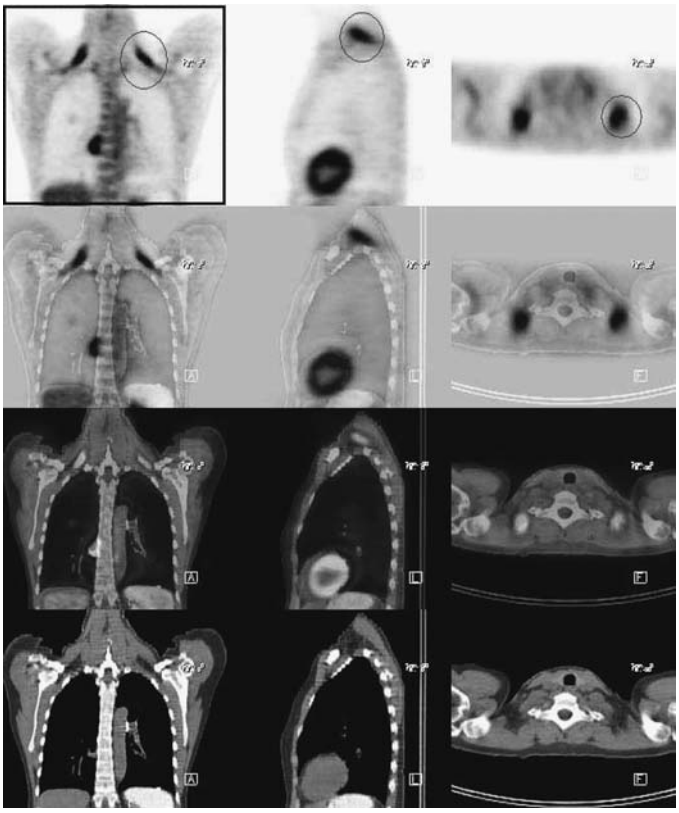

FIGURE 6.3.6.

Impression

1. Three hypermetabolic right pulmonary nodules highly suspicious for metastatic disease.
2. No evidence for locally recurrent disease in the pelvis.
3. Probable distal esophagitis.
4. Other presumed benign findings as described above.

Pearls and Pitfalls

- *The sensitivity and specificity of lymphangiography, as an alternative to surgical staging, are 79% and 73%, respectively.*[1]
- *The sensitivity and specificity of CT are 34% and 96% based on size and morphology criteria.*[1]
- *In contrast, ultrasonography demonstrates a sensitivity of 19% and specificity of 99%.*[1]
- *PET FDG has a sensitivity of 75% and specificity of 92%.*[1]

Discussion

Cervical cancer is staged clinically based on the FIGO system. The tumor generally spreads from the primary cervical lesion follow by the pelvic lymph nodes, para-aortic lymph nodes, and supraclavicular lymph node. Hematogenous metastases to lung, liver, and bone are seen in advanced disease.

Carcinoma in situ (CIS) and microinvasive cervical cancer (stage IA) are not associated with lymph node metastases. Therefore, intracavitary brachytherapy alone, delivering approximately 5500 cGy, can control 100% of CIS and stage IA disease and

is an acceptable alternative to surgery for patients who cannot undergo surgery because of their medical condition. Concurrent radiotherapy and chemotherapy (cisplatin-based) with or without adjuvant hysterectomy are standard treatments for bulky (≥8 cm) IB2 cervical cancer. For stage IIA-IVA disease without para-aortic lymph node metastases, pelvic external radiation (4000 cGy–5000 cGy) should be used, followed by intracavitary brachytherapy (4000 cGy–5000 cGy), for a total dose of 8000 cGy–9000 cGy.

Case 6.4

History

32-year-old female status post hysterectomy and right oophorectomy for uterine cancer. She now has a biopsy-proven left upper lung mass with histology of adenocarcinoma. The exam is for staging.

Findings

The large left upper lobe pulmonary mass (*Figures 6.4.1 and 6.4.2*) is intensely hypermetabolic, consistent with adenocarcinoma. This could either be primary or metastatic from the uterine disease. There is some focal disease in the left costophrenic sulcus (*Figure 6.4.3*). There are also small deposits in each adrenal area (*Figure 6.4.4*). The dominant findings, however, are extensive skeletal metastases. These are concentrated in the thoracolumbar spine, pelvis, proximal femora (*Figure 6.4.5*), and proximal

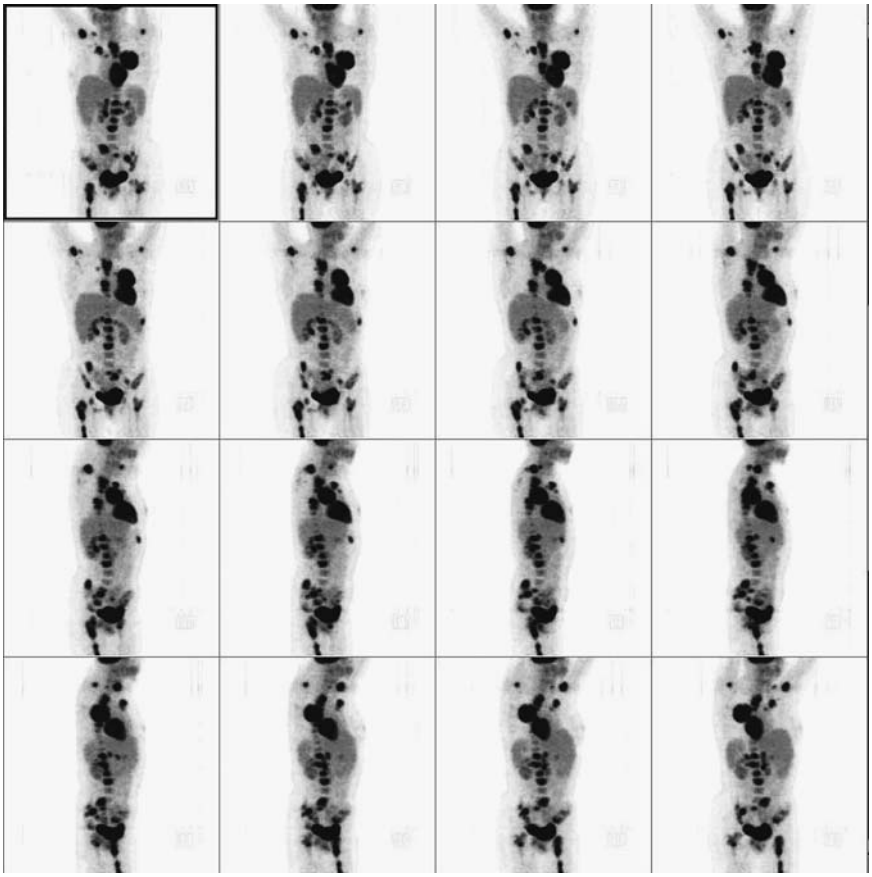

FIGURE 6.4.1.

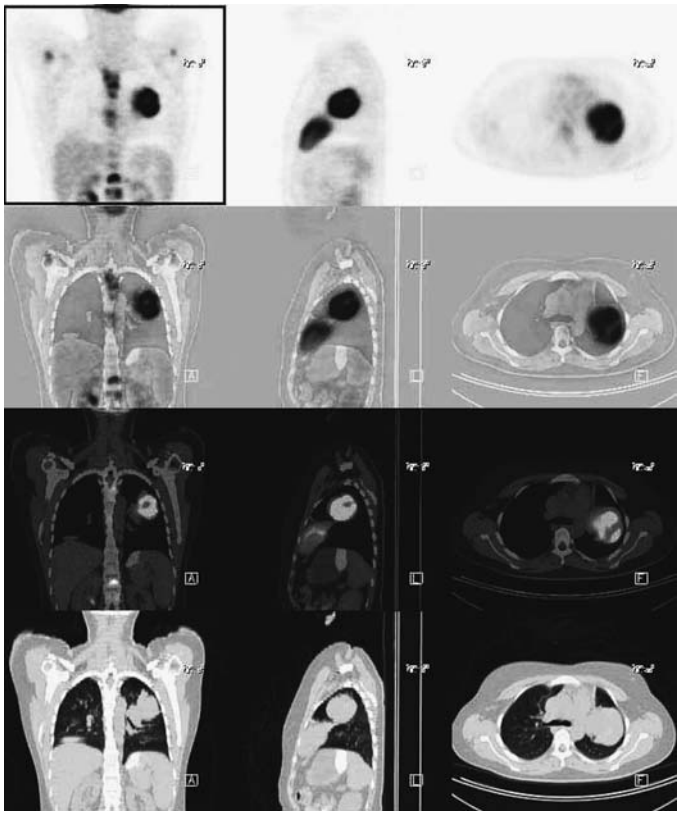

FIGURE 6.4.2.

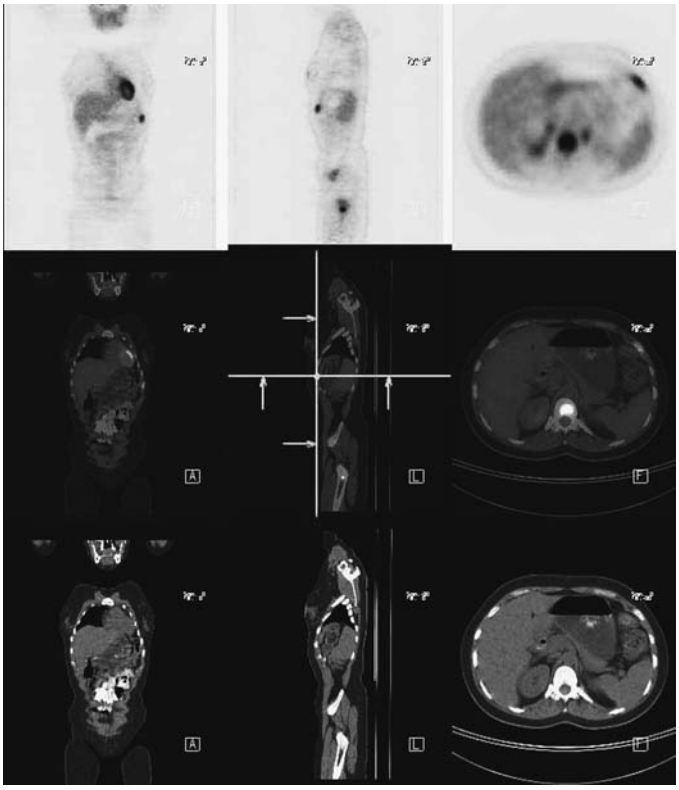

FIGURE 6.4.3.

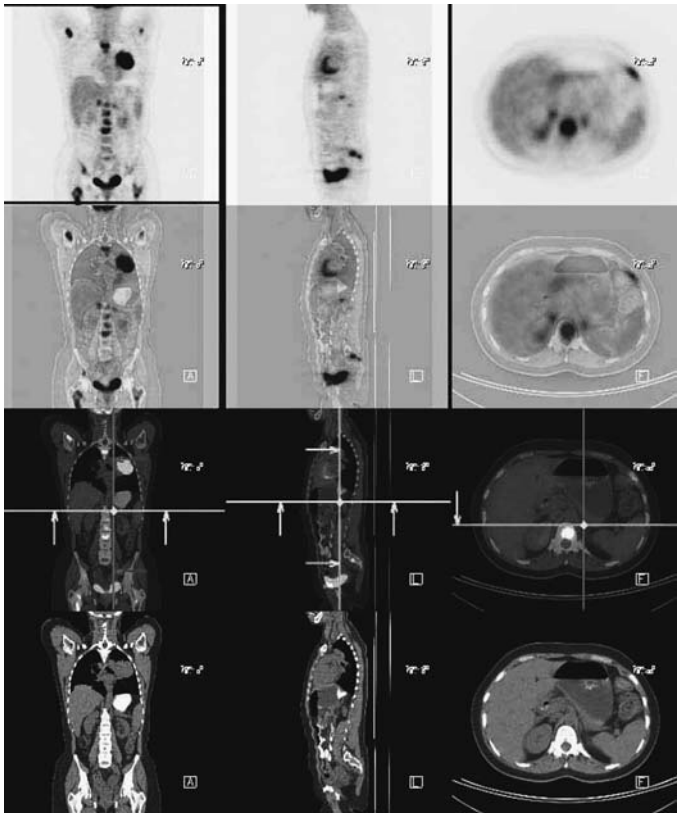

FIGURE 6.4.4.

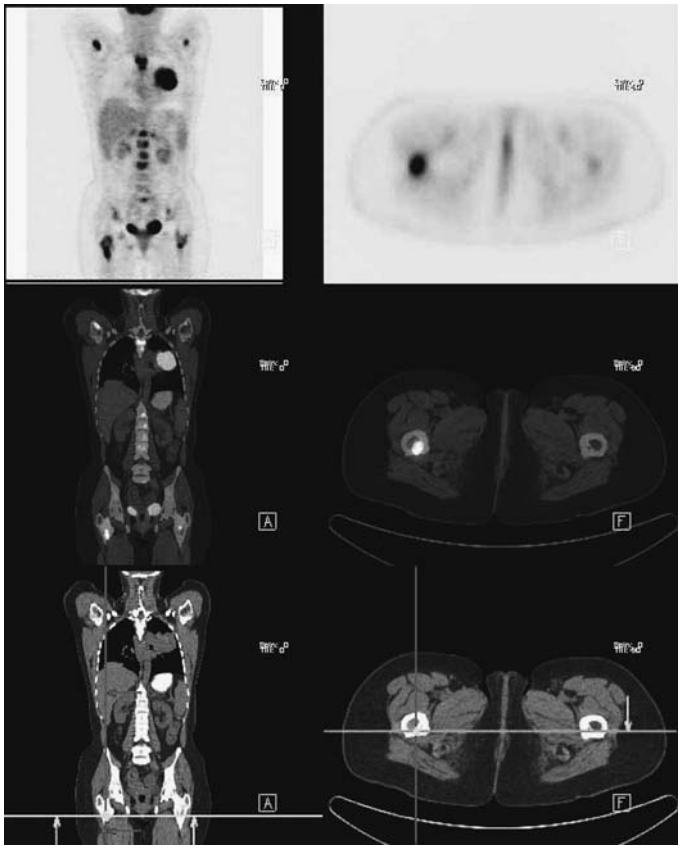

FIGURE 6.4.5.

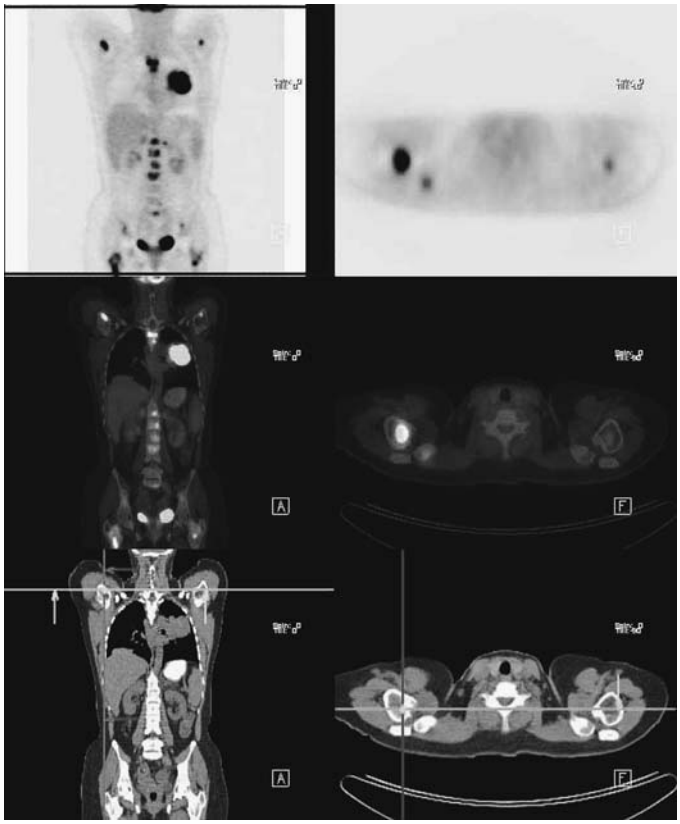

FIGURE 6.4.6.

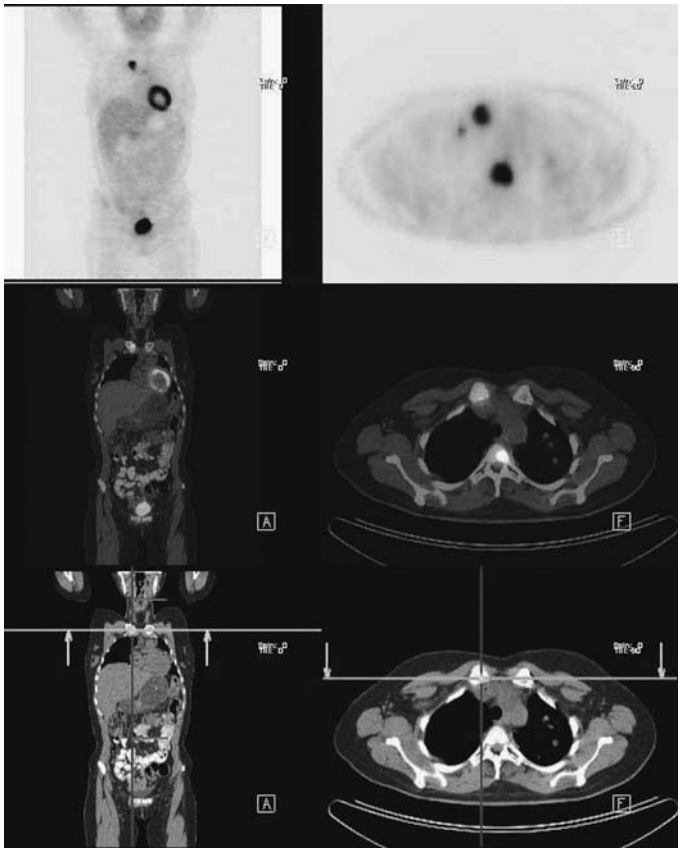

FIGURE 6.4.7.

humeri (*Figure 6.4.6*). There are also lesions in the right medial clavicle (*Figure 6.4.7*) and manubrium (*Figure 6.4.8*), as well as a number of small lesions in bones elsewhere. There is little apparent osteolysis evident at the present time. Nonetheless, baseline radiography of the thoracolumbar spine, pelvis, and proximal extremities may still be an appropriate consideration as a baseline to judge progression of disease.

Impression

1. The large left upper lung mass is intensely hypermetabolic, consistent with known adenocarcinoma.
2. There are a few soft tissue deposits, but the dominant finding is one of advanced skeletal metastases, concentrated in the central skeleton and proximal peripheral skeleton.

Pearls and Pitfalls

- *FDG PET has high sensitivity and specificity during surveillance of endometrial cancer following therapy.*[6]
- *C-11 methionine accumulates in uterine cancer and has a direct correlation with tissue grade based on SUV level.*[3]
- *Continuous bladder irrigation with 18-FDG may eliminate potential artifacts from the urinary bladder and help characterize malignant and nonmalignant lesions.*[2]

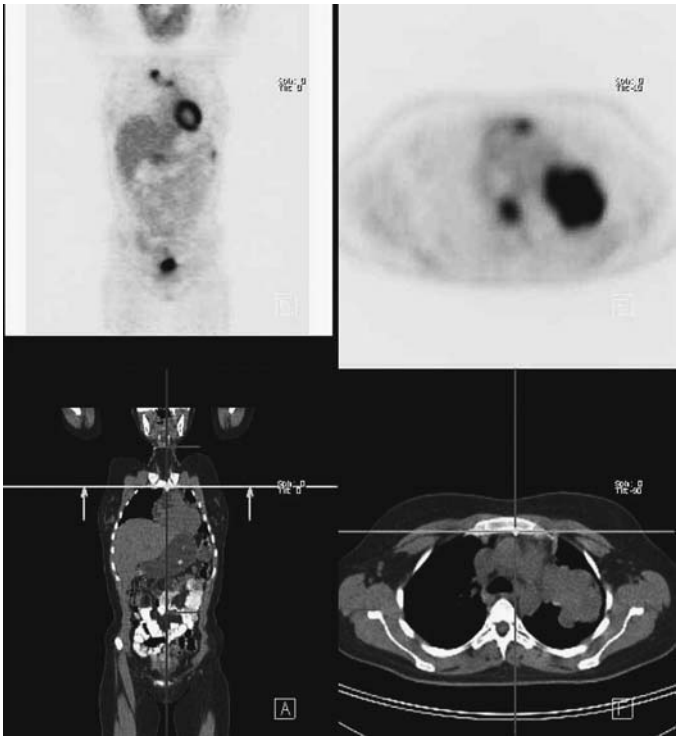

FIGURE 6.4.8.

Discussion

Uterine cancer is the most common cancer of the female pelvic organs. The most common cancer in the uterus is adenocarcinoma. Postmenopausal bleeding is the most common presentation in 90% of the patient. Of the female population, 70% to 75% are diagnosed with surgical stage I disease. Obesity, chronic anovulation, diabetes mellitus, and hypertension are risk factors. CA-125 is useful for surveillance. Transvaginal ultrasound can devaluate the endometrial stripe thickness. Chest radiography is helpful to rule out distant metastases. CT-MR can reveal local vs. metastatic disease. Endometrial biopsy is the definitive diagnosis. Direct local extension in the majority of cases is seen beyond the uterus. Lymphatic spread can occur to the pelvis and para-aortic lymph nodes. Hematogeneous spread is seen to the lungs, liver, bone, and brain. Clinical staging underestimates the extent of disease and thus the FIGO staging system requires surgical and histopathologic evaluation. Most endometrial cancers are diagnosed in stage I and surgery alone is adequate. Beyond that, adjuvant radiotherapy may be necessary for treatment. The 5-year survival rate for endometrial carcinoma in stage I is 74% to 92% depending on histologic grade.

Case 6.5

History

78-year-old female who has a history of vulvar cancer positive from left groin lymph node biopsy. She was status postvulvectomy and local radiotherapy. The ultrasonography revealed a subcutaneous mass in the left groin; scar vs. recurrent tumor. Evaluation for possible recurrence is requested.

FIGURE 6.5.1.

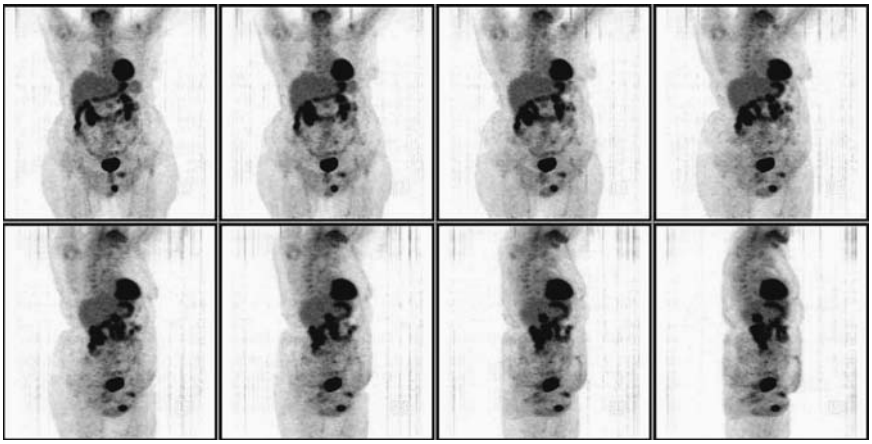

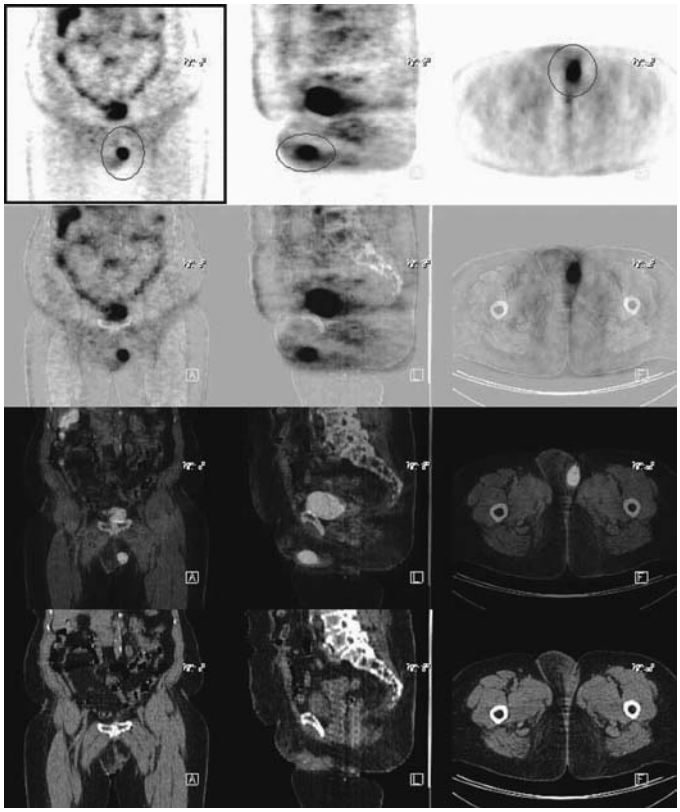

FIGURE 6.5.2.

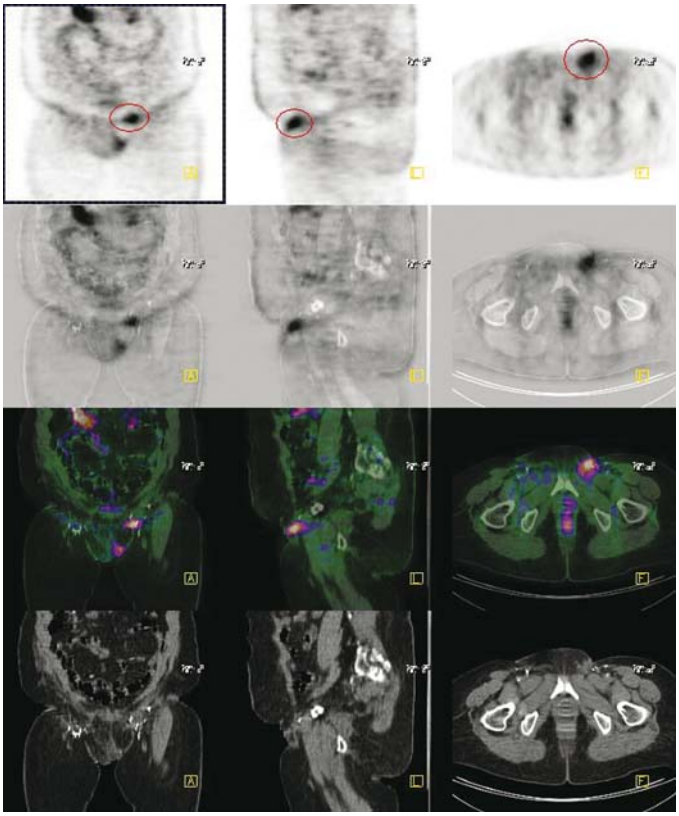

FIGURE 6.5.3.

Findings

There is a vulvar mass (*Figures 6.5.1 and 6.5.2*) on CT that is hypermetabolic to the left of midline consistent with locally recurrent tumor. There is an ill-defined mass in the left groin (*Figure 6.5.3*) suspicious for metastatic disease. A focus of activity seen in a para-aortic node (*Figure 6.5.4*) above the bifurcation of the iliac vessels is noted. A mass anterior to the left kidney in the para-aortic area (*Figure 6.5.5*) on CT likely represents a lymph node. The activity in the shoulders is likely inflammatory joint disease. The scattered bowel uptake is physiologic.

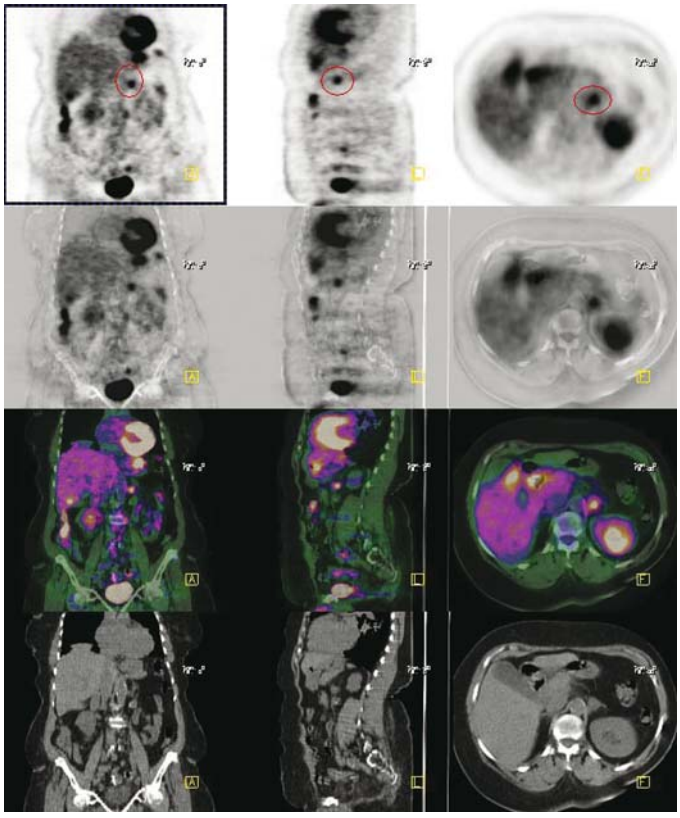

FIGURE 6.5.4.

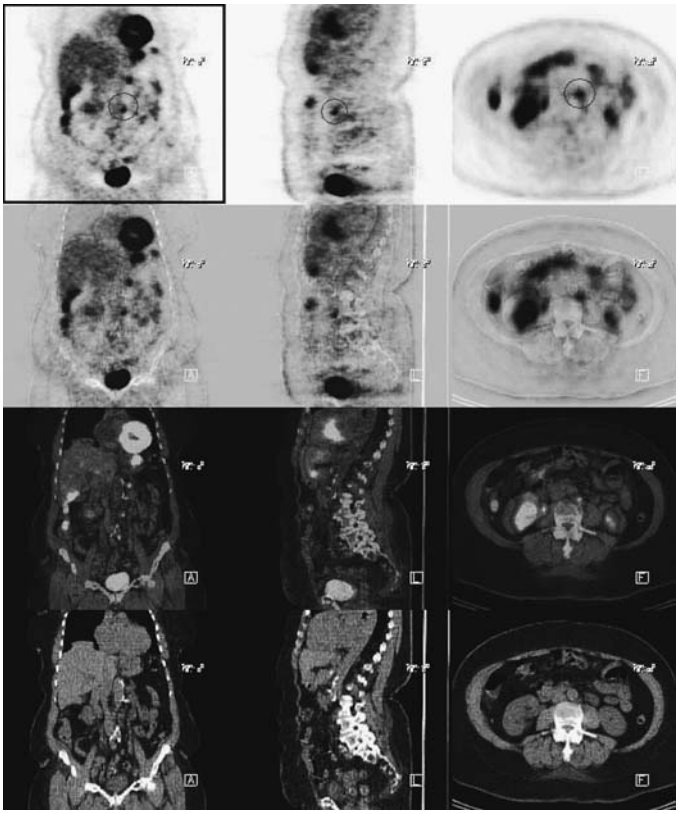

FIGURE 6.5.5.

Impression

Local and regional abnormalities consistent with primary recurrent malignancy with distant metastatic disease.

Pearls and Pitfalls

- *PET scanning has the ability to identify small nodal metastasis.*[6]
- *Currently, there is no data in the literature to evaluate the sensitivity and specificity of PET for detecting vulvar carcinoma.*

Discussion

Vulvar carcinoma represents 1% of the female genital cancers. The majority arises in the labia majora and minora. Vulvar carcinoma includes squamous cell carcinoma, adenocarcinoma and melanoma. Human papilloma virus, sexually transmitted disease, smoking, and multiple sexual partners are risk factors. Patients may be asymptomatic or present with a mass, pruritus, bleeding, or pain. Biopsy is the most diagnostic test. Imaging studies may be helpful. CT can evaluate adenopathy with a sensitivity of 30%. MR may evaluate lymphatic involvement. PET can detect small nodal metastasis. Radical primary tumor excision and en bloc lymph nodes dissection is the treatment of choice. Cure rate is 80% if malignancy is contained in stage I and II. Stage III has a 68% 5-year survival rate vs. stage IV with 20%.

7 Colorectal Cancers

Robert W. Henderson

Case 7.1A

History

62-year-old male who has a history of colon cancer diagnosed two years prior to the current study. He was treated with chemotherapy. His recent CT demonstrated stable mediastinal lymph nodes, while his last PET one year ago revealed multiple sites of lymphadenopathy. The patient is having a repeat PET study for restaging.

Findings

The hypermetabolism involving the subcarinal (*Figures 7.1A.1 and 7.1A.2*), as well as the celiac axis node is again seen with a very slight increase since the previous PET study. The small right midline focus of uptake below the level of the renal arteries is unchanged from the prior study. There is a newly apparent small hypermetabolic focus in the right paracolic gutter (*Figure 7.1A.3*), which represents an implant on the peritoneal surface.

Impression

Progression of disease with increased activity in the mediastinal and retroperitoneal nodes, with a new peritoneal implant.

Pearls and Pitfalls

- *FDG PET has a sensitivity ranging from 81% to 91% for recurrent colorectal cancer.*[5,7]
- *PET is more accurate than CT for the detection of liver metastases.*[19]
- *FDG imaging as an alternative to conventional imaging is by far the superior method for detection of extrahepatic metastases (sensitivity 94% vs. 67%).*[1,2,14,15,18,20]

Discussion

Common indications for a FDG PET scan include a rising CEA tumor marker from an occult tumor, equivocal lesion on conventional imaging, detection of hepatic or extrahepatic metastases, preoperative staging for a recurrent disease resection, char-

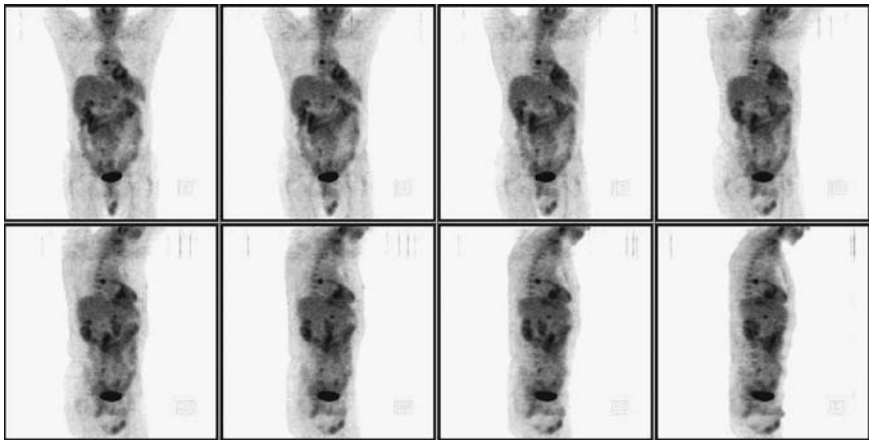

FIGURE 7.1A.1.

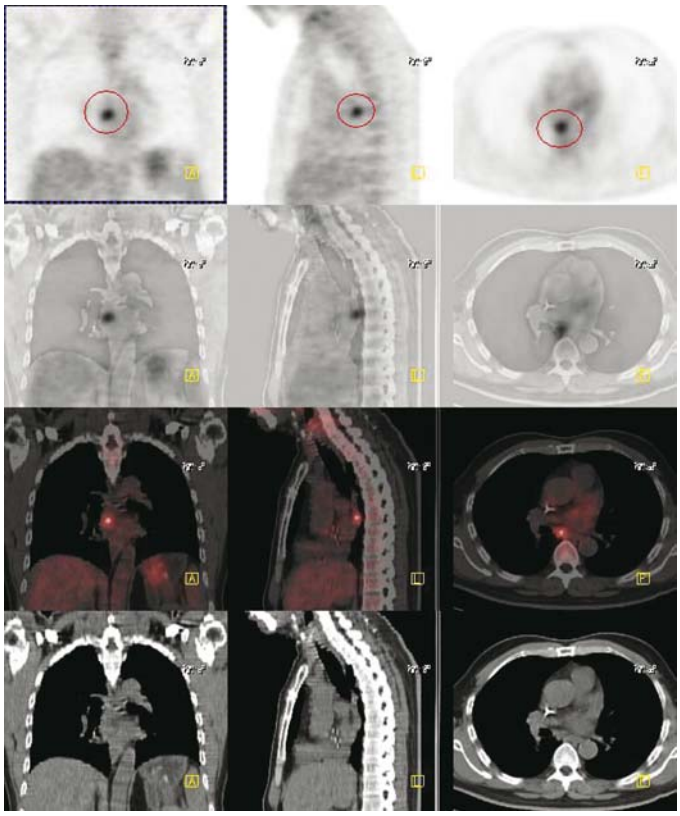

FIGURE 7.1A.2.

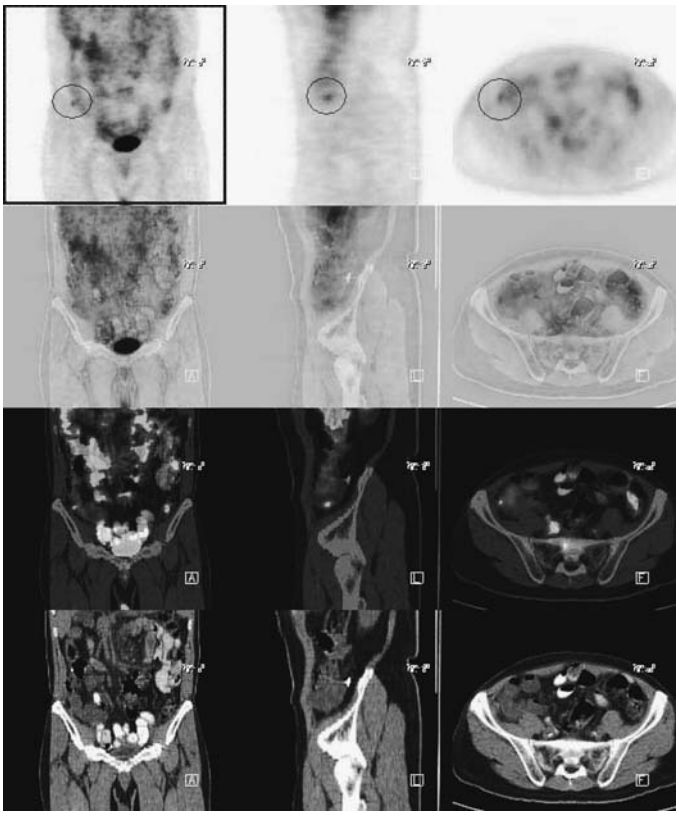

FIGURE 7.1A.3.

acterization of a local recurrence from postoperative scar and assessment of treatment response. The reduction of tumor FDG uptake also correlates with therapy outcome.

Case 7.1B

History

63-year-old male with known metastatic colon carcinoma. The current study is done to evaluate extent of disease and is compared to a prior PET-CT from six months ago.

FIGURE 7.1B.1.

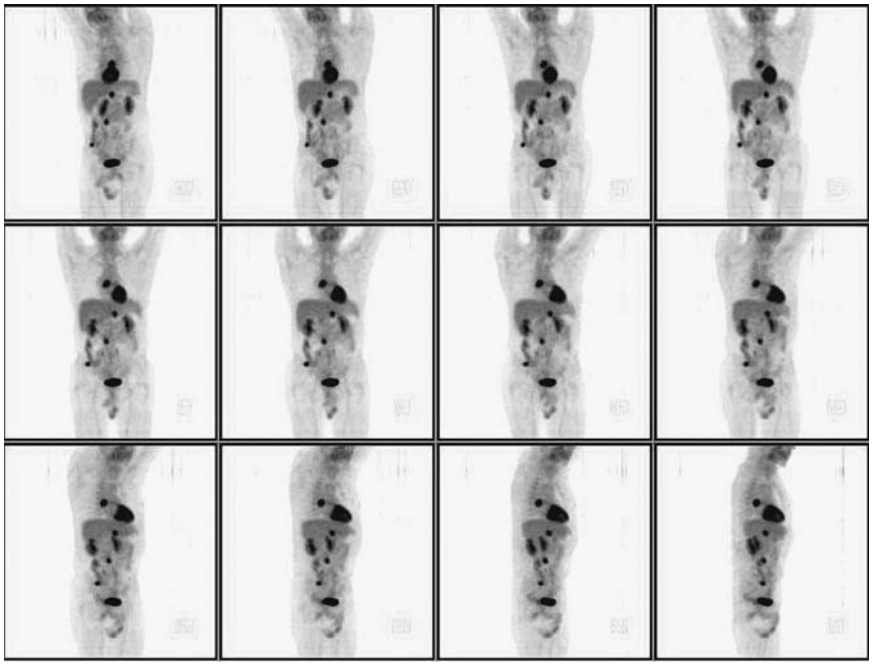

Findings

The current examination has four pathologic foci consistent with metastatic disease and identical in locations with the prior examination (*Figure 7.1B.1*). All four lesions, subcarcinal, left of the celiac axis, precaval/peripancreatic node, and peritoneal deposit in the right paracolic gutter adjacent to the cecum in the right iliac fossa, have increased in size and activity. No new foci are apparent and the patient remains negative for hepatic metastasis.

Impression

Metastatic disease with four scattered metastatic deposits with progression based on size of the individual lesions but not in number.

Pearls and Pitfalls

- *FDG PET has the potential to change colorectal patient management in 26% to 65% of cases.*[4,6]
- *The sensitivity for the detection of recurrent colorectal cancer disease is between 93% and 100%.*[5]
- *The liver is the primary site of hematogenous metastases in colorectal cancer.*[2,14,18]
- *Existence of one to four metastases confined to one lobe of the liver is an indication for liver resection if no other pathologic adenopathy or metastatic disease is present.*

Discussion

PET-CT is an ideal way to follow scattered metastatic deposits, in this case, mediastinum, retroperitoneum, and peritoneum. Because increased relative activity increases the apparent size of a lesion, small changes in size and activity are more confidently identified than small changes in size alone on anatomical imaging.

Case 7.2

History

56-year-old female with a history of colon CA currently receiving chemotherapy via infusion pump and status postradiofrequency ablation in the liver six months prior to this study. She has a slightly elevated and rising CEA and an elevated CA19-9, and is being evaluated for tumor recurrence.

Findings

There are two photopenic areas representing treated areas in the liver (*Figure 7.2.1*). One is in the posterior dome (*Figure 7.2.2*). This photopenic area has no associated surrounding hypermetabolic activity. However, the second treated area, in the anterior dome in the upper liver while photopenic has an adjacent hypermetabolic focus medial to it on the anterior surface of the liver (*Figure 7.2.3*). This is consistent with recurrent disease within the liver. There is obvious and moderately advanced metastatic disease to bone. The lesion of most immediate importance would appear to be a T-12 posterior element/epidural lesion (*Figure 7.2.4*). Further anatomic imaging with MRI and possible local therapy would be appropriate in this area. Other deposits have a potential for future pathologic fracture although they have no major osteolysis at the present time. There is a large lesion in the right medial ileum. Of concern also for future pathologic fracture would be a large lesion in the right lower ileum near the acetabulum (*Figure 7.2.5*) and several lesions in the proximal femora (*Figure 7.2.6*), larger on the right than the left. These involve the femoral neck and intertrochanteric areas. An

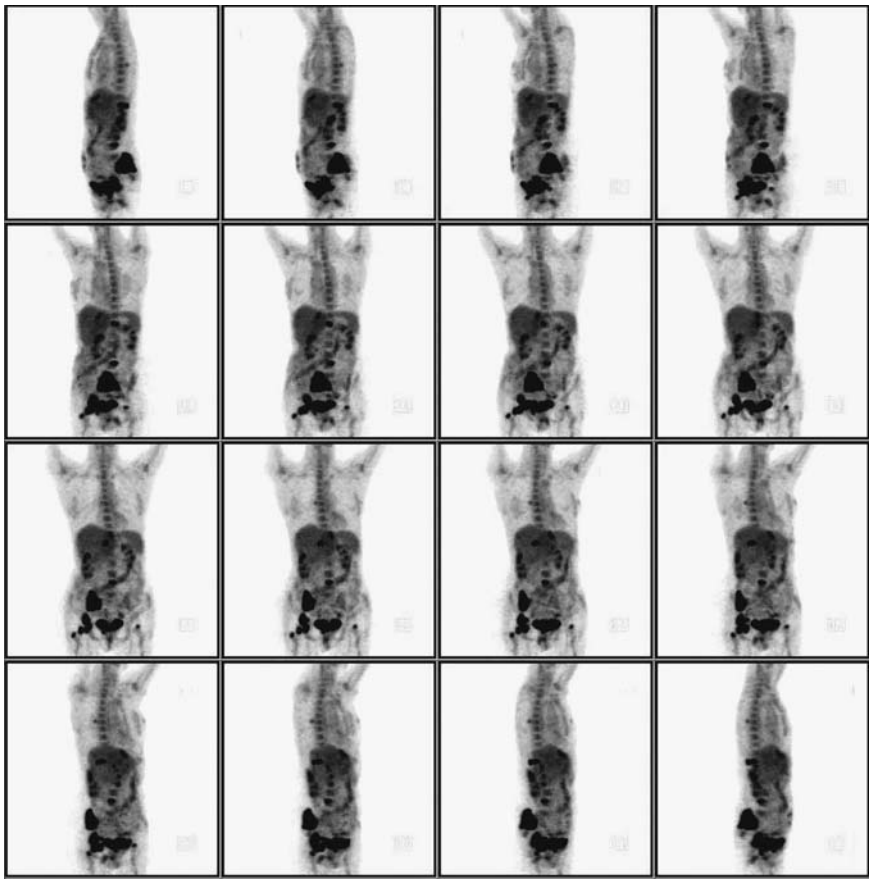

FIGURE 7.2.1.

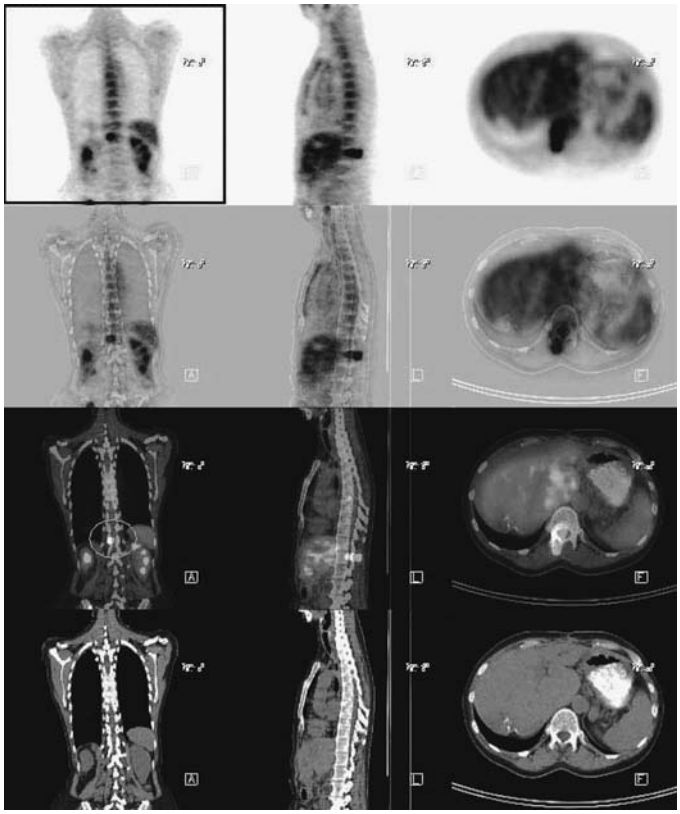

FIGURE 7.2.2.

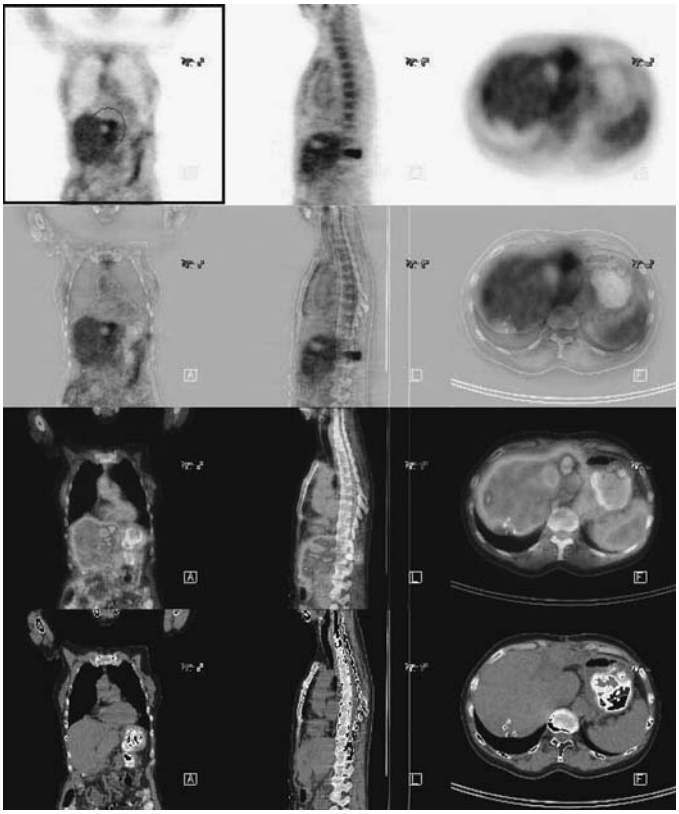

FIGURE 7.2.3.

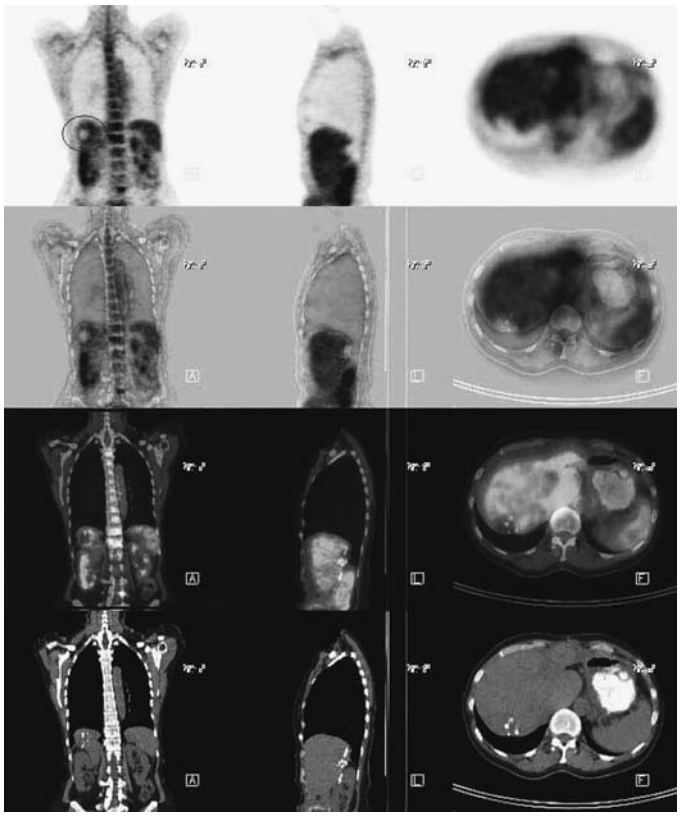

FIGURE 7.2.4.

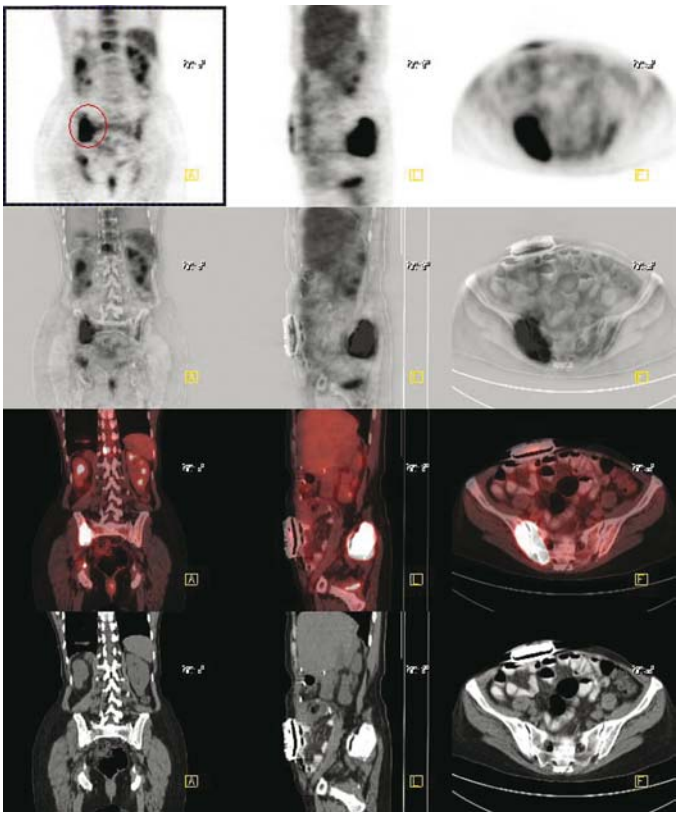

FIGURE 7.2.5.

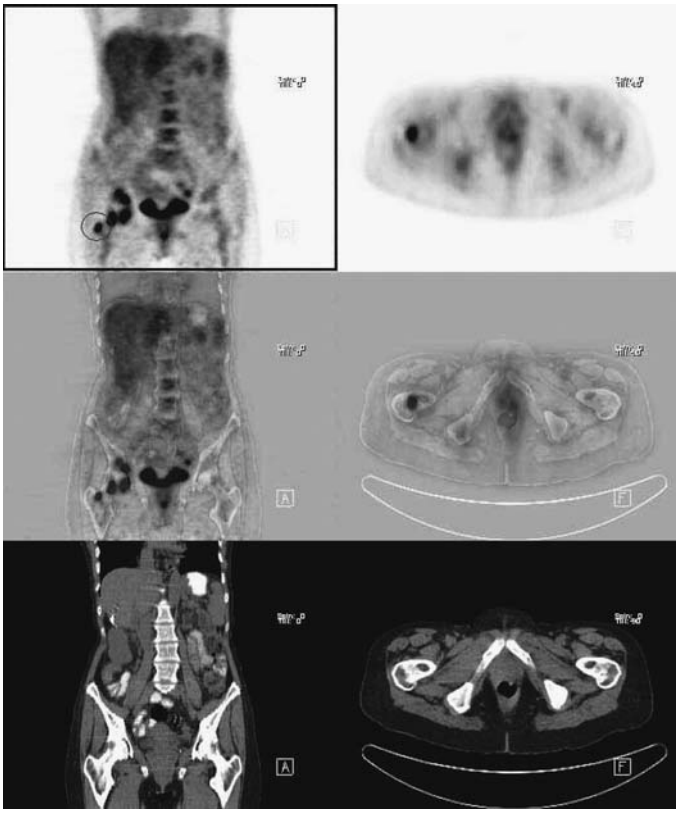

FIGURE 7.2.6.

additional lesion is present in the lumbar spine at L-4. There is a left costovertebral junction focus in the midthoracic spine which is small. There is moderate segmental sigmoid colon activity; in the absence of either symptoms of colitis or wall thickening this is presumed physiologic.

Impression

1. Moderately advanced metastatic disease to the skeleton, with the most important lesion being a posterior element/epidural lesion at T-12. There are also multiple proximal femoral and pelvic metastases discussed above.
2. There are two treated photopenic areas in the liver, one posterior VII segment and one anterior near the dome. The posterior one is unassociated with hypermetabolic activity. The anterior lesion has a focal area of hypermetabolism medial to it which is consistent with residual/recurrent disease within the liver.

Pearls and Pitfalls

- *FDG PET imaging is more accurate than CT in distinguishing post therapy changes from residual tumor in patients treated with radiofrequency ablation therapy.*[10,12,16]
- *PET-CT is very useful for differentiating local recurrence from scarring following surgery/radiation therapy.*[5,8]

Discussion

Skeletal metastases of colon origin are uncommon but not rare. CT allows assessment of osteolysis/fracture potential. PET-CT is very helpful to assess post ablation status

of liver metastases. False-positive FDG uptake can be seen immediately after radiation therapy due to inflammation and increased FDG uptake within irradiated tumor cells. A minimum of 2 to 3 months following radiation therapy is usually necessary for an accurate assessment on follow-up imaging.

Case 7.3

History

59-year-old male who has a history of colon cancer status post left hemicolectomy. His CA 19-9 is 57. His CEA level is 15.7 and rising. The patient is now being restaged with PET-CT.

Findings

There is a significant amount of perirectal stranding (*Figures 7.3.1 and 7.3.2*) on CT anterior to the sacrum and involving the perineum that is hypermetabolically active on PET consistent with local infiltration from recurrence. A band of activity is seen to extend posteriorly beyond the level of the coccyx (*Figures 7.3.3A and 7.3.3B*) extending into the midline gluteal subcutaneous fat. There is probable destruction of the coccyx on CT. There is involvement with obstruction of the distal right ureter. There is retroperitoneal paracaval adenopathy. The activity involving the ostomy (*Figures 7.3.4A and 7.3.4B*) and the scattered bowel uptake is likely inflammatory (*Figure 7.3.5*) and physiologic respectively. No other abnormality is seen in the chest or liver.

Impression

1. There is an anastamotic recurrence of low rectal carcinoma with local coccygeal destruction and posterior subcutaneous extension. There is right retroperitoneal paracaval metastatic adenopathy with ureteral obstruction.
2. There is intense but probably physiologic colon activity including the stoma.

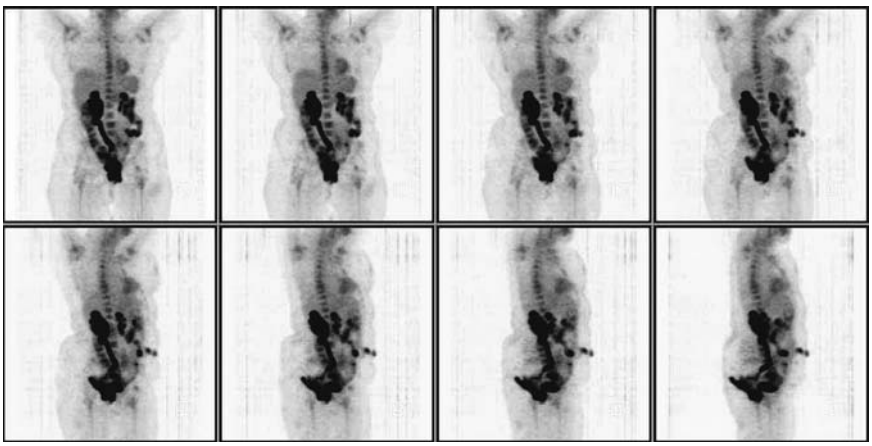

FIGURE 7.3.1.

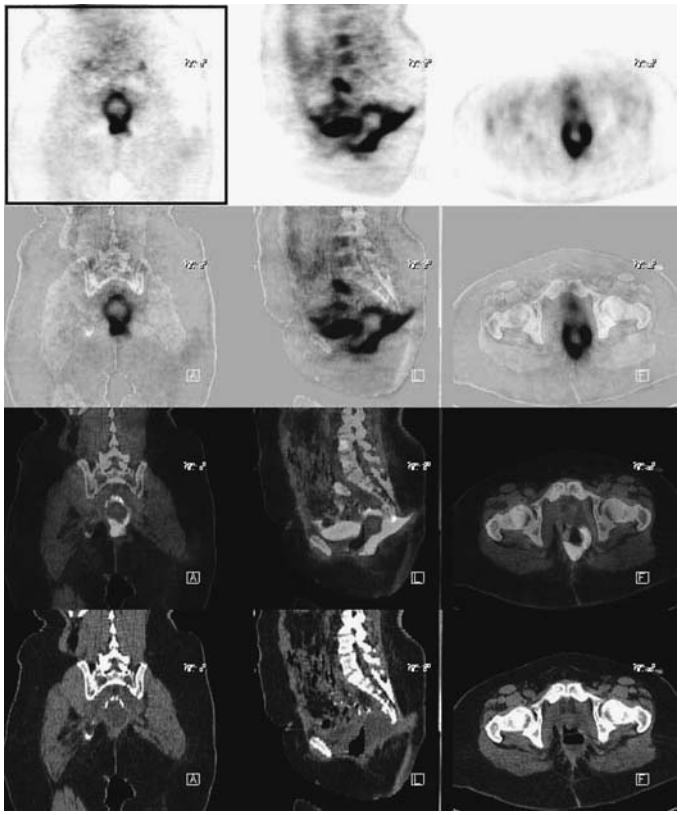

FIGURE 7.3.2.

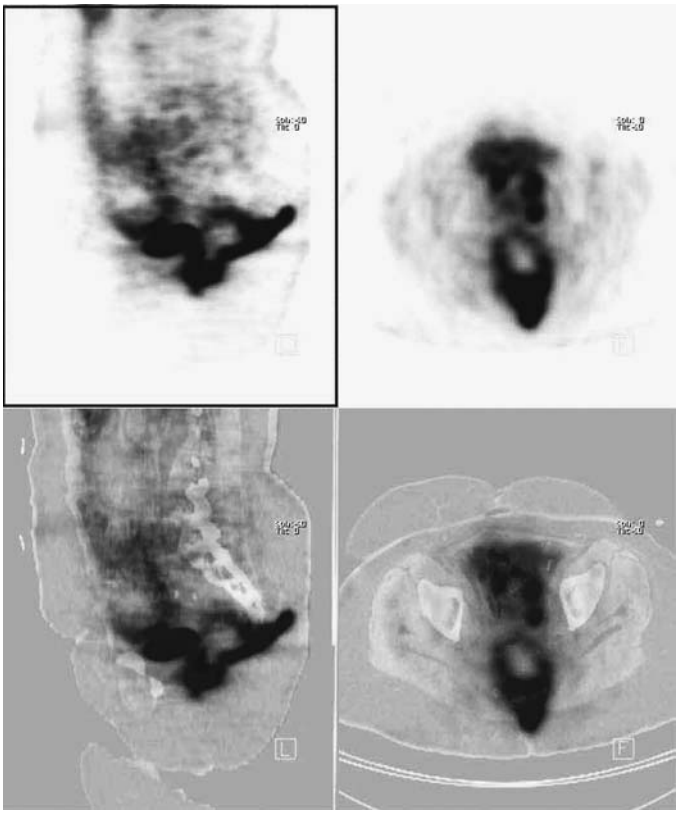

FIGURE 7.3.3A.

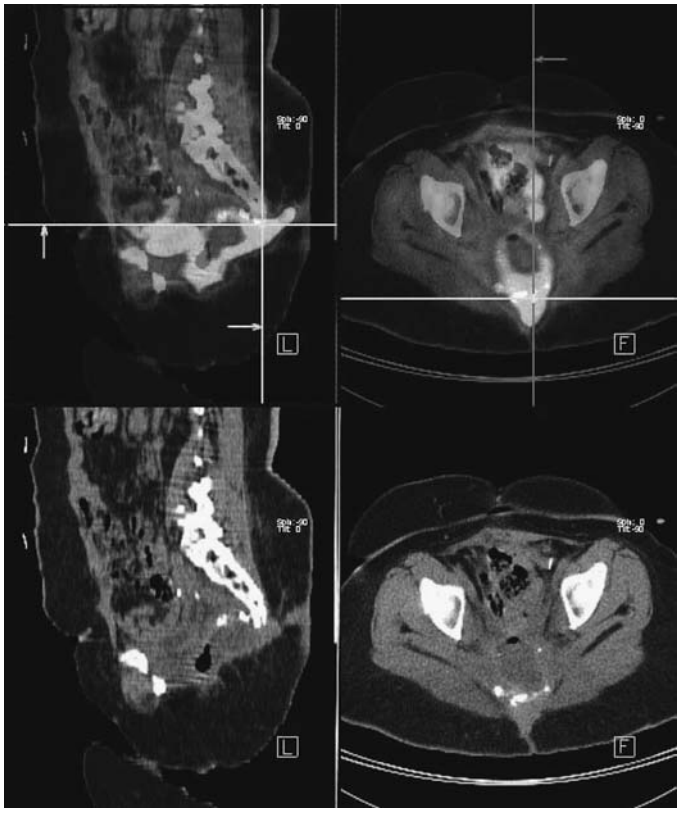

FIGURE 7.3.3B.

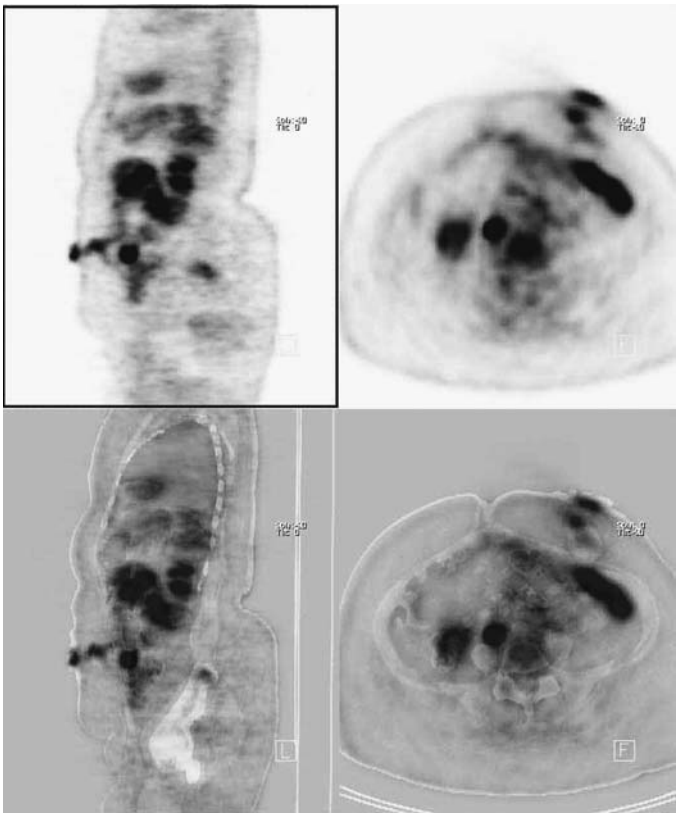

FIGURE 7.3.4A.

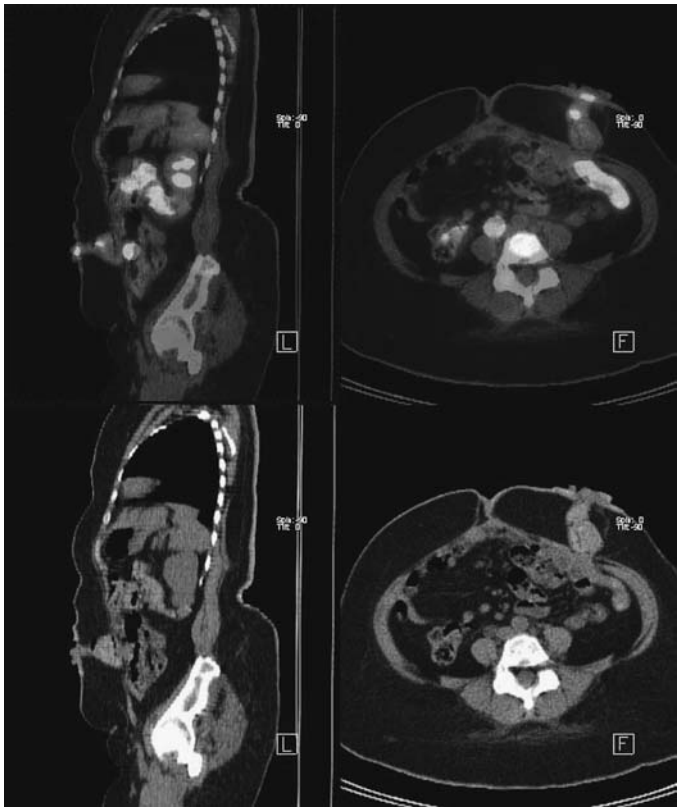

FIGURE 7.3.4B.

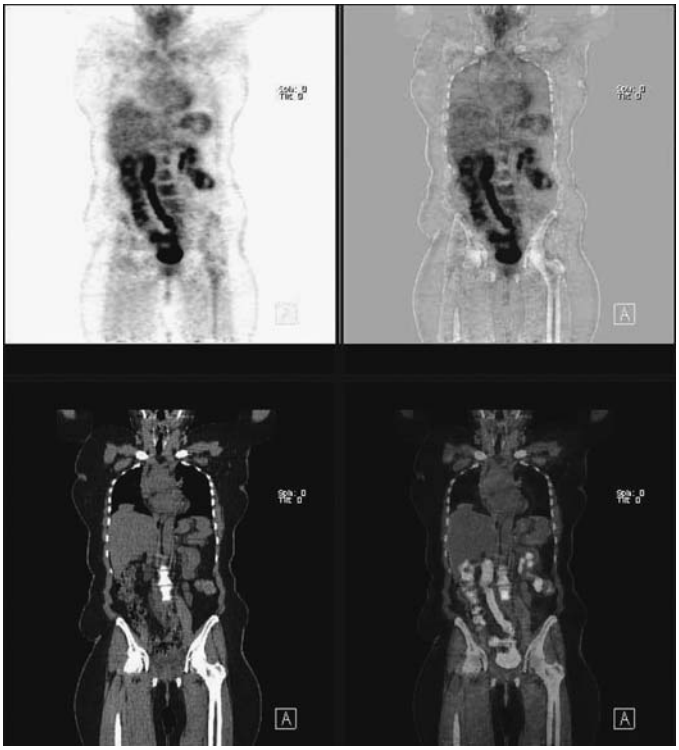

FIGURE 7.3.5.

Pearls and Pitfalls

- *The presence of recurrent disease can be detected using serum levels of carcinoembryonic antigen (CEA) with a sensitivity of 59%, and a specificity of 84%. A limitation of the CEA test is that it cannot localize the site of recurrent disease.*[9]
- *15% to 20% of patients with locally recurrent disease are cured by reresection.*[18]
- *Roughly 35% of patients have long-term survival after the curative resection for metastatic or locally recurrent tumor. This is probably due to undetected metastatic disease at other sites.*[3,11,17]

Discussion

Diffuse colon activity is usually physiologic even when intense. Segmental intense colon activity frequently indicates colitis. Focal intense colon activity frequently indicates adenomatous polyp or adenocarcinoma.

Case 7.4

History

51-year-old female with known metastatic disease from colon carcinoma. The current exam is compared with the most recent PET scintigraphy from one year ago and is being done for restaging.

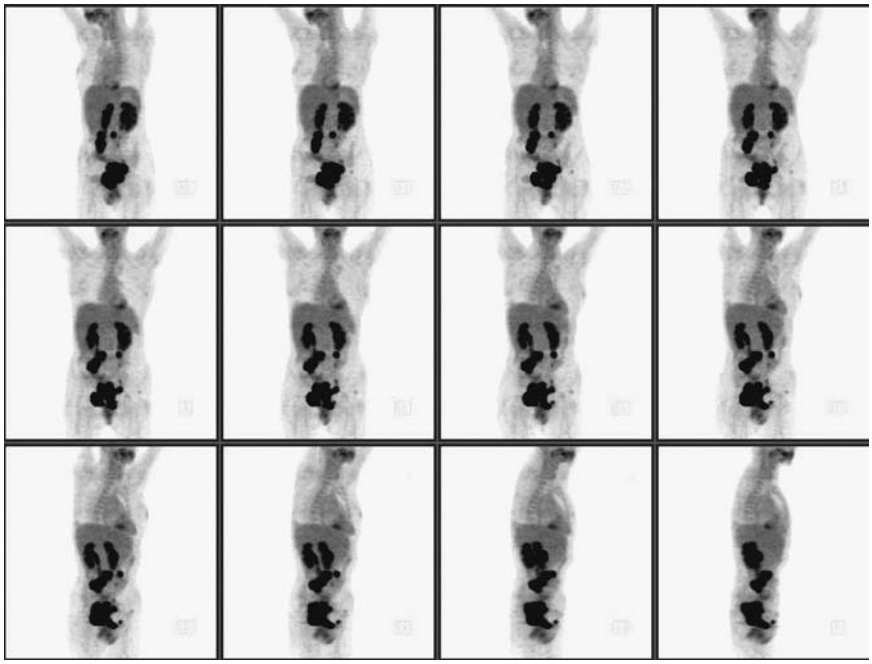

FIGURE 7.4.1.

Findings

Since the prior exam, there has been progression of abdominal disease, but no disease is evident above the diaphragm (*Figure 7.4.1*). There appear to be postsurgical changes at the right lung base, but there is no hypermetabolism evident above the diaphragm. As with the prior exam, there is bulky abdominal retroperitoneal and pelvic extraperitoneal disease (*Figure 7.4.2*). The individual lesions appear significantly larger than previously seen. The lesion in the right abdominal retroperitoneum, which had obstructed the right ureter, is now seen to engulf the ureter by virtue of a stent passing through it (*Figure 7.4.3*). This mass is 5.5 cm in maximum dimension. There is also a retroperitoneal lesion on the left at the same level as the lesion obstructing the right ureter of smaller size, about 3.3 cm (*Figure 7.4.4*). The disease is even bulkier in the pelvis. There is a large, lobulated mass which is anterior to the rectum and superior to the urinary bladder, which compresses the urinary bladder and displaces it anteriorly. This mass is about 7.5 cm in both maximum oblique dimensions. A small left iliac deposit of about 1.7 cm is evident just below the iliac bifurcation. One additional extraperitoneal implant is evident anteriorly just above the left pubic symphysis. Incidental notation is made of thoracolumbar scoliosis.

Impression

There has been significant interval progression of bulky retroperitoneal/extraperitoneal disease. There is a large, lobular mass above and compressing the urinary bladder and a large right pelvic extraperitoneal mass with intimate relationship to the right ureter. Several smaller pelvic extraperitoneal deposits are apparent. There has also been progression of the right retroperitoneal deposit which has obstructed the right ureter, now seen in intimate relationship to the stent, which passes through a portion of it. There is a smaller deposit at the same level, near the left ureter.

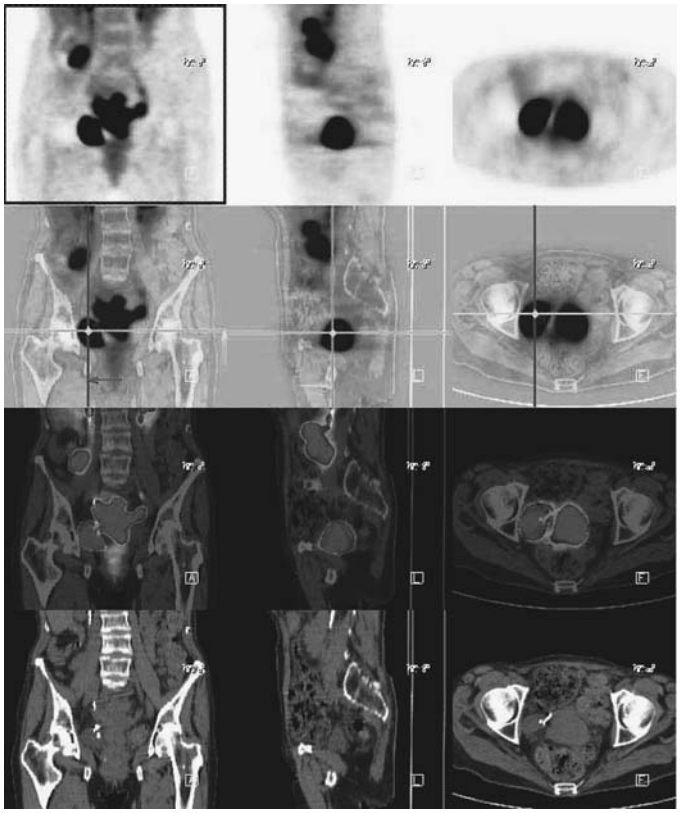

FIGURE 7.4.2.

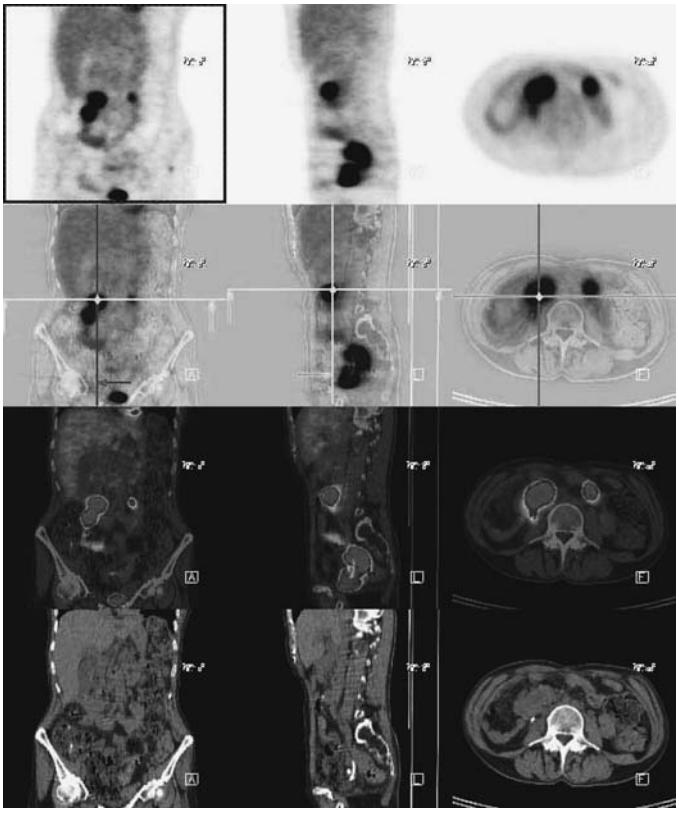

FIGURE 7.4.3.

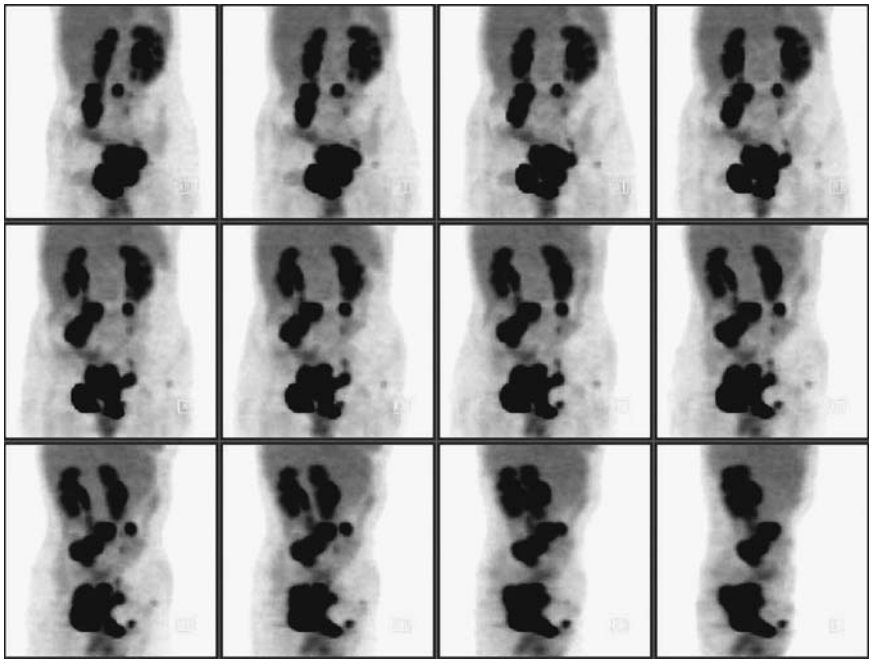

FIGURE 7.4.4.

Pearls and Pitfalls

- *The 5-year survival rate following salvage surgery for locally recurrent disease is roughly 35%.*[18]
- *In the detection of hepatic metastases, FDG PET has a sensitivity of 87% (compared to 73% for conventional imaging [CT/MR]).*[2,15]
- *Extrahepatic metastases can be identified in 18% to 43% of the patients in therapy leading to treatment alteration.*[18]
- *Local recurrence can be detected by PET with an accuracy of 90% to 100%, compared to 48% to 65% accuracy by CT.*[19]

Discussion

Ureteral stents are helpful to mark the course of ureters obstructed by tumor.

Case 7.5

History

42-year-old male with a recent diagnosis of low rectal tumor by biopsy. The current exam is for staging.

Findings

There is a single, intense focal area of colonic 18-FDG activity in the low rectum (*Figure 7.5.1*). An outside CT reported this as a 2-cm lesion from the anal verge. The hypermetabolism appears to be centered 3 cm above the anal verge (*Figure 7.5.2*). This is very consistent with the primary tumor. No pathologic regional nodal activity is evident. There is no evidence for hepatic metastasis or distant metastasis elsewhere. There is moderately intense diffuse activity in the distal sigmoid loop and upper rectum (*Figure 7.5.3*). There is dense barium on the CT in this segment. No wall thickening is apparent. In the absence of wall thickening, this is more likely physiologic than due to colitis or tumor.

Impression

1. Isolated focal abnormal activity in the low rectum centered 3 cm above the anal verge judging from CT. This appears as isolated abnormality with no evident nodal or distant metastases. The staging by PET-CT would be Dukes A or B.
2. Diffuse distal sigmoid loop and upper rectal activity, probably physiologic; air in the urinary bladder, unassociated with other abnormality, is likely related to recently discontinued Foley catheter.

Pearls and Pitfalls

- *Nonspecific inflammation from abscess or post radiation treatment can produce a false-positive PET exam.*[1,13]
- *PET may upstage or downstage the disease and thereby affect patient management.*[4,6,11,12]

FIGURE 7.5.1.

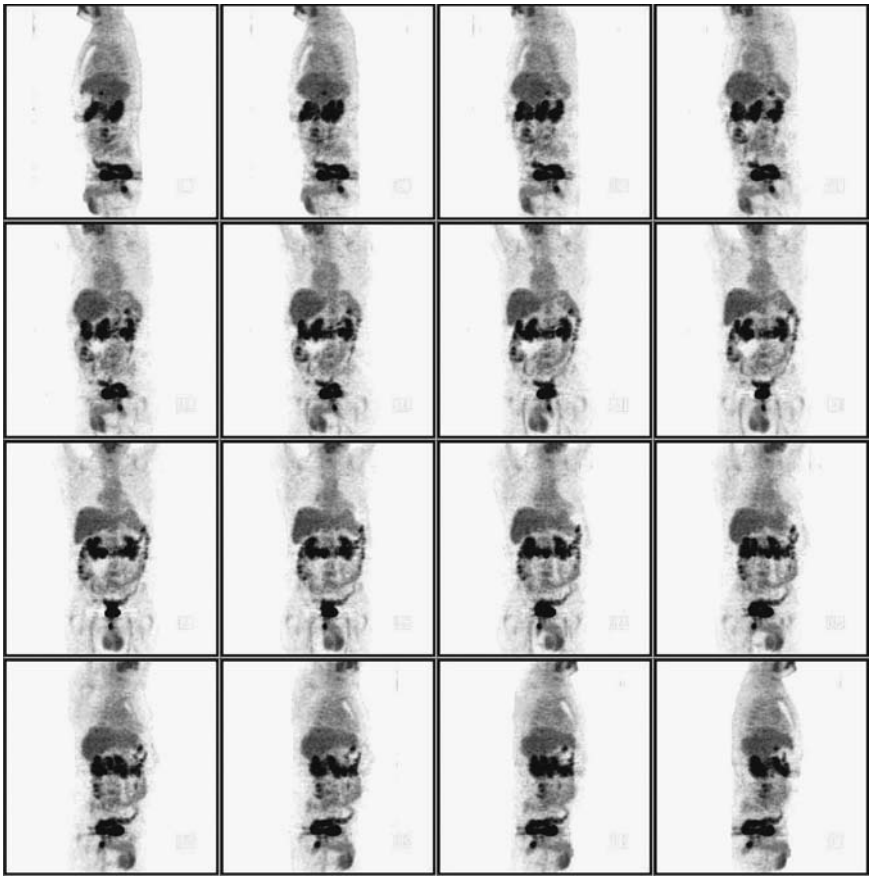

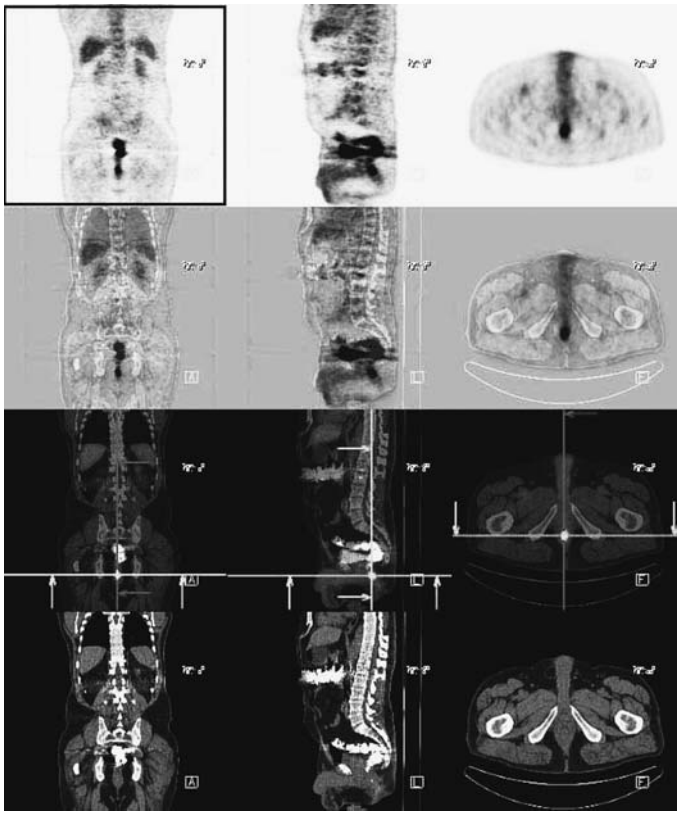

FIGURE 7.5.2.

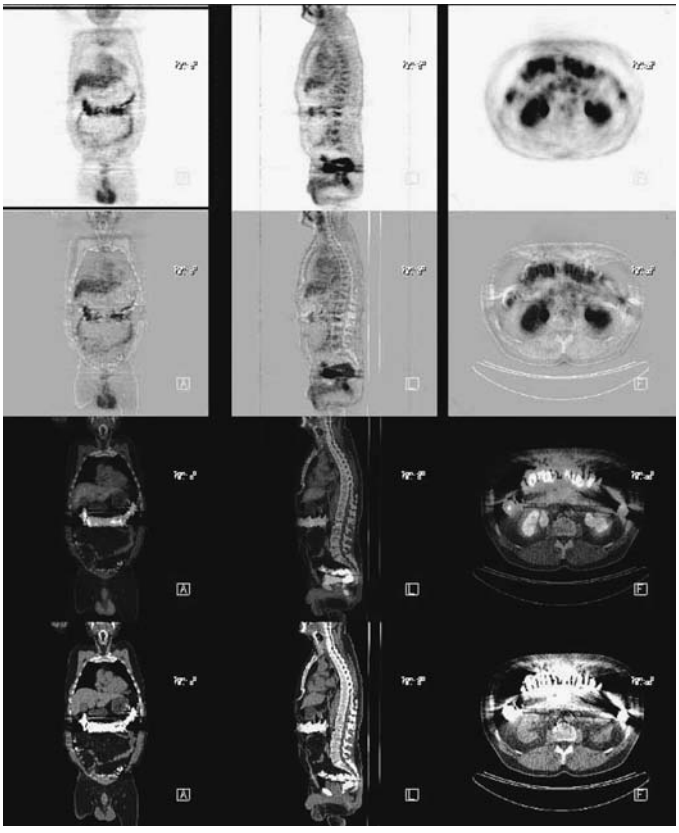

FIGURE 7.5.3.

Discussion

Distance from the anal verge is of obvious importance to the colorectal surgeon and must be assessed on CT if PET-CT is the sole staging procedure. Dense barium causes artifacts on CT-corrected PET but dilute barium does not. Dense barium is frequently associated with intense physiologic 18-FDG activity in bowel.

8 Cholangiocarcinoma

Heidi R. Wassef

Case 8.1

History

74-year-old male who has a history of extrahepatic cholangiocarcinoma diagnosed 5 years ago with a known metastasis to the liver found three years ago. The patient had a Whipple procedure and a partial liver resection. His liver malignancy recurred two years ago and he was subsequently treated with chemotherapy. Radioablation therapy was later performed on the liver tumor. The patient's recent CA 19-9 level is 697.3 and is rising. He is being evaluated for extent of disease.

Findings

In the chest, there is right upper lobe focus of activity that is hypermetabolic which corresponds to the lesion seen on CT (*Figures 8.1.1 and 8.1.2*). The right apex has two small foci of abnormal activity. A right paratracheal node is active (*Figure 8.1.3*). A second node more inferior is also active but less well defined on CT. In the abdomen, there is a large region of intense abnormal activity in the right lobe of the liver near the IVC. In addition, there are smaller sites of hypermetabolism involving the posterior, posterolateral, and the right lateral aspect of the liver. The right lateral aspect of the liver is the region of prior surgical resection. Small nodes around the pancreas exhibit elevated uptake (*Figure 8.1.4*). The gastric wall (*Figure 8.1.5*) demonstrates physiological activity. The intense uptake in the loop of colon near the hepatic flexure is either in the colon, or on the surface. This is suspicious for metastasis, implants, or inflammatory bowel disease. A small focus in the rectum maybe a polyp; endoscopic evaluation is advised. The lower thoracic, upper lumber spine hypoactivity is consistent with prior radiation therapy. The generalized increased marrow activity in other areas may be due to anemia or residual hyperplasia from chemotherapy.

Impression

Multiple sites of hypermetabolism involving the liver and the lung parenchyma as described above consistent with metastatic and locally recurrent disease.

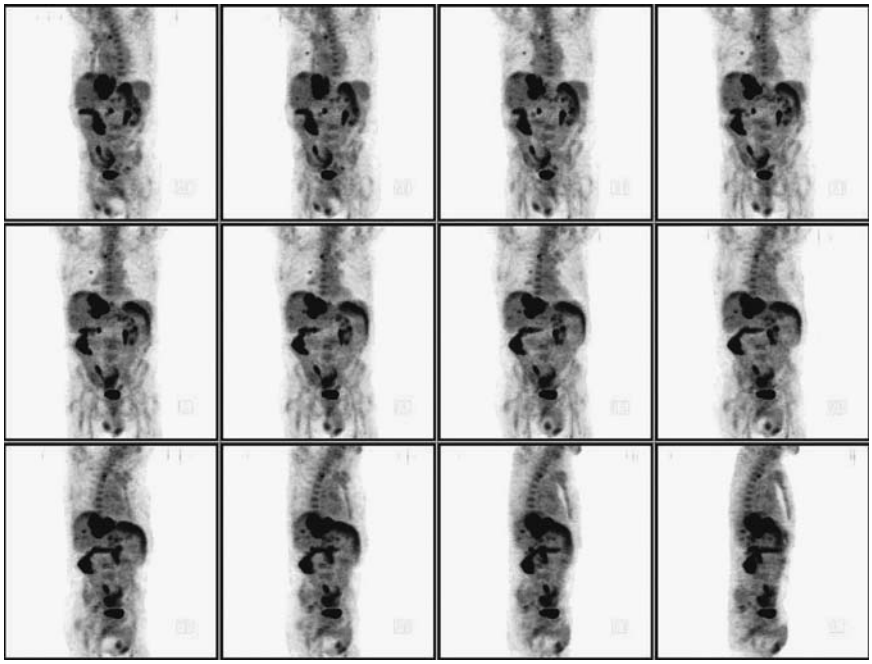

FIGURE 8.1.1.

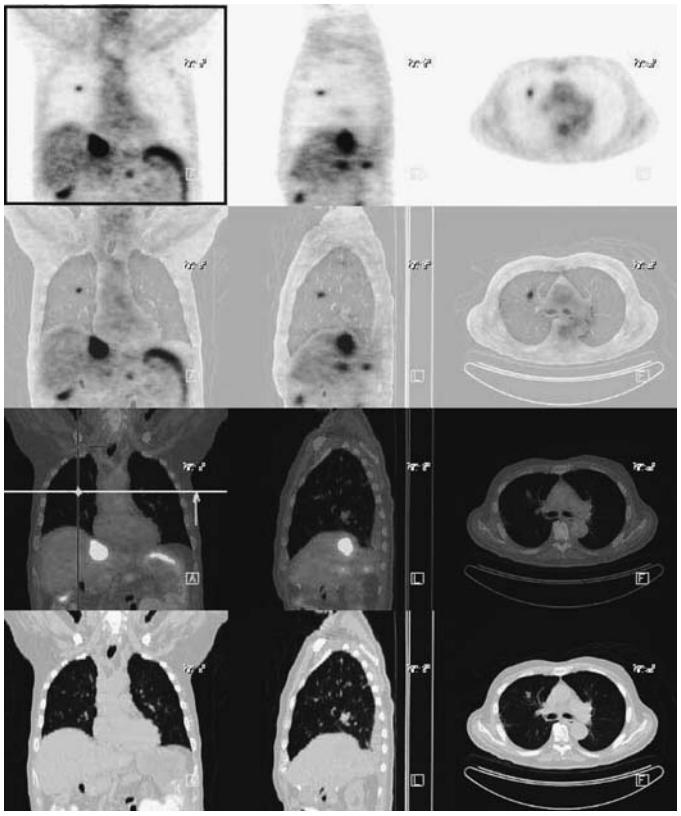

FIGURE 8.1.2.

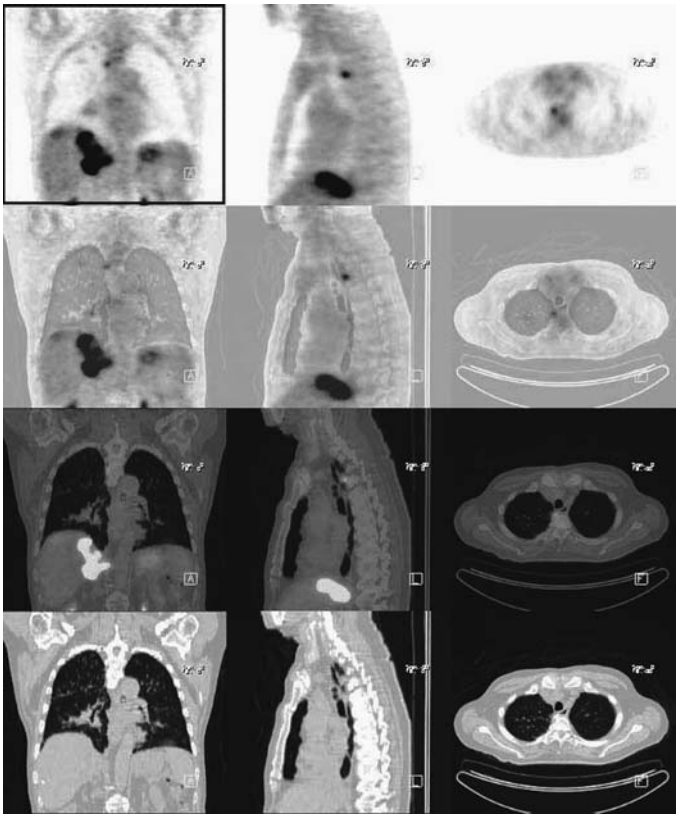

FIGURE 8.1.3.

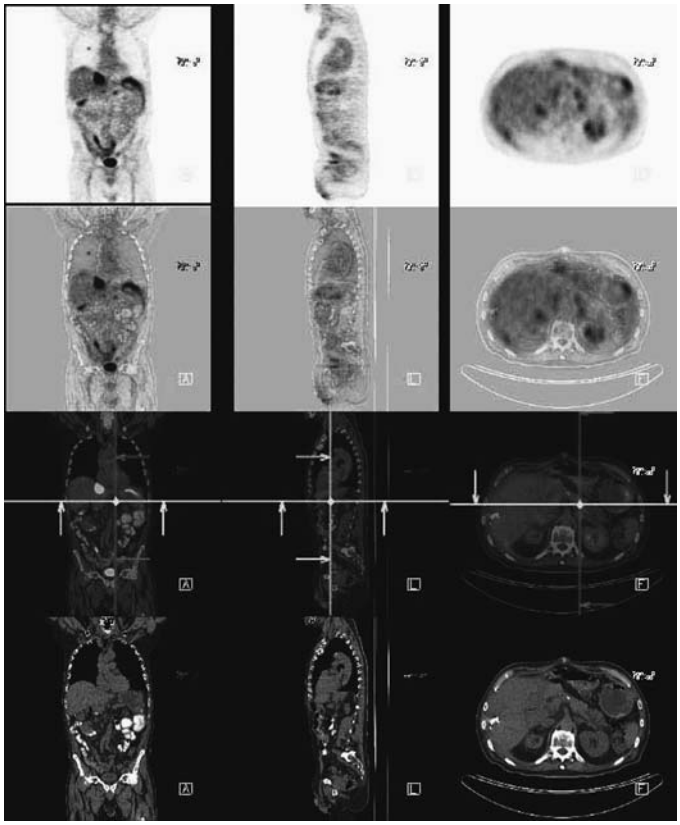

FIGURE 8.1.4.

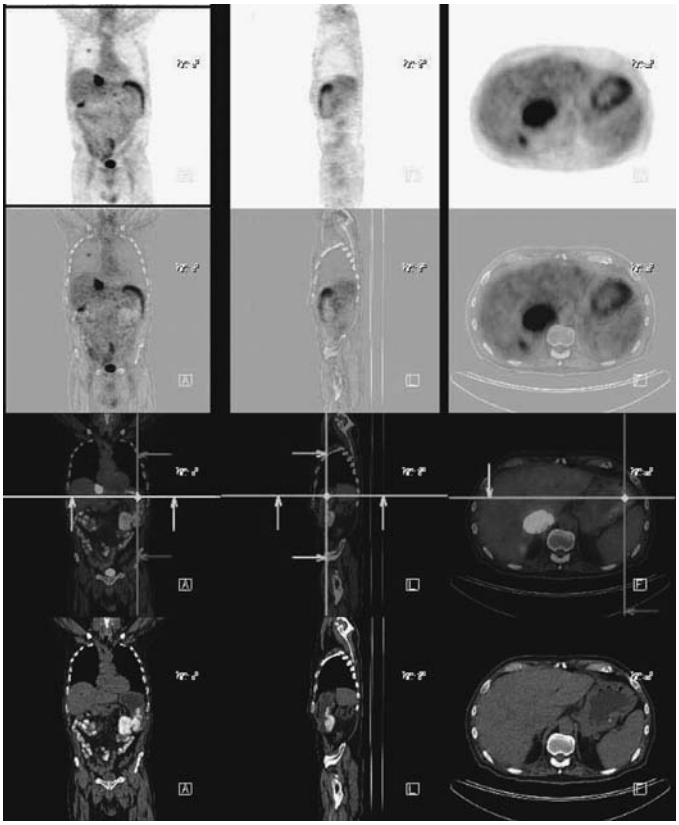

FIGURE 8.1.5.

Pearls and Pitfalls

- *The overall prognosis for cholangiocarcinoma is 10% 5-year survival.*[1,3]
- *Tc-99m sulfur colloid and Tc-99m acetanilide iminodiacetic acid analogs may be alternatives to PET in cholangiocarcinoma imaging, but are less effective.*

Discussion

Cholangiocarcinoma is the second most common primary hepatic tumor after hepatoma. Bacteria-induced carcinogens are believed to be related. Primary sclerosing cholangitis and oriental cholangiohepatitis are predisposing factors. Of the tumors, 87% to 92% are intrahepatic and only 8% to 13% are extrahepatic. Abdominal tenderness, palpable masses, weight loss, and painless jaundice are the typical clinical presentations. Ultrasonography to the right upper quadrant is the best initial noninvasive examination. CT infrequently depicts the tumor well but asymmetrical right vs. left biliary dilatation is typical for biliary hilar cholangioma (Klatskin tumor). PET is helpful for defining viable tumor. MRCP is very helpful for surgical or interventional radiology procedure planning. ERCP is the definitive test.

Case 8.2

History

60-year-old male who has a history of gallbladder carcinoma diagnosed two years ago status post cholecystectomy and partial hepatectomy with Roux-en-Y choledochoje-

junostomy at that time. A previous PET at the time of diagnosis revealed hypermetabolism in the gallbladder fossa and right midabdomen suggestive of serosal implantation. The PET scan is now being done for restaging.

Findings

There is an area of intense hypermetabolism in the right lower abdominal quadrant (*Figure 8.2.1*) that corresponds with a soft tissue mass in the right paracolic gutter (*Figure 8.2.2*) adjacent to the iliac crest on CT compatible with a peritoneal deposit or implant. Another site of more diffuse area of increased tracer uptake is seen in the right lower quadrant anteriorly, corresponding to the bowel without wall thickening,

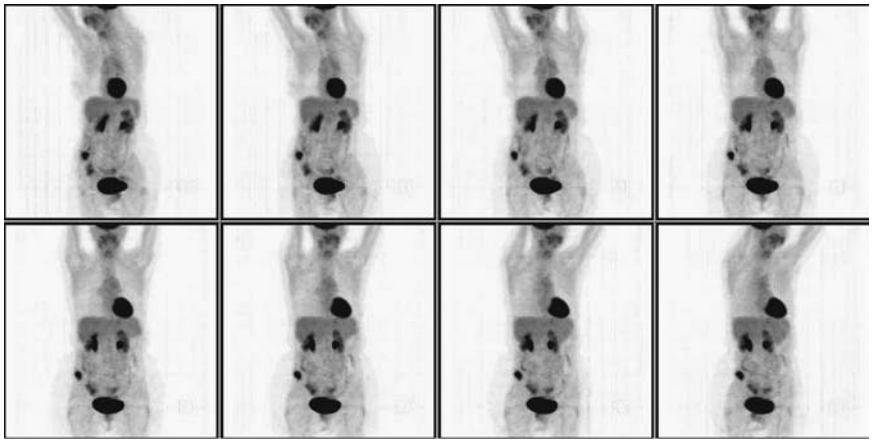

FIGURE 8.2.1.

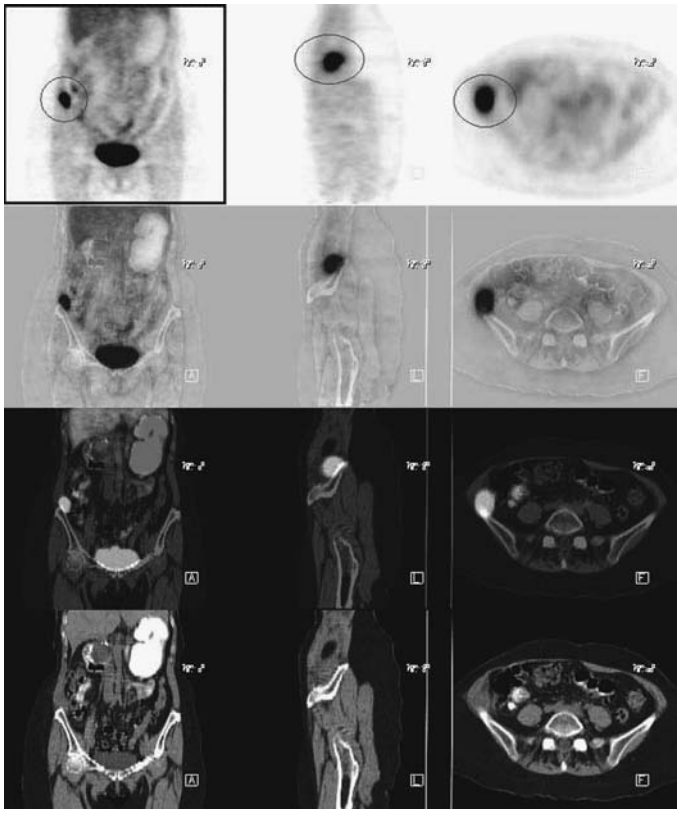

FIGURE 8.2.2.

likely due to physiologic activity. There is also a pulmonary nodule in the anterobasal segment of the right lower lobe which is metabolically inactive and considered benign. No abnormal activity is seen in the gallbladder surgical bed.

Impression

1. Interval development of an intensely hypermetabolic right paracolic gutter metastatic deposit.
2. No evidence for locally recurrent disease in the gallbladder surgical bed.
3. Anterobasal right lower lobe pulmonary nodule without abnormal metabolic activity, considered benign (e.g. hamartoma, old granuloma).

Pearls and Pitfalls

- *PET is an excellent diagnostic tool in detecting unsuspected distant metastases from GI cancers.*[1,2]

Discussion

Gallbladder cancer is the fifth most prevalent cancer of the gastrointestinal tract. Of these patients, 80% are diagnosed with the presence of gallstones. Porcelain gallbladder is an advanced stage of cholecystitis. Females age >70 and Native American heritage are risk factors. Pain, jaundice, weight loss, and ascites are usually present late in the disease. Ninety percent of the patients will eventually die of the disease. Fifty percent of the gallbladder cancers are detected with ultrasonography. CT can detect liver metastasis in 70% to 80% of the cases. MRCP and MRA can assist preoperative planning. ERCP with biliary stent is a palliative treatment for jaundice. Surgery is the only cure, although chemotherapy such as 5-FU and gemcitabine may be useful in the adjuvant setting.

Change in Treatment

There is a definite change in the pre- and post-PET management for this patient. Surgery was done and the malignancy was found to be confined to the mass in the abdomen.

9 Esophageal Carcinoma

Hossein Jadvar and Shahram Bouyadlou

Case 9.1

History

52-year-old male status post esophagectomy for esophageal carcinoma. He has had subsequent radiation and chemotherapy. The current examination is to evaluate a new right adrenal mass (adenoma vs. metastasis) seen on prior anatomic imaging.

Findings

The right adrenal tumor is intensely hypermetabolic (*Figures 9.1.1 and 9.1.2*) and consistent with metastasis. No other metastatic disease is evident on the current exam. The CT shows the surgery to be a gastric pull-up. Thyroid lobe activity is unusually intense (*Figure 9.1.3*). This could be physiologic but a TSH value is suggested if not recently performed to evaluate for functional significance.

Impression

1. Right adrenal metastasis as the isolated manifestation of metastatic disease of esophageal origin.
2. Unusually intense thyroid uptake as discussed above.

Pearls and Pitfalls

- *PET is useful for tumor staging prior to surgical intervention in esophageal cancer.*[3,4,6]
- *Endoscopy and conventional CT are primarily used for local staging; PET is primarily used for detection of metastases.*[3,4,5,6]

Discussion

Ninety percent of the initial presentations in esophageal cancer include dysphagia and weight loss. Most early stages of disease are asymptomatic. Seventy-five percent are discovered in advanced stages with lymph node metastases. The basic workup includes barium esophagram and esophagoscopy with ultrasound. For early-stage disease, the 5-year survival is 57% to 78%. But overall, most patients have a 10% 5-year survival

FIGURE 9.1.1.

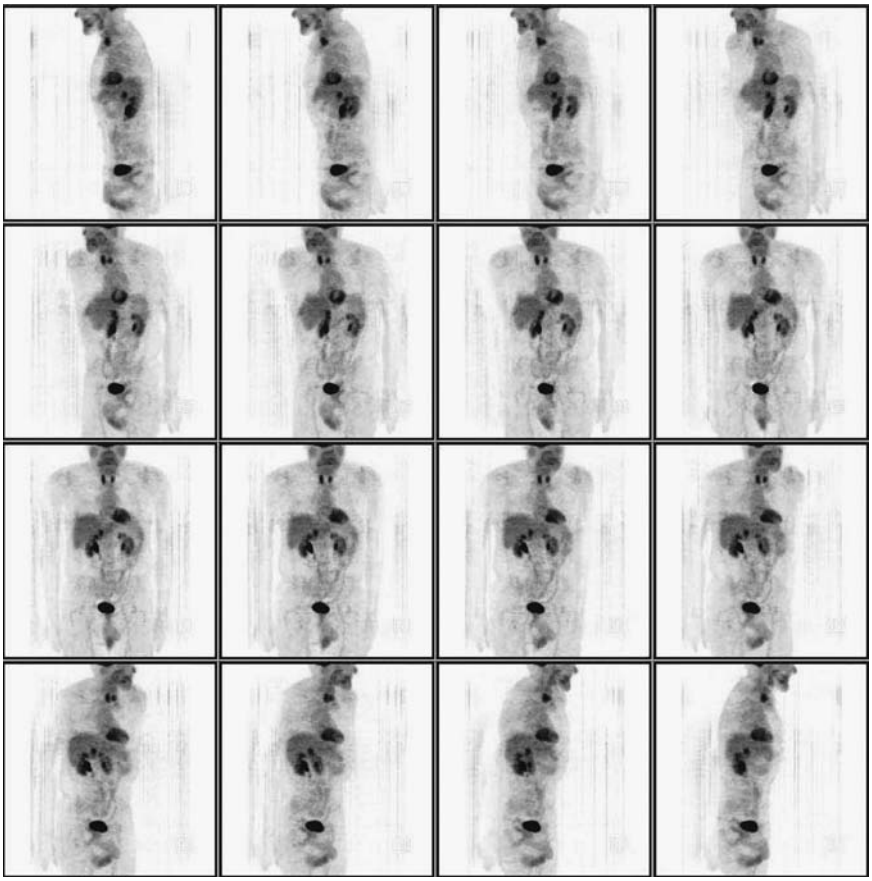

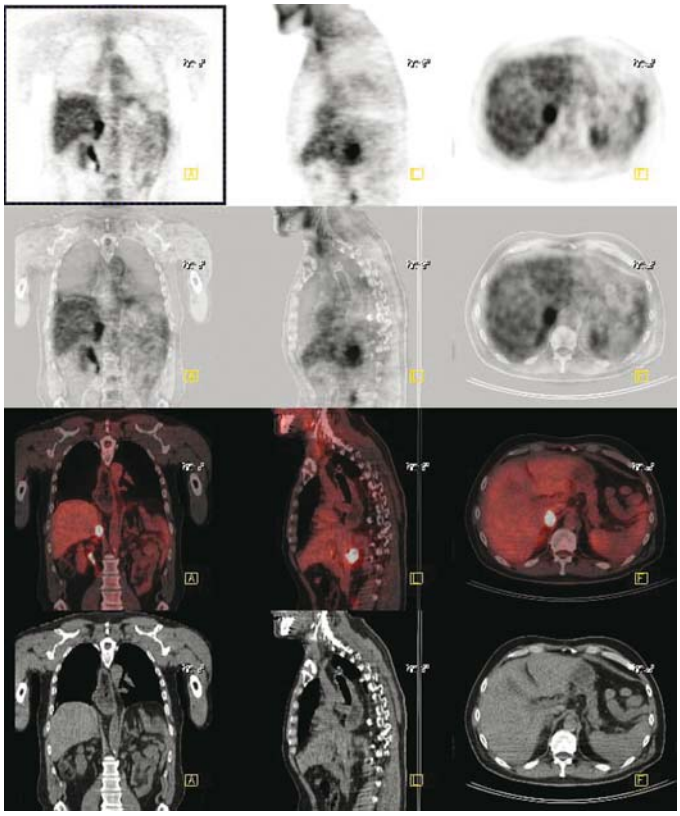

FIGURE 9.1.2.

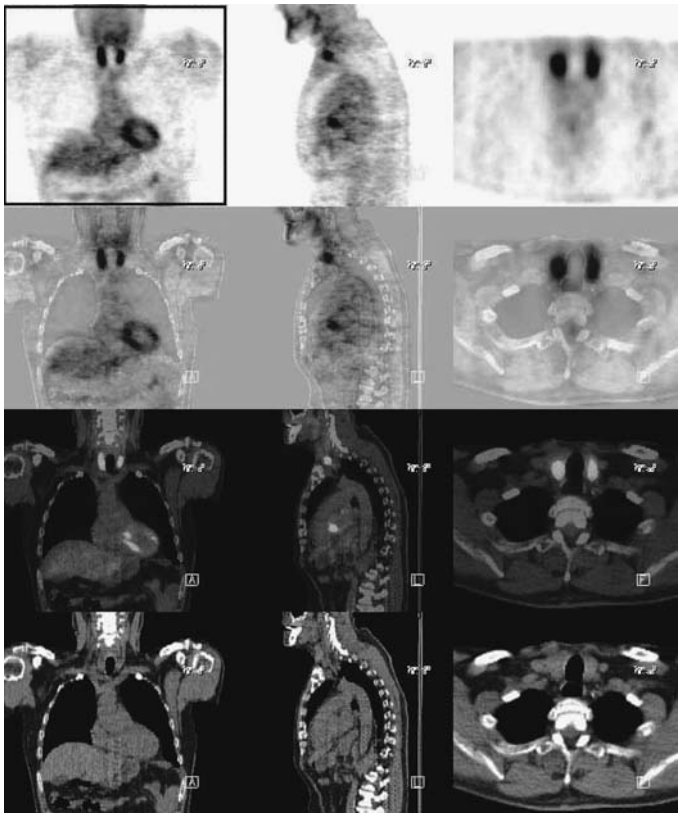

FIGURE 9.1.3.

rate. Surgery or external beam irradiation and chemotherapy are currently the standards of care for limited esophageal cancer.

Case 9.2

History

51-year-old male with a recent diagnosis of esophageal cancer with a 1-cm lesion endoscopically biopsied as positive. Outside CT had shown two small nodules in the left upper lobe. The current examination is for staging.

Findings

In the chest, review of the CT scan reveals two small nodules in the left upper lobe, one 3 mm and one 2 mm. No abnormal activity is seen in relationship to these small nodules, but they may well be below the resolution of PET, particularly in view of the quiet respiration status during acquisition. However, there are numerously intensely active lymph nodes within the mediastinum (*Figure 9.2.1*). These lymph nodes are normal by size criteria on CT but abnormal by PET scintigraphy. Numerous right superior mediastinal, prevascular, bilateral peribronchial, precarinal, subcarinal, and lower middle mediastinal nodes are apparent (*Figure 9.2.2*). There are also bihilar and infrahilar lymph nodes (*Figure 9.2.3*). There are two focal hypermetabolic areas in the lower esophageal area. One is probably the primary tumor. The other may be a second lesion with a skip metastasis or an adjacent posterior mediastinal lymph node. The lymphadenopathy distribution and extent would be unusual for metastatic esophageal CA at presentation; the possibility of incidental granulomatous disease is considered. Bronchoscopy prior to surgery might be helpful in this regard. Incidental notation is made of minor circumflex coronary calcification and a small Bochdalek's defect in the left diaphragm. Minimal activity in the inguinal nodes is not pathologic and is probably reactive.

Impression

1. There is one focus consistent with a primary esophageal carcinoma in the lower esophagus. There is either a skip metastasis above it or an adjacent lymph node.
2. Extensive superior and middle mediastinal and bihilar hypermetabolic lymphadenopathy. This could either represent metastatic esophageal CA or active granulomatous disease.

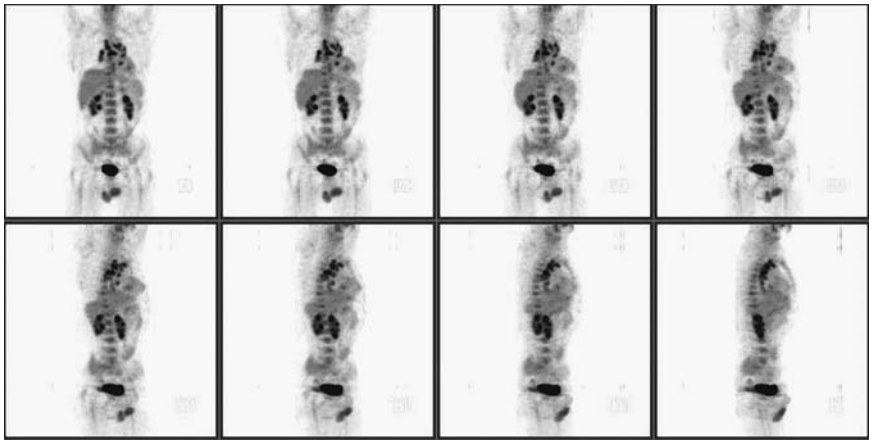

FIGURE 9.2.1.

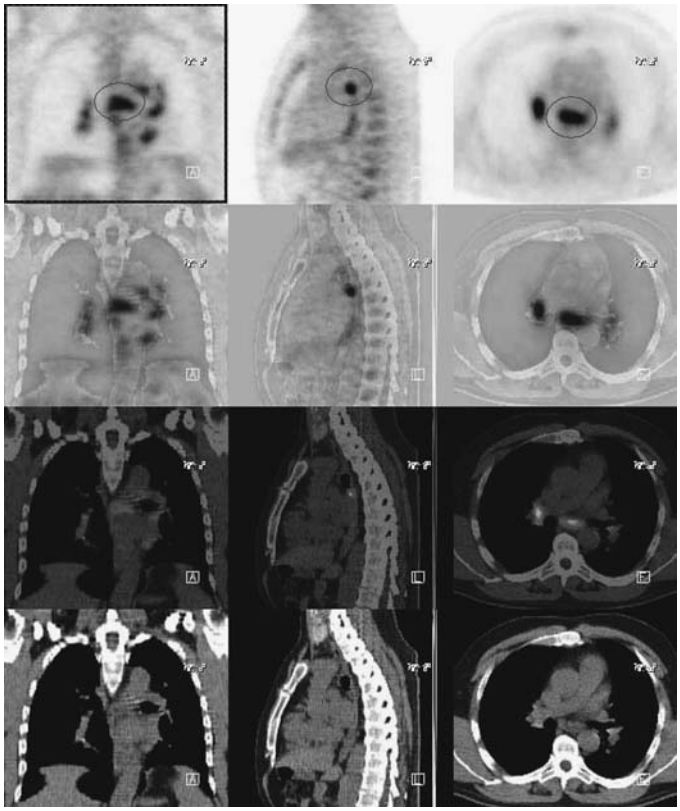

FIGURE 9.2.2.

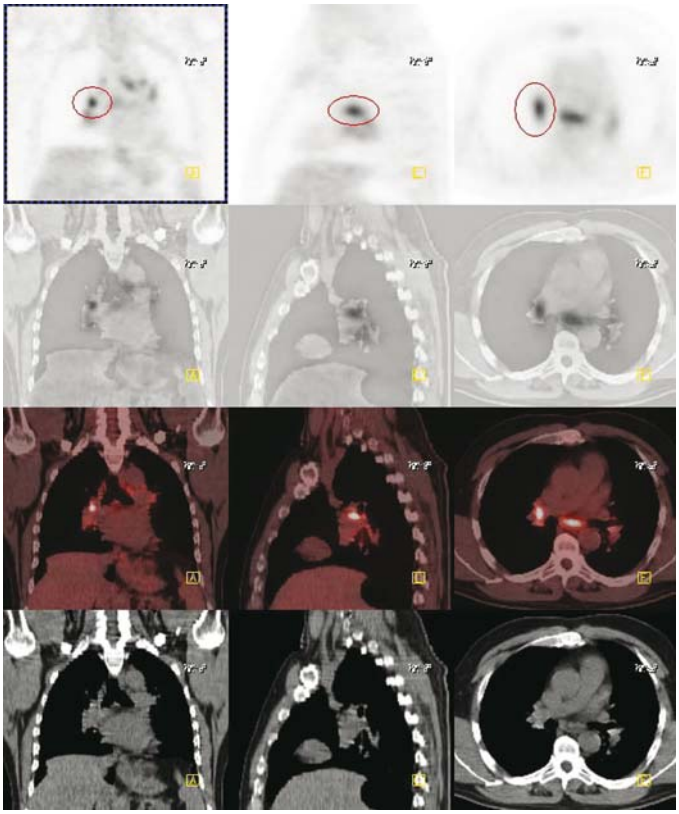

FIGURE 9.2.3.

3. The small pulmonary nodules are not visualized on PET but are probably below the threshold of resolution.

Pearls and Pitfalls

- *The sensitivity for primary esophageal cancer is 91% to 100%.*[5,8]
- *PET is not sensitive enough to assess local invasion.*[4,8,9]
- *Carcinoma-in-situ and T1 small cancers are predisposing factors for a false-negative PET result.*[4,8,9]
- *False-positive test results can occur with patients who have esophageal inflammation.*[4,8,9]
- *The accuracy for nodal metastases in CT is 40% to 73%, as opposed to 24% to 90% for PET.*[7,9,10]

Discussion

Of the esophageal cancers, 50% to 60% are squamous cell carcinoma. There has been a surge in number of adenocarcinomas in recent years. Once the malignancy extends beyond the esophageal wall, a good radial resection is hard to achieve. The tumor usually spreads longitudinally and may present with skip metastases. Ten to fifteen percent of the patients will relapse despite clear margins on resection; 50% to 70% of the patients will have lymph node involvement; and 20% to 30% will involve supraclavicular nodes that are nonpalpable.

Case 9.3

History

65-year-old male who has a history of esophageal and liver cancer diagnosed within a few months of each other. An earlier PET scan revealed hypermetabolism involving the liver and esophagus. He was treated subsequently with chemotherapy. Evaluation for treatment response is requested.

Findings

There are four hypermetabolic foci seen in the liver (*Figures 9.3.1 and 9.3.2*); two on the right and two on the left, corresponding with the previous PET findings. There is focal short segment of activity at the level of the original gastroesophageal junction (*Figure 9.3.3*) that may represent local recurrent residual tumor. The mild bihilar activity is probably inflammatory (*Figure 9.3.4*) in nature. The tracer localization at the base of the neck is fat or muscle activity (*Figure 9.3.5*). No pulmonary metastasis or discrete mediastinal lymph node pathology is seen.

Impression

1. Hypermetabolism in the liver compatible with metastatic disease.
2. Abnormal activity at the level of the gastroesophageal junction compatible with local recurrence; inflammatory disease at this site must also be considered.
3. Overall, findings represent a poor response to chemotherapy.

Pearls and Pitfalls

- *CEA is an effective tumor marker for monitoring patient response to treatment.*
- *PET is a useful tool for detecting nodal metastases.*
- *Patients with limited and local disease have a higher survival rate (60%) than those patients with distant metastasis (20%) over a 2 to 3 year period.*[4,8,10]
- *PET has the potential to alter patient management in 22% of the cases.*[1,2,3,5]

Discussion

Patients with distant metastases are considered nonresectable. Most metastatic lesions in the liver and lung are subcentimeter in size. PET has a sensitivity of 69% to 100%,

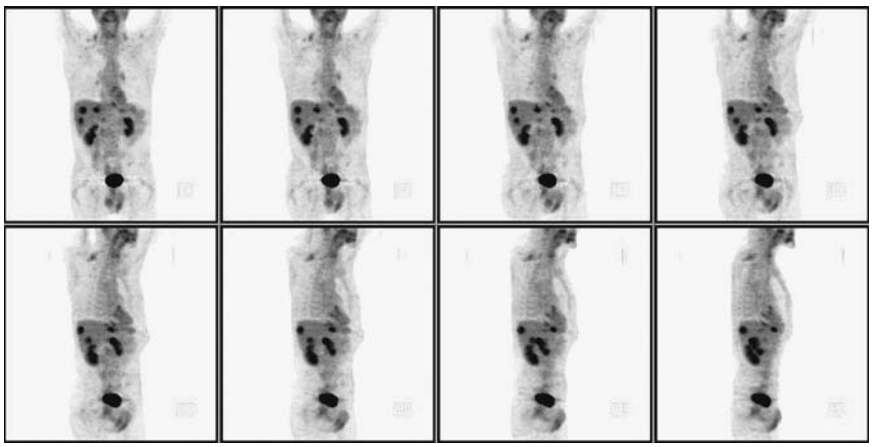

FIGURE 9.3.1.

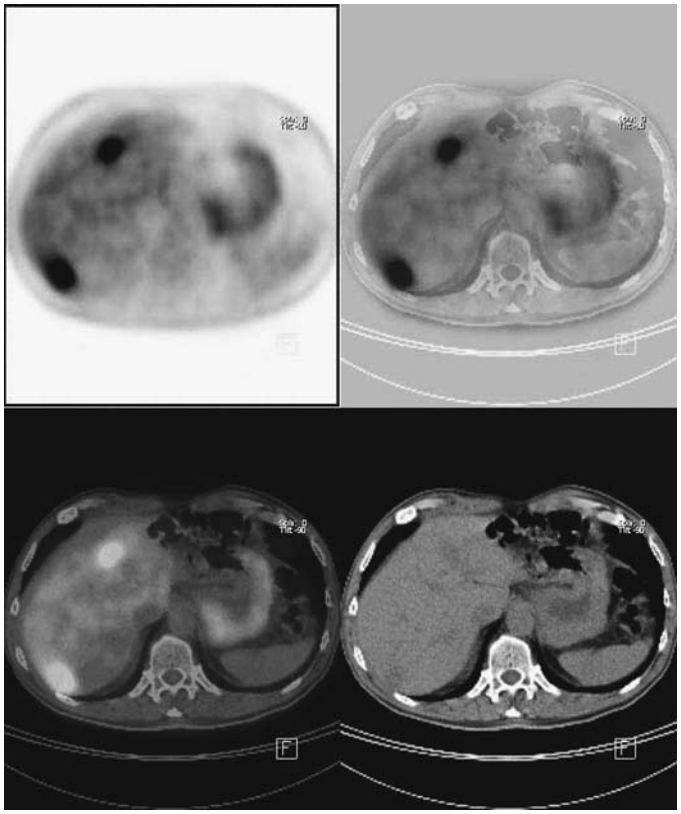

FIGURE 9.3.2.

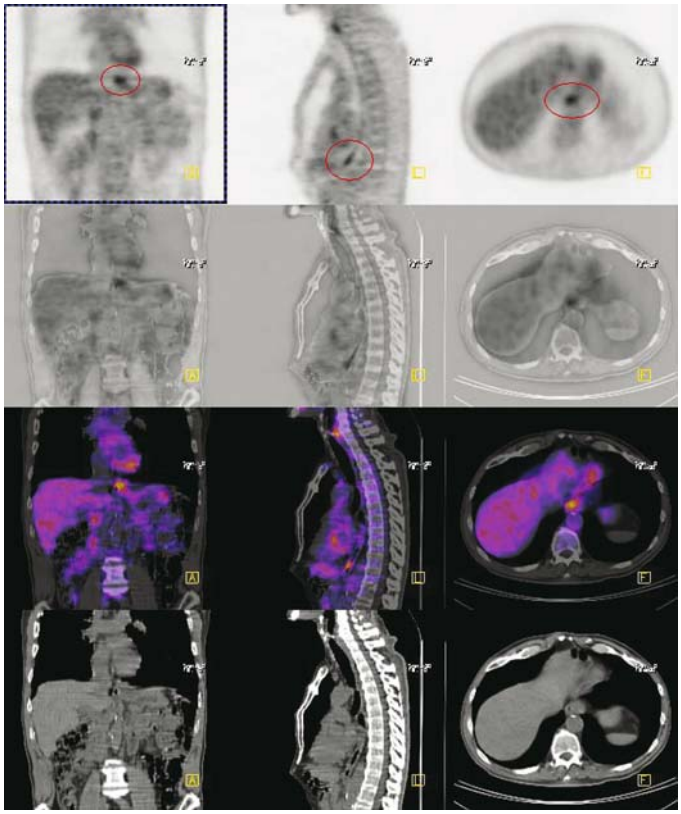

FIGURE 9.3.3.

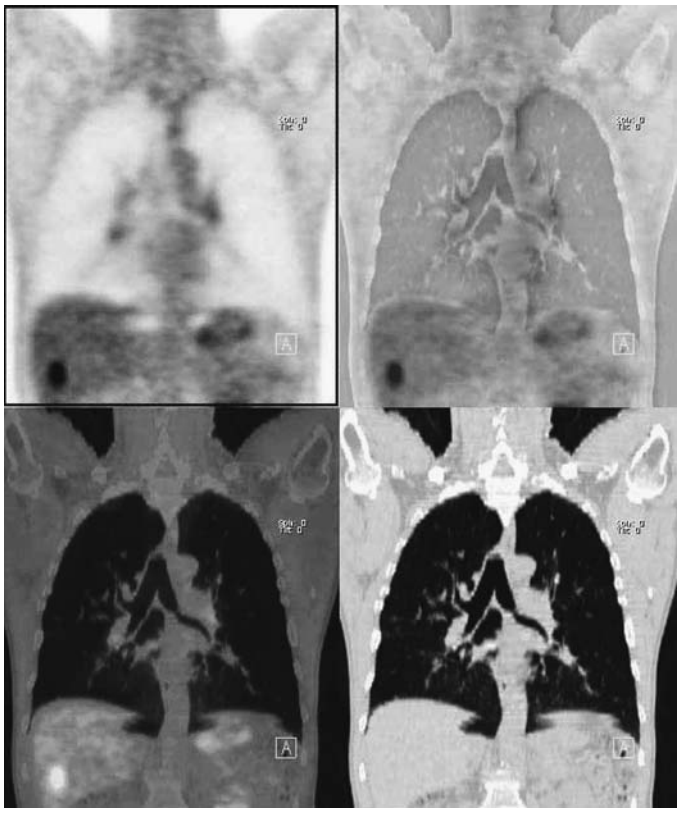

FIGURE 9.3.4.

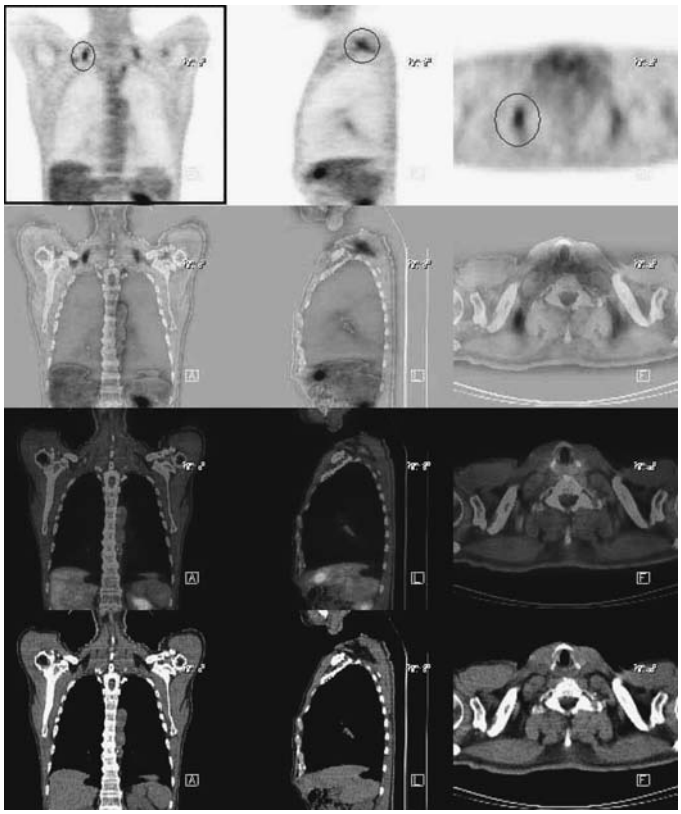

FIGURE 9.3.5.

specificity of 84% to 90%, and accuracy of 84% to 91% for detecting metastases, whereas CT has a reported sensitivity for distant metastases of 46%. Comparing the two modalities, PET scored higher for the detection of distant metastases compared to CT, 84% vs. 63%, respectively.

Case 9.4

History

63-year-old female status post esophagectomy with gastric pull-up for esophageal carcinoma. The patient is being seen for restaging.

Findings

The most striking finding of the exam is the intensely hypermetabolic confluent bulky subcarinal (*Figure 9.4.1*) and left hilar adenopathy with a few smaller left peribronchial intensely active nodes (*Figure 9.4.2*). This is consistent with metastatic regional adenopathy of esophageal origin. There is some peripheral atelectasis in the left midlung, which is likely related to the hilar adenopathy with bronchial compression. There are a few mildly active nodes in the superior mediastinum between the posterior margin of the left pulmonary artery and the aorta. The modest activity at the right AC joint is presumed inflammatory in character.

In the abdomen, there is unusually active but probably physiologic distal colon activity diffusely. There is one separate focus which is probably also colon rather than an iliac lymph node. There is no evidence for adrenal or hepatic metastasis. Multiple findings corresponding to surgical history and incidental notation of sigmoid diverticulosis.

Impression

1. With regard to the history of esophageal carcinoma, there is bulky, intensely hypermetabolic subcarinal, left hilar, and left peribronchial adenopathy with some secondary peripheral atelectasis.
2. There is unusually intense but probably physiologic distal colon activity. A single intense focus more proximally is somewhat suspect but not definite for polyp/tumor.

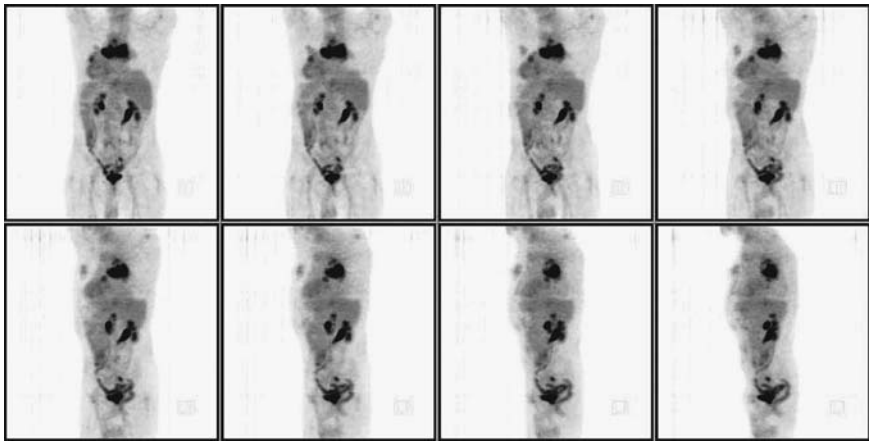

FIGURE 9.4.1.

FIGURE 9.4.2.

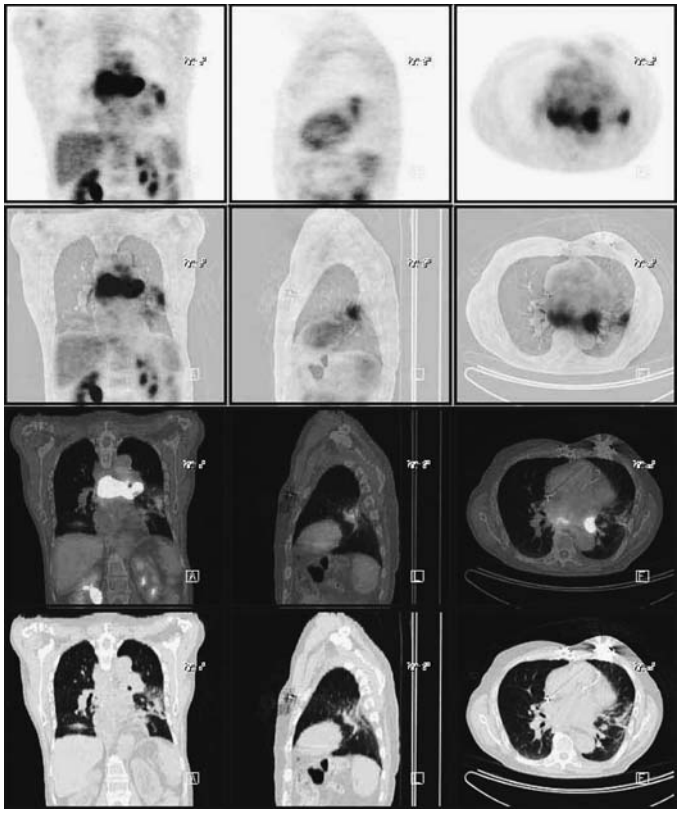

Pearls and Pitfalls

- *PET has a higher accuracy (88%) for determining utility of surgical resection than CT (65%).*[1,2,3,6,8]
- *PET is a cost-effective imaging procedure since it will select patients more appropriately suited for surgery.*[3,6,8]

Discussion

Only 40% of esophageal cancer patients are candidates for surgical resection. Residual tumors are frequently seen at the margins of the resection. The postoperative mortality is 20% from fistulas, abscesses, and respiratory complications. The 5-year survival after a total esophagectomy is less than 20%.

Case 9.5

History

62-year-old male who has a history of esophageal cancer three years ago status post en bloc esophagectomy and gastric pull-up. His CT was unremarkable and his CEA level was 1.0. The patient presents with dysphasia and is being evaluated for recurrence.

Findings

There is an intensely hypermetabolic mass (*Figures 9.5.1 and 9.5.2*) posterior to the trachea and lateral to the gastric pull-up within the superior mediastinum. This corresponds to a soft tissue mass in this region. No regional adenopathy is seen.

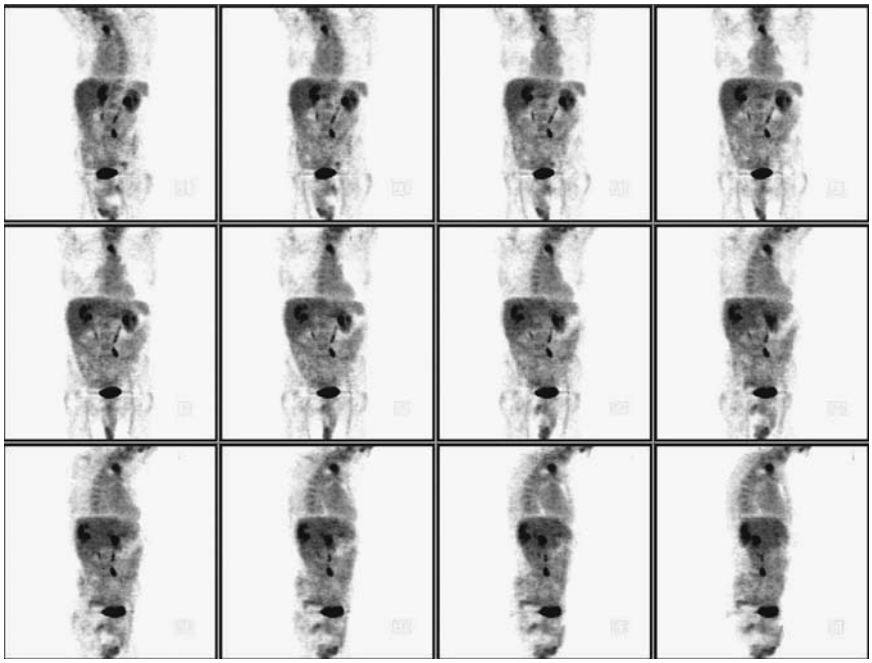

FIGURE 9.5.1.

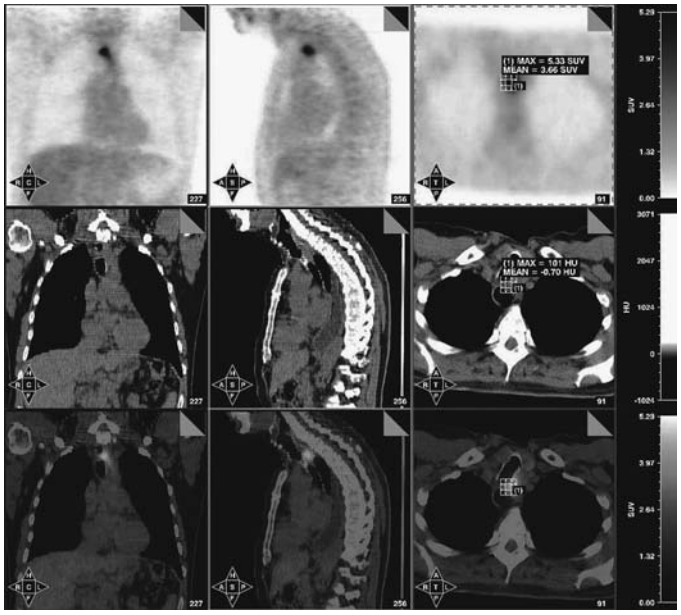

FIGURE 9.5.2.

Impression

Evidence for tumor recurrence adjacent to the gastric pull-up anastomosis in the superior mediastinum near the esophagogastric anastamosis.

Pearls and Pitfalls

- *PET can evaluate patient response to therapy.*[1,2]
- *Recurrence is most common near the esophagogastric anastamosis.*[4,9,10]

10 Gastric Cancer

Hossein Jadvar and Shahram Bouyadlou

Case 10.1

History

64-year-old male with a history of gastric cancer, status post partial gastrectomy, with subsequent radiotherapy and chemotherapy one year ago. A recent CT demonstrated a suspicious area in the medial segment of the left lobe of the liver. This study is performed to evaluate for evidence of metastatic disease.

Findings

The pulmonary exam is negative by 18-FDG PET scintigraphy. Scattered atelectasis is evident on CT as well as a left-lung base cystic area in the lung. No pulmonary nodule is apparent. The mediastinum is negative. The abdomen is remarkable for a liver dome lesion which is intensely hypermetabolic (*Figure 10.1.1*) with central hypoactivity consistent with central necrosis (*Figure 10.1.2*). This is somewhat ill-defined on the noncontrast CT but it is measured at about 3.3 cm in diameter. No other hepatic lesion is apparent. Multiple upper abdominal surgical clips are consistent with the history. There is moderate calcification in the normal caliber abdominal aorta. There is prominent but presumed physiologic diffuse bowel activity. In the pelvis, the urinary bladder appears more distended than usually seen on a post-voiding exam. This may reflect prostate enlargement.

Impression

1. Solitary liver dome metastasis of approximately 3.3 cm diameter with central necrosis. There is no other evidence for metastatic disease by PET scintigraphy with CT attenuation correction.
2. Increased postvoiding residual in the urinary bladder; prior partial gastrectomy with multiple upper abdominal surgical clips; scattered pulmonary atelectasis and left lung base cyst.

Pearls and Pitfalls

- *PET may be useful in the evaluation of recurrent gastric cancer and localize the disease where CT is nondiagnostic.*[1,2]
- *PET can alter the clinical management of patients with recurrent gastric cancer.*[1,2,3]

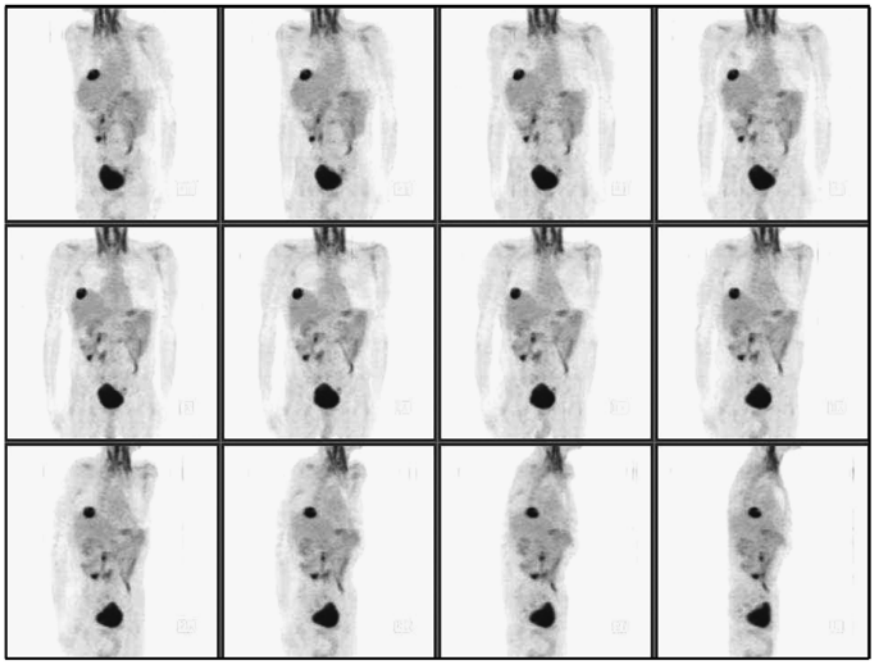

FIGURE 10.1.1.

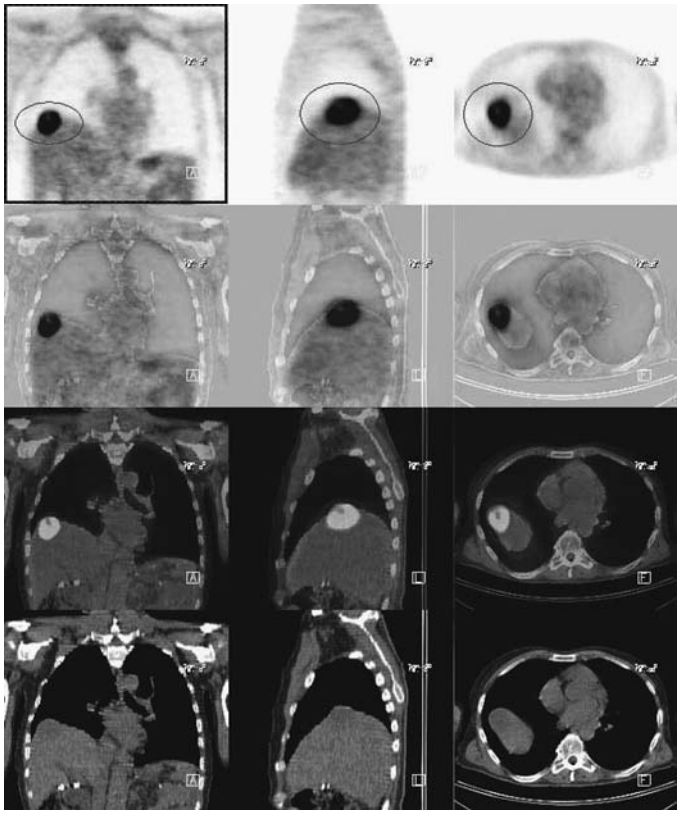

FIGURE 10.1.2.

- *In a retrospective study, PET demonstrates a sensitivity of 62% and specificity of 60% for a group of primary tumors with signet cell differentiation.*[1,2,3]
- *The positive predictive value of PET in gastric cancer is 78% as opposed to a negative predictive value of 60%.*[1,2,3]
- *Due to the poor sensitivity and negative predictive value, most authorities agree PET imaging is not a useful screening tool for gastric cancer.*[1,2,3]

Discussion

Gastric cancer ranked fourteenth among major malignancies in the US and remains the least studied malignancy with F-18 FDG PET imaging. Studies suggest that exposure to an etiologic agent at an early age (H. pylori infection, cigarette smoking, and low levels of dietary vitamin C) may be responsible for gastric cancer that eventually leads to up-regulation of expression of cox-2 enzyme.

Early satiety and abdominal tenderness are some of early-stage nonspecific signs for stomach cancer. Weight loss or palpable mass is late in the course of the disease. Endoscopy, gastric cytology washing, and barium x-ray are commonly used for diagnosis. Resection is the cornerstone for cure. Chemotherapy may be used for palliative treatment. Prognosis is good only if the malignancy is limited to the mucosa and submucosa.

Case 10.2

History

63-year-old male who has a history of gastric cancer diagnosed status post chemotherapy two years ago. His most recent CT revealed a suspicious lesion in the medial aspect of the inferior portion of the liver. The patient is being evaluated for metastatic disease.

Findings

In the abdomen, there are several small hepatic metastases (*Figures 10.2.1 and 10.2.2*). There is a large subhepatic (*Figure 10.2.3*) and several other large peritoneal implants (*Figures 10.2.4 and 10.2.5*). The low left pelvic focus is probably a peritoneal implant in the rectovesical recess (*Figure 10.2.6*). The chest is clear.

Impression

Multiple lesions found in the liver and the abdomen consistent with disseminated implants from known gastric cancer.

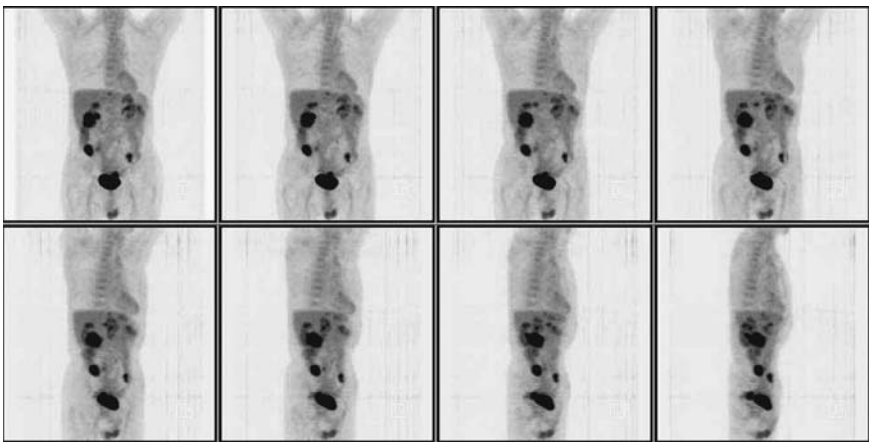

FIGURE 10.2.1.

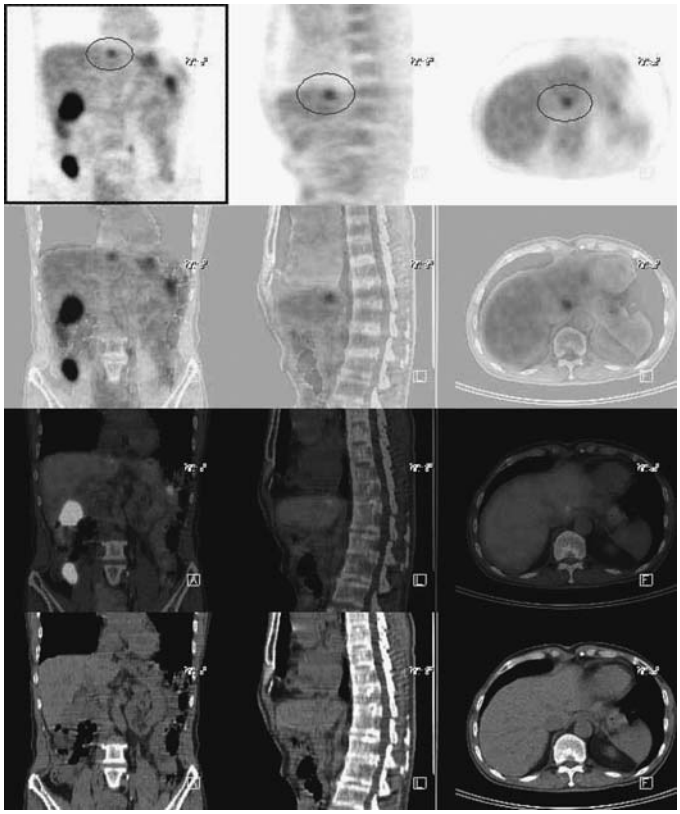

FIGURE 10.2.2.

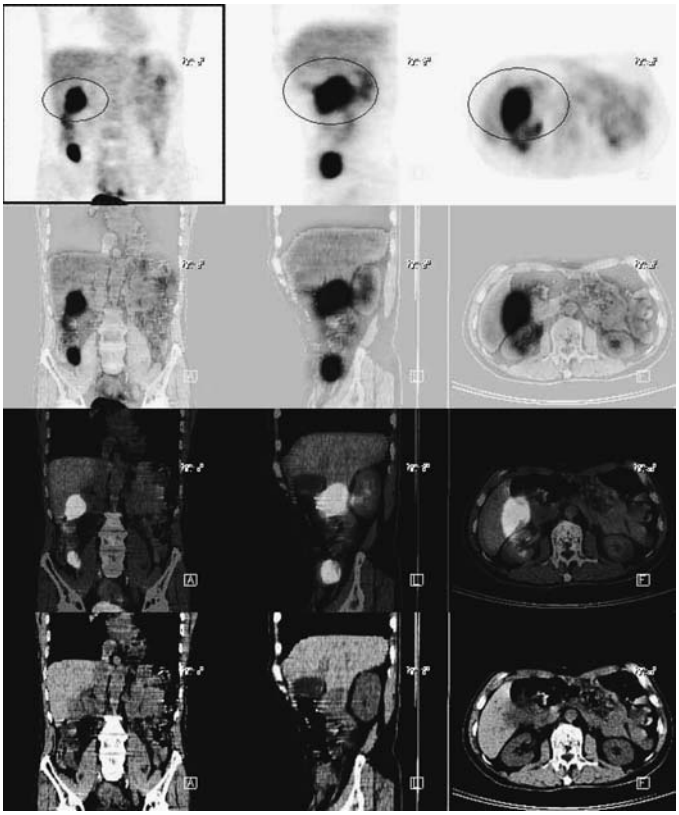

FIGURE 10.2.3.

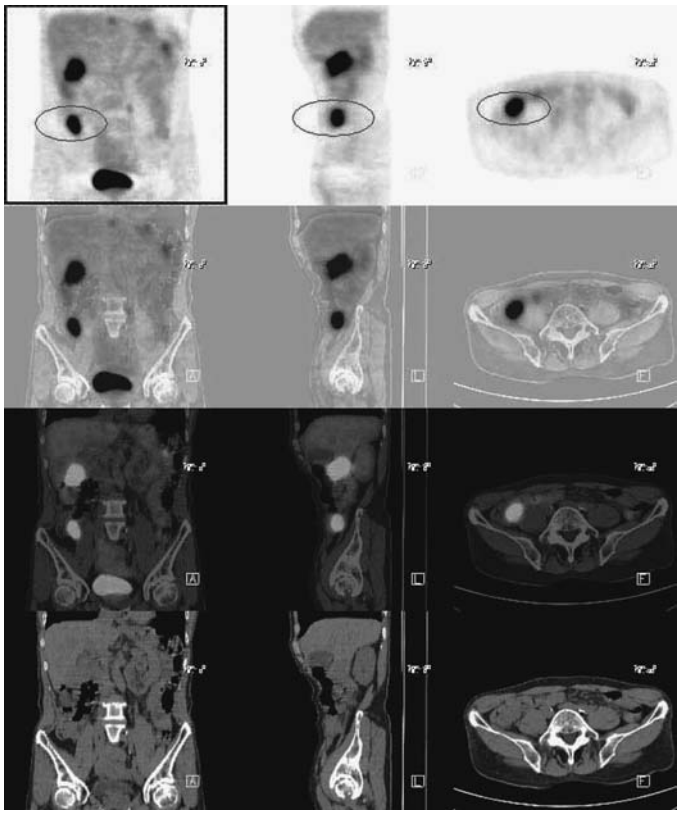

FIGURE 10.2.4.

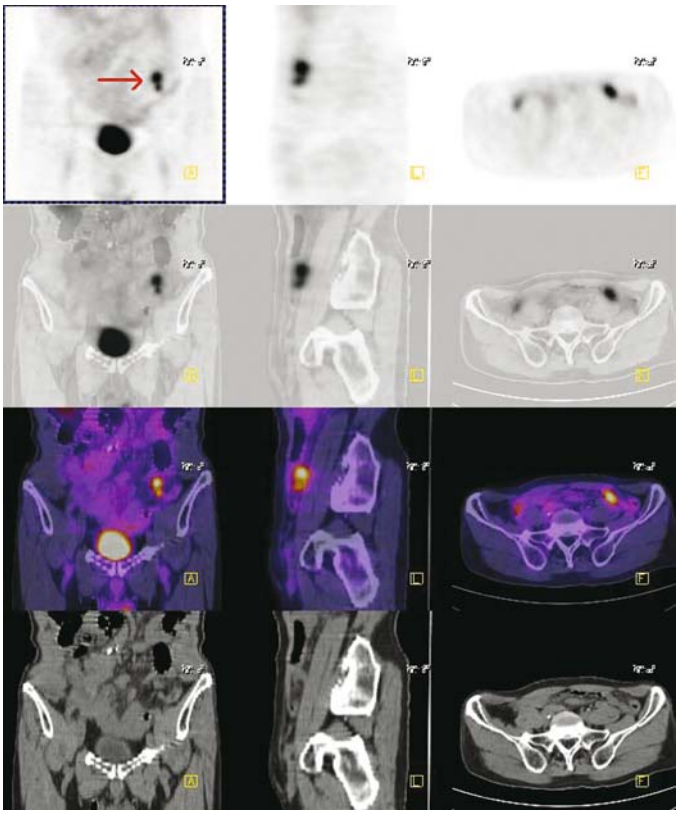

FIGURE 10.2.5.

FIGURE 10.2.6.

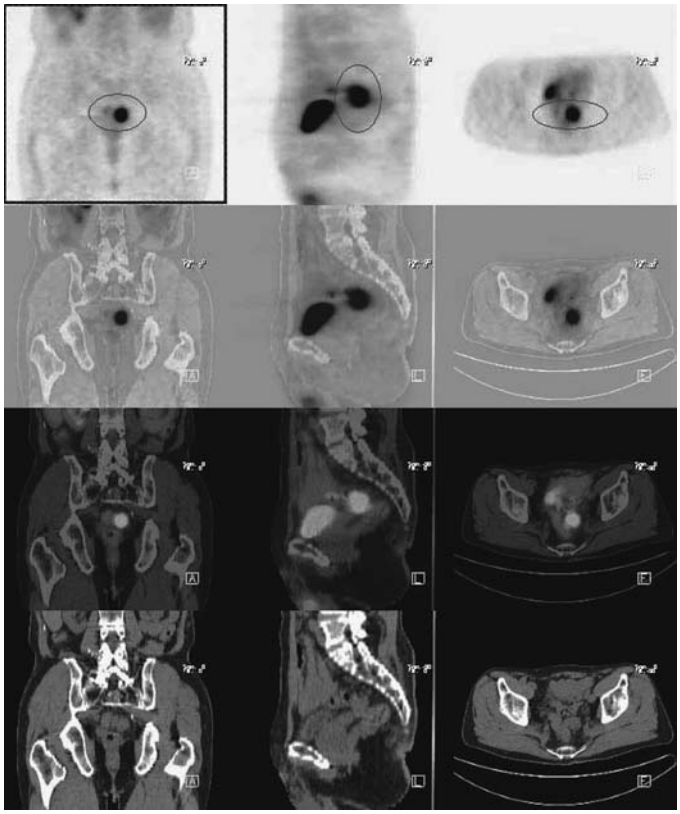

Pearls and Pitfalls

- *PET-negative patients have a higher survival rate than PET-positive patients, 18.5 months vs. 6.9 months, respectively.*[1,3]

Discussion

PET scintigraphy is useful for imaging in advanced, metastatic, or recurrent disease, although there is no direct correlation between uptake and histopathological appearance. F-18 FDG is an important tool in staging, treatment planning, and in assessing response to therapy.

Change in Treatment

There is a definite pre- and post-PET management change in this patient. The patient initially refuses chemotherapy due to its side effect profile and would prefer radiotherapy instead. After the PET findings, the patient was convinced that chemotherapy would be the best therapeutic approach to his therapy planning.

11 Gastrointestinal Tumors

Heidi R. Wassef

Case 11.1

History

43-year-old male who has a history of gastrointestinal stromal tumor diagnosed status postexploratory laparotomy. Evaluation for metastatic diseases is requested.

Findings

There is a single abnormality in the loop of bowel below the umbilicus deep (*Figures 11.1.1 and 11.1.2*) in the abdomen that is moderately hypermetabolic with wall thickening on CT consistent with malignancy. The ground glass density on CT in the right pulmonary apex is mildly active probably representing inflammatory changes. The prominent activity in the right colon is physiologic. The activity near the cervical vertebrae posteriorly is consistent with fat mobilization (*Figure 11.1.3*).

Impression

1. Hypermetabolism in a thickened loop of bowel as described above compatible with known malignancy.
2. Presumed inflammation in right pulmonary apex.
3. No evidence of metastatic disease.

Discussion

Gastrointestinal stromal tumors (GISTs) are a group of rare soft tissue tumors that constitutes 80% of the GI mesenchymal tumors. This represents less than 3% of all GI malignancies. Both men and women are affected between the ages of 40 and 70 years. Fifty to seventy percent of the GISTs occur in the stomach, 33% in the small bowel, and 5% to 15% in the colorectal.

The typical symptoms include abdominal discomfort (or pain), vomiting, fecal blood, and fatigue secondary to anemia.

CT with contrast can provide information regarding the location of the abnormal growth. It is also very sensitive in detecting any metastatic involvement including the liver, peritoneum, and lungs. MRI is used to evaluate soft tissue mass and lesion vascularity. Ultrasound guided biopsy follow by immunohistochemical staining will provide additional character of the tumor. PET can determine if any other malignancy is involved where CT (MR) might have missed the diagnosis. Special diagnostic kits

FIGURE 11.1.1.

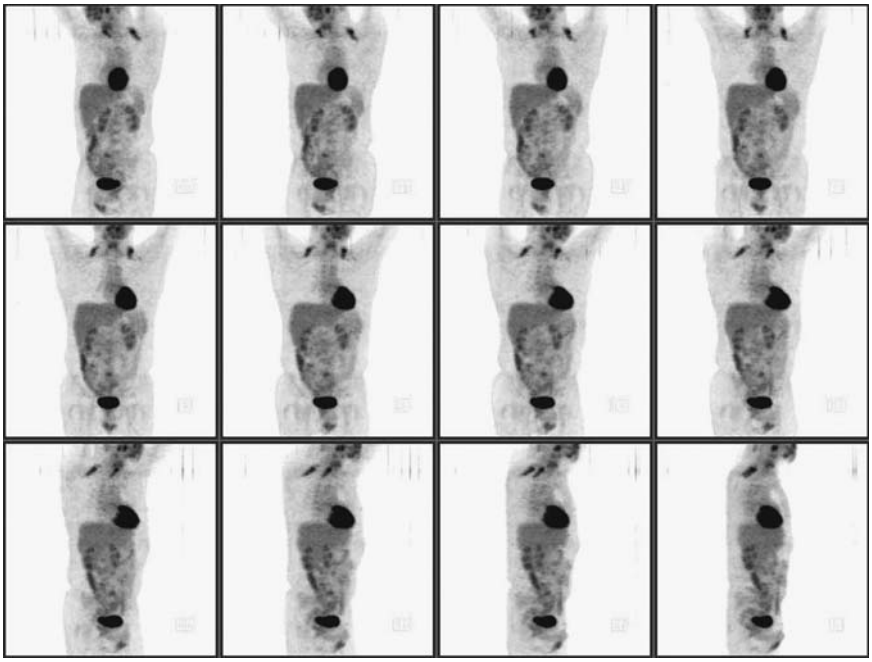

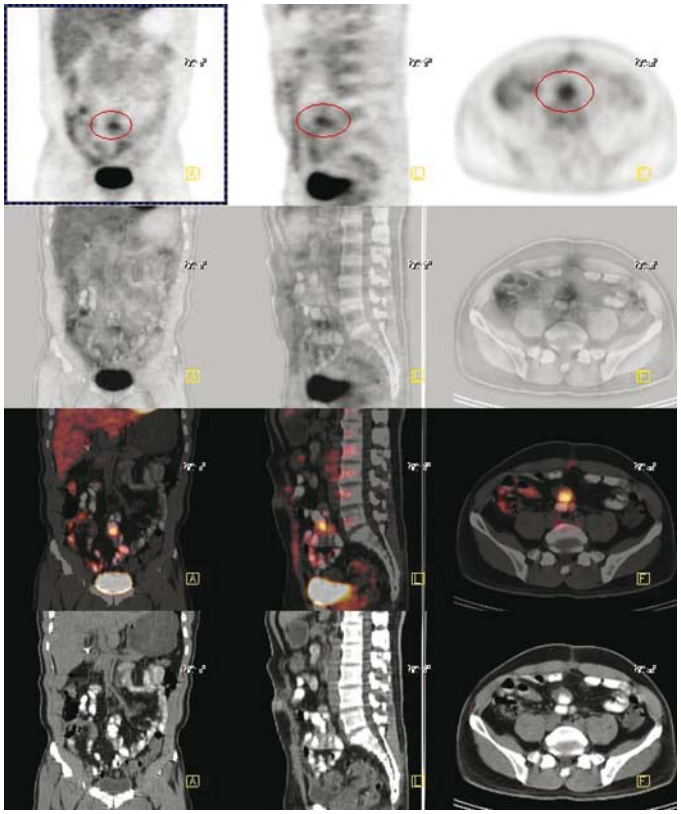

FIGURE 11.1.2.

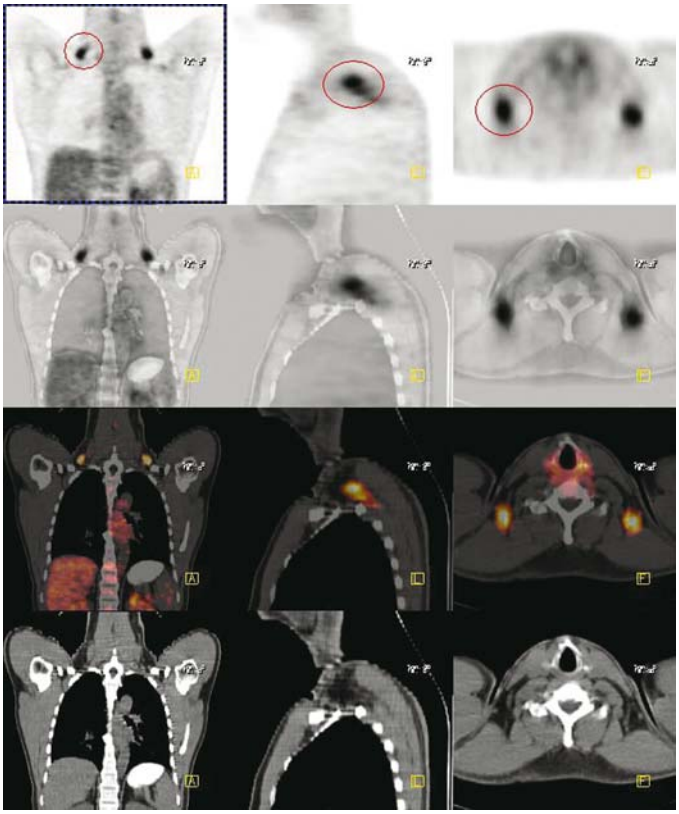

FIGURE 11.1.3.

are now commercially available to detect GISTs with CD-117 (and CD-34 antigen) surface tissue expression.

The treatment of GISTs is primarily surgical. Only 10% of patients will remain symptom free after treatment. As a rule of thumb, small GISTs (<1 cm in size) rarely metastasize; whereas larger GISTs (>15 cm) will inevitably spread.

The overall 1-year survival rate of GISTs is 69%. The 3-year survival rate is 29% to 35% and 5-year is 29% to 35%.

Follow-up

In this case scenario, PET has successfully downstaged the original malignancy suggested from CT.

Case 11.2

History

67-year-old male who presented with jaundice. A biliary stent was placed endoscopically and an ulcerative mass noted in the post-bulbar duodenum and confirmed on CT. The current evaluation is for staging.

Findings

There is thickening of the medial wall of the descending duodenum with accompanying intense hypermetabolism (*Figures 11.2.1 and Figure 11.2.2*), between the duodenal lumen and the stent. The lesion is about 2 cm in diameter and the intense hypermetabolism is consistent with malignancy. Additionally, there is a focal area of intense hypermetabolism of about 1.5 cm dimension in the posteromedial cortex of the upper right kidney. An apparent cortical lesion appears to be a misregistered prominent

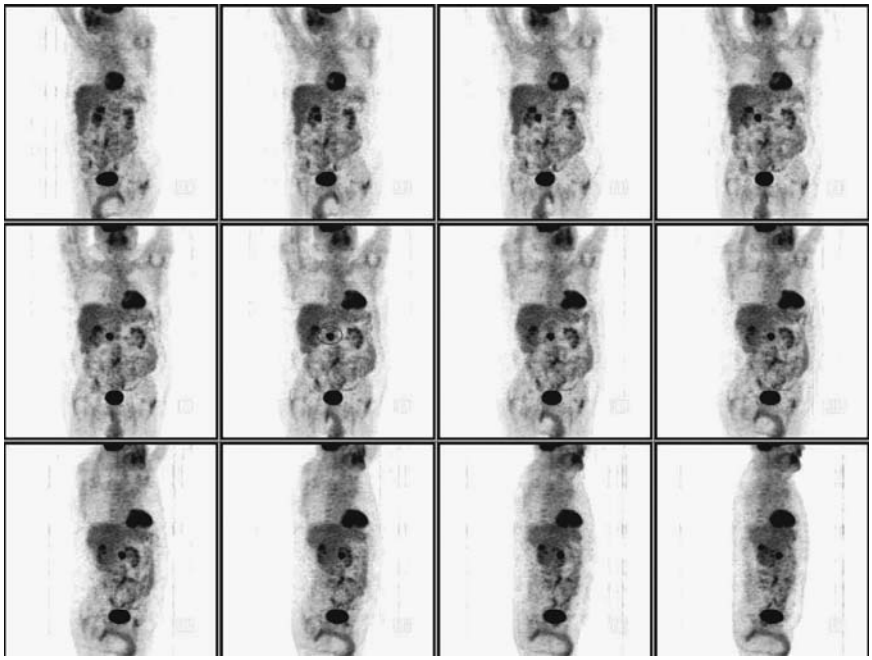

FIGURE 11.2.1.

FIGURE 11.2.2.

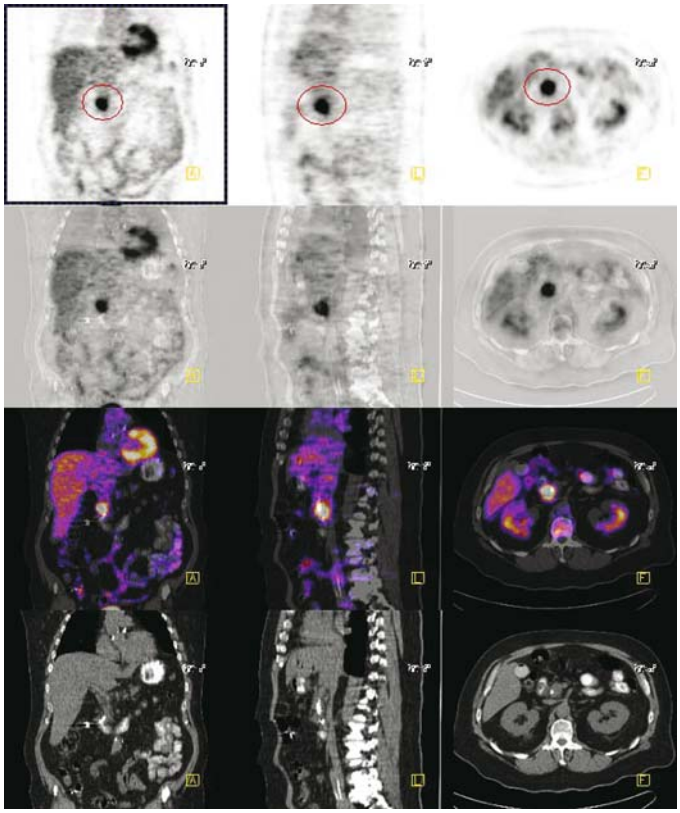

upper pole calyx. There are a few scattered peripheral radiodensities that are interpreted as minor atelectasis on CT. Incidental notations are made of pneumobilia related to the stent and high-density material in the gallbladder, which is probably contrast from a previous radiographic exam.

Impression

1. Intense hypermetabolism of the wall thickening of the left/medial aspect of the descending duodenum, between the duodenal lumen and the biliary stent, consistent with malignancy.
2. No evidence of regional or distant metastatic disease.

12 Head and Neck Cancers

John L. Go

Case 12.1

History

35-year-old female who is status post left modified radical neck dissection with a diagnosis of buccal cavity squamous cell carcinoma. She is being evaluated for locally recurrent and metastatic disease.

Findings

In the head and neck examination, there are two areas of intense hypermetabolism (*Figures 12.1.1 and 12.1.1A*). The first area is within and extending inward from an osteolytic defect at the internal cortex of the proximal left mandibular ramus (*Figure 12.1.2*) near the angle of the jaw. There are multiple surgical clips in this area, but this intense hypermetabolism at 15 months after surgery is likely to represent locally recurrent neoplasm (rather than postoperative changes). The other area of intense hypermetabolism is the soft palate (*Figure 12.1.3*). This is most likely physiologic. Also noted in the head and neck is moderately increased right gingival margin activity along multiple teeth in the right maxilla likely representing gingival inflammation. At the same level, there is more intense right than left posterior tongue activity, which may reflect asymmetric muscular activity. Also noted as striking in the head and neck is increased fat activity in the neck and shoulders. This is suspected to be related to mobilization of fat, as the patient reports significant recent weight loss. Vocal cord activity is slightly asymmetrical, left greater than right, but no pathologic significance is attributed to this finding. The lung window images on the chest CT are negative, with no evident pulmonary nodules.

Impression

1. Intense hypermetabolism within and extending inward from a defect in the internal cortex of the left mandibular ramus. At more than one-year post surgery this is most likely recurrent neoplasm.
2. Intense soft palate and right greater than left posterior tongue activity, probably physiologic.
3. Negative for metastatic disease on whole-body examination.

FIGURE 12.1.1.

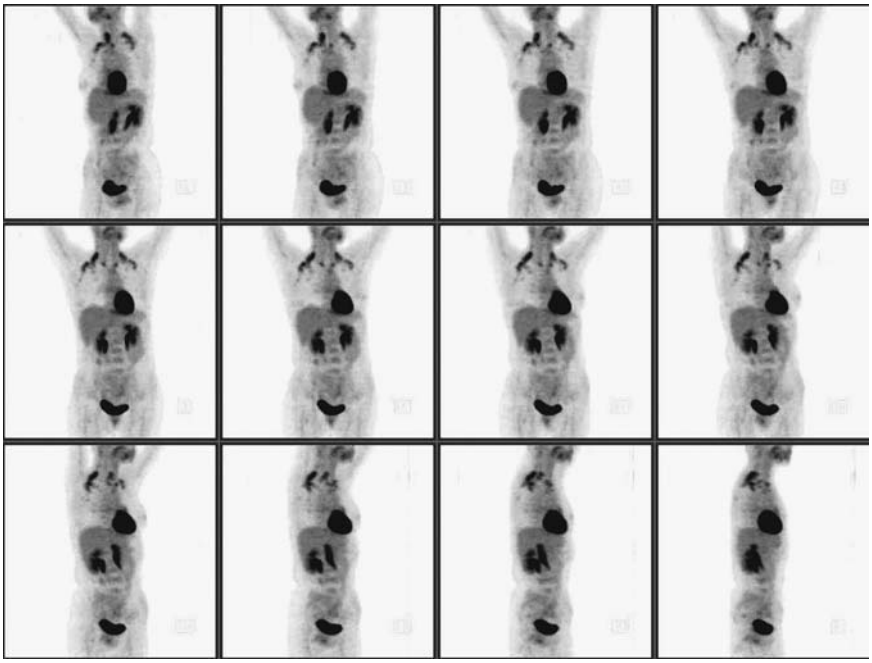

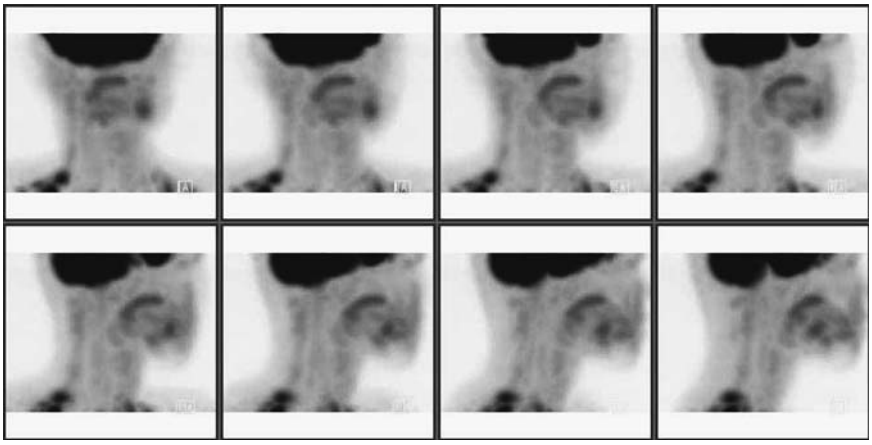

FIGURE 12.1.1A.

Pearls and Pitfalls

- *PET has an accuracy of 81% in distinguishing residual tumor from scar in head and neck cancers, whereas for CT (or MR) are 42%.*[4,5,7,9]

Discussion

Squamous cell carcinoma (SCC) of the buccal mucosa is a rare form of oral cavity cancer. It is a very aggressive disease that is associated with a high rate of locoregional recurrence and poor survival. The 5-year survival with patients of T1 or T2 tumors is only 78% and 66%, respectively. Extracapsular lymphadenopathy, muscle invasion, and Stensen's duct involvement are poor prognosticators. Surgical salvage for patients with locoregional recurrence after radiation therapy is rarely successful.

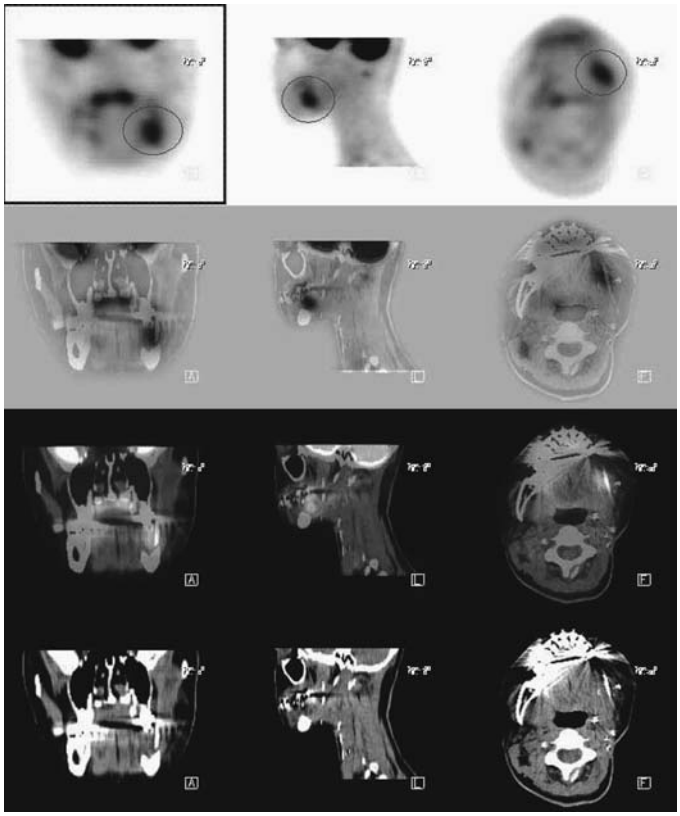

FIGURE 12.1.2.

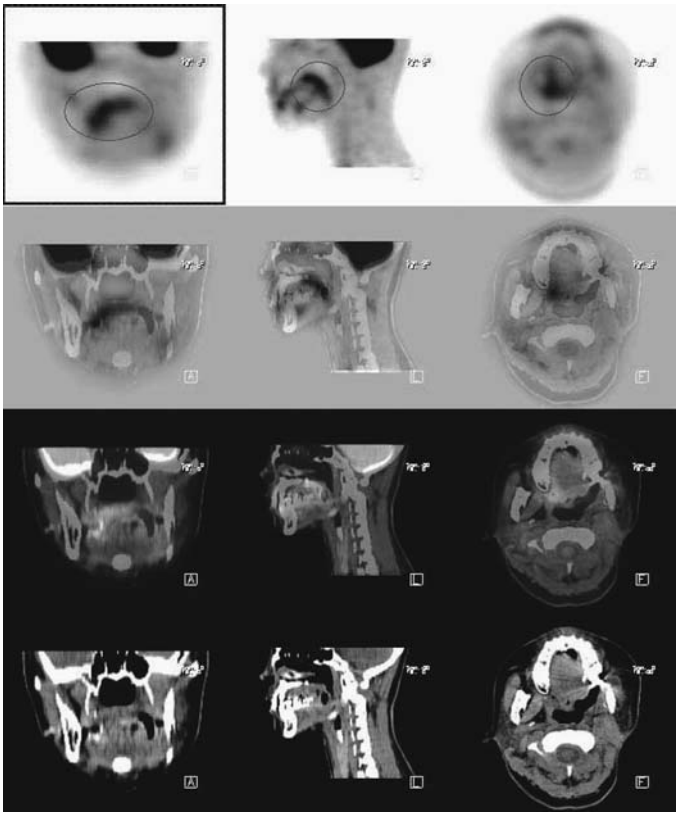

FIGURE 12.1.3.

Case 12.2

History

62-year-old male who has a history of squamous cell carcinoma on the face with known metastasis to the brain. His most recent MR demonstrated suspicious lesions involving the right lateral pons, right internal auditory canal, and left infratemporal fossa. Evaluation for extent of disease is requested.

Findings

On the rotating images, no bulky adenopathy is seen (*Figure 12.2.1*). There is slight increased activity in the right pons (*Figures 12.2.2 and 12.2.2A*) when compared to the left with evidence of ipsilateral diaschesis in the cerebellum. The rest of the brain parenchyma is within limits. In the chest, a linear band of activity is seen posterior to the right perihilar region (*Figure 12.2.3*) with a slightly prominent focus laterally. This is suspicious for inflammatory lung disease. There is small focus of activity on the lateral chest wall underneath the right axilla on the medial aspect of the arm that may represent a skin mole. Right urinary stasis is seen near the pelvis brim. There is mild caliectasis in the right renal collecting system.

FIGURE 12.2.1.

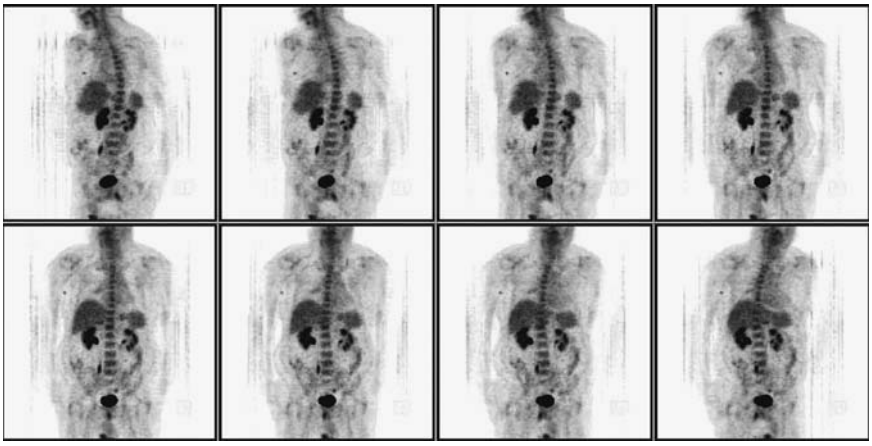

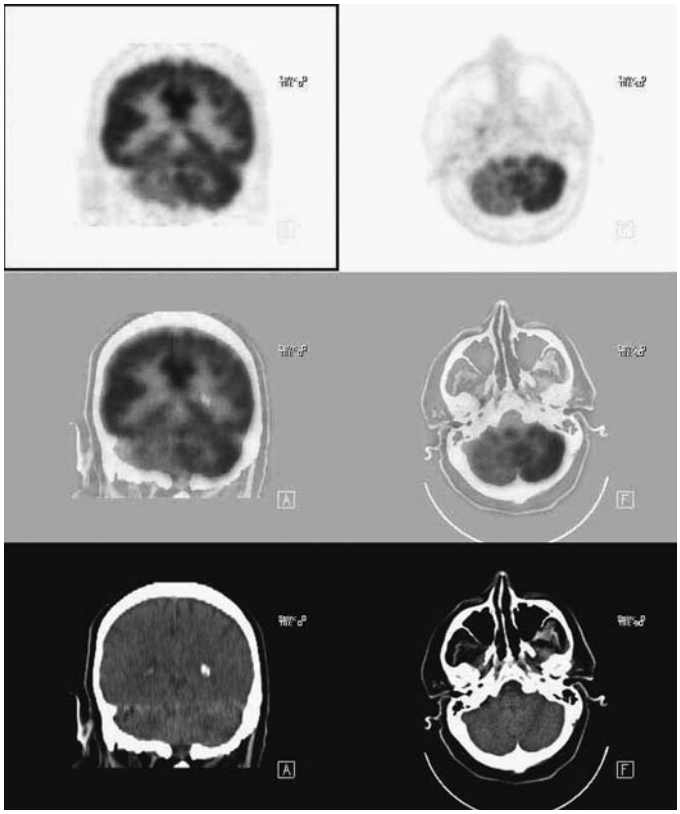

FIGURE 12.2.2.

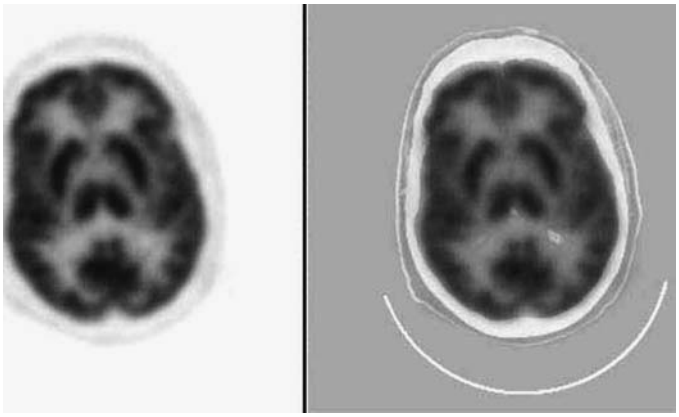

FIGURE 12.2.2A.

Impression

1. PET evidence for malignancy involving the right pons.
2. Suspicious activity on the right lateral chest or medial arm warrants additional clinical examination.

Pearls and Pitfalls

- *CT is useful in identifying the extent of primary and nodal involvement. It can also assess for pulmonary and hepatic metastasis.*[4,7]

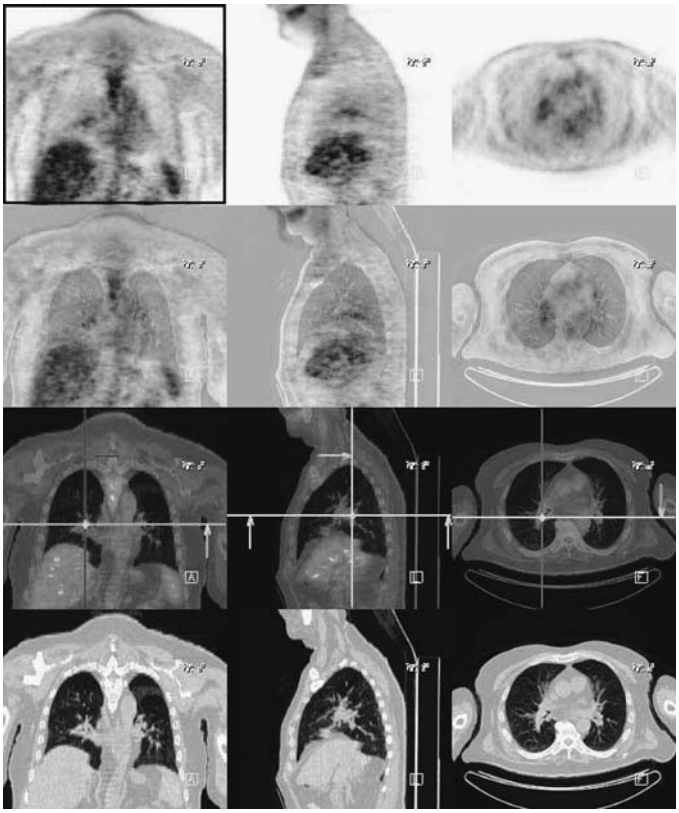

FIGURE 12.2.3.

- *MRI is recommended for evaluation of brain metastases due to higher sensitivity compared to other imaging modalities; PET can be used in this setting to improve specificity.*[7,9]

Discussion

Squamous cell carcinoma of the skin involves malignancy of the keratinocytes arising from the epidermis with evidence of dermal histological invasion. People with fair skin color are more susceptible to this disease. The prognosis corresponds to the location, the size, and the depth of the invasion. Local excision is the initial treatment. Radiotherapy after surgery is used to treat local recurrence.

This patient has a known history of squamous cell carcinoma of the face. Although rare, malignancy on the face can potentially spread to the central nervous system by lymphatic drainage.

Case 12.3

History

44-year-old female with a history of treated nasopharyngeal carcinoma. She is currently being restaged.

Findings

There is intense pathologic activity in the midline and left of midline at the posterior nasopharynx level. On CT, there is lytic destruction of the clivus (sphenooccipital clivus

FIGURE 12.3.1.

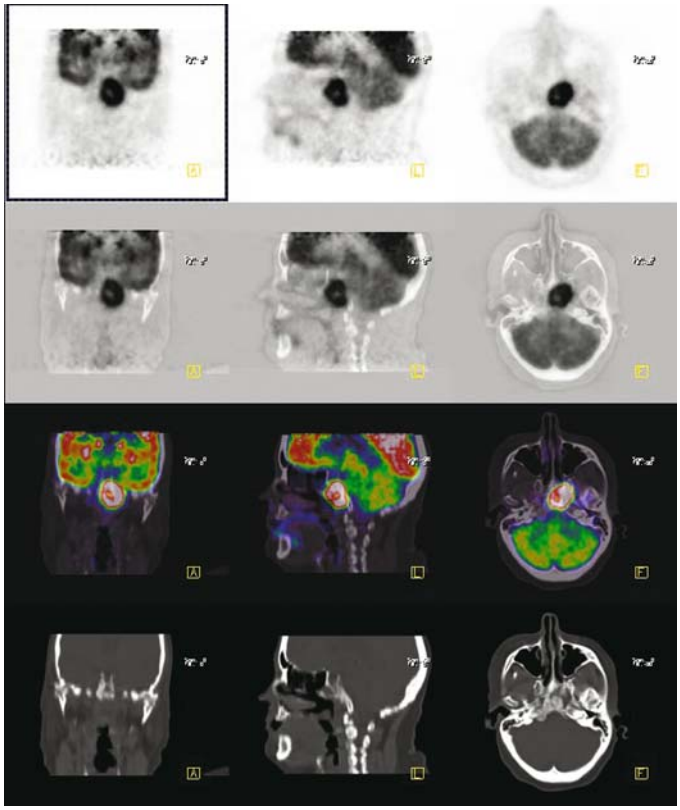

and body of sphenoid) with permeative infiltration of the adjacent remaining bone, midline and left of midline (*Figure 12.3.1*). There is involvement of the foramen ovale but no inferior extension into the masticatory space. There is involvement of medial margin of the carotid canal (horizontal portion of the petrous segment). This extends to the upper left paramedian soft tissues anterior to the foramen magnum. No regional adenopathy is evident.

The torso exam is unremarkable in appearance by 18-FDG PET scintigraphy. There is physiologic cardiac, GU, hepatic, and splenic activity as well as physiologic marrow activity. The liver has a long right lobe, consistent with Reidel's lobe.

Impression

1. Primary nasopharyngeal carcinoma involving the left neck without evidence of distant metastatic disease. Recurrence in the left posterior and posterolateral nasopharyngeal carcinoma extends posteriorly and superiorly to involve the skull base.
2. Negative for regional adenopathy and distant metastatic disease.

Pearls and Pitfalls

- *A SUV of greater than 5.5 has been used by some groups to identify patients in need of aggressive treatment.*[1,6]

Discussion

Nasopharyngeal carcinoma is a common malignant disease in Southeast Asia. In the Western population, it is 0.19% per 100,000 persons each year. Although the etiology

of this disease is unclear, both genetic and environmental elements may be contributing factors. The incidence mostly occurs in males with the age of onset at 30 to 40 and 50 to 60 years of age. Most cases go undetected until late in disease course with presentation of a neck mass at the time of diagnosis. Approximately 60% to 85% of the patients are first diagnosed with the disease already having cervical metastasis.

Epstein-Barr virus is associated with the disease. Most (80% to 90%) of the patients have an elevated level of immunoglobulin A (IgA) antibodies to the viral capsid antigen (VCA) and early antigen (EA). Transnasal biopsy is the gold standard to diagnose the nasopharyngeal mass, although fine-needle aspiration may suffice in the detection of occult primary tumor. External beam radiation is the common approach to treat nasopharyngeal cancer. Chemotherapy may serve as an adjuvant treatment when metastasis is detected. The 3-year survival for locoregional disease is 34% to 48%. The distant failure rate has been reported as 18% to 35%.

Case 12.4

History

63-year-old male who has a history of squamous oral cancer. His most recent CEA level is 6.3 and has been rising. His last PET study demonstrates elevated uptake in the left parotid gland. He now presents with an enlarged left neck lymph node and a right upper jaw pain. Evaluation for malignancy is requested.

Findings

There is a large area of mildly intense hypermetabolic activity in the left parotid (*Figures 12.4.1 and 12.4.2*) as well as the submandibular gland (*Figure 12.4.3*) consistent with inflammatory changes. There is evidence of right mandibular surgery with graft and plate placement. The right parotid gland has been surgically removed. There is no evidence of significant hypermetabolic activity on the right neck to indicate residual or recurrent tumor. In the abdomen, there is mildly intense activity along the distribution of the GI tract considered to be physiological. There is mildly increased activity in the left hip consistent with inflammatory arthritis.

Impression

1. No evidence of residual or recurrent tumor in the head and neck region.
2. Mildly increased activity in the left parotid and submandibular gland consistent with inflammatory changes.

Pearls and Pitfalls

- *The overall diagnostic accuracy of PET in head and neck cancer is 86% depending on the type of cancer and area evaluated.*[3,5,8,11,12]

Discussion

False-positive findings with FDG imaging are commonly seen with inflammatory processes, such as with infections, granulomas, abscesses, and postsurgical changes.

FIGURE 12.4.1.

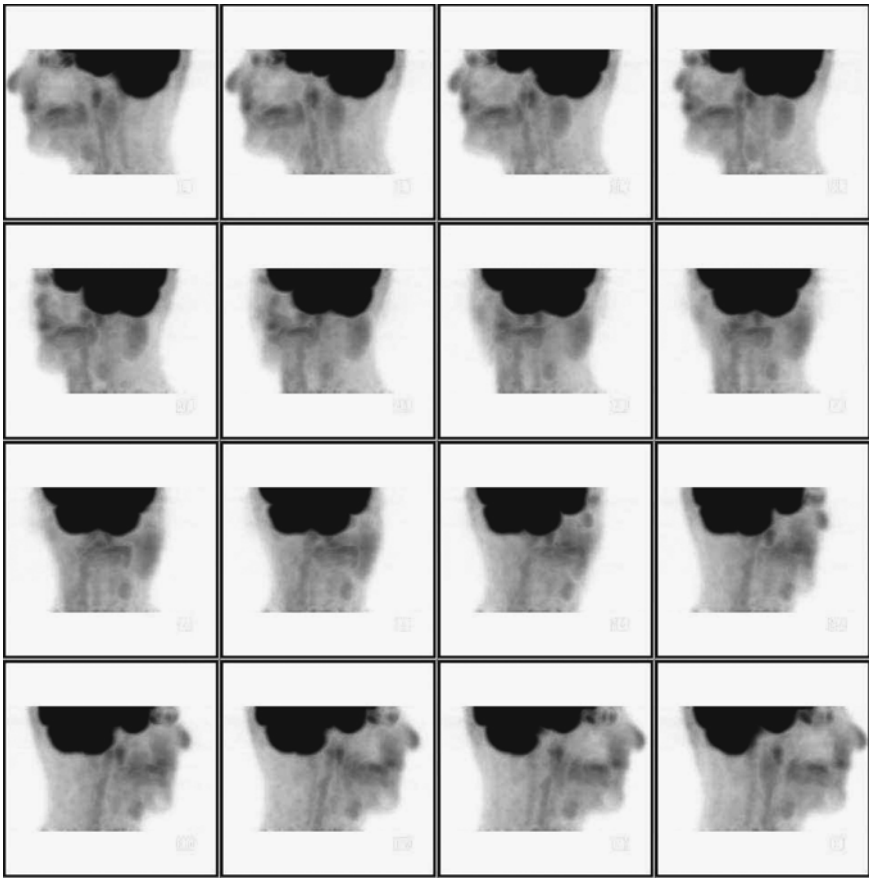

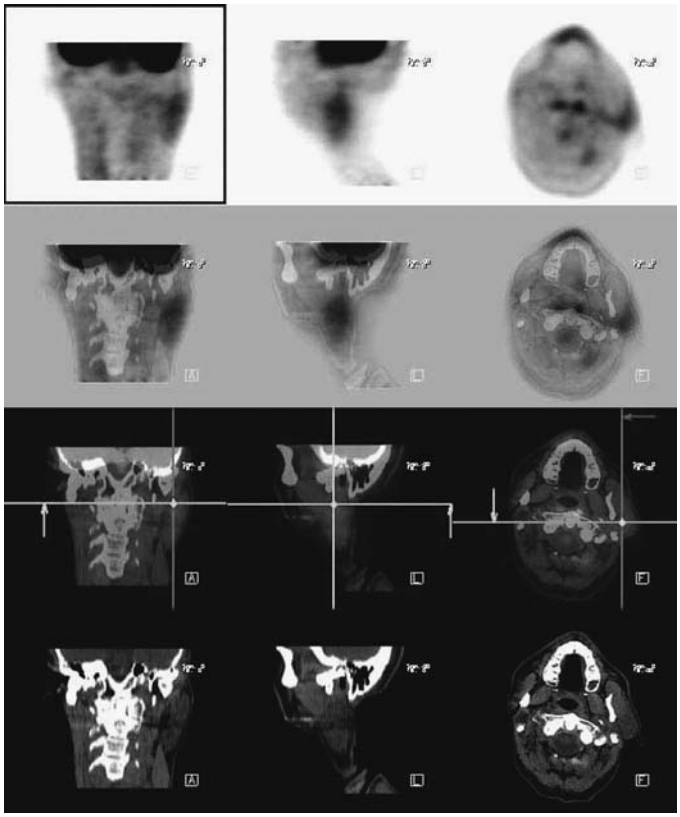

FIGURE 12.4.2.

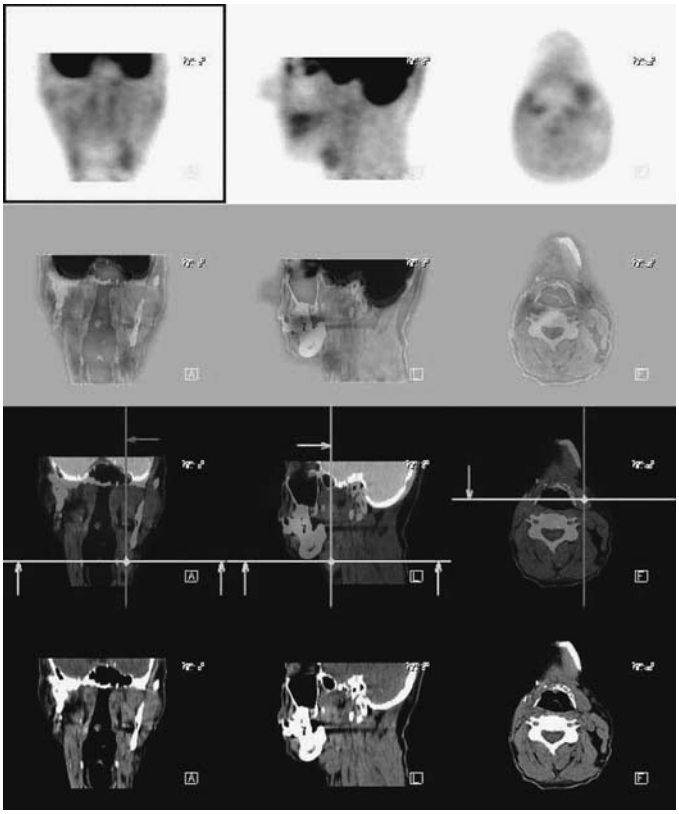

FIGURE 12.4.3.

These are benign processes that accumulate FDG and can easily be confused with malignant lesions.

Case 12.5

History

50-year-old male who has a history of oral squamous cell carcinoma status post resection. Evaluation for recurrence is requested.

Findings

There is a hypermetabolic mass in the right posterior liver (*Figures 12.5.1 and 12.5.2*) that corresponds to a poorly visualized lesion on non-contrast CT compatible with either primary hepatoma or metastatic disease. There is asymmetric uptake involving the larynx, more on the right (*Figure 12.5.3*), that corresponds to minimal soft tissue fullness on CT, suspicious for malignancy or metastasis from the known primary cancer. The paraspinal activity is related to muscular uptake (*Figure 12.5.4*) and is considered physiologic.

Impression

Hypermetabolism involving the right posterior hepatic mass and soft tissue fullness in the right larynx consistent with malignancy.

Pearls and Pitfalls

- *PET is useful for identifying distant metastatic disease in head and neck cancers.*[2,3,10,11,13,14]

Discussion

The TNM staging system of the American Joint Committee on Cancer (AJCC) maintains uniformity in the staging of head and neck tumors. Prognosis correlates strongly

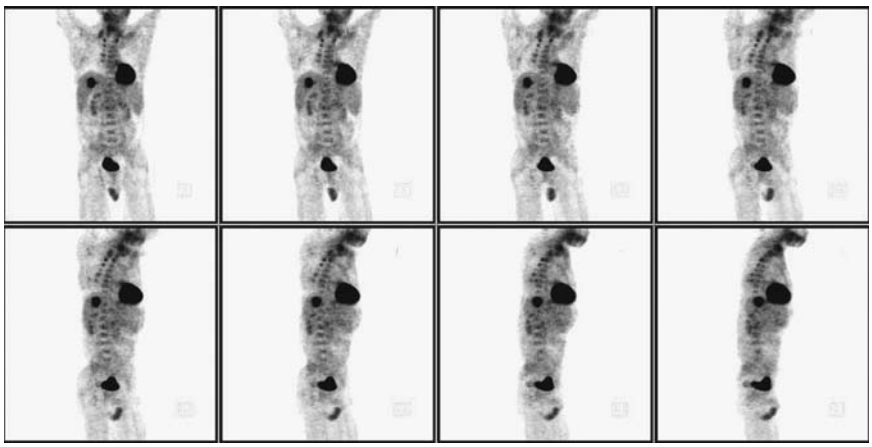

FIGURE 12.5.1.

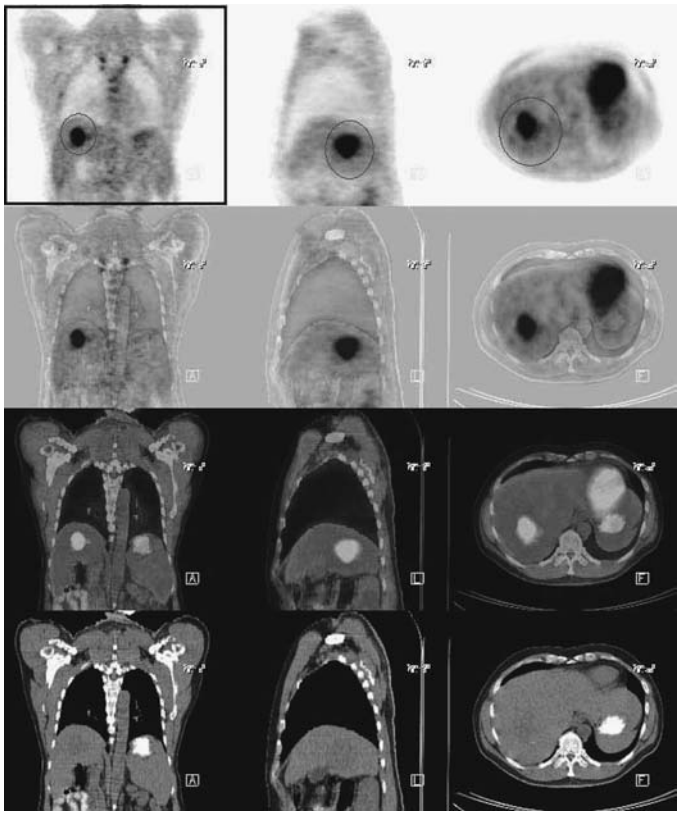

FIGURE 12.5.2.

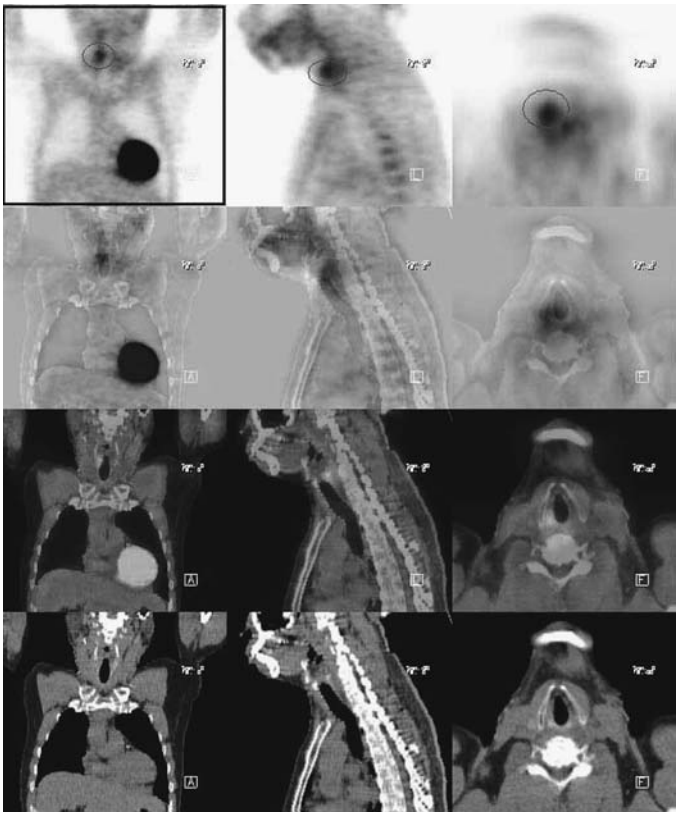

FIGURE 12.5.3.

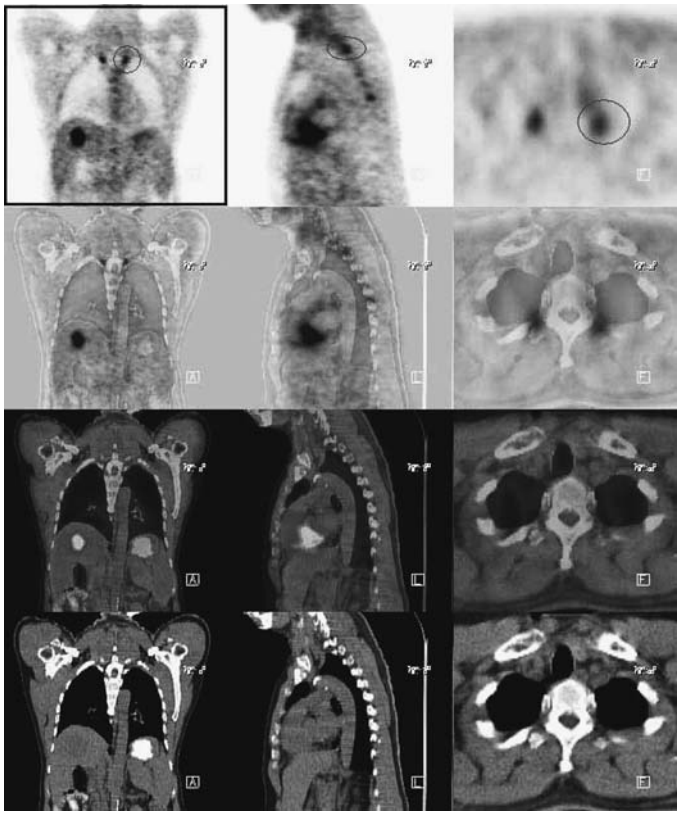

FIGURE 12.5.4.

with stage at diagnosis. For many head and neck cancer sites, survival for patients with stage I disease exceeds 80%. For patients with locally advanced disease at the time of diagnosis, stages III and IV, survival drops below 40%. Development of nodal metastases reduces survival of a small primary tumor by ≈50. Involvement of even a single lymph node is associated with a marked decline in survival. Most patients with head and neck cancer have stage III or IV disease at diagnosis.

Case 12.6

History

44-year-old female who had the diagnosis of palate carcinoma seven years ago with recurrence. She is status post radiation therapy, resection of recurrent tumor twenty months ago, and status post recent gamma knife therapy. An MR demonstrated a right infratemporal fossa tumor recurrence with right mandible infiltration and two lymph nodes in the submandibular area.

Findings

The examination of the head and neck is abnormal. There is a curvilinear band of abnormal activity in the right infratemporal fossa (*Figures 12.6.1 and 12.6.2*), consistent with metastatic disease. It is parallel to and probably involving the upper right mandibular ramus. There are also two weakly positive subcutaneous nodes near the angle of the right mandible. The middle cranial fossa finding reported on MR is not seen on PET-CT. Decreased temporal cortical activity consistent with prior radiation is noted on PET. Also noted was a right posterolateral tracheal focus of either adherent mucus or, less likely, a polyp. No pulmonary nodules are apparent.

The torso exam appears negative. No distant metastases are apparent. The CT shows relatively low iodine content of the thyroid isodense with muscular tissue. A TSH is suggested to evaluate for functionally significant thyroid disease, if not recently performed.

Impression

1. Abnormal activity consistent with regional metastasis to the infratemporal fossa along and probably involving the upper right mandibular ramus.

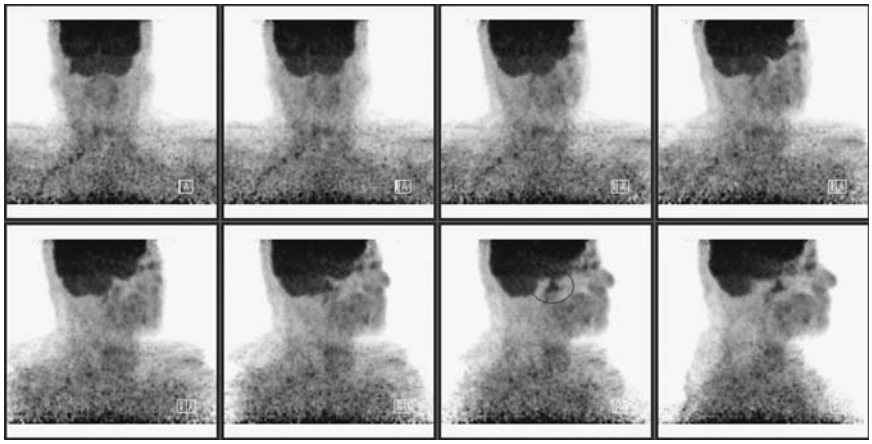

FIGURE 12.6.1.

FIGURE 12.6.2.

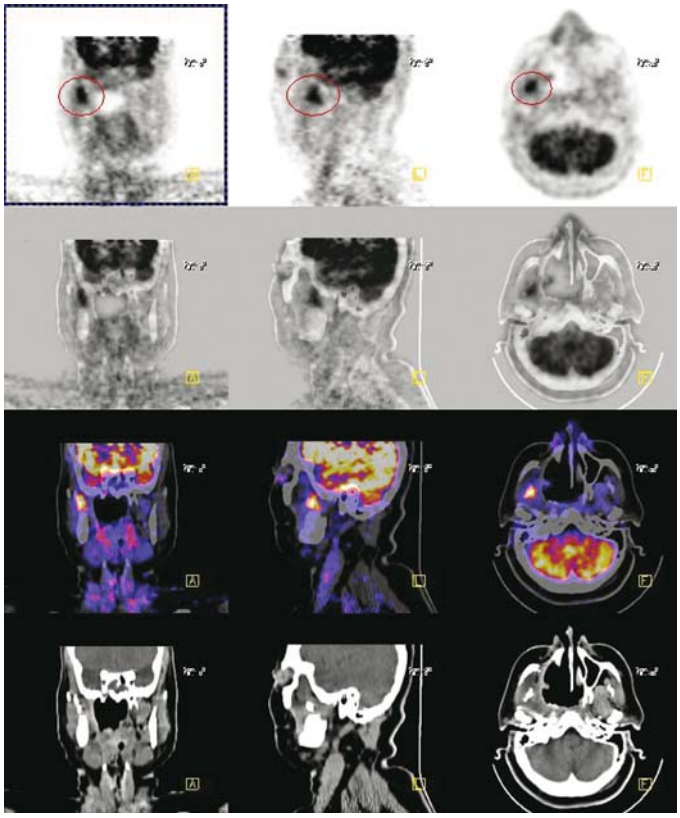

2. Two subcutaneous nodes near the angle of the right mandible are weakly positive and also suspicious for metastasis.
3. Post radiation changes in right temporal cortical activity.

Pearls and Pitfalls

- *CT is best to assess bony invasion of the palate, maxillary sinus, and its adjacent structures. It is an invaluable for staging. Contrast infusion can assess for cervical nodal involvement. MRI can be used to evaluate for perineural invasion.*[4,7]

Discussion

The palate is divided into the hard palate and the soft palate. Two percent of the head and neck malignancies involve the soft palate; 80% of the cancers are squamous cell carcinoma. Tobacco and alcohol are predisposing factors. Most patients are asymptomatic in early stage disease. Only in advance stage disease will the patient present with painful ulceration, bleeding, and dysphagia.

Ten to fifteen percent of the patients with squamous cell carcinoma of the head and neck have a synchronous second primary cancer in the upper aerodigestive tract. It is important to perform panendoscopy to assess for either synchronous or metachronous lesions. Local biopsy is typically performed under local anesthesia to evaluate the extent of locoregional tumor involvement.

Case 12.7

History

73-year-old male with a history of soft palate surgery. He is status post maxillary sinus surgery.

Findings

There has been resection of the medial wall of the left maxillary sinus (*Figure 12.7.1*). The most intense regional hypermetabolism, however, is in the left maxillary alveolar ridge (*Figure 12.7.2*) in the molar area, centered in the bone and probably of dental or osseous origin. There is moderate hypermetabolism of the walls of the left maxillary sinus as well as of the soft tissues of the face anterior to the left maxillary sinus. The fact that the most intense hypermetabolism is in the left maxillary alveolar ridge favors a dental origin. In the chest, there is ground glass density in the posterior segment of the right upper lobe (*Figure 12.7.3*). This is moderately hypermetabolic on 18-FDG PET scintigraphy. In view of the history of recent surgery, this may well represent alveolitis associated with aspiration. However, follow-up CT would be recommended, because differential diagnosis for ground glass density in this location with moderate hypermetabolism would also include active granulomatous disease and bronchioalveolar type neoplasm. There are several incidental findings in the lung, with a calcification at the dome of the left base, a small linear density in the anterior segment of the left upper lobe, both findings of doubtful clinical significance. In the abdomen, there are multiple bilateral renal cysts. Two small cysts on the left are more than water density. Ultrasound is recommended if not previously performed to exclude a solid lesion. There is also a small cyst in the lateral segment of the left lobe of the liver, an incidental notation of degenerative disc disease and facet arthropathy at the lumbosacral junction.

Impression

1. Intense focal hypermetabolism of the molar area of the left maxillary alveolar ridge. There is moderate general activity of the base of the left maxillary sinus and of its walls, as well as soft tissue anterior to the sinus in the face. Findings indicate a likely dental origin and infection and tumor are both in the differential diagnosis.
2. Ground glass density of moderate hypermetabolism in the posterior segment of the right upper lobe, for which follow-up is needed.
3. Two of the left renal cysts are greater than water density.

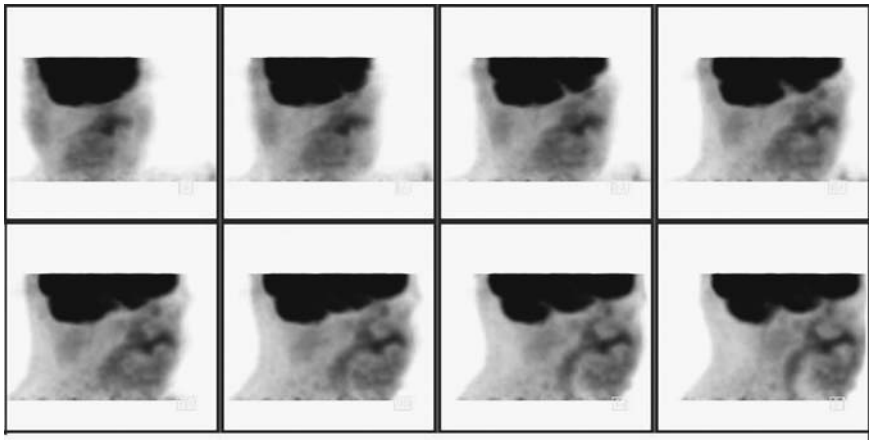

FIGURE 12.7.1.

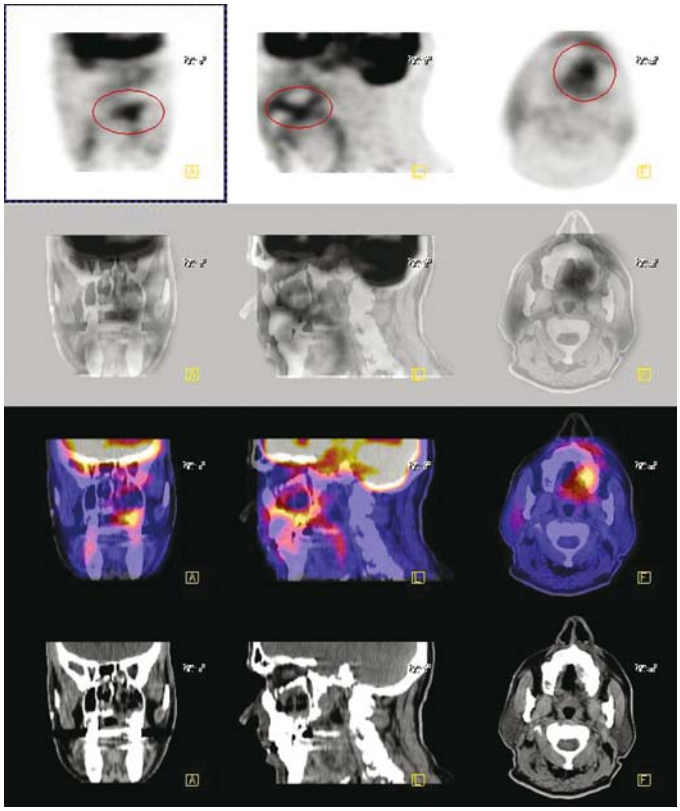

FIGURE 12.7.2.

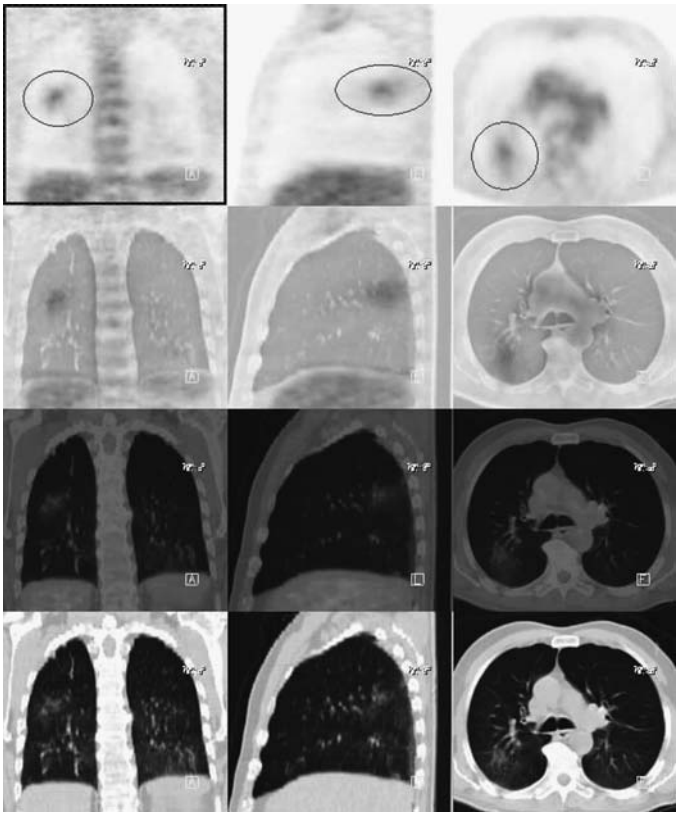

FIGURE 12.7.3.

Pearls and Pitfalls

- *MRI with gadolinium can determine the extent of brain parenchymal involvement as well as its associated structures, in particular the foramen ovales, spinosum, and lacerum. The carotid canal and the jugular foramen are also places to examine for metastasis. PET can offer additional way to examine the nasopharynx and the skull base when CT and MRI are in doubt.*[3,4,7]

Discussion

The treatment of squamous cell carcinoma of the hard palate is primarily resection. Radiation therapy may be an alternate approach for more extensive invasion. The treatment of soft palate tumor depends on the extent of tumor spread, with radiation therapy being the mainstay of treatment. For advanced lesions, chemotherapy is used as an adjunctive treatment.

Case 12.8

History

59-year-old male who has a history of right parotid cancer followed by resection. Evaluation for metastasis is requested.

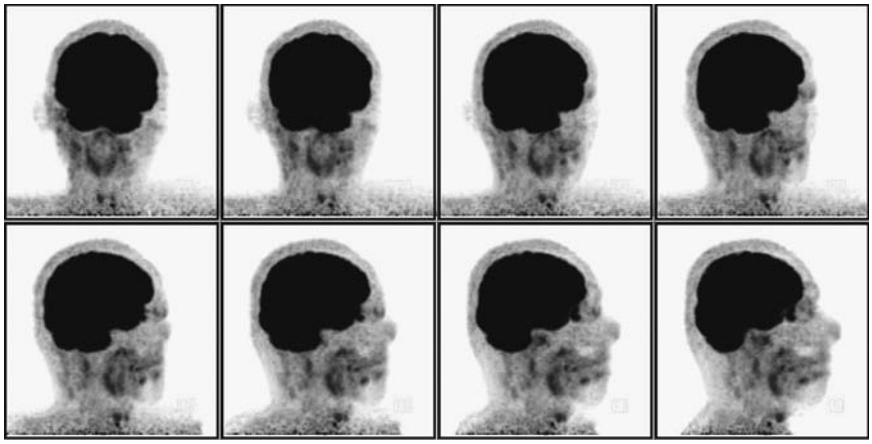

FIGURE 12.8.1.

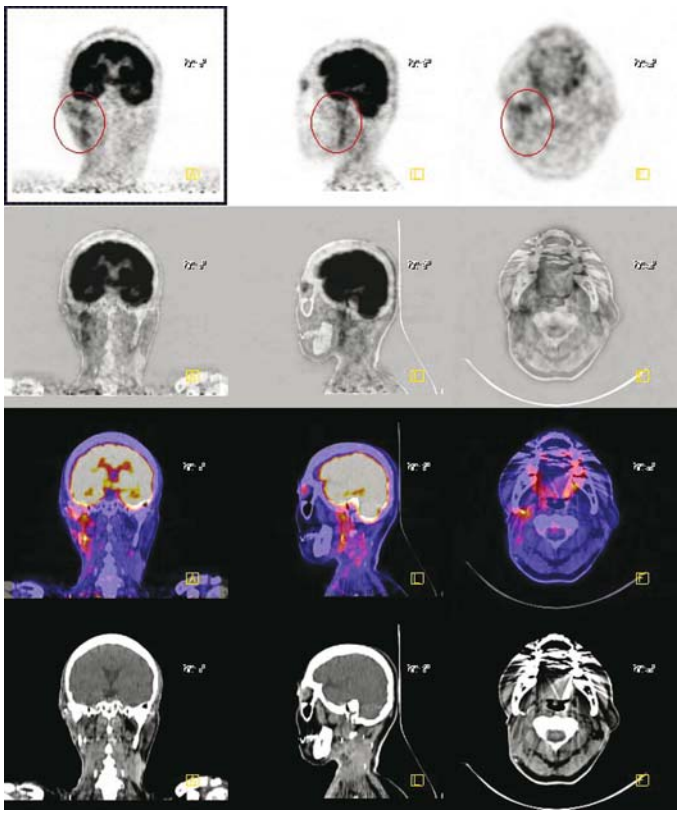

FIGURE 12.8.2.

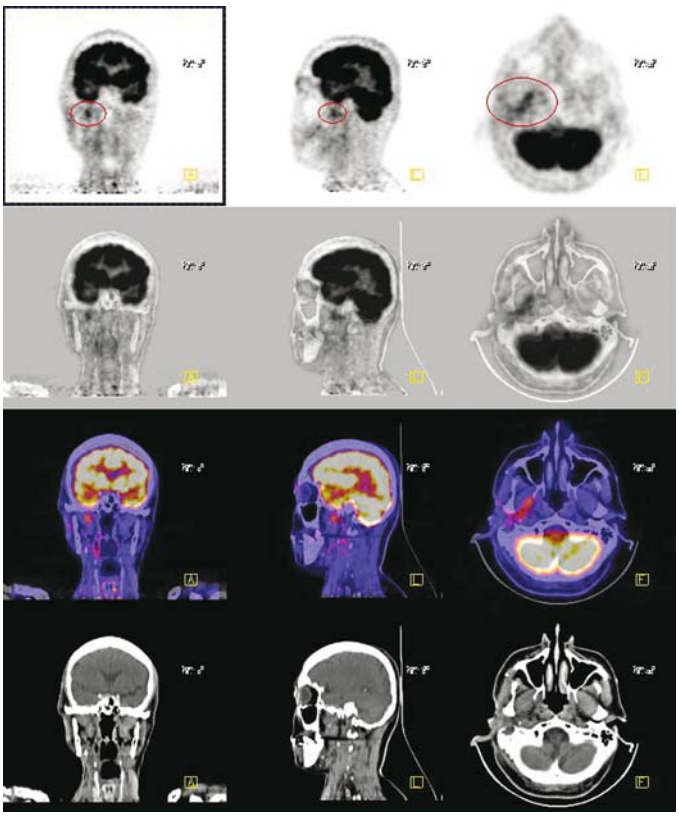

FIGURE 12.8.3.

Findings

Abnormal uptake on the right side deep to the angle of the mandible to the right of the parotid is noted (*Figures 12.8.1, 12.8.2, and 12.8.3*). However, because there is no recent manipulation in this area, the uptake is most likely related to metastasis or locally recurrent disease. Bilateral hilar adenopathy with mild elevated uptake is noted (*Figures 12.8.4 and 12.8.5*). The mild uptake in the left upper chest is consistent with a pacemaker (*Figure 12.8.6*). The mild activity in the wall of esophagus is likely secondary to inflammation.

FIGURE 12.8.4.

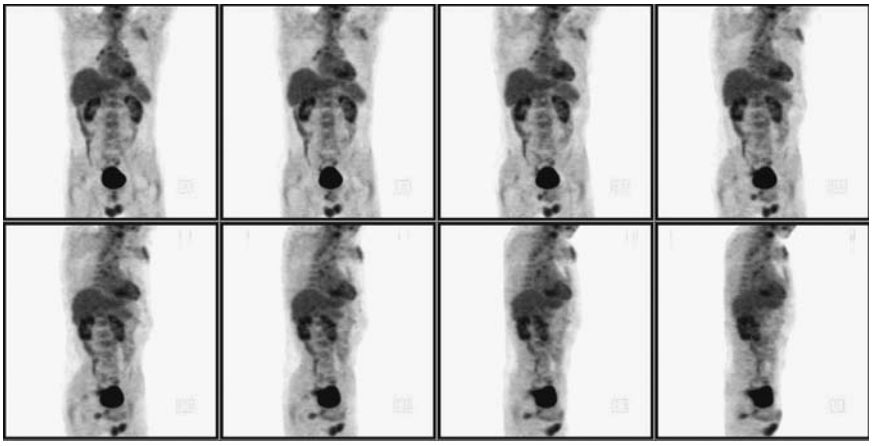

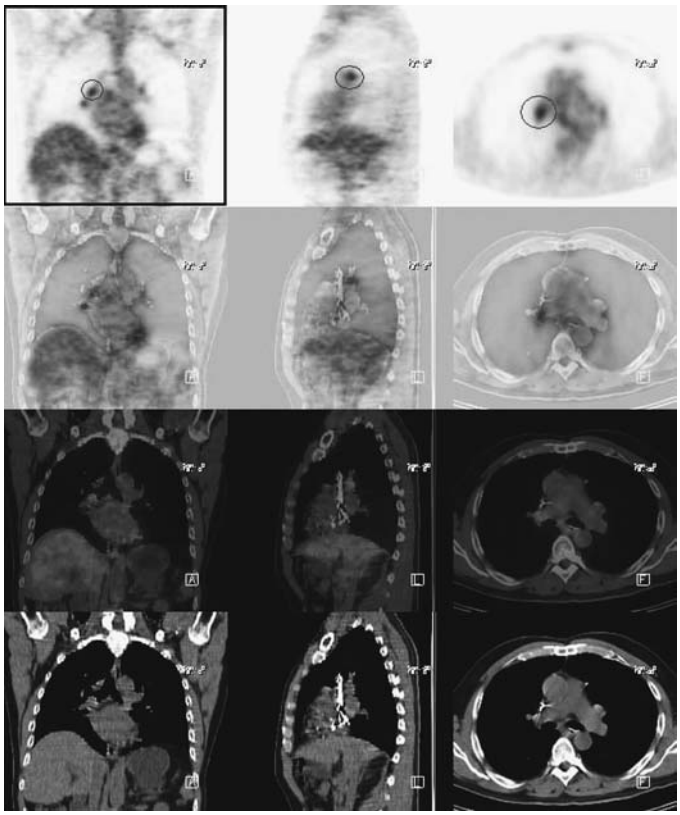

FIGURE 12.8.5.

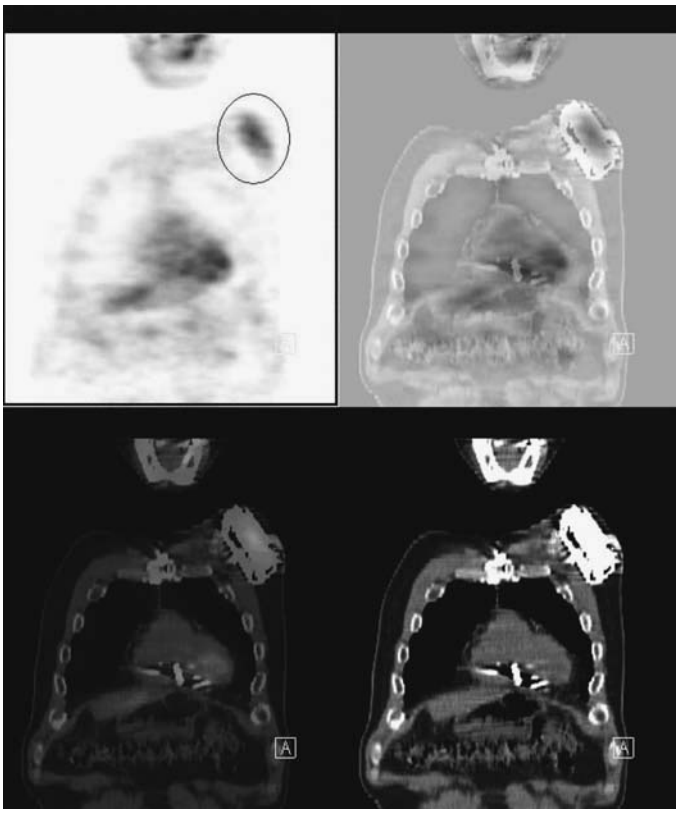

FIGURE 12.8.6.

Impression

1. Suspicious uptake near the region of the right parotid gland, deep to the angle of the mandible. A repeat PET-CT is indicated in 3 months if the decision is to observe the patient.
2. Bilateral hilar adenopathy is probably related to inflammatory changes.
3. Mild uptake in the left upper chest is consistent with inflammation associated with a pacemaker.
4. Mild esophageal uptake secondary to inflammation.

Pearls and Pitfalls

- *Parotid cancers are not uncommonly identified by PET as a source of primary head and neck cancer.*[3,12,14]

Discussion

Eighty-five percent of the salivary gland tumors arise from parotid glands, and 75% are benign. The most common nonneoplastic cases include cysts, parotitis, and lymphoepithelial lesions associated with benign hypertrophy, collagen vascular diseases, and AIDS.

A painless, asymptomatic mass is the most common initial presentation. Eighty percent of the masses involve the cheek. Malignancy is likely when there is evidence for perineural invasion. Facial nerve paralysis is a poor prognostic indicator; 80% of these patients will have nodal metastatic involvement with a 10-year survival rate of 14% to 26%. Trismus and dysphagia are also indicators for malignancy.

Case 12.9

History

72-year-old male who has a history of squamous cell carcinoma involving the right parotid gland. He was treated with radiotherapy and resection, with facial reconstructions. Evaluation for recurrence is requested.

Findings

There is intense hypermetabolism in the right parotid region (*Figures 12.9.1 and 12.9.2*) highly suspicious for locally recurrent disease. There is asymmetric hypermetabolism involving the left posterior aspect of the hard palate (*Figure 12.9.3*). The right Rosenmüller's fossa is also hypermetabolic with associated soft tissue irregularity on CT. There is slight asymmetry in the tonsillar activity, considered physiologic. Dental metallic implant artifact is present. No hypermetabolic distant lesions are seen.

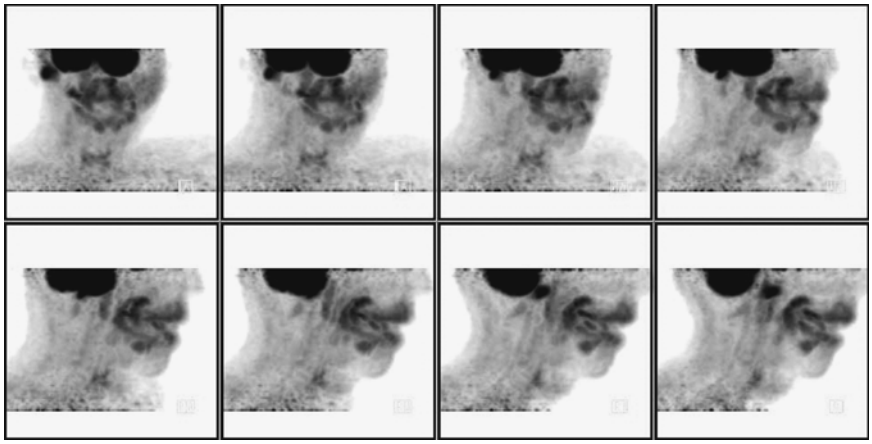

FIGURE 12.9.1.

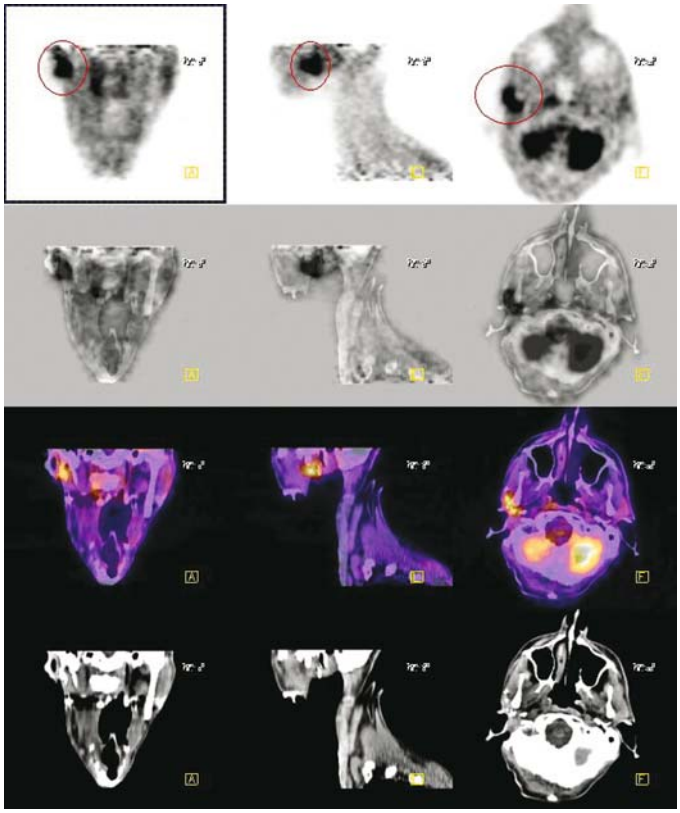

FIGURE 12.9.2.

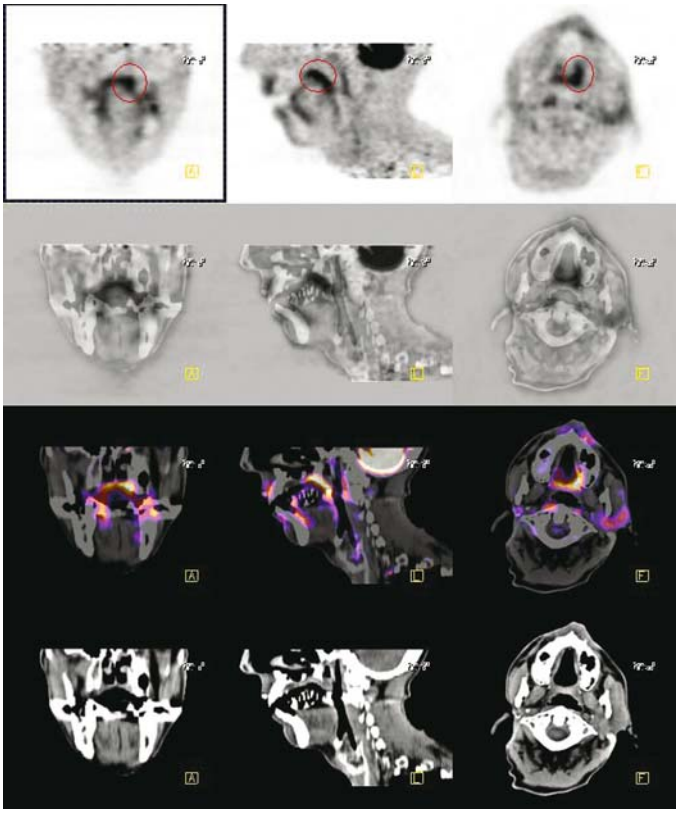

FIGURE 12.9.3.

Impression

1. Intense hypermetabolism involving the right parotid region highly suspicious for locally recurrent tumor.
2. The hypermetabolism in the left posterior hard palate and the right Rosenmüller's fossa may be related to infection, evolving post therapy inflammation, or spread of malignancy. Direct endoscopic examination would be helpful.
3. No evidence for distant metastatic disease.

Pearls and Pitfalls

- *False-positive PET for benign parotid tumor such as Warthin's tumor and pleomorphic adenomas can limit the specificity (reported as 63%) from true malignancy.*[1,3,14]
- *CT scan can determine the extent of lymph node metastasis by size criteria, particularly in those lesions larger than 1 cm to 1.5 cm, multiple enlarging lymph nodes, and nodes with central necrosis.*[4,13]
- *MRI can assess the size of the soft tissue mass. It can reveal the extent of tumor invasion to the adjacent tissue and parapharyngeal space.*[9,11,14]

Discussion

Most parotid tumors are in the superficial lobe. Surgery followed by radiation therapy is currently the mainstay of treatment. As in this case, only superficial parotid lobectomy is needed. This is especially true with tumors confined to the superficial lobe, low

grade by histology, and less than 4-cm in size without evidence for local invasion. The overall 5-year survival for all stages is 62% and the 5-year survival for recurrent disease is 37%.

Case 12.10A

History

51-year-old male who has a history of tonsillar and submandibular cancer. The patient was later treated with radiation therapy. Evaluation for recurrence is requested.

Findings

A focal site of intense uptake is noted superficially anterior to the sternum. This is probably related to an implant. On CT, multiple staples are noted in the anterior triangle of the left neck consistent with prior surgery. Mild to moderate multifocal activity in muscle is seen, likely physiologic in nature. Due to the patient's known prior malignancy, this might obscure any abnormalities within this region. No abnormal uptake is seen in the mediastinum, abdomen, or pelvis. No residual tumor in the neck is observed (*Figure 12.10A.1*).

Impression

1. No evidence for primary local recurrence or metastasis.
2. A repeat scan is advised in three months.

Pearls and Pitfalls

- *A mean reduction of 82% from the baseline SUV is suggestive of a favorable outcome after therapy.*[8,11,14]
- *Premedication with 10 mg–20 mg of a benzodiazepine (e.g. Valium) can reduce physiological muscle uptake.*

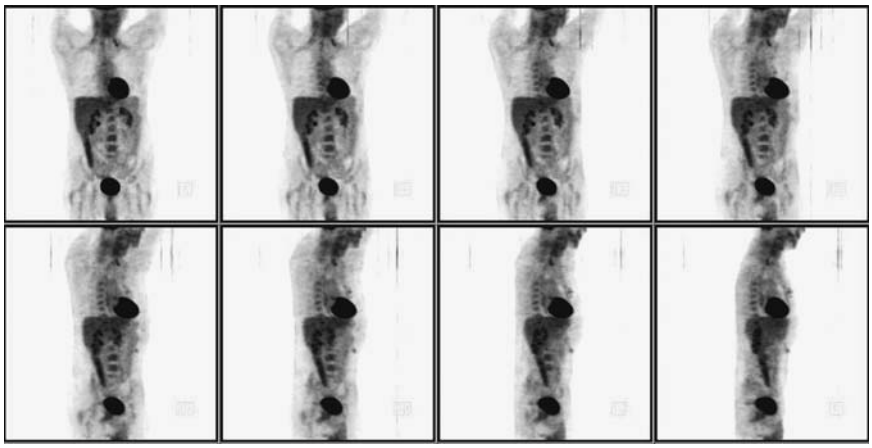

FIGURE 12.10A.1.

Discussion

Radiation therapy with curative intent usually involves daily treatment for 6 to 7 weeks (total dose, 60 Gy–70 Gy). Although there is no tissue loss with radiation therapy, complications include dry mouth, tissue fibrosis, trismus, bone necrosis, and hypothyroidism. Some problems are very common and sufficiently debilitating to warrant significant concern in treatment planning for head and neck cancer. Surgery often produces less morbidity.

Case 12.10B

History

52-year-old male status post surgery for tonsillar cancer. He underwent left neck dissection and flap. He has received radiation therapy. The study is being done to evaluate for tumor recurrence.

Findings

The head and neck evaluation is very limited due to patient motion and dental artifacts (*Figures 12.10B.1 and 12.10B.2*). There is evidence for left neck dissection. There is a large and intensely hypermetabolic mass located to the right of midline in the area of the tongue consistent with tumor recurrence (*Figure 12.10B.3*). No evidence of regional lymphadenopathy seen. There is some hypermetabolic activity (*Figure 12.10B.4*) anterior to the left of midline likely related to post surgical reconstruction. In the abdomen, there is mild hypermetabolic activity located just left of midline consistent with a percutaneous feeding tube (*Figure 12.10B.5*). No evidence for hypermetabolic activity in the pancreas and adrenals to indicate metastatic disease. Activity in the kidney and GI tract is physiologic.

Impression

Intense hypermetabolic activity in the left tongue, compatible with tumor recurrence.

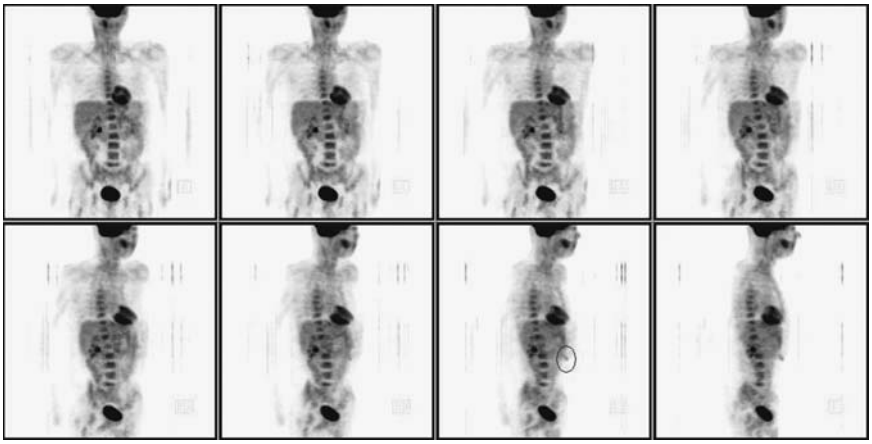

FIGURE 12.10B.1.

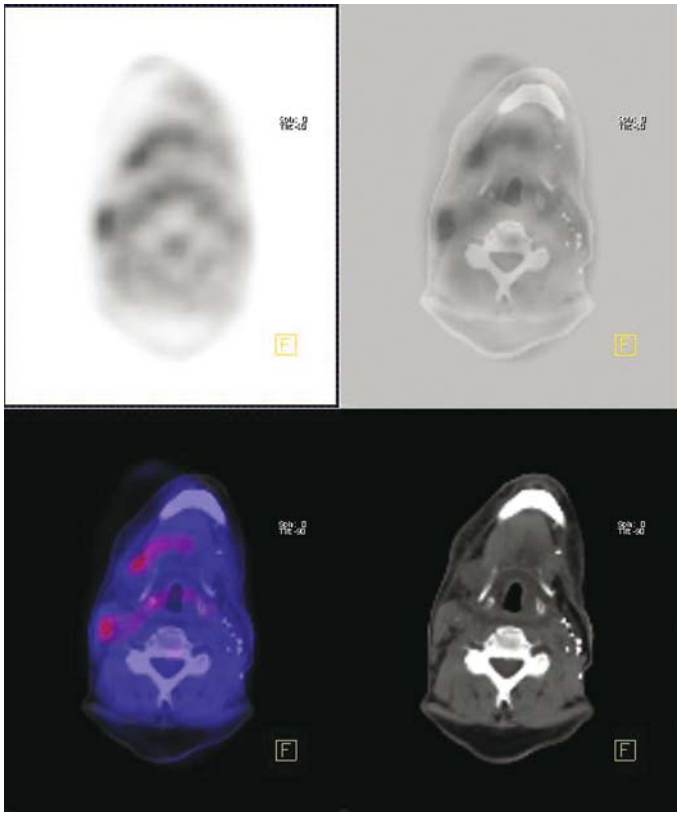

FIGURE 12.10B.2.

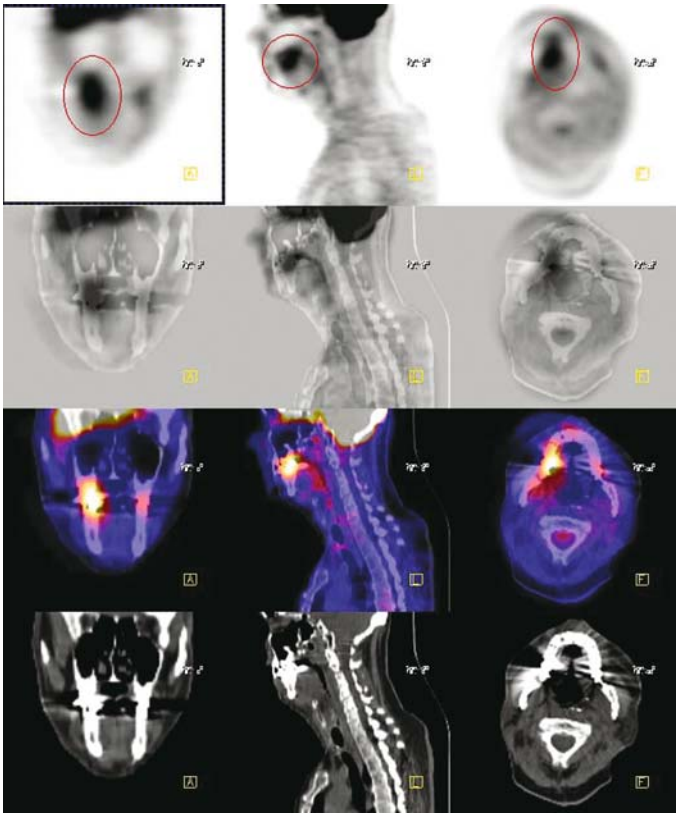

FIGURE 12.10B.3.

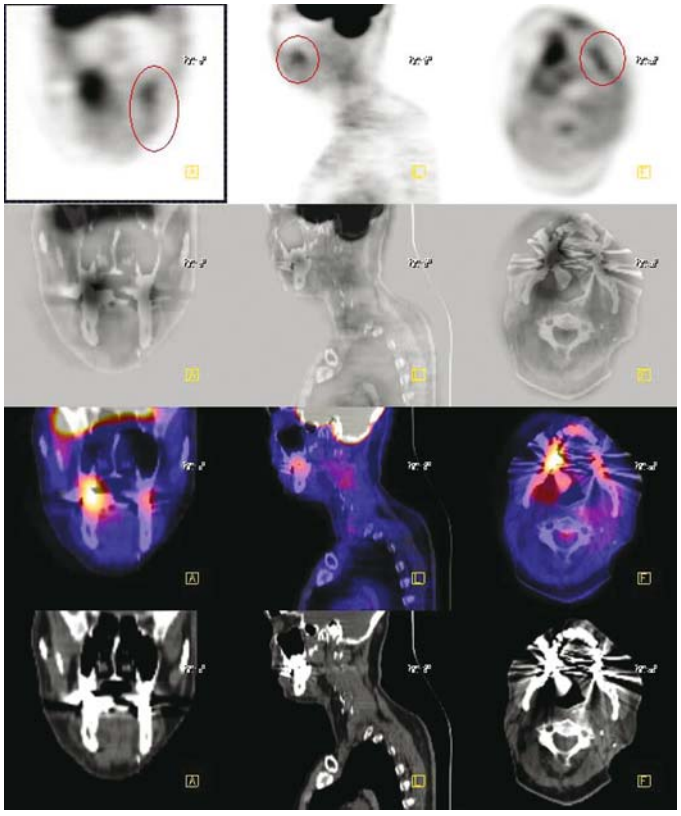

FIGURE 12.10B.4.

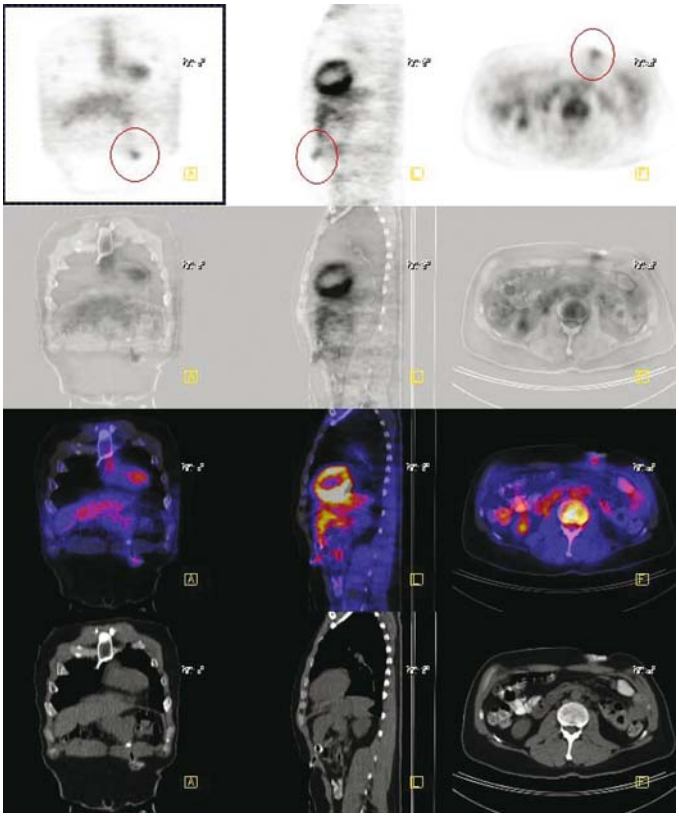

FIGURE 12.10B.5.

Pearls and Pitfalls

- *To avoid a false-positive PET study due to inflammatory changes, a waiting period of 5–7 days is recommended following needle biopsy and at least two weeks following surgical resection.*[3,5,12]

Discussion

Stages I and II disease at most sites may be treated with either resection or radiation therapy. The best therapeutic approach for the primary tumor depends on the anatomic site. The approach to treatment of the neck also varies with site and treatment of the primary tumor. A neck dissection in a clinically negative neck might be considered optional for primary tumor of the oral cavity, but would typically be performed in association with pharynx operations since resection would require incision/dissection in the neck. Neck dissection should remain standardized (i.e., complete anatomic dissections, as opposed to "berry picking" or random biopsy) in these settings so as to avoid incomplete surgery.

13 Heart Viability

Lalitha Ramanna

Case 13.1

History

55-year-old male who has a history of coronary artery disease status post CABG. The rest and stress thallium examination revealed mild apicolateral wall ischemia and transmural scar involving the inferior, inferoapical walls. Evaluation for heart viability is requested.

Findings

There is hypometabolism seen involving the midportion of the inferior wall consistent with transmural infarction and matching the resting perfusion exam results (*Figures 13.1.1 and 13.1.2*). There is viability present in the inferoapical and proximal posterior wall (*Figures 13.1.3 and 13.1.4*). These findings are suggestive of a significant circumflex artery deficit with the presence of scar in a third of the inferior posterior wall. The remaining two-thirds of the posterior wall is metabolically preserved but compromised.

Impression

Nonviable myocardium in the mid inferior wall.

Pearls and Pitfalls

- *FDG will be trapped in the myocardium since the phosphorylated form cannot be further metabolized.*[4,11]
- *The myocardium is considered viable if uptake of FDG is present even in the absence of resting perfusion.*[1,3,4,6,8]
- *80% to 85% of the myocardial ischemic patients will improve following revascularization.*[3,4,11]

Discussion

The myocardium preferentially oxidizes the fatty acids and lactate as energy substrates in the fasting state. When perfusion is compromised, this will increase the glycolytic

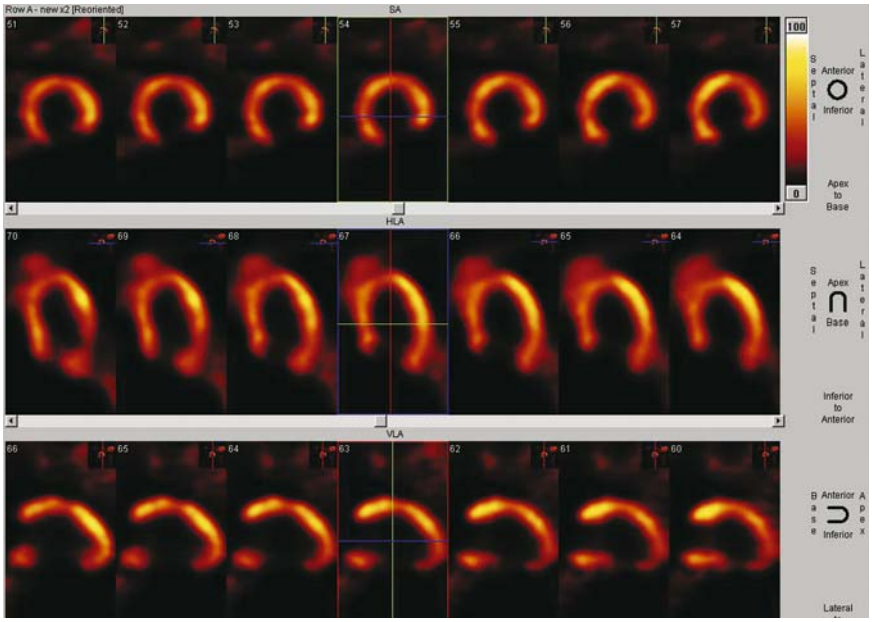

FIGURE 13.1.1.

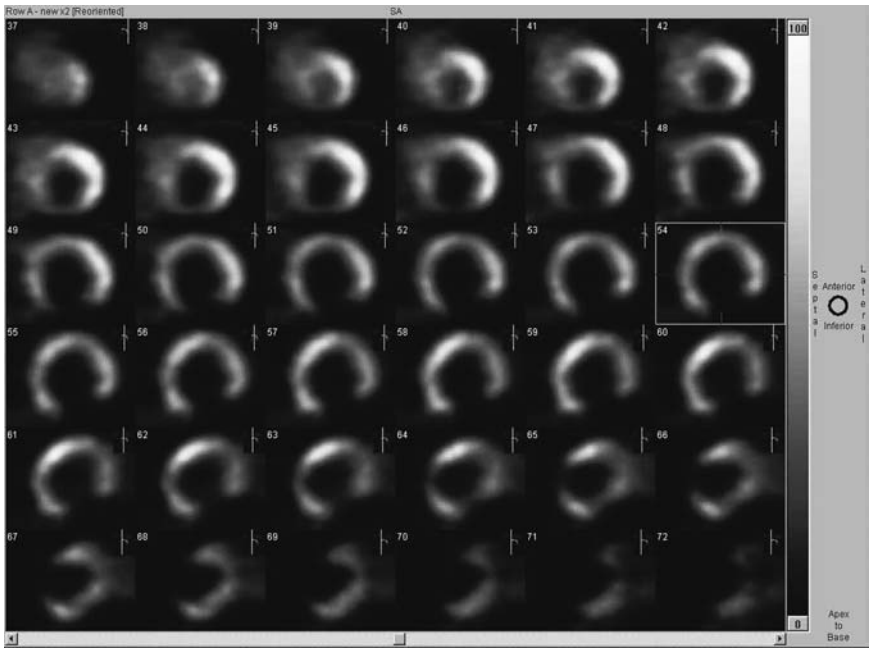

FIGURE 13.1.2.

flux and will increase exogenous glucose utilization. The myocyte can only maintain glycolysis if lactate and hydrogen ions do not accumulate to toxic levels. When the myocardium is still viable but incapable of sustaining mechanical work, it is considered in the state of hibernation. This is reflected in a perfusion-metabolism mismatch where resting perfusion is lost or reduced and glucose uptake is preserved. Contractility will improve with revascularization.

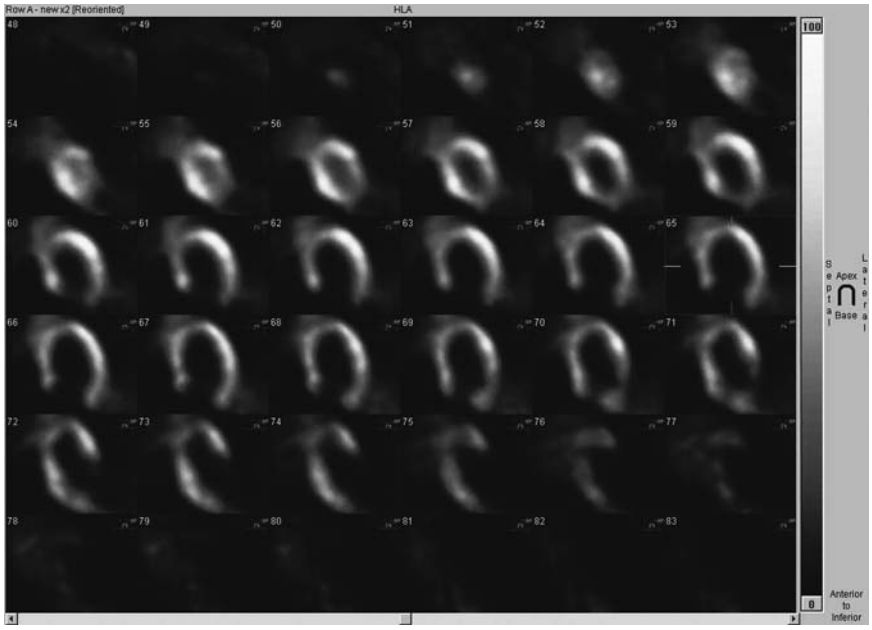

FIGURE 13.1.3.

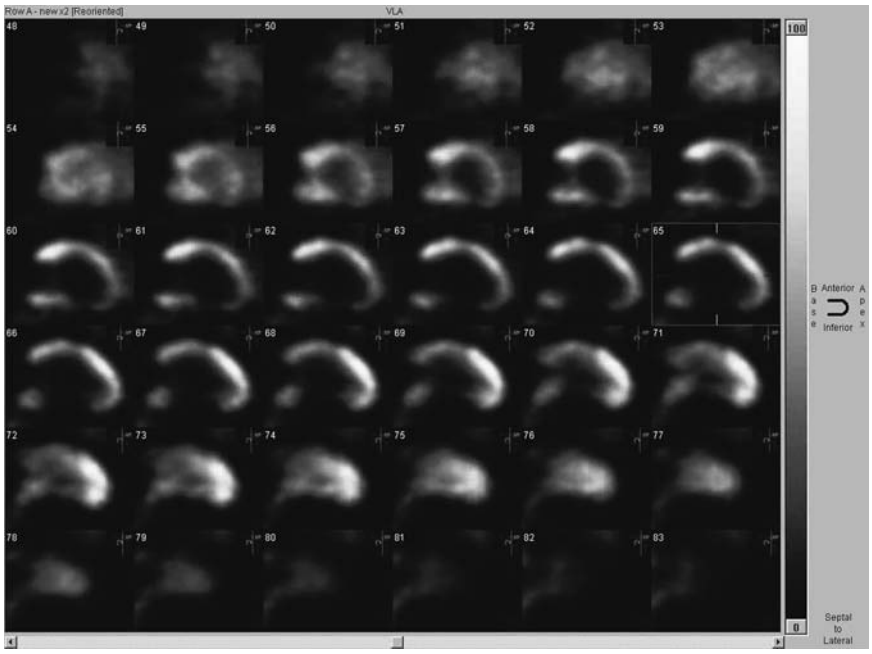

FIGURE 13.1.4.

Case 13.2

History

73-year-old female who has a history of coronary artery disease status post myocardial infarction involving the anterior and inferior wall. Her most recent thallium perfusion scan demonstrated transmural infarction involving the anteroseptal and anterolateral wall of the apical myocardium. There was mild to moderate ischemia in the infero-posterior wall. Evaluation for viability is requested.

FIGURE 13.2.1.

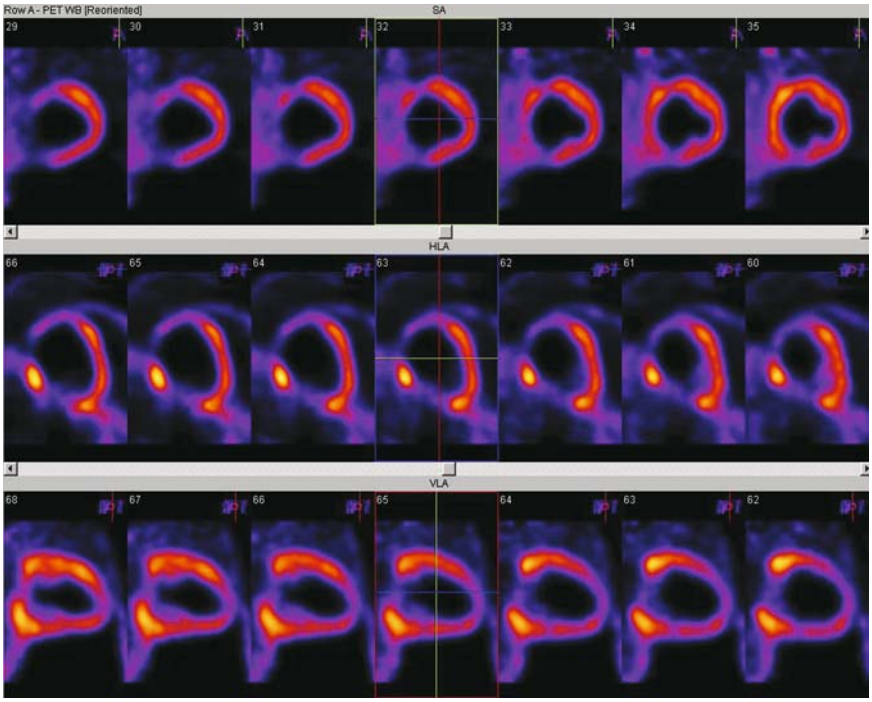

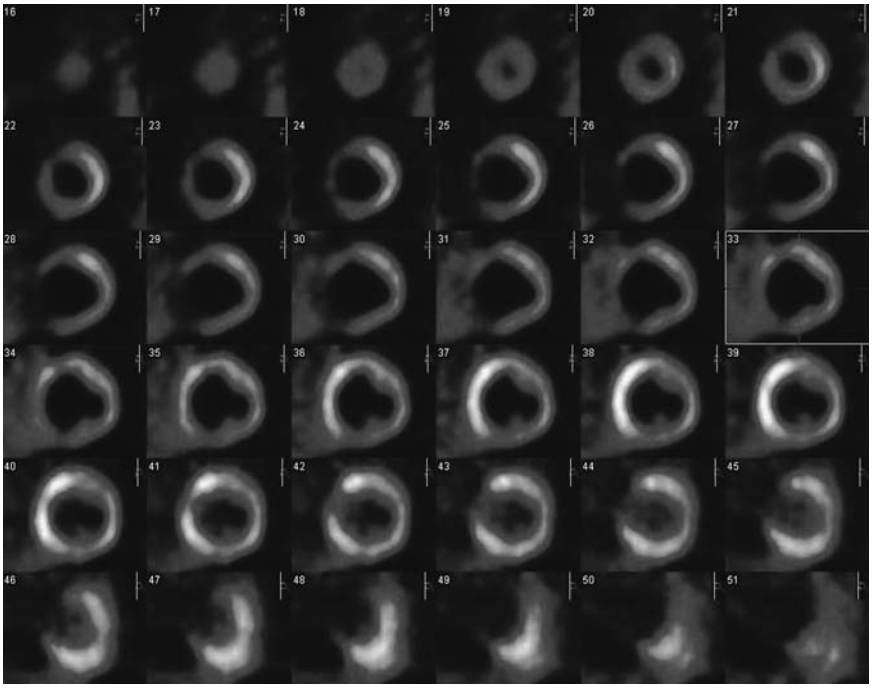

FIGURE 13.2.2.

Findings

There is a significant focal metabolic defect involving the mid anterior wall extending to the apicoseptal wall (*Figures 13.2.1 and 13.2.2*) similar to the anteroseptal defect seen in the SPECT myocardial perfusion study. There is also a small segment of focal pronounced defect involving the middle third of the inferior wall (*Figures 13.2.3 and 13.2.4*). These focal abnormalities represent nonviable tissue but only ten percent of

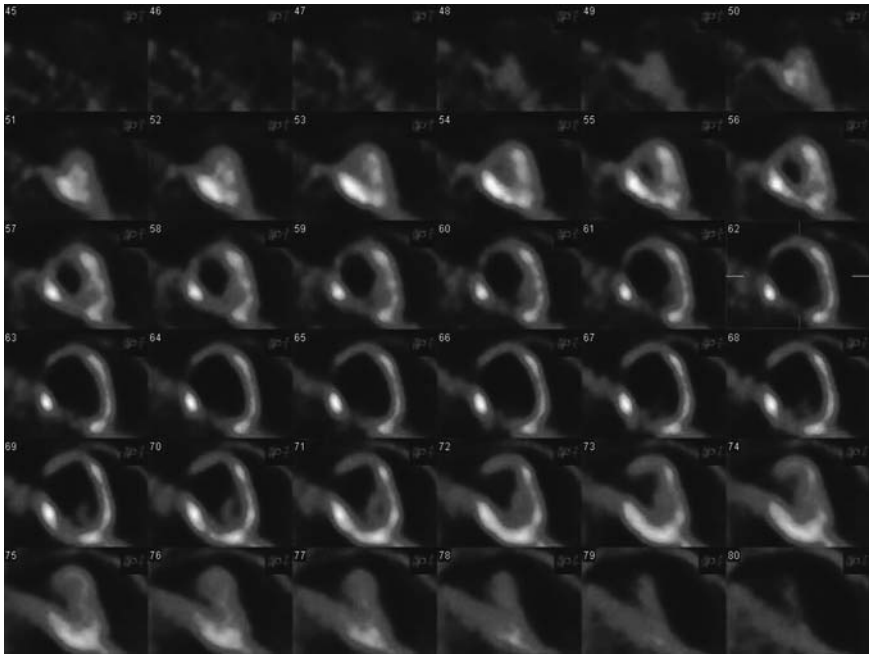

FIGURE 13.2.3.

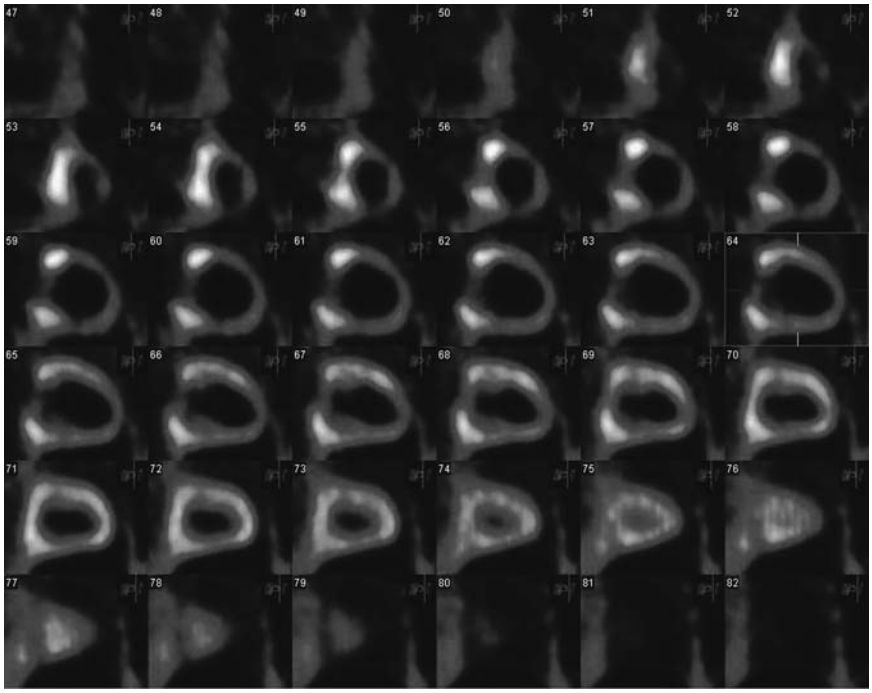

FIGURE 13.2.4.

the total left ventricular myocardium. The ischemia described on SPECT in the inferoposterior wall demonstrates preserved metabolism.

Impression

Significant metabolic defect involving the distal anteroseptal wall as well as the middle third of the inferior wall, compatible with infarction. This region is nonviable, but represents about 10% of the total left ventricular myocardium.

Pearls and Pitfalls

- *Oral glucose loading and hyperinsulinemic-euglycemic clamping are some of the ways used to optimize the image quality.*[2,5,8,9,10]
- *Nonviable tissue is considered a scar when both flow and metabolism demonstrate matched reduction.*[7]
- *PET can overestimate the potential for recovery in post-MI patients within one week of the initial event since the function of the myocardium may still be widely variable.*[1]

14 Inflammatory Disease and Infection

Lalitha Ramanna

Case 14.1

History

77-year-old female who has a history of ulcerative colitis status post colectomy, Koch pouch, and cholecystectomy. Her recent CT demonstrated significant dilatation involving the biliary ducts and colon. Evaluation for malignancy is requested.

Findings

There are multiple sites of hypermetabolism involving the glenohumeral joints (*Figures 14.1.1, 14.1.2A, and 14.1.2B*), right sternoclavicular joint (*Figure 14.1.3*), and humeri bilaterally. The sternoclavicular joints, more on the right, are also involved. The tracer localization to the metacarpal-carpal bones, more on the right, is also noted. Uptake in the hips, more prominent on the left, is noted. These findings are consistent with inflammatory joint disease. There is right renal stasis with evidence of caliectasis (*Figure 14.1.4*). The superficial lower right abdominal uptake is compatible with Koch's pouch (*Figure 14.1.5*). The activity at the base of the neck bilaterally is muscular uptake and is considered physiologic.

Impression

1. Multifocal inflammatory joint disease.
2. Koch's pouch.

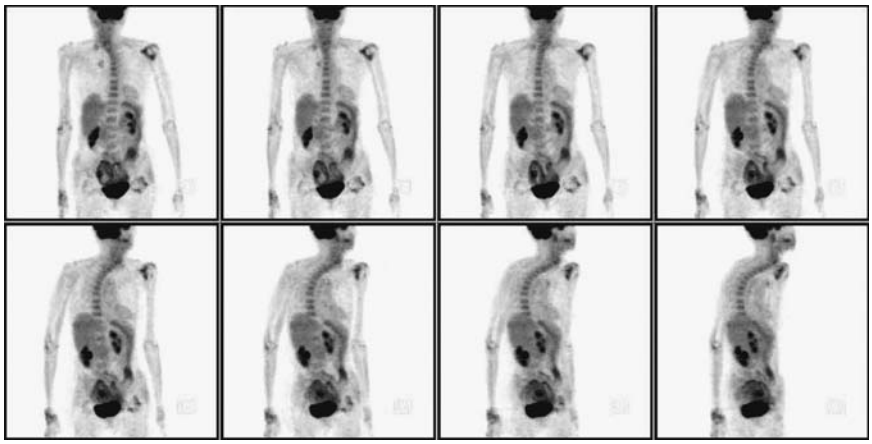

FIGURE 14.1.1.

FIGURE 14.1.2A.

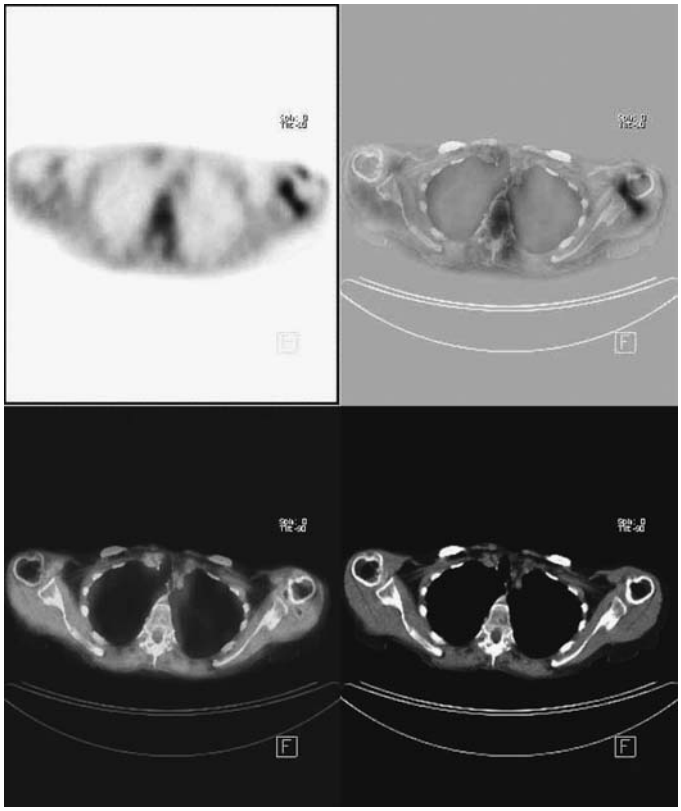

FIGURE 14.1.2B.

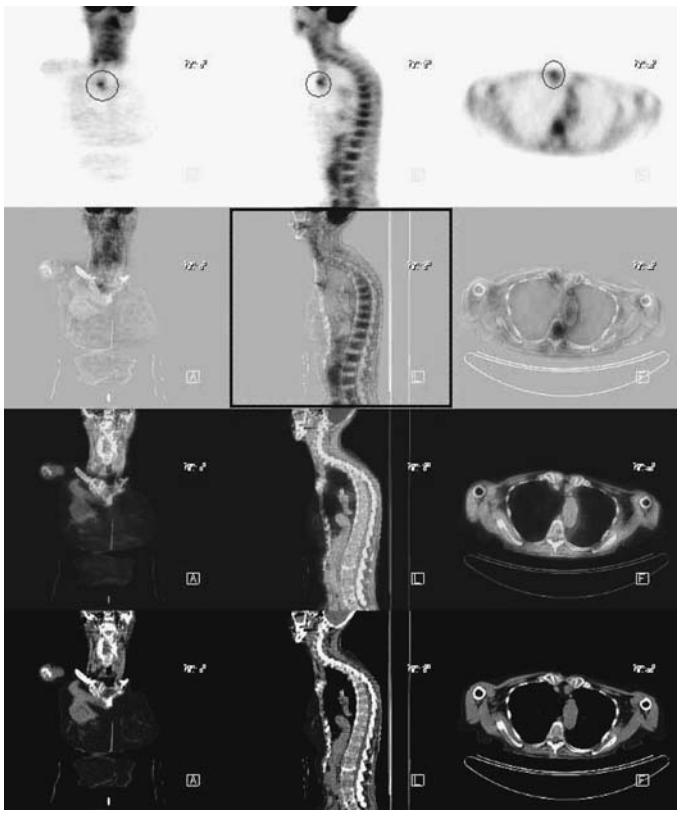

FIGURE 14.1.3.

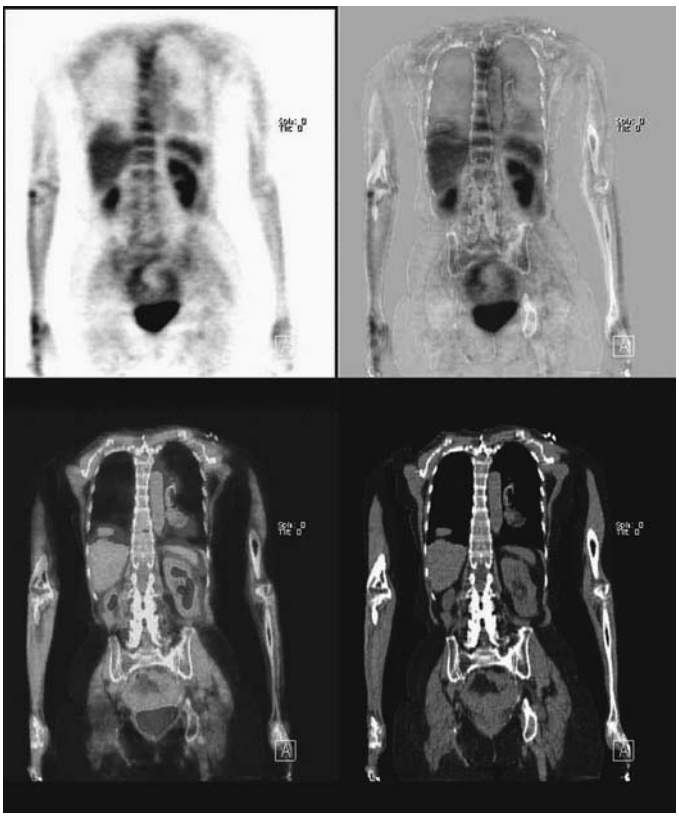

FIGURE 14.1.4.

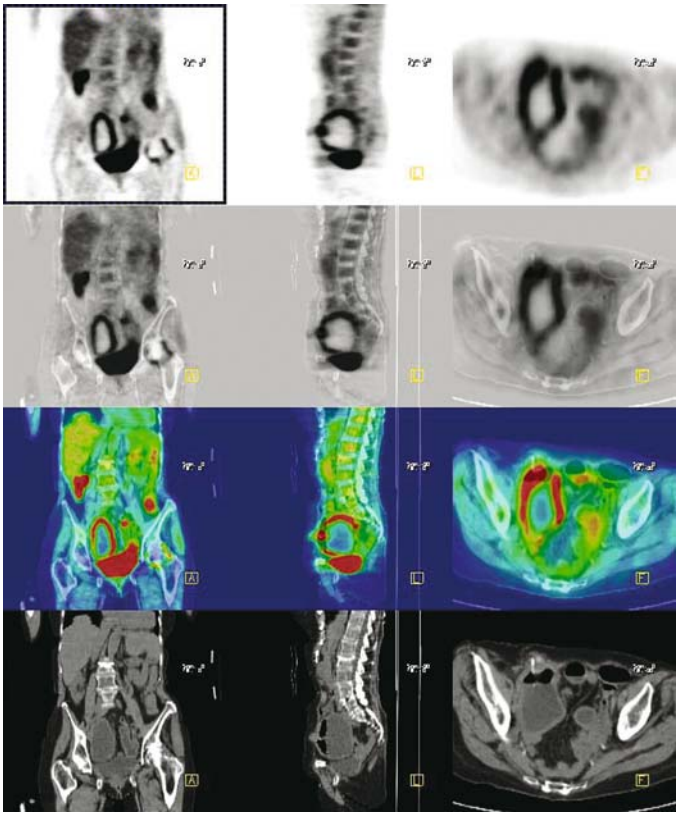

FIGURE 14.1.5.

Pearls and Pitfalls

- *Patients with bone prostheses may present with a false-positive PET study for infection since a loosening may be associated with elevated uptake. FDG uptake specifically in the synovial joint is considered synovitis.*[1,2,3]
- *50% of the joint accumulations are seen in the acromio-clavicular joint, 80% in the glenohumeral joint, 50% in the hip joint, 90% in the knee joint, and 80% in the talotibial joints.*[3]
- *FDG accumulations in the joints are frequent and usually asymptomatic.*
- *There is a strong correlation between the amount of FDG uptake and age.*[4,5,6]
- *Subclinical inflammatory proliferation in the synovial joint and chronic inflammatory processes is commonly seen in elderly patients.*[3]

15 Unknown Primary Tumors

Shahram Bouyadlou and Peter S. Conti

Case 15.1

History

38-year-old male who has a history of low-grade fever and episodic night sweats presents with an abnormal CT. Evaluation for malignancy is requested.

Findings

There is extensive adenopathy within the mediastinum involving the paratracheal, subcarinal, pericardial, and the AP window nodes (*Figure 15.1.1*). There are also hypermetabolic nodes within the gallbladder fossa adjacent to the pancreatic head near the common bile duct. A right internal mammary, as well as a perigastric node, are moderately positive. The periaortic nodes within the celiac axis are also active. There is abnormal activity involving the pleural base and possibly soft tissue on the left of the chest wall. No abnormalities are seen in the liver and spleen. No definite bony lesions are seen.

Impression

Extensive metastatic lymphadenopathy along with soft tissue disease. Differential diagnosis included lymphoma vs. metastatic disease from an unknown primary. Disseminated granulomatous disease is a less likely possibility.

Discussion

A patient should be considered to have carcinoma of unknown primary site when a tumor is detected at one or more metastatic sites and routine evaluation fails to define a primary tumor site. In evaluation of a patient with suspected malignancy, history would be the key to develop the differential diagnosis. The clinical findings along with imaging studies are complementary.

In this case the patient is a young male with constitutional symptoms of night sweats and low-grade fever. The initial diagnosis of infection (most likely TB) is more likely. The abnormal mediastinal lymphadenopathy on CT without lung involvement leads more toward malignancy. The anatomically based imaging modalities have significant shortcomings, particularly their lack of specificity when abnormal findings are present.

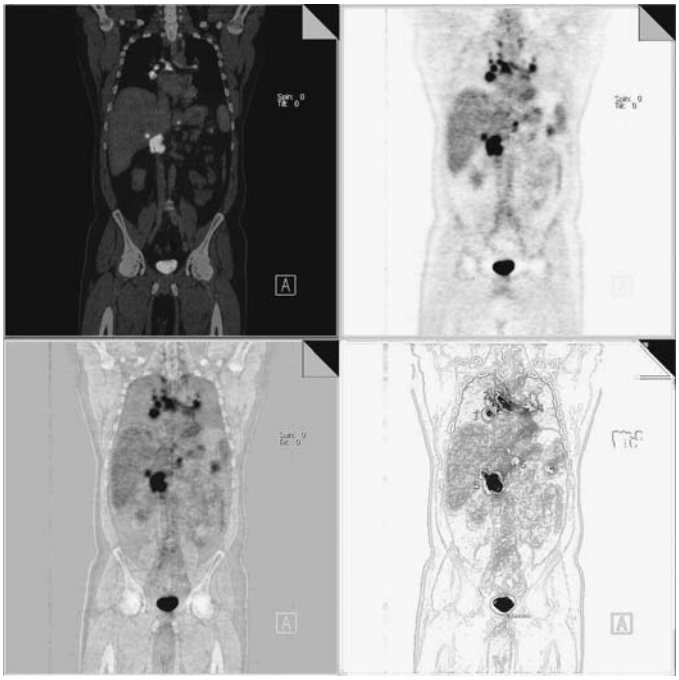

FIGURE 15.1.1.

Lymphoma may be multifocal and widespread, where there is a need for a non-invasive whole body imaging capability. Ga-67 has been successfully used for high-grade lymphoma but carries limitations for abdominal evaluation. With the introduction of F-18 FDG PET these limitations have been overcome. Studies have demonstrated that FDG shows good visualization of Hodgkin's and non-Hodgkin's lymphoma, and that there is a direct correlation between quantitative FDG uptake and poor prognosis. The highest FDG uptake is seen in the most clinically aggressive tumors.

The clinical presentation and imaging findings will place this case in the category of highly suspicious for malignancy (lymphoma preferably), however one must still consider infection (e.g., advanced TB) in this case.

Case 15.2

History

44-year-old male who has a history of an inflammed left buttock. The CT revealed swelling in multiple muscles in the pelvis. Evaluation for malignancy is requested.

Findings

There is extensive hypermetabolism in the left obturator internis piriformis muscle (*Figure 15.2.1*) extending to the gluteus minimis and left iliacus muscles which presents as an irregular border soft tissue mass adjacent to the sclerotic iliac/ischium lesion on CT (*Figure 15.2.2*). There is also a focus of intense activity in a right inguinal node (*Figure 15.2.3*).

The generalized uptake in the left lower extremity (*Figure 15.2.4*), more in the calf, is suggestive of venous stasis, possibly thrombophlebitis secondary to a pelvic

FIGURE 15.2.1.

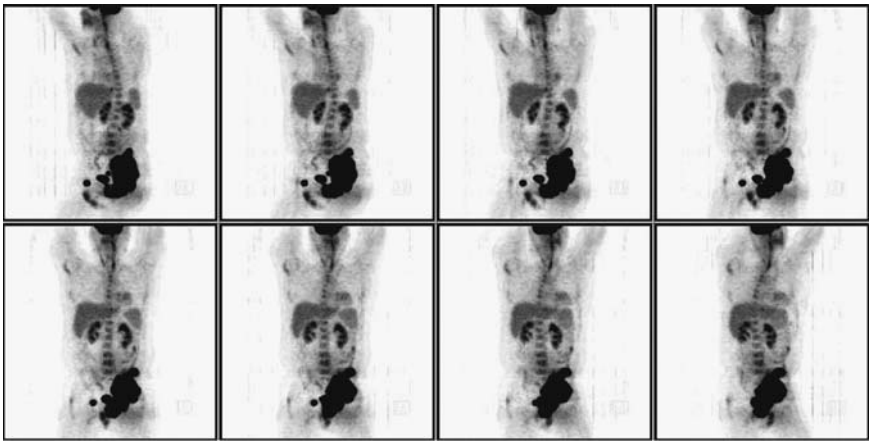

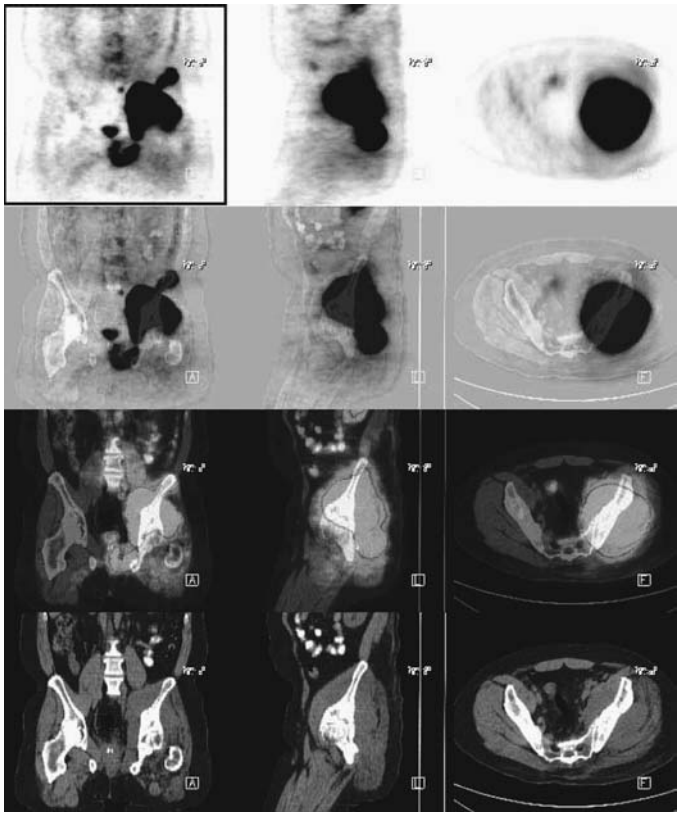

FIGURE 15.2.2.

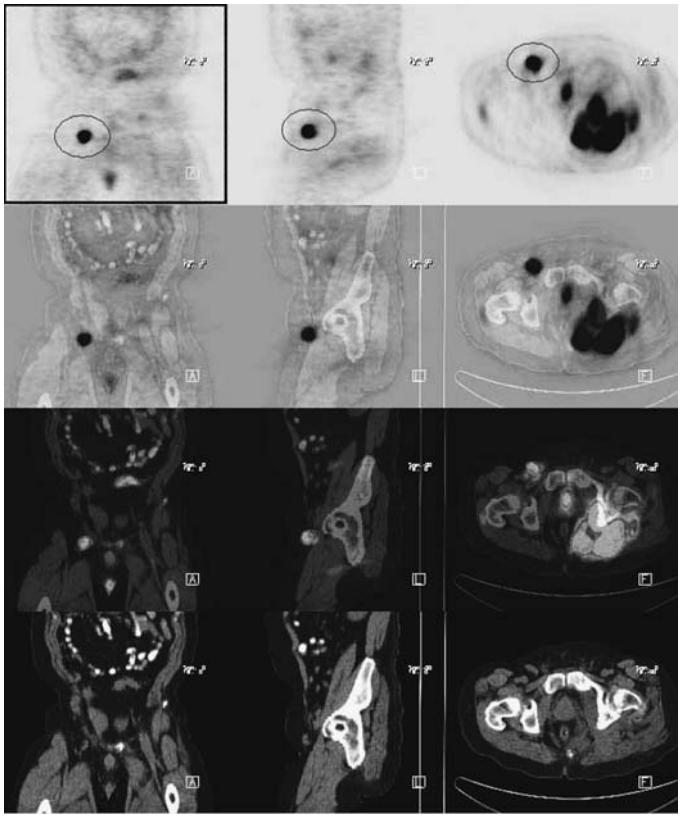

FIGURE 15.2.3.

FIGURE 15.2.4.

malignancy superiorly. The mild uptake in the gastroesophageal junction is due to inflammatory changes.

Impression

Bulky adenopathy seen involving the muscle groups mentioned above with additional right groin lymphadenopathy, compatible with lymphoma vs. sarcoma.

16 Liver Cancer

Heidi R. Wassef

Case 16.1

History

67-year-old male who has a history of hepatic ductal cancer with liver resection. He is currently on chemotherapy. The patient is being evaluated for recurrence in a suspicious lesion on CT.

Findings

On CT, the multiple clips in the liver inferiorly are consistent with prior liver resection. There are two discrete hypermetabolic nodules in the right posterior liver next to the kidney in the region of surgical clips consistent with local recurrence (*Figures 16.1.1, 16.1.2, and Figure 16.1.3*). Curvilinear uptake in the bowel is physiologic. No active adenopathy is evident above or below the diaphragm.

Impression

Evidence for hypermetabolism in the right posterior liver consistent with local recurrence.

Pearls and Pitfalls

- *In primary liver cancer, there is a strong correlation between high-grade histopathology and intratumoral fibrosis, but not with necrosis or cirrhosis.*[1,2,6]

Discussion

Hepatocellular carcinoma (HCC) is one of the most common malignancies worldwide. Most cases occur in individuals older than 40 years of age. It is more common in males than in females. Hepatitis B, hepatitis C, cirrhosis, aflatoxin, and Thorotrast are risk factors for HCC. AFP and ultrasonography are useful screening tools. AFP is usually present in 75% of the symptomatic cases, but AFP alone cannot distinguish between benign from malignant disease. Helical CT is a useful tool for subcentimeter lesion detection without the problems of respiratory misregistration. Angiographically assisted CT can characterize the lesions for resectability. Sonography is useful for

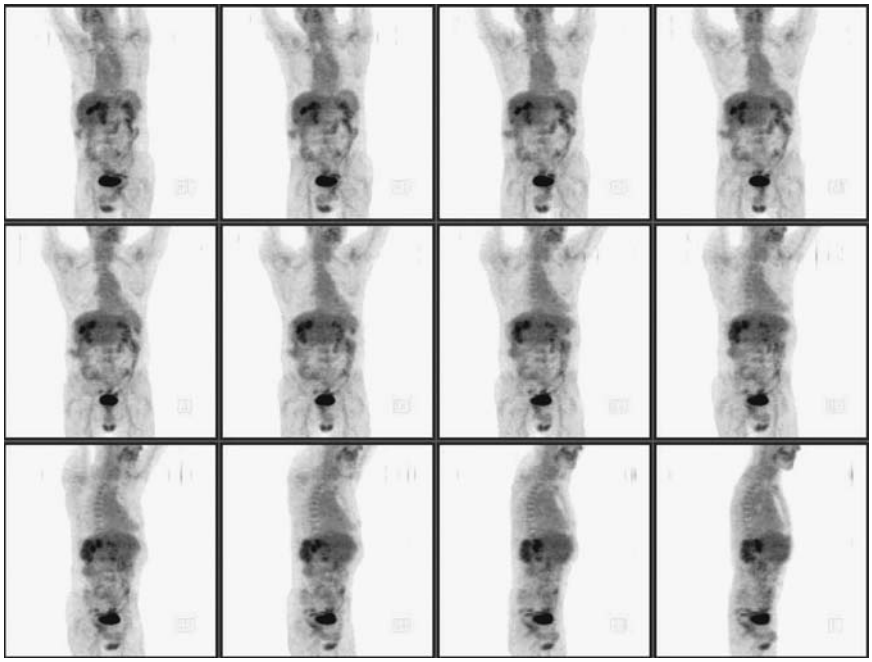

FIGURE 16.1.1.

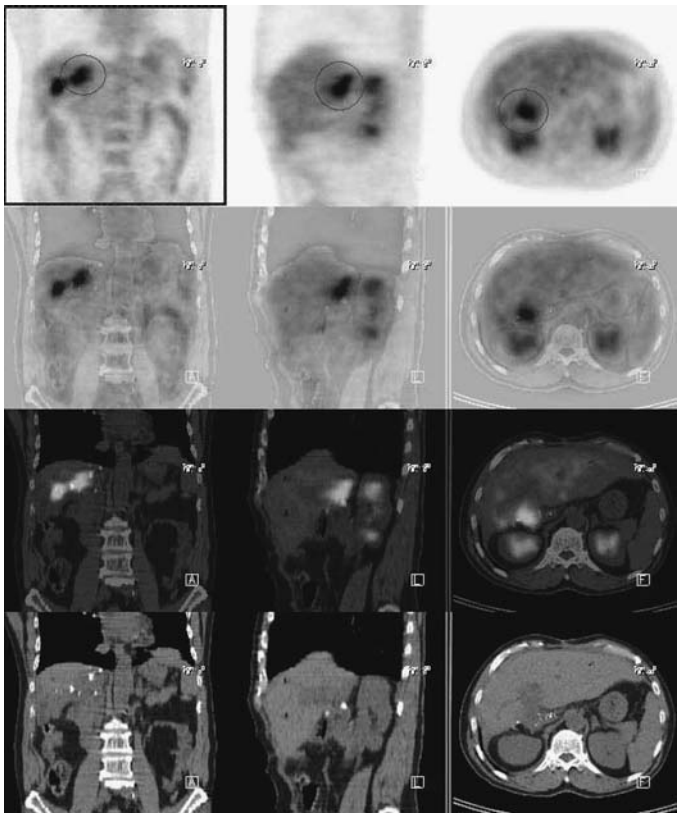

FIGURE 16.1.2.

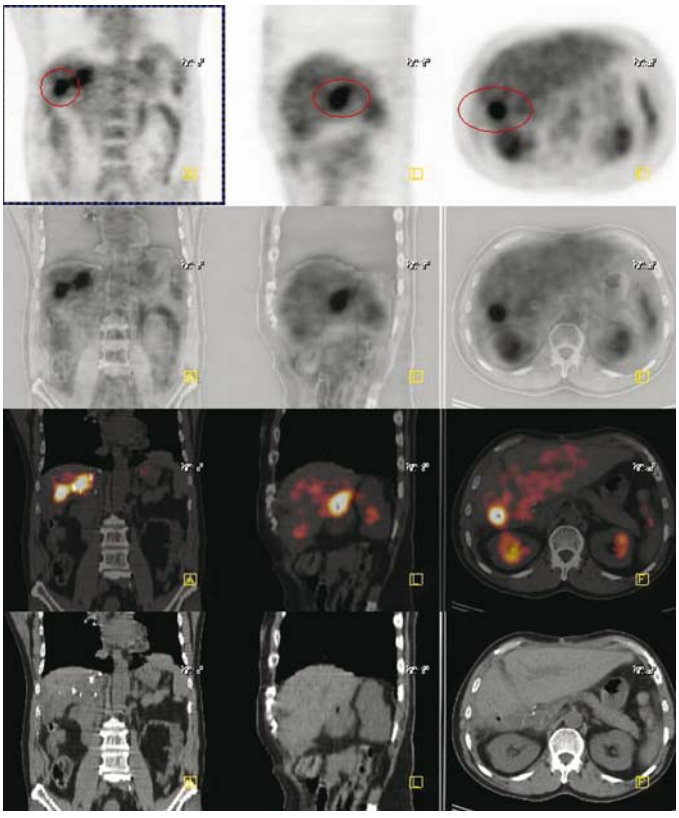

FIGURE 16.1.3.

detecting hyperechoic lesions. Duplex and color Doppler are useful for the detection of vascular invasion. MRI with gadolinium enhancement is also useful for early detection of HCC.

Case 16.2

History

68-year-old male who has a history of liver cancer status post liver transplant and chemotherapy. His most recent MRI study demonstrated suspicious lesions involving the right hepatic dome and right posterior lobe of the liver. Evaluation for recurrence is requested.

Findings

There is an intense focus of hypermetabolism in the dome of the liver laterally (*Figures 16.2.1 and 16.2.2*), which does not corresponds to a definite CT (noncontrast) abnormality. The surgical sutures in the right upper quadrant (*Figure 16.2.3*) are consistent with prior liver transplant. Abnormal multifocal sites of hypermetabolism are also seen within the mediastinum including the hila, prevascular space (*Figure 16.2.4*), AP window, right paratracheal, precarinal, and subcarcinal regions, highly suspicious for metastatic nodal disease. There is an approximately 1-cm noncalcified nodule (*Figures 16.2.5 and 16.2.5A*) seen in the posterior aspect of the left lower lobe, which is mildly hypermetabolic. Incidentally noted are three superficial hypermetabolic lesions in the buttocks (*Figure 16.2.6*) presumably inflammatory injection sites, two superior and one right inferior in location. Another separate superficial focus of hypermetabolism is seen located in the posterolateral aspect of the abdominal wall corresponding to subcutaneous soft tissue thickening on CT attributed to probable inflammation. Inferior and posterior to the bladder in the prostate bed, there is moderate hypermetabolism, which probably represents benign prostatic hypertrophy (*Figure 16.2.7*); other prostate pathology cannot be excluded. The thickened gastric wall (*Figure 16.2.8*) with associated hypermetabolism is compatible with gastritis. The spleen is prominent in size with heterogeneous tracer localization. The aortic wall is calcified. There is symmetric high tracer uptake in the larynx which is considered physiologic. The activities in the rectum and testes are also considered physiologic. An artifact in relation to the metallic dental work is noted.

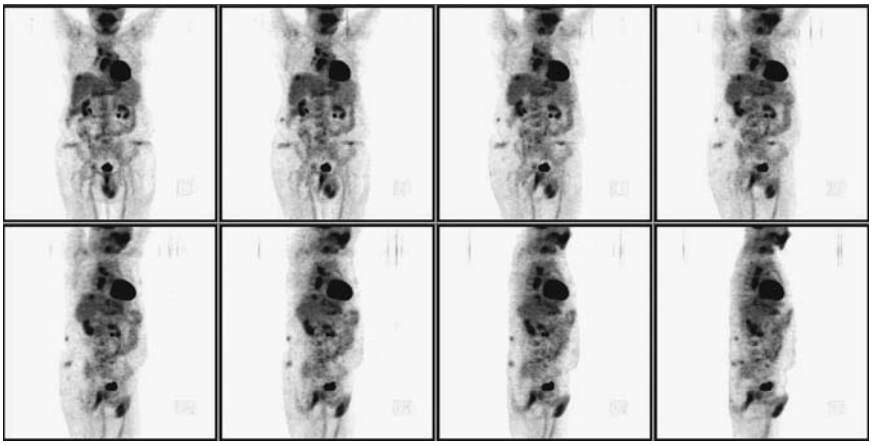

FIGURE 16.2.1.

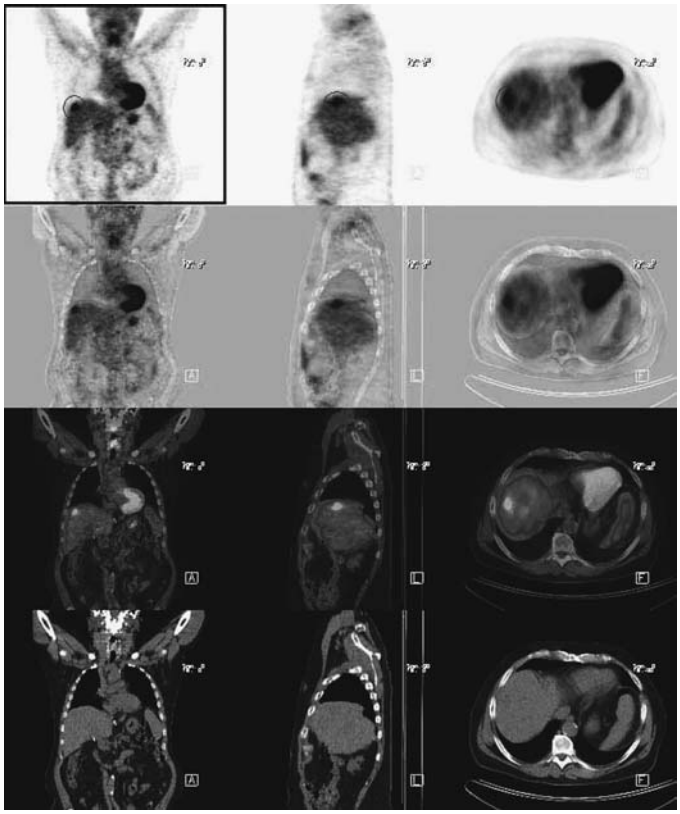

FIGURE 16.2.2.

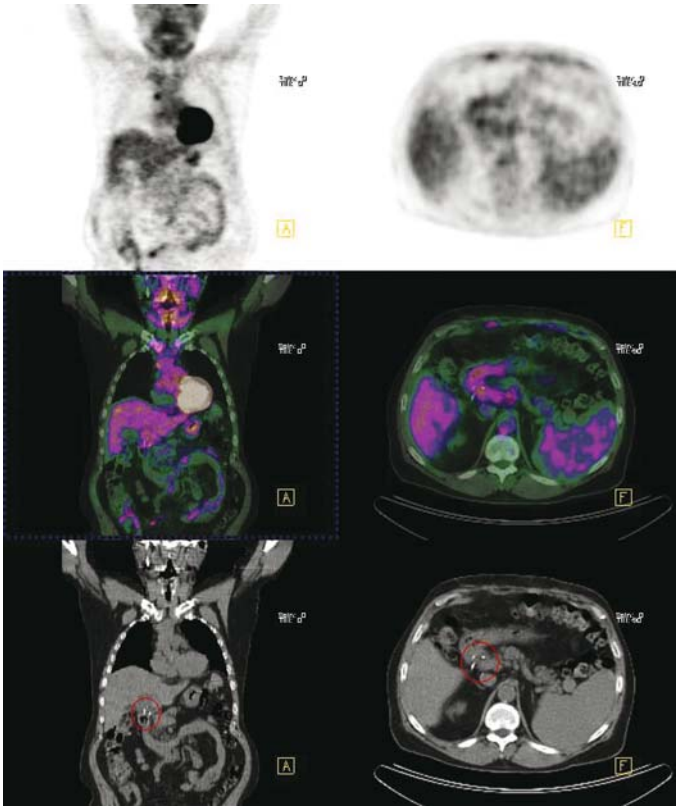

FIGURE 16.2.3.

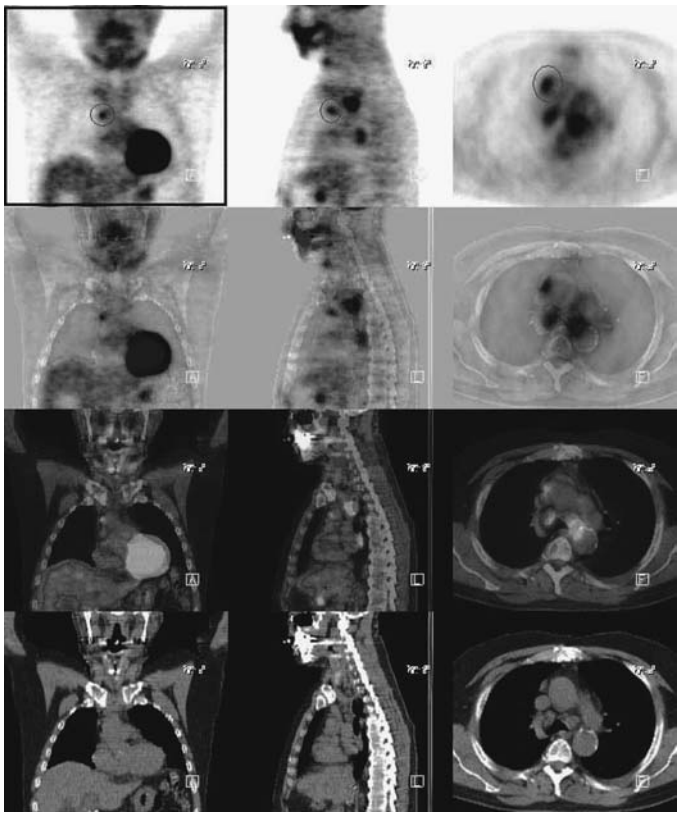

FIGURE 16.2.4.

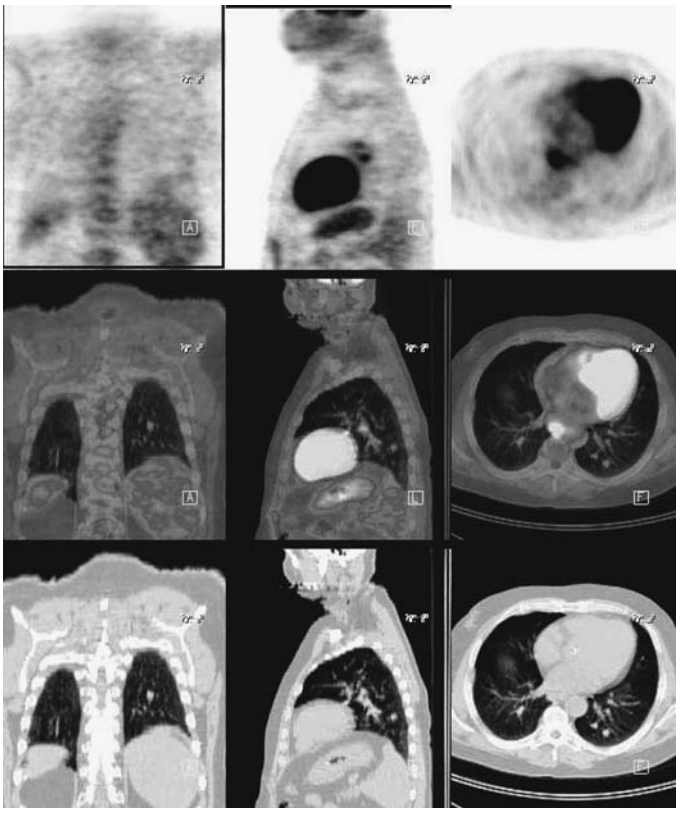

FIGURE 16.2.5.

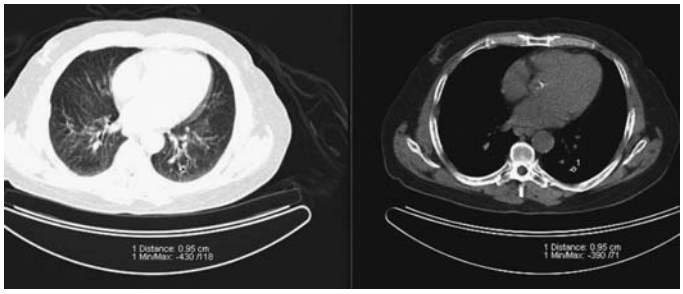

FIGURE 16.2.5A.

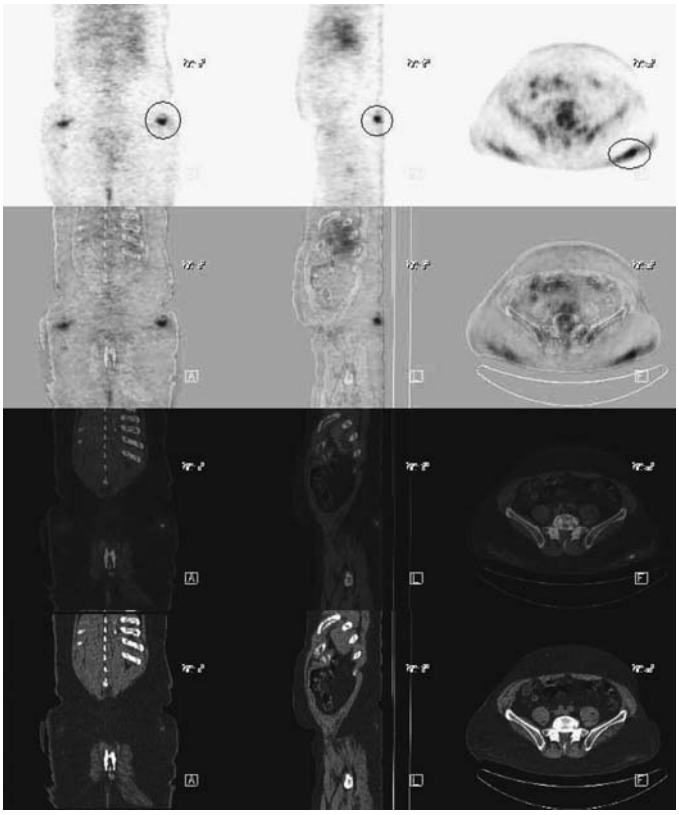

FIGURE 16.2.6.

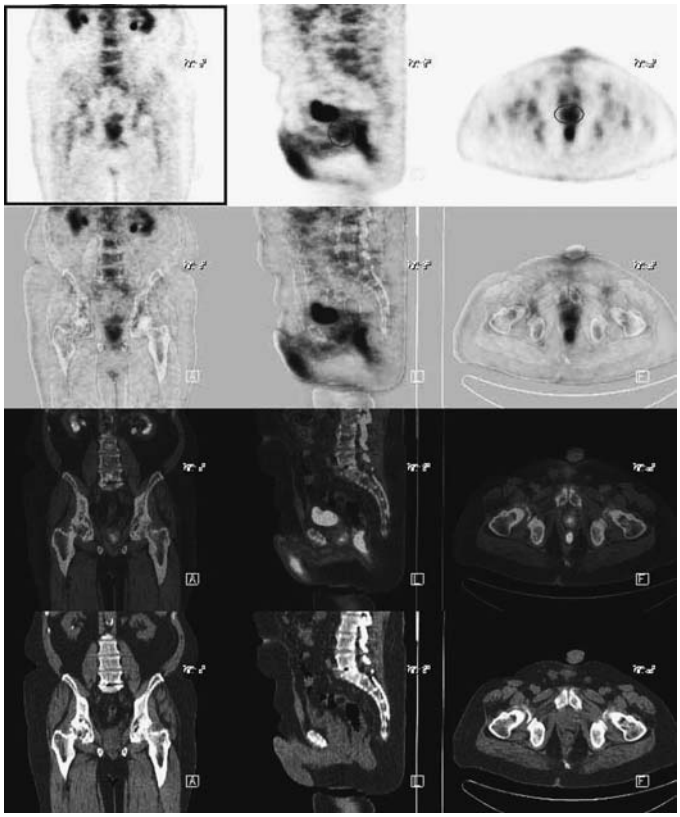

FIGURE 16.2.7.

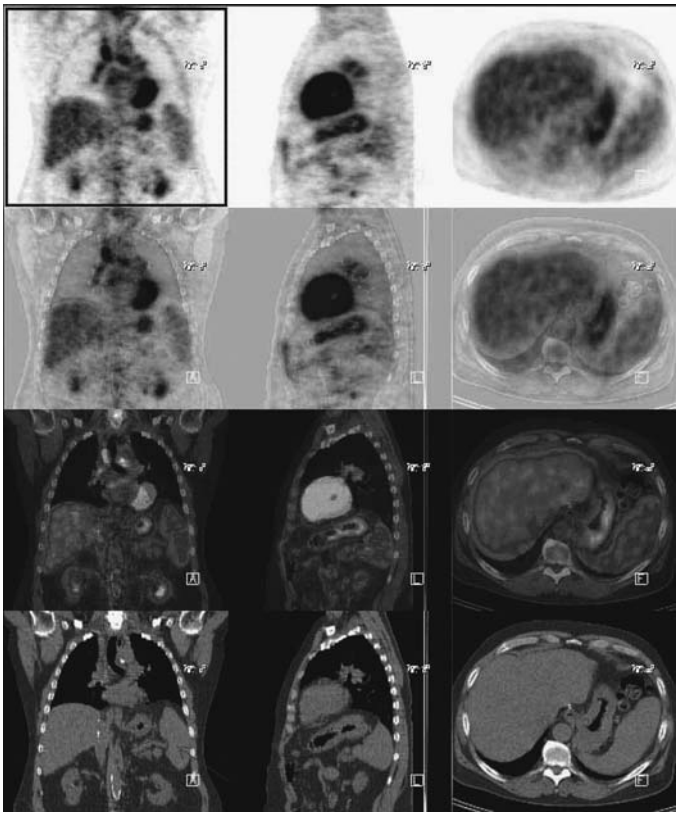

FIGURE 16.2.8.

Impression

1. Markedly abnormal study demonstrating at least one focal intensely hypermetabolic lesion at the dome of the liver, hypermetabolic multinodal disease in the chest and a noncalcified pulmonary nodule in the posterior left lower lobe, all suspicious for recurrent metastatic disease. The differential diagnosis also includes post transplant lymphoproliferative disease.
2. Splenomegaly.
3. Moderate prostate hypermetabolism probably related to benign prostate hyperplasia/hypertrophy; malignancy cannot be excluded.
4. Thickened gastric wall with moderate hypermetabolism suggestive of gastritis.
5. Probable injection site superficial inflammation in the buttocks.

Pearls and Pitfalls

- *64% of HCC lesions accumulate FDG.*[2,8]
- *PET can alter management in 28% of patients.*[1,2,8]
- *PET-CT may potentially mislocate a lesion particularly at the dome of the liver and base of the lung owing to respiratory motion artifact. It is highly recommended to obtain breath-hold CT views for comparison.*[6]

Case 16.3

History

59-year-old male who has a history of liver cancer status post liver transplant and was later treated with chemotherapy. His most recent AFP is 119 and is rising. Evaluation for recurrence is requested.

Findings

There is a large right upper quadrant focus in the sub hepatic region (*Figures 16.3.1, 16.3.1A, and 16.3.2*) along the bowel distribution that is metabolically active. Another smaller lesion is seen in the right lower quadrant (*Figure 16.3.3*). A third focus of activity is also noted in the mid-abdomen just right of midline (*Figure 16.3.4*). These findings appear both intense and focal and are suspicious for serosal, bowel, or omental involvement with metastatic disease. Other bowel pathology such as inflammatory bowel disease or polyposis also should to be considered. The surgical bed in the liver (*Figure 16.3.5*) is mildly active consistent most likely with post-surgical changes. The mild activity in the stomach is likely gastritis (*Figure 16.3.6*).

Impression

Multiple intense hypermetabolic foci in the abdomen as described above suspicious for serosal, bowel, or omental involvement with malignant process.

Pearls and Pitfalls

- *CEA is not a sensitive indicator for liver cancer recurrence. Only 59% of recurrent disease demonstrates an elevated serum CEA level.*[1,2]

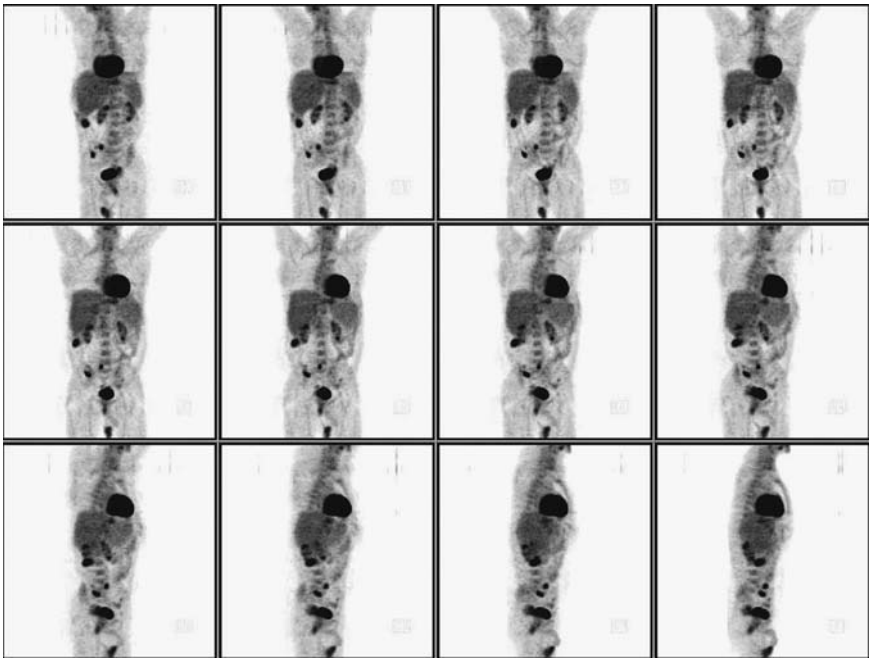

FIGURE 16.3.1.

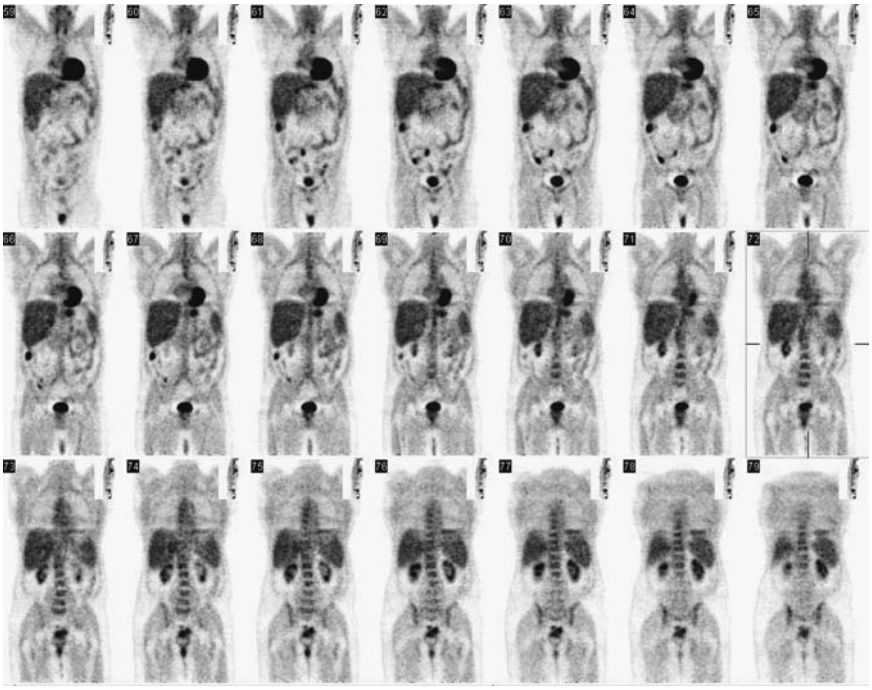

FIGURE 16.3.1A.

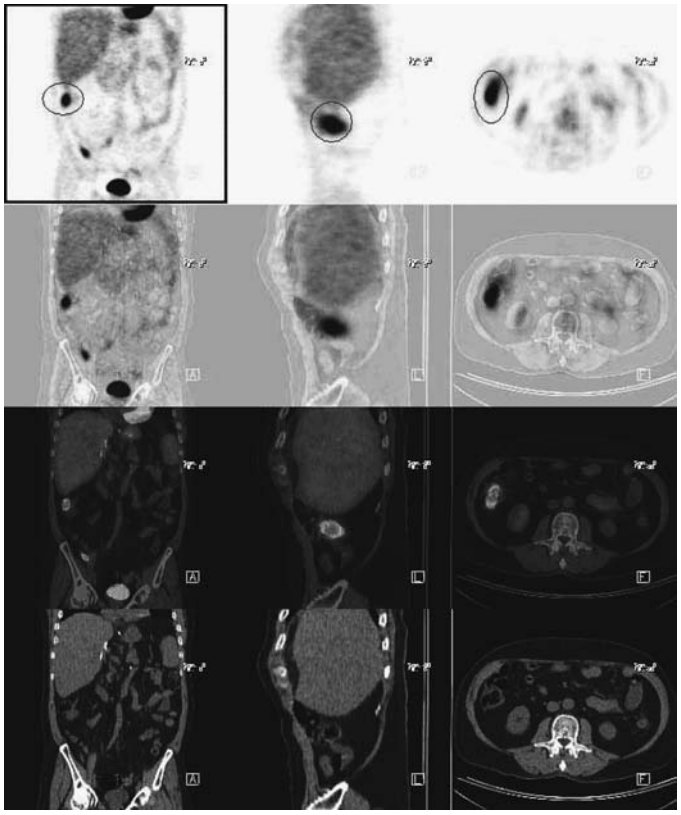

FIGURE 16.3.2.

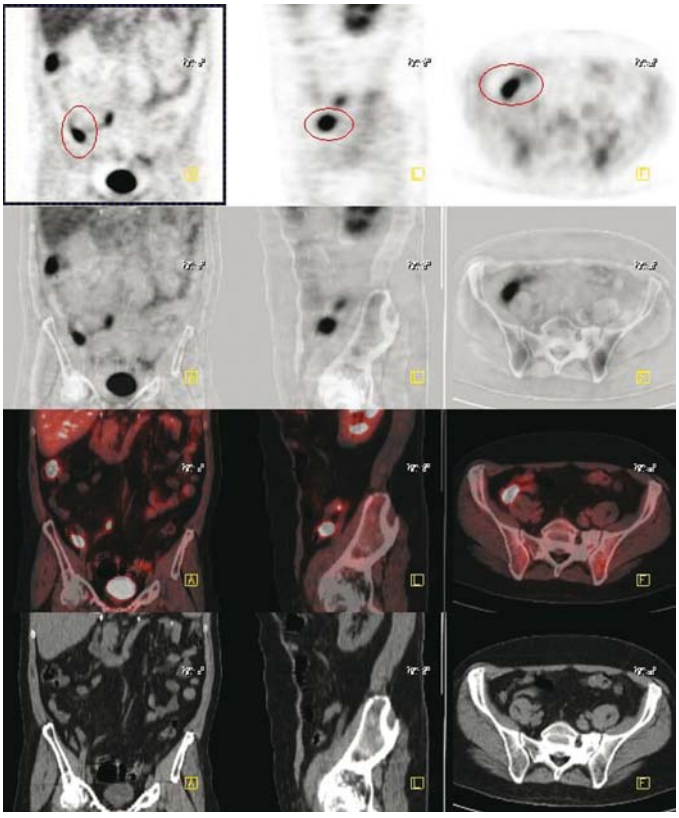

FIGURE 16.3.3.

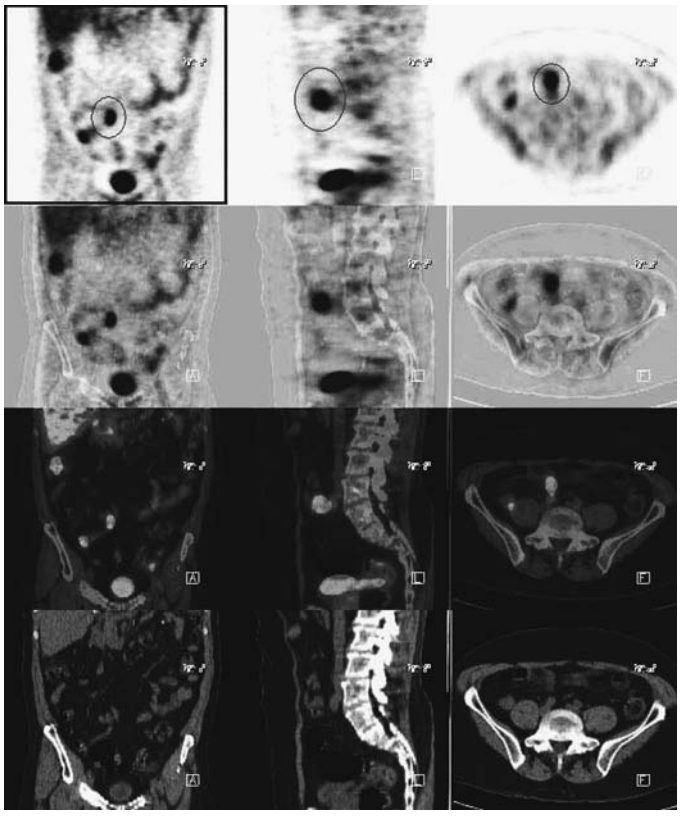

FIGURE 16.3.4.

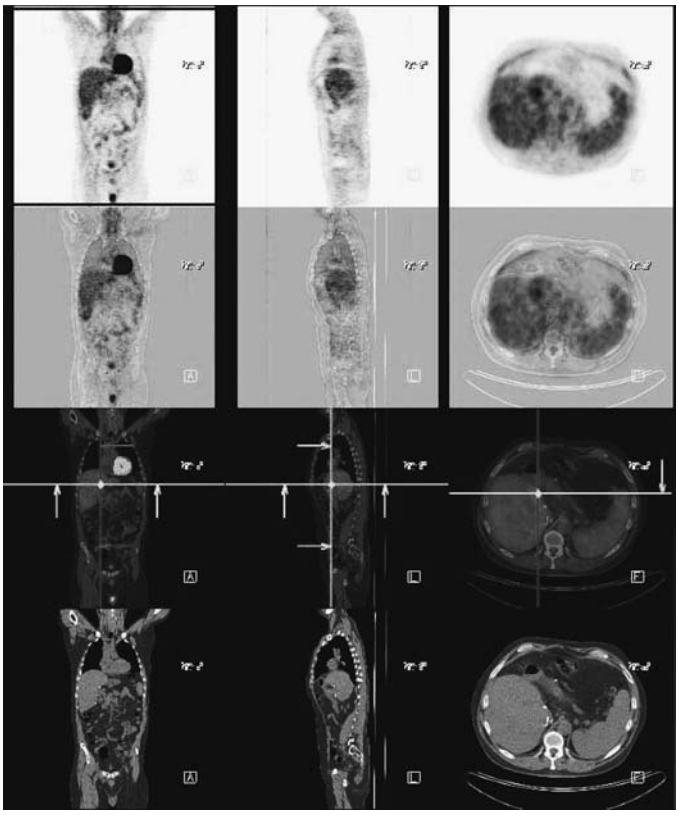

FIGURE 16.3.5.

FIGURE 16.3.6.

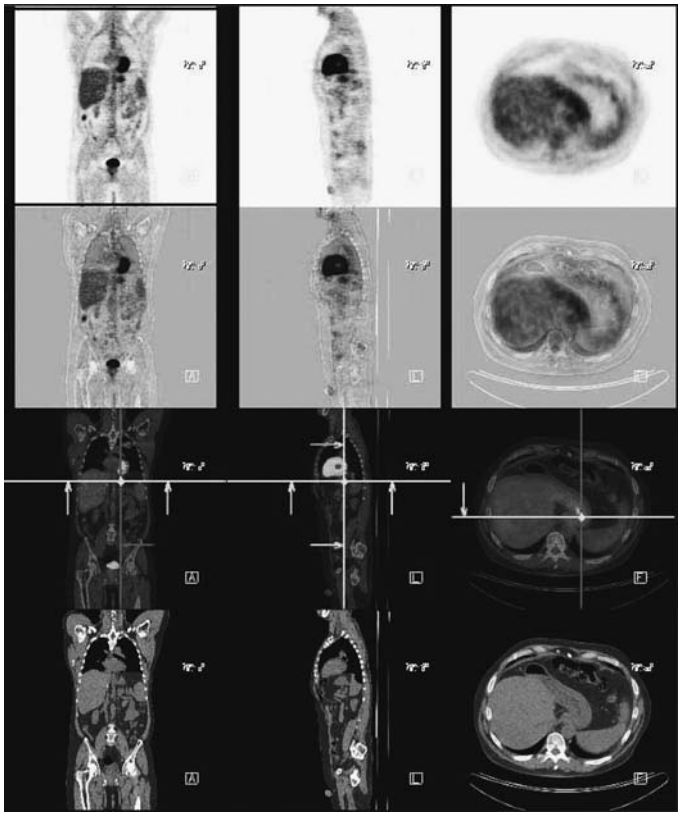

- *The positive predictive value for detecting a locally recurrent lesion after treatment with PET is 80%; the negative predictive value is 100%.*[5,7,8]

Case 16.4A

History

58-year-old male with a history of liver cancer status post partial liver resection. He was later treated with radiotherapy and chemotherapy. His AFP level has increased from 11.0 to 53.9. Evaluation for recurrence is requested.

Findings

There is a focus of activity near the anterior abdominal wall left of midline (*Figures 16.4A.1 and 16.4A.2*), which corresponds to a mass seen below the liver on CT. This is new compared to a previous PET done 5 months ago. This is suspicious for metastases either from an implant on the transverse colon wall or peritoneal surface. The mild to moderate focal hypermetabolism along the liver edge (*Figure 16.4A.3*) near the surgical resection noted is minimally increased since the last PET study. A loop of bowel is seen as protruding into the right hepatic cavity consistent with the history of right hepatic lobe resection.

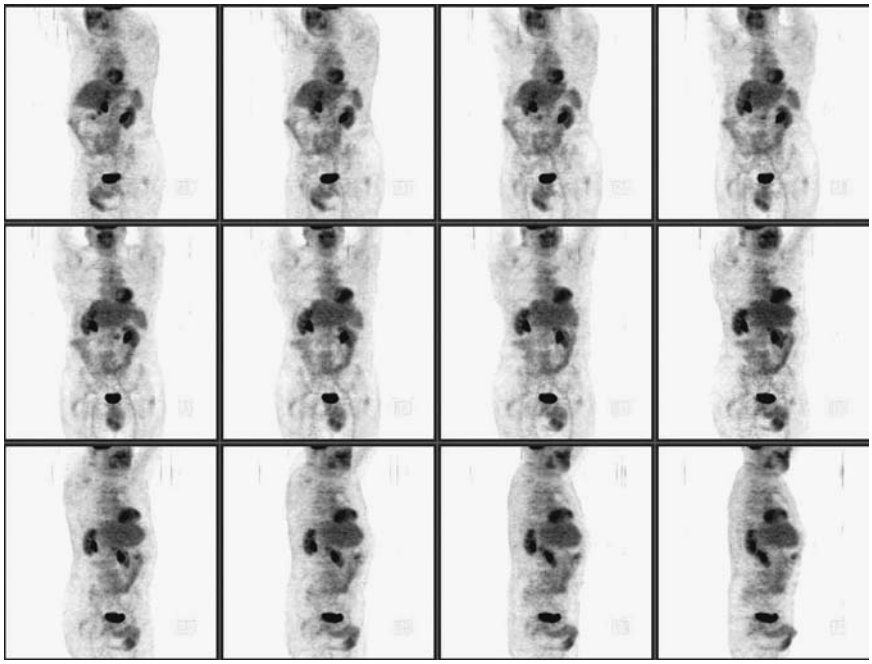

FIGURE 16.4A.1.

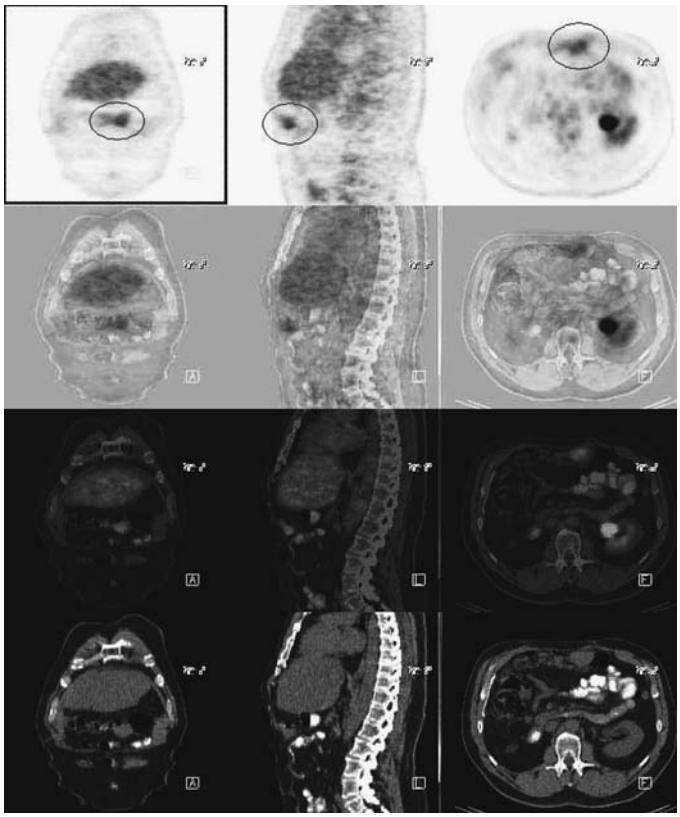

FIGURE 16.4A.2.

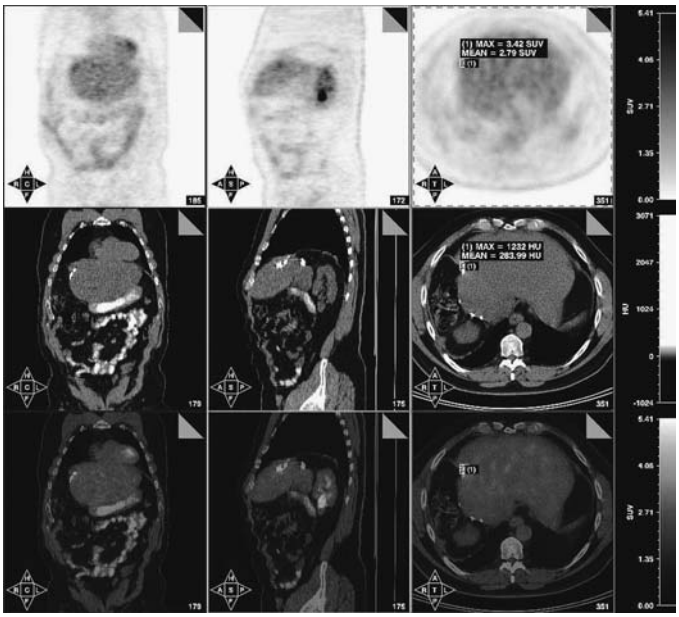

FIGURE 16.4A.3.

Impression

1. New malignancy seen in the anterior abdominal wall left of midline with modest increased activity in the hepatic surgical bed.
1. Possible locally recurrent disease at the surgical margin as described above.

Discussion

The degree of tumor differentiation is closely related to the rate of proliferation in hepatocellular carcinoma. Patients with the worst prognosis tend to have histologically undifferentiated lesions and lesion size exceeding 1 cm in diameter. The 5-year survival rate of HCC is 90% if the lesion is 1 cm in diameter or less and well differentiated. A high cure rate is possible only with resection. Fifty percent of the patients with advanced disease will benefit from liver transplantation as the most salient treatment for a cure.

Case 16.4B

History

58-year-old male who has a history of liver cancer with the prior PET demonstrating hypermetabolism involving the left anterior abdominal wall and liver. He later underwent anterior abdominal wall resection. Evaluation for malignancy is requested.

Findings

There is a small focus of activity along the superolateral aspect of the residual liver (*Figures 16.4B.1 and 16.4B.2*) at the site of the surgical resection and clips that is unchanged from the prior study. The lesion in the left anterior abdominal wall is no longer visible.

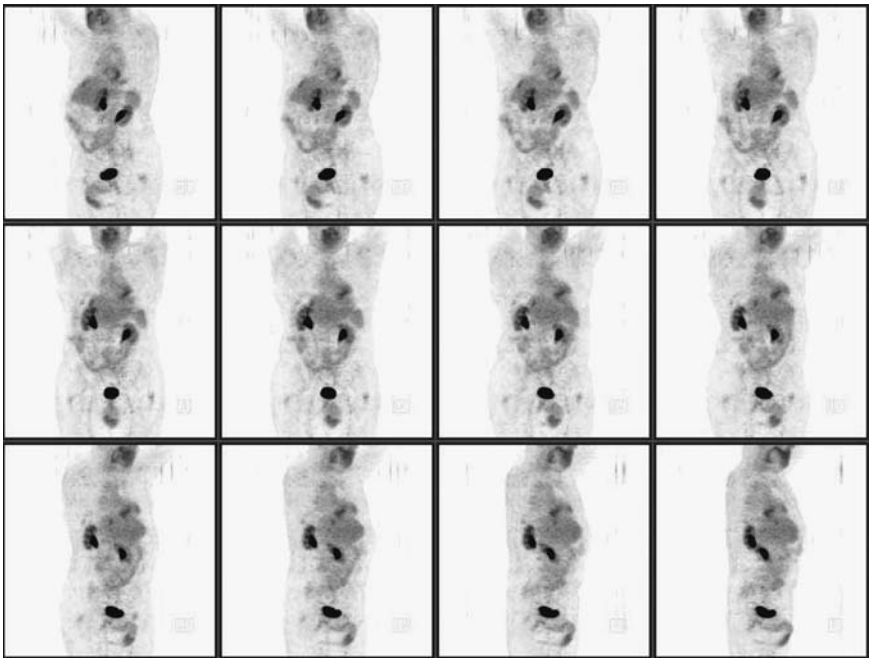

FIGURE 16.4B.1.

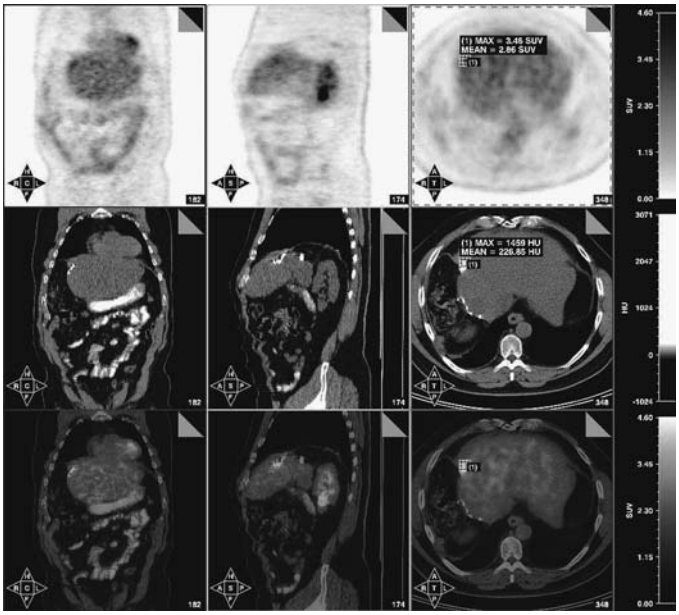

FIGURE 16.4B.2.

Impression

Interval resolution involving the left anterior abdominal wall abnormality with residual liver activity suspicious from post surgical changes; suggest a repeat scan in 3 months to monitor for disease progression.

Pearls and Pitfalls

- *FDG accumulation varies with the degree of tumor differentiation.*[1,2]
- *^{11}C-acetate may be used as an alternative to ^{18}F-FDG since it demonstrates a detection sensitivity of 87.3% as opposed to 47.3% in the detection of individual tumor lesions using FDG.*[3,4]

Discussion

In normal hepatocytes, glucose-6-phosphatase degrades the phosphorylated FDG resulting in poor intracellular accumulation of the tracer. Well-differentiated HCC contains an abundance of glucose-6-phosphatase, accounting for decreased accumulation.

Only 55% of the malignant tumors have been reported to have a higher intensity of FDG uptake than normal livers. Thirty percent of the malignant tumors have an uptake intensity equal to uptake intensity in normal liver and 15% have uptake less than that of normal liver.

Case 16.5

History

41-year-old patient with cirrhosis secondary to hepatitis-B and known hepatoma status post embolization therapy. The current exam is to evaluate for metastatic disease and consideration for potential liver transplant.

FIGURE 16.5.1.

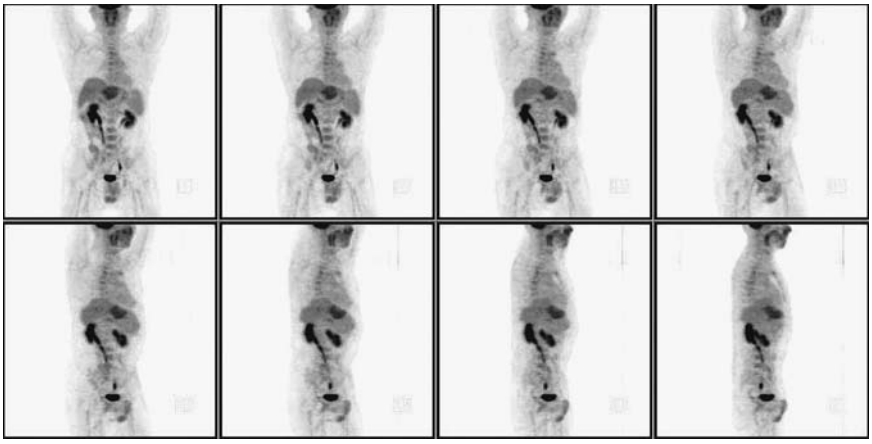

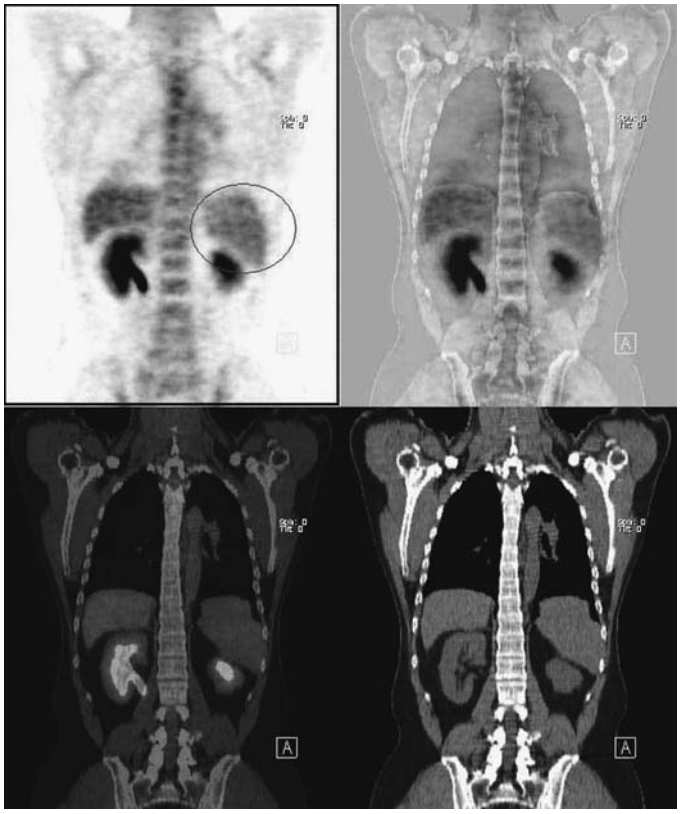

FIGURE 16.5.2.

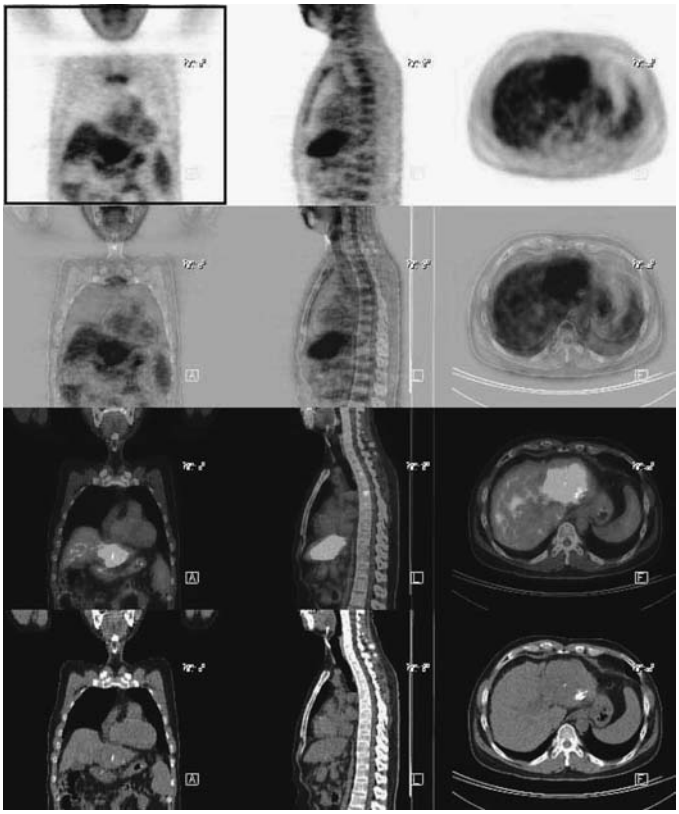

FIGURE 16.5.3.

Findings

On CT the liver surface is irregular, and the spleen mildly enlarged (*Figures 16.5.1 and 16.5.2*) with some omental portosystemic collaterals. These are consistent with the history of cirrhosis. The primary hepatocellular carcinoma is visible as a hypermetabolic mass replacing much of the lateral segment of the left lobe of the liver (*Figure 16.5.3*). Radiodensities within the lateral segment on CT are consistent with contrast given with chemoembolization. The largest contrast collection is devoid of activity. A small collection is seen within the tumor, which has a hypometabolic center and a hypermetabolic periphery, consistent with treated hepatocellular carcinoma with

viable tumor at the periphery. No other hypermetabolic liver lesion is apparent. The remainder of the study appears normal with prominent but symmetrical presumed physiologic tonsillar, bowel, and testicular activity. There is no evidence for skeletal metastatic disease. Lung window images of the chest were reviewed, and there is no evidence for pulmonary metastasis.

Impression

Moderately intense hypermetabolism within the lateral segment of the left lobe of the liver with central photopenia, consistent with hepatocellular carcinoma status post embolization therapy. There is a background of cirrhosis with portal hypertension. However, there is no evidence for metastatic disease.

Discussion

PET imaging can guide the biopsy of large, metabolically active tumors, identify distant metastases, monitor patient response to treatment for hepatic chemoembolization, and detect recurrent disease.

17 Lung Tumors

Hossein Jadvar and Sherief Gamie

Case 17.1

History

57-year-old male with known right-sided malignant mesothelioma. The current study is being done to evaluate extent of disease.

Findings

There is intensely hypermetabolic right-sided pleural disease. There is a linear band of tumor activity in the midsagittal plane of the right lung, extending over the anterior surface and over the posterior surface of the lung (*Figure 17.1.1*). The band-like distribution probably reflects tumor spread with background pleural adhesive disease. Additionally, there is disease in the right costophrenic angle along the lateral right major fissure, and the minor fissure. No distant disease is evident outside the right thorax. There is minimal dot-dash pleural involvement of the medial posterior pleura.

Impression

Malignant right-sided mesothelioma with the most dramatic disease in the lung base/costophrenic angle and liver dome and along the lateral fissures.

Pearls and Pitfalls

- *The overall sensitivity, specificity, and accuracy are 97%, 80%, and 94% in detecting malignant mesothelioma.*[8,9]
- *CT cannot reliably distinguish benign pleural thickening from malignant mesothelioma.*
- *PET can define the extent of disease in patients with diffuse malignant mesothelioma.*[1,7,8,10,13]
- *Patients with highly active FDG uptake have a poor long-term prognosis.*[5,11,12]
- *Pleuritis may produce a false-positive response on FDG PET imaging.*
- *Mesothelioma tends to have low FDG uptake early in the disease process.*[1,2,3,13]

Discussion

Mesothelioma is an occupational disease. Ninety percent of the patients are exposed to asbestos once in their lifetimes. Pleural mesotheliomas spread diffusely over the

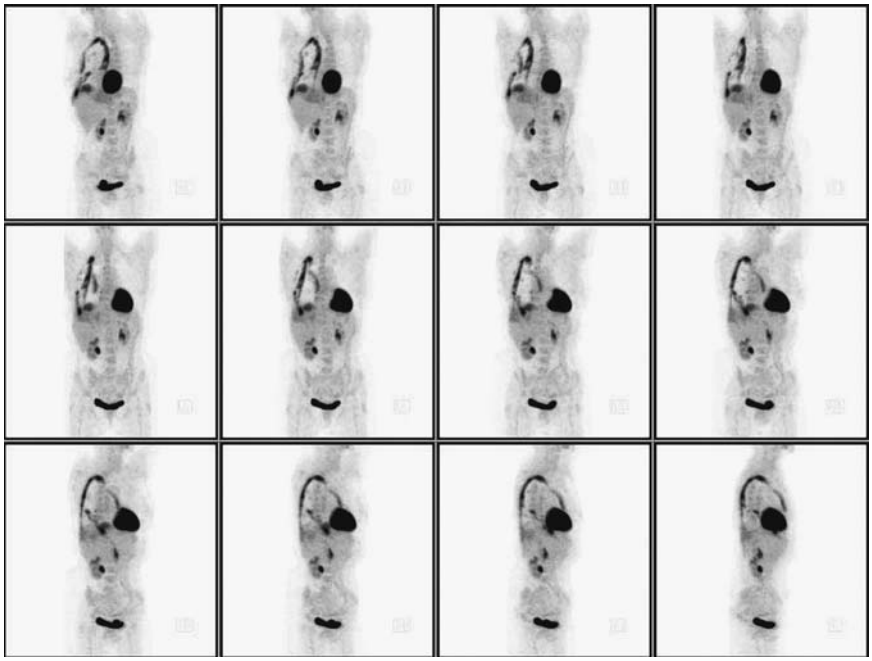

FIGURE 17.1.1.

lung surface and invade the pulmonary parenchyma. The prognosis is poor and the mean survival is usually less than two years after the initial diagnosis. The irregular sheet-like lesions wrapping around the lung makes this especially challenging for conventional imaging.

Follow-up

The patient was subsequently treated with chemotherapy and is currently improving. A follow-up PET scan was done to monitor treatment response and revealed a partial resolution in disease involving the right hemidiaphragm.

Case 17.2A

History

55-year-old male who has a history of lung cancer status post left lung biopsy three weeks ago. The patient is scheduled to start chemotherapy and is being staged with PET.

Findings

There is a bulky hypermetabolic mass involving the left hilum (*Figures 17.2A.1 and 17.2A.2*) with subcarinal, right paratracheal region anterior mediastinal adenopathy left of midline. The vertebral uptake in the right pedicle at the level of T-7 (*Figure 17.2A.3*) indicates this is Stage IV disease. There is no pathology visible in the brain or adrenal glands.

FIGURE 17.2A.1.

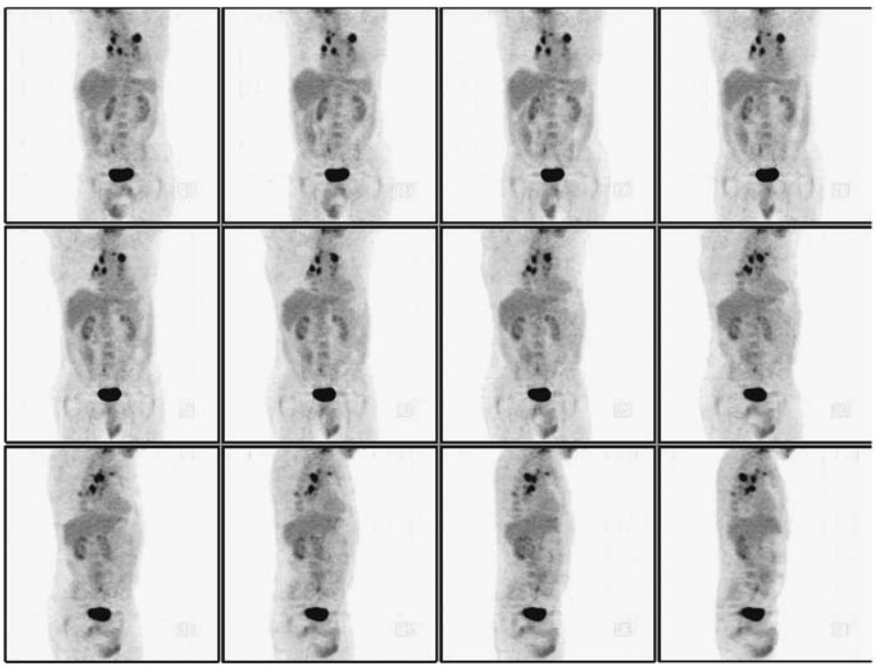

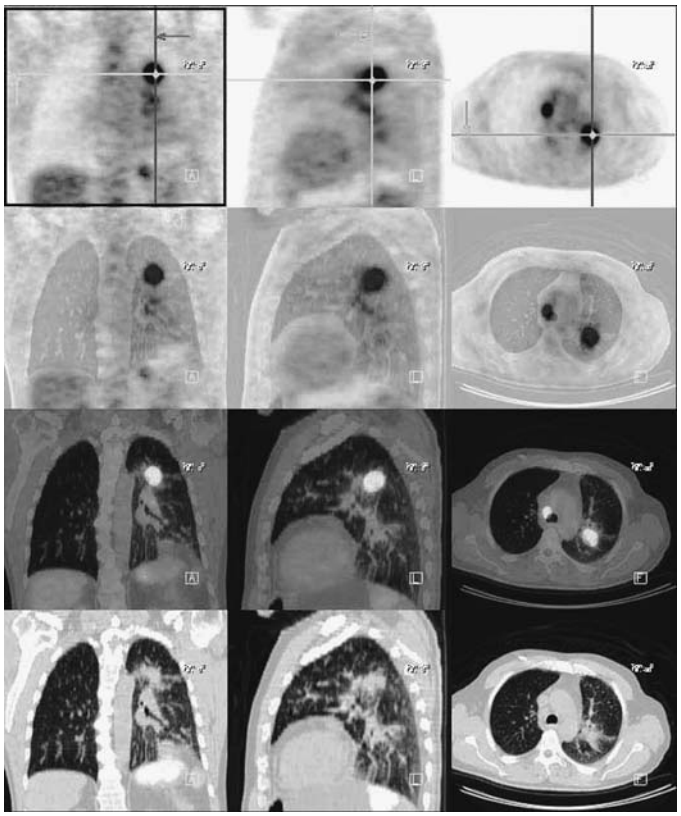

FIGURE 17.2A.2.

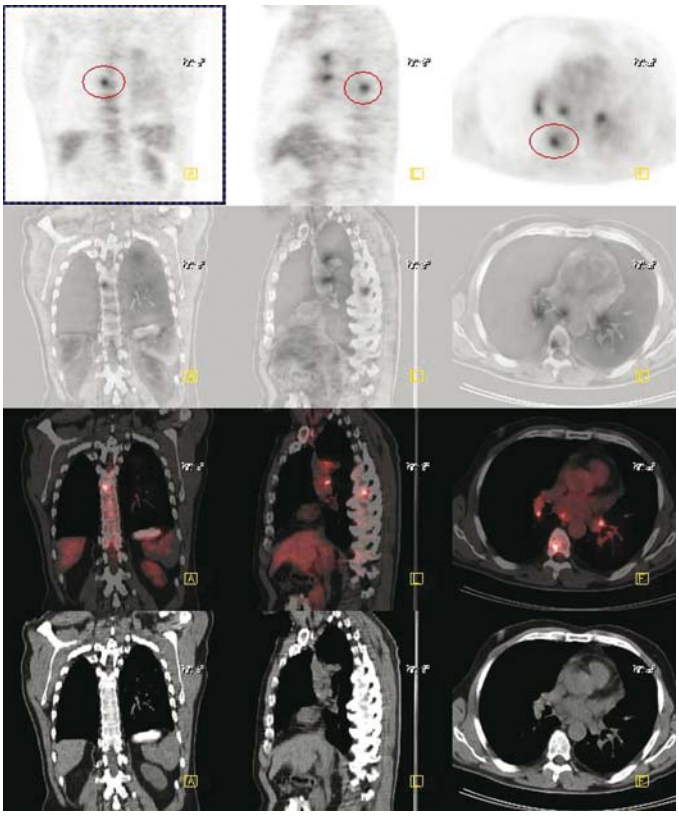

FIGURE 17.2A.3.

Impression

1. Primary left lung cancer with disseminated metastases involving the mediastinum and vertebral column.
2. Negative for brain and adrenal metastases by PET.

Pearls and Pitfalls

- *Conventional imaging, specifically MRI, is still the initial method of choice in the evaluation of brain metastases. A normal brain has substantial glucose uptake on PET scan. This may potentially mask small metastatic foci.*[3,6]

Discussion

PET can change treatment planning in 39% of patients. It can alter staging in 44% of the cases, upstaging 29%, and downstaging 15%. As a result, PET has been observed to change patient management in 35% to 67% of the time.

PET is capable of identifying twice as many patients with unresectable disease than conventional imaging.

Case 17.2B

History

55-year-old male who has a history of lung cancer with known metastatic disease to the brain. He is status post chemotherapy. His previous PET demonstrated hypermetabolism involving the mediastinum and vertebral column consistent with malignancy. His MR revealed several suspicious lesions involving the brain, for which he received gamma knife treatment. Evaluation for restaging is requested.

Findings

In comparison with the previous PET scan, there is no interval change in metastatic disease (*Figure 17.2B.1*) with regard to the number, size, and intensity of the lesions in the mediastinum (*Figures 17.2B.2, 17.2B.3, 17.2B.4*). There is a region of photopenia in the right posterior temporal lobe of the brain likely related to gamma knife treatment (*Figure 17.2B.5*). The other lesions described on the MR of the brain are nonvisualized.

Impression

1. Persistent hypermetabolism involving the mediastinum consistent with metastatic disease unchanged since the prior PET study.
2. No PET evidence of residual metastatic disease in brain.

FIGURE 17.2B.1.

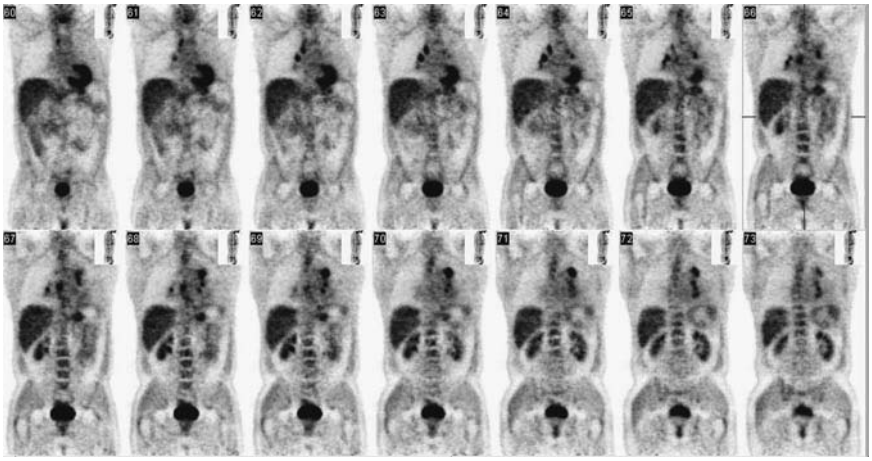

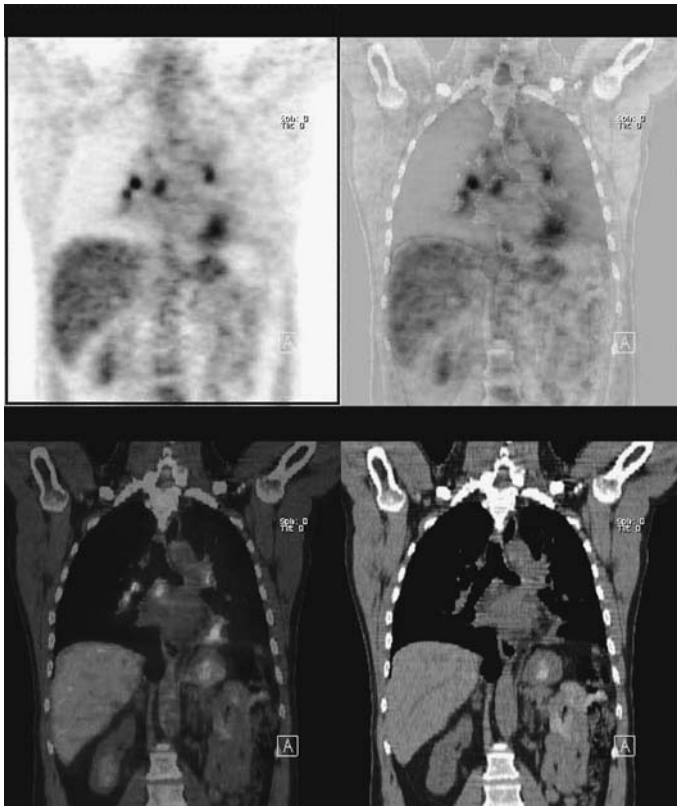

FIGURE 17.2B.2.

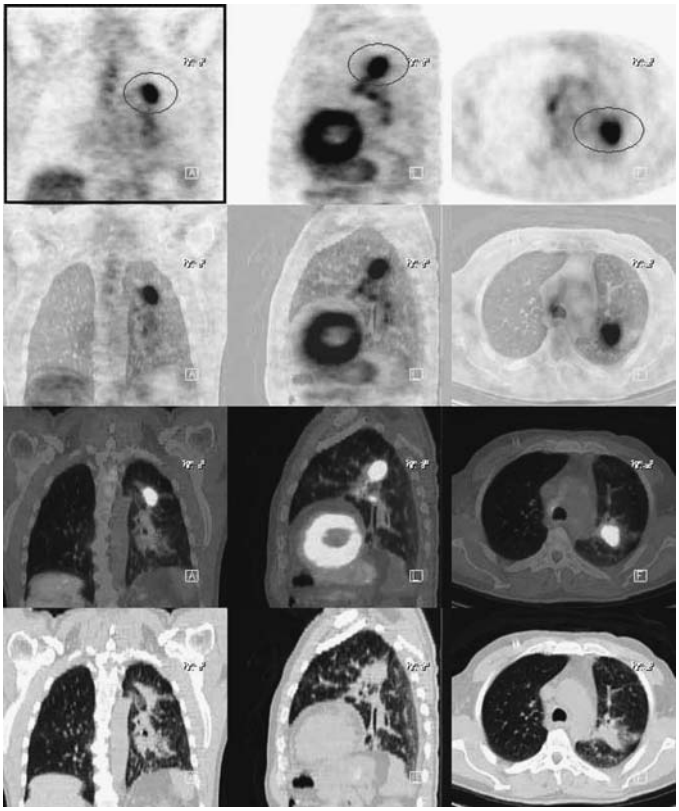

FIGURE 17.2B.3.

Pearls and Pitfalls

- *The 5-year survival rate for Stage IV lung cancer patient is 1%.*
- *MRI should be a consideration when evaluating for brain metastases.*[14,23]

Discussion

Solitary brain metastasis may present synchronously or metachronously. Postoperative radiation to the lesion in the brain may improve survival.

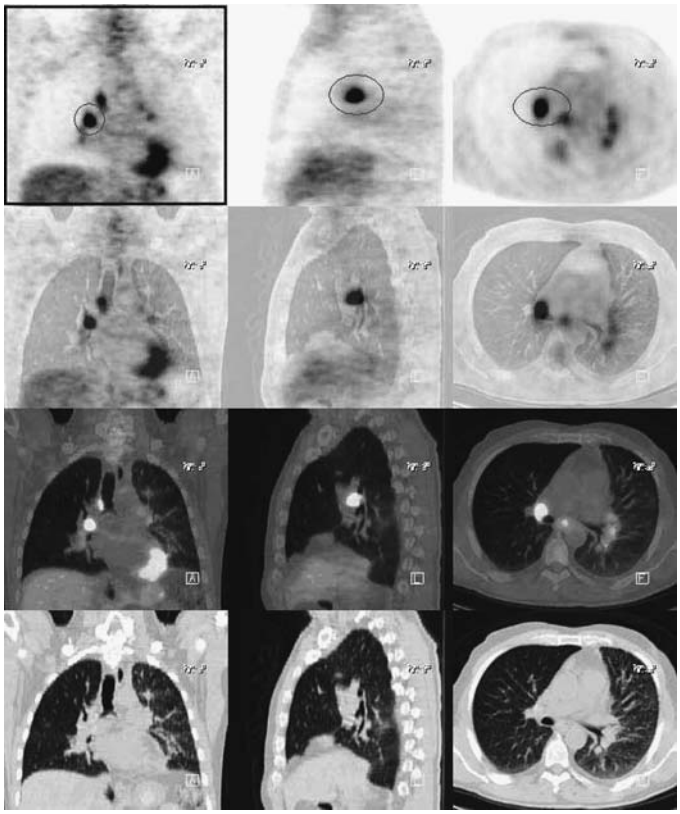

FIGURE 17.2B.4.

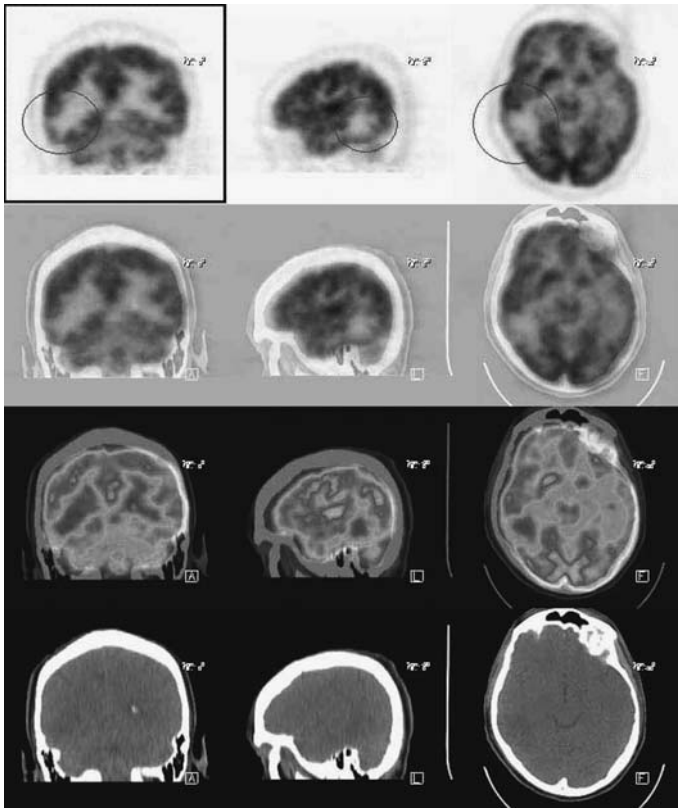

FIGURE 17.2B.5.

Case 17.3

History

85-year-old female who has a large mass in the left midlung suspicious for malignancy. There was also lymphadenopathy seen involving the left hilum, subcarcinal area, and the azygoesophageal space on a recent chest CT study. Evaluation for staging is requested.

Findings

There is a large intensely hypermetabolic mass (*Figure 17.3.1*) in the left midlung extending medially to the mediastinum and laterally to the pleural surface (*Figure 17.3.2*). There is also extensive hypermetabolic pathology seen involving the AP window, prevascular space (*Figure 17.3.3*), right paratracheal region, subcarina, and the right supraclavicular area. No evidence for distant hypermetabolic lesions. The vocal cord uptake is physiological. The hyperactivity in the shoulders is likely related to degenerative changes.

Impression

Large intensely hypermetabolic left lung mass extending to left pleural surface and mediastinum with evidence for multiple hypermetabolic lymph nodes highly suspicious for at least stage III-B lung cancer.

FIGURE 17.3.1.

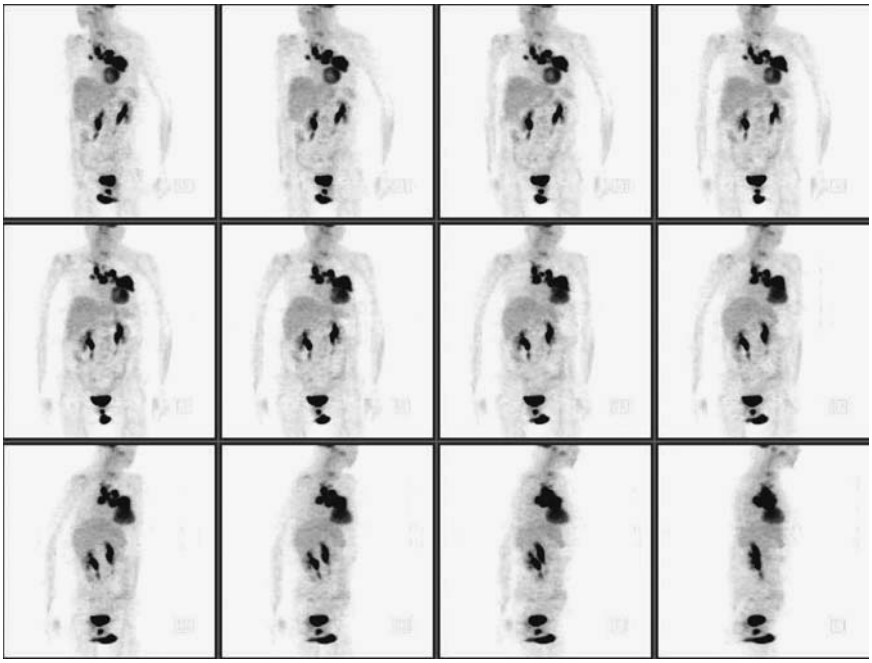

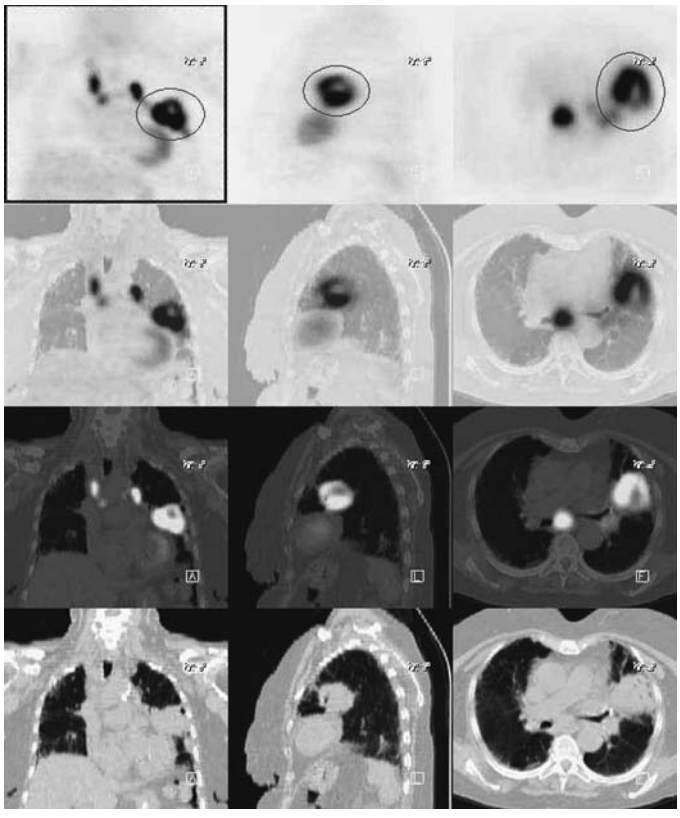

FIGURE 17.3.2.

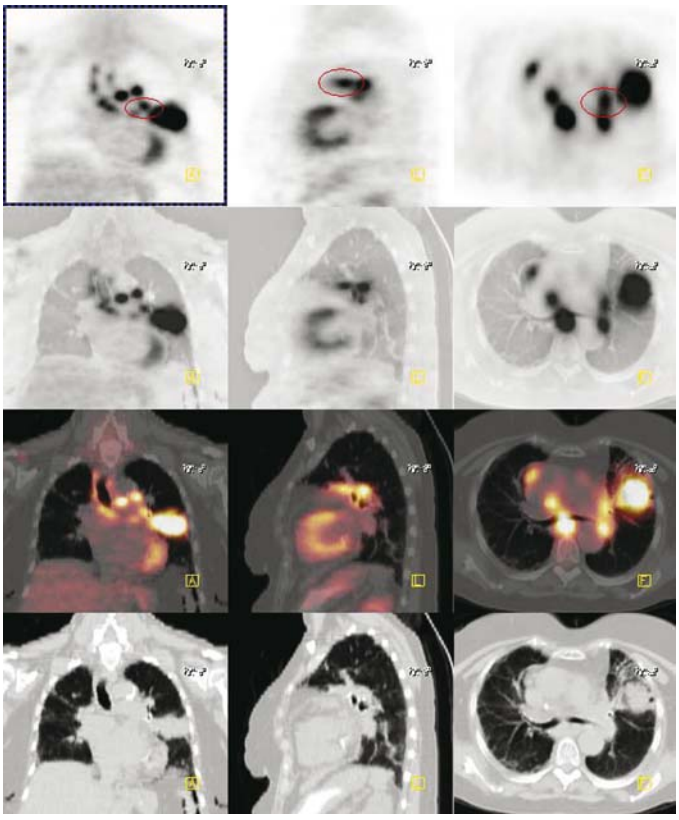

FIGURE 17.3.3.

Pearls and Pitfalls

- *Effusion (T4 staging) is best visualized with CT with malignant pleural lesions seen well on PET.*[1,2,7,8]

Discussion

CT scanning is still the method of choice in determining the size of the tumor. PET plays a limited role in evaluating the extent of the tumor's invasion to its adjacent structures. In the detection of mediastinal lymphadenopathy, however, the sensitivity for PET is reported as 67% to 92% and specificity as 97% to 100%.

Case 17.4

History

59-year-old male who has a history of lung cancer. The CT chest revealed a large neoplastic mass in the right upper lobe with supraclavicular adenopathy. Evaluation for malignancy is requested.

Findings

There is a large hypermetabolic mass with central photopenia (*Figure 17.4.1*) consistent with central necrosis in the right upper chest abutting the mediastinum (*Figure 17.4.2*). There is pericarinal adenopathy noted. Mild scoliosis is noted in the mid-thoracic spine. There is activity in the right ureter compatible with urinary stasis. No abnormality seen in the adrenal glands.

Impression

Bulky hypermetabolic mass in the right upper chest with adjacent pericarinal adenopathy consistent with stage III-B lung cancer.

Pearls and Pitfalls

- *Stage III-B cancer patients are generally not candidates for surgical intervention. The 5-year survival rate is 7% to 18%. The treatment of choice is chemotherapy and radiation therapy.*[4,7,13]
- *Some authorities have claimed the 4-year survival rate may increase to 46% with surgical intervention by resection of III-B disease.*[4,7,13]

Discussion

The distinction of primary malignant tumor and hilar or mediastinal adenopathy can be successfully assessed with PET-CT fusion imaging. The ability to superimpose metabolic abnormalities detected with PET with anatomic CT images is very helpful in this scenario. The pericarinal lymphadenopathy could have been mistaken as parenchymal disease.

FIGURE 17.4.1.

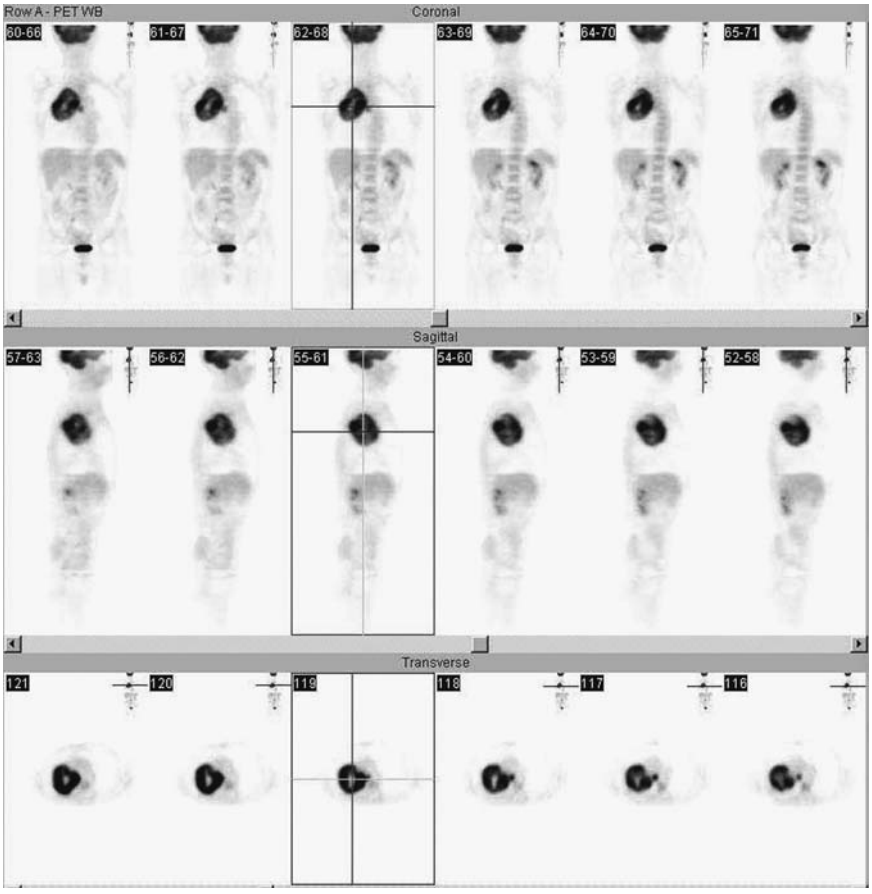

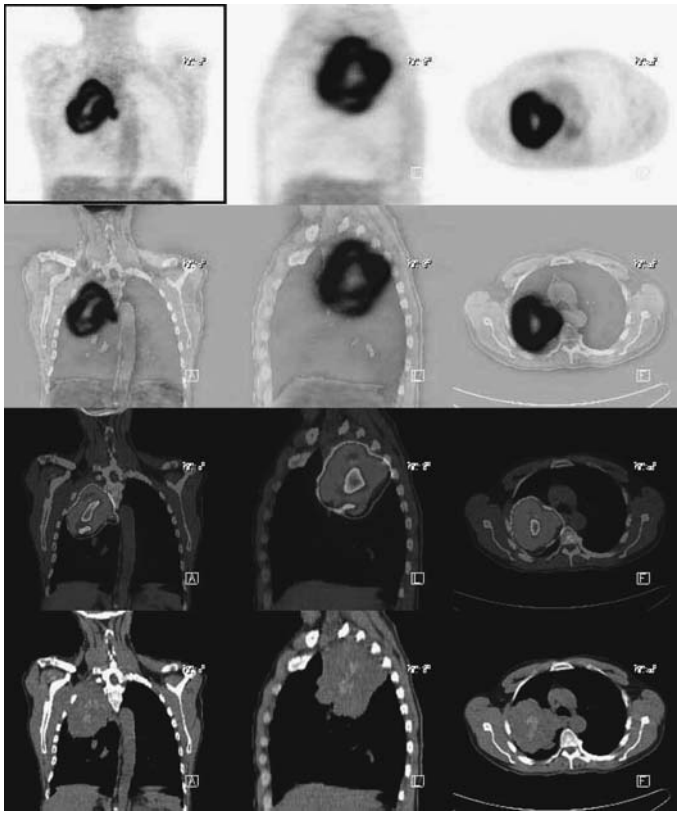

FIGURE 17.4.2.

Case 17.5

History

72-year-old female who has a history of lung cancer positive by bronchoscopy. The patient is being evaluated for staging.

Findings

Heterogeneous hypermetabolism in the right hilum, right upper, and right middle lobe (*Figure 17.5.1*) is present in the area of consolidation/mass seen on CT (*Figure 17.5.2*). There is intense hypermetabolism in the soft tissue mass in the right lung base posteriorly (*Figure 17.5.3*). Hypermetabolism in the lower tip of the left lobe of the liver just anterolateral to the gall bladder is suggestive of a metastasis; ultrasonography is advised as it is not definitely seen on CT and is superficial. The mild hyperactivity in the right supraclavicular region is a lymph node measured 1.40 × 1.35 cm. There is apparent wall thickening in a small bowel loop in the left lower quadrant, likely distal ileum, of uncertain etiology.

Impression

1. Extensive active disease involving a right lung base, right hilum, and right upper and middle lobes mass. It is difficult to accurately differentiate tumor burden from associated postobstructive pneumonia.
2. Possible hepatic metastasis as described above. Recommend ultrasonography.
3. Right supraclavicular lymphadenopathy suggestive of metastatic disease.

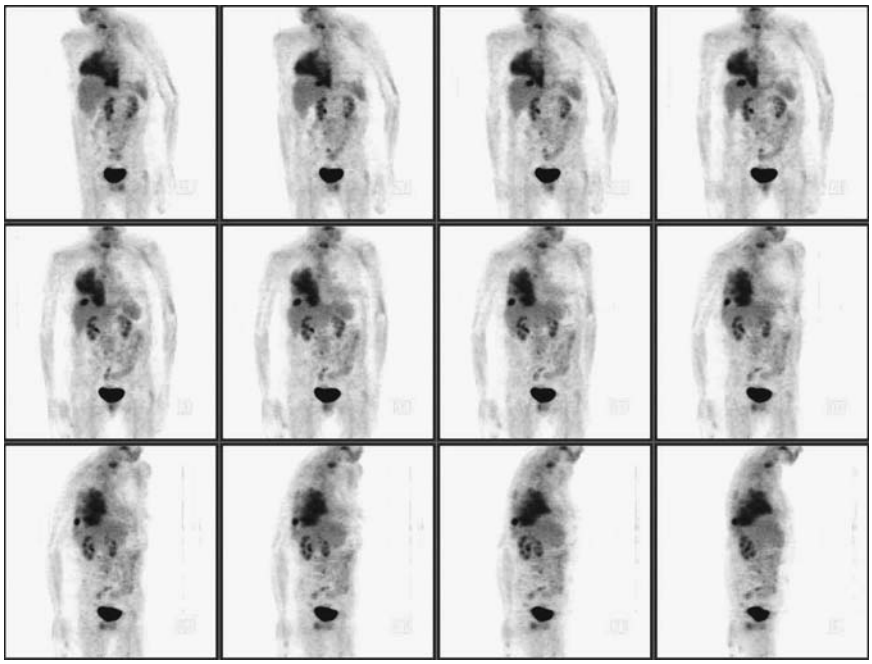

FIGURE 17.5.1.

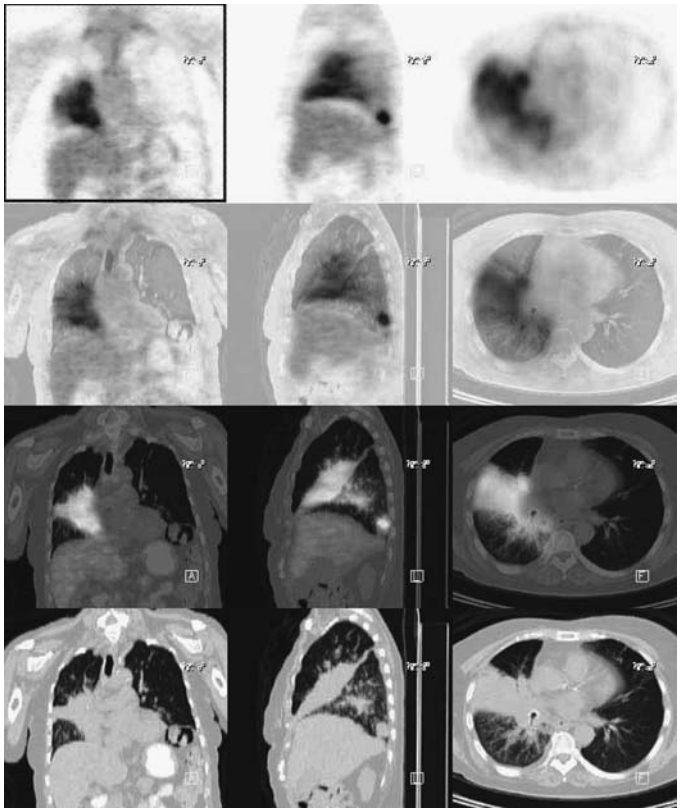

FIGURE 17.5.2.

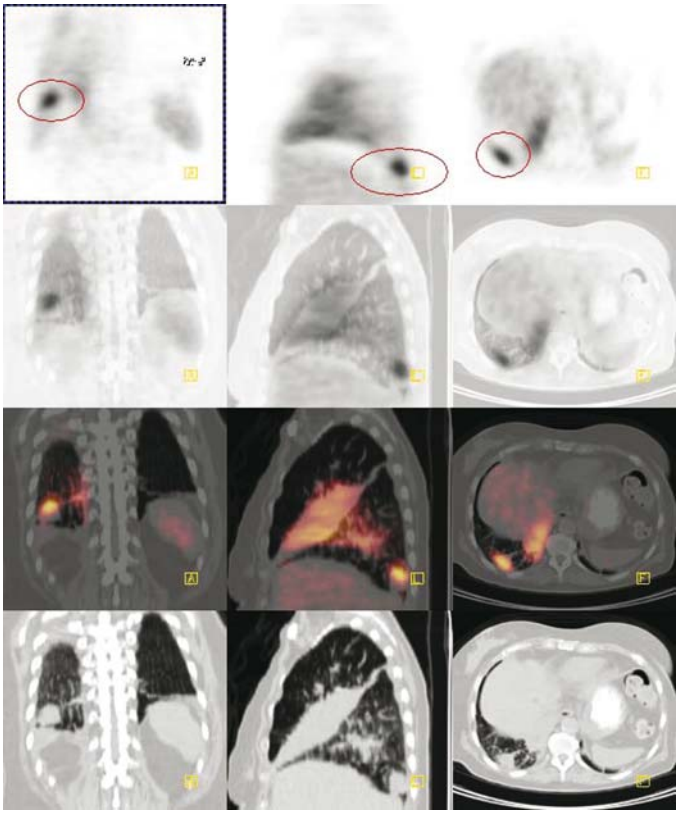

FIGURE 17.5.3.

Pearls and Pitfalls

- *The sensitivity of PET for malignant pleural disease with effusion is 95%.*[10,13]
- *Sputum cytology may be useful for diagnoses since 50% to 60% of the squamous cell carcinomas are proximal and involve the hila.*[7,8]

Discussion

A false-positive PET can sometimes be observed as reactive lymphadenopathy from post-obstructive pneumonitis. Malignant pleural disease associated with effusion is commonly FDG avid.

Case 17.6

History

65-year-old male with known small cell lung carcinoma is being evaluated for staging.

Findings

There is a left midlung mass of 2.8 × 2.8 cm dimension in the midcoronal plane at the hilar level (*Figures 17.6.1, 17.6.2, 17.6.3*). There is an adjacent 2.6 cm left hilar mass.

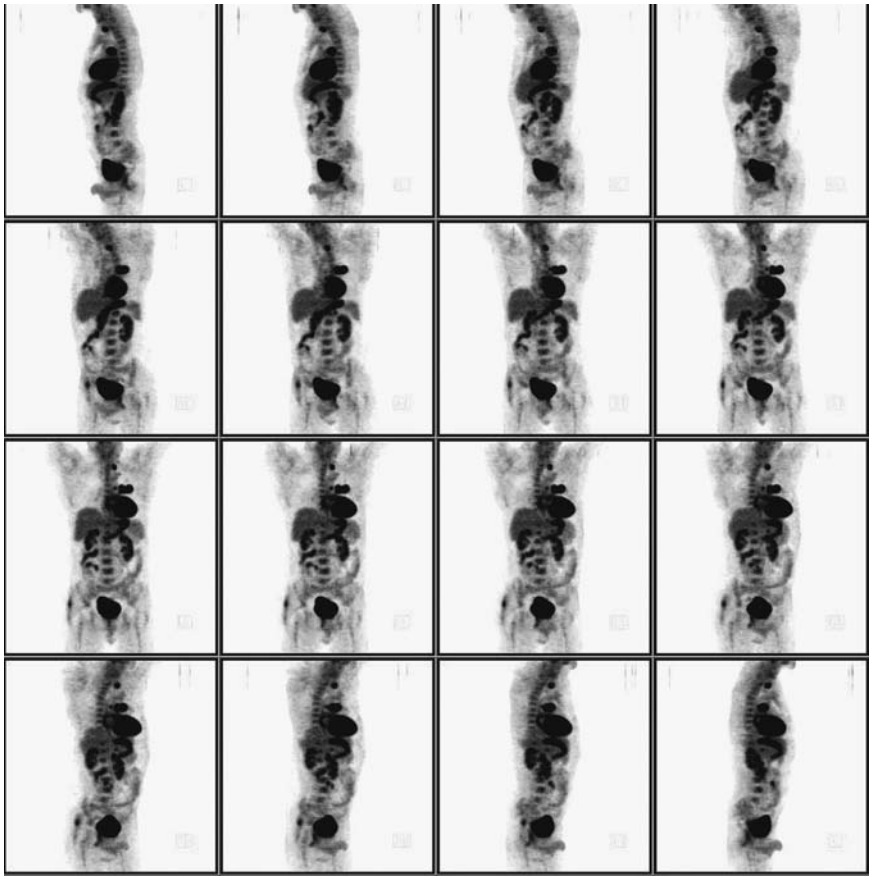

FIGURE 17.6.1.

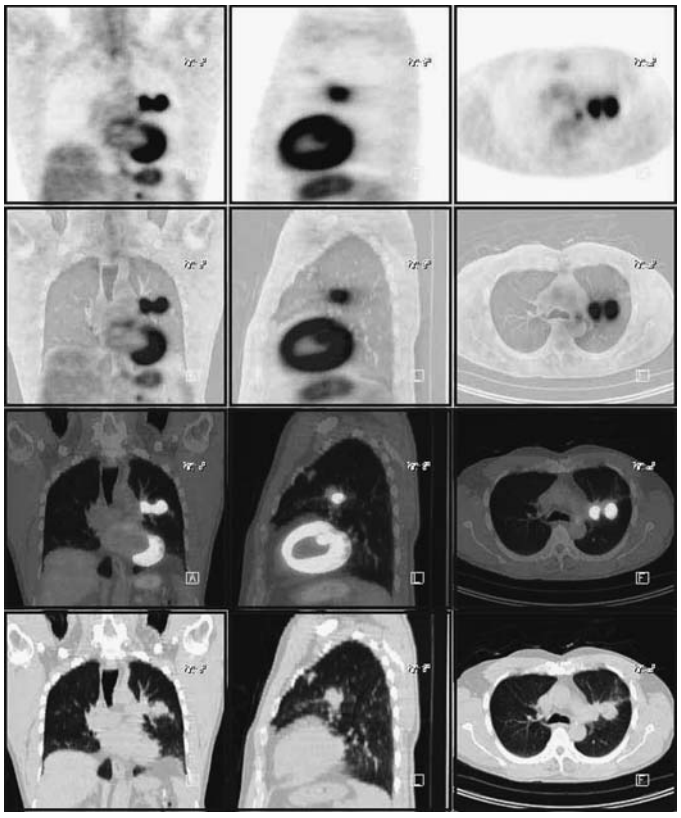

FIGURE 17.6.2.

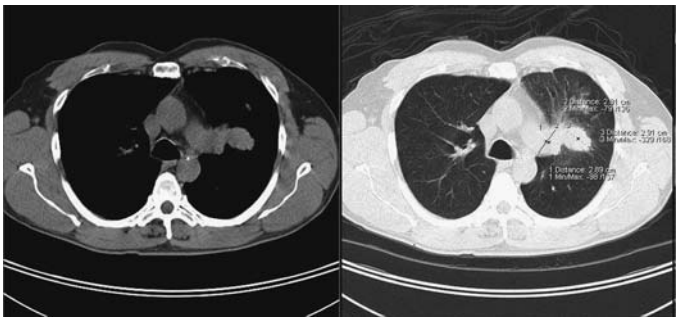

FIGURE 17.6.3.

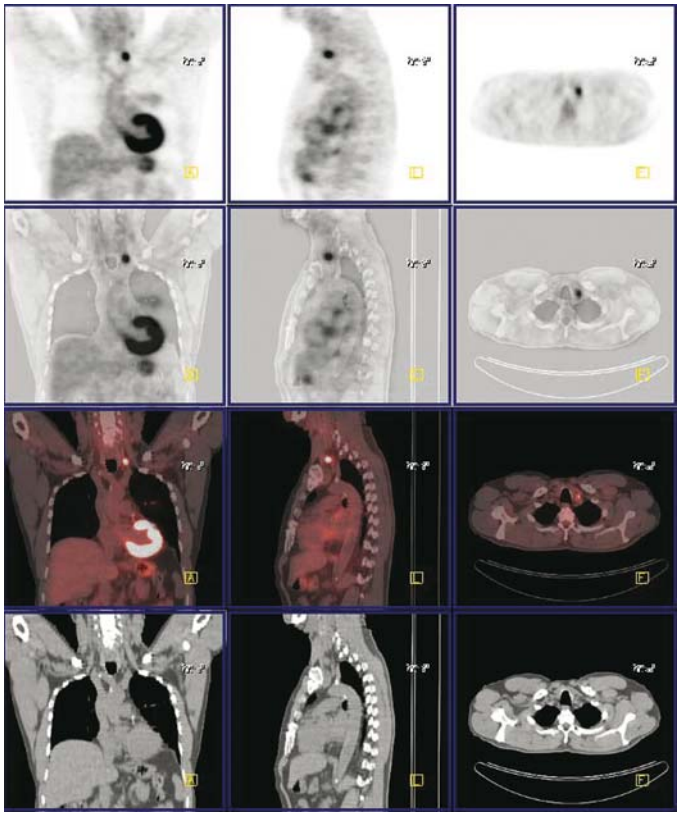

FIGURE 17.6.4.

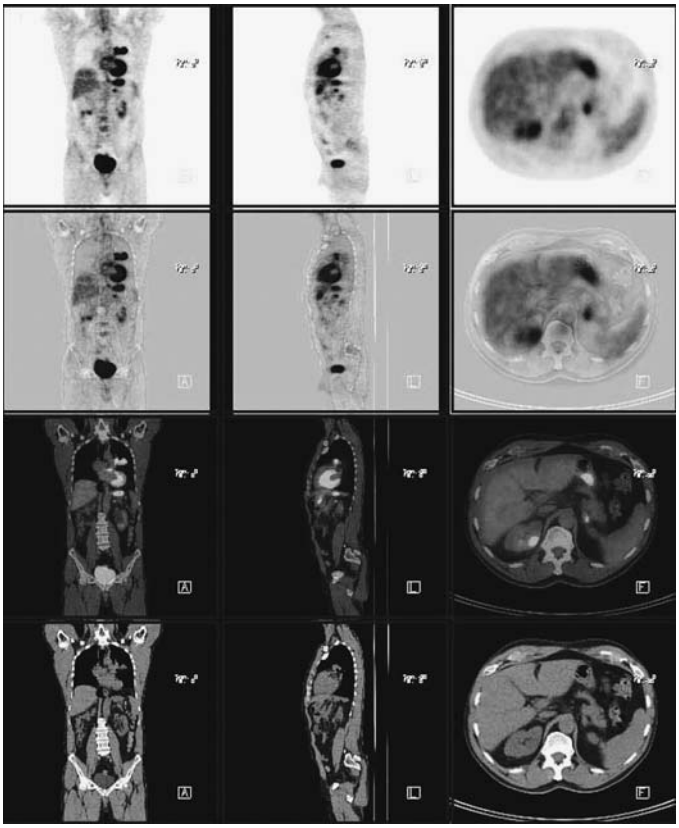

FIGURE 17.6.5.

There are several satellite nodules around the midlung mass, as well as a small nodule in the anterior segment of the left upper lobe near the apex. There is a small left peribronchial node (*Figure 17.6.4*) central to the left hilar mass. A definite distant metastasis is present in the left adrenal gland (*Figure 17.6.5*). There is an involved left supraclavicular node immediately lateral to the left thyroid lobe of 1.1 cm short axis dimension. There is a very small node of about 3 mm which is probably involved in the left jugular area at the vocal cord level. There is a focal area of hypermetabolism within the right gluteal musculature with lesser activity extending superior and inferior to it along the fascial plane. This most likely represents a muscular injection site. There is prominent but probably physiologic gastric activity.

Impression

1. The left midlung mass is intensely hypermetabolic, consistent with neoplasm. There is an adjacent hypermetabolic hilar mass, as well as a small left peribronchial node. There are also multiple satellite nodules near the mass and a small metastasis to the left pulmonary apex. Distant metastasis is evident in the left adrenal gland and left supraclavicular area, as well as a small probable 3-mm left jugular node.
2. There is focal hypermetabolism in the right gluteal musculature most likely representing an injection site for prior therapy.

Pearls and Pitfalls

- *11% of the small cell carcinoma patients are found to be in the advanced stages of their disease through PET imaging although they had been initially staged at I or II by conventional imaging.*[8,13,14]
- *PET imaging has the ability to detect extrathoracic malignancy using a whole body imaging approach. This valuable aspect of PET imaging allows it to detect extrathoracic metastases that are not otherwise suspected in 6% to 24% of the patients.*[8,10]

Discussion

Small cell carcinoma tends to be disseminated at the time of diagnosis. It is an aggressive and rapid growing tumor. Twenty-five percent of the patients will have thoracic involvement. Lung, liver, adrenal gland, bone, CNS, and locoregional lymph nodes are the most common sites for metastases. Chemotherapy is the therapy of choice.

18 Hematologic Malignancies: Lymphoma, Leukemia, Multiple Myeloma

Robert W. Henderson

Case 18.1

History

67-year-old male status post left neck biopsy proven to be lymphoma. The patient has not received any treatment yet. The PET study is requested for staging.

Findings

Examination of the head and neck area reveal multiple sites of lymphadenopathy bilaterally. This includes level-2 bilaterally, level-3 on the right side with a node on the left side at the same level, and level-4 on the right side. In addition, extranodal hypermetabolic activity is seen bilaterally in the lingual, palatine tonsil, and parotid glands (*Figure 18.1.1*). There are multiple bilateral axillary sites of lymphadenopathy (*Figures 18.1.2 and 18.1.3*). No evidence for hilar adenopathy. Mild activity in the mediastinal area is not clearly pathological. In the abdomen, there is focal uptake in the right upper quadrant in the gastric area most likely representing a physiologic finding. No evidence of para-aortic lymphadenopathy is seen. There is a curvilinear area of hypermetabolic activity in the lower quadrant most likely related to physiologic bowel activity (*Figure 18.1.4*). Focal activity in the right inguinal region would be consistent with a pathologic node.

Impression

Extensive lymphadenopathy predominantly involving the lymph node basins above the diaphragm with a node below the diaphragm in the right inguinal region consistent with stage III disease.

Pearls and Pitfalls

- *A single inguinal node upstages this patient from stage II to stage III.*[1,7,12,18]

Discussion

PET is a useful tool for detecting abnormal lymph nodes with lymphoma and usually identifies all lesions seen on CT. This includes disease in mesenteric lymph nodes where

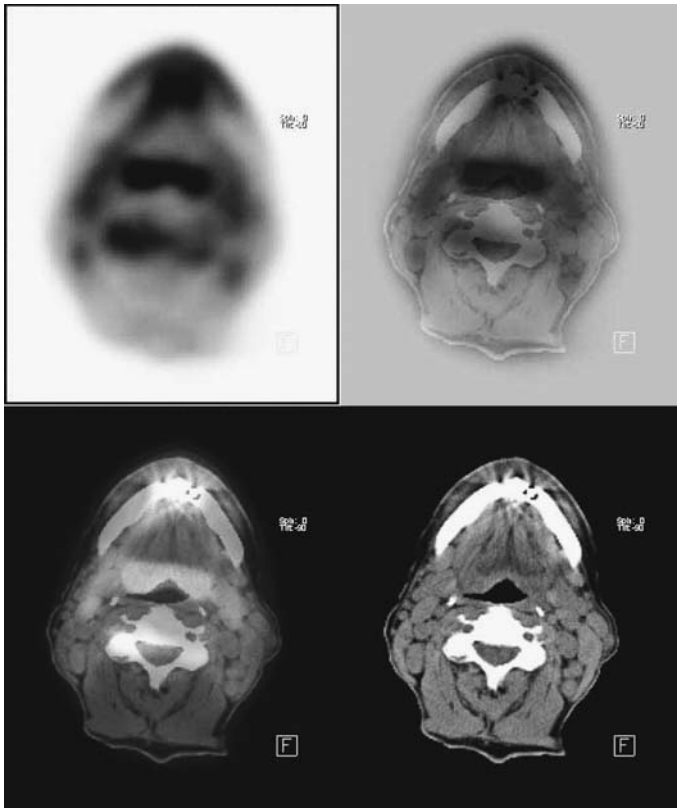

FIGURE 18.1.1.

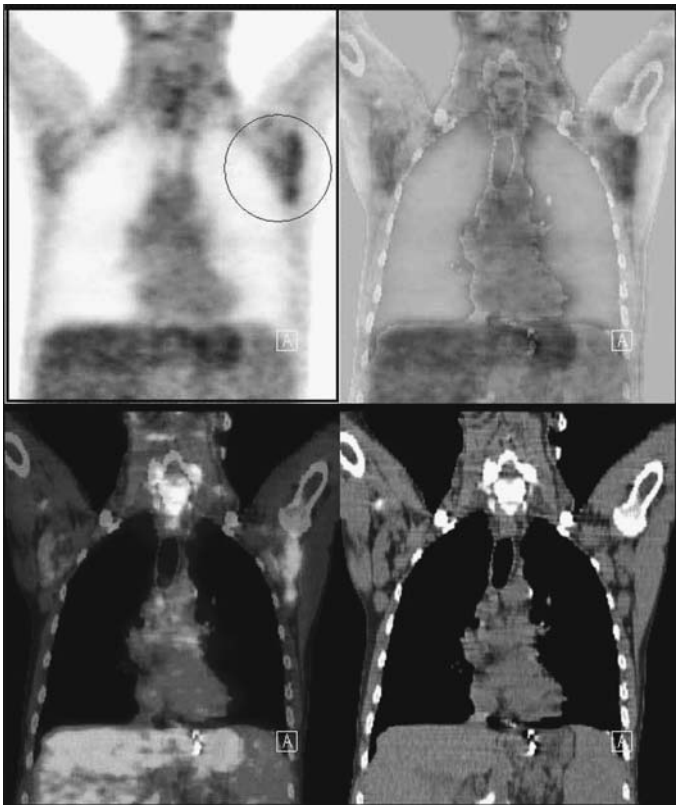

FIGURE 18.1.2.

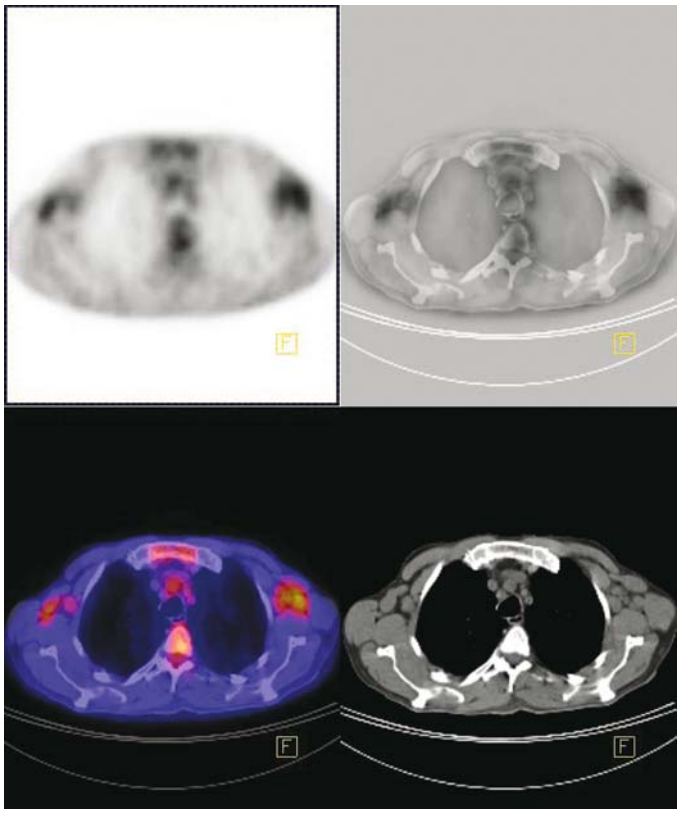

FIGURE 18.1.3.

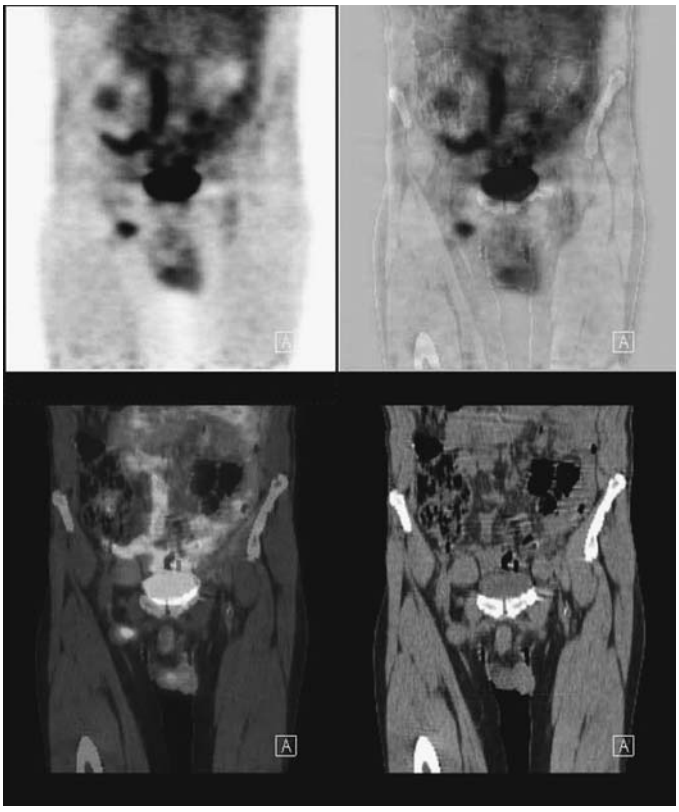

FIGURE 18.1.4.

CT may be inadequate. The sensitivity of PET for nodal disease is 62% to 100% based on the histology type and grade.

Case 18.2

History

62-year-old female with a history of lymphoma who presents with several suspicious nodules in the abdominal cavity. The CT of the pelvis was unremarkable. The patient is being seen for restaging of recurrent disease.

Findings

In the chest wall, bilateral breast implants are noted. There is a mass compressing the anterior medial aspect of the right implant (*Figures 18.2.1 and 18.2.2*) that is hypermetabolic. A focus of activity in the upper abdomen midline (*Figure 18.2.3*) is seen corresponding to a mesenteric node on CT. Along the right anterior lateral aspect of the abdomen adjacent to the wall of the ascending colon is another pathological lymph node. There is a mesenteric lymph node in the pelvis, not well defined on CT. A cluster of metabolic nodes is seen in the midline of the anterior pelvis. The linear activity in the left acromioclavicular joint is likely degenerative joint disease. The intense uptake below the left elbow medially is likely contamination. In the lower extremities, there are numerous superficial nodules seen scattered throughout both thighs (*Figures 18.2.4 and 18.2.5*), right greater than left, that are unusually metabolically active compatible with soft tissue tumor deposits. Two other nodules are noted in the upper thigh on the left.

Impression

Hypermetabolism involving the right breast, abdomen, pelvis, and lower extremities bilaterally compatible with disseminated lymphoma.

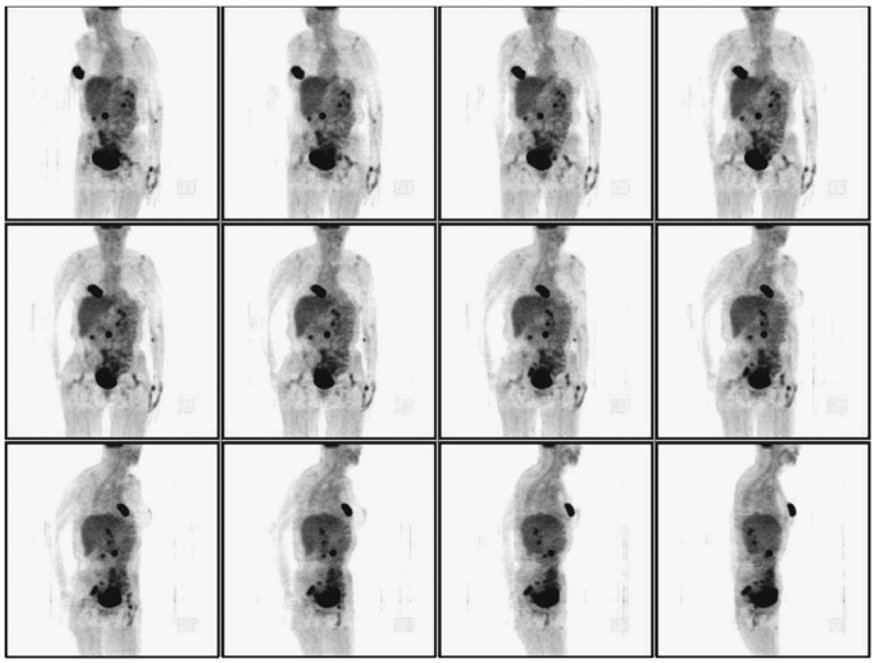

FIGURE 18.2.1.

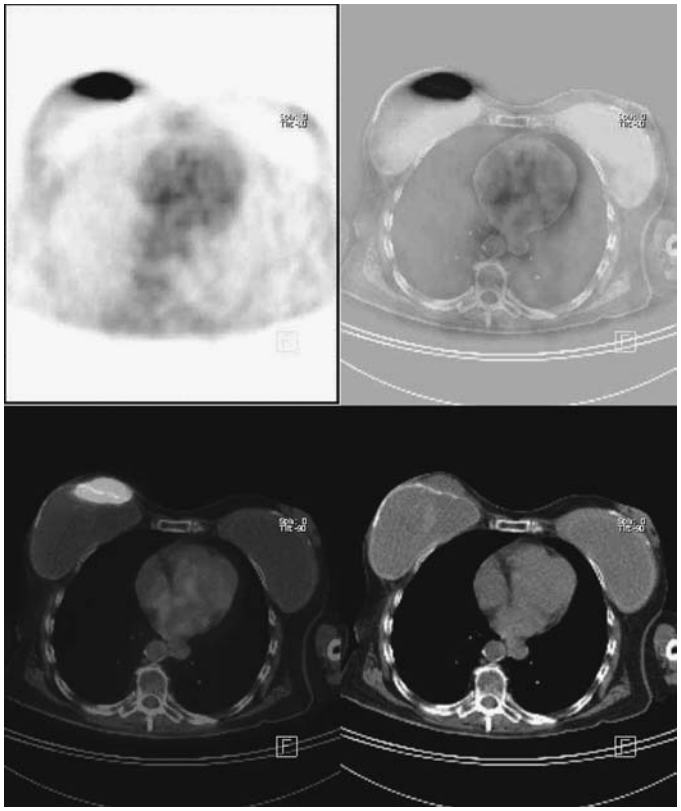

FIGURE 18.2.2.

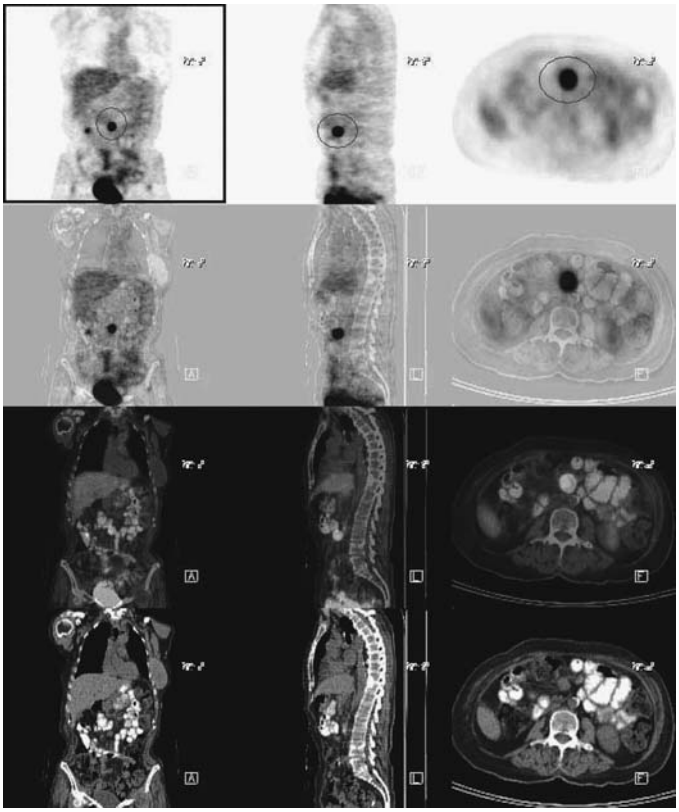

FIGURE 18.2.3.

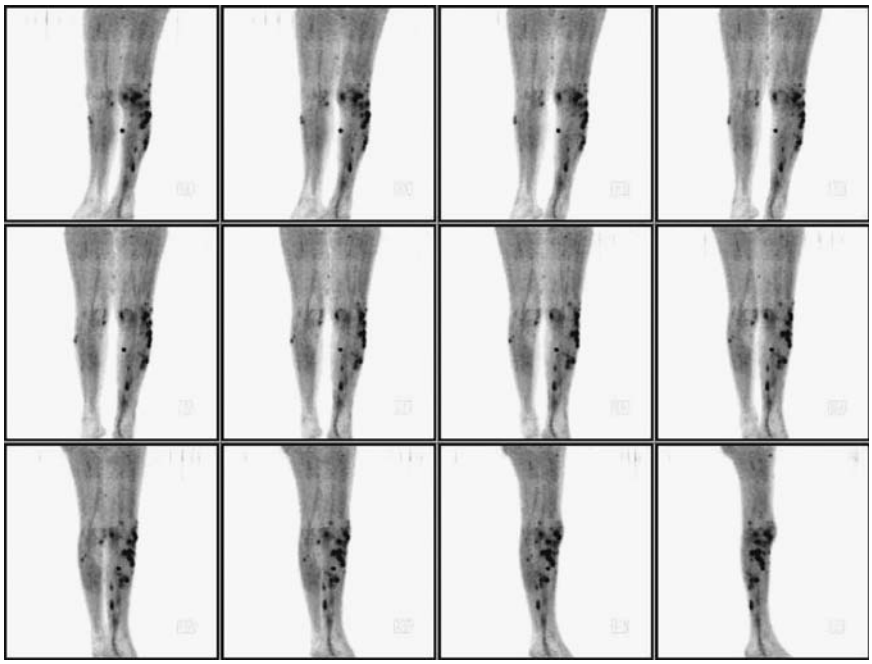

FIGURE 18.2.4.

FIGURE 18.2.5.

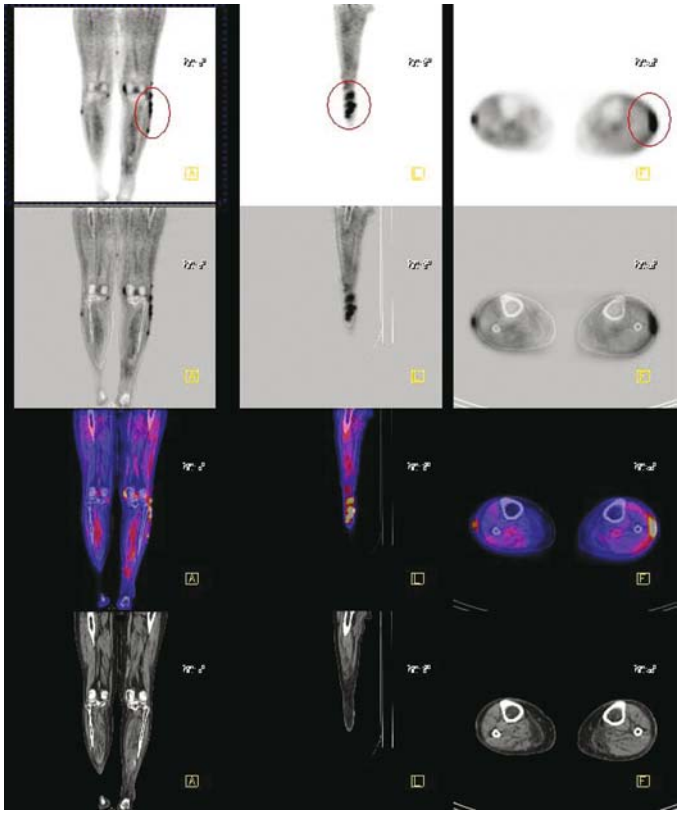

Pearls and Pitfalls

- *PET can isolate 57% more extranodal diseases than CT.*[12,15,21]

Discussion

In the staging of lymphoma, FDG PET is more accurate than CT. This is especially true when the lesions are nodally and extra-nodally involved where CT/MR has a limited value. Patients with splenic, hepatic, and bone marrow involvement tend to have a poor prognosis in comparison with isolated nodal disease. Cutaneous/subcutaneous lymphoma is much better appreciated on PET than CT.

Case 18.3A

History

64-year-old female with a recent diagnosis of lymphoma. The study is being done for disease staging.

Findings

The PET scintigraphy demonstrates bilateral cervical and supraclavicular pathologic adenopathy, which is intensely hypermetabolic (*Figure 18.3A.1*). There is bulky patho-

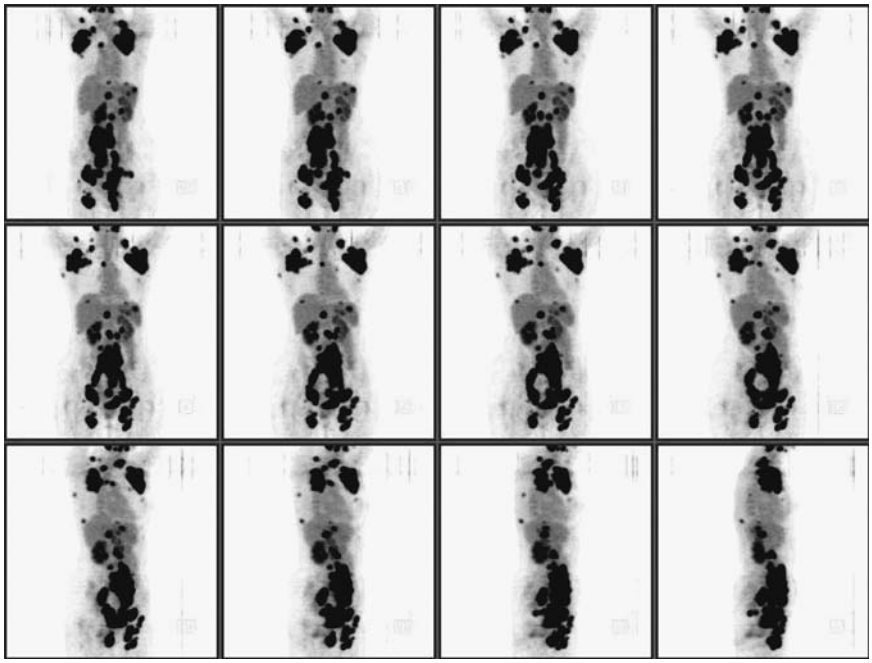

FIGURE 18.3A.1.

logic biaxillary adenopathy; all nodes are very intensely hypermetabolic. In the abdomen, there is pathologic retrocrural adenopathy (*Figure 18.3A.2*) and abdominal retroperitoneal adenopathy. There is a fairly bulky confluent mesenteric mass of pathologic hypermetabolic adenopathy (*Figure 18.3A.3*). There is a virtual chain of pathologic adenopathy throughout the common external and inguinal lymph node chains, with additional left internal iliac adenopathy.

Impression

There is bulky intense hypermetabolic adenopathy, both above and below the diaphragm. Above the diaphragm and within the thorax, the disease is limited to a right superior mediastinal and a left internal mammary node. However, there is bulky bilateral axillary, bilateral cervical, and bilateral supraclavicular adenopathy. There is virtually continuous disease below the diaphragm from the retrocrural space to the inguinal areas bilaterally.

Pearls and Pitfalls

- *Extent of widespread lymphoma is easier to visualize with PET than CT.*[15,16]

Discussion

Laparotomy has an important role in staging. It has the ability to detect 20% to 30% of the patients with presumed only supradiaphragmatic disease also with infradiaphragmatic involvement. One major disadvantage of laparotomy is that it is a inva-

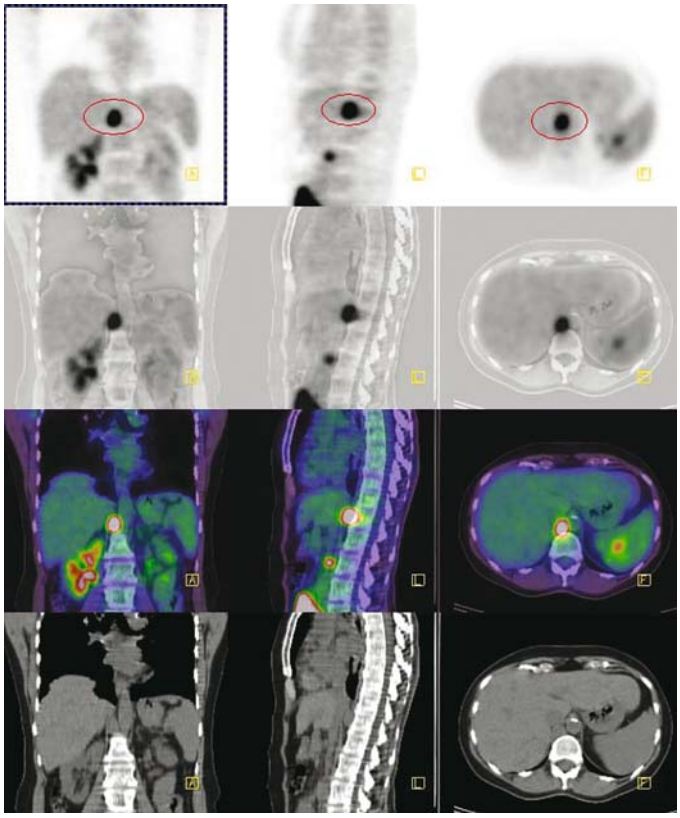

FIGURE 18.3A.2.

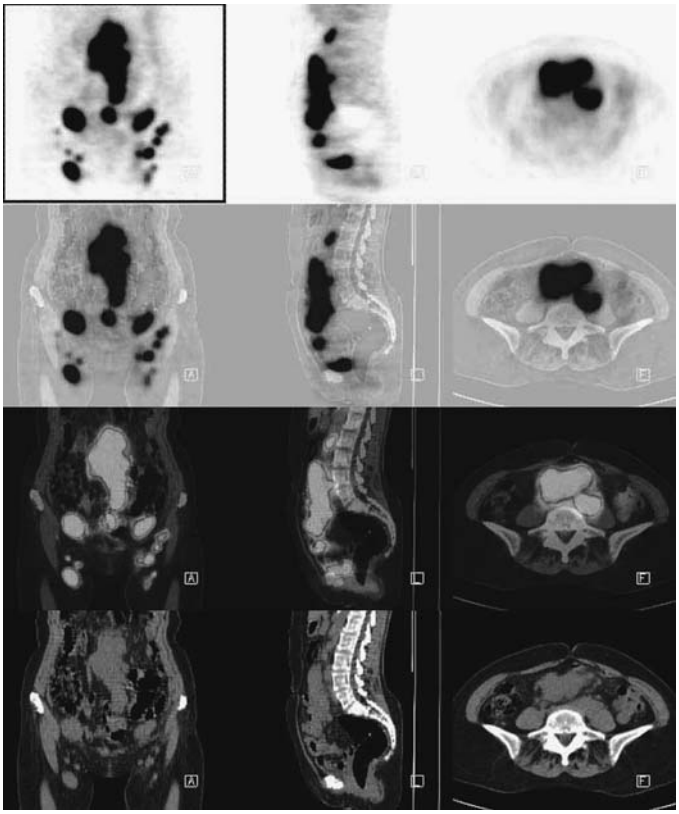

FIGURE 18.3A.3.

sive procedure. PET has the potential to identify these lesions without any long-term complications.

Case 18.3B

History

64-year-old female with a history of lymphoma being evaluated for restaging. The current exam is compared directly with the prior PET scintigraphy.

Findings

There is bulky pathologic biaxillary adenopathy (*Figure 18.3B.1*). There are a few small remaining supraclavicular nodes, but there has been a significant regression in supraclavicular disease since the prior exam. The hepatic and splenic lesions have resolved. However, the reduction in bulk of the axillary adenopathy is modest. Likewise, there has been only a moderate decrease in the bulk of the bilateral common iliac, right posterior internal iliac and external iliac adenopathy. The overall impression is one of a moderate interval partial response to therapy, with the smallest nodes, such as the superior mediastinum and internal mammary no longer visible, and the bulkiest disease in the axilla and iliac areas showing only modest improvement. The most dramatic improvement is the resolution of the hepatic and splenic lesions. Overall, the bulk of the disease has decreased on the order of 50% to 60%.

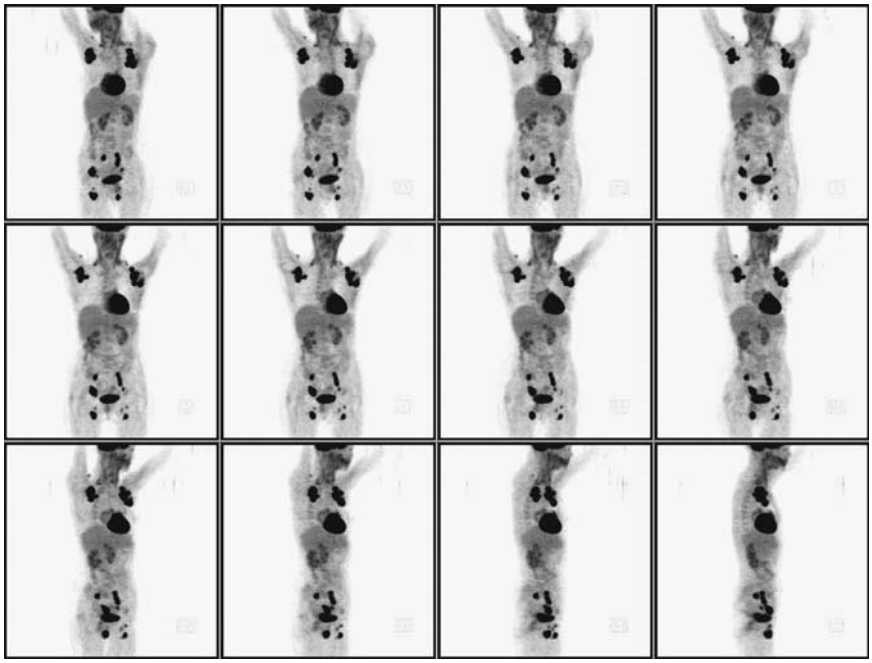

FIGURE 18.3B.1.

Impression

Interval significant partial response to interval therapy as detailed above.

Pearls and Pitfalls

- *62% to 100% of the FDG positive patients will relapse after first-line chemotherapy; in contrast, only 4% to 16% of the patients with negative PET will relapse.*[9,18,20]
- *30% to 64% of the residual masses will remain viable following the completion of therapy, demonstrating persistent metabolic uptake.*[9,18,20,23]
- *Patients with a negative PET will relapse in 16% to 25% on a long-term followup.*[10,13,16,22]
- *80% of the patients who relapse do so in another site.*[10,13,16,22]

Discussion

Response to therapy is easier to conceptualize with the whole body images. Complete remission is very important after first-line chemotherapy since it has a higher rate for progression-free survival than partial remission. Conventional imaging is inferior to PET in differentiating residual malignancy vs. fibrotic tissue. It has a high predictive value for relapse and determining the overall prognosis when comparing with patients without FDG uptake. One limitation of PET is that uptake from thymic hyperplasia and histiocytic reaction can cause false-positive results.

Case 18.4

History

47-year-old male with diagnosis of solitary plasmocytoma of the T-10 vertebral body. He has had subsequent proton therapy to the thoracic spine and chemotherapy and is status post decompressive T-10 laminectomy.

FIGURE 18.4.1.

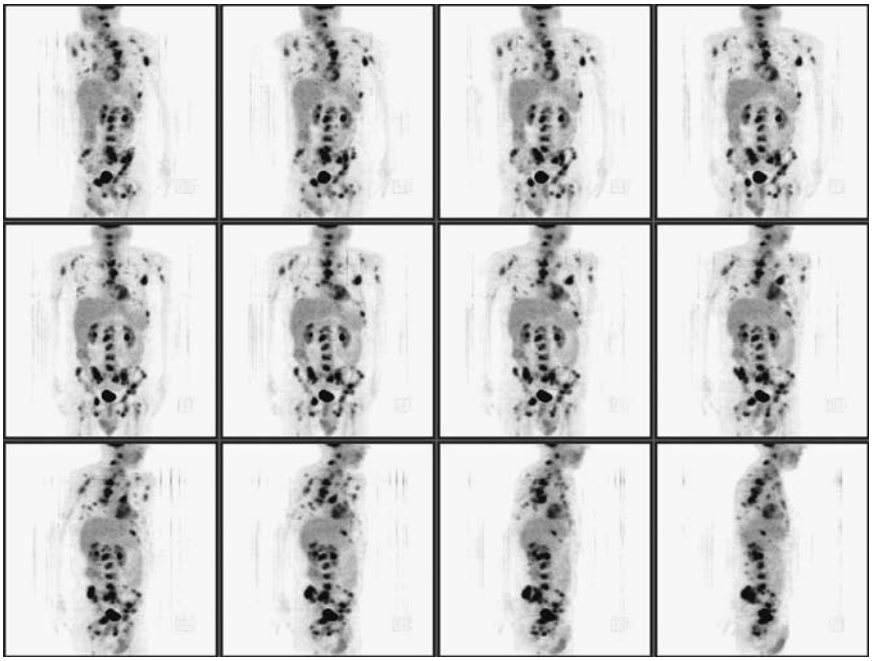

Findings

There are numerous intensely active randomly distributed pathologic hypermetabolic foci within the central skeleton on the PET scintigraphy (*Figure 18.4.1*). This is consistent with extensive active multiple myeloma and correlates with lytic disease, evident on the concurrent CT. There is also left scapular involvement. There is heavy involvement of the central posterior pelvis bilaterally in the medial iliac bones and in the sacral wings (*Figure 18.4.2*). There is also bilateral ischial uptake. In the spine, there is heavy involvement of L-2 through L-5 (*Figure 18.4.3*) and on CT there appears to be a right-sided pathologic fracture at L-3 (*Figure 18.4.4*). In the thoracic spine, there is lytic disease but no hypermetabolism at the level of T-10 where there had been decompressive laminectomy and fusion. In the upper thoracic spine, there are multiple lesions. In the upper thoracic spine, probably T-3, there is involvement of the left anterior aspect of the bony spinal canal with possible epidural involvement. There is a cortical infraction at the posterior aspect of the mid thoracic vertebra, about T-7, with a cortical infraction into the bony spinal canal. There are both C-2 vertebral body involvement (*Figure 18.4.5*) and multiple areas of cervical posterior element involvement. MR with contrast would be an appropriate consideration to evaluate epidural disease, particularly in the cervical and thoracic areas and particularly if there were long tract signs. Also noted on the CT scan is some dependent lower lung atelectasis, several lytic rib lesions, a small hiatus hernia, and the mentioned lytic disease of the thoracolumbar spine.

Impression

Widespread and advanced disease of bone, consistent with multiple myeloma with heaviest involvement in the spine and pelvis as detailed above.

Pearls and Pitfalls

- *Focal and diffuse osseous involvement is a common finding for multiple myeloma.*
- *25% of the PET positive patients will have a negative plain film.*[8,14,19]

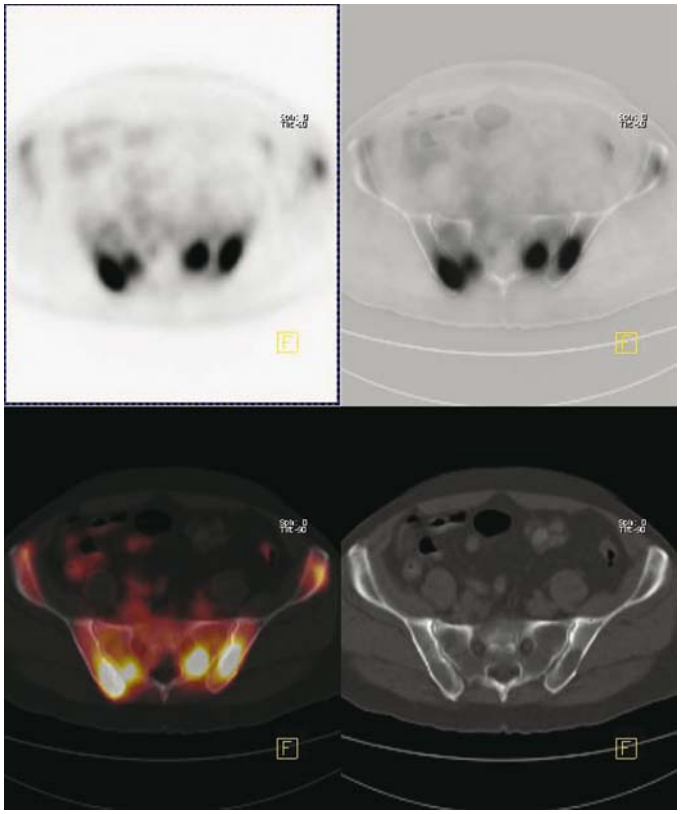

FIGURE 18.4.2.

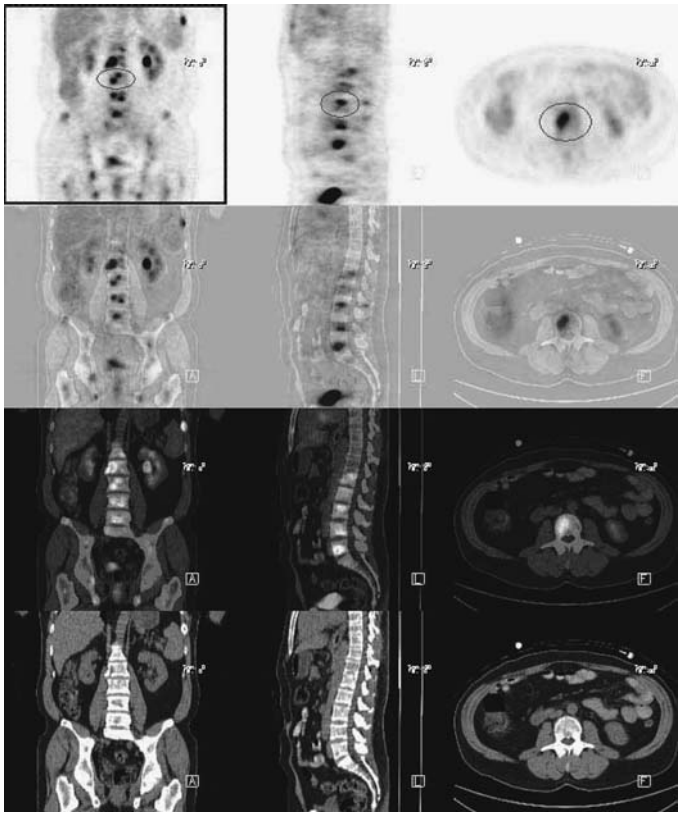

FIGURE 18.4.3.

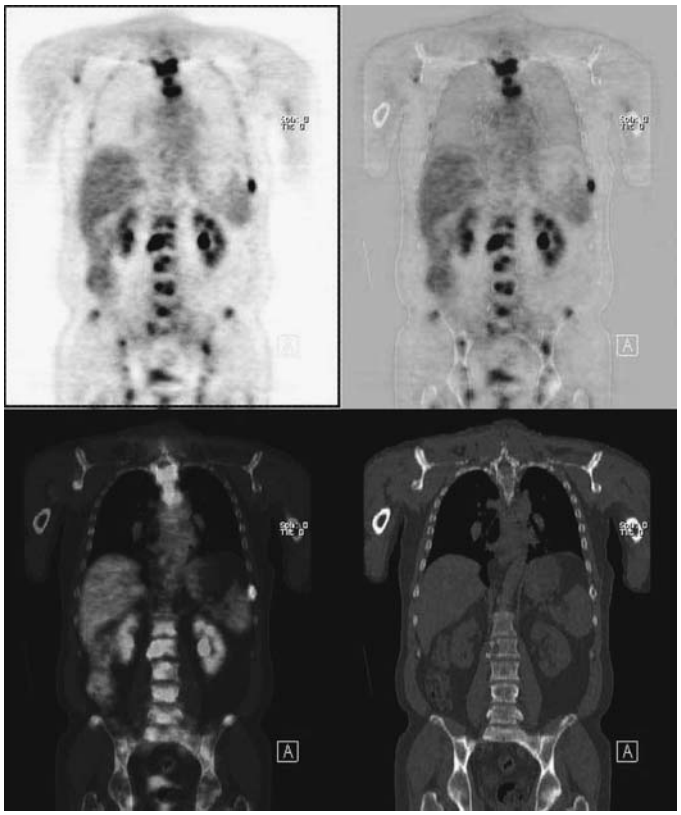

FIGURE 18.4.4.

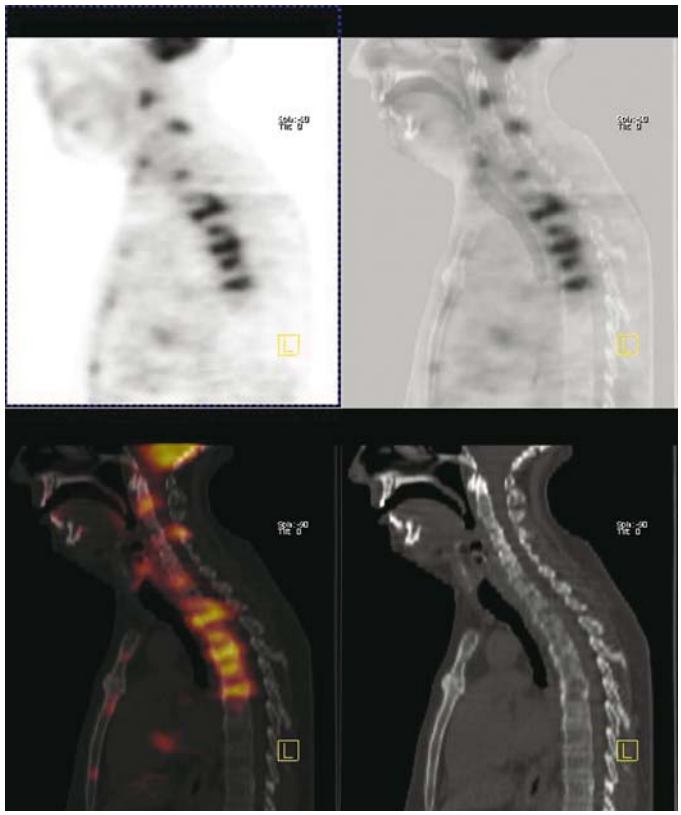

FIGURE 18.4.5.

- *25% of the time, PET will identify focal extramedullary disease that was not previously suspected, indicating a poor prognosis irrespective of treatment.*

Discussion

Multiple myeloma is a plasma cell neoplasm. The management is primarily based on staging and monitoring. Skeletal survey is commonly for staging and unfortunately tends to underestimate bone marrow involvement. Bone scintilligraphy and gallium study may be useful but they are unreliable for staging and monitoring. MR is good for assessment of local disease. CT fails to differentiate active disease from scar. PET can detect early marrow involvement of multiple myeloma. It is useful in assessing the extent of active disease at the time of initial presentation and in evaluating treatment response.

Case 18.5

History

42-year-old male with a history of acute myelocytic leukemia. He had a left neck lymph node biopsy which was inconclusive for malignancy. His bone marrow biopsy was positive for AML. The patient is being evaluated for recurrence.

Findings

In the left neck, there is a single left jugular node below the angle of the jaw and deep to the anterior sternocleidomastoid muscle (*Figures 18.5.1 and 18.5.2*). It is inseparable from the carotid sheath by CT, but appears to be between the carotid sheath and the anterior aspect of the sternocleidomastoid muscle on PET. It is estimated on PET to be spherical in shape and just over 1 cm in dimension. The remainder of the head and neck activity appears modestly active with some submandibular activity asymmetry, right greater than left. The right submandibular gland is somewhat larger than the left. This probably represents some inflammation of the right submandibular gland. Parotid activity is symmetrical. There is vocal activity noted. The whole body study is unremarkable other than notation of two findings. There is increased central marrow activity with some heterogeneity of activity (*Figure 18.5.3*), consistent with AML and its treatment. The second finding is focal hypermetabolism which is located by CT to be in close proximity to the anterior margin of the left hip joint (*Figure 18.5.4*). There

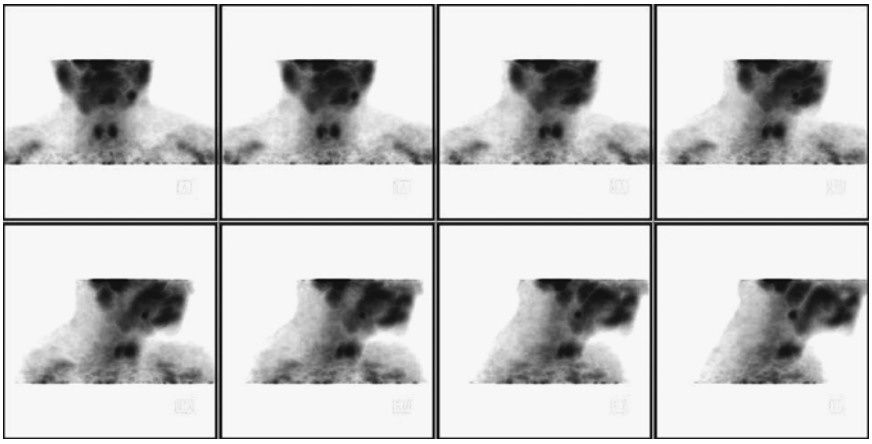

FIGURE 18.5.1.

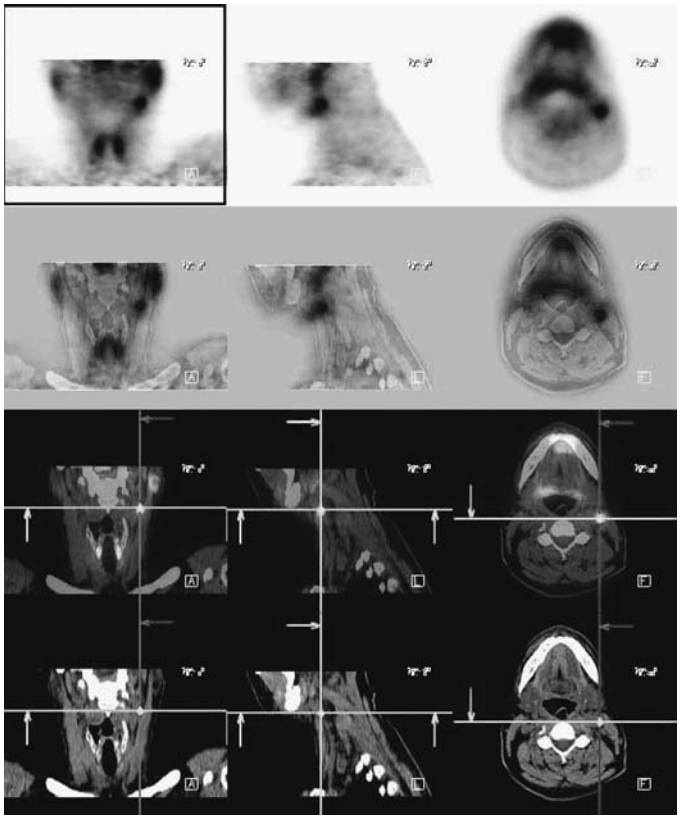

FIGURE 18.5.2.

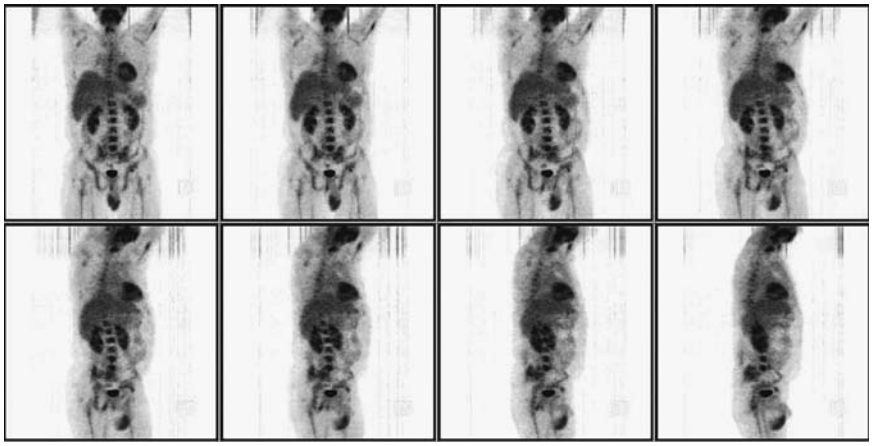

FIGURE 18.5.3.

is modest activity within the hip joints bilaterally. The location of the left-sided focus favors synovitis/synovial cyst. No abnormal nodal uptake is evident in the torso.

Impression

1. There is a single hypermetabolic lymph node in the left jugular chain, appearing to be lateral to the carotid and deep to the anterior aspect of the sternocleidomastoid muscle.

FIGURE 18.5.4.

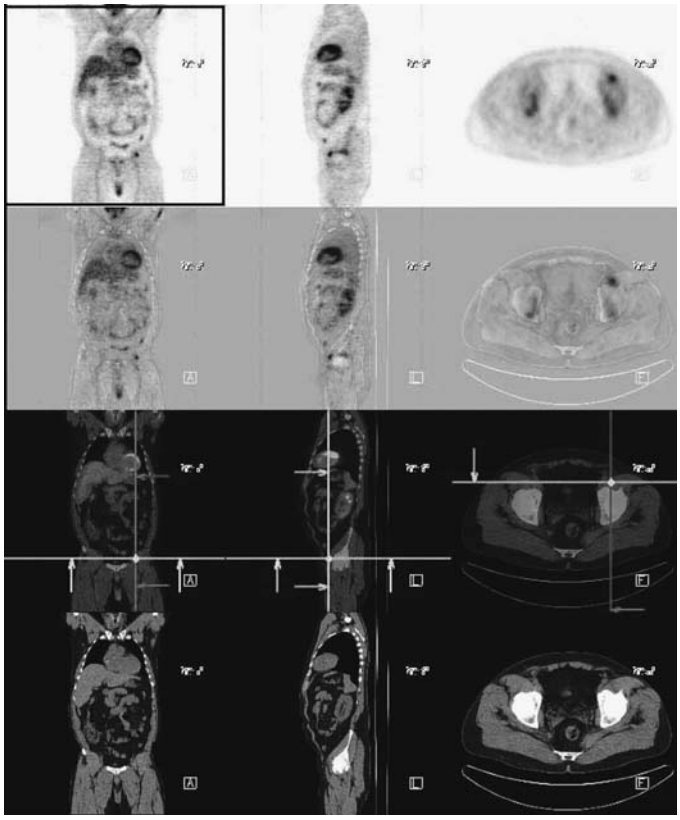

2. Heterogeneity of and increased activity of the central marrow, consistent with AML/treatment.
3. Focal activity anterior to the left hip joint, likely related to synovitis by location.

Pearls and Pitfalls

- *The intense FDG uptake in the lingual tonsil and vocalis muscle is physiologic.*[2,3]
- *The moderate symmetrical uptake in the salivary gland activity is physiologic.*[2,3]
- *CT scan can distinguish inflammatory joint activity in the hip from inflammatory activity in the external iliac node.*[25]

Discussion

Twenty percent of new leukemia diagnosed in children is acute myelocytic leukemia (AML). In adults males, Caucasians, and patients with a median age of 65 are predisposing factors. Some other etiology to this disease includes prior radiation exposure, toxins, and genetics. Fatigue, fever, and dyspnea are common clinical features. Blood count and smear is the best initial screening test. Anemia, neutropenia, and thrombocytopenia are usually seen. Chemistry profile may reveal an LDH elevation. Bone marrow is the definitive diagnosis. CT can detect any suspicious large bowel thickening from infection. Echocardiogram for baseline cardiac function prior to chemotherapy. Technetium bone scan is for occult osteomyelitis and Gallium study is for occult deep tissue infection. PET is to monitor treatment response and restaging.

Chemotherapy is the cornerstone for treatment. Radiation for oncologic emergency such as cord compression fracture. Bone marrow transplant may be an effective approach for cure.

The 5-year survival for age <60 is 25% to 30% and fewer than 10% will appear in older population. The long-term survival rate of pediatric patients is 50%. Seventy-five percent of the patients will be disease free.

Case 18.6A

History

27-year-old female who has a history of Castleman's disease presenting with retroperitoneal adenopathy in the abdomen on CT. Evaluation for staging is requested.

Findings

There is a large hypermetabolic mass in the left pelvis with two smaller lesions noted inferiorly and to the right of midline (*Figures 18.6A.1 and 18.6A.2*) compatible with known Castleman's bowel wall lymphoid infiltrates. There is a smaller para-aortic node superiorly that is hypermetabolic. Very mild bilateral hilar uptake is noted which may represent minimum disease involvement vs. nonspecific inflammatory disease.

Impression

Multifocal sites of hypermetabolism in the left pelvis as described above compatible with known Castleman's disease.

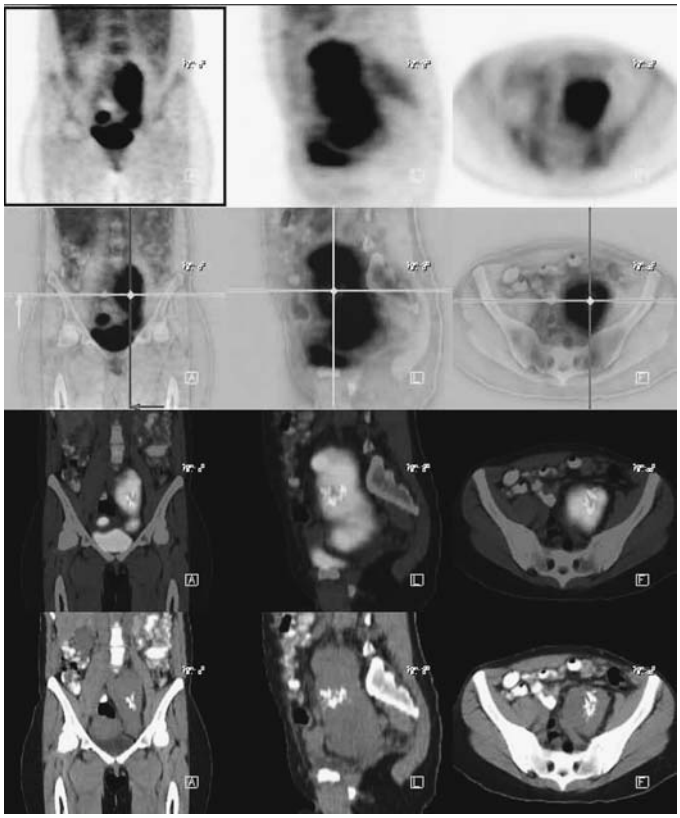

FIGURE 18.6A.1.

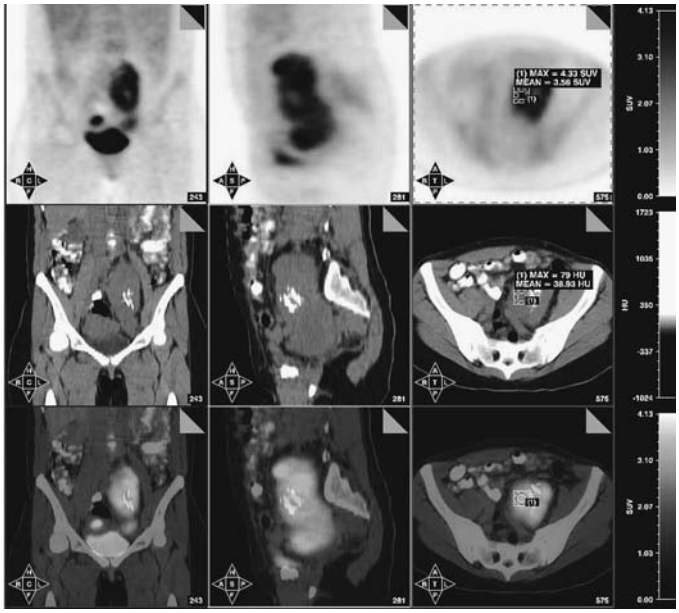

FIGURE 18.6A.2.

Pearls and Pitfalls

- *This patient is a good candidate for Rituxan treatment because she exhibits a CD-20 positive cytology on biopsy.*[4,5,24]

Discussion

Castleman's disease, more specifically, the hyaline vascular type, is an angiofollicular lymph node hyperplasia most frequently observed pathologically as hypervascular hyaline germinal centers and extensive capillary proliferation in the nodes. Majority of the patients are young (age < 30 yrs), and usually asymptomatic. The most common site is in the chest, stomach, neck, and mediastinum; and less commonly in the axilla, pelvis, and pancreas. This asymptomatic 27-year-old female had incidental retroperitoneal adenopathy on an abdominal on CT (initially mistaken as an ovarian cyst on routine clinical examination) and a positive biopsy confirmed for Castleman's disease, with positive CD-20 cytology.

Case 18.6B

History

27-year-old female with a diagnosis of bulky left pelvic Castleman's disease, which is CD-20 positive. There has been interval Rituxan therapy since the baseline exam.

Findings

In the abdomen, there is again seen bulk disease in the left pelvis (*Figures 18.6B.1 and 18.6B.2*). The three-dimensional images show a definite reduction in bulk between the two exams. The measured difference at the level of the greatest depiction of the central stellate calcification are less impressive than the three-dimensional images, with dimensions decreasing from 5.7 cm × 5.1 cm to 5.3 cm × 4.7 cm in maximum oblique axial measurements. The findings on the current exam are isolated to bulky confluent, common iliac and external iliac adenopathy with stellate central calcification. On the prior exam there had been another intense focus above the urinary bladder that localized to bowel which is not seen on the current exam. The central stellate calcification is typical for Castleman's adenopathy. There is atrophy of the left abdominal rectus muscle and the psoas component of the iliopsoas muscle. Aside from the bulk left pelvis disease, the exam currently is otherwise negative. There is intense but presumed physiologic tonsillar and anterior tongue activity. There is supraclavicular fat activity. These findings are considered physiologic.

Impression

Substantial interval partial response to Rituxan therapy with decrease in bulk of the remaining confluent left pelvic iliac adenopathy with typical central stellate calcification.

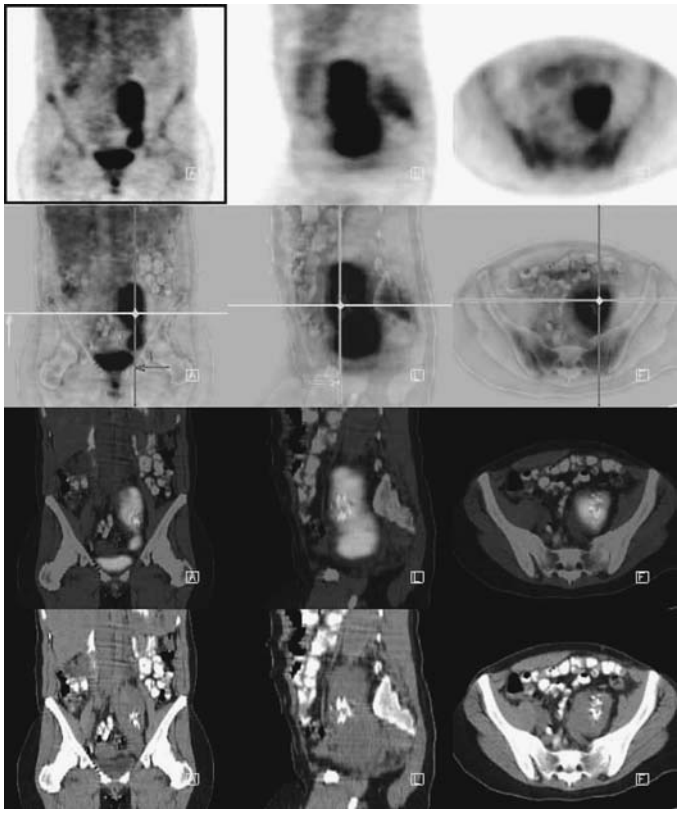

FIGURE 18.6B.1.

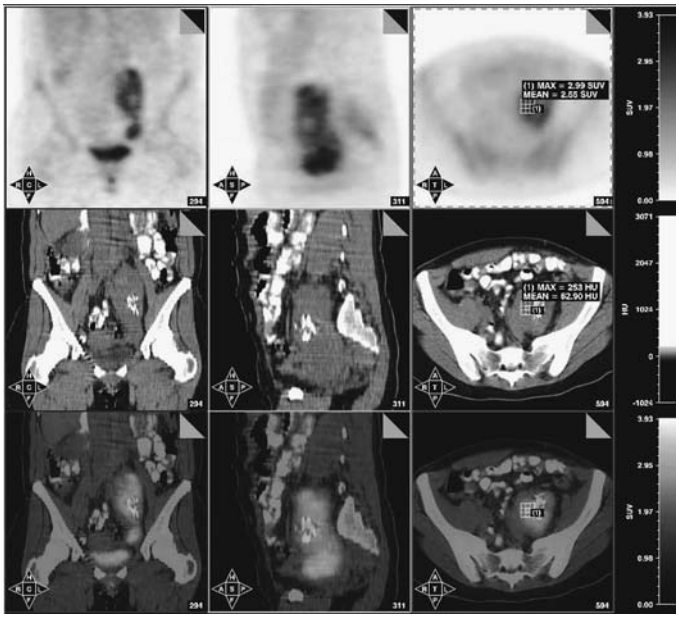

FIGURE 18.6B.2.

Case 18.7

History

58-year-old male who has a history of lymphoma and recently presents with several suspicious lesions involving the lung, liver, and spleen on CT. The patient is being staged.

Findings

There is a widespread hypermetabolism involving the axial and appendicular skeletons (*Figure 18.7.1*). Multiple punctate lesions are also seen in the lungs, liver, and spleen. Left periclavicular and anterior base of the neck adenopathy is noted. There are several scattered omental nodes also seen.

Impression

Widespread metastatic disease involving bone and soft tissue as described above.

Pearls and Pitfalls

- *The sensitivity of FDG PET for lymphomatous involvement of the bone marrow ranges from 81% to 88% and the specificity is 100%. FDG imaging is superior to*

FIGURE 18.7.1.

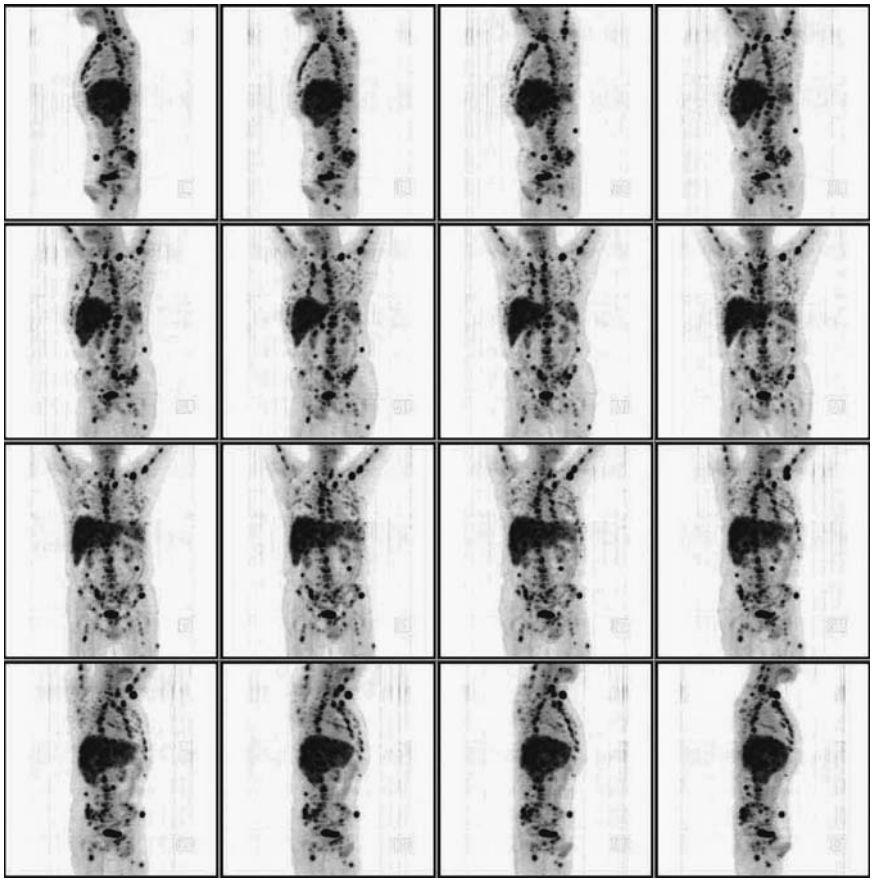

^{99m}Tc-MDP bone scintigraphy, detecting an additional 42% more osseous lesions than the latter.[11]

- *Disseminated osseous lymphoma is well visualized on PET whole body images.*[1,2,3,6,17,23]

Discussion

Lymphoma patients with bone marrow involvement have a poor prognosis. Five to fifteen percent (avg. 10%) of the Hodgkin's lymphoma patients will have bone marrow involvement on the initial presentation, compared to 19% to 83% (avg. 25%) of those with NHL.

PET has the advantage in detecting asymptomatic patient with infiltrative marrow involvement without bony destruction. Conversely, CT detection of osseous involvement requires the presence of bony destruction.

The degree of FDG uptake declines in a lower grade of malignancy. False-negative PET can occur in low- or intermediate-grade lymphomas with only discrete displacement (up to 10%) of normal marrow. Five percent of patients not detected by FDG PET imaging are bone marrow biopsy positive for tumor involvement.

19 Melanoma

Heidi R. Wassef

Case 19.1

History

69-year-old female with a history of melanoma of the right heel. After several recurrences, the patient underwent right inguinal lymph node biopsy with three of seven positive nodes. More recently, she underwent resection of three lesions in the right leg, anterior shin, lateral leg, and foot. The current exam is being done for staging.

Findings

The exam of the lower extremities reveals focal hypermetabolism in the subcutaneous soft tissues of the right lateral foot (*Figure 19.1.1*). There is a second focus in the dorsum of the right midfoot. There is subcutaneous focal disease in the lateral soft tissues of the right lower leg above the ankle. There is also moderate hypermetabolism in the deep subcutaneous tissues adjacent to the tibia (*Figures 19.1.2 and 19.1.3*) at the junction of its proximal middle third anterolaterally, more on the lateral than the medial side. On the contralateral left foot, there is a focus at the left plantar forefoot which is probably urine contamination. Increased synovial activity at the left knee probably represents synovitis. There is intense hypermetabolism in multiple areas in the anterior left thigh (*Figure 19.1.4*) and left lateral gluteal soft tissues (*Figure 19.1.5*). These correspond to reticular changes in the subcutaneous fat on CT. The findings are suspicious for cellulitis and could be related to injection.

In the whole body exam (*Figure 19.1.6*), there is intense hypermetabolism corresponding to confluent right external iliac adenopathy, similar to that reported on recent CT. There is prominent gastric activity but this is presumed physiologic. A small nodular lesion is noted on the CT in the right lower lung which is negative by PET scintigraphy and has the appearance of a small AVM on CT. There is no evidence for skeletal or pulmonary metastasis or hepatic metastasis.

Impression

1. There are multiple areas in the right lower extremity which appear subcutaneous in location and are fairly intensely hypermetabolic, consistent with metastatic disease: right lateral foot; right dorsal midfoot; right lateral lower leg above the ankle; and right shin in the tissues around the tibia at the junction of the proximal and middle third.
2. Intensely hypermetabolic pathologic confluent right external iliac adenopathy.

FIGURE 19.1.1.

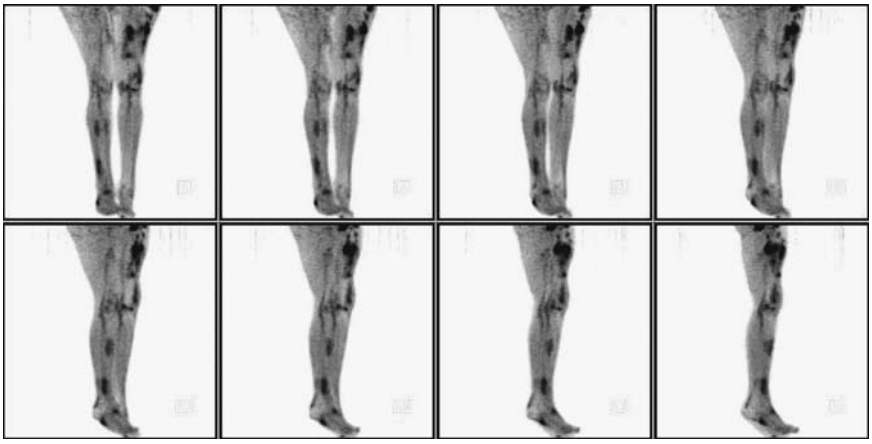

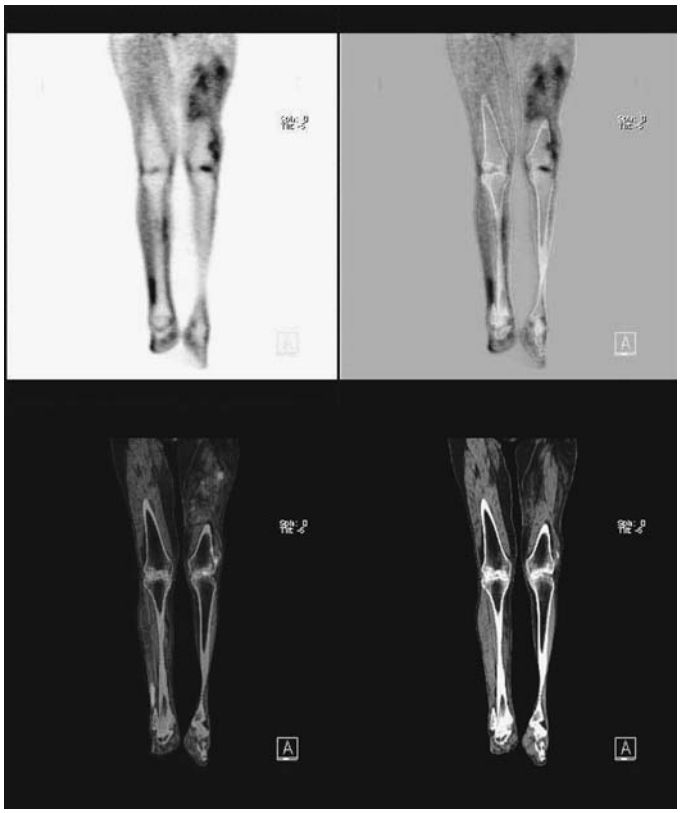

FIGURE 19.1.2.

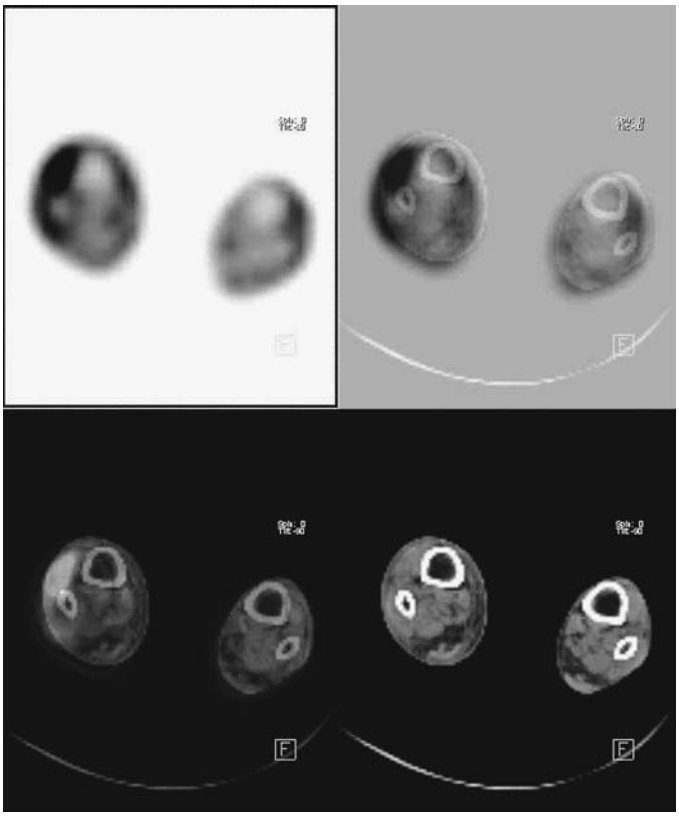

FIGURE 19.1.3.

3. Reticular changes in the fat with hypermetabolism of the left thigh and lateral gluteal subcutaneous soft tissues, likely cellulitis and possibly related to injections.
4. 18-FDG PET negative right lower lobe pulmonary finding, probably an AVM.
5. Negative for skeletal, hepatic, or pulmonary metastasis.

Pearls and Pitfalls

- *Breslow thickness is a good indicator for recurrence and prognosis.*
- *Lymphoscintigraphy and sentinel node biopsy have a sensitivity of 94% and specificity of 100% for the detection of occult regional metastases.*[3,5,6]

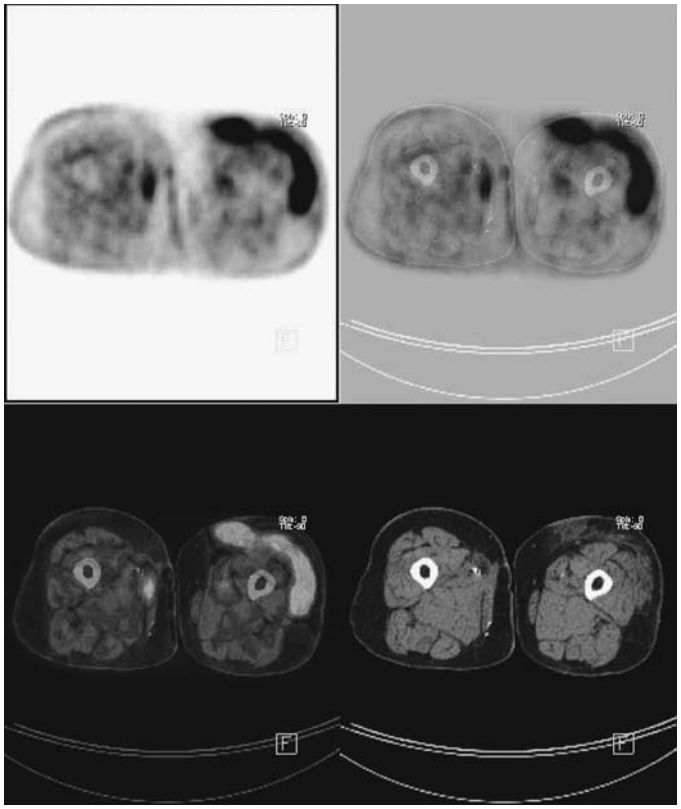

FIGURE 19.1.4.

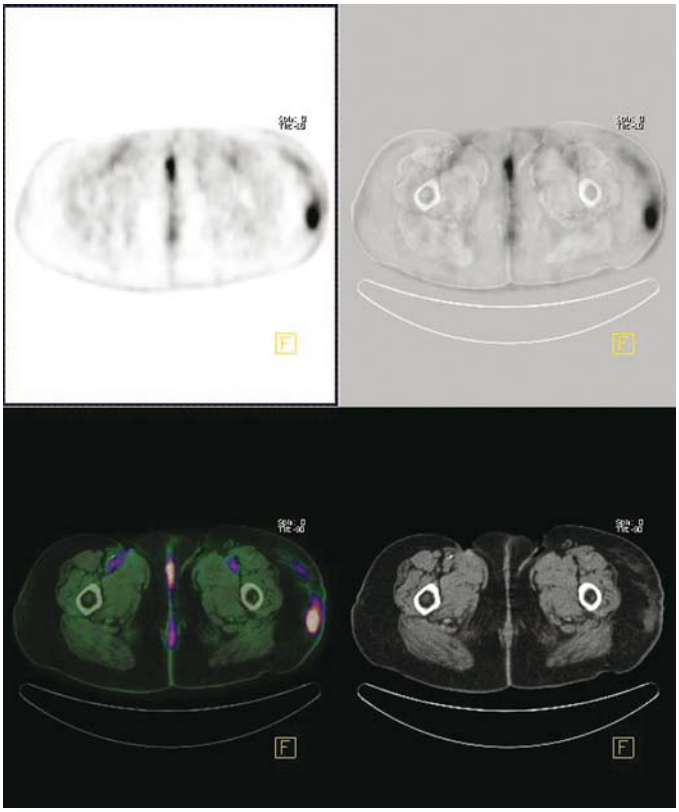

FIGURE 19.1.5.

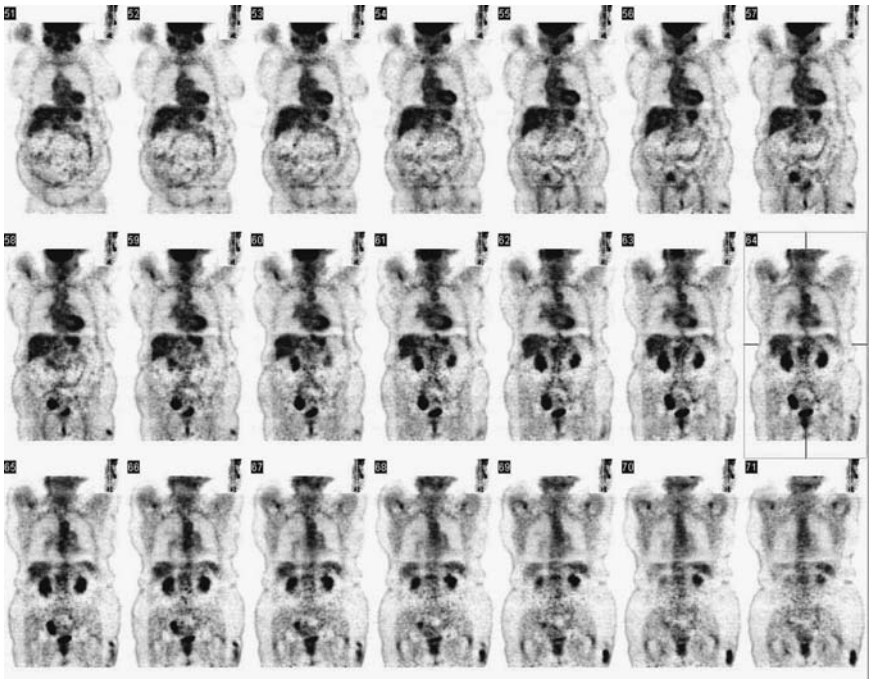

FIGURE 19.1.6.

- *PET is currently used for extranodal staging, restaging, and recurrent melanoma.*[7,9,10]
- *The sensitivity of PET for skin metastases less than 3 mm in diameter is 79% and the specificity is 86%.*[1,8,10]

Discussion

Malignant melanomas are cutaneous tumors which develop from melanocytes. Melanoma can involve the eye, central nervous system, respiratory, gastrointestinal, and genitourinary tracts. It is now the fifth most common tumor and second to lung cancer for mortality. Ninety percent of malignant melanoma is curable if discovered early. The overall cure rate is 80%.

Case 19.2

History

75-year-old male who has a history of malignant melanoma twenty years ago. A CT demonstrated new multifocal metastases in the right posterior 6th rib, liver, and lungs bilaterally. Evaluation of extent of disease is requested.

Findings

There is a focus of sternal hyperactivity associated with a soft tissue component and bony destruction in comparison with the CT. A rib lesion on the left upper lateral chest wall is noted (*Figures 19.2.1 and 19.2.2*). A right anterior lateral rib is also involved. The posterior elements in a left upper thoracic spine are involved with metastatic deposits with activity seen on the right projecting to the pleural surface. The T-7 vertebral body displays a lytic lesion with a soft tissue mass possibly compressing the spinal cord (*Figure 19.2.3*). Another smaller vertebral lesion at the level of T-12 on the right is also seen. There is a large destructive lesion associate with soft tissue mass in the posterior aspect of the right ilium. Multiple sites of hypermetabolism are noted on the medial aspect of the right lobe of the liver extending from the dome to the caudate lobe, representing multiple coalescing nodules corresponding to the abnormalities described on the earlier CT (*Figure 19.2.4*). The activity in the shoulders bilaterally, right greater than left, is likely inflammatory arthritis. There is mild focal

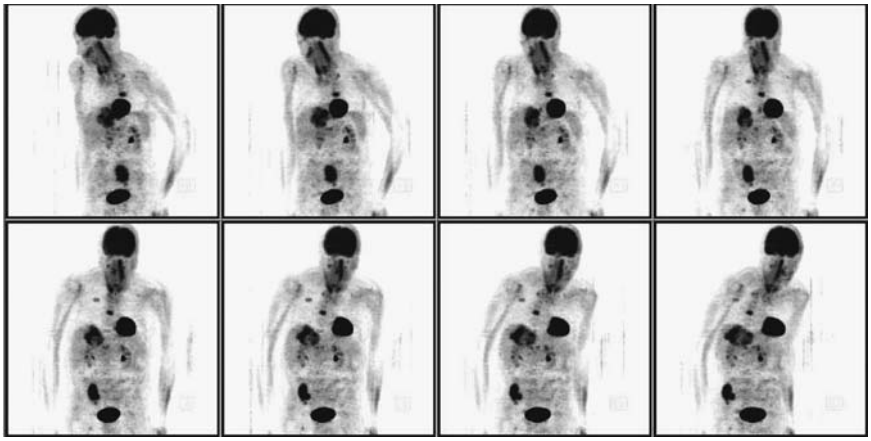

FIGURE 19.2.1.

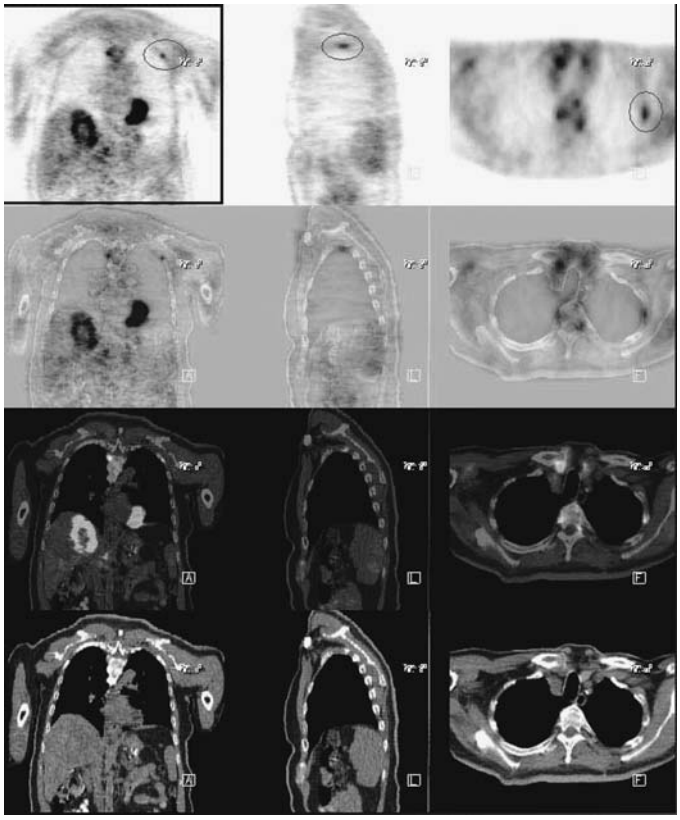

FIGURE 19.2.2.

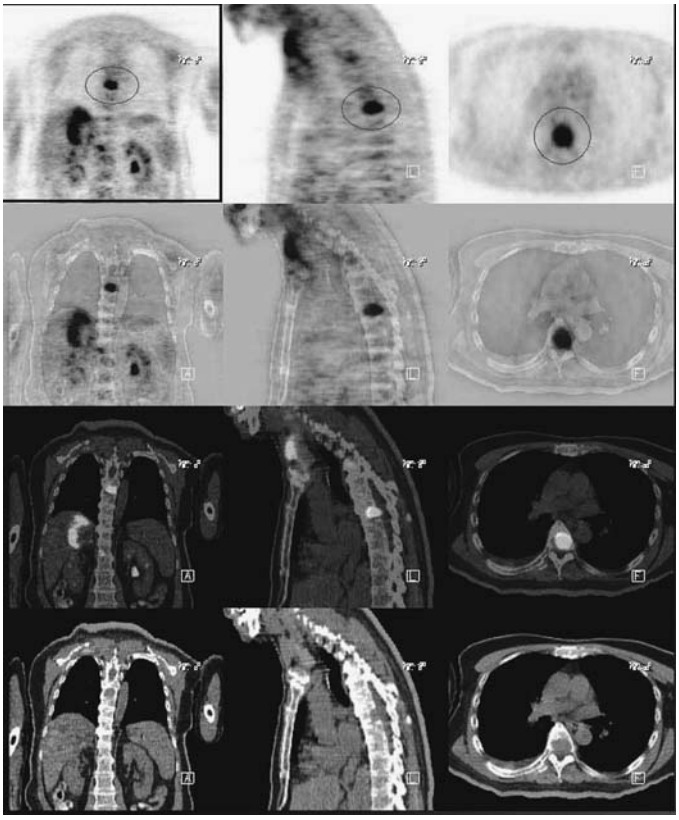

FIGURE 19.2.3.

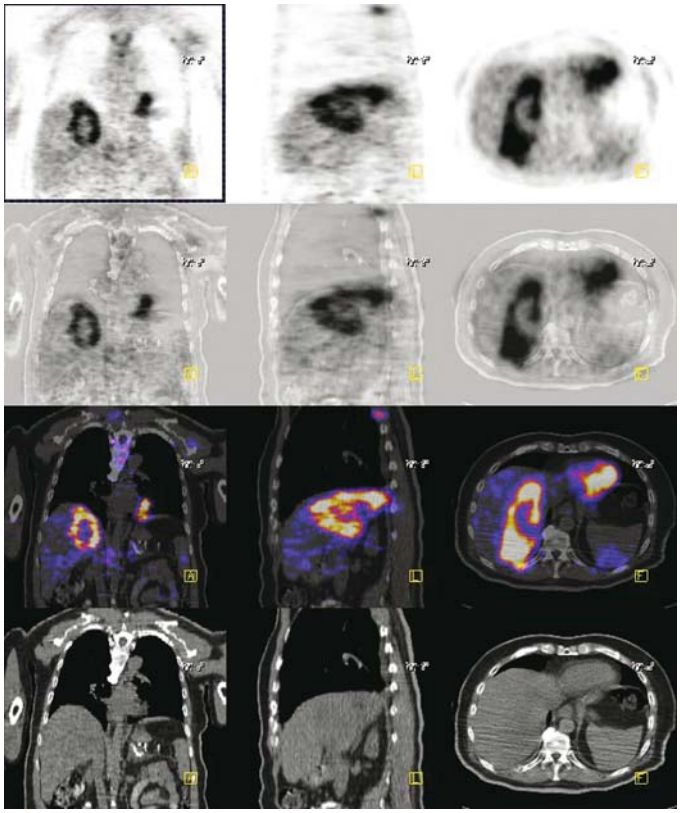

FIGURE 19.2.4.

patchy ill-defined activity on the right lateral thigh which may represent local skin inflammation.

Impression

1. Multiple bony metastasis as described above, in particular the vertebral body at the level of T-7 with a soft tissue mass which may be compressing the spinal cord.
2. Multifocal sites hypermetabolism in the right lobe of the liver consistent with metastatic disease.
3. Ill-defined right lateral thigh uptake, likely inflammatory in nature.

Pearls and Pitfalls

- *PET-CT is very helpful in identifying spinal cord or nerve root compression secondary to metastatic disease.*[2,9,10]
- *FDG PET alters clinical management in up to 50% of the patients with melanoma.*[7,9]

Discussion

The highest prevalence of disease is in young females between the ages of 25 and 29, with the age range of 15 to 39. Red-haired, blond, light-skinned individuals, sun exposure, race, nevus, family history, and xeroderma pigmentosum are other risk factors. There are 4 major subtypes of malignant melanoma: the lentigo maligna melanoma (4%–15%), superficial spreading melanoma (70%), nodular melanoma (12%–30%), and acral lentiginous melanoma (2%–8%). Staging is based on the TNM classification system which requires histologic correlation of (T stage) and depth and level of invasion as described by Breslow and Clark.

Case 19.3

History

75-year-old female who has stage-III melanoma. The original resection was from the toe. She is status post ipsilateral right inguinal lymph node dissection. The current examination is for restaging.

Findings

There is a single pathologic hypermetabolic focus corresponding to a normal-to-borderline size deep left axillary lymph node (*Figure 19.3.1*), near the chest wall, which is measured on the CT at 1 cm × 2 cm. This is a solitary hypermetabolic focus. It is consistent with a solitary axillary lymph node metastasis. The right inguinal area is weakly positive (*Figure 19.3.2*), consistent with recent (5-month) scar. The lower extremities are negative with notation of muscular activity in the right medial calf (*Figure 19.3.3*). No hepatic lesion or pulmonary lesion is apparent.

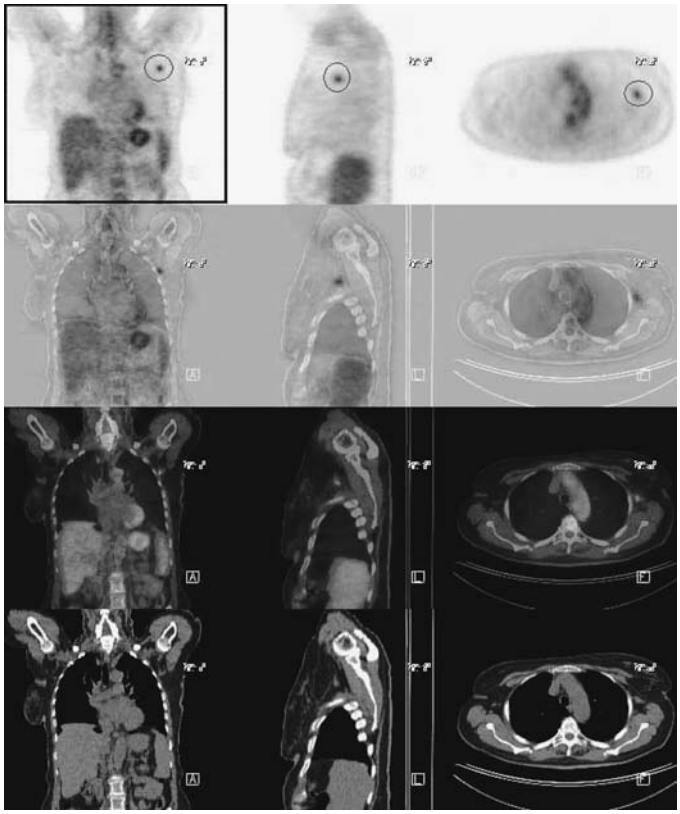

FIGURE 19.3.1.

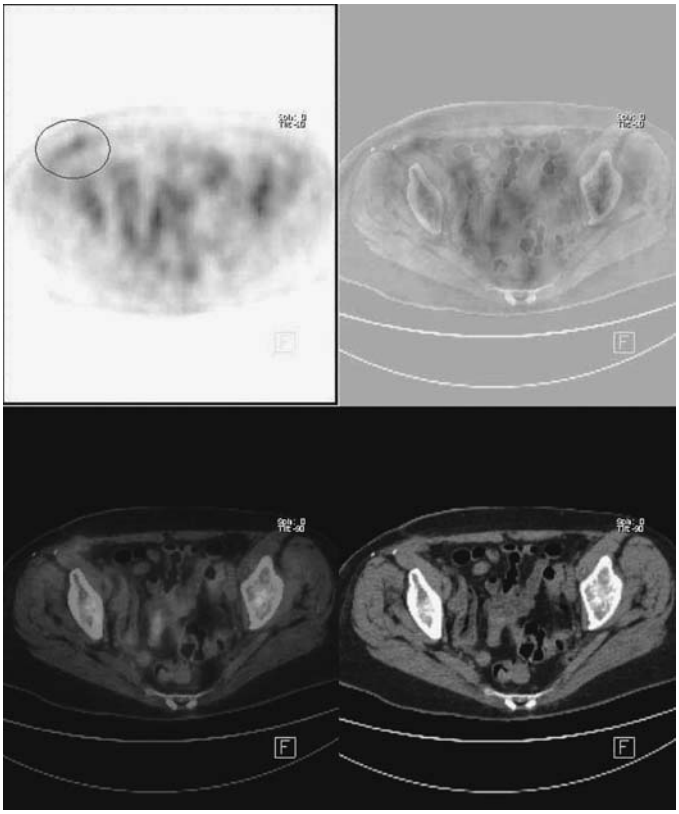

FIGURE 19.3.2.

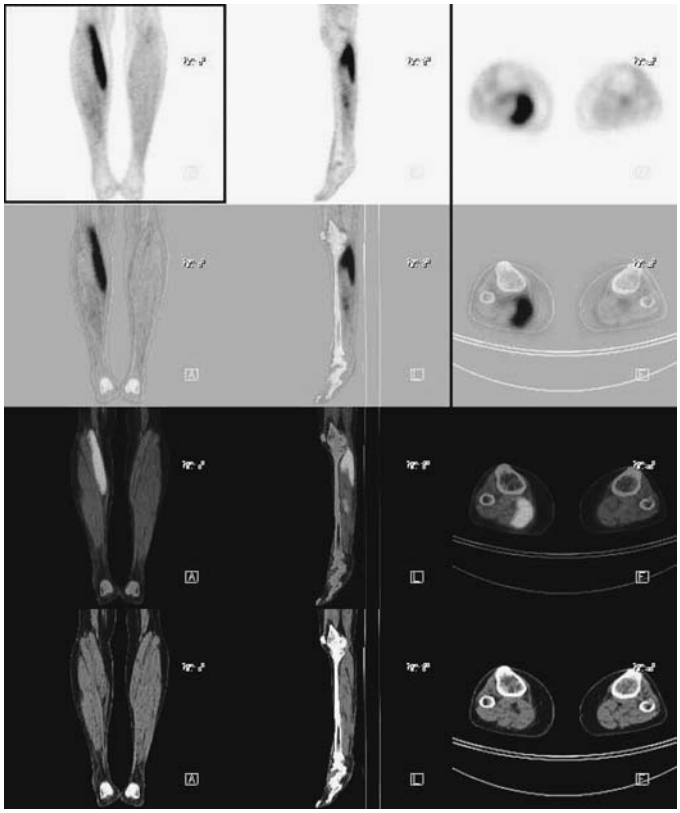

FIGURE 19.3.3.

Impression

1. Apparently solitary hypermetabolic focus corresponding to a deep left axillary lymph node near the chest wall, measuring 1 cm × 2 cm. No other evidence for metastasis is evident by PET scintigraphy, inclusive of the liver and lungs.
2. Weak activity corresponding to the right inguinal scar, consistent with recent scar formation.
3. Right medial calf muscular activity. No pathologic significance is attributed to this finding.

Pearls and Pitfalls

- *3% to 5% of patients presenting with malignant melanoma will develop a second primary melanoma within 3 years of treatment.*[1,3,4]
- *PET is a useful tool for evaluating recurrent or metastatic disease in patients with Stage III and IV disease.*[4,10]
- *Sentinel node biopsy has a sensitivity of 95% for initial melanoma staging.*[6]

Discussion

Early surgical resection is the mainstay of treatment. This is followed by sentinal node mapping with either blue dye or technetium-labeled ultrafiltered sulfur colloid or both. If the nodal basin is positive for cancerous cells, radical lymph node dissection may be necessary. PET is more accurate than regional lymph node staging and is used for systematic staging of disease.

20 Thyroid Carcinoma

Lalitha Ramanna

Case 20.1

History

74-year-old female who is status post thyroidectomy and status post subsequent radioiodine × 2. She is currently being evaluated for recurrent disease because of elevated thyroglobulin of 14.

Findings

Breath hold images of the lung show a number of peripheral areas of atelectasis in the lingula and middle lobe which suggest a background of chronic bronchial disease. There is also some postinflammatory linear scarring at the left base. However, no pulmonary nodules are apparent. One tiny pleural nodule is rectangular in shape and is probably a postinflammatory lesion. The 18-FDG whole body PET scintigraphy is negative in the chest and abdomen. There is one moderately hypermetabolic focus in the neck (*Figure 20.1.1*). The neck dissection was on the right (*Figure 20.1.2*). The focus is on the left, just posterior to the inferior posterior ala of the thyroid cartilage (*Figure 20.1.3*). No recognizable lymph node is evident on the unenhanced CT. All of the tissue is the same density on CT at this level.

Impression

1. Single moderately hypermetabolic focus in the deep left neck, just posterior to the posterior inferior left thyroid cartilage ala, compatible with recurrent thyroid cancer.
2. Negative scintigraphy in the chest, abdomen and pelvis.

Pearls and Pitfalls

- *Only 50% to 60% of papillary thyroid carcinomas and 64% to 67% of follicular cancers are iodine avid.*[4,5]
- *PET is not indicated for primary thyroid malignancy detection since FDG can accumulate in normal thyroid tissue (~30% of patients) and in certain benign thyroid diseases.*[3,7]
- *A PET study will usually be positive in patients with thyroglobulin level higher than 100 ug/L. PET will detect true positive disease in 11%, 50%, and 93% of patients with hTg levels of <10 ug/L, 10 to 20 ug/L, and >100 ug/L.*[6,8]

FIGURE 20.1.1.

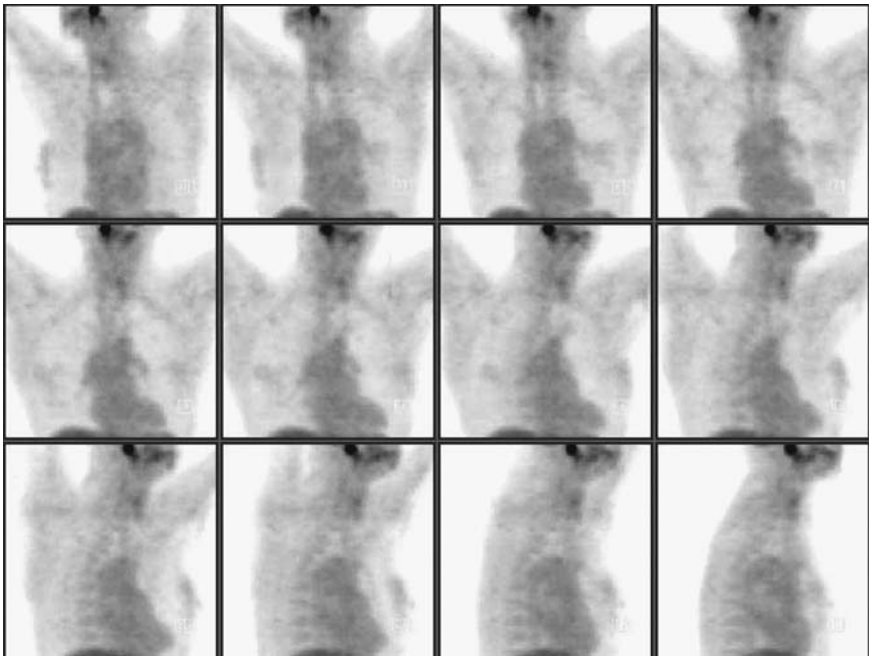

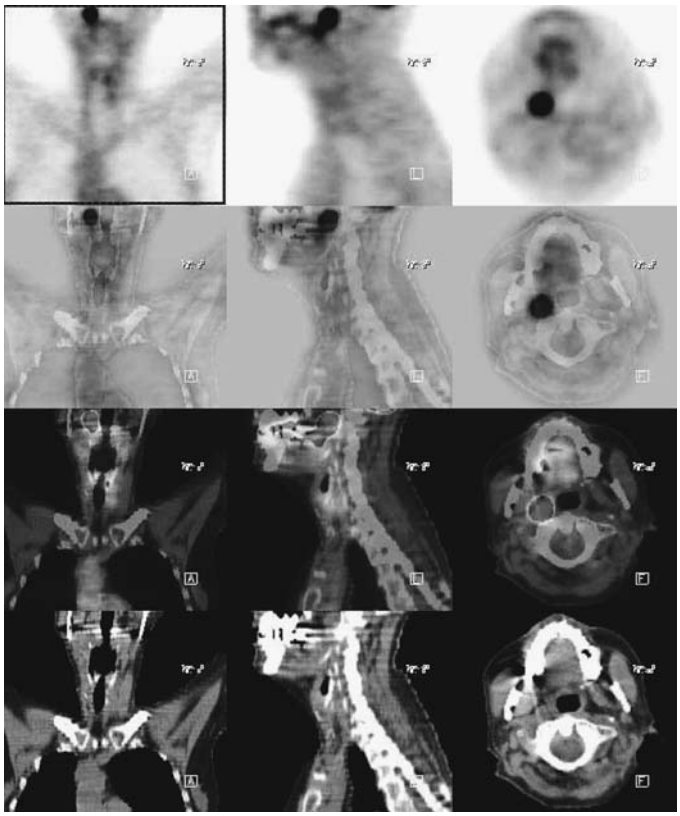

FIGURE 20.1.2.

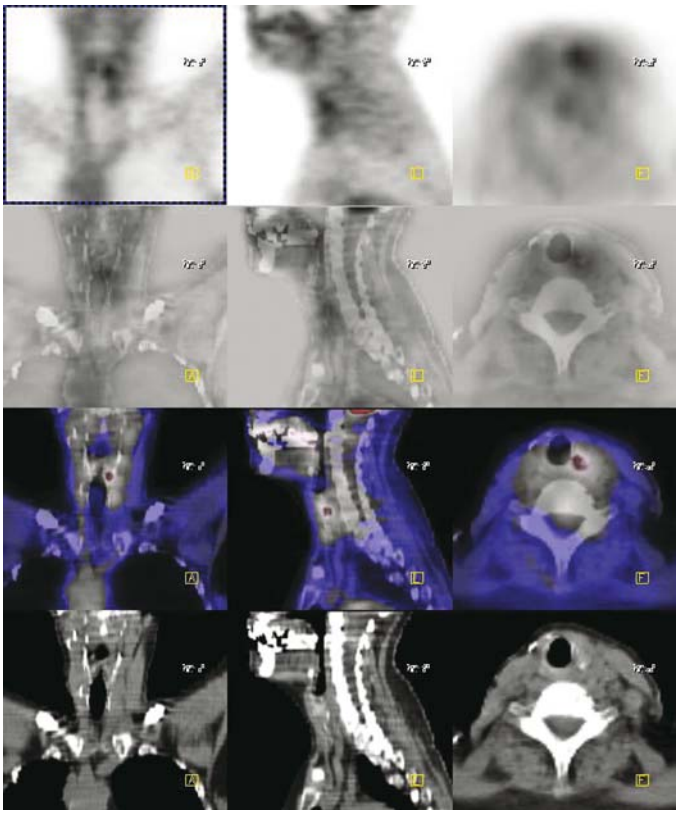

FIGURE 20.1.3.

- *FDG is indicated for a known, differentiated, and recurrent papillary/follicular thyroid cancer patient with a negative I-131 scan. Increased expression of GLUT-1 is associated with the loss of radioactive iodine uptake in metastases.*[10,14]

Discussion

Less than 1% of all cancer deaths are from thyroid cancer. Most differentiated thyroid cancers have an indolent course with low morbidity and mortality. 12% to 15% of the photopenic lesions seen on technetium-99m or radioiodine studies are malignant. Most malignant lesions are solid on ultrasonography. Fine needle aspiration is best for accurate diagnosis. The treatment of papillary and follicular thyroid cancers are surgery complemented with I-131 therapy.

Thyroid cancers are mostly in females with the age range of 45 to 50 years old. In countries where iodine intake is normal, 80% of the thyroid cancers are of papillary and follicular histology. In countries of low iodine intake, follicular and anaplastic histology are more common. Previous external irradiation is a risk factor for papillary carcinoma, whereas previous I-131 administration is not. Less than 10% of all thyroid cancers are undifferentiated anaplastic cancers, mostly occurring in elderly patients. Medullary carcinoma constitutes the rest of the 10% cancers. These cancers have a high predisposition for MEN (multiple endocrine neoplastic) syndromes. The principle treatment of papillary and follicular (Hürthle cell) carcinoma is surgery followed by I-131 radioablation 4 to 6 weeks postop and a whole body scan 4 to 7 days later. External radiotherapy is reserved for elderly patients who have contraindications for surgery and I-131 treatment. Anaplastic cancers are treated with combination therapy of systemic chemotherapy and external radiotherapy. The treatment of medullary thyroid cancer is surgery, provided the presence of pheochromocytoma has been ruled out.

Case 20.2

History

49-year-old female who has a history of papillary thyroid cancer treated with radiotherapy and limited neck dissection. The patient is being seen for evaluation for metastatic disease.

Findings

There is focal hypermetabolism within the upper posterior triangle of the right neck (*Figure 20.2.1*) that corresponds to a lymph node on CT. Additionally two moderately positive hypermetabolic nodes are seen bilaterally in the superior mediastinum with the more prominent one on the right (*Figure 20.2.2*, *right column*). Inferiorly, there is hyperactivity in the thymus (*Figure 20.2.2*, *left column*) corresponding to prominence on CT; differential diagnosis includes thyroid metastases at this site.

Impression

Evidence for distant metastasis involving the right upper posterior triangle of the neck, the superior mediastinum, and possibly the anterior mediastinum.

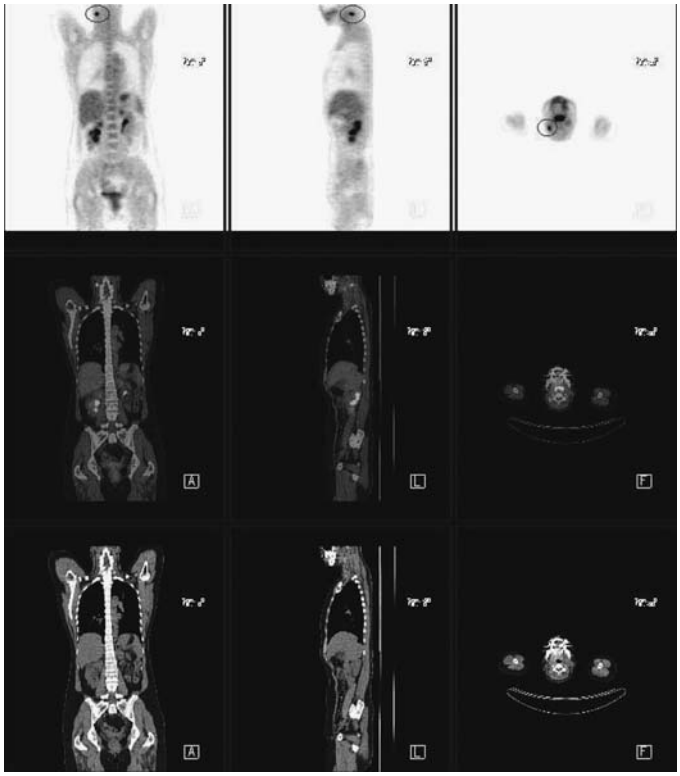

FIGURE 20.2.1.

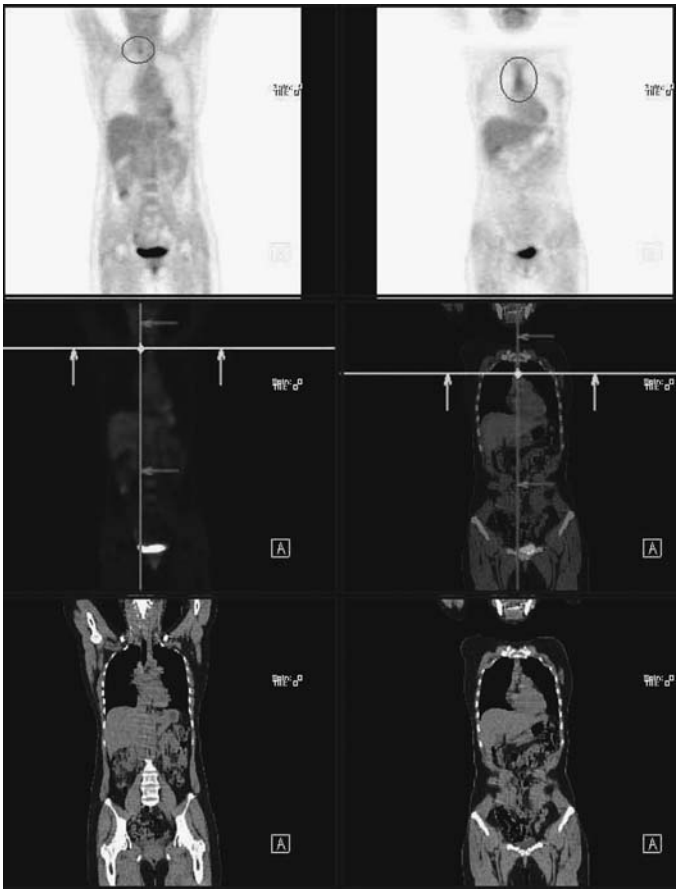

FIGURE 20.2.2.

Pearls and Pitfalls

- *In differentiated thyroid carcinoma, PET can detect recurrence and metastases with a sensitivity of 80% to 90%.*[11]
- *Removal of exogenous thyroid hormone in addition to TSH stimulation may improve the detection of unsuspected lesions.*[5,7]
- *The 3-year survival rate of a thyroid carcinoma patient with a positive PET scan is 60% as opposed to 98% survival of the same patient with a negative PET scan.*[1,6,7,8]
- *Thymic hyperplasia can cause false-positive PET results in the anterior mediastinum.*

Discussion

Differentiated cancers, papillary or follicular, are highly treatable and usually curable. Poorly differentiated cancers, medullary or anaplastic, are less common but aggressive, metastasize early, and have a poorer prognosis.

Case 20.3

History

62-year-old male who has a history of undifferentiated thyroid carcinoma and esophageal cancer. A prior PET demonstrated several sites of hypermetabolism involv-

ing the neck and lung. His most recent CT confirmed the right neck pathology. He was treated with radiotherapy and chemotherapy. Evaluation for metastases is requested.

Findings

There is hypermetabolism posterior to the left hyoid bone in the prevertebral space (*Figures 20.3.1 and 20.3.2*) that exhibits soft tissue asymmetry with lower density on the left side without evidence of a discrete mass on CT. This may represent residual normal thyroid tissue or metastatic disease. There is a band of activity in the paravertebral region on the right (*Figure 20.3.3*) that corresponds to nodular pleural

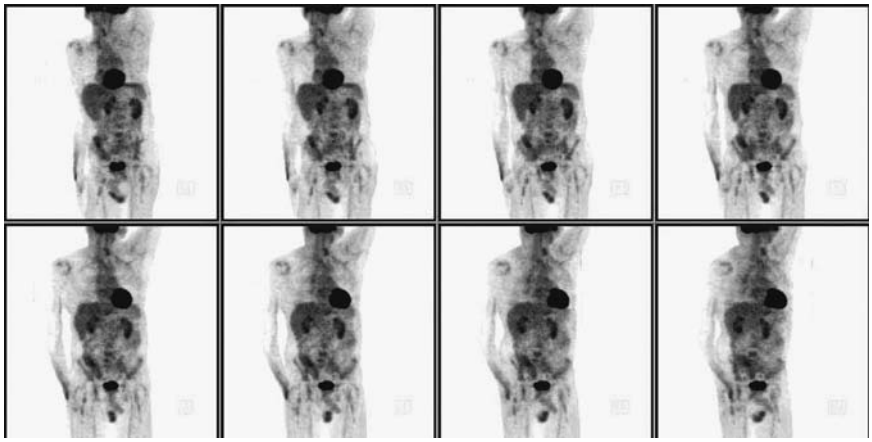

FIGURE 20.3.1.

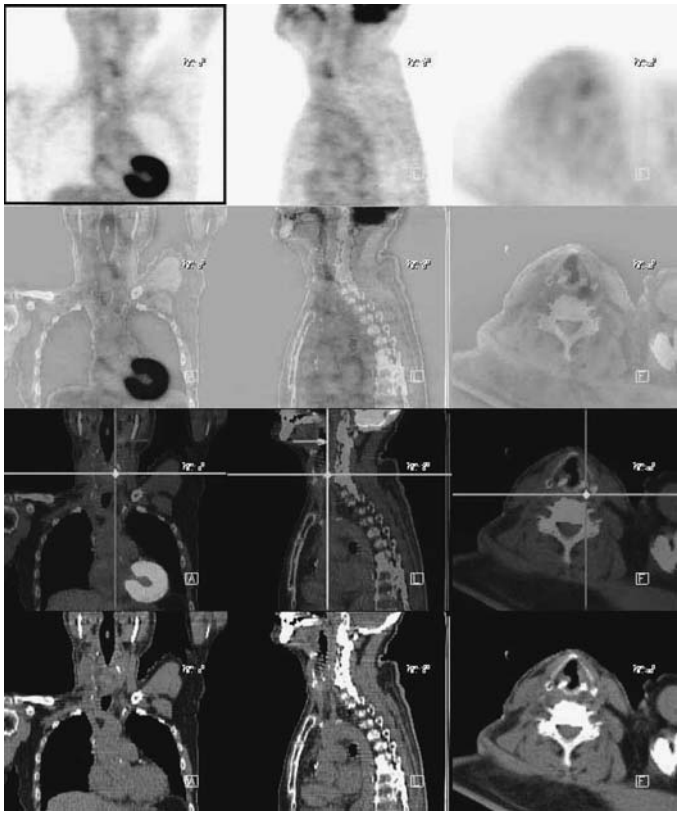

FIGURE 20.3.2.

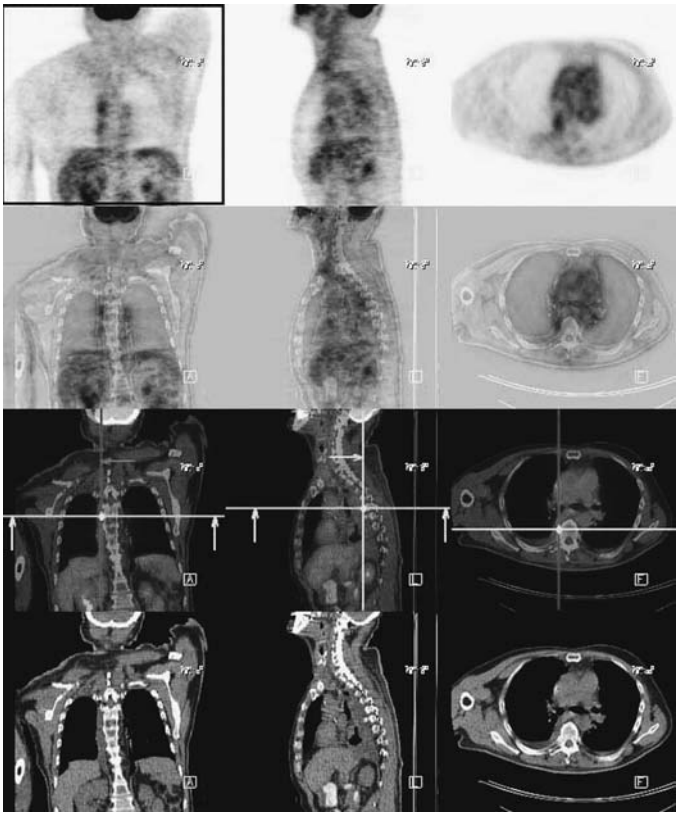

FIGURE 20.3.3.

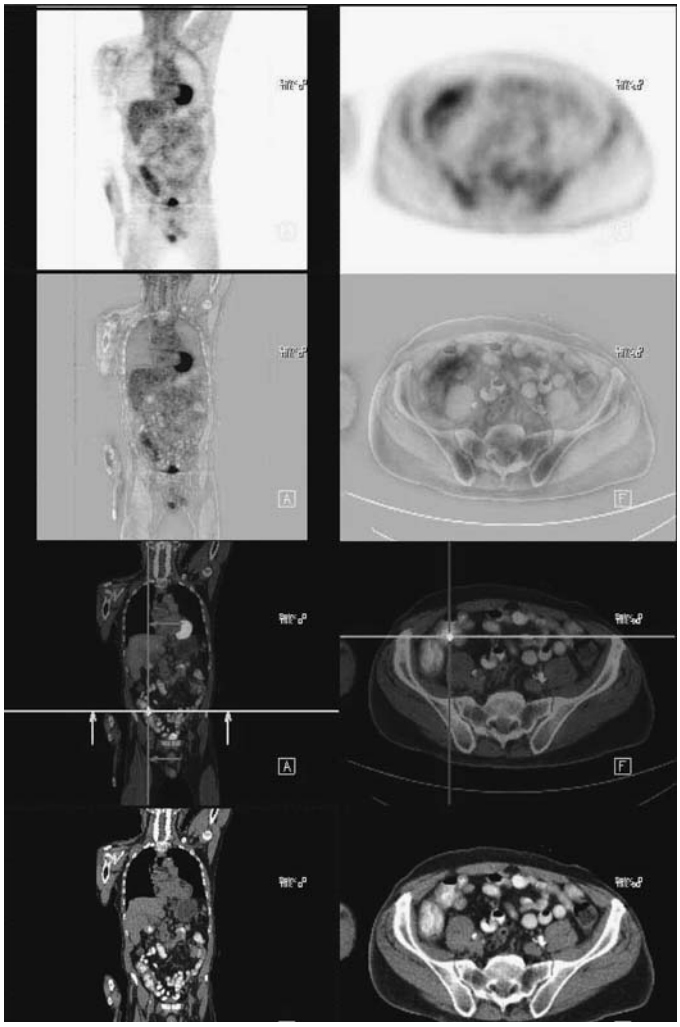

FIGURE 20.3.4.

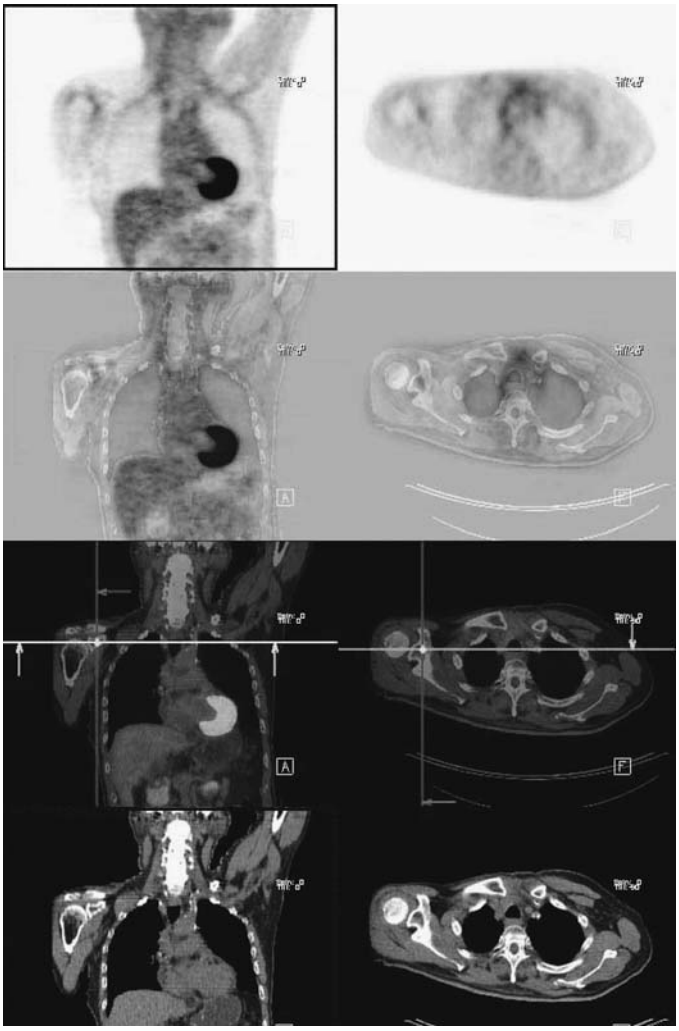

FIGURE 20.3.5.

thickening on CT, compatible with metastatic disease vs. pleuritis. This latter finding has decreased from the prior PET examination. The left band of activity is no longer visible. There is no interval change in the thyroid bed activity left of midline, consistent with residual thyroid tissue vs. tumor. The focus of activity in the cecum (*Figure 20.3.4*) indicates possible pathology and endoscopic evaluation is recommended. The halo of activity around the glenohumeral joint (*Figure 20.3.5*) is likely the result of inflammatory joint disease. The abnormal lung activity from prior study has resolved.

Impression

1. Suspicious sites of mediastinal uptake involving the neck and chest with some interval improvement. The findings are most consistent with residual metastatic disease from either of the two known primary cancers.
2. The focal activity in the cecum is suspicious; endoscopic evaluation is advised.

Pearls and Pitfalls

- *CT is superior to PET in the detection of small lung lesions less than one centimeter in diameter. Low FDG uptake makes even large lesions difficult to detect on PET.*[11,15]

- *Highly differentiated thyroid cancer is usually I-131 positive and may display low FDG uptake; in contrast, poorly differentiated thyroid cancer will be I-131 negative and FDG positive.*[10]
- *Retinoic acids and somatostatin therapy are alternate treatments for undifferentiated thyroid cancer showing persistent serum thyroglobulin levels if I-131 therapy proves ineffective.*[2,9,13]

Discussion

In medullary thyroid cancer (MTC), 71% to 80% of the cases present with loco-regional metastases and 20% have distant metastases. FDG may also be indicated for medullary thyroid cancer with rising calcitonin level, or CEA level, and a negative study on octreotide or MIBG scan.

Case 20.4

History

The patient has a remote history of thyroid carcinoma, status post thyroidectomy and I-131 ablation. He is now being evaluated for a soft tissue abnormality on CT near the thyroid bed, possibly representing recurrence.

Findings

There is active tissue in the right thyroid bed (*Figures 20.4.1 and Figure 20.4.2*). The tissue, which is moderately metabolically active, is below the thyroid cartilage and about 2 cm above the suprasternal notch. It is triangular in shape and adjacent to the trachea. It is modestly more active than the usual malignancy, but it should be noted that thyroid carcinoma is quite variable in its 18-FDG metabolic activity. It is so remote

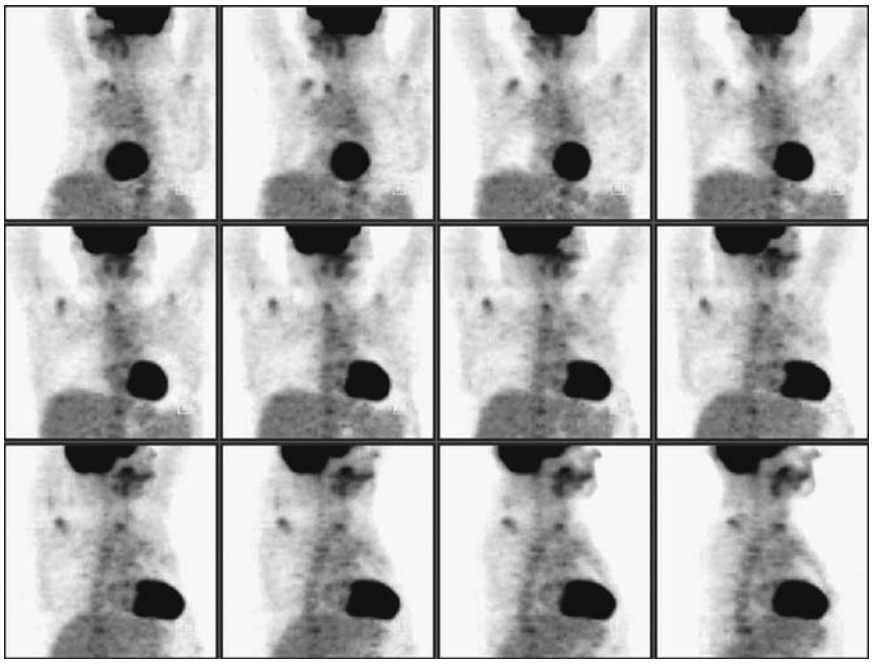

FIGURE 20.4.1.

FIGURE 20.4.2.

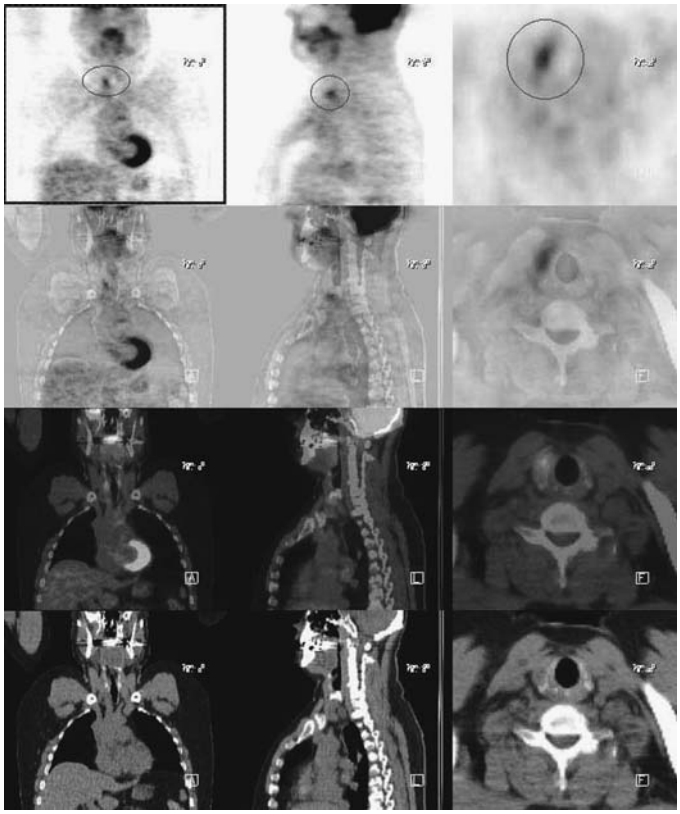

from surgery that it is considered unlikely to represent scar activity. No other metabolically active abnormality is evident on the torso exam.

Impression

Active soft tissue of about 2 cm dimension in the right paratracheal area in the right thyroid bed, status post remote bilateral thyroidectomy, suspicious for recurrent thyroid cancer.

Pearls and Pitfalls

- *The sensitivity and specificity of PET for recurrent tumor ranges from 69% to 94% and 42% to 95%, respectively.*[15]
- *70% of the normal lymph nodes are detected with PET.*[7,12]
- *50% of the changes in patient management are directly related to results obtained from PET imaging.*[6,7]
- *20% of the differentiated thyroid cancers recur.*

21 Muscular Skeletal Tumors

Lalitha Ramanna and Sherief Gamie

Case 21.1

History

52-year-old female who has a history of sarcoma in the right thigh. The patient is being seen for staging.

Findings

There is a bulky mass displaying hypermetabolism with central necrosis (*Figures 21.1.1, 21.1.2, and 21.1.2A*) seen in the right mid posterior thigh compatible with known malignancy. Multiple sites of photopenia are noted in the liver (*Figures 21.1.3 and 21.1.3A*) involving the left and right lobes consistent with hepatic cysts seen on CT. No abnormal uptake is seen in the chest. There is a focus of activity in the sigmoid colon (*Figure 21.1.4*) suspicious for a polyp or tumor; recommend flexible sigmoidoscopy.

Impression

1. Hypermetabolism in the right mid posterior thigh compatible with history of sarcoma, without evidence of metastatic disease.
2. Abnormal activity in the sigmoid colon; advise endoscopy.

Pearls and Pitfalls

- *Total whole body PET-CT is helpful in detecting distant metastases. High-grade sarcomas are generally more FDG-avid than a low-grade lesions.*[2,5,8]

Discussion

The histopathology of this mass in this patient was proven later to be a liposarcoma. Liposarcoma is a malignant tumor that can occur anywhere fat is present. This tumor most typically presents between 40 and 60 years of age. Histologic subtype is a significant prognostic indicator. Myxoid liposarcoma is often classified as an intermediate-grade tumor with a large metastatic potential. The treatment of choice is resection with a wide surgical margin. Liposarcoma is radioresponsive. Adjuvant radiation therapy can be given, either preoperatively or postoperatively, depending on the margin status.

FIGURE 21.1.1.

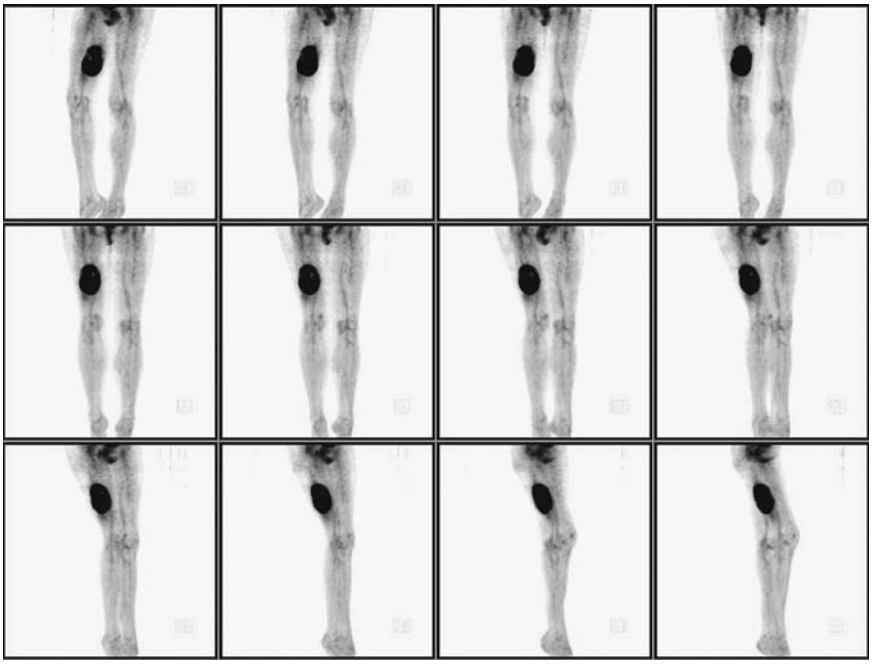

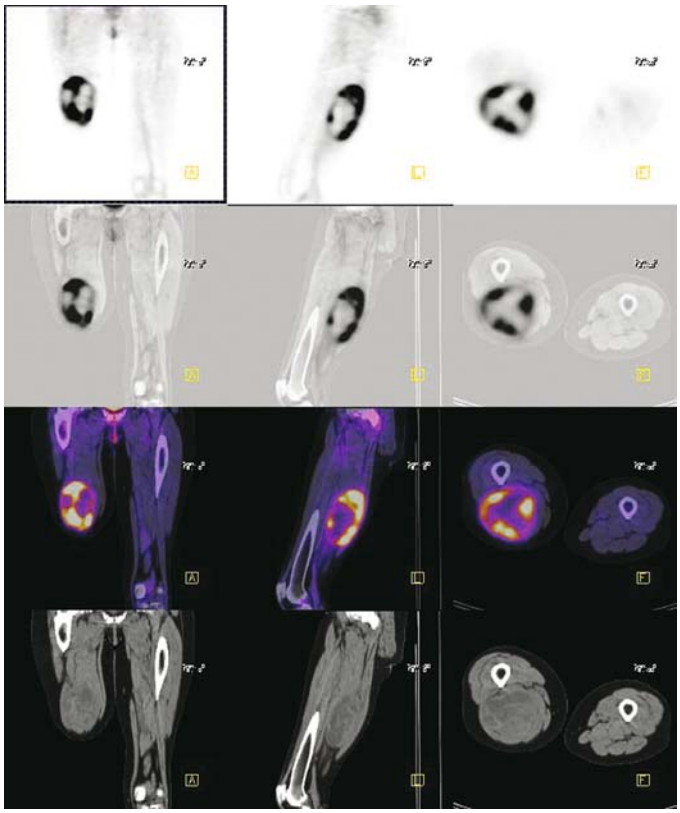

FIGURE 21.1.2.

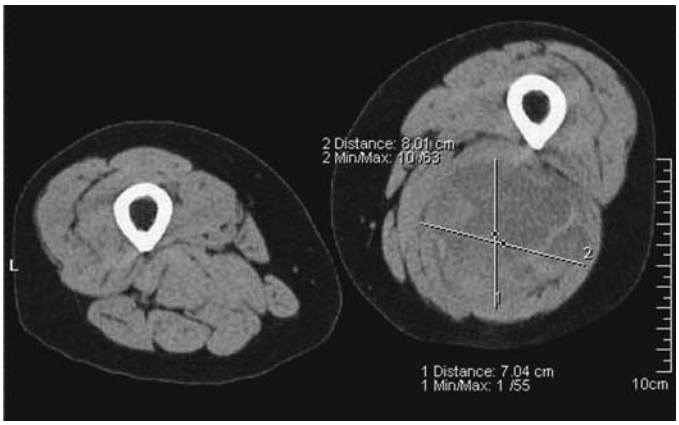

FIGURE 21.1.2A.

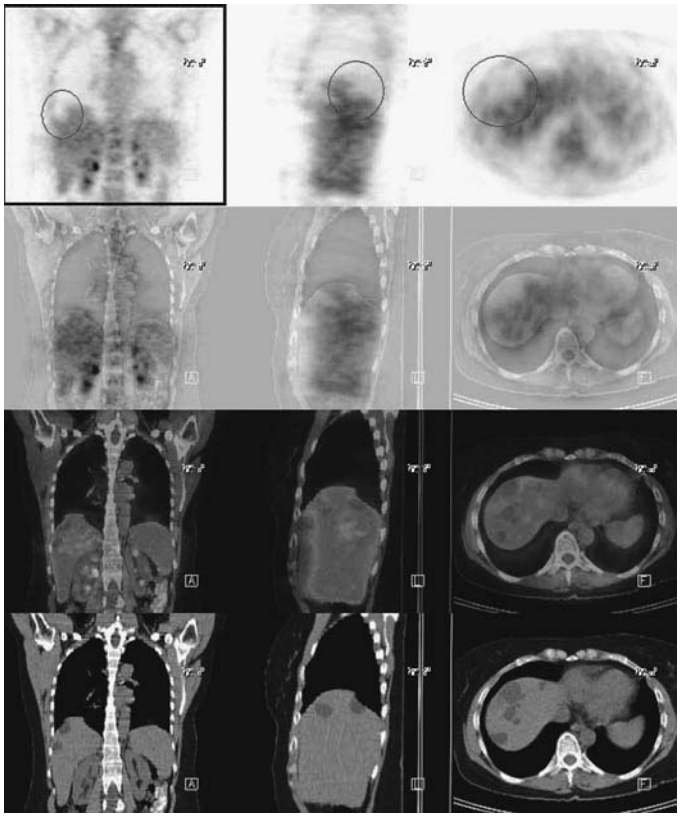

FIGURE 21.1.3.

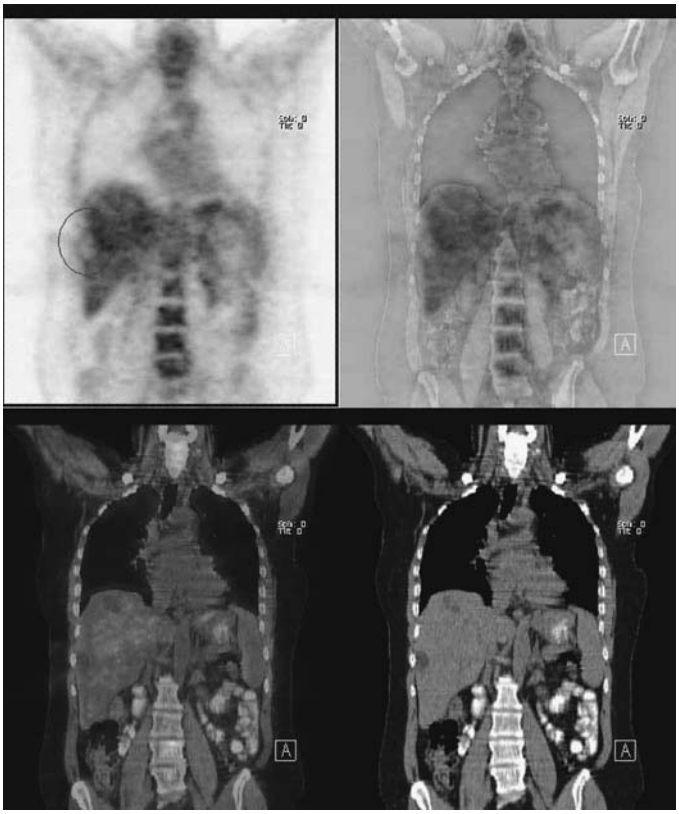

FIGURE 21.1.3A.

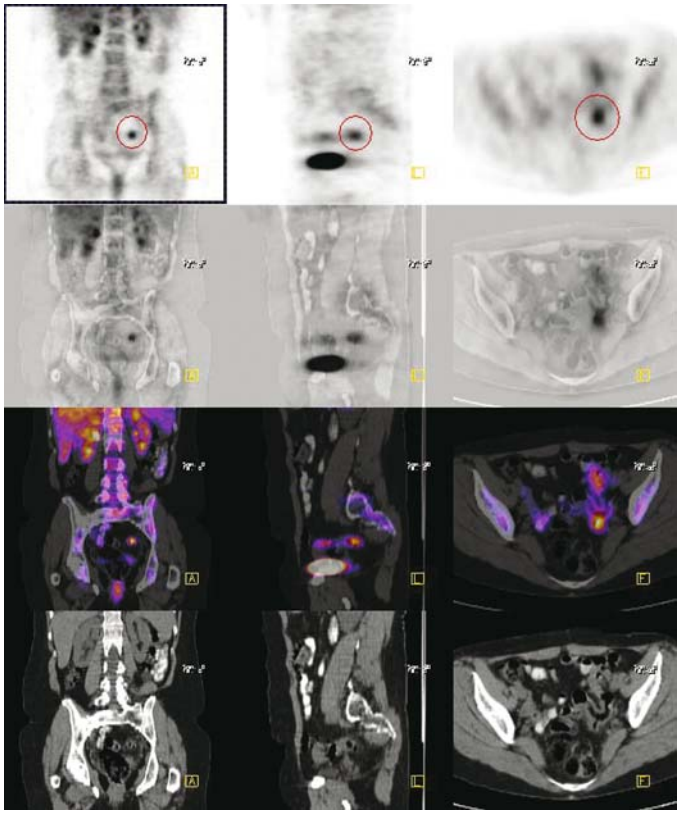

FIGURE 21.1.4.

Certain variants of liposarcoma have shown a higher incidence of regional nodal and extrapulmonary metastases. Regional adenopathy is generally well depicted with PET.

Case 21.2

History

80-year-old female with a history of recurrent leiomyosarcoma. The current exam is being done to evaluate extent of disease.

Findings

There is a large pelvic mass (*Figure 21.2.1*) corresponding to the 8 cm × 8.3 cm low pelvic mass demonstrated on recent CT (*Figure 21.2.2*). This is seen to be between an anastomotic bowel staple line and the urinary bladder, superior to and compressing the urinary bladder. The mass is moderately and heterogeneously hypermetabolic with greater hypermetabolism at its periphery than at its center. There are three small nodular densities extending from or adjacent to the mass. Any one of these could be a separate mesenteric mass. All of these peripheral lobulations or adjacent nodular densities are intensely hypermetabolic. There is physiologic bowel activity. No abnormal focus is seen above the central midpelvic mass. Sigmoid diverticular disease and low-density liver lesions are noted. No abnormal hepatic activity is evident, consistent

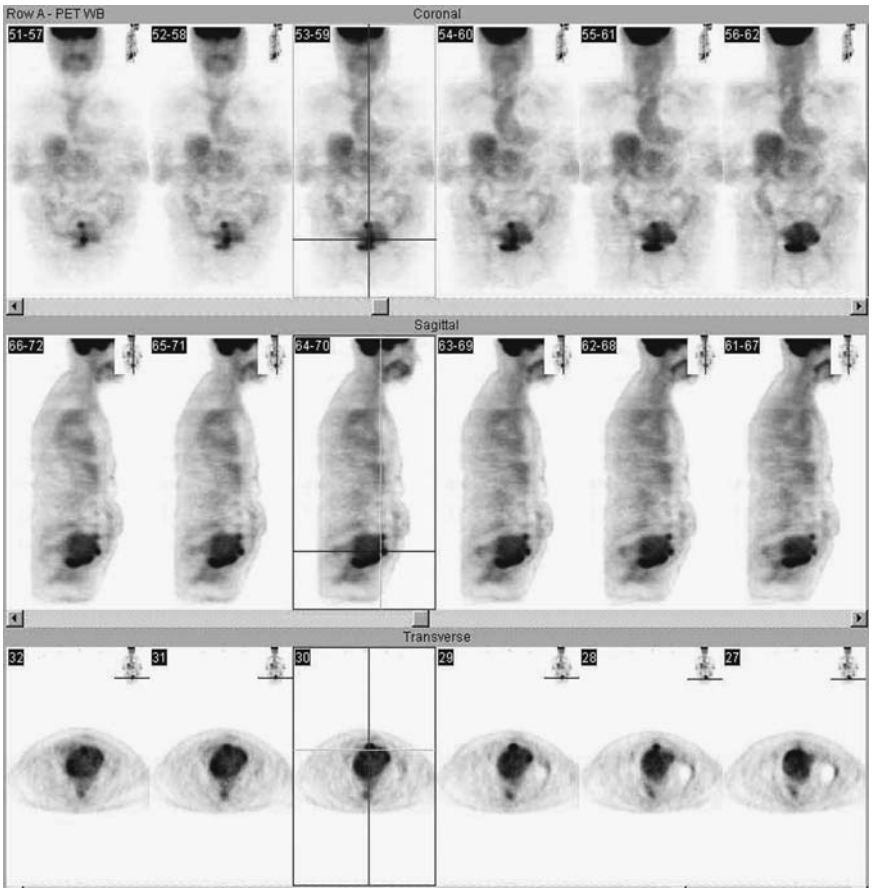

FIGURE 21.2.1.

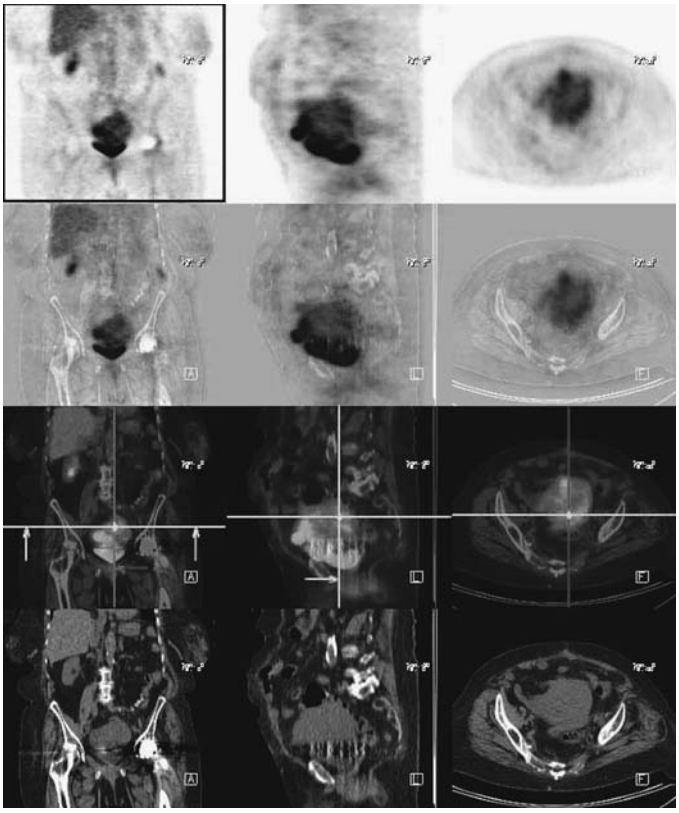

FIGURE 21.2.2.

with cysts. The subcarinal soft tissue noted on CT is negative by 18-FDG PET scintigraphy. Incidental findings include sigmoid diverticulosis and atherosclerotic vascular disease. Multilevel degenerative disease in the lumbar spine is noted.

Impression

There is a large central pelvic mass above and compressing the urinary bladder and just below an anastomotic staple line. This is heterogeneous in activity with moderate activity centrally and multifocal sites of peripheral intense hypermetabolism. Several lobulations or adjacent nodular densities are intensely hypermetabolic. No distant disease is evident.

Pearls and Pitfalls

- *Heterogeneous uptake of FDG is typical for pelvic leiomyosarcoma.*[2,5,8]

Discussion

Leiomyosarcoma is a subgroup of sarcoma and is more commonly seen in gynecologic malignancies. The mean patient age at diagnosis is about 60 years old. Leiomyosarcoma frequently is diagnosed after a hysterectomy is performed for a presumed leiomyomatous uterus. Pure leiomyosarcomas constitute about 20% to 50% of uterine sarcomas. Leiomyosarcomas are relatively radio-insensitive to treatment. Chemotherapy has limited success rate. Cisplatin has a total response rate of only a 3% with leiomyosarcomas. Newer agents, such as Ifosfamide, have been used in phase II trials for advanced or recurrent tumor, with a response rate of 17%.

The 5-year survival rate for leiomyosarcomas can range from 17% to 65% based on mitotic rate. The recurrence rate is 71%.

Case 21.3A

History

19-year-old male who has a history of a left ankle mass. A biopsy was positive for osteosarcoma. His MR demonstrated a left calcaneus mass measuring 3.2 cm. An outside CT chest was unremarkable. The patient is being seen for staging.

Findings

There is a large and well-demarcated hypermetabolic mass (*Figure 21.3A.1*) seen involving the medial and lateral aspect of the left calcaneus (*Figures 21.3A.2 and 21.3A.3*) and tarsal bone (*Figure 21.3A.4*) with corresponding soft tissue mass and bony destruction on CT. There is mild soft tissue uptake involving right lateral foot compatible with pressure from altered weight bearing. The mild activity in the thymus (*Figure 21.3A.5*) is considered normal for age. CT of the chest demonstrates no evidence of metastatic disease.

Impression

Hypermetabolism involving the left calcaneus and tarsal bone consistent with malignancy, without evidence of regional or distant metastases.

Pearls and Pitfalls

- *Low-grade osteosarcomas can produce false-negative results on PET because FDG uptake tends to be low.*[2,5,8]
- *PET has the ability to identify recurrent tumor earlier than conventional imaging.*[9]
- *FDG imaging can accurately depict histopathologic response to therapy.*[1,4,6]
- *The sensitivity for soft tissue tumors is 87% and specificity 79%. The positive predictive value for high-grade tumors is higher than that for lower-grade tumors.*[2,5,8]

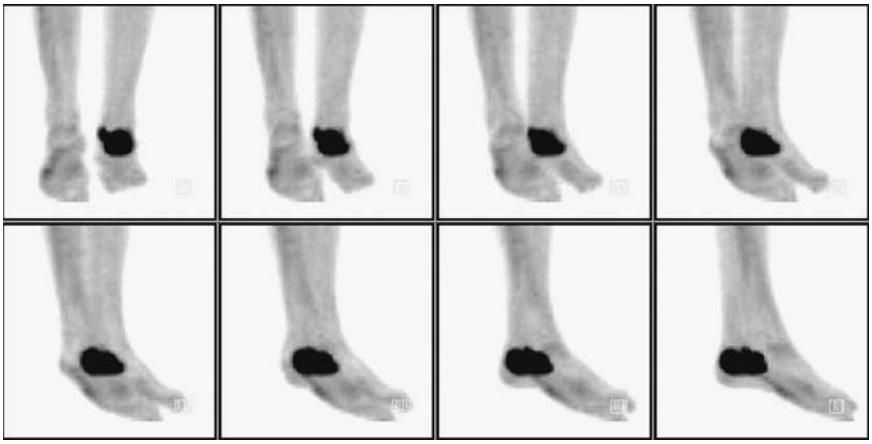

FIGURE 21.3A.1.

FIGURE 21.3A.2.

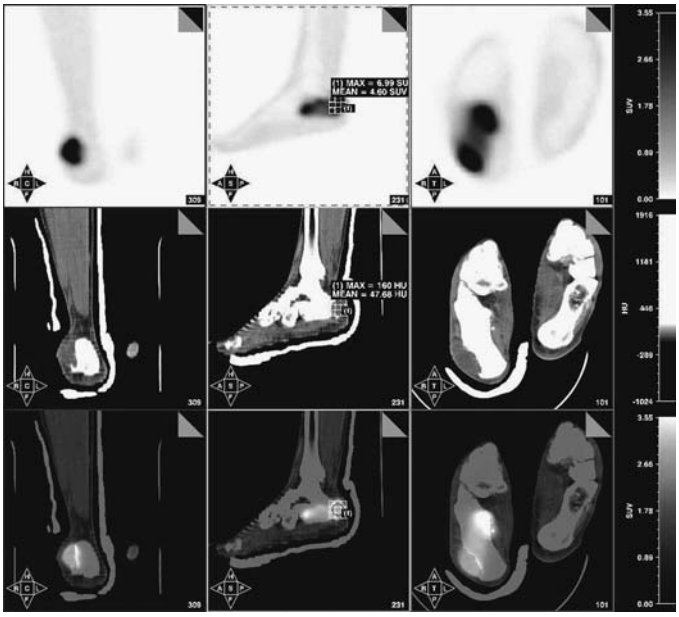

FIGURE 21.3A.3.

FIGURE 21.3A.4.

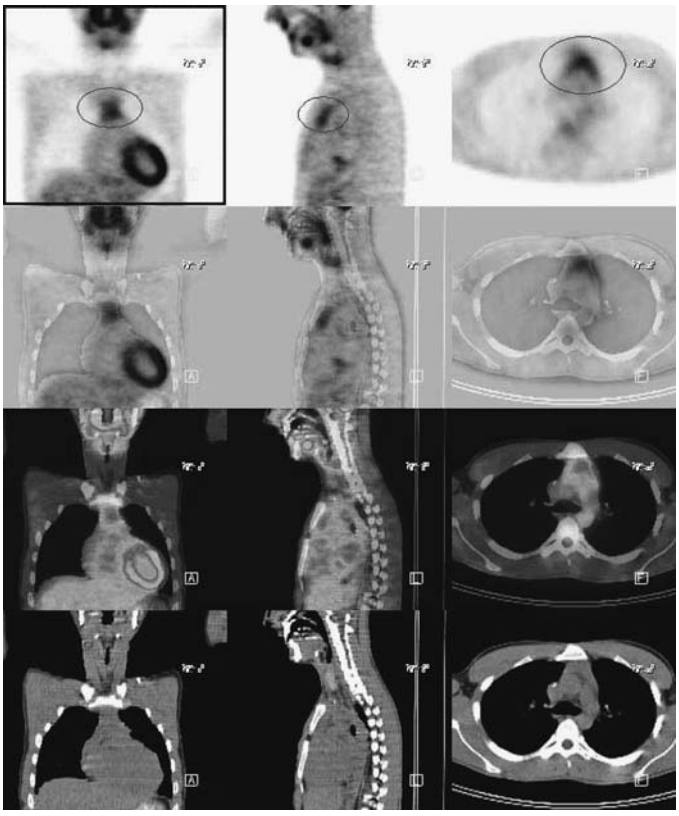

FIGURE 21.3A.5.

Discussion

Osteogenic sarcoma is a rapidly proliferating tumor and usually presents as a primary malignant bone tumor. It is the most common bone tumor encountered in the first three decades of life and has an incidence rate of 2.6% of all childhood cancers. It is more common in males. The peak incidence is at 13 to 14 years of age. The incidence of osteogenic sarcoma is increased in patients with Paget's disease and bones that have previously been irradiated. This is why there is a second prevalence peak in older individuals. Pain is the most common presentation as well as palpable masses, swelling, and limitation of motion.

Conventional imaging shows bone destruction and periosteal new bone formation. A "sunburst" appearance, and soft tissue swelling is sometime seen. MRI imaging of the involved region is recommended because the MRI scan can then be used to plan resection and subsequent reconstruction. Arteriography is considered for limb salvage procedures. Chest x-ray and CT scan are used to detect metastatic disease in the lungs. Technetium-99m or F-18 fluoride bone scans can outline the primary tumor, and FDG PET can detect unsuspected metastatic lesions.

Case 21.3B

History

19-year-old male with osteosarcoma of the left calcaneus. The current PET study is compared with the prior exam to evaluate response to chemotherapy.

Findings

There is again seen intense hypermetabolism in the body of the left os calcis (*Figures 21.3B.1 and 21.3B.2*). The tumor appears to involve all but the most posterior, superior, and anterior portions of the calcaneus, roughly 80% with intense hypermetabolism. There appears to be extension into the soft tissues medially, laterally, and inferiorly. The relative intensity is similar to the prior exam (SUV=4.3 prior, 3.8 current) (*Figures 21.3B.3 and 21.3B.4*). No other hypermetabolic focus in the lower extremities is apparent. Incidental notation is made of interval appearance of treatment-related marrow hyperplasia (*Figures 21.3B.5 and 21.3B.6*) of the distal femora and proximal tibias. The torso exam is negative for metastatic disease.

FIGURE 21.3B.1.

FIGURE 21.3B.2.

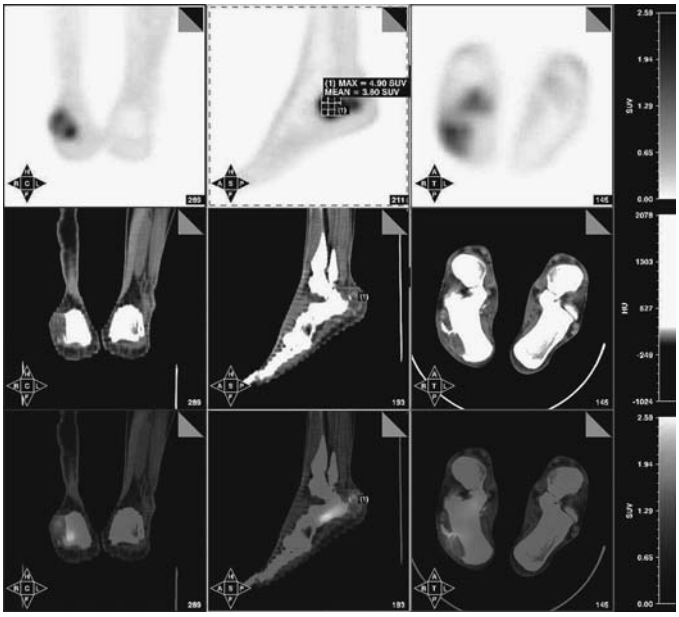

FIGURE 21.3B.3.

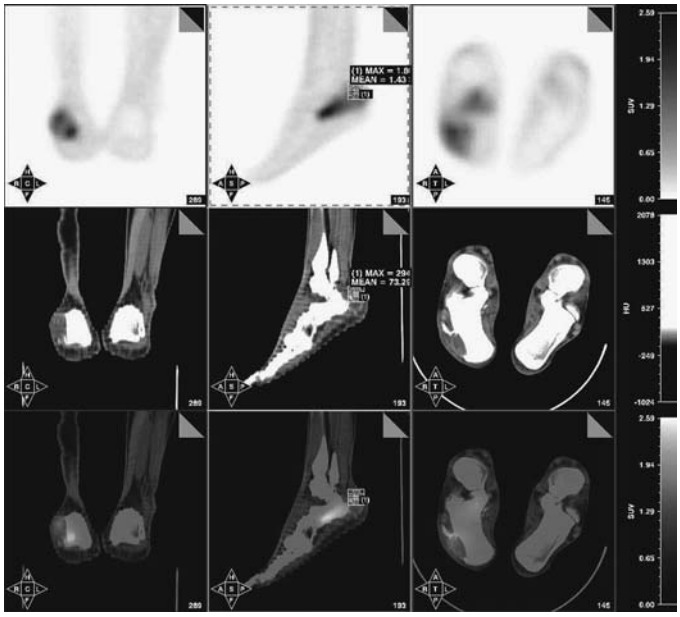

FIGURE 21.3B.4.

Impression

Persistent intense hypermetabolism of the left os calcis osteosarcoma, with no visible improvement since the prior exam. There is symmetric FDG uptake in bilateral neck, upper chest, and paraspinal area representing fat uptake.

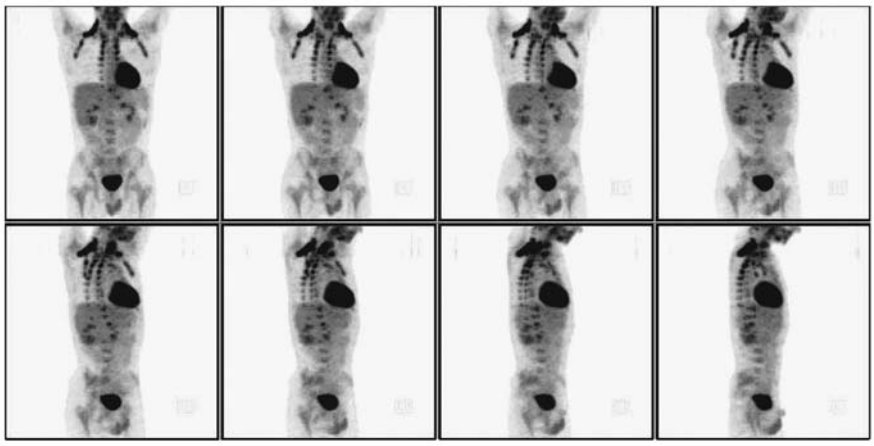

FIGURE 21.3B.5.

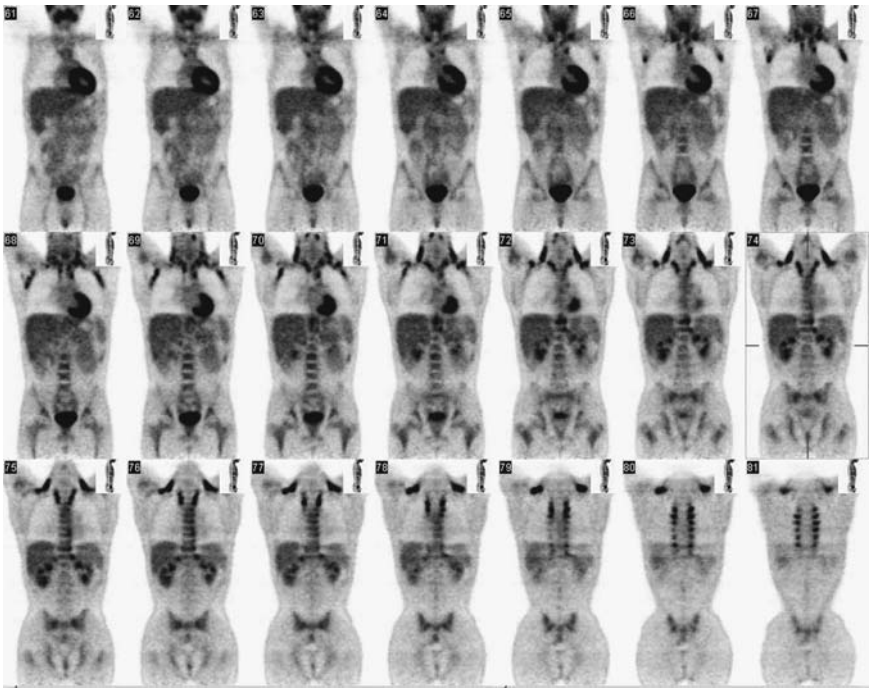

FIGURE 21.3B.6.

Pearls and Pitfalls

- *FDG PET is extremely valuable in monitoring patient response to chemotherapy, changing management in many patients considered surgical candidates.*[3,6]

Discussion

Certain forms of chemotherapy may cause an apparent increase in or persistently high SUV value if images are obtained within the first few weeks to one month after treatment. Residual high uptake of FDG is most commonly due to poor response to treatment, but may also occur with development of an inflammatory reaction in the tumor bed, mimicking tumor progression or lack of treatment response. An additional short-term follow-up imaging study may help clarify whether there is response if immediate surgery or biopsy is not contemplated: persistent uptake after 2 to 3 months is more likely to reflect poor treatment response as inflammatory changes tend to subside over

time. In this case a third examination done 3 months after the first examination continued to demonstrate high tumor uptake, consistent with pathologically proven residual tumor.

Case 21.4

History

43-year-old female who has a history of right thigh angiosarcoma status post resection. Her radiotherapy ended several months ago and is currently treated with chemotherapy. The patient is being seen to evaluate for recurrence.

Findings

There is heterogeneous hypermetabolism in the upper medial aspect of the right lower extremity (*Figures 21.4.1 and 21.4.2*). The lesion extends from the surgical clips superiorly to the level of the medial femoral condyle inferiorly consistent with recurrent tumor. Mild to moderate bone marrow activity is also noted in the central skeleton (*Figure 21.4.3*).

Impression

1. Hypermetabolism in the right lower extremity suggestive of recurrent malignancy.
2. Central skeletal marrow hyperplasia consistent with chemotherapy-related marrow response.

Pearls and Pitfalls

- *Prominent bone marrow activity is noted and explained by post treatment changes.*[3,6]

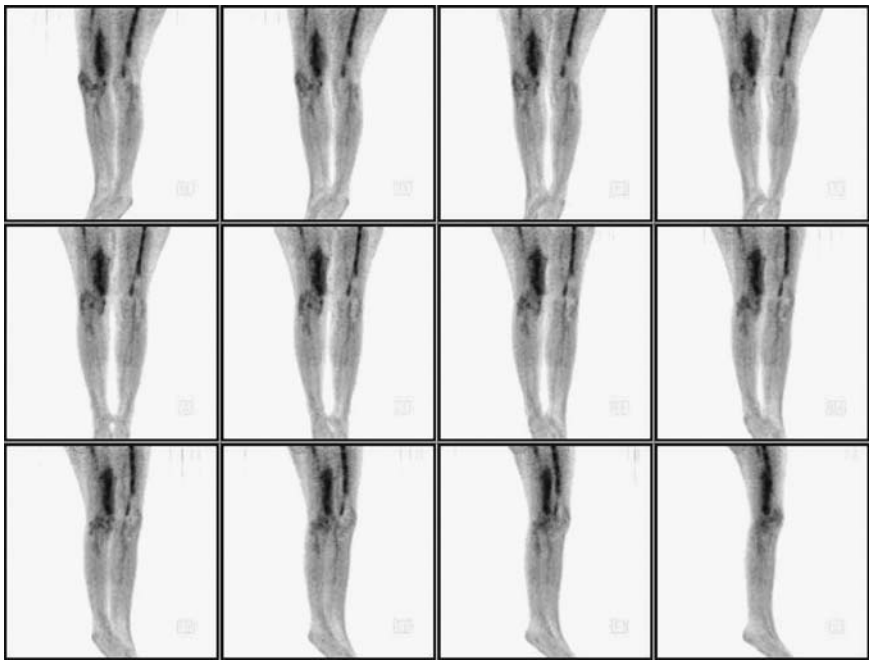

FIGURE 21.4.1.

FIGURE 21.4.2.

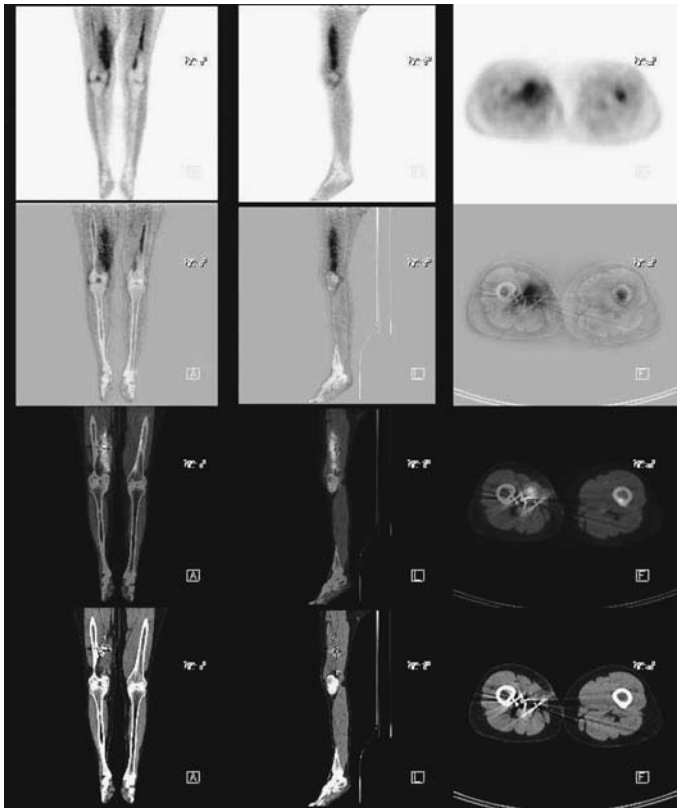

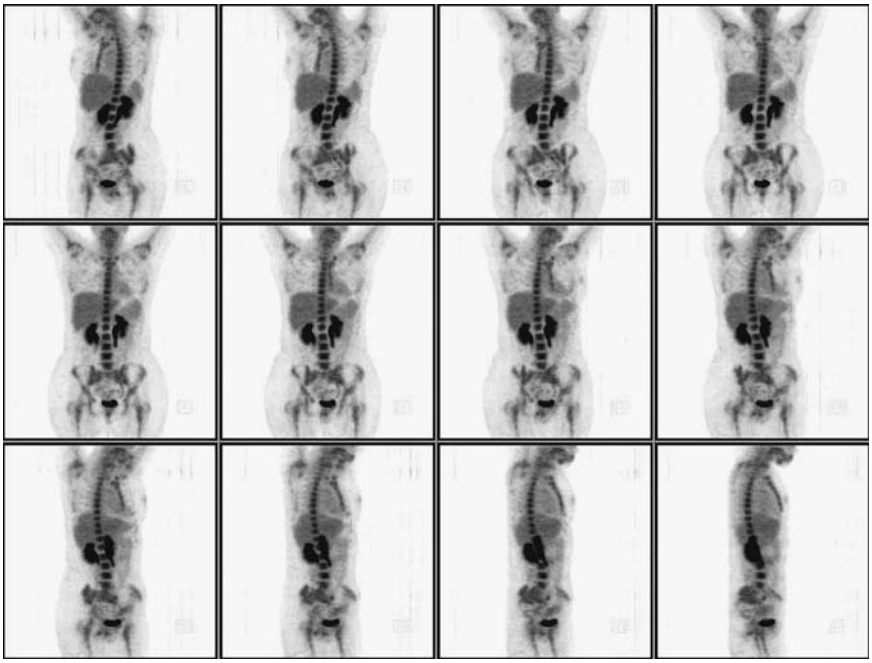

FIGURE 21.4.3.

Discussion

Angiosarcomas are a group of rare and high-grade tumors derived from vascular endothelial cells. Angiosarcomas frequently have been associated with previous irradiation sites. The prognosis of angiosarcoma is poor. The progression is frequently described as relentless. The standard approach is surgical resection. A few studies have reported limited success with adjunctive chemotherapy.

This patient has a right thigh angiosarcoma. Prior to PET, the patient had her right thigh mass resected followed by external beam radiation. Four months later, PET evaluation was requested to evaluate for metastatic disease. The CT examination failed to detect any trace of residual disease. On the PET study, the recurrence was clearly visible.

Case 21.5

History

25-year-old male who has a history of a lateral right knee mass increasing in size. The patient is being seen to evaluate for extent of disease.

Findings

There is intense hypermetabolism in the popliteal fossa (*Figure 21.5.1*) corresponding to a mass on CT. There is also an additional site of hypermetabolism in the muscular compartment surrounding the proximal right tibia that is irregular posteriorly and confluent anterolaterally, corresponding to a large lobulated mass on CT. There are small high-density foci in the posterior aspect of the large mass which are curvilinear inferiorly, suggestive of calcifications within the wall of the lobules. A separate focally intense hypermetabolic lesion is noted more superiorly and posteriorly adjacent to the superior portion of the right fibula (*Figure 21.5.2*). There is some asymmetry in the surrounding vocal cord which may represents pharyngeal uptake and is physiologic. Physiologic activity is seen in the heart, lung, liver, bowel, and testicles. No metastases are present in the lung.

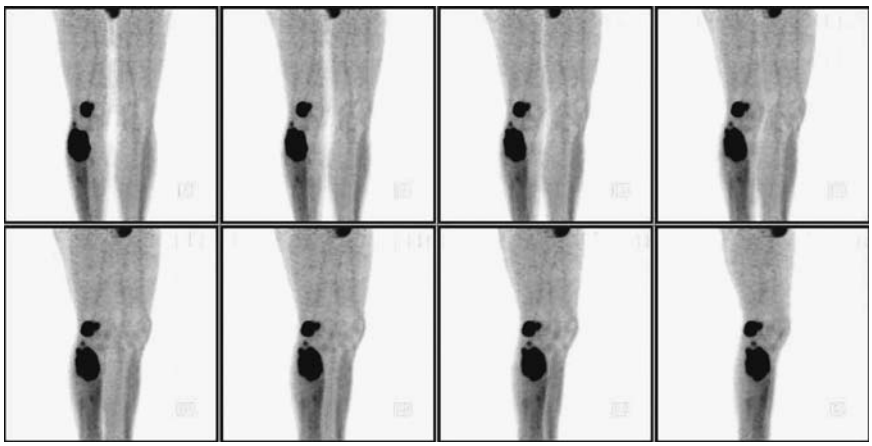

FIGURE 21.5.1.

FIGURE 21.5.2.

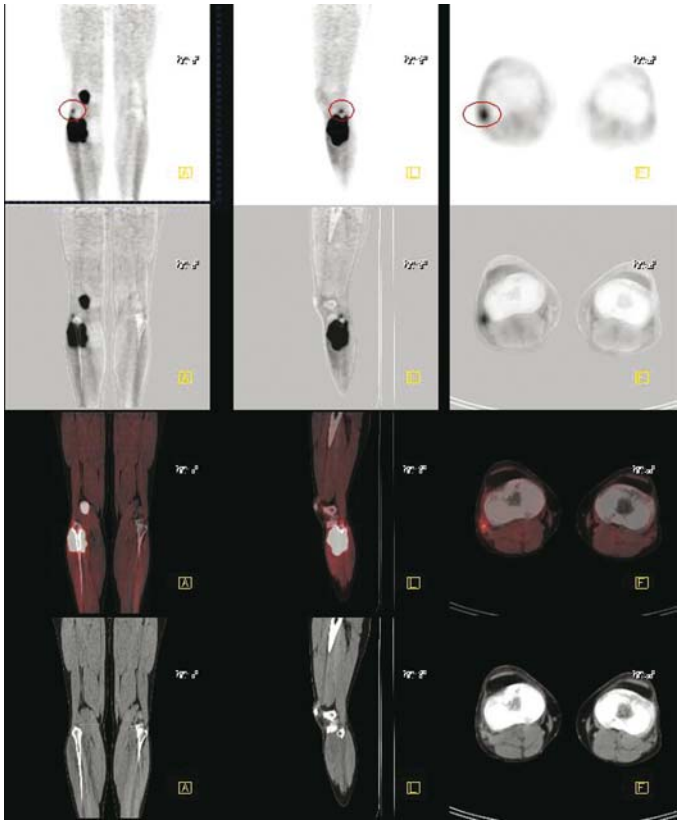

Impression

1. There is a large intensely hypermetabolic mass surrounding the right proximal tibia with additional satellite lesions adjacent to the right proximal fibula and in the popliteal fossa consistent with malignancy.
2. No evidence for distant disease.

Pearls and Pitfalls

- *Synovial sarcoma is highly FDG avid because of the tumor's inherent aggressive behavior.*[7,10]

Discussion

In this patient, the histopathology was subsequently found to be consistent with synovial sarcoma. Synovial sarcoma belongs to a group of sarcomas that usually grow by local extension, infiltrate adjacent tissues, and extend along tissue planes. Ninety percent of these sarcoma patients will have localized disease but the tumor eventually spreads to distant sites. More than 50% will develop disease in the lung as the first distant metastatic site. Chromosomal analysis, histology, and immunohistochemistry are some of the techniques available to identify the types of soft tissue sarcomas.

22 Urinary Malignancies: Renal Cell Carcinoma and Bladder Cancer

Lalitha Ramanna

Case 22.1

History

55-year-old male who has a history of renal cell carcinoma status post left nephrectomy and chemotherapy. His outside CT revealed a left renal bed mass consistent with recurrent renal cell carcinoma. There is a 2-cm nodule in the right lower lobe of the lung, which is a new finding. The patient is being evaluated for metastatic disease.

Findings

There is local recurrence of disease in the left renal bed, which is hypermetabolic on PET. The right lower lobe nodule (*Figures 22.1.1 and 22.1.2*) on CT is once again seen as an intense hypermetabolic foci on PET. There is also uptake in the left lower rib anteriorly (*Figure 22.1.3*), which suggest metastasis. The mild uptake in the right lower anterior wall (*Figure 22.1.4*) is likely due to myositis. There is a mild activity in the right buttock (*Figure 22.1.5*) possibly related to an injection site.

Impression

Evidence for local tumor in the left renal bed and metastasis in the right lower lobe and left lower rib anteriorly.

Pearls and Pitfalls

- *77% of the renal cell carcinomas are identified correctly with PET.*[6,7]
- *The diagnostic accuracy for staging is 84%.*[6,7]
- *The sensitivity is 82% and specificity is 88%.*[6,7]
- *PET reveals lesions not previously suspected in 69% of the cases.*[6,7]
- *In contrast to bone scan, PET has a sensitivity and accuracy of 100% and 100% for detecting metastatic bone lesions; bone scintigraphy has a sensitivity and specificity of 77.5% and 59.6%, respectively.*[6,7]

FIGURE 22.1.1.

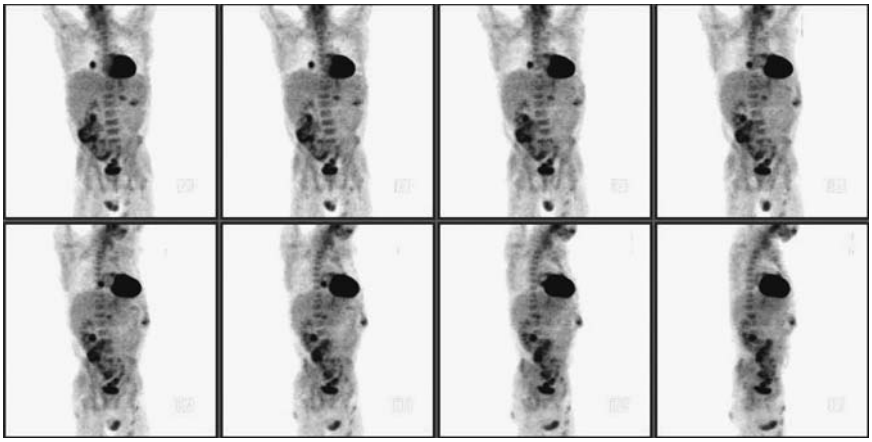

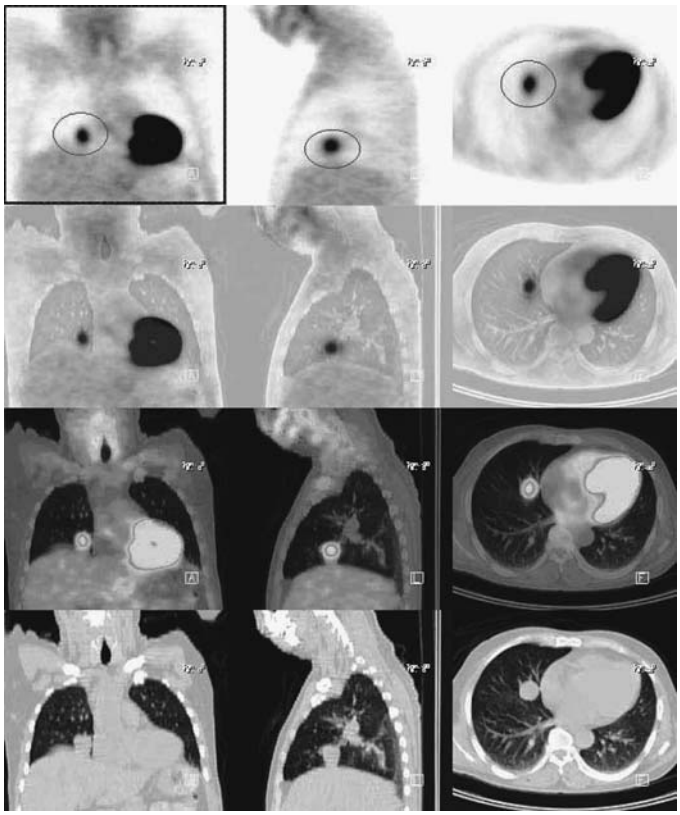

FIGURE 22.1.2.

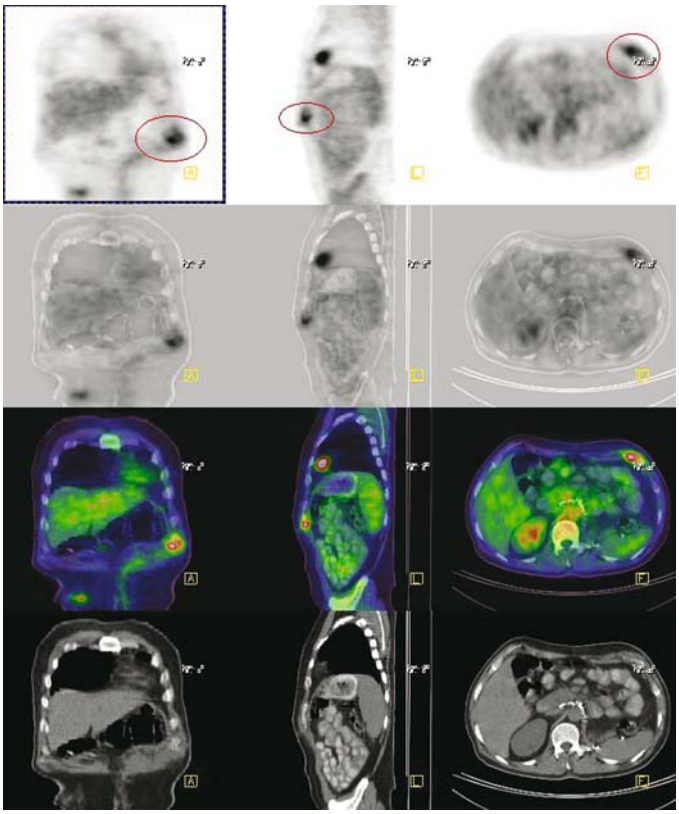

FIGURE 22.1.3.

Discussion

Renal cell carcinoma represents 3% of all cancers in the adult population. Commonly occur in men and within the age range of 50 to 70 years of age. Most patients are detected incidentally with ultrasonography and CT. Surgery is the modality of choice.

Metastatic renal cell carcinoma has a median survival of 10 months despite of nephrectomy. A shortcoming regarding FDG PET is that its success is highly dependent on the glucose transporter 1 (GLUT-1) expression. This protein molecule is an early marker for cellular malignant transformation. It has been reported that some renal tumors fail to express this protein, thereby lowering the detectability of disease.

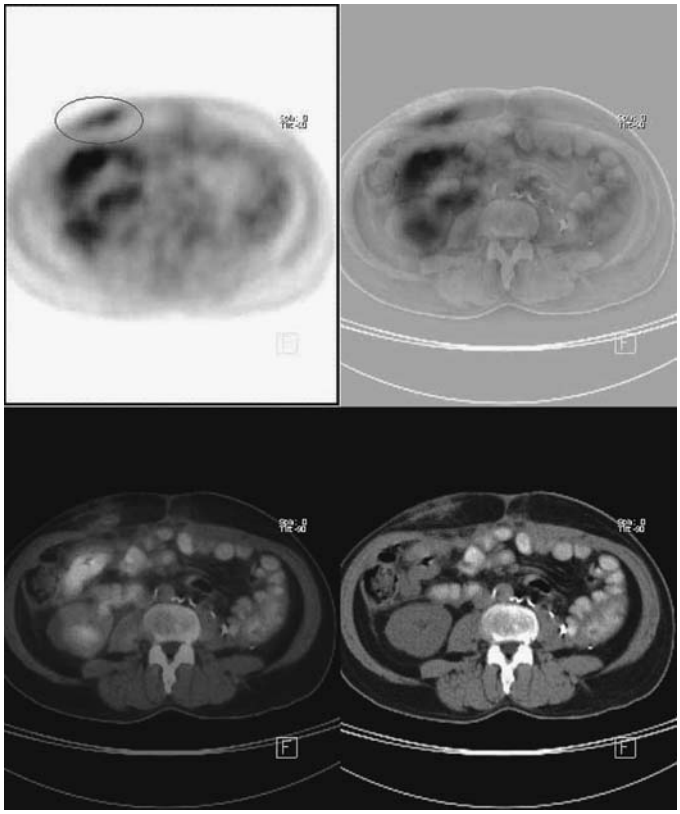

FIGURE 22.1.4.

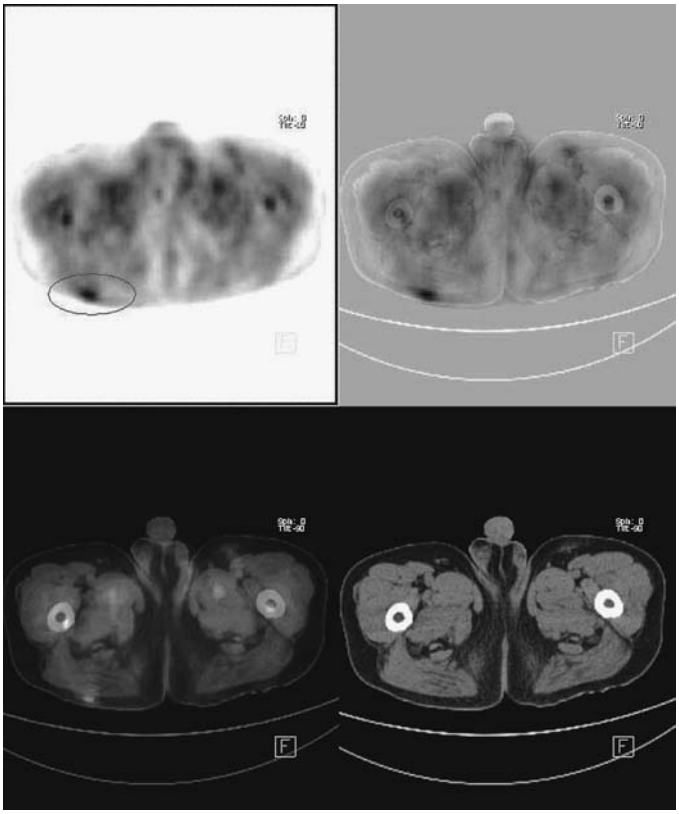

FIGURE 22.1.5.

Case 22.2

History

76-year-old male with a remote history of laryngeal cancer status post radiation therapy and total laryngectomy. Subsequently, he developed right flank symptoms and was diagnosed with renal cell carcinoma of the right kidney. The current study is being done to evaluate for metastatic disease.

Findings

There is a large mass intrinsic to the right kidney which has intense peripheral hypermetabolism (*Figures 22.2.1 and 22.2.2*). The mass measures 10.5 cm in diameter. There is extensive central photopenia with more necrosis than viable tumor. No regional or distant metastatic disease is apparent, however. One pulmonary nodule at the left base is not active by 18-FDG PET scintigraphy.

Impression

1. 10.5-cm right renal cell carcinoma with peripheral hypermetabolism but predominant central necrosis. There is no evidence for metastatic disease within the neck, chest, abdomen, or pelvis.
2. Mild hypermetabolism at the right shoulder joint, likely representing some synovitis.
3. 1-cm pulmonary nodule in the lingula, not active by 18-FDG PET scintigraphy, is likely benign.

FIGURE 22.2.1.

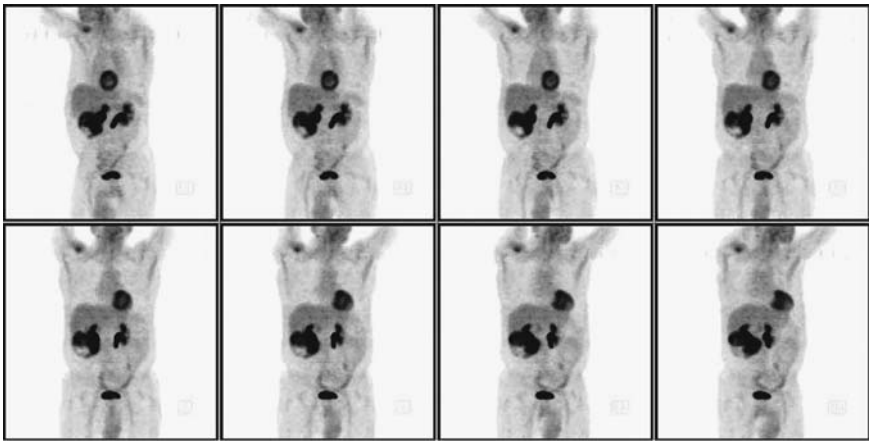

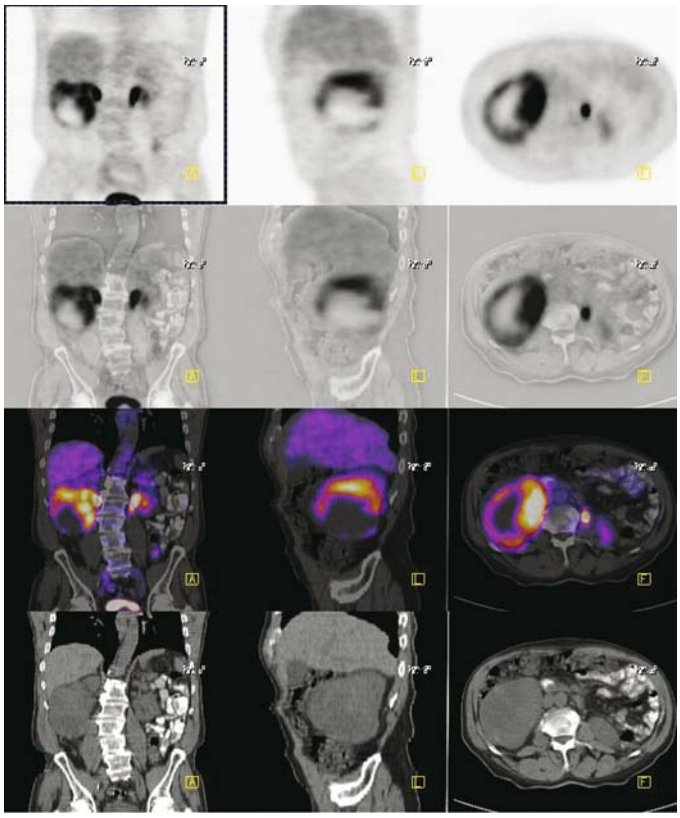

FIGURE 22.2.2.

Pearls and Pitfalls

- *Both PET and CT performed well in detecting metastatic lesions, 69% as opposed to 70% respectively.*[7]
- *PET can alter patient management in 40% of the cases.*[5]

Case 22.3

History

82-year-old male status post left nephrectomy and cystectomy for bladder cancer. He is currently being evaluated for a left chest mass.

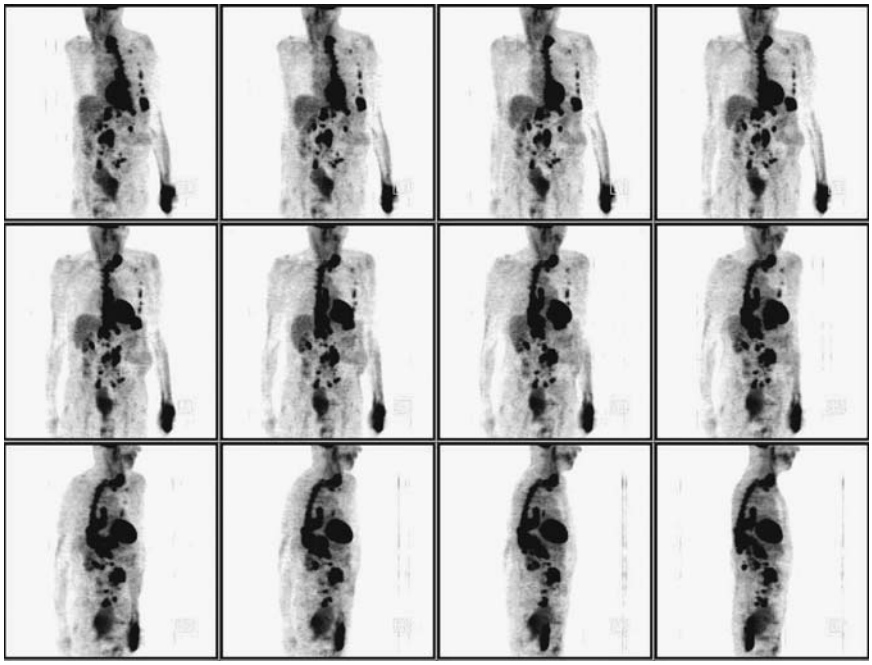

FIGURE 22.3.1.

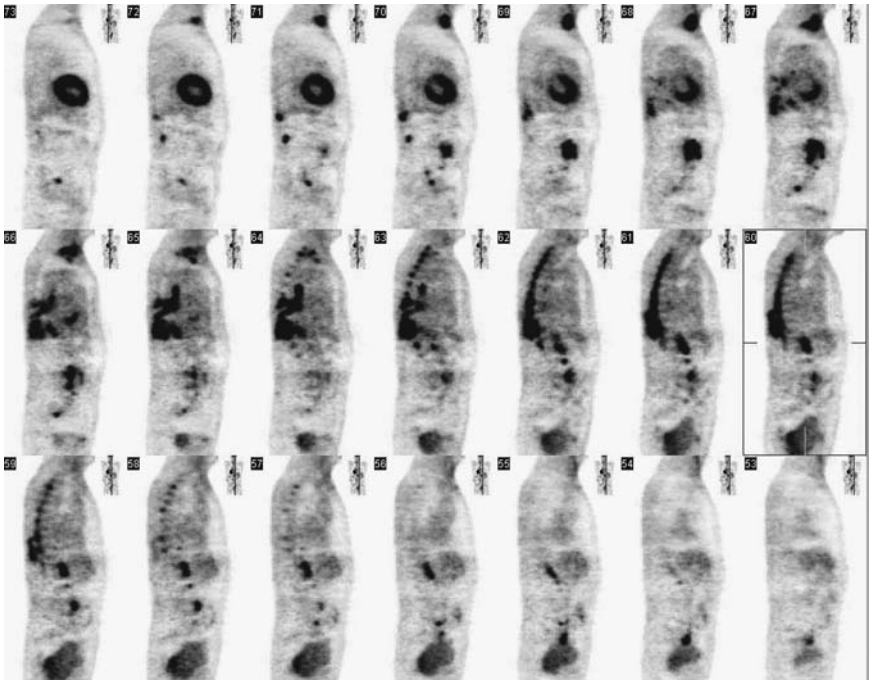

FIGURE 22.3.1A.

Findings

The activity in the face and upper neck appears physiologic with some pre-cervical normal-variant muscular activity and tonsillar activity (*Figures 22.3.1 and 22.3.1A*). However, there is intense hypermetabolism in a left neck supraclavicular mass (*Figure 22.3.2*). This has a discernible tail, which extends posteriorly into the left T-2 neural foramen. This connects to an extensive region of epidural hypermetabolism which is nearly continuous from T-1 to T-10 (*Figure 22.3.3*). There is extension along the proximal left posterior ribs at multiple levels, indicating likelihood for perineural spread (*Figure 22.3.4*).

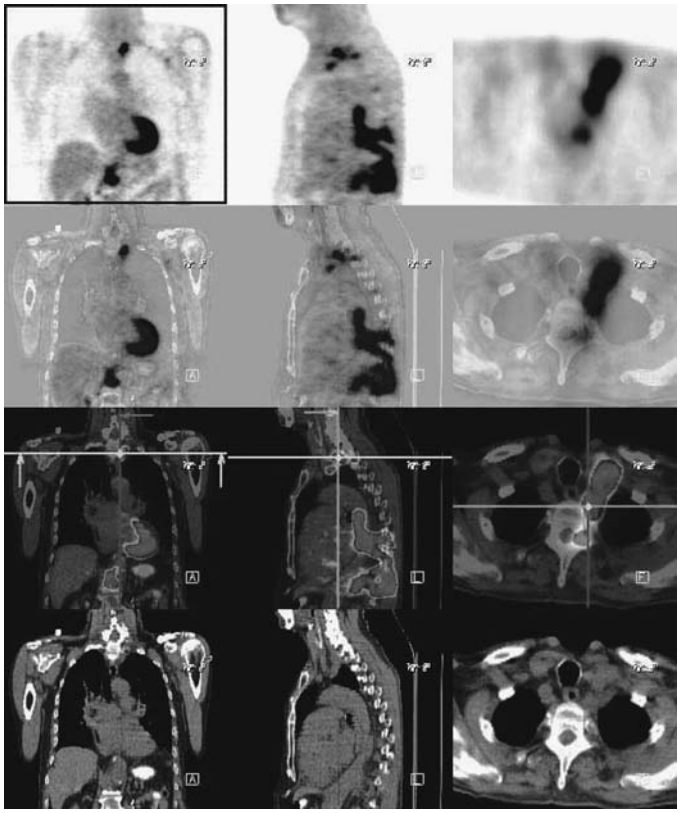

FIGURE 22.3.2.

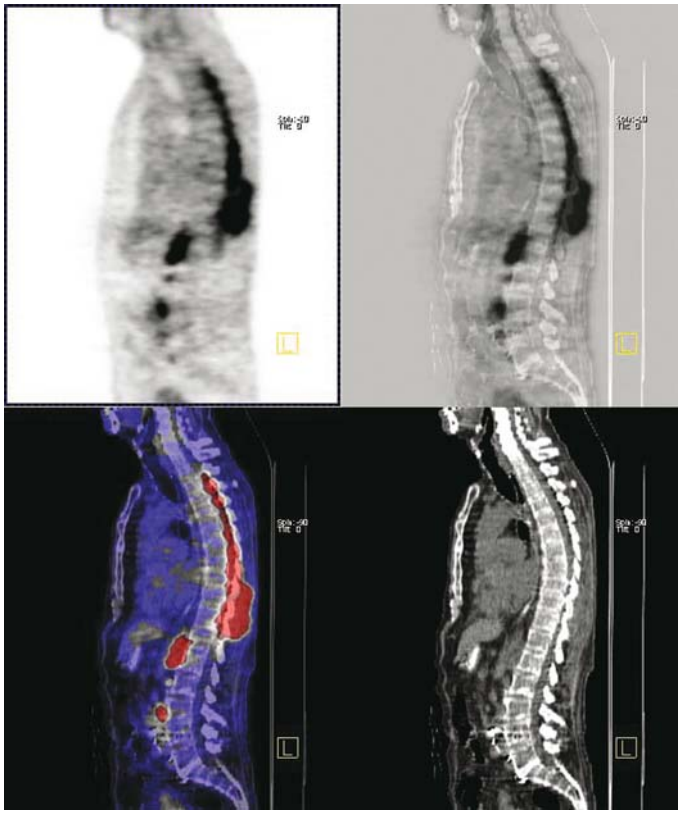

FIGURE 22.3.3.

The epidural disease also appears to extend into the left posterior mediastinum at the midthoracic level and is continuous in the posterior mediastinal, the left aspect of the vertebral bodies and the right aspect of the descending aorta from the carina downward to the left retrocrural space (*Figure 22.3.5*). Involvement of vertebral foramina may be a consequence of spread from epidural disease. The left pleural effusion does not have associated hypermetabolism. However, there appears to be some left paraspinous musculature and left latissimus dorsi musculature hypermetabolism. The paraspinous disease appears continuous with the posterior mediastinal disease. The retrocrural hypermetabolism extends caudally and is continuous with upper abdominal retroperitoneal adenopathy, which is hypermetabolic. One other small paraspinous muscular deposit is evident at about L-2.

There is one small hypermetabolic deposit in a lymph node in the high left axilla. There is also a small focus in the left common iliac area bilaterally which probably also represents metastatic adenopathy.

Impression

1. Extensive hypermetabolic disease in an unusual distribution with apparent epidural disease from T-1 to T-10 and perineural extensions at multiple thoracic levels, as well as into the left supraclavicular neck. There is extension into the lower posterior mediastinum with continuous disease from the carina through the retrocrural space, into the upper abdominal retroperitoneum. There are also a few nodes in the common iliac chains and left axilla.
2. The epidural disease is of concern and MR would be an appropriate consideration to evaluate the status of the thoracic cord.

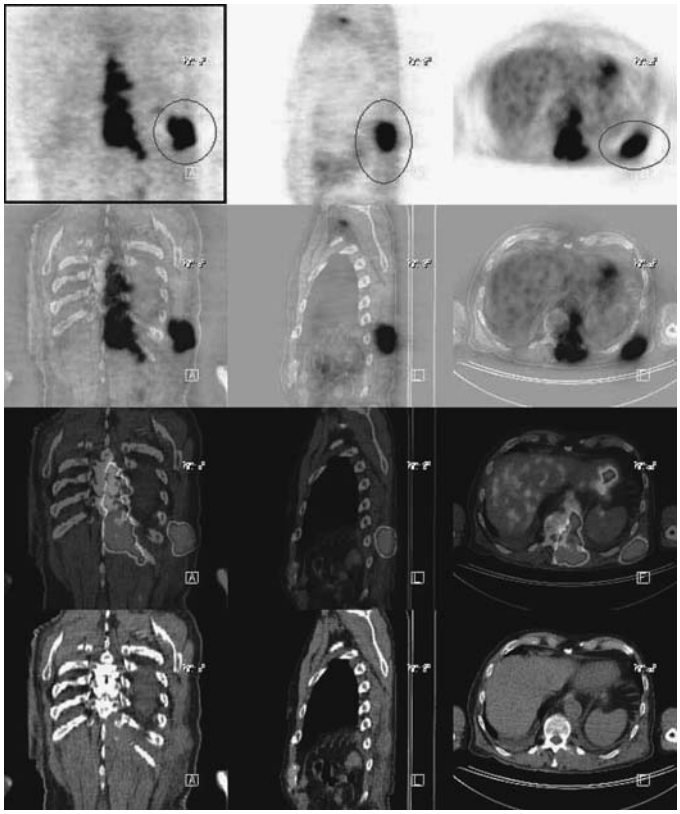

FIGURE 22.3.4.

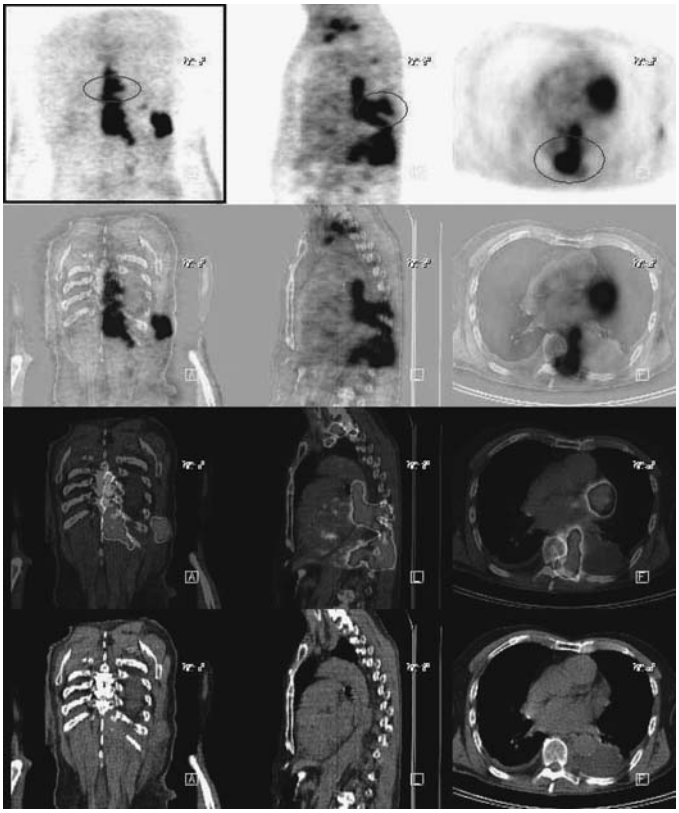

FIGURE 22.3.5.

Pearls and Pitfalls

- *FDG is not generally used for the detection of primary bladder cancer since the tracer is mostly excreted through urine. However, distant metastatic disease is usually well seen.*
- *Radiolabeled choline and acetate have potential for bladder tumor imaging because they are not excreted in the urine.*[3]
- *PET has a sensitivity of 67%, specificity of 86%, and an accuracy of 80% for bladder cancer.*[1,2,4]

Discussion

Bladder cancer is the fourth common cancer in men. Most cases are transitional cell carcinoma. It is more common in whites than blacks. The median age is 68 years. Smoking, industrial carcinogen exposure, and prior radiation are risk factors. Microscopic hematuria is a common finding. IVP can be used image the upper-tract urothelium in patient presenting with hematuria. CT and ultrasonography can be effective for lesion detection but they can miss urothelial tumors in the upper tract. Cystoscopy and urine cytology are diagnostic. More than 70% of the cancers are carcinoma in situ. Intravesical immunotherapy and intravesical chemotherapy are common treatment modalities. The methotrexate, vinblastine, Adriamycin, and cisplatin combination is the standard treatment for metastatic bladder cancer. For superficial bladder cancer, the 5-year survival is 82% to 100%. For T-2, T-3, and T-4 tumors, the 5-year survival rates are 63% to 83%, 455 to 55%, and 0% to 22%.

Recognition of epidural disease should prompt urgent consultation to initiate local therapy (radiation or surgery) if there is compromise of the spinal cord on MRI.

23 Nerve Tumors

Lalitha Ramanna

Case 23.1

History

63-year-old female who has a history of high-grade malignant peripheral nerve sheath tumor of the right facial nerve. She is status post right superficial parotidectomy and treatment with adjuvant radiotherapy. Her CT revealed multiple lesions in the bilateral lung parenchyma suspicious for malignancy. The fine needle aspiration of the right middle lobe demonstrated malignant spindle cell components consistent with metastasis from the parotid gland. Evaluation for metastasis is requested.

Findings

There is a large hypermetabolic mass in the right midlung (*Figures 23.1.1 and 23.1.2*) associated with a soft tissue mass on CT. Another smaller lesion in the right anterior lateral lung field (*Figure 23.1.3*) is seen adjacent to the pleural surface and also corresponds to a mass on CT. Within the left anterior lateral midlung (*Figure 23.1.4*), there is a lesion seen with corresponding soft tissue mass that is hypermetabolic. The photopenia in the region of the right parotid (*Figure 23.1.5*) is from prior radiotherapy. The activity in the stomach is physiologic. Dedicated brain scan is within normal limits for age.

Impression

Abnormal hypermetabolism seen in the lung parenchymal nodules bilaterally, consistent with metastatic disease.

Pearls and Pitfalls

- *An imaging delay of 3 hours can be helpful for distinguishing malignant lesions from background activity due to continued washout of tracer from normal organ and progressive accumulation in tumor.*

Discussion

With more than 4% of the neurofibromatosis 1 (NF-1) patients are at risk of developing malignant peripheral nerve sheath tumor (MPNST) from preexisting plexiform

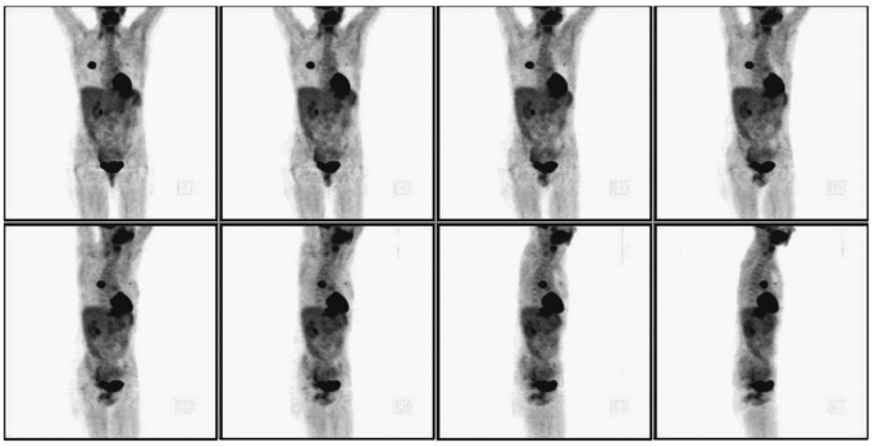

Figure 23.1.1.

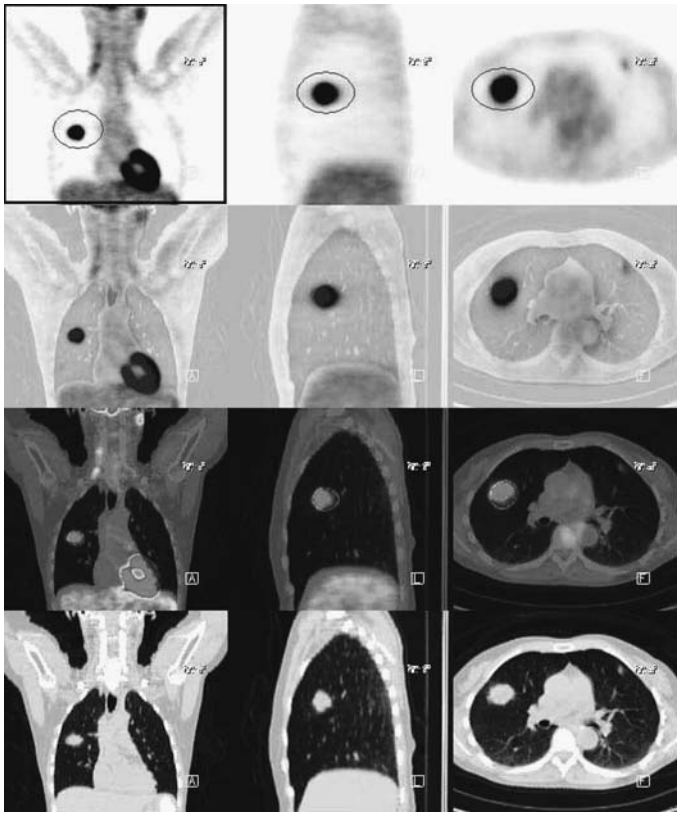

Figure 23.1.2.

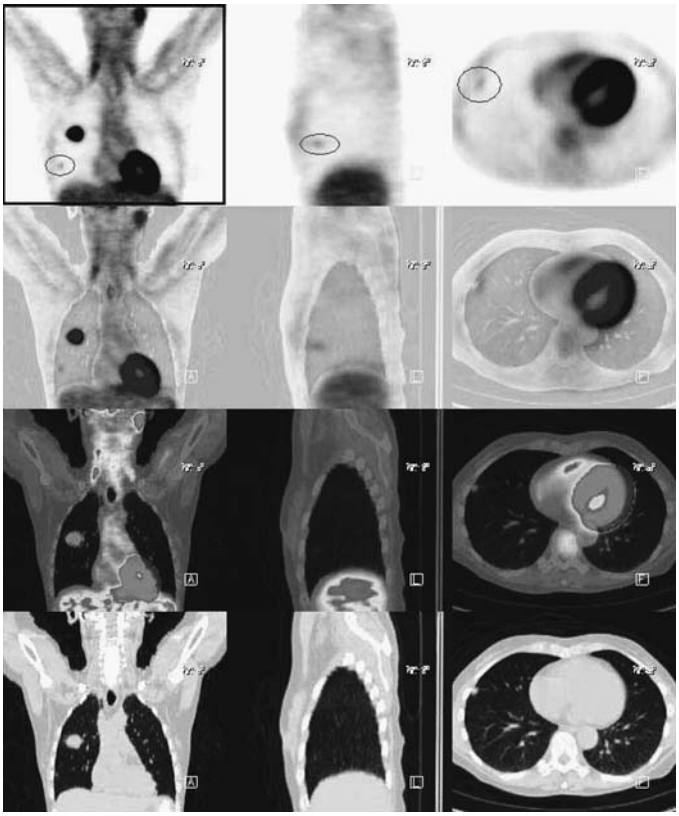

Figure 23.1.3.

neurofibromas. Previous radiotherapy, family history, and microdeletion of the NF-1 locus are predisposition factors. The disease may metastasize widely to the lung, brain, liver, and retroperitoneum. The prognosis is poor. Pain, changing texture, increasing size, and neurological deficit are some of the nonspecific indicators for malignancy. MR can assess the extent of plexiform neurofibroma involvement. PET can determine the degree of malignancy based on metabolism. Surgery is the treatment of choice. Adjuvant radiotherapy may be used for intermediate to high grade MPNST. Ifosfamide and doxorubicin are for palliation.

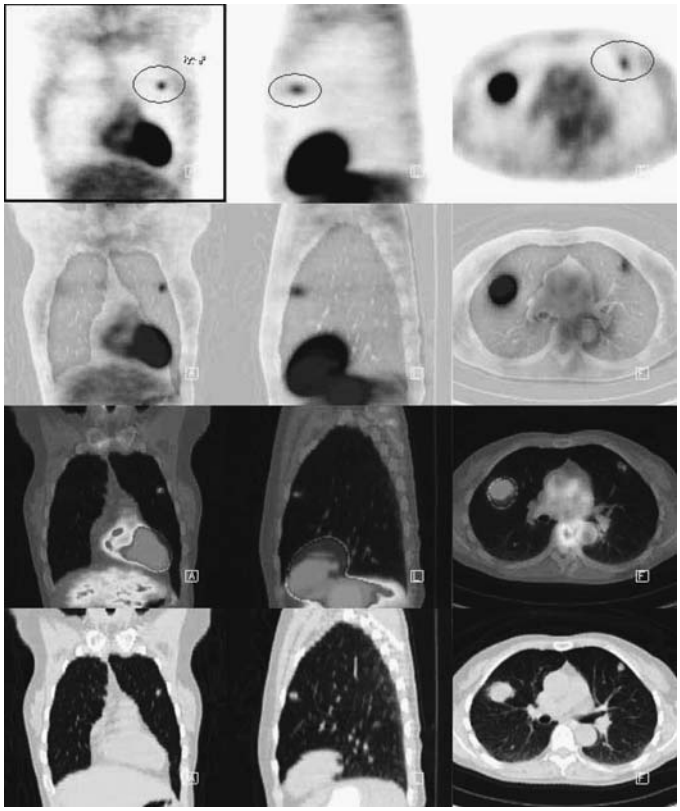

FIGURE 23.1.4.

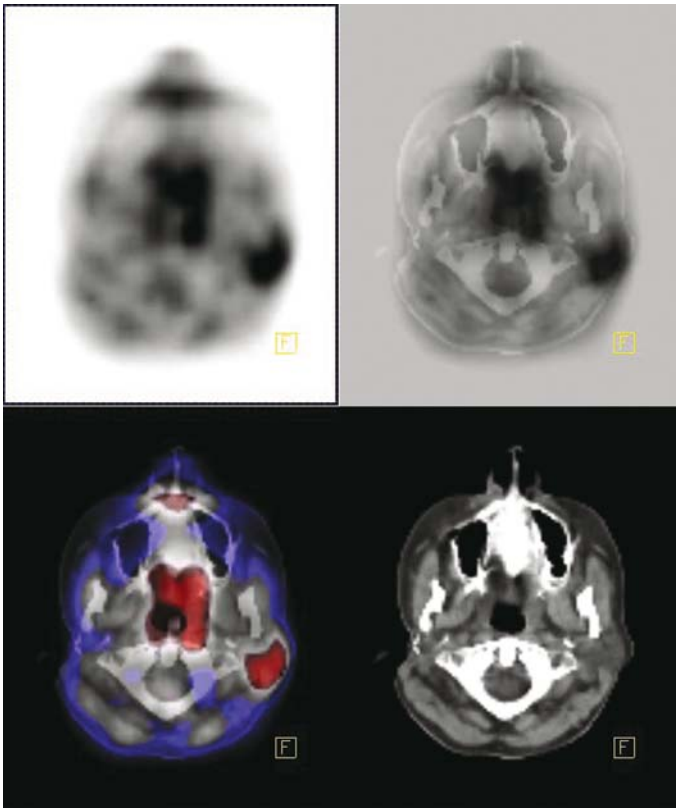

FIGURE 23.1.5.

Case 23.2A

History

48-year-old male status post resection of a right ulnar mass which was proven to be primitive neuroectodermal tumor (PNET). PET study is requested for staging.

Findings

There is moderately intense hypermetabolic activity in the right distal arm/elbow area (*Figures 23.2A.1 and 23.2A.2*) consistent with recurrent tumor. In the neck and chest area, there is bilateral and symmetric metabolic activity in the lower neck consistent with muscle uptake. No hypermetabolic foci are seen in the parenchyma to indicate pulmonary metastatic disease. In the abdomen, no hypermetabolic foci are seen in the liver and adrenals. Tubular shaped activity along the distribution of the GI track is attributed to physiologic tracer accumulation. No evidence for adenopathy is seen. In the lower extremity, there is an elongated segment of hypermetabolic activity in the lateral muscular compartment of the left leg attributed to physiologic activity (*Figure 23.2A.3*).

Impression

1. FDG uptake in the right distal arm mass consistent with recurrent tumor.
2. PET scan is negative for metastatic disease.

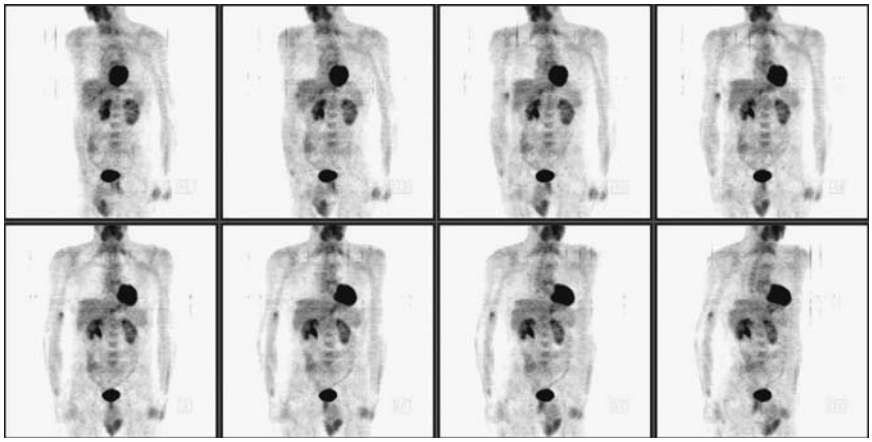

FIGURE 23.2A.1.

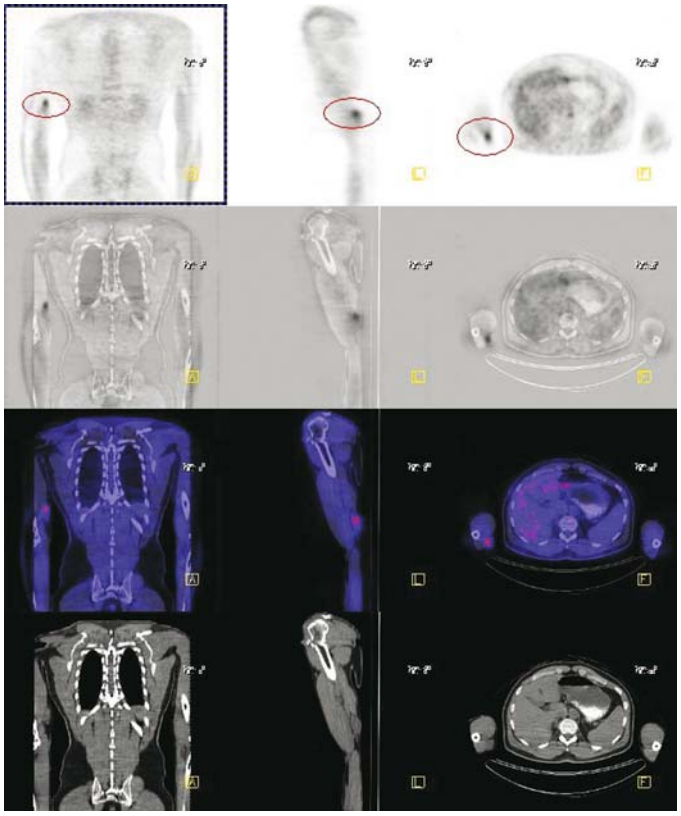

FIGURE 23.2A.2.

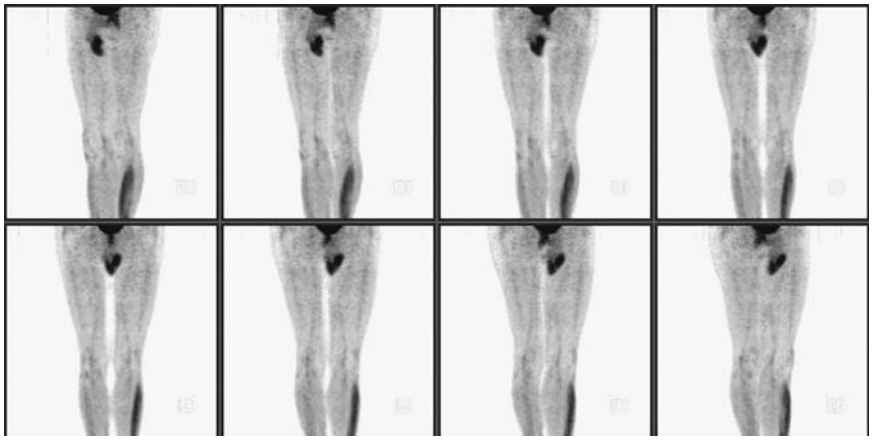

FIGURE 23.2A.3.

Pearls and Pitfalls

- *PET is a useful method to detect distant metastases.*

Discussion

Ewing's sarcoma (primitive neuroectodermal tumor) is a rare malignant bone tumor found mostly in the pelvis, femur, humerus, and ribs. Pain and stiffness are the most common presentations. Biopsy is the definitive diagnosis. Early diagnosis offers the best prognosis. The cancer can spread to the lung and bone marrow. Recurrent tumor can occur regionally from the site of prior resection or distally in a new location. Surgery is the treatment of choice. Additional radiation or chemotherapy may be needed for metastatic disease.

Case 23.2B

History

48-year-old male who is status post resection of right arm mass proven to be a primitive neuroectodermal tumor (PNET). He has now received chemotherapy and is being evaluated for treatment response. The current exam is compared with the prior exam which had shown a regional hypermetabolic focus in the medial soft tissues of the right arm above the elbow.

Findings

There has been interval regression of the focal hypermetabolism previously demonstrated in the soft tissues of the right arm above the elbow (*Figure 23.2B.1*). There is a smaller focus of lesser hypermetabolism evident in this area on the current exam.

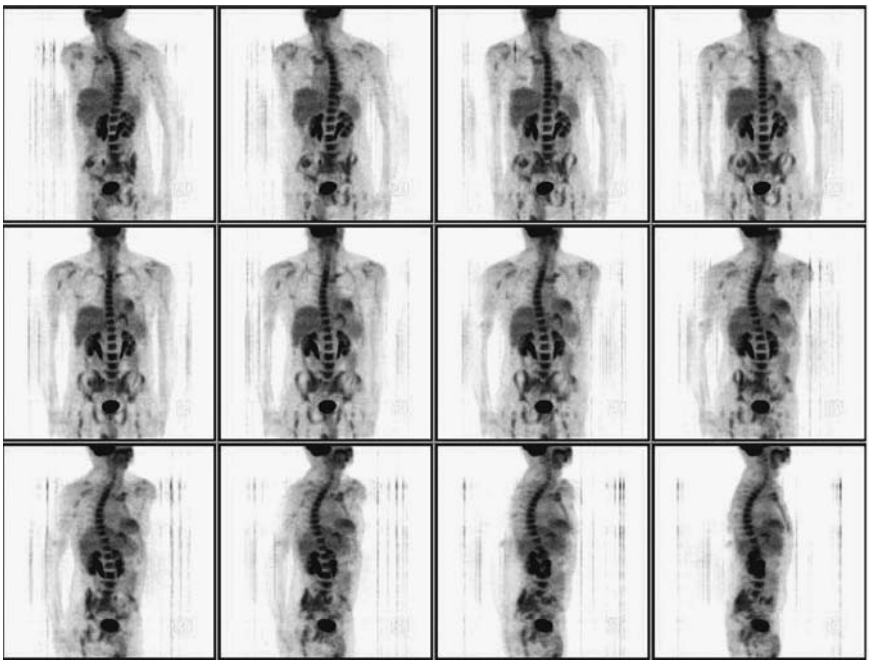

FIGURE 23.2B.1.

There is no evidence of pathologic axillary adenopathy or mediastinal adenopathy. The lungs appear negative both by 18-FDG PET scintigraphy and by CT with lung window settings with no pulmonary lesions identified. No skeletal metastases are identified. There is some marrow hyperplasia. Incidental notation is made of a left subcutaneous pectoral port for central venous catheter which terminates in the right atrium.

Impression

With regard to the history of right upper extremity primitive neuroectodermal tumor, there has been a significant interval decrease in the apparent size and relative intensity of the right arm lesion since the prior exam. The patient remains free of evident disease elsewhere.

Pearls and Pitfalls

- *FDG is more sensitive when compared to other modalities in evaluating patient responses to treatment.*

Case 23.3

History

39-year-old male who has a history of schwannoma with a recent left inguinal resection for multiple masses. The patient is being evaluated for extent of disease.

Findings

Hypermetabolic nodal uptake is seen near the site of recent biopsy in the left medial inguinal region (*Figures 23.3.1 and 23.3.2*) corresponding to nodes seen on CT. This is likely local recurrence of the patient's previous tumor. Asymmetrical substernal uptake is also noted possibly representing thyroid gland uptake (*Figure 23.3.3*); further thyroid work up is recommended. The prominent uptake in the stomach is likely due to inflammatory disease. Bilateral prominent muscle uptake in legs is physiological.

Impression

1. Abnormal uptake in the left medial inguinal region is consistent with recurrent tumor plus inflammation associated with recent surgery.
2. Prominent stomach activity is likely related to an inflammatory process; suggest clinical correlation.

Pearls and Pitfalls

- *Wide resection is the primary treatment for malignant schwannoma.*[1,2,3,4]

FIGURE 23.3.1.

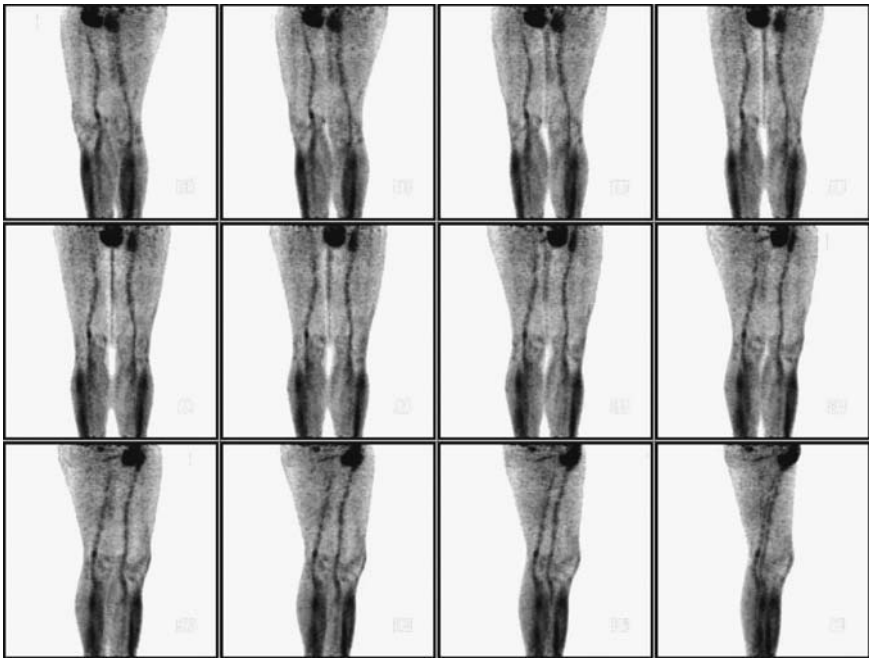

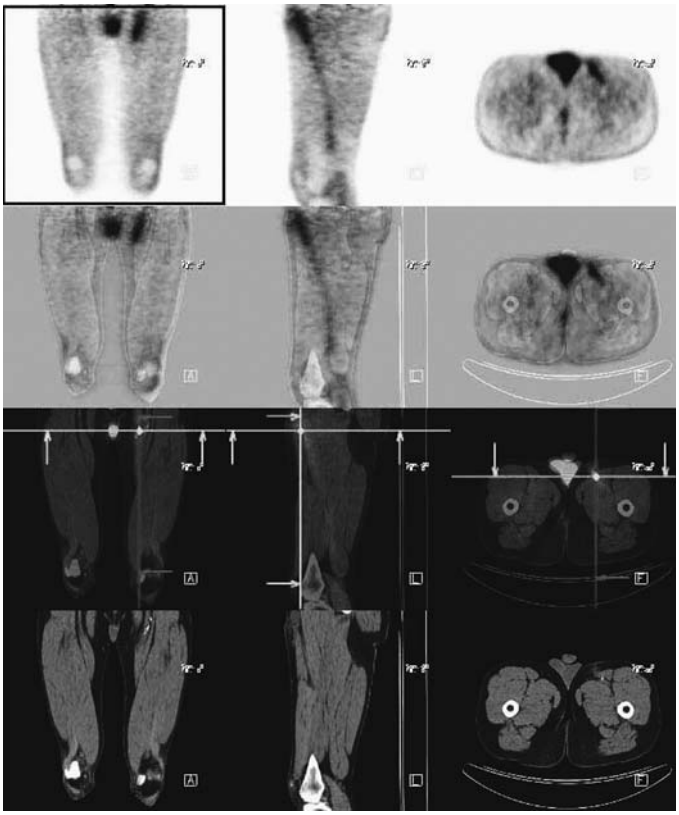

FIGURE 23.3.2.

Discussion

Schwannoma is a tumor that forms from a group of cells around the peripheral nerve fibers which normally produce the myelin sheath. The most common schwannoma is acoustic neuroma involving the eighth cranial nerve. Neurilemmoma and melanocytic

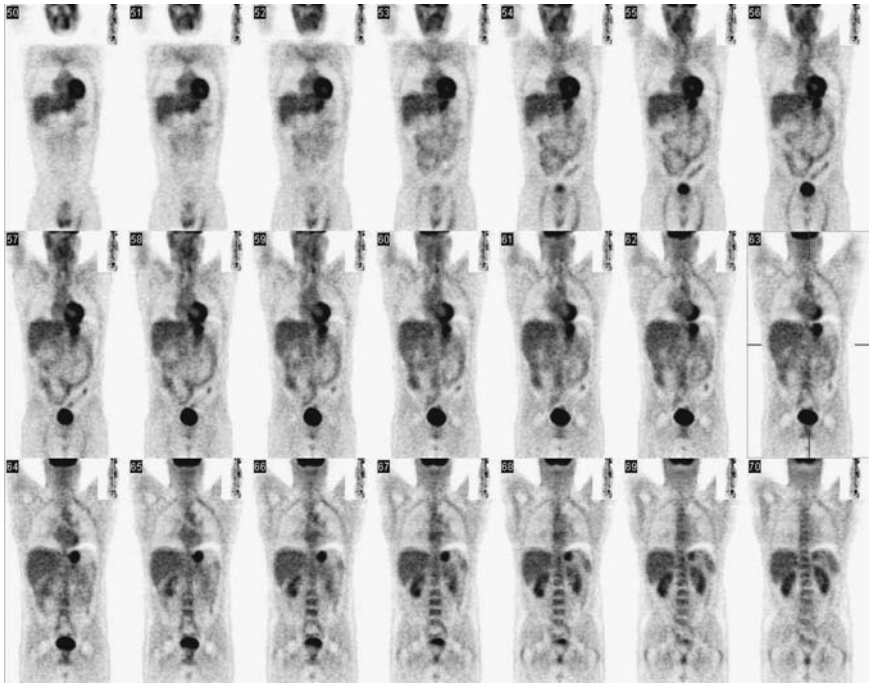

FIGURE 23.3.3.

schwannoma are benign tumors, as opposed to malignant peripheral nerve sheath tumor (MPNST) and malignant melanocytic schwannoma. CT is used to determine pulmonary metastases and hepatic involvement. MR is best to define the tumor and adjacent anatomic structures. The definitive diagnosis is biopsy. Staging is based on a GTNM (grading, tumor, node, metastases) system. Surgical resection is used for localized tumor and medical treatment with chemotherapy is generally reserved for high-grade tumor.

Case 23.4

History

32-year-old male presents with a left calf tumor. Evaluation for metabolic activity and metastatic disease is requested.

Findings

The torso study is negative other than notation of vocalis muscle activity at the vocal cord level. This is unusual as it is asymmetrical, right much more than left. However, the vocal cords appear normal by CT. If there were any symptoms referable to phonation, indirect laryngoscopy would be an appropriate consideration. The lower extremity images demonstrate an intensely hypermetabolic left calf lesion (*Figures 23.4.1 and 23.4.2*). This is much longer than it is around. It is adjacent to and parallel to the proximal to middiaphysis of the left fibula. The shape of the tumor is quite consistent with a tumor of peroneal nerve origin. The intense hypermetabolism does not imply malignancy, as benign neural tumors can be quite hypermetabolic by 18-FDG PET scintigraphy.

FIGURE 23.4.1.

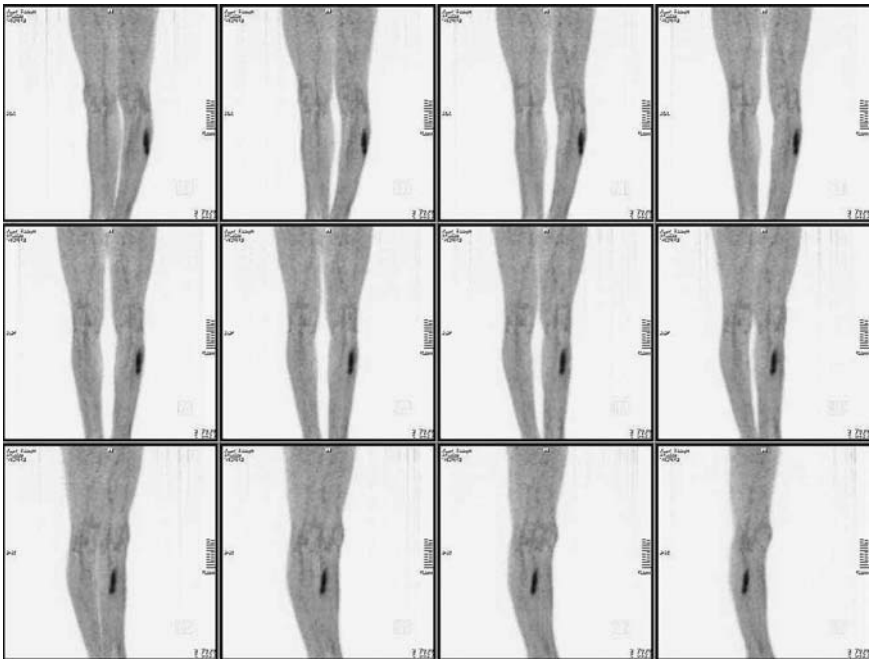

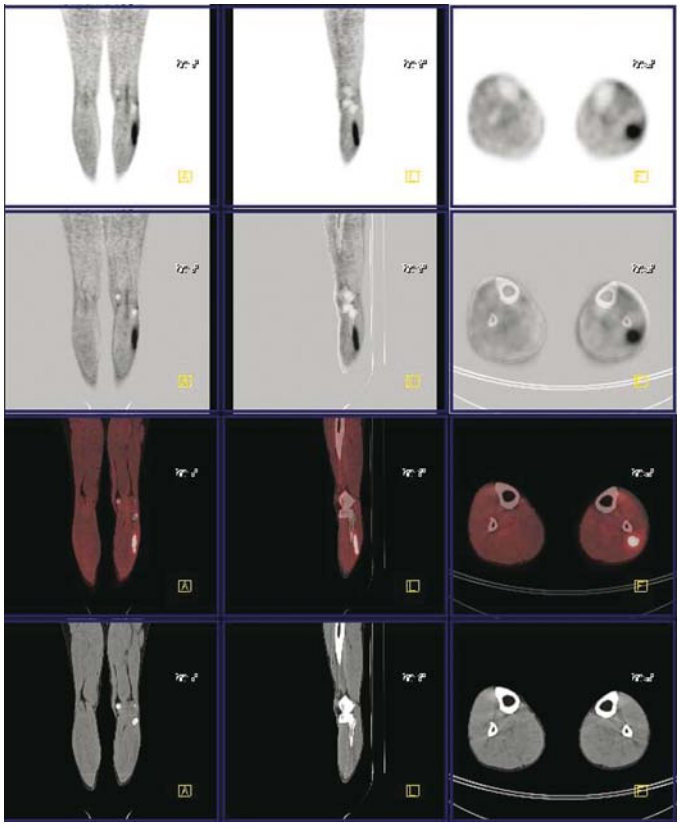

FIGURE 23.4.2.

Impression

1. The left calf tumor is intensely hypermetabolic and much longer than it is around. It parallels the fibula and is most likely a tumor of peroneal nerve origin. A benign tumor is likely even though the tumor is intensely hypermetabolic.
2. Negative torso study, other than notation of rather asymmetric vocalis activity at the vocal cord level.

24 Ovarian Cancer

Hossein Jadvar

Case 24.1

History

73-year-old female who has a history of ovarian cancer, who is also status post right gluteal resection for sarcoma. Her recent CA-125 is 71 and a new right iliac mass was found on the recent CT study. The patient is evaluated for extent of disease.

Findings

There is a moderately intense focus of hypermetabolism in the right gluteal soft tissue consistent with locally recurrent sarcoma (*Figures 24.1.1 and 24.1.2*). This corresponds with the recent enhanced CT clearly delineating the soft tissue density within the water density collection in the area of resection. The right psoas muscle is also hypermetabolically active (*Figure 24.1.3*) in the region of the common iliac vessels indicating metastases. The bladder is displaced by the feces-filled rectum and is extending to the right psoas area. The right colonic activity is prominent but probably physiologic. The tongue uptake is also probably physiologic. No other active lesions are noted above the diaphragm.

Impression

1. Interval multifocal gluteal recurrence consistent with the enhanced gluteal lesions on CT.
2. Interval appearance of bulky right psoas muscle metastasis consistent with mass on CT.

Pearls and Pitfalls

- *PET has the sensitivity of 80% to 90%, specificity of 92% to 100%, and accuracy of 79% to 92% for detecting recurrent ovarian tumor.*[2,6,7,8]
- *PET has the ability to change patient management by 40%.*

Discussion

A PET negative exam tends to have a longer relapse-free interval than a positive PET study. This patient has a recurrent tumor. Most authorities recommend a followup post chemotherapy in 6 months with imaging.

FIGURE 24.1.1.

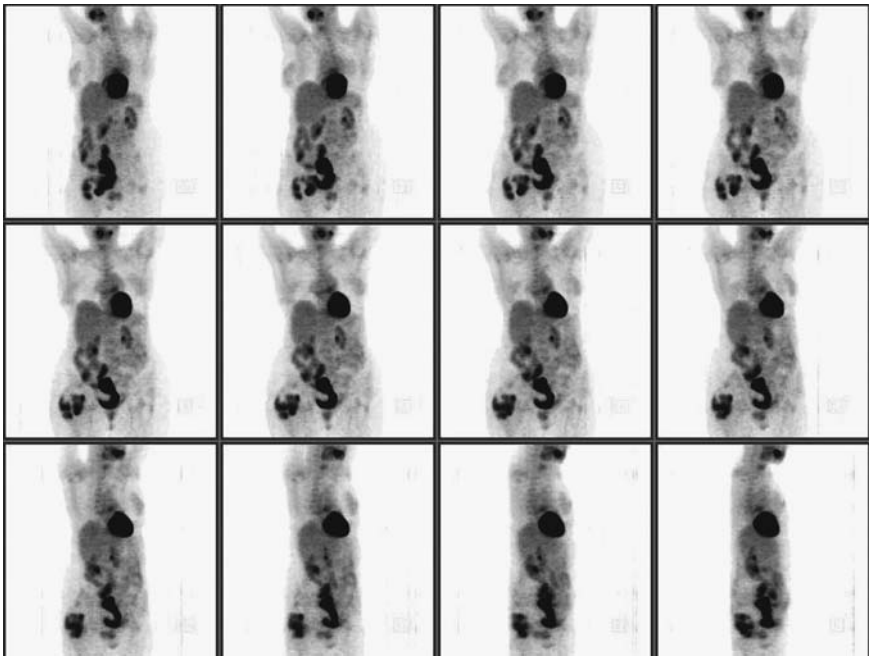

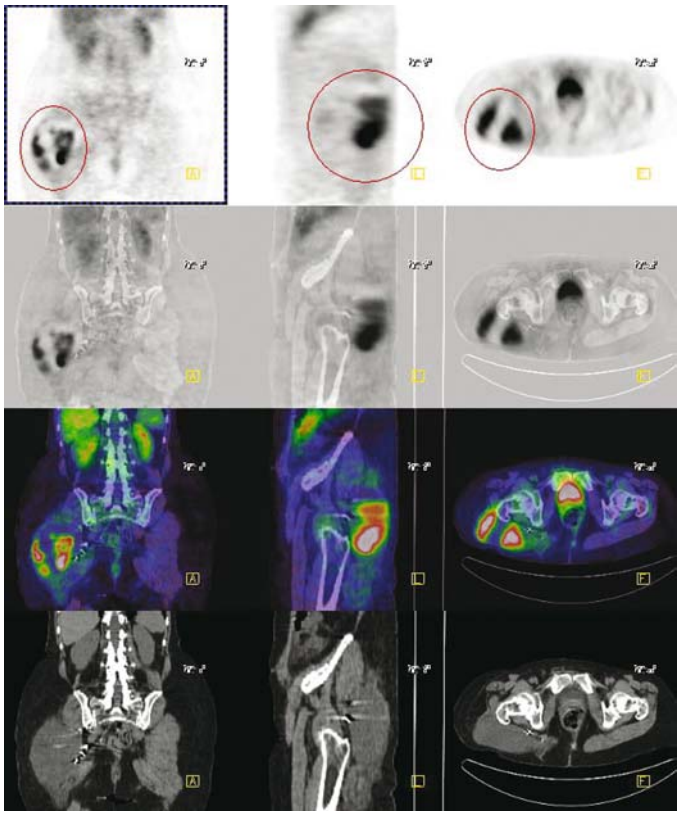

FIGURE 24.1.2.

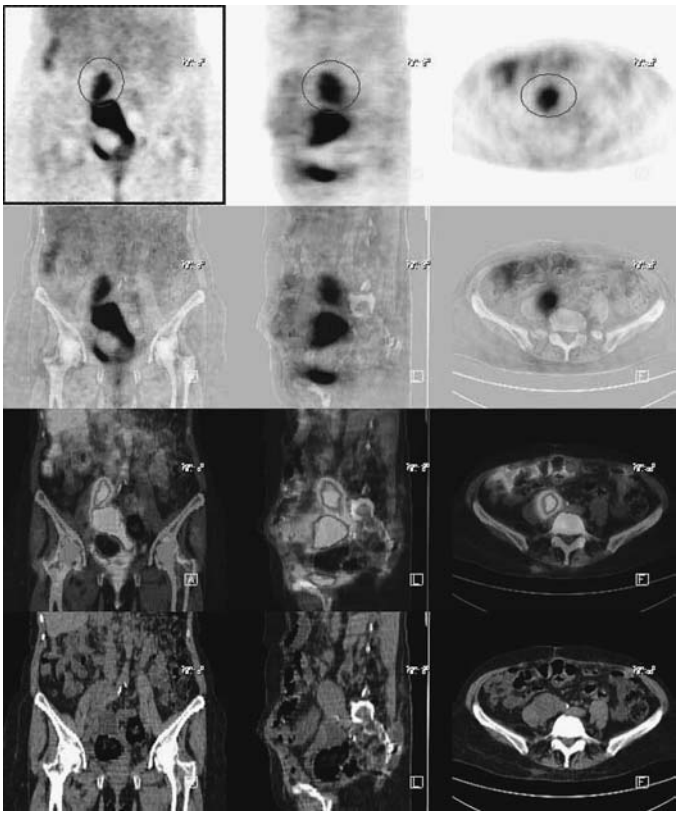

FIGURE 24.1.3.

Case 24.2

History

74-year-old female who has a history of ovarian cancer with elevated CA-125 at 2522. Patient underwent hysterectomy, bilateral salpingo-oophorectomy, and omentectomy. Pelvic washing was positive for cancer. She was treated with chemotherapy. Her last CT revealed some residual paraaortic adenopathy and a right pelvic lymphocele. Her most current CA-125 was 19. Evaluation for residual disease is requested.

Findings

There are multiple extensive sites of lymphadenopathy along the left para-aortic (*Figures 24.2.1 and 24.2.2*) and left iliac chains (*Figure 24.2.3*). Another intense focus of hypermetabolism is also noted in the left lower cervical node (*Figure 24.2.4*). These findings are consistent with metastasis. There is photopenia (*Figure 24.2.5*) in the right superior aspect of the bladder consistent with the right pelvic lymphocyst seen on the CT. The symmetric activity in the vocal cord (*Figure 24.2.6*) is physiologic. No other adenopathy seen above or below the diaphragm. Moderately intense tubular shaped uptake in the right abdomen may be related to either normal bowel uptake or metastatic serosal/omental tumor implants.

Impression

1. Evidence for distant metastasis in a lower cervical lymph node.
2. Extensive lymphadenopathy in the left para-aortic and left iliac chain.
3. Photopenic right lymphocyst as noted on CT.

Pearls and Pitfalls

- *PET has a sensitivity of 73%, specificity of 92%, and accuracy of 86% for detecting lymph node involvement.*[3,4]
- *The positive predictive value and negative predictive value are 89% and 86% respectively.*[1,3,4]
- *The sensitivity of CT for detecting lymph node involvement ranges from 40% to 63%; the specificity of CT for detecting the same ranges from 81% to 83%.*[1,3,4]

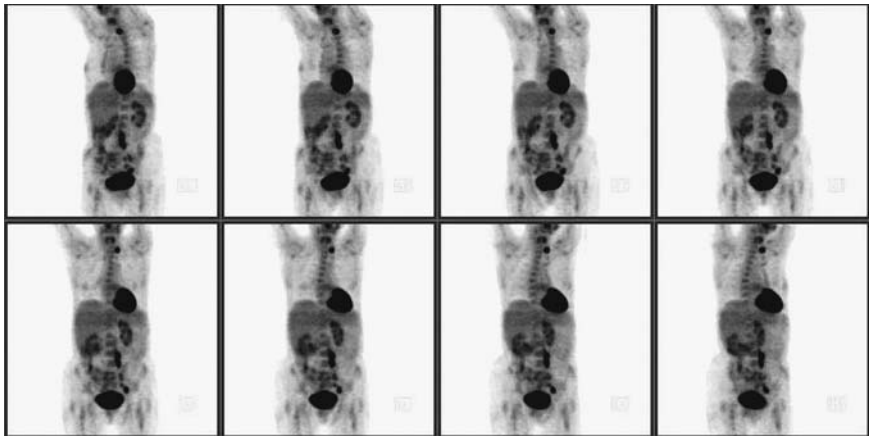

FIGURE 24.2.1.

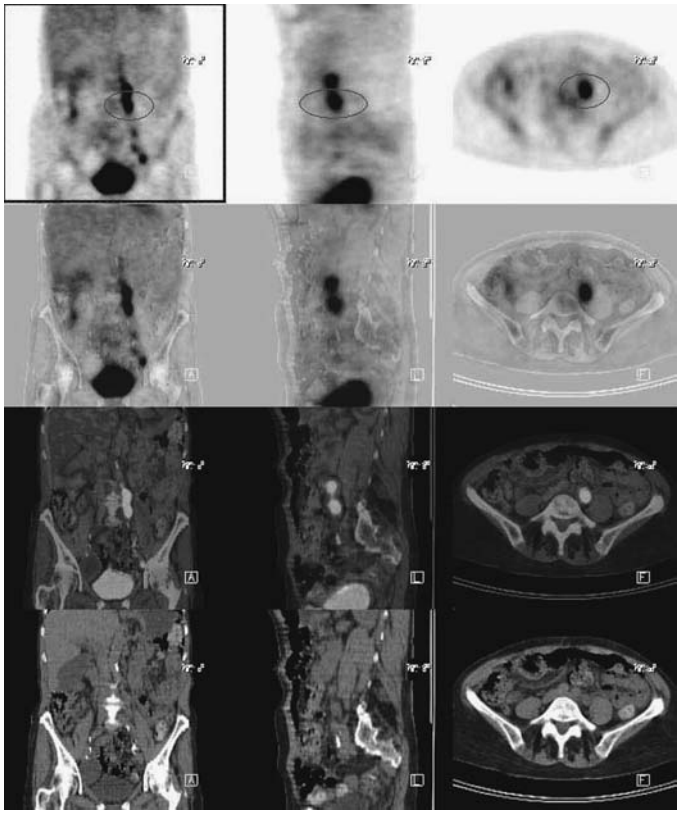

FIGURE 24.2.2.

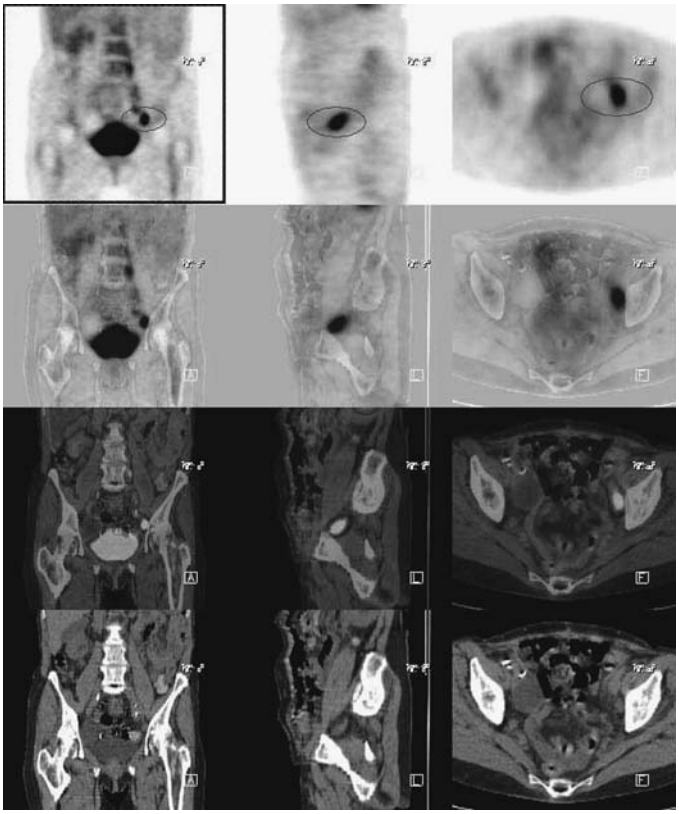

FIGURE 24.2.3.

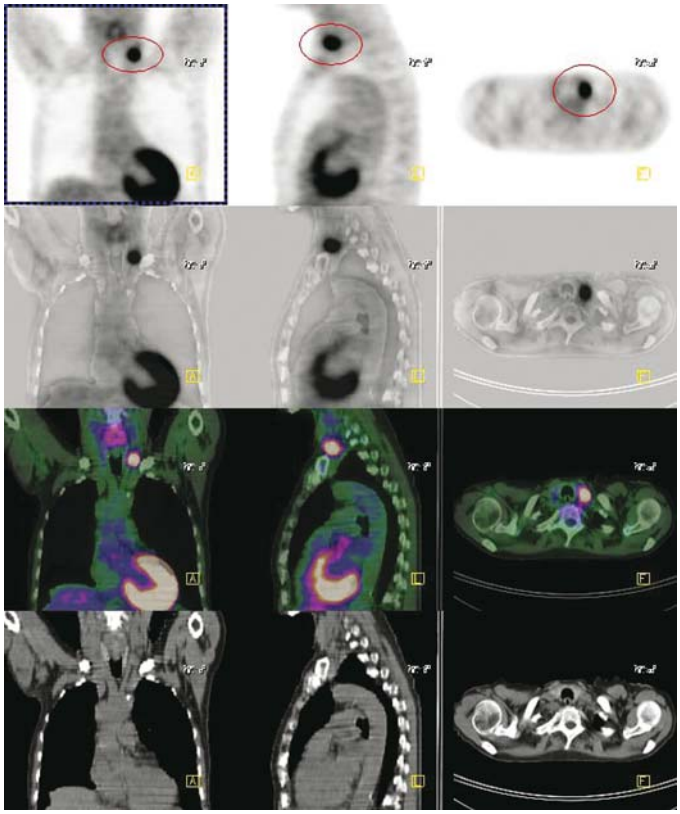

FIGURE 24.2.4.

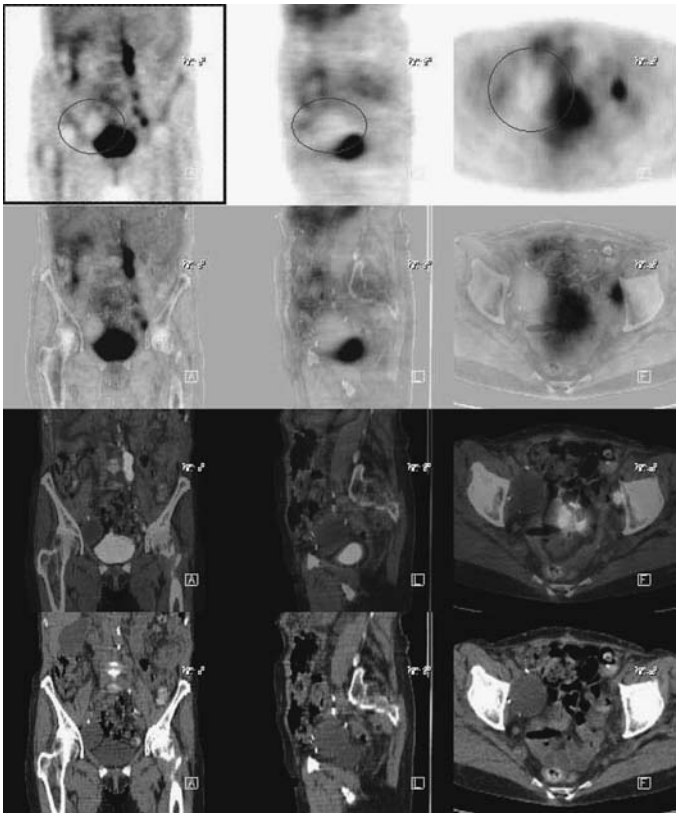

FIGURE 24.2.5.

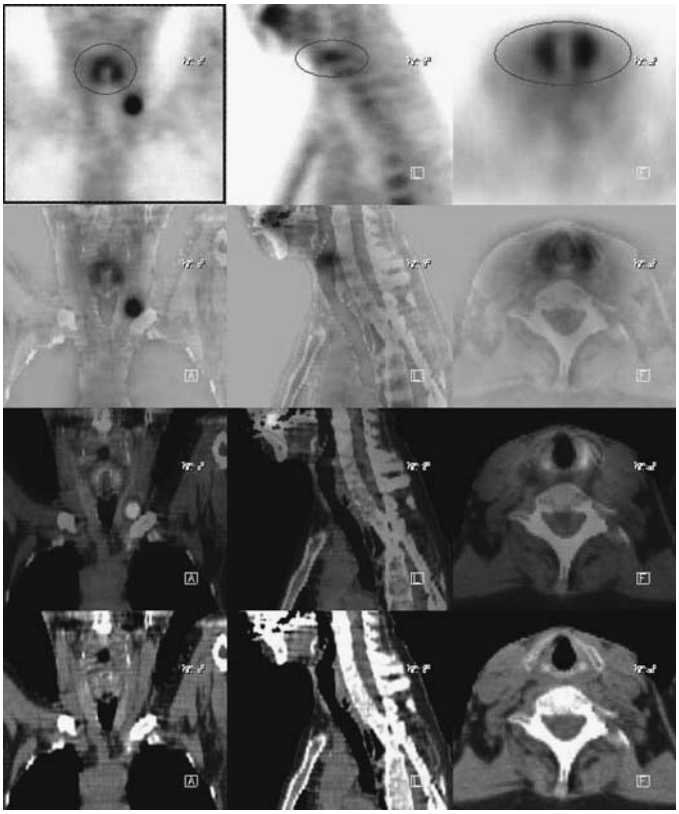

FIGURE 24.2.6.

Discussion

CA-125 is a serum marker to monitor recurrent tumor. The sensitivity of CA-125 is 90% to 100%. However, it can be falsely negative in 25% to 50% of the cases. Also, it does not provide the site of recurrence.

Case 24.3

History

69-year-old female who has a history of ovarian cancer currently on Cytoxan therapy. The patient is being evaluated for using CA-125 level and disease recurrence.

Findings

There are retroperitoneal (*Figures 24.3.1 and 24.3.2*), common iliac (*Figures 24.3.3 and 24.3.4*), and distal external iliac nodes. There is a left paracolic gutter peritoneal implant (*Figure 24.3.5*). There are multiple hypermetabolic liver metastases (*Figures 24.3.6 and 24.3.7*), some with calcification, indicating mucinous histology.

Impression

Metastatic mucinous ovarian carcinoma to the liver parenchyma, retroperitoneum, and peritoneum.

FIGURE 24.3.1.

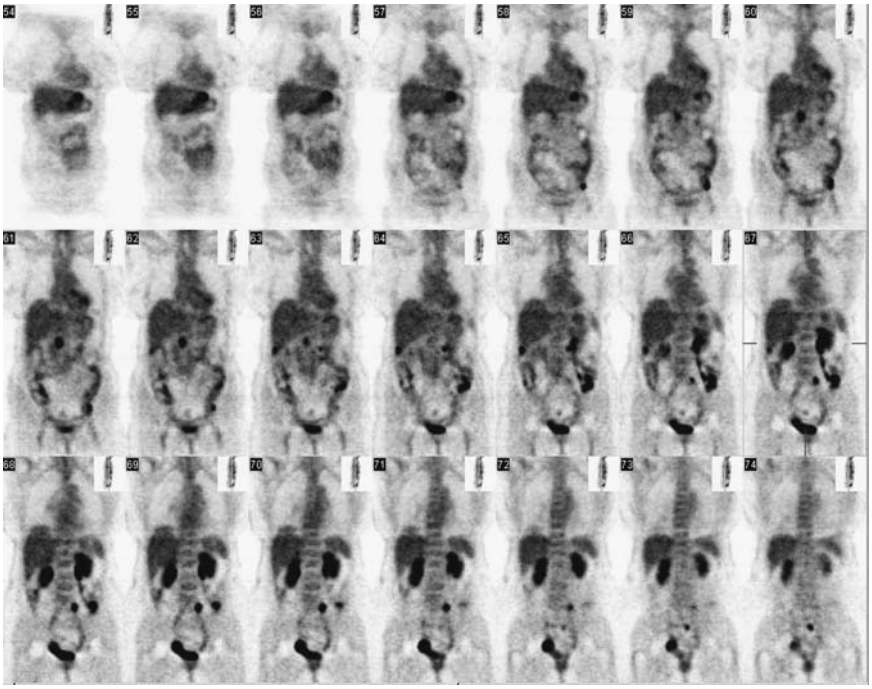

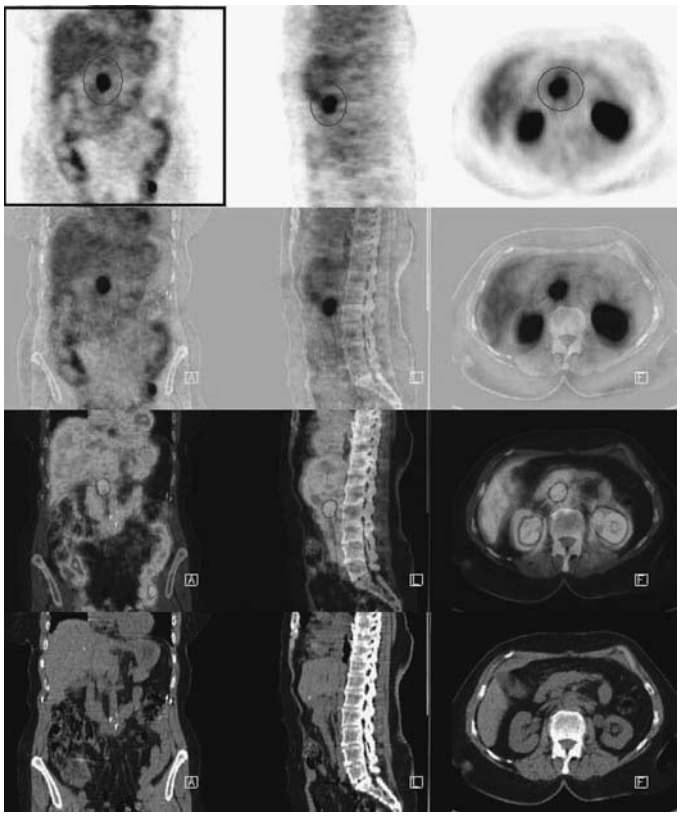

FIGURE 24.3.2.

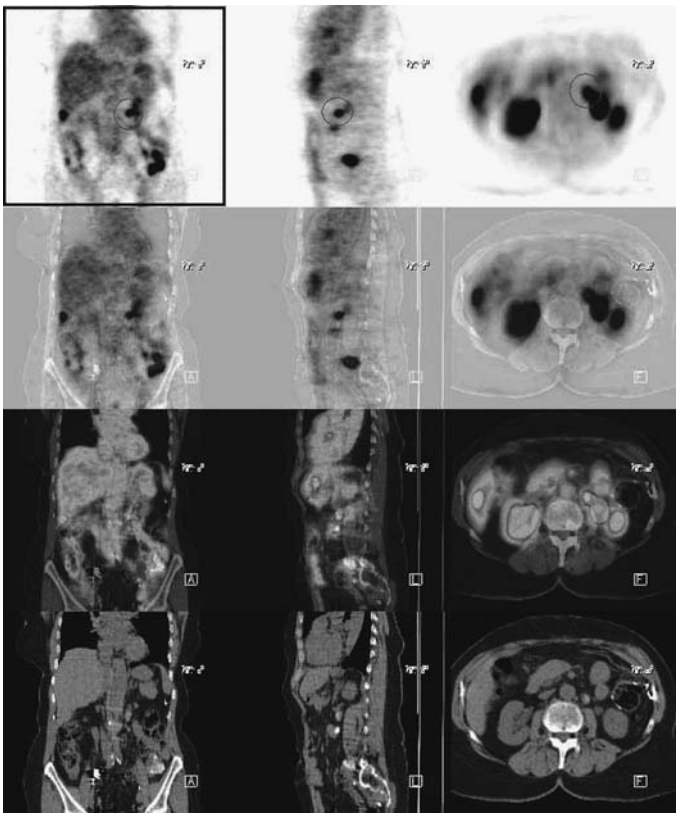

FIGURE 24.3.3.

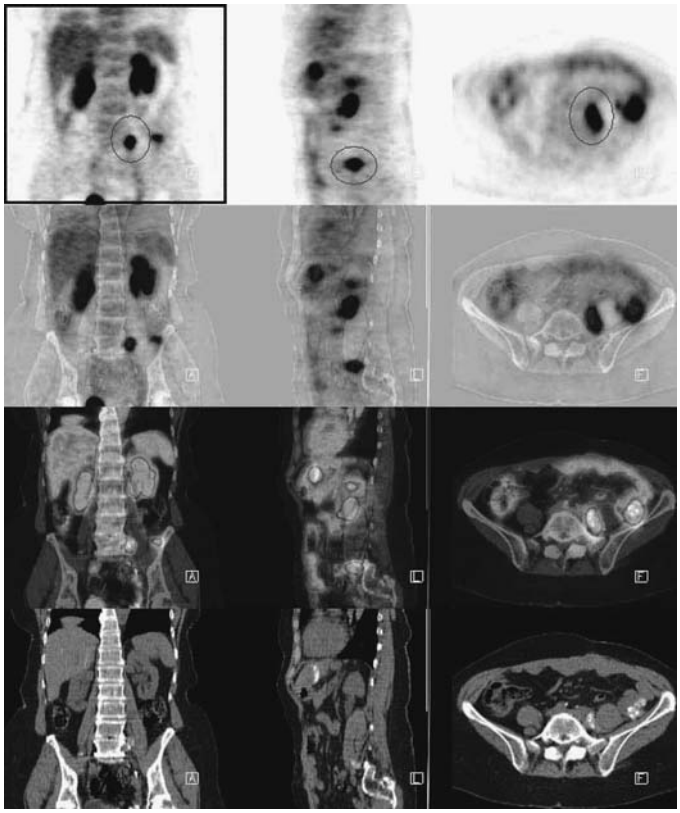

FIGURE 24.3.4.

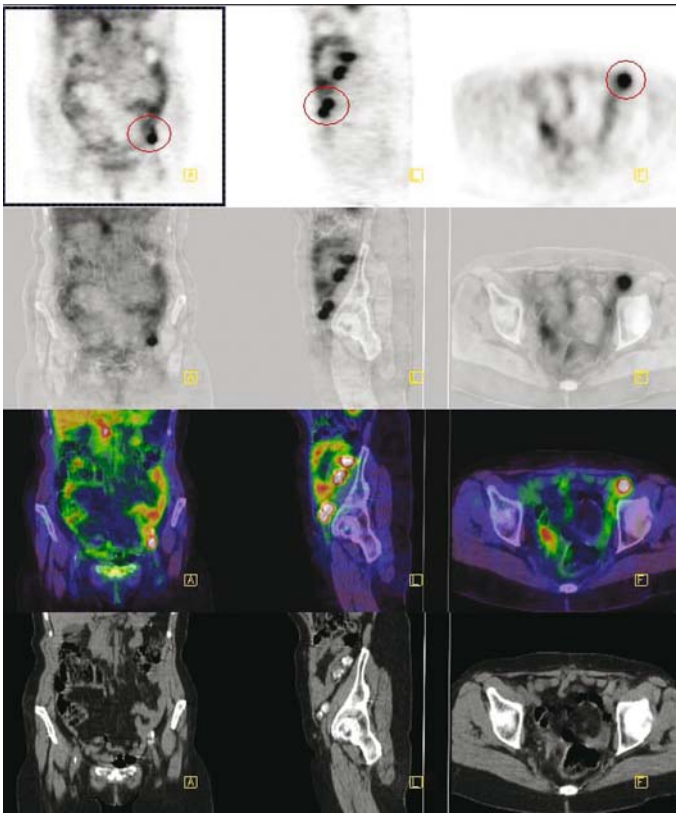

FIGURE 24.3.5.

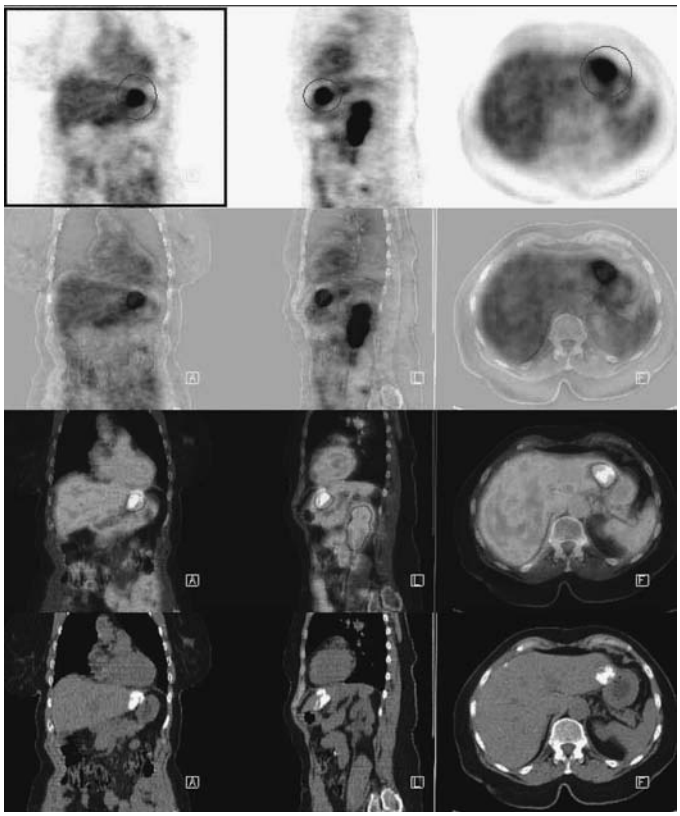

FIGURE 24.3.6.

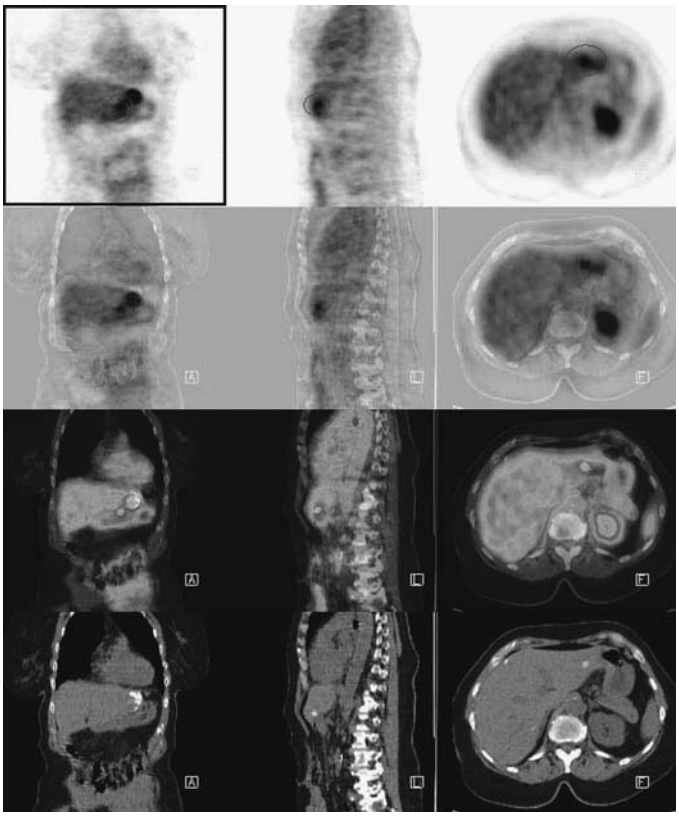

FIGURE 24.3.7.

Pearls and Pitfalls

- *FDG PET has a sensitivity of 71%, specificity of 100%, positive predictive value of 100%, negative predictive value of 76%, and an accuracy of 85% in the detection of peritoneal carcinomatosis.*[5]
- *Calcifying metastases is typical of mucinous cystadenocarcinoma histology.*

Discussion

Early detection of recurrent disease is a reliable indicator for a second-line therapy. PET can detect an intra-abdominal relapse with peritoneal carcinomatosis in 40% to 60% of the cases. Most recurrent ovarian carcinomas present with peritoneal seeding from para-arotic or peritoneal lymphatics. Unfortunately, false-positive examinations can occur with associated nonmalignancy physiology including inflammatory adnexal mass or corpus luteum. Urine activity can also potentially mask the lesions. Some institutions recommend the use of bladder lavage in order to minimize this artifact.

25 Pancreatic Cancer

Heidi R. Wassef

Case 25.1

History

47-year-old male with a history of pancreatic cancer and liver lesions on CT. The study is being done to evaluate extent of disease.

Findings

The breath hold CT chest images show some concave focal posterior pleural thickening on the right. No pleural fluid is apparent. No pathologic mediastinal adenopathy is evident. In the abdomen, there is increased metabolism in the body and tail of the pancreas (*Figure 25.1.1*), consistent with primary carcinoma of the body/tail of the pancreas (*Figure 25.1.2*). There are numerous hypermetabolic lesions within the hepatic parenchyma, panlobar (*Figure 25.1.3*). A disproportionate number of these small liver lesions are surface lesions. This is seen in conjunction with some moderate hyperactivity in the omentum. These features suggest that there is also peritoneal carcinomatosis.

Impression

Primary carcinoma of the body and tail of the pancreas with panlobar liver metastases and probable peritoneal carcinomatosis.

Pearls and Pitfalls

- *The role of PET imaging is to distinguish benign pancreatic masses from cancer, stage nodal involvement and liver metastasis, and assess patient response to chemotherapy.*[1,2,3,5]
- *It is estimated that PET can alter patient management in 50% of the patients with pancreatic carcinoma.*[1,2,3,5]

Discussion

Pancreatic cancer is the third most common gastrointestinal malignancy in the United States. It is the fifth leading cause of cancer-related mortality. Black, male, and age over

FIGURE 25.1.1.

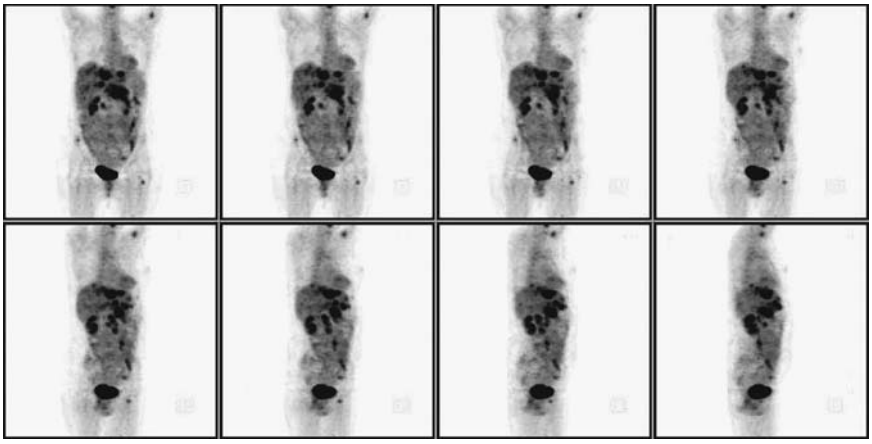

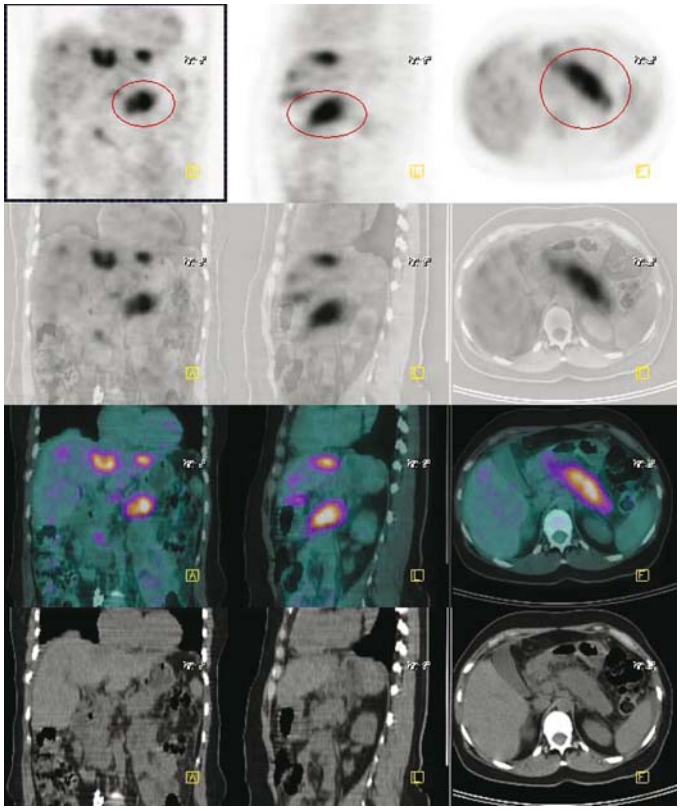

FIGURE 25.1.2.

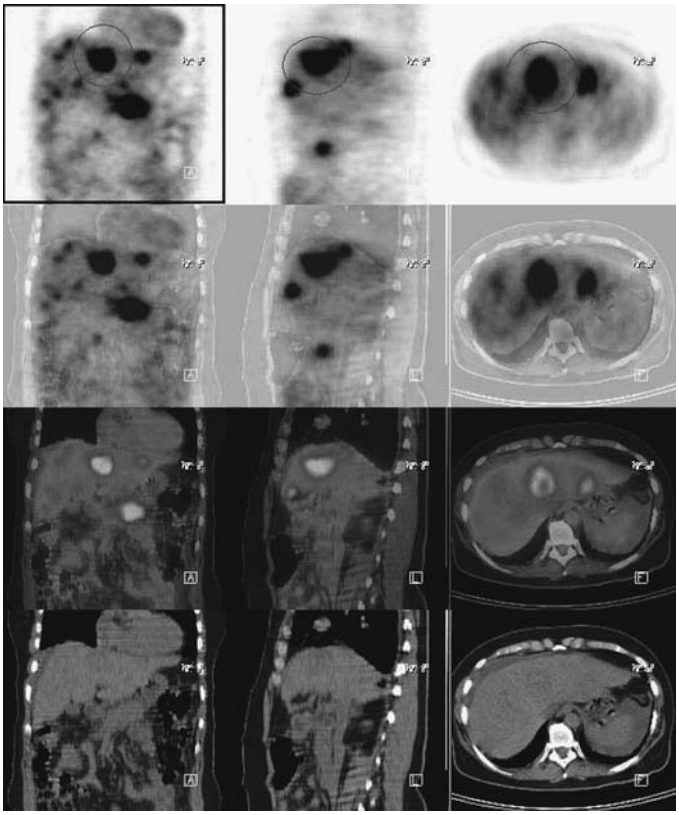

FIGURE 25.1.3.

45 are predispositing factors. Patients are asymptomatic. By the time symptomology surfaces, most patients are incurable. Midepigastric abdominal tenderness and weight loss are the most common symptoms. Smoking, alcohol, diabetes, chronic pancreatitis, and family history are all risk factors. Seventy-five percent of the cancers involve the head or neck of the pancreas. Approximately 95% of the pancreatic cancer arises from the exocrine portion. The tumor first spread to regional lymph nodes, then to the liver, and then to the lungs. CEA will be elevated in 40% to 45% and CA 19-9 will elevated in 75% to 85%. CT is useful, with 70% to 80% of lesions detected. Percutaneous ultrasound will detect 60% to 70% of the cancers. Endoscopic ultrasound and ERCP will detect 99% to 100% and 90% to 95% of the cases, respectively.

Case 25.2

History

82-year-old male who has a history of pancreatic cancer. His recent CT demonstrates fullness in the pancreatic head with bilateral suspicious cavitary pulmonary nodules. Evaluation for metastasis in the lung is requested.

Findings

There is a hypermetabolic focus on PET which corresponds to the fullness in the pancreatic head (*Figures 25.2.1 and 25.2.2*) previously described on CT. This appears to

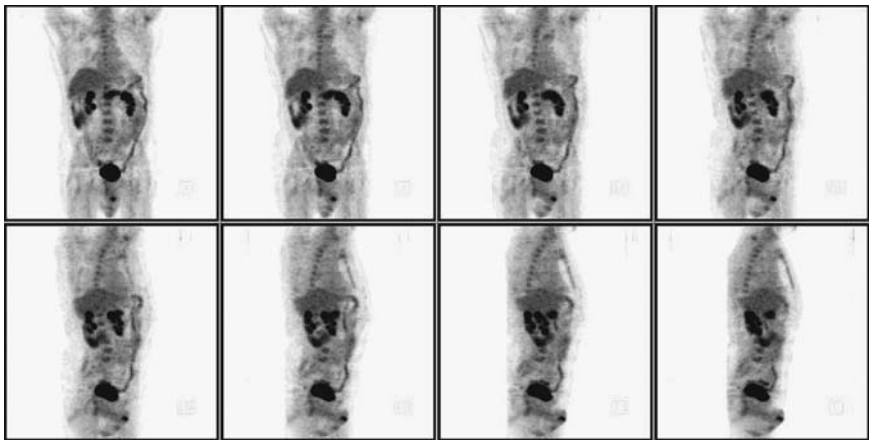

FIGURE 25.2.1.

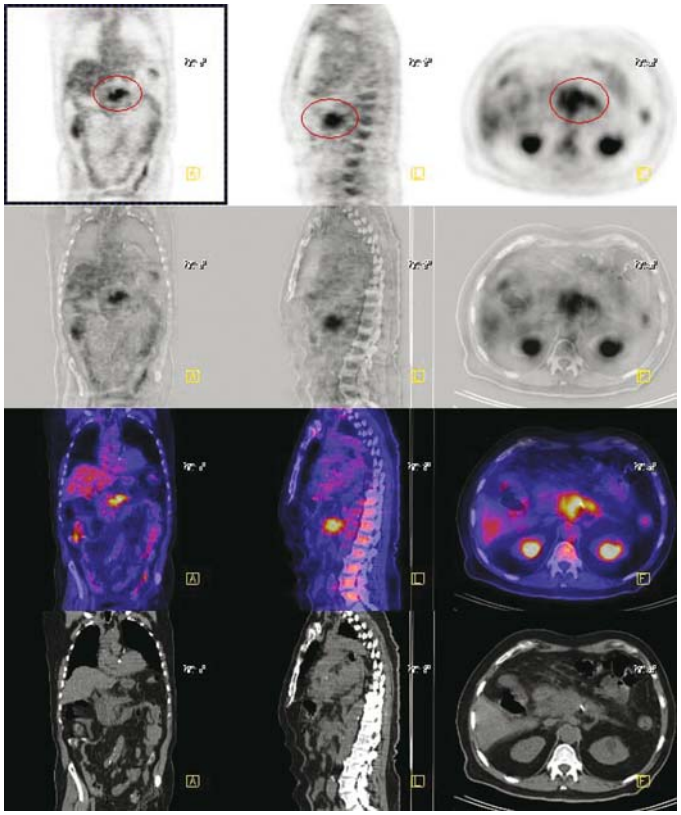

FIGURE 25.2.2.

extend into the tail of the pancreas. The nonrandom clusters and smooth wall pulmonary nodules on CT are metabolically negative on PET and are probably inflammatory rather than neoplastic. The weakly positive activity in the right perihilar node, or medial midlung parenchyma, is probably inflammatory. The retention in the upper pole of the collecting system is due to urinary stasis. The curvilinear activity in the bowel is physiologic.

Impression

1. Hypermetabolic focus in the region of the pancreatic head consistent with history of pancreatic malignancy.
2. The nodules in the lung are not FDG avid and therefore are considered non-neoplastic.

Pearls and Pitfalls

- *Pancreatic cancer displays a higher expression of glucose transporter 1 (Glut-1) vs. glucose transporter 4 (Glut-4) in comparison to chronic mass-forming pancreatitis.*[4]
- *The overall sensitivity and specificity for pancreatic cancer by SUV analysis is 94% and 88%, respectively.*[1,2,3,5]
- *When using the SUV cutoff criteria of 1.53, PET has a better sensitivity and specificity than CT for detecting cancer, 93% PET sensitivity as opposed to 80% CT sensitivity, and 93% PET specificity as opposed to 74% CT specificity.*[1,2,3,5]
- *Chronic active pancreatitis and serous cystadenoma are common causes for false-positive PET results.*
- *PET helps accurately stage the disease, making it helpful in planning the appropriate therapy.*[1,2,3,5]

Discussion

Histologically, 80% of the pancreatic cancers are adenocarcinomas. Staging is based on a TNM staging system. At initial presentation, 20% of the patients are in stage I, 40% are in stage II, and 40% are in stage III and IV. Whipple pancreaticoduodenectomy is usually performed. 5FU and gemcitabine may improve overall survival. Palliative therapy is usually employed for analgesia. The overall 5-year survival rate is less than 5%. In patients who are fortunate enough to have a successful curative resection, the 5-year survival rate is 15% to 20%.

Case 25.3

History

64-year-old female with a history of pancreatic cancer ten years ago, status post Whipple procedure. There is a history of thyroidectomy for thyroid cancer eight years ago. The current study is being done to evaluate for recurrence.

Findings

There is focal hypermetabolism in the neck (*Figure 25.3.1*). The focal hypermetabolism is midline and retrotracheal in location (*Figure 25.3.2*), centered 2 cm below the

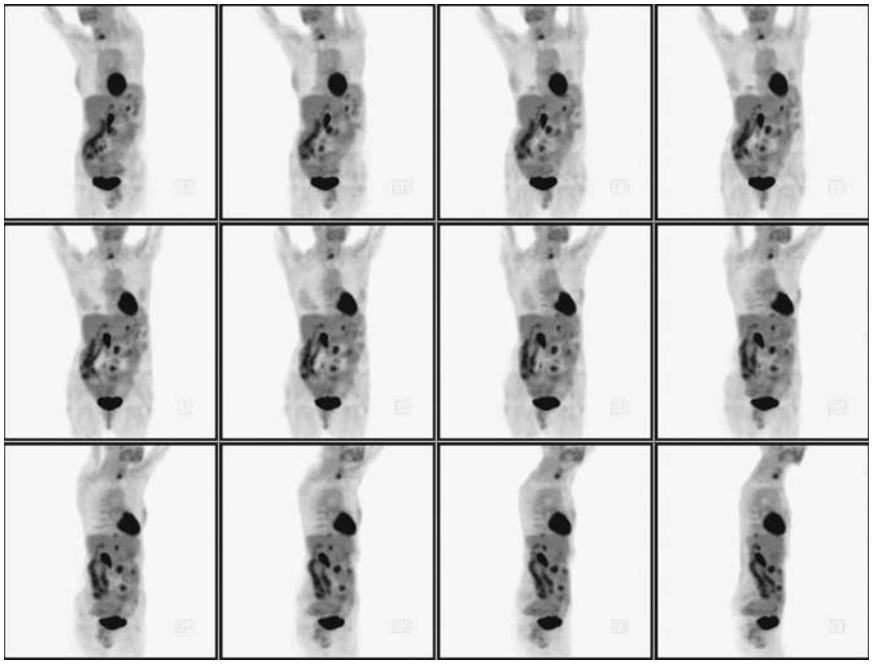

FIGURE 25.3.1.

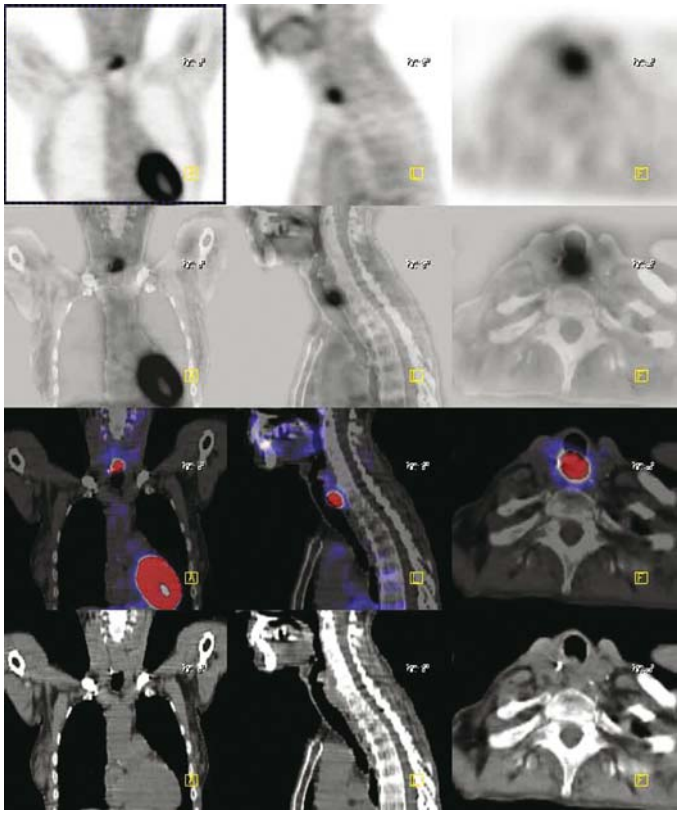

FIGURE 25.3.2.

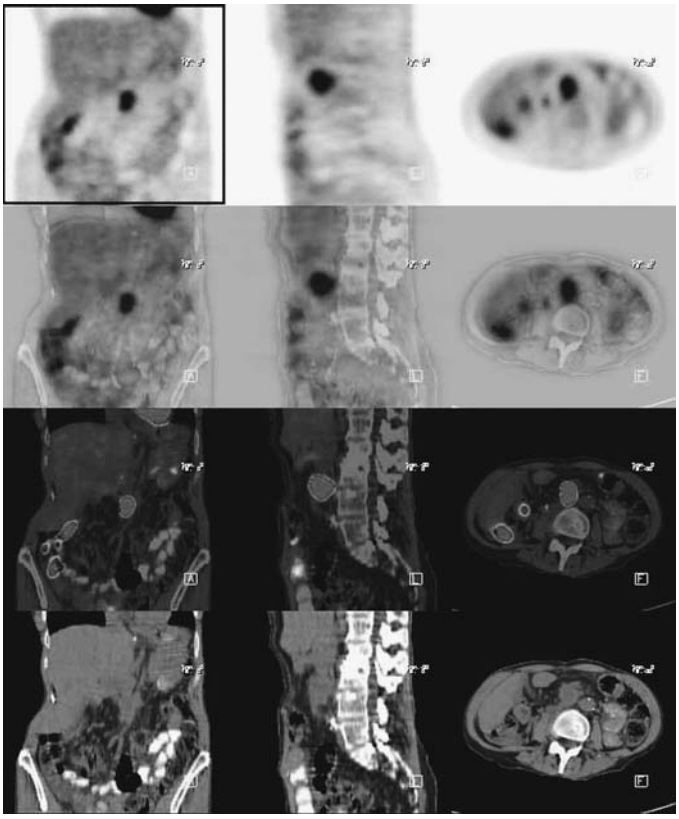

FIGURE 25.3.3.

FIGURE 25.3.4.

vocal cord and centered at the level of the only surgical clip right of midline. This may represent metastatic disease or recurrent thyroid carcinoma. An elevated thyroglobulin would favor the latter.

There is intense focal hypermetabolism of the 3-cm mass at the root of the mesentery (*Figures 25.3.3 and 25.3.4*), which was shown to be heterogeneously enhancing on prior CT. This is consistent with recurrent pancreatic carcinoma by location but unusual in time frame from diagnosis. It is potentially approachable by percutaneous biopsy.

No abnormal hypermetabolism is evident in the chest. There is no increase in activity related to the fibrotic changes in the pulmonary apices.

Impression

1. Single midline, approximately 1-cm retrotracheal cervical focus, corresponding to increased retrotracheal soft tissues, centered at the level of the only rightsided surgical clip. This could be due to recurrent thyroid carcinoma or metastatic disease.
2. Intensely hypermetabolic 3-cm mesenteric root mass consistent with recurrent pancreatic cancer.

Pearls and Pitfalls

- *FDG PET cannot be used to differentiate types of cancer although the level of uptake may correlate with tumor grade in certain types of malignancies.*

Discussion

FDG PET is useful in staging and determination of resectability of pancreatic masses at the time of initial diagnosis as well as in reevaluation of patients after therapy and differentiating malignancy from chronic pancreatitis.

26 Prostate Cancer

Hossein Jadvar

Case 26.1

History

50-year-old male who is being evaluated because of a prevertebral soft tissue mass at T-9 on CT.

Findings

The intense 18-FDG activity at T-9 is seen on the sagittal images to involve both the prevertebral soft tissues and the vertebral body at T-9 (*Figure 26.1.1*). There is no osteolysis and slight medullary sclerosis of this vertebral body. This appears on 18-FDG to be only one of many randomly scattered pathologically intense osseous foci (*Figures 26.1.2 and 26.1.3*). There is a small focus in the left ischium, involvement of the right subtrochanteric femoral medullary cavity (*Figure 26.1.4*), a small focus in the right anterior superior ilium, abnormal activity in the right proximal humeral diaphyses (*Figure 26.1.5*), and a possible small lesion near the right AC joint. Each of these lesions is characterized by slight sclerosis without osteolysis. The multiplicity of the lesions is indicative of likelihood for metastatic disease of unknown primary. Pertinent to this is the intense hypermetabolism in the posterior midline prostate gland (*Figure 26.1.6*). If this proves to be prostate carcinoma with osseous metastasis at presentation, it would appear to represent an aggressive prostate lesion. Serum PSA is recommended as a first initial step with subsequent prostate biopsy if positive.

Impression

The T-9 prevertebral soft tissue appears to represent coexistent involvement of the T-9 vertebral body as one of several scattered osseous metastases with slight sclerosis. There is an intense midline posterior lobe prostate activity, consistent with an aggressive primary prostate carcinoma. Other diagnoses such as myeloma and lymphoma are considered less likely.

Pearls and Pitfalls

- *80% of expired prostate cancer patients have osseous metastases.*
- *The sensitivity of PET for prostate cancer is 50%.*[1]
- *PET has a detection rate of 18% to 65% for metastatic disease.*[1]

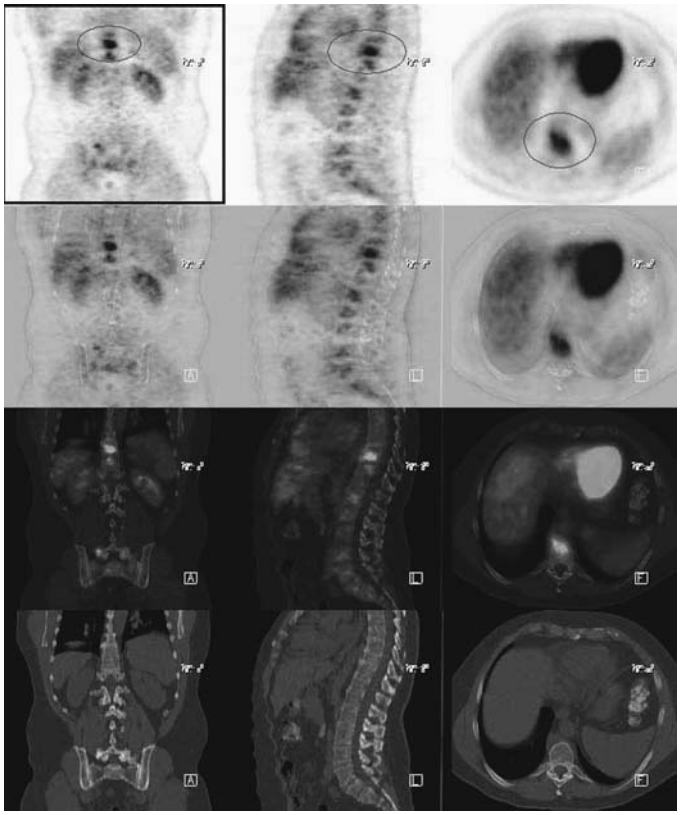

FIGURE 26.1.1.

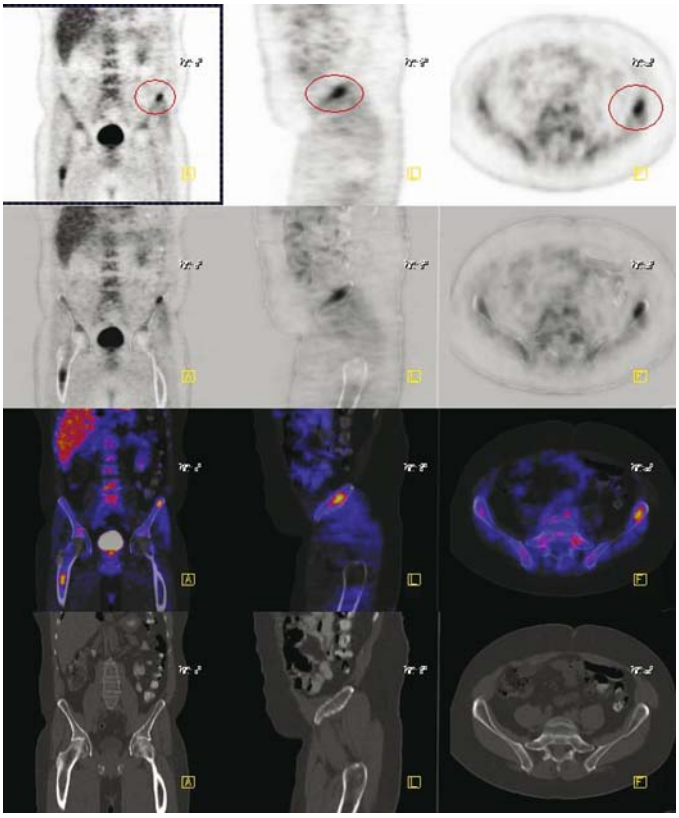

FIGURE 26.1.2.

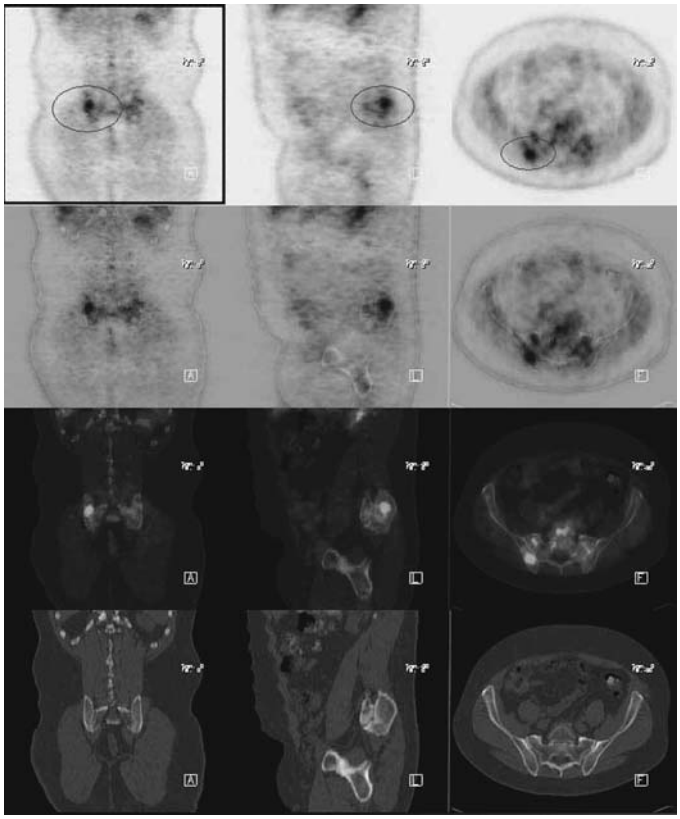

FIGURE 26.1.3.

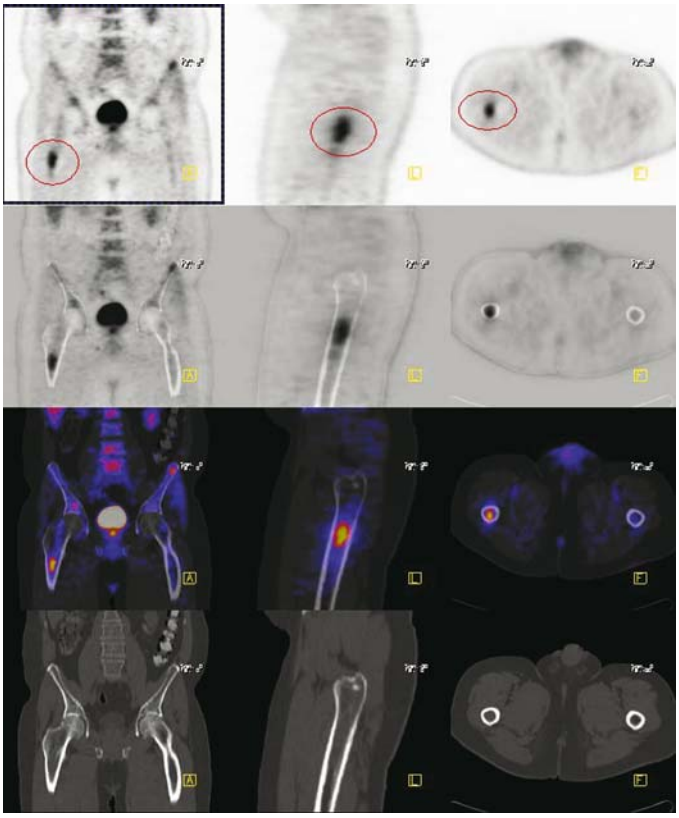

FIGURE 26.1.4.

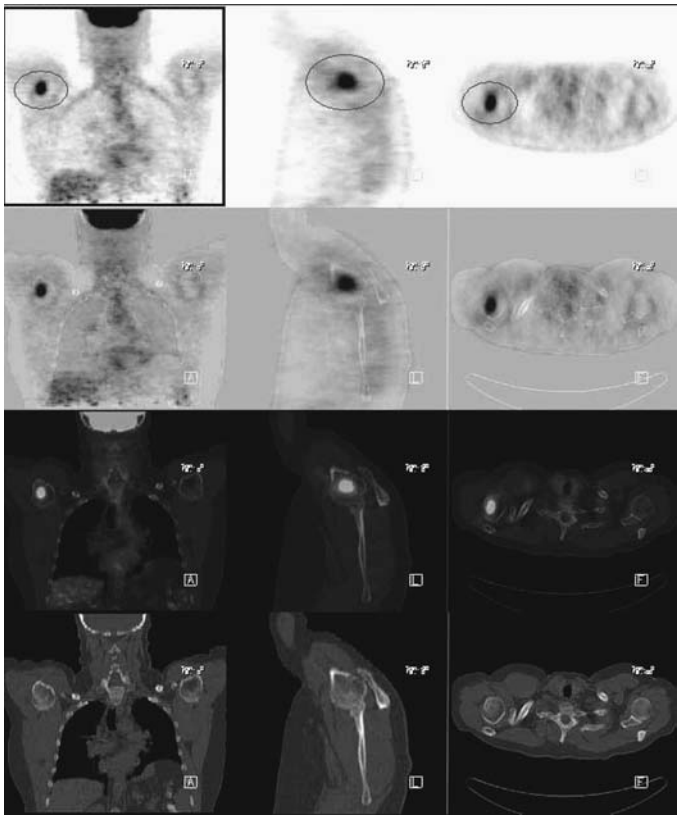

FIGURE 26.1.5.

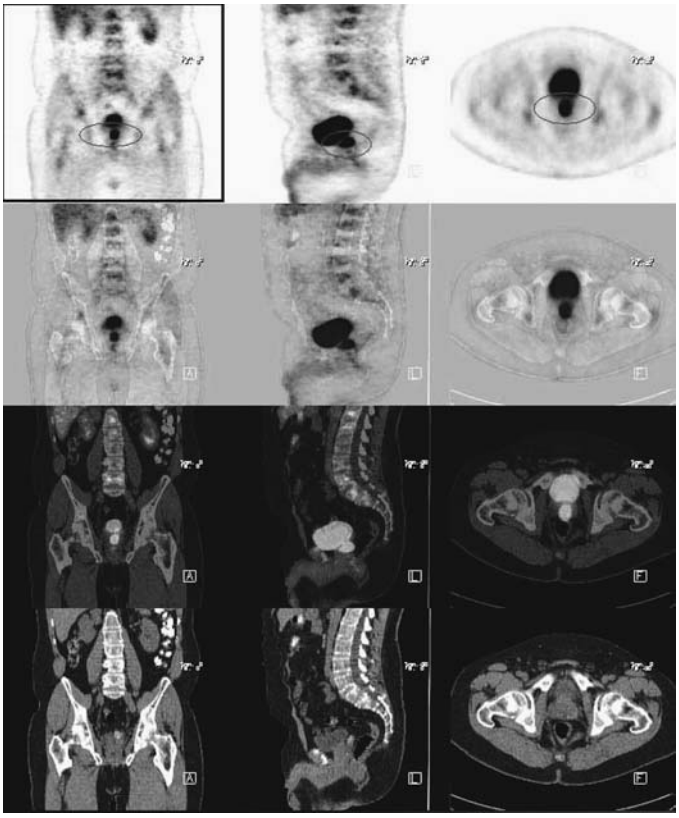

FIGURE 26.1.6.

- *PET imaging is a valuable tool for identifying lymph node metastases since it is a whole body exam.*
- *PET is currently useful in monitoring patient response to treatment for prostate cancer in patients with positive baseline examinations.*[3]

Discussion

A problem with FDG imaging is that it does not accumulate well in some prostate cancers presumably due to a low glucose metabolic rate. Another problem with the tracer is that it is excreted in the urine which will potentially mask lesions in the vicinity of the prostate.

^{11}C-choline may provide an alternative way for prostate cancer imaging. Choline is an important component of phospholipids in cell membrane integrity. Most prostate cancer display a high proliferation rate and increases production of cellular components for choline uptake. Choline may be superior than FDG because it does not accumulate in urine. The sensitivity of ^{11}C-choline PET and conventional imaging is 80% vs. 47%, in histologically proven cases. The specificity is 96% vs. 98% and accuracy 93% vs. 86%, respectively. Micrometastases and bowel activity are common reasons for a false-negative exam.

^{11}C-acetate also may be useful in the detection of recurrent prostate cancer. It can accumulate in prostate cancer and has a sensitivity higher than that of FDG. A problem with this agent is that it can also accumulate in normal prostate gland and benign prostate hyperplasia. This may lower the specificity of this exam.

27 ^{18}F Fluoride Bone Scintigraphy

Peter S. Conti

Case 27.1A

History

37-year-old male with a history of osteosarcoma of the left upper maxilla status post resection followed by radiation and chemotherapy. The patient had recurrence in the L-4 vertebra and was treated with chemotherapy. Outside bone scan revealed abnormal uptake at L-4 and left mastoid.

Findings

On the FDG PET scan there is a large hypermetabolic sclerotic lesion in the vertebral body of L-4 with an expansile mass beyond the vertebral body and a soft tissue component on the left side with extensive calcification consistent with high-grade sarcoma (*Figures 27.1A.1, 27.1A.2, and 27.1A.3*). There are sclerotic lesions involving the left posterior iliac bone, right iliac wing, sacrum, and multiple lesions in T-9, T-10, and T-11 (*Figure 27.1A.4*). There are additional sclerotic lesions throughout the cervical, thoracic, and lumbar spine, too small to characterize but hypermetabolic in the PET scan. There are small sclerotic foci in the left sternomanubrial joint and right third rib posteriorly. There is asymmetry in the soft tissue in the right groin, possibly due to a small lymph node. The tiny nodules in both lungs are not metabolically active and may be below the resolution of the scanner. There is a large area of photopenia in the left

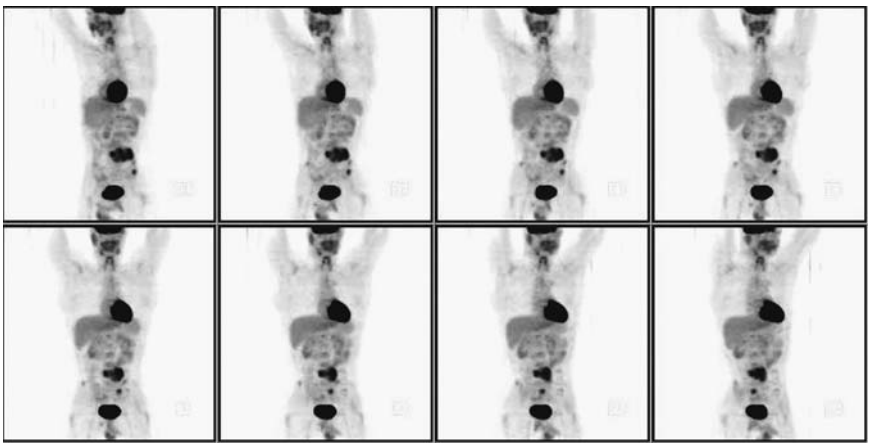

FIGURE 27.1A.1.

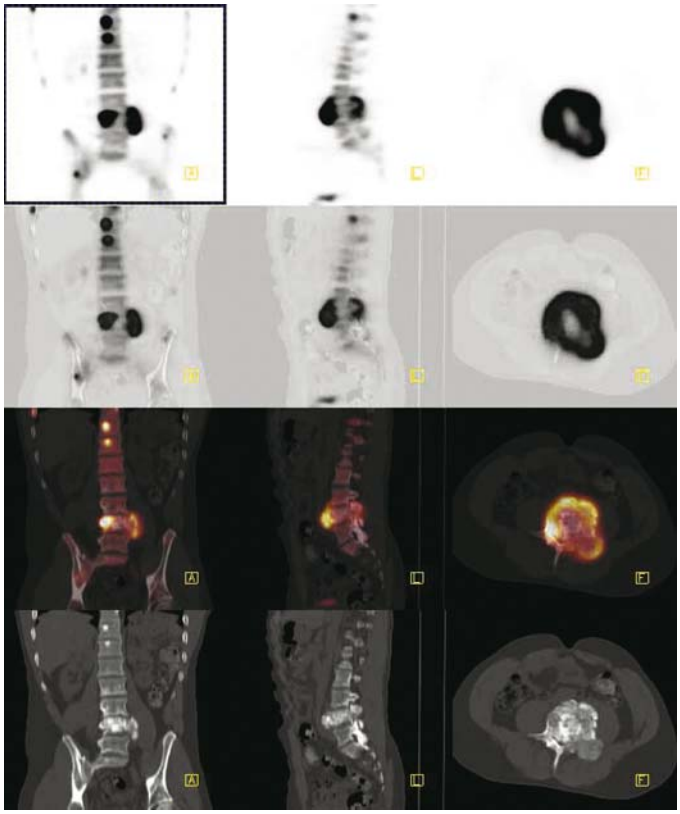

FIGURE 27.1A.2.

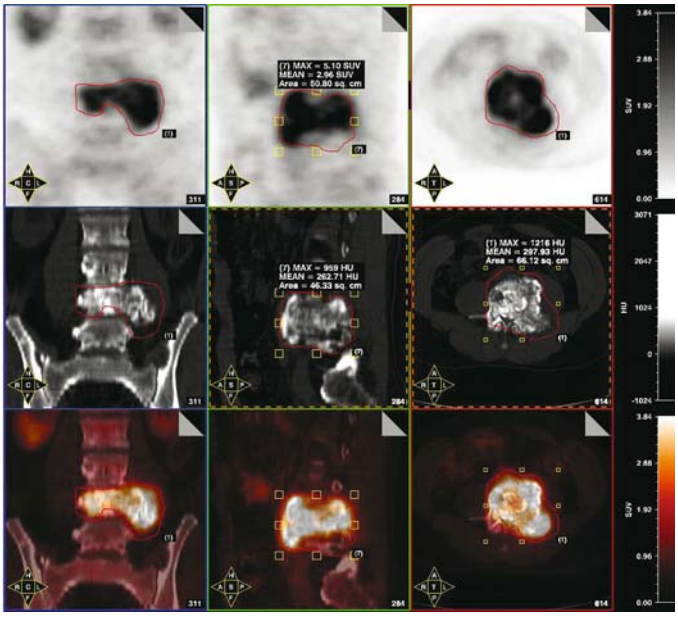

FIGURE 27.1A.3.

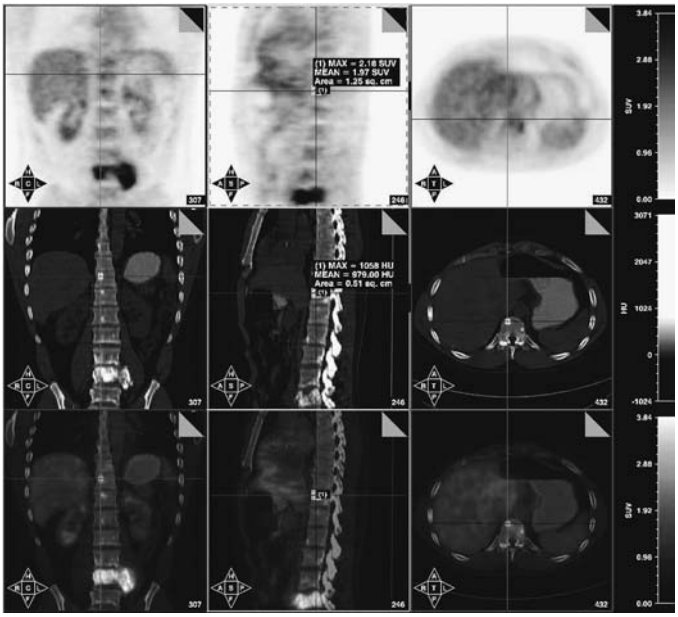

FIGURE 27.1A.4.

maxilla compatible with the surgical defect. Low-level uptake is seen lateral to the surgical margin with no focal increase in tracer activity suggestive of post treatment changes rather than recurrence. There is no discrete focus of regional adenopathy in the neck.

Impression

1. Evidence of extensive metastases to the skeleton and possibly the right groin and lungs.
2. Large surgical defect in the left maxilla without definite evidence of local recurrence or pathologic adenopathy in the neck.

Case 27.1B

History

37-year-old female with a history of osteosarcoma in the left maxilla status post resection with recurrence in L-4 vertebra follow by chemotherapy. Her previous FDG PET scan is abnormal, and this study is being done with 18-F fluoride bone scintilligraphy to evaluate response extent of bony disease and treatment.

Findings

There is bony uptake with some thickening in the right maxilla with little activity in the posterior maxillary anthrum probably associated with small osteitis or maxillary infection (*Figure 27.1B.1*). Evidence of postsurgical maxillary remnant is seen in the left maxillary region. There are foci of increased radiotracer uptake involving the left scapula proximal to the glenoid, right glenoid, left side of the manubrium, right fourth or fifth costocartilaginous junction, anterior left midrib, right ninth lateral rib, left posterolateral sixth rib, left second costovertebral junction, left fifth costovertebral junction, right eighth costovertebral junction, and left T-11 costovertebral junction. Increased tracer activity is seen in the vertebral bodies of T-7, T-9, T-11, L-1, L-4, and the coccyx. There is increased radiotracer uptake involving the right iliac wing, right acetabulum, inferior left sacroiliac joint, and left medial iliac crest. There are degenerative changes around the right knee joint with some remodeling of the bone. There is no evidence of metastasis in the lower extremities.

Impression

1. Evidence of extensive and progressive bony metastases, suggesting poor response to chemotherapy.

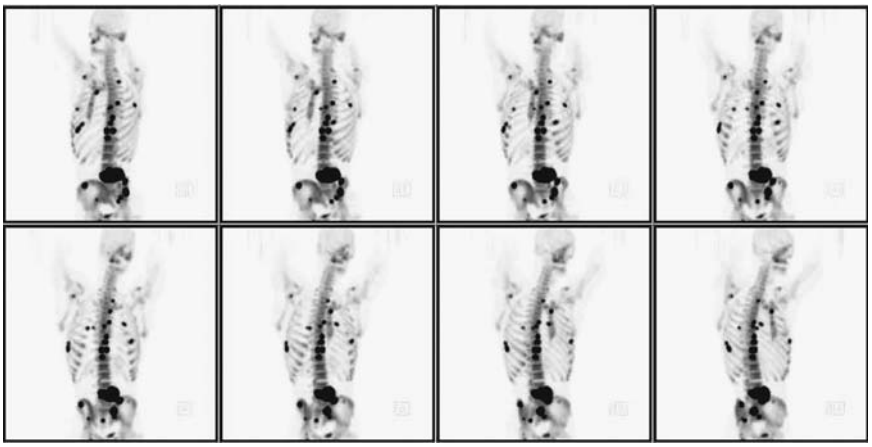

FIGURE 27.1B.1.

2. Probable osteitis or sinus infection in the right maxillary region.
3. Postsurgical changes in the left maxilla.
4. Degenerative changes in the right knee.

Pearls and Pitfalls

- *^{18}F Fluoride PET can quantitatively estimates metabolic activity in bone.*[2]
- *Fluoride studies can reduce the number of invasive bone biopsies and facilitate subsequent follow up in patients with metabolic bone diseases.*
- *Very early bone reaction in small bone metastases can be seen with F-18 fluoride scintigraphy.*[1]

Discussion

[^{18}F] flouride bone scintigraphy with PET offers a high resolution, quantitative alternative to planar and SPECT scintigraphy with Tc–99m based radiotracers. Images are generally acquired 2 hours following injection of radiotracer, and no pre-injection fasting is required by the patient. Correlation with the companion CT acquisition allows for precise registration of abnormal activity with bony structures.

References

Chapter 2 Adrenal Cancer

1. Lawson MA. Role of molecular imaging in management of nonhypersecreting adrenal masses. J Nucl Med 2001;42:893–894.
2. Maurea S, Klain M, Mainolfi C, Ziviello M, Salvatore M. The diagnostic role of radionuclide imaging in evaluation of patients with nonhypersecreting adrenal masses. J Nucl Med 2001;42:884–892.
3. Yun M, Kim W, Alnafisi N, Lacorte L, Jang S, Alavi A. 18F-FDG PET in characterizing adrenal lesions detected on CT or MRI. J Nucl Med 2001;42(12):1795–1799.

Chapter 3 Germ Cell Tumors

1. Bourguet P, Groupe de Travail SOR. Standards, Options and Recommendations for the use of PET-FDG in cancerology. Results in urological cancers. Bulletin du Cancer 2003;90: S80–87.
2. De Santis M, Bokemeyer C, Becherer A, Stoiber F, Oechsle K, Kletter K, Dohmen BM, Dittrich C, Pont J. Predictive impact of 2-18fluoro-2-deoxy-D-glucose positron emission tomography for residual postchemotherapy masses in patients with bulky seminoma. J Clin Oncol 2001;19(23):4355.
3. Hebart H, Erley C, Kaskas B, et al. Positron emission tomography helps to diagnose tumor emboli and residual disease in choriocarcinoma. Ann Oncol 1996;7(4):416–418.
4. Hellerstedt BA, Pienta KJ. Testicular cancer. Curr Opin Oncol 2002;14(3):260–264.
5. Kalvin B, Marian T, Galuska L, et al. Positron emission tomography in the investigation of malignant testicular tumors. Orvosi Hetilap 2002;143(21 Suppl 3):1286–1289.
6. Oyama N, Miller TR, Deddashti F, et al. ^{11}C-acetate PET imaging of prostate cancer: detection of recurrent disease at PSA relapse. J Nucl Med 2003;44:549–555.
7. Dejong IJ, Pruim J, Elsinga PH, Vaalburg W, Mensink HJ. Preoperative staging of pelvic lymph nodes in prostate cancer by ^{11}C-choline PET. J Nucl Med 2003;44:331–335.
8. Shvarts O, Han KR, Seltzer M, Pantuck AJ, Belldegrun AS. Positron emission tomography in urologic oncology. Cancer Control 2002;9(4):335–342.
9. Spermon JR, De Geus-Oei LF, Kiemeney LA, Witjes JA, Oyen WJ. The role of (18) fluoro-2-deoxyglucose positron emission tomography in initial staging and re-staging after chemotherapy for testicular germ cell tumours. BJU Int 2002;89(6):549–556.
10. Trubenbach J, Pereira PL, Huppert PE, et al. Primary choriocarcinoma of the pulmonary artery mimicking pulmonary embolism. Br J Radiol 1997;70(836):843–845.
11. Zhuang H, Yamamoto AJ, Ghesani N, Alavi A. Detection of choriocarcinoma in the lung by FDG positron emission tomography. Clin Nucl Med 2001;26(8):723.

Chapter 4 Brain

1. Delbeke D. Oncological applications of FDG PET imaging: Brain tumors, colorectal cancer, lymphoma, and melanoma. J Nucl Med 1999;40:591–603.

2. Dethy S, Laute MA, Blecic S, Luxen A, Hildebrand J, Goldman S. Carbon-11-methionine and fluorine-18-FDG PET study in brain hematoma. J Nucl Med 1994;35(7):1162–1166.
3. Hagge RJ, Wong TZ, Colman RE. Positron emission tomography. Brain tumors and lung cancer. Radiol Clin North Am 2001;39:871–881.
4. Ishii K, Ogawa T, Hatazawa J, et al. High L-methyl-[11C] methionine uptake in brain abscess: a PET study. J Comput Assist Tomogr 1993;17:660–661.
5. Langleben DD, Segall GM. PET in differentiation of recurrent brain tumor from radiation injury. J Nucl Med 2001;41:1861–1867.
6. Massager N. [Usefulness of PET scan guidance in stereotaxic radioneurosurgery using a gamma knife]. Bull Mem Acad R Med Bel 2002;157(7–9):355–369.
7. Ogawa T, Hatazawa J, Inugami A, et al. Carbon-11-methionine PET evaluation of intracerebral hematoma: Distinguishing neoplastic from non-neoplastic hematoma. J Nucl Med 1995;36(12):2175–2179.
8. Ogawa T, Kanno I, Shishido F, et al. Clinical value of PET with 18F-fluorodeoxyglucose and L-methyl-11C-methionine for diagnosis of recurrent brain tumor and radiation injury. Acta Radiol 1991;32:197–202.
9. Petrella JR, Coleman RE, Doraiswamy PM. Neuroimaging and early diagnosis of Alzheimer disease: a look to the future. Radiology 2003;226:315–336.
10. Seo DW, Park MS, Hong SB, Hong SC, Suh YL. Combined temporal and frontal epileptogenic foci in meningioangiomatosis. Eur Neurol 2003;49(3):184–186.
11. Tsuyuguchi N, Sunada I, Iwai Y, et al. Methionine positron emission tomography of recurrent metastatic brain tumor and radiation necrosis after stereotactic radiosurgery: is a differential diagnosis possible? J Neurosurg 2003;98(5):1056–1064.
12. Wong TZ, van der Westhuizen GJ, Coleman RE. Positron emission tomography imaging of brain tumors. Neuroimag Clin North Am 2002;12(4):615–626.

Chapter 5 Breast Cancer

1. Avril N, Rose CA, Schelling M, et al. Breast imaging with positron emission tomography and fluorine-18 fluorodeoxyglucose: use and limitations. J Clin Oncol 2000;18:3495–3502.
2. Avril N, Menzel M, Dose J, et al. Glucose metabolism of breast cancer assessed by 18F-FDG PET: Histologic and immunohistochemical tissue analysis. J Nucl Med 2001;42:9–16.
3. Bos R, van Der Hoeven JJ, van Der Wall, et al. Biologic correlates of ^{18}Fluorodeoxyglucose uptake in human breast cancer measured by positron emission tomography. J Clin Oncol 2002;20:379–387.
4. Buck A, Schirrmeister H, Kuhn T, et al. FDG uptake in breast cancer: correlation with biological and clinical prognostic parameters. Eur J Nucl Med Mol Imag 2002;29(10):1317–1323.
5. Cook GJ, Houston S, Rubens R, Maisey MN, Fogey I. Detection of bone metastases in breast cancer by ^{18}FDG PET: differing metabolic activity in osteoblastic and osteolytic lesions. J Clin Oncol 1998;16:3375–3379.
6. Dehdashti F, Flanagan FL, Mortimer JE, Katzenellenbogen JA, Welch MJ, Siegel BA. Positron emission tomographic assessment of "metabolic flare" to predict response of metastatic breast cancer to antiestrogen therapy. Eur J Nucl Med 1999;26:51–56.
7. Dehdashti F, Siegel BA. Evaluation of breast and gynecologic cancers by positron emission tomography. Semin Roentgenol. 2002;37(2):151–168.
8. Eubank WB, Mankoff DA, Takasugi J, et al. ^{18}Fluorodeoxyglucose positron emission tomography to detect mediastinal or internal mammary metastases in breast cancer. J Clin Oncol 2001;19:3516–3523.
9. Greco M, Crippa F, Agresti R, et al. Axillary lymph node staging in breast cancer by 2-fluoro-2-deoxy-D-glucose-positron emission tomography: clinical evaluation and alternative management. J Natl Cancer Inst 2001;93:630–635.
10. Hathaway PB, Mankoff DA, Maravilla KR, et al. Value of FDG PET and MR imaging in the evaluation of suspected recurrent local-regional breast cancer: preliminary experience. Radiology 1999;210:807–814.
11. Ilknur AK, et al. Positron emission tomography with 2-[18F] fluoro-2-deoxy-D-glucose in oncology: Part II: The clinical value in detecting and staging primary tumours. J Cancer Res Clin Oncol 2000;126:560–574.

12. Lin WY, Tsai SC, Cheng KY, Yen RF, Kao CH. Fluorine-18 FDG-PET in detecting local and distant metastases in breast cancer—Taiwanese experience. Cancer Invest 2002;20: 725–729.
13. Pisano ED, Parham CA. Digital mammography, sestamibi breast scintigraphy, and positron emission tomography breast imaging. Radiol Clin North Am 2000;38:861–869.
14. Hubner KF, Smith GT, Thie JA, Bell JL, Nelson HS, Hanna WT. Potential of F-18-FDG PET in breast cancer. Detection of primary lesions, axillary lymph node metastases, or distant metastases. Clin Positron Imaging 2000;3:197–205.
15. Van der Hoeven JJ, Hoekstra OS, Comans EF, et al. Determinants of diagnostic performance of [F-18] fluorodeoxyglucose positron emission tomography for axillary staging in breast cancer. Ann Surg 2002;236:619–624.
16. Vranjesevic D, Filmont JE, Meta J, et al. Whole-body ^{18}FDG PET and conventional imaging for predicting outcome in previously treated breast cancer patients. J Nucl Med 2002;43: 325–329.
17. Yap CS, Seltzer MA, Schiepers C, et al. Impact of whole-body 18F-FDG PET on staging and managing patients with breast cancer: The referring physicians perspective. J Nucl Med 2001;42:1334–1337.
18. Zimny M, Siggelkow W. Positron emission tomography scanning in gynecologic and breast cancers. Curr Opin Obstet Gynecol 2003;15(1):69–75.

Chapter 6 Gynecologic Malignancies

1. Kaur H, Silverman PM, Iyer RB, Verschraegen CF, Eifel PJ, Charnsangavej C. Diagnosis, staging, and surveillance of cervical carcinoma. AJR Am J Roentgenol 2003;180:1621–1632.
2. Koyama K, Okamura T, Kawabe J, et al. Evaluation of ^{18}F-FDG PET with bladder irrigation in patients with uterine and ovarian tumors. J Nucl Med 2003;44:353–358.
3. Lapela M, Leskinen-Kallio S, Varpula M, et al. Imaging of uterine carcinoma by carbon-11-methionine and PET. J Nucl Med 1994;35(10):1618–1623.
4. Ryu SY, Kim MH, Choi SC, Choi CW, Lee KH. Detection of early recurrence with 18F-FDG PET in patients with cervical cancer. J Nucl Med 2003;44(3):347–352.
5. Ryu SY, Kim MH, Choi SC, Choi CW, Lee KH. Detection of early recurrence with ^{18}F-FDG PET in patients with cervical cancer. J Nucl Med 2003;44:347–352.
6. Gambhir SS, Czernin J, Schwimmer J, Silverman DS, Coleman RE, Phelps ME. A tabulated summary of the FDG PET literature. J Nucl Med 2001;42:1S–93S.

Chapter 7 Colorectal Cancers

1. Anderson GS, Brinkman F, Soulen MC, Alavi A, Zhuang H. FDG positron emission tomography in the surveillance of hepatic tumors treated with radiofrequency ablation. Clin Nucl Med 2003;28:192–197.
2. Boykin KN, Zibari GB, Lilien DL, McMillan RW, Aultman DF, MacDonald JC. The use of FDG-positron emission tomography for the evaluation of colorectal metastases of the liver. Am Surg 1999;65:1183–1185.
3. Delbeke D, Martin WH. Positron emission tomography in oncology. Radiol Clin N Am 2001;39:883–917.
4. Dobos N, Rubesin SE. Radiologic imaging modalities in the diagnosis and management of colorectal cancer. Hematol Oncol Clin North Am 2002;16(4):875–895.
5. Fukunaga H, Sekimoto M, Tatsumi M, et al. Clinical relevance of fusion images using (18) F-2-fluoro-2-deoxy-D-glucose positron emission tomography in local recurrence of rectal cancer. Int J Oncol 2002;20(4):691–695.
6. Horton KM, Corl FM, Fishman EK. Spiral CT of colon cancer: Imaging features and role in management. Radiographics 2000;20:419–430.
7. Kaliff V, et al. The clinical impact of ^{18}F-FDG PET in patients with suspected or confirmed recurrence of colorectal cancer: A prospective study. J Nucl Med 2002;43:492–499.
8. Kostakoglu L, Goldsmith SJ. ^{18}F-FDG PET evaluation of the response to therapy for lymphoma and for breast, lung, and colorectal carcinoma. J Nucl Med 2003;44:224–239.

9. Lechner P, Lind P, Goldenberg DM. Can postoperative surveillance with serial CEA immunoscintigraphy detect resectable rectal cancer recurrence and potentially improve tumor-free survival? J Am Coll Surg 2000;191:511–518.
10. Lonneux M, Van Beers BE, Kartheuser A. Positive F-18 FDG positron emission tomography in the perineum after anorectal reconstruction. Clin Nucl Med 2002;27(5):363–364.
11. Meta J, Seltzer M, Schiepers C, et al. Impact of 18F-FDG PET on managing patients with colorectal cancer: The referring physician's perspective. J Nucl Med 2001;42:586–590.
12. Oku S, Nakagawa K, Momose T, et al. FDG-PET after radiotherapy is a good prognostic indicator of rectal cancer. Ann Nucl Med 2002;16(6):409–416.
13. Osman MM, Cohade C, Nakamoto Y, Marshall LT, Leal JP, Wahl RL. Clinically significant inaccurate localization of lesions with PET/CT: frequency in 300 patients. J Nucl Med 2003;44(2):240–243.
14. Ruers TJ, Langenhoff BS, Neeleman N, et al. Value of positron emission tomography with [F-18] Fluorodeoxyglucose in patients with colorectal liver metastases: A prospective study. J Clin Oncol 2002;20:388–395.
15. Rydzewski B, Dehdashti F, Gordon BA, Teefey SA, Strasberg SM, Siegel BA. Usefulness of intraoperative sonography for revealing hepatic metastases from colorectal cancer in patients selected for surgery after undergoing FDG PET. Am J Roentgenol 2002;178: 353–358.
16. Strasberg SM, Dehdashti F, Siegel BA, Drebin JA, Linehan D. Survival of patients evaluated by FDG-PET before hepatic resection for metastatic colorectal carcinoma: A prospective database study. Ann Surg 2001;233:293–299.
17. Thoeni RF. Colorectal cancer. Radiologic staging. Radiol Clin North Am 1997;35:457–485.
18. Whiteford MH, Whiteford HM, Yee LF, et al. Usefulness of FDG-PET scan in the assessment of suspected metastatic or recurrent adenocarcinoma of the colon and rectum. Dis Colon Rectum 2000;53:759–770.
19. Yasuda S, Fujii H, Nakahara T, et al. 18F-FDG PET detection of colonic adenomas. J Nucl Med 2001;42:989–992.
20. Yoshoka T, et al. FDG PET evaluation of residual masses and regrowth of abdominal lymph node metastases from colon cancer compared with CT during chemotherapy. Clin Nucl Med 1999;24:261–263.

Chapter 8 Cholangiocarcinoma

1. Kluge R, Schmidt F, Caca K, et al. Positron emission tomography with [(18) F] fluoro-2-deoxy-D-glucose for diagnosis and staging of bile duct cancer. Hepatology 2001;33(5): 1029–1035.
2. Teefey SA, Hildeboldt CC, Dehdashti F, et al. Detection of primary hepatic malignancy in liver transplant candidates: prospective comparison of CT, MR imaging, US and PET. Radiology 2003;226(2):533–542.
3. Torok N, Gores GJ. Cholangiocarcinoma. Semin Gastroint Dis 2001;12(2):125–132.

Chapter 9 Esophageal Carcinoma

1. Couper GW, Park KG. Detection of response to neoadjuvant therapy of esophageal squamous cell carcinoma by positron emission tomography (PET). Annals of Surgery. 2003;237(2):289–290.
2. Downey RJ, Akhurst T, Ilson D, et al. Whole body 18FDG-PET and the response of esophageal cancer to induction therapy: results of a prospective trial. J Clin Oncol 2003;21(3):428–432.
3. Flamen P, Lerut A, Van Cutsem E, et al. The utility of positron emission tomography for the diagnosis and staging of recurrent esophageal cancer. J Thorac Cardiovasc Surg 2000;120:1085–1092.
4. Iyer RB, Silverman PM, Tamm EP, Dunnington JS, DuBrow RA. Diagnosis, staging, and follow-up of esophageal cancer. AJR Am J Roentgenol 2003;181:785–793.
5. Kostakoglu L, Agress H Jr, Goldsmith SJ. Clinical role of FDG PET in evaluation of cancer patients. Radiographics 2003;23:315–340.

6. Lowe VJ, Naunheim KS. Current role of positron emission tomography in thoracic oncology. Thorax 1998;53:703–712.
7. Luketich JD, Friedman DM, Weigel TL, et al. Evaluation of distant metastases in esophgeal cancer: 100 consecutive positron emission tomography scans. Ann Thorac Surg 1999; 68:1133–1137.
8. Moadel RM, Blaufox MD, Freeman LM. The role of positron emission tomography in gastrointestinal imaging. Gastroenterol Clin North Am 2002;31(3):841–861.
9. Skehan S, Brown AL, Thompson M, Young JE, Coates G, Nahmias C. Imaging features of primary and recurrent esophageal cancer at FDG PET. Radiographics 2000;20:713–723.
10. Yoon YC, Lee KS, Shim YM, Kim BT, Kim K, Kim TS. Metastasis to regional lymph nodes in patients with esophageal squamous cell carcinoma: CT versus FDG PET for presurgical detection—prospective study. Radiology 2003;227:764–770.

Chapter 10 Gastric Cancer

1. De Potter T, Flamen P, Van Cutsem E, et al. Whole-body PET with FDG for the diagnosis of recurrent gastric cancer. European Journal of Nuclear Medicine & Molecular Imaging. 2002;29(4):525–529.
2. Jadvar H, Tatlidil R, Garcia AA, Conti PS. Evaluation of recurrent gastric malignancy with [F-18]-FDG positron emission tomography. Clin Radiol 2003;58(3): 215–221.
3. Yoshioka T, Yamaguchi K, Kubota K, et al. Evaluation of ^{18}F-FDG PET in patients with advanced, metastatic, or recurrent gastric cancer. J Nucl Med 2003;44:690–699.

Chapter 11 Gastrointestinal Tumors

1. Muler JH, Baker L, Zalupski MM. Gastrointestinal stromal tumors: Chemotherapy and imatinib. Curr Oncol Rep 2002;4(6):499–503.
2. Gambhir SS, Czernin J, Schwimmer J, Silverman D, Coleman RE, Phelps ME. A tabulated summary of the FDG PET literature. J Nucl Med 2001;42:1S–93S.

Chapter 12 Head and Neck Cancers

1. Allal AS, Dulguerov P, Allaoua M, et al. Standardized uptake value of 2-[^{18}F] fluoro-2-deoxy-D-glucose in predicting outcome in head and neck carcinomas treated by radiotherapy with or without chemotherapy. J Clin Oncol 2002;20:1398–1404.
2. Braams JW, Pruim J, Freling NJ, et al. Detection of lymph node metastases of squamous-cell cancer of the head and neck with FDG-PET and MRI. J Nucl Med 1995;36:211–216.
3. Delbeke D. Oncological applications of FDG PET imaging: Brain tumors, colorectal cancer, lymphoma, and melanoma. J Nucl Med 1999;40:591–603.
4. Dresel S, Schwenzer K, Brinkbaumer K, et al. [F-18] FDG imaging of head and neck tumors: Comparison of hybrid PET, dedicated PET and CT. Nuklearmedizin 2001;40(5): 172–178.
5. Ilknur AK, et al. Positron emission tomography with 2-[18F] fluoro-2-deoxy-D-glucose in oncology: Part II: The clinical value in detecting and staging primary tumours. J Cancer Res Clin Oncol 2000;126:560–574.
6. de Boer JR, Pruim J, van der Laan B, et al. L-1-^{11}C-Tyrosine PET in patients with laryngeal carcinomas: Comparison of standardized uptake value and protein synthesis rate. J Nucl Med 2003;44:341–346.
7. Kitagawa Y, Nishizawa S, Sano K, et al. Prospective comparison of 18F-FDG PET with conventional imaging modalities (MRI, CT, and 67Ga scintigraphy) in assessment of combined intraarterial chemotherapy and radiotherapy for head and neck carcinoma. J Nucl Med 2003;44(2):198–206.
8. Kostakoglu L, Agress H Jr, Goldsmith SJ, et al. Clinical role of FDG PET in evaluation of cancer patients. Radiographics 2003;23:315–340.
9. Laubenbacher C, Saumweber D, Wagner-Manslau C, et al. Comparison of fluorine-18-fluorodeoxyglucose PET, MRI, and endoscopy for staging head and neck squamous-cell carcinomas. J Nucl Med 1995;36:1747–1757.

10. Lonneux M, Lawson G, Ide C, Bausart R, Remacle M, Pauwels S. Positron emission tomography with fluorodeoxyglucose for suspected head and neck tumor recurrence in the symptomatic patient. Laryngoscope. 2000;110(9):1493–1497.
11. Lowe VJ, Boyd JH, Dunphy FR, et al. Surveillance for recurrent head and neck cancer using positron emission tomography. J Clin Oncol 2000;18(3):651–658.
12. Lowe VJ, Stack BC Jr. Esophageal cancer and head and neck cancer. Sem Roentgenol 2002;37(2):140–150.
13. Ojiri H, Mancuso AA, Mendenhall WM, Stringer SP. Lymph nodes of patients with regional metastases from head and neck squamous cell carcinoma as a predictor of pathologic outcome: size changes at CT before and after radiation therapy. Am J Neuroradiol 2002;23(10):1627–1631.
14. Teknos TN, Rosenthal EL, Lee D, Taylor R, Marn S. Positron emission tomography in the evaluation of stage III and IV head and neck cancer. Head Neck 2001;23:1056–1060.

Chapter 13 Heart Viability

1. Bergmann SR. Use and limitations of metabolic tracers labeled with positron-emitting radionuclides in the identification of viable myocardium. J Nucl Med 1994;35(4 Suppl): 15S–22S.
2. Brink I, Nitzsche EU, Mix M, et al. Appropriate uptake period for myocardial PET imaging with 18F-FDG after oral glucose loading. Nuklearmedizin. 2003;42(1):39–44.
3. Grandin C, Wijns W, Melin JA, et al. Delineation of myocardial viability with PET. J Nucl Med 1995;36(9):1543–1552.
4. Maddahi J. Cardiovascular nuclear medicine: state-of-the-art. J Nucl Med 1994; 35(4):672–673.
5. Schelbert HR, Beanlands R, Bengel F, et al. PET myocardial perfusion and glucose metabolism imaging: Part 2-guidelines for interpretation and reporting. J Nucl Cardiol 2003; 10:557–571.
6. Schelbert HR. Metabolic imaging to assess myocardial viability. J Nucl Med 1994;35 (4 Suppl):8S–14S.
7. Schinkel AFL, Bax JJ, van Domburg R, et al. Dobutamine-induced contractile reserve in stunned, hibernating, and scarred myocardium in patients with ischemic cardiomyopathy. J Nucl Med 2003;44:127–133.
8. Schinkel AFL, Bax JJ, Valkema R, et al. Effect of diabetes mellitus on myocardial ^{18}F-FDG SPECT using acipimox for the assessment of myocardial viability. J Nucl Med 2003;44:877–883.
9. Tamaki N, Morita K, Kuge Y, Tsukamoto E. The role of fatty acids in cardiac imaging. J Nucl Med 2000;41:1525–1534.
10. Vitale GD, deKempe RA, Ruddy TD, Williams K, Beanlands RS. Myocardial glucose utilization and optimization of ^{18}F-FDG imaging in patients with non-insulin-dependent diabetes mellitus, coronary artery disease, and left ventricular dysfunction. J Nucl Med 2001;42:1730–1736.
11. Zhang X, et al. Clinical outcome of patients with previous myocardial infarction and left ventricular dysfunction assessed with myocardial 99mTc-MIBI SPECT and 18F-FDG PET. J Nucl Med 2001;42:1166–1173.

Chapter 14 Inflammatory Disease

1. Beckers C, Foidart J, Thiry A, Malaise MG. Synovial metastases from colonic cancer presenting as arthritis of the knee. Characterization by 18FDG PET scan. Revue Medicale de Liege 2002;57(7):467–474.
2. Palestro CJ. Nuclear medicine, the painful prosthetic joint, and orthopedic infection. J Nucl Med 2003;44:927–929.
3. Zhuang H, Pourdehnad M, Lambright ES, et al. Dual time point ^{18}F-FDG PET imaging for differentiating malignant from inflammatory processes. J Nucl Med 2001;42:1412–1417.
4. Bakheet SM, Powe J. Fluorine-18-fluorodeoxyglucose uptake in rheumatoid arthritis-associated lung disease in a patient with thyroid cancer. J Nucl Med.1998;39:234–236.

5. Wipke BT, Wang Z, Kim J, McCarthy TJ, Allen PM. Dynamic visualization of a joint-specific autoimmune response through positron emission tomography. Nature Immunol 2002;3(4):366–372.
6. Yun M, Kim W, Adam LE, Alnafisi N, Herman C, Alavi A. F-18 FDG uptake in a patient with psoriatic arthritis: imaging correlation with patient symptoms. Clin Nucl Med 2001;26(8):692–693.

Chapter 15 Unknown Primary Tumors

1. Delgado-Bolton RC, Fernando-Perez C, Gonzalez-Mate A, Carreras JL. Meta-analysis of the performance of ^{18}F-FDG PET in primary tumor detection in unknown primary tumors. J Nucl Med 2003;44:1301–1314.
2. Okada J, Yoshikawa K, Imazeki K, et al. The use of FDG-PET in the detection and management of malignant lymphoma: Correlation of uptake with prognosis. J Nucl Med 1991;32;686–691.
3. Okada J, Yoshikawa K, Itami M, et al. Positron emission tomography using fluorine-18 fluorodeoxyglucose in malignant lymphoma: a comparison with proliferative activity. J Nucl Med 1992;33;325–329.
4. Paul R. Comparison of fluorine-18 2-fluorodeoxyglucose and gallium-67 citrate imaging for detection of lymphoma. J Nucl Med 1987;28;288–292.
5. Stoeckli SJ, Mosna-Firlejczyk K, Goerres GW. Lymph node metastasis of squamous cell carcinoma from an unknown primary: impact of positron emission tomography. Eur J Nucl Med Mol Imaging 2003;30(3):411–416.

Chapter 16 Liver Cancer

1. Bourguet P, Groupe de Travail SOR. Standards, options and recommendations for the use of PET-FDG in cancerology. Results in digestive system neoplasms. Bulletin du Cancer 2003;90S56–S66.
2. Delbeke D, Martin WH. Positron emission tomography in oncology. Radiol Clin North Am 2001;39:883–917.
3. Delbeke D. ^{11}C-acetate: a new tracer for the evaluation of hepatocellular carcinoma. J Nucl Med 2003;44:222–223.
4. Ho CL, et al. ^{11}C-acetate PET imaging in hepatocellular carcinoma and other liver masses. J Nucl Med 2003;44:213–221.
5. Langenhoff BS, Oyen WJ, Jager GJ, et al. Efficacy of fluorine-18-deoxyglucose positron emission tomography in detecting tumor recurrence after local ablative therapy for liver metastases: A prospective study. J Clin Oncol 2002;20(22):4453–4458.
6. Osman MM, Cohade C, Nakamoto Y, Marshall LT, Leal JP, Wahl RL. Clinically significant inaccurate localization of lesions with PET/CT: frequency in 300 patients. J Nucl Med 2003;44:240–243.
7. Teefey SA, Hildeboldt CC, Dehdashti F, et al. Detection of primary hepatic malignancy in liver transplant candidates: prospective comparison of CT, MR, US, and PET. Radiology 2003;226:533–542.
8. Wudel LJ Jr, Delbeke D, Morris D, et al. The role of [18F] fluorodeoxyglucose positron emission tomography imaging in the evaluation of hepatocellular carcinoma. Am Surg 2003;69(2):117–124.

Chapter 17 Lung Tumors

1. Delbeke D. Oncological applications of FDG PET imaging: brain tumors, colorectal cancer, lymphoma, and melanoma. J Nucl Med 1999;40:591–603.
2. Erasmus JJ, McAdams HP, Patz EF Jr, Goodman PC, Coleman RE. Thoracic FDG PET: state of the art. Radiographics 1998;18:5–20.
3. Hagge RJ, Wong TZ, Coleman RE. Positron emission tomography. Brain tumors and lung cancer. Radiol Clin North Am 2001;39:871–881.

4. Hauber HP, Bohuslavizki KH, Lund CH, Fritscher-Ravens A, Meyer A, Pforte A. Positron emission tomography in the staging of small-cell lung cancer. A preliminary study. Chest 2001;119:950–954.
5. Higashi K, Ueda Y, Arisaka Y, et al. ^{18}F-FDG uptake as a biologic prognostic factor for recurrence in patients with surgically resected non-small cell lung cancer. J Nucl Med 2002;43:39–45.
6. Komori T, Delbeke D. Leptomeningeal carcinomatosis and intramedullary spinal cord metastases from lung cancer: detection with FDG positron emission tomography. Clin Nucl Med 2001;26(11):905–907.
7. Kostakoglu L, Agress H Jr, Goldsmith SJ. Clinical role of FDG PET in evaluation of cancer patients. Radiographics 2003;23:315–340.
8. Lowe VJ, Naunheim KS. Current role of positron emission tomography in thoracic oncology. Thorax 1998;53:703–712.
9. Mastin ST, Drane WE, Harman EM, Fenton JJ, Quesenberry L. FDG SPECT in patients with lung masses. Chest 1999;115:1012–1017.
10. McCain TW, Dunagan DP, Chin R Jr, Oaks T, Harkness BA, Haponik EF. The usefulness of positron emission tomography in evaluating patients for pulmonary malignancies. Chest 2000;118:1610–1615.
11. Patz EF Jr, Connelly J, Herndon J. Prognostic value of thoracic FDG PET imaging after treatment for non-small cell lung cancer. AJR Am J Roentgenol 2000;174:769–774.
12. Hicks RJ, Kalff V, MacManus MP, et al. ^{18}F-FDG PET provides high-impact and powerful prognostic stratification in staging newly diagnosed non-small cell lung cancer. J Nucl Med 2001;42:1596–1604.
13. Shon IH, O'doherty MJ, Maisey MN. Positron emission tomography in lung cancer. Sem Nucl Med 2002;32(4):240–271.
14. Demura Y, Tsuchida T, Ishizaki T, et al. ^{18}F-FDG accumulation with PET for differentiation between benign and malignant lesions in the thorax. J Nucl Med 2003;44:540–548.

Chapter 18 Hematologic Malignancies

1. Bangerter M, Kotzerke J, Griesshammer M, Elsner K, Reske SN, Bergmann L. Positron emission tomography with 18-Fluorodeoxyglucose in the staging and follow-up of lymphoma in the chest. Acta Oncol 1999;38(6):799–804.
2. Delbeke D, Martin WH. Positron emission tomography in oncology. Radiol Clin North Am 2001;39:883–917.
3. Delbeke D. Oncological applications of FDG PET imaging: Brain tumors, colorectal cancer, lymphoma, and melanoma. J Nucl Med 1999;40:591–603.
4. Wiseman GA, Kornmehl E, Leigh B, et al. Radiation dosimetry results and safety correlations from ^{90}Y-Ibritumomab tiuxetan radioimmunotherapy for relapsed or refractory non-Hodgkin's lymphoma: combined data from 4 clinical trials. J Nucl Med 2003;44:465–474.
5. Wagner HN Jr, Wiseman GA, Marcus CS, et al. Administration guidelines for radioimmunotherapy of non-Hodgkin's lymphoma with ^{90}Y-Labeled anti-CD20 monoclonal antibody. J Nucl Med 2002;43:267–272.
6. Hoffmann M, Kletter K, Becherer A, Jager U, Chott A, Raderer M. 18F-fluorodeoxyglucose positron emission tomography (18F-FDG-PET) for staging and follow-up of marginal zone B-cell lymphoma. Oncology 2003;64(4):336–340.
7. Ilknur AK, et al. Positron emission tomography with 2-[18F] fluoro-2-deoxy-D-glucose in oncology: Part II: The clinical value in detecting and staging primary tumours. J Cancer Res Clin Oncol 2000;126:560–574.
8. Jadvar H, Conti PS. Diagnostic utility of FDG PET in multiple myeloma. Skeletal Radiol 2002;31(12):690–694.
9. Kostakoglu L, Coleman M, Leonard JP, Kuji I, Zoe H, Goldsmith SJ. PET predicts prognosis after 1 cycle of chemotherapy in aggressive lymphoma and Hodgkin's disease. J Nucl Med 2002;43:1018–1027.
10. Kostakoglu L, Goldsmith SJ. ^{18}F-FDG PET evaluation of the response to therapy for lymphoma and for breast, lung, and colorectal carcinoma. J Nucl Med 2003;44:224–239.
11. Lee J. Dichotomy between Tc-99m MDP bone scan and Fluorine-18 fluorodeoxyglucose coincidence detection positron emission tomography in patients with non-Hodgkin's lymphoma. Clin Nucl Med 2000;25:532–535.

12. Tatsumi M, Kitayama H, Sugahara H, et al. Whole-body hybrid PET with ^{18}F-FDG in the staging of non-Hodgkin's lymphoma. J Nucl Med 2001;42:601–608.
13. Naumann R, Vaic A, Beuthien-Baumann B, et al. Prognostic value of positron emission tomography in the evaluation of post-treatment residual mass in patients with Hodgkin's disease and non-Hodgkin's lymphoma. Br J Haematol 2001;115:793–800.
14. Orchard K, Barrington S, Buscombe J, Hilson A, Prentice HG, Mehta A. Fluoro-deoxyglucose positron emission tomography imaging for the detection of occult disease in multiple myeloma. Br J Haematol 2002;117(1):133–135.
15. Rini JN, Leonidas JC, Tomas MB, et al. 18F-FDG PET versus CT for evaluating the spleen during initial staging of lymphoma. J Nucl Med 2003;44:1072–1074.
16. Romer W, Schwaiger N. Positron emission tomography in diagnosis and therapy monitoring of patients with lymphoma. Clin Positron Imaging 1998;1(2):101–110.
17. Romer W, Hanauske AR, Ziegler S, et al. Positron emission tomography in non-Hodgkin's lymphoma: Assesment of chemotherapy with fluorodeoxyglucose. Blood 1998;91:4464–4471.
18. Sasaki M, Kuwabara Y, Koga H, et al. Clinical impact of whole body FDG-PET on the staging and therapeutic decision-making for malignant lymphoma. Ann Nucl Med 2002;16(5):337–345.
19. Schirrmeister H, Bommer M, Buck AK, et al. Initial results in the assessment of multiple myeloma using 18F-FDG PET. Eur J Nucl Med Mol Imag 2002;29(3):361–366.
20. Schoder H, Meta J, Yap C, et al. Effect of whole-body ^{18}F-FDG PET imaging on clinical staging and management of patients with malignant lymphoma. J Nucl Med 2001;42: 1139–1143.
21. Shen YY, Wu Hs, Huang WS, et al. Comparison of 18F-fluoro-2-deoxyglucose positron emission tomography and gallium-67 citrate scintigraphy for detecting malignant lymphoma. Oncol Rep 2002;9:321–325.
22. Spaepen K, Stroobants S, Dupont P, et al. Prognostic value of positron emission tomography (PET) with fluorine-18 fluorodeoxyglucose ([^{18}F] FDG) after first-line chemotherapy in non-Hodgkin's lymphoma: is [^{18}F] FDG-PET a valid alternative to conventional diagnostic methods? J Clin Oncol 2001;19:414–419.
23. Lowe VJ, Wiseman GA. Assessment of lymphoma therapy using ^{18}F-FDG PET. J Nucl Med 2002;43:1028–1030.
24. Wiseman GA, White CA, Sparks RB, et al. Biodistribution and dosimetry results from a phase III prospectively randomized controlled trial of Zevalin radioimmunotherapy for low-grade, follicular, or transformed B-cell non-Hodgkin's lymphoma. Crit Rev Oncol Hematol 2001;39(1–2):181–194.
25. Zhuang H, Alavi A. 18-fluorodeoxyglucose positron emission tomographic imaging in the detection and monitoring of infection and inflammation. Sem Nucl Med 2002;32(1): 47–59.

Chapter 19 Melanoma

1. Bourguet P, Groupe de Travail SOR. Standards, options and recommendations for the use of PET-FDG in cancerology. Results in skin and ocular melanoma. Bulletin du Cancer 2003;90:S42–S46.
2. Damian DL, Fulham MJ, Thompson E, Thompson JF. Positron emission tomography in the detection and management of metastatic melanoma. Melanoma Res 1996;6:325–329.
3. Delbeke D. Oncological applications of FDG PET imaging: Brain tumors, colorectal cancer, lymphoma, and melanoma. J Nucl Med 1999;40:591–603.
4. Gritters LS, Francis IR, Zasadny KR, Wahl RL. Initial assessment of positron emission tomography using 2-fluorine-18-fluor-2-deoxy-D-glucose in the imaging of malignant melanoma. J Nucl Med 1993;34:1420–1427.
5. Ilknur AK, et al. Positron emission tomography with 2-[18F] fluoro-2-deoxy-D-glucose in oncology: Part II: The clinical value in detecting and staging primary tumours. J Cancer Res Clin Oncol 2000;126:560–574.
6. Mijnhout GS, Hoekstra OS, van Tulder MW, Teule GJ, Deville WL. Systematic review of the diagnostic accuracy of 18F-Fluorodeoxyglucose positron emission tomography in melanoma patients. Cancer 2001;91:1530–1542.

7. Mijnhout GS, Hoekstra OS, van Lingen A, et al. How morphometric analysis of metastatic load predicts the (un) usefulness of PET scanning: The case of lymph node staging in melanoma. J Clin Pathol 2003;56(4):283–286.
8. Rinne D, Baum RP, Hor G, Kaufmann R. Primary staging and follow-up of high-risk melanoma patients with whole-body 18-F-fluorodeoxyglucose positron emission tomography: Results of a prospective study of 100 patients. Cancer 1998;82:1664–1671.
9. Stas M, Stroobants S, Dupont P, et al. 18-FDG PET scan in the staging of recurrent melanoma: additional value and therapeutic impact. Melanoma Res 2002;12(5):479–490.
10. Wagner JD. PET detection of melanoma metastases in lymph nodes. J Nucl Med 2003; 44(3):486.

Chapter 20 Thyroid Carcinoma

1. Alnafisi NS, Driedger AA, Coates G, Moote DJ, Raphael SJ. FDG PET of recurrent or metastatic 131I-negative papillary thyroid carcinoma. J Nucl Med 2000;41:1010–1015.
2. Helal BO, Merlet P, Toubert ME, et al. Clinical impact of ^{18}F-FDG PET in thyroid carcinoma patients with elevated thyroglobulin levels and negative ^{131}I scanning results after therapy. J Nucl Med 2001;42:1464–1469.
3. Bourguet P, Groupe de Travail SOR. Standards, Options and Recommendations for the use of PET-FDG in cancerology. Results in cancer of the thyroid. Bulletin du Cancer 2003;90;S105–S109.
4. Chung JK, So Y, Lee JS, et al. Value of FDG PET in papillary thyroid carcinoma with negative I-131 whole body scans. J Nucl Med 1999;40:986–992.
5. Clark OH, Hoelting L. Managament of patients with differentiated thyroid cancer who have positive serum thyroglobulin levels and negative radioiodine scans. Thyroid 1994; 4 (4):501–505.
6. Helal BO, Merlet P, Toubert ME, et al. Clinical impact of 18F-FDG PET in thyroid carcinoma patients with elevated thyroglobulin levels and negative 131I scanning results after therapy. J Nucl Med 2001;42:1464–1469.
7. Macapinlac HA. Clinical usefulness of FDG PET in differentiated thyroid cancer. J Nucl Med 2001;42:77–78.
8. Lind P, Kresnik E, Kumnig G, et al. 18F-FDG-PET in the follow-up of thyroid cancer. Acta Medica Austriaca. 2003;30(1):17–21.
9. Moog F, Linke R, Manthey N, et al. Influence of thyroid-stimulating hormone levels on uptake of FDG in recurrent and metastatic differentiated thyroid carcinoma. J Nucl Med 2000;41:1989–1995.
10. Schonberger J, Ruschoff J, Grimm D, et al. Glucose transporter 1 gene expression is related to thyroid neoplasms with an unfavorable prognosis: an immunohistochemical study. Thyroid 2002;12(9):747–754.
11. Shiga T. Comparison of 18F-FDG, 131I-Na, and 201-Tl in diagnosis of recurrent or metastatic thyroid cancer. J Nucl Med 2001;42:414–419.
12. Szakall S Jr, Esik O, Bajzik G, et al. ^{18}F-FDG PET detection of lymph node metastases in medullary thyroid carcinoma. J Nucl Med 2002;43:66–71.
13. Van Tol KM, Jager PL, Piers DA, et al. Better yield of (18) fluorodeoxyglucose-positron emission tomography in patients with metastatic differentiated thyroid carcinoma during thyrotropin stimulation. Thyroid 2002;12(5):381–387.
14. Yeo JS, Chung JK, So Y, et al. F-18-fluorodeoxyglucose positron emission tomography as a presurgical evaluation modality for i-131 scan-negative thyroid carcinoma patients with local recurrence in cervical lymph nodes. Head Neck 2001;23:94–103.
15. Zimmer LA, McCook B, Meltzer C, et al. Combined positron emission tomography/computed tomography imaging of recurrent thyroid cancer. Otolaryngol Head Neck Surg 2003;128(2):178–184.

Chapter 21 Muscular Skeletal Tumors

1. Bredella MA, Caputo GR, Steinbach LS. Value of FDG positron emission tomography in conjunction with MR imaging for evaluating therapy response in patients with musculoskeletal sarcomas. Am J Roentgenol 2002;179:1145–1150.

2. Dimitrakopoulou-Strauss A, Strauss LG, Schwarzbach M, et al. Dynamic PET ^{18}F-FDG studies in patients with primary and recurrent soft-tissue sarcomas: Impact on diagnosis and correlation with grading. J Nucl Med 2001;42:713–720.
3. Franzius C, Sciuk J, Brinkschmidt C, Jurgens H, Schober O. Evaluation of chemotherapy response in primary bone tumors with F-18 FDG positron emission tomography compared with histologically assessed tumor necrosis. Clin Nucl Med 2000;25:874–881.
4. Franzius C, Bielack S, Flege S, Sciuk J, Jurgens H, Schober O. Prognostic significance of ^{18}F-FDG and ^{99m}Tc-methylene diphosphonate uptake in primary osteosarcoma. J Nucl Med 2002;43:1012–1017.
5. Ioannidis JPA, Lau J. ^{18}F-FDG PET for the diagnosis and grading of soft-tissue sarcoma: a meta-analysis. J Nucl Med 2003;44:717–724.
6. Jones DN, McCowage GB, Sostman HD, et al. Monitoring of neoadjuvant therapy response of soft-tissue and musculoskeletal sarcoma using fluorine-18-FDG PET. J Nucl Med. 1996;37(9):1438–1444.
7. Messa C, Landoni C, Pozzato C, Fazio F. Is there a role for FDG PET in the diagnosis of musculoskeletal neoplasms? J Nucl Med 2000;41(10):1702–1703.
8. Schulte M, Brech-Krauss D, Heymer B, et al. Grading of tumors and tumor like lesions of bone: Evaluation by FDG PET. J Nucl Med 2000;41:1695–1701.
9. Schwarzbach M, Willeke F, Dimitrakopoulou-Strauss A, et al. Functional imaging and detection of local recurrence in soft tissue sarcomas by positron emission tomography Anticancer Res 1999;19(2B):1343–1349.
10. Brenner W, Bohuslavizki KH, Eary JF. PET imaging of osteosarcoma. J Nucl Med 2003;44:930–942.

Chapter 22 Urinary Malignancies

1. Ahlstrom H, Malmstrom PU, Letocha H, Andersson J, Langstrom B, Nilsson S. Positron emission tomography in the diagnosis and staging of urinary bladder cancer. Acta Radiologica 1996;37(2):180–185.
2. Bachor R, Kotzerke J, Reske SN, Hautmann R. Lymph node staging of bladder neck carcinoma with positron emission tomography. Urologe 1999;38(1):46–50.
3. de Jong IJ, Pruim J, Elsinga PH, Jongen MM, Mensink HJ, Vaalburg W. Visualisation of bladder cancer using (11) C-choline PET: first clinical experience. Eur J Nucl Med Mol Imag 2002;29(10):1283–1288.
4. Heicappell R, Muller-Mattheis V, Reinhardt M, et al. Staging of pelvic lymph nodes in neoplasms of the bladder and prostate by positron emission tomography with 2-[(18) F]-2-deoxy-D-glucose. Eur Urol 1999;36(6):582–587.
5. Ramdave S, Thomas GW, Berlangieri SU, et al. Clinical role of F-18 fluorodeoxyglucose positron emission tomography for detection and management of renal cell carcinoma. J Urol 2001;166(3):825–830.
6. Shvarts O, Han KR, Seltzer M, Pantuck AJ, Belldegrun AS. Positron emission tomography in urologic oncology. Cancer Control 2002;9(4):335–342.
7. Steffens MG, Mulders PF, Brouwers AH, Oyen WJ. Re: Clinical role of F-18 fluorodeoxyglucose positron emission tomography for detection and management of renal cell carcinoma. J Urol 2002;168(5):2127–2128.

Chapter 23 Nerve Tumors

1. Ahmed AR, Watanabe H, Aoki J, et al. Schwannoma of the extremities: The role of PET in preoperative planning. Eur J Nucl Med 2001;28(10):1541–1551.
2. Antoch G, Egelhof T, Korfee S, Frings M, Forsting M, Bockisch A. Recurrent schwannoma: Diagnosis with PET/CT. Neurology. 2002;59(8):1240.
3. Ferner RE. O'Doherty MJ. Neurofibroma and schwannoma. Curr Opin Neurol 2002;15(6):679–684.
4. Shah N, Sibtain A, Saunders MI, Townsend E, Wong WL. High FDG uptake in a schwannoma: A PET study. J Comput Assist Tomogr 2000;24(1):55–56.

Chapter 24 Ovarian Cancer

1. Cho SM, Ha HK, Byun JY, et al. Usefulness of FDG PET for assessment of early recurrent epithelial ovarian cancer. AJR 2002;179:391–395.
2. Kubik-Huch RA, et al. Value of (18F)-FDG positron emission tomography, computed tomography, and magnetic resonance imaging in diagnosing primary and recurrent ovarian carcinoma. Eur Radiol 2000;10:761–767.
3. Nakamoto Y. Clinical value of positron emission tomography with FDG for recurrent ovarian cancer. AJR Am J Roentgenol 2001;176:1449–1454.
4. Torizuka T, Nobezawa S, Kanno T, et al. Ovarian cancer recurrence: role of whole-body positron emission tomography using 2-[fluorine-18]-fluoro-2-deoxy- D-glucose. Eur J Nucl Med Mol Imag 2002;29(6):797–803.
5. Turlakow A, Yeung HW, Salmon AS, Macapinlac HA, Larson SM. Peritoneal carcinomatosis: role of ^{18}F-FDG-PET. J Nucl Med 2003;44:1407–1412.
6. Yen RF, Sun SS, Shen YY, Changlai SP, Kao A. Whole body positron emission tomography with 18F-fluoro-2-deoxyglucose for the detection of recurrent ovarian cancer. Anticancer Res 2001;21(5):3691–3694.
7. Wang PH, Liu RS, Li YF, Ng HT, Yuan CC. Whole-body PET with (Fluorine-18)-2-deoxyglucose for detecting recurrent ovarian carcinoma. Initial report. Gynecol Oncol 2000;44:775–778.
8. Zimny M, Siggelkow W, Schroder W, et al. 2-[Fluorine-18]-fluoro-2-deoxy-d-glucose positron emission tomography in the diagnosis of recurrent ovarian cancer. Gynecol Oncol 2001;83:310–315.

Chapter 25 Pancreatic Cancer

1. Kalra MK, Maher MM, Prasad SR, et al. Correlation of positron emission tomography and CT in evaluating pancreatic tumors: technical and clinical implications. AJR Am J Roentgenol 2003;181:387–393.
2. Moadel RM, Blaufox MD, Freeman LM. The role of positron emission tomography in gastrointestinal imaging. Gastroenterol Clin North Am 2002;31(3):841–861.
3. Iyer RB, Silverman PM, Tamm EP, Dunnington JS, DuBrow RA. Diagnosis, staging, and surveillance of pancreatic cancer. AJR Am J Roentgenol 2003;180:1311–1323.
4. Higashi T, Saga T, Nakamoto Y, et al. Relationship between retention index in dual-phase ^{18}F-FDG PET, and hexokinase-II and glucose transporter-1 expression in pancreatic cancer. J Nucl Med 2002;43:173–180.
5. Valinas R, Barrier A, Montravers F, Houry S, Talbot JN, Huguier M. 18 F-fluorodeoxyglucose positron emission tomography for characterization and initial staging of pancreatic tumors. Gastroenterol Clin Biol 2002;26(10):888–892.

Chapter 26 Prostate Cancer

1. Kotzerke J, Gschwend JE, Neumaier B. PET for prostate cancer imaging: still a quandary or the ultimate solution? J Nucl Med 2002;43:200–202.

Chapter 27 ^{18}F Fluoride Bone Scintigraphy

1. Cook GJ, Fogelman I. The role of positron emission tomography in the management of bone metastases. Cancer 2000;88(12 Suppl):2927–2233.
2. Piert M, Machulla HJ, Jahn M, Stahlschmidt A, Becker GA, Zittel TT. Coupling of porcine bone blood flow and metabolism in high-turnover bone disease measured by [(15) O] H(2)O and [(18)F]fluoride ion positron emission tomography. Eur J Nucl Med Mol Imag 2002;29(7):907–914.

Appendixes

I PET and PET-CT Reimbursement

Jennifer S. Keppler

PET and PET-CT have become important tools in the clinical management of patients with cancer, neurologic disorders, and coronary artery disease. Numerous peer-reviewed publications support the value of FDG PET in patients with many different types of cancer. Summaries of this literature show that the sensitivity and specificity of FDG PET range on average between 80% and 90%, and that patient management is changed with the introduction of PET into clinical decision-making in up to 40% of patients (Conti 1996). In neurology applications, FDG PET has demonstrated value in patients with primary brain tumors, epilepsy, and dementia. PET also provides earlier and more accurate detection of primary brain tumor regrowth than MRI (DiChiro 1986; Patronas 1982, 1985; Coleman 1991; Conti 1995a, 1995b). In patients with complex partial epilepsy, FDG PET scan results indicating a unilateral foci of hypometabolism is correlated with a high likelihood of the patient benefiting from surgical resection (Gambhir 2001). Studies have shown that patterns of FDG uptake in the brain can predict both progressive cognitive impairment and the histopathologic diagnosis of Alzheimer's disease at early stages of disease, with a sensitivity, specificity, and accuracy of 94%, 75%, and 90% respectively. In the heart, using the short-lived radiotracers of [N-13] Ammonia or [Rb-82] Chloride, PET is an effective way to assess perfusion of the heart, at rest or with pharmacological stress, for management of patients with known or suspected coronary artery disease (Schelbert 1982; Gould 1986). Finally, the use of FDG to demonstrate the presence of myocardial viability before a revascularization procedure has been shown to predict postsurgical functional improvement and better survival (Tillisch 1986; Schöder 1999). Despite the substantial and growing peer-reviewed literature support for this technology, public and private reimbursement for PET continues to lag behind its demonstrated utility.

Reimbursement for a medical test or procedure is conditional on a combination of factors, including any required *Food and Drug Administration (FDA) approvals*, peer-reviewed documentation of *clinical utility*, as well as acceptance of *medical necessity* within the clinician and payer communities. Recently, the Center for Medicare and Medicaid Services (CMS), which sets coverage guidelines for Medicare beneficiaries, has focused intently on the quality of the published literature as well as on its own assessment of medical necessity. Given that recent data suggest that the utilization of imaging is growing at a rate of 4.5% and the relative value units for imaging procedures are growing at 6% per year, we can expect continued scrutiny of the necessity of imaging procedures in clinical patient management (Dehn 2003).

FDA Approval for PET Scanners and Radiopharmaceuticals

The FDA is charged with ensuring the safety and effectiveness of drugs and medical devices used in the United States. For PET, this includes the use of both the *PET scanners*, as well as the *PET radiopharmaceuticals*. Operationally, other regulatory approvals may be required to maintain compliance or facilitate reimbursement contracting (e.g., Nuclear Regulatory Commission or an equivalent state radiation regulatory agency for handling or using radioactive materials, Environmental Protection Agency for monitoring of effluent release, and practice accreditation through State or private agencies); however, a discussion of these issues is outside of the scope of this appendix.

For reimbursement to be made on behalf of services provided to Medicare patients, CMS requires that the equipment used to perform the PET scans be "approved" or "cleared for marketing" by the FDA (Medicare Coverage Issues Manual 50–36). This is not an unusual requirement; the FDA must clear all medical devices before a vendor can legally market the device. The FDA provides this "approval to market," which in the case of PET scanners is "510K Clearance," in the form of a letter addressed to the manufacturer of scanner. Having 510 K Clearance is required before a device can be marketed and sold. In general, all commercially available PET scanners have been cleared for the use of "imaging radionuclide emissions from the body."

FDA approval of the radiopharmaceutical has always been a stated prerequisite for Medicare reimbursement for PET. This was a significant roadblock for PET reimbursement for many years, because traditional pathways of gaining FDA approval were not easily applied to most PET drugs. The FDA did approve one PET drug in 1989, Rubidium-82 for cardiac rest and stress imaging. Rubidium-82 is manufactured centrally, and then shipped to sites via a generator. This central manufacturing concept is better aligned with the traditional pathways of FDA approval, than is the distributed model of manufacturing FDG at regionally-based cyclotrons. Rubidium-82 (Rb-82) was afforded coverage by the CMS for Medicare beneficiaries (then, the Health Care Financing Administration, HCFA) in 1994. This first Medicare coverage statement restricted payments to only these Rb-82 applications, noting that all other PET radiopharmaceuticals and indications for PET were to be considered experimental. Subsequently in 1994, the FDA reviewed and approved a single application for the use of FDG and approved its production and use in epilepsy. However, Medicare reimbursement did not follow this additional FDA approval. Changes in the regulatory mechanisms of PET would be required in order for this technology to be made widely available to the public.

The FDA Modernization and Accountability Act of 1997 ("FDAMA") provided the basis for the FDA to develop these new regulatory mechanisms for PET and equally important, for CMS to expand public sector reimbursement. FDAMA contained specific language requiring that "appropriate" procedures for approval of New Drug Applications (NDA) and abbreviated NDAs for PET radiopharmaceuticals, as well as "appropriate" Current Good Manufacturing Practices (CGMPs) for the production of PET compounds be developed. FDAMA also stated the mechanism by which PET drugs could be legally produced in the interim until final FDA approvals were in place. This opened the way for expansion of Medicare reimbursement. Shortly thereafter, CMS (then, HCFA) revised its national coverage policy, providing coverage as of January 1, 1998 to Medicare beneficiaries for PET scans to characterize solitary pulmonary nodules and to initially stage certain types of lung cancer. CMS (then HCFA) developed several temporary HCPCs codes (G-codes assigned by diagnosis) to provide the coding for payment. This was the first of several steps taken by the HCFA toward a controlled expansion of PET reimbursement.

In March of 2000, the FDA released its assessment of the safety and efficacy of FDG [FR 65(48)]. In summary, the FDA concluded:

- FDG is safe and effective in PET imaging for assessment of abnormal glucose metabolism to assist in the evaluation of malignancy in patients with known or suspected abnormalities found by other testing modalities or in patients with existing diagnoses of cancer.
- FDG is safe and effective in PET imaging in patients with coronary artery disease and left ventricular dysfunction, when used together with myocardial perfusion imaging, to examine myocardial glucose metabolism, and to identify myocardium with reversible loss of systolic function.
- NH3 is safe and effective in PET imaging of the myocardium under rest or pharmacological stress conditions to evaluate myocardial perfusion in patients with suspected or existing coronary artery disease.

These findings supplemented the FDA's previous favorable conclusions of the efficacy of positron emitting drugs, including:

- Sodium fluoride F 18 injection is safe and effective as a bone imaging agent to define areas of altered osteogenic activity.
- FDG F 18 injection is safe and effective for the identification of regions of abnormal glucose metabolism associated with foci of epileptic seizures.
- Rb-82 Chloride is safe and effective as a myocardial perfusion agent that is useful in distinguishing normal from abnormal myocardium in patients with suspected myocardial infarction.

FDA publication of these findings opened up the path for expansion of PET reimbursement.

Reimbursement for PET

Although FDA approval is a prerequisite for reimbursement for Medicare and many private insurance carriers, FDA approval does not guarantee a drug or procedure will be covered. In the private sector, each independent insurance company determines the benefits offered to its subscribers. Payments by insurance companies for a service or procedure may be influenced by a number of factors, including published technology assessments, FDA approval, peer-reviewed literature, and standard medical practice in an area or region. In the public sector, CMS is the government entity that defines coverage benefits for Medicare beneficiaries. The current view of PET reimbursement is outlined below.

CMS implements Medicare coverage through contracts with private insurance carriers, also known as Medicare Carriers and/or Fiscal Intermediaries ("Medicare Contractors"). CMS determines what services will be eligible for coverage (i.e., that it deems to be "reasonable and necessary") by defining a "National Coverage Decision" *or* by delegating a coverage decision to its Medicare Contractors. National coverage decisions are policies that provide for or restrict Medicare coverage for a particular medical service and generate obligatory benefits for all Medicare beneficiaries [FR 64(80)]. These local contracting companies that insure the Medicare beneficiaries may also publish their own local medical review policies to clarify when an item or service will be considered "reasonable and necessary" and thus eligible for coverage under the Medicare. These local policies, however, cannot conflict with a national coverage decision published by CMS.

A *National Coverage Decision* has been issued for PET scanning; that is, there is a national definition of the types of PET scans that Medicare beneficiaries are eligible to receive (Medicare Coverage Issues Manual 50–36). As compared with most other radiology services, PET is unique in this regard; however, national coverage determinations exist for many medical services, including magnetic resonance angiography (Medicare Coverage Issues Manual 50–14), and use of cardiac rehabilitation therapy

(Medicare Coverage Issues Manual 35–25). Most of the published coverage instructions for other tests and treatments have fewer constraints than those published for PET, which contributes to the difficulty that some of the Medicare Contractors have had in the implementation of the PET guidelines. Nonetheless, the nationwide coverage assures that all Medicare patients are eligible for PET scans in certain diagnoses and clinical situations. The Medicare Contractor does not have the authority to expand this coverage, even if the national guidelines fall behind the utility demonstrated in the peer-reviewed literature or local medical practice. Local Medicare Carriers and Fiscal Intermediaries that provide payment for Medicare beneficiaries around the country must follow this policy and do not have latitude to make changes to it. Providers of services are obligated prior to billing for the services to ascertain whether the patient meets the prescriptive criteria. Efforts are underway to remove the national coverage restriction to allow local Medicare Contractors to assess and define coverage needs for their beneficiaries.

CMS has been very cautious with its expansion of coverage for PET. Their coverage decisions not only have restricted the scope of eligible diagnoses, but also have limited clinical eligibility within a covered diagnosis based on their strict interpretation of the indication demonstrated by portions of the published literature. More recently, CMS has restricted coverage of PET scans performed on coincidence gamma camera devices, requiring that most of these procedures be performed on full or partial ring PET Scanners (Medicare Coverage Issues Manual 50–36). Professional societies have taken the lead in petitioning CMS to expand coverage so that appropriate clinical situations are included in the coverage guidelines; however many petitions have been denied by CMS. Several formal requests are currently pending.

Current Medicare Coverage Guidelines

Guidelines for reimbursement of PET are described in Medicare's Coverage Instruction Manual (CIM) Section 50–36. CMS places the responsibility for ensuring that the patient qualifies on the referring physician (Medicare Coverage Issues Manual 50–36); however PET providers also have a responsibility to ascertain whether the patient meets the prescriptive criteria, prior to billing for the services. A summary of the current Medicare coverage guidelines is shown in Table A1.1 and described below.

Within the cancer indications, Medicare has defined the terms "diagnosis," "staging," "restaging," and has outlined the scenarios in which they consider a scan to be "rea-

Table A1.1. Summary of clinical conditions covered by Medicare

Clinical Condition	**Coverage (*within the guidelines of CIM 50–36*)**
Lung cancer (Non-Small Cell)	Diagnosis, Staging & Restaging
Esophageal Cancer	Diagnosis, Staging & Restaging
Colorectal Cancer	Diagnosis, Staging & Restaging
Lymphoma	Diagnosis, Staging & Restaging
Melanoma	Diagnosis, Staging & Restaging
Head and Neck Cancer (excludes CNS & thyroid)	Diagnosis, Staging & Restaging
Breast Cancer	Restaging, Monitoring Response to Therapy
Thyroid Cancer (Follicular Cell Origin; not medullary)	Restaging
Single Pulmonary Nodule (≤4 cm diameter)	Characterization of indeterminate nodule
Coronary Artery Disease	Assess rest & stress myocardial perfusion; assess myocardial viability
Refractory Seizures	Presurgical Evaluation

sonable and necessary," or more specifically, payable. For the cancer indications, the policy states that:

Diagnosis: PET is covered only in clinical situations in which the PET results may assist in avoiding an invasive diagnostic procedure, or in which the PET results may assist in determining the optimal anatomical location to perform an invasive diagnostic procedure . . . PET scans following a tissue diagnosis are performed for the purpose of staging, not diagnosis.

Staging and or Restaging: PET is covered in clinical situations in which:
1) (a) the stage of the cancer remains in doubt after completion of a standard diagnostic workup, including conventional imaging (computed tomography, magnetic resonance imaging, or ultrasound); or (b) the use of PET would also be considered reasonable and necessary if it could potentially replace one or more conventional imaging studies when it is expected that conventional study information is insufficient for the clinical management of the patient; and 2) clinical management of the patient would differ depending on the stage of the cancer identified (Medicare Coverage Issues Manual 50–36).

The Coverage Instructions add to the definition of when PET will be covered in restaging and monitoring, indicating that use of PET is appropriate in restaging only after the completion of treatment for the purpose of detecting residual disease, for detecting suspected recurrence or to determine the extent of a known recurrence. Use of PET would also be considered reasonable and necessary if it could potentially replace one or more conventional imaging studies when it is expected that conventional study information is insufficient for the clinical management of the patient (Medicare Coverage Issues Manual 50–36).

For monitoring a patient's cancer, the "use of PET to monitor tumor response during the planned course of therapy (i.e. when no change in therapy is being contemplated) is not covered. A PET scan for monitoring therapy may be considered reasonable and necessary when change of therapy is being considered" (Medicare Coverage Issues Manual 50–36). Furthermore, by these definitions, "Restaging only occurs after a course of treatment is completed . . . subject to the conditions above" (Medicare Coverage Issues Manual 50–36).

Medicare patients with a solitary pulmonary nodule may also be eligible for a PET scan under the Medicare system. If other diagnostic studies, such as CT scans or a chest x-ray are inconclusive about the malignancy status of a lesion, then a PET scan may be done to help characterize it, if the lesion is ≤4 cm in diameter. It is important to note that if the PET scan is negative, then, since all other diagnostic studies have as well been inconclusive, a biopsy procedure also would not be routinely covered in that patient (Medicare Coverage Issues Manual 50–36).

CMS defines a number of clinical exceptions to their stated coverage. Specifically, in lung cancer, eligibility is restricted to patients with demonstrated "non-small cell" pathology. In addition, although some Medicare patients with breast cancer are eligible for PET scans, as shown in Table A1.1, CMS will not cover a PET scan for the "diagnosis" or "initial (presurgical) staging" of the axillary lymph nodes in patients with breast cancer. PET scans may be performed, however, for staging or restaging of patients with distant metastasis or locoregional recurrence. Importantly, FDG PET scans may be used in women with locally advanced or metastatic breast cancer to monitor the tumor's response to the treatment, as long as a change in therapy is being considered. Breast cancer is currently the only type of cancer in which Medicare recognizes the role of PET in monitoring response to treatment (Medicare Coverage Issues Manual 50–36).

The guidelines are also extremely specific with respect to the eligibility of patients with a history of thyroid cancer. Those patients who are Medicare beneficiaries must have been previously treated by thyroidectomy and radioiodine ablation, have a negative I-131 whole body scan and currently have a serum thyroglobulin >10 ng/ml, in order to be eligible for PET scans for restaging. Futhermore, this coverage is limited

to the types of thyroid cancer with a follicular cell origin, so patients with medullary thyroid cancers are excluded from coverage for PET scans (Medicare Coverage Issues Manual 50–36).

In addition to oncology applications, clinical indications in neurology and cardiology are covered for Medicare beneficiaries. The only neurology indication that is covered by CMS currently is in epilepsy. The clinical scenario for coverage is very specific; the PET scan is covered if it is done as a part of a presurgical evaluation of patient with medically refractory seizures, with the intent of localize one of more seizure foci. In cardiology, two types of procedures are covered for Medicare beneficiaries. These include myocardial perfusion imaging (stress and/or rest using either Rb-82 Chloride or N-13 Ammonia), as well as a study to ascertain myocardial viability. The myocardial perfusion exams are covered instead of a conventional SPECT myocardial perfusion procedure or following an inconclusive SPECT myocardial perfusion scan. For the PET myocardial viability scan, the scan is covered either as a front line test to assess cardiac myocardial viability, or following an inconclusive myocardial perfusion test. For each of these indications, Medicare imposes certain conditions and restrictions for coverage (Medicare Coverage Issues Manual 50–36).

Like most diagnostic tests, PET scans are not covered for "screening" defined as testing patients without specific signs and symptoms of disease. The coverage guideline also affirms that PET is not covered for other diagnostic uses, thereby preventing Medicare contractors from expanding coverage beyond the national coverage policy (Medicare Coverage Issues Manual 50–36).

CMS continuously reevaluates its coverage policy for PET. Therefore, it is important to review the Medicare Coverage Issues Manual, Section 50–36 to gain a complete understanding of Medicare's coverage policy for PET for all these indications and to consult with your local Medicare carrier or fiscal intermediary for clarification of local or regional policies.

There are several pending applications for coverage. A request for evaluation of diagnostic imaging in patients with suspected Alzheimer's disease recently has been approved. Although the detail have not been finalized at the time of this writing, coverage under this application would be restricted to patients who have had a gradual decline in one or more cognitive domain over a 6 month period, do not suffer from a severe dementia, have no other documented cause by laboratory testing or anatomical imaging, and in whom the diagnosis would have a specific impact on life planning decisions.

Private Insurance Coverage Guidelines

Private payer's reimbursement policies for coverage of PET will vary by company, depending on a variety of factors. Each private insurance payer makes an independent decision on which procedures to cover. While some private payers may rely on Medicare coverage guidelines as the basis for their reimbursement policies, others may choose to set coverage that is either more or less restrictive. Most companies have published policies, which you may be able to access from your local PET center. The keys to working with private insurance carriers is to understand their existing coverage policies, and their process for deciding whether a test is covered or not. Developing good relationships with the decision-maker in the Insurance Carrier will help ensure that they have the proper information with which to decide on PET coverage.

Coding

One of the challenges to securing appropriate reimbursement for PET is learning to use the billing codes appropriately. CMS reimbursement relies on "Healthcare Common Procedure Coding System" (HCPCS) codes. For PET, CMS has established Level II codes for reimbursement. These codes are more specific than CPT® codes and allow tracking of utilization by both the clinical diagnosis and the stage of disease man-

agement, or in the case of the cardiology procedures, by the prior testing that has been completed. These Level II HCPCS codes describe the services in much more detail than Level I (existing CPT codes) and must be used in lieu of the CPT codes in billing for Medicare procedures. Tables A1.2 and A1.3 outline the HCPCS codes that should be used for billing PET procedures to Medicare.

Private insurance carriers may accept the Level II HCPCS coding required by Medicare; others may rely on CPT or other codes for the billing of PET services. It is important to work with each private payer in your area to determine the appropriate billing codes for a given company. CPT codes for PET, which describe the procedures in much more general terms than the CMS developed codes, can be obtained through private insurance companies, professional societies, or directly from CMS.

Coverage and Coding for PET-CT

No specific coverage guidelines exist for scans performed on combined PET-CT scanners in either the private or the public sector. The American College of Radiology (ACR) has issued a position statement describing guidelines for performing and billing for combined PET and CT images acquired in a single imaging session. First, in order to bill for both the PET and the CT scans performed, it is essential that both procedures are medically necessary, as documented by the orders from the referring clinician. This means that the referring clinician must specifically order the diagnostic CT scans to be performed at the time of the PET scan, providing the necessary history and clinical indication. Additionally, the CT scan should be performed using the generally acceptable diagnostic parameters common in the community. Separate reports should be rendered. Currently, ACR guidelines recommend that separate PET and CT codes be used to charge for the procedures.

In early 2004, the American Medical Association (AMA) approved the addition of six new CPT codes for PET and PET/CT to be published in January 2005. These new codes (numbers to be determined) have been developed to reflect more accurately the current practice of PET and PET-CT. Two of the codes will reflect a limited PET scan, performed with or without anatomical correlation. These codes would cover a one or two bed position PET scan. Another two codes will reflect a standard torso PET scan, performed with or without anatomical correlation. The vignettes sent to the AMA described these scans as being performed from "eyes to thighs" to indicate that the neck and full pelvis would be included in these types of PET scans. Finally, the last two codes will reflect a whole body PET scan, performed with or without anatomical correlation. These codes would be used to reflect PET scans performed from head to toe, such as what might be required in an assessment of melanoma.

Implications of Coverage Guidelines on PET Operations

It is important that a PET Center prequalify a patient for services based upon his/her clinical background. To do this, it will be important to obtain detailed information on the patient to determine eligibility under their insurance guidelines. Table A1.4 describes the type of information that should be obtained in order to assess whether or not the patient will qualify under insurance guidelines. Assign an expert within the Center to review the documentation to make an accurate assessment of whether or not the patient is eligible under Medicare and what billing code should be used to assure payment. Then, the PET Center can communicate with the clinician's office office, as well as with the patient as to whether or not Medicare or the private insurance company will cover the PET scan.

Most of the clinical information that is needed prior to scheduling the exam will be in the patient's medical chart. With private insurance, it is important to determine if a preauthorization for the PET scan is needed. With respect to ascertaining Medicare eligibility or obtaining a pre-authorization, the latest "History and Physical", current progress notes, and reports of recent radiographs and blood tests should provide

TABLE A1.2. 2004 Medicare codes for procedures performed on a Full/Partial Ring PET scanner

Code	HCPCS description
G0125	PET Imaging regional or whole body; single pulmonary nodule; full-and partial-ring PET scanners only
G0210	PET Imaging whole body; full- and partial-ring PET scanners only, diagnosis; lung cancer, non-small cell
G0211	PET Imaging whole body; full- and partial-ring PET scanners only, initial staging; lung cancer; non-small cell
G0212	PET Imaging whole body; full- and partial-ring PET scanners only, restaging; lung cancer; non-small cell
G0213	PET Imaging whole body; full- and partial-ring PET scanners only, diagnosis; colorectal cancer
G0214	PET Imaging whole body; full- and partial-ring PET scanners only, initial staging; colorectal cancer
G0215	PET Imaging whole body; full- and partial-ring PET scanners only, restaging, colorectal cancer
G0216	PET Imaging whole body; full- and partial-ring PET scanners only, diagnosis; melanoma
G0217	PET Imaging whole body; full- and partial-ring PET scanners only, initial staging; melanoma
G0218	PET Imaging whole body; full- and partial-ring PET scanners only, restaging; melanoma
G0219	PET Imaging whole body; full- and partial-ring PET scanners only, melanoma for non-covered indications
G0220	PET Imaging whole body; full- and partial-ring PET scanners only, diagnosis; lymphoma
G0221	PET Imaging whole body; full- and partial-ring PET scanners only, initial staging; lymphoma
G0222	PET Imaging whole body; full- and partial-ring PET scanners only, restaging; lymphoma (replaces G0164)
G0223	PET Imaging whole body or regional; full- and partial-ring PET scanners only, diagnosis; head and neck cancer; excluding thyroid and CNS cancers
G0224	PET Imaging whole body or regional; full- and partial-ring PET scanners only, initial staging; head and neck cancer; excluding thyroid and CNS cancers
G0225	PET Imaging whole body or regional; full- and partial-ring PET scanners only, restaging; head and neck cancer, excluding thyroid and CNS cancers
G0226	PET Imaging whole body; full- and partial-ring PET scanners only, diagnosis; esophageal cancer
G0227	PET Imaging whole body; full- and partial-ring PET scanners only, initial staging; esophageal cancer
G0228	PET Imaging whole body; full- and partial-ring PET scanners only, restaging; esophageal cancer
G0229	PET Imaging; Metabolic brain imaging for pre-surgical evaluation of refractory seizures; full- and partial-ring PET scanners only
G0230	PET Imaging; Metabolic assessment for myocardial viability following inconclusive SPECT study; full- and partial-ring PET scanners only
G0252	PET imaging, full and partial-ring PET scanners only, for initial diagnosis of breast cancer and/or surgical planning for breast cancer (e.g., initial staging of axillary lymph nodes), **not covered by Medicare**
G0253	PET imaging for breast cancer, full and partial-ring PET scanners only, staging/restaging of local regional recurrence or distant metastases, i.e., staging/restaging after or prior to course of treatment
G0254	PET imaging for breast cancer, full and partial-ring PET scanners only, evaluation of response to treatment, performed during course of treatment
78459	Myocardial imaging, positron emission tomography (PET), metabolic evaluation
G0296	PET Imaging, full and partial ring PET scanner only, for restaging of previously treated thyroid cancer of follicular cell origin following negative I-131 whole body scan
C1775	FDG, per dose (4–40 mCi/ml)

Source: Data from Medicare Program; Changes to the Hospital Outpatient Prospective Payment System and Calendar Year 2004 Payment Rate; Final Rule, 42 CFR Parts 410 and 419, Federal Register, Friday Nov 7, 2003 (CMS-1471-FC).

Table A1.3. 2004 Medicare codes for cardiac procedures performed on a Full/Partial Ring PET scanner

Code	HCPCS description
G0030	PET myocardial perfusion imaging, (following previous PET, G0030-G0047); single study, rest or stress (exercise and/or pharmacologic)
G0031	multiple studies, rest or stress (exercise and/or pharmacologic)
G0032	PET myocardial perfusion imaging, (following rest SPECT, 78464); single study, rest or stress (exercise and/or pharmacologic)
G0033	multiple studies, rest or stress (exercise and/or pharmacologic)
G0034	PET myocardial perfusion imaging, (following rest SPECT, 78465); single study, rest or stress (exercise and/or pharmacologic)
G0035	multiple studies, rest or stress (exercise and/or pharmacologic)
G0036	PET myocardial perfusion imaging (following coronary angiography, (93510–93529); single study, rest or stress (exercise and/or pharmacologic)
G0037	multiple studies, rest or stress (exercise and/or pharmacologic)
G0038	PET myocardial perfusion imaging (following stress planar myocardial perfusion 78460); single study, rest or stress (exercise and/or pharmacologic)
G0039	multiple studies, rest or stress (exercise and/or pharmacologic)
G0040	PET myocardial perfusion imaging (following stress echocardiogram, 93350); single study, rest or stress (exercise and/or pharmacologic)
G0041	multiple studies, rest or stress (exercise and/or pharmacologic)
G0042	PET myocardial perfusion imaging (following stress nuclear ventriculogram 78481 or 78483); single study, rest or stress (exercise and/or pharmacologic)
G0043	multiple studies, rest or stress (exercise and/or pharmacologic)
G0044	PET myocardial perfusion imaging (following rest ECG 93000); single study, rest or stress (exercise and/or pharmacologic)
G0045	multiple studies, rest or stress (exercise and/or pharmacologic)
G0046	PET myocardial perfusion imaging (following stress ECG 93015); single study, rest or stress (exercise and/or pharmacologic)
G0047	multiple studies, rest or stress (exercise and/or pharmacologic)
78459	Myocardial imaging, positron emission tomography (PET), metabolic evaluation
Q3000	Supply of radiopharmaceutical diagnostic imaging agent, Rubidium-82 per dose
Q4078	Supply of radiopharmaceutical diagnostic imaging agent, Ammonia N-13, per dose

Source: Data from Medicare Program; Changes to the Hospital Outpatient Prospective Payment System and Calendar Year 2004 Payment Rates; Final Rule, 42 CFR Parts 410 and 419, Federal Register, Friday Nov 7, 2004 (CMS-1471-FC).

Table A1.4. Information needed to assess patient eligibility

Patient data to be collected at scheduling:

- Patient name, height and weight
- Age of patient (if pediatric)
- Insurance card/information
- Diagnosis and H & P
  - *Including history of diabetes, if any*
- Dates of recent surgery and treatments
- Reports of recent radiographs and blood work, if any
- How the clinician plans to use the PET results in the care of the patient (*to help justify medical necessity*)

an adequate picture of the patients' clinical history. If possible, determine how the clinician plans to use the PET scan results in the management of the patient (such as to differentiate between alternative courses of treatment). This will further document patient eligibility under Medicare and may help justify any required pre-authorization.

Having a National Coverage Policy for PET clarifies which Medicare patients are eligible for a PET scan. Unfortunately, patients are not eligible for coverage might be referred for a PET scan. In these cases, the patient must sign an "Advanced Beneficiary Notification" (ABN), which will inform him/her of the financial responsibility for the scan (Medicare Carriers Manual 30–50). Medicare can be billed, if needed in order to obtain a denial of services, however, the claim form must indicate that the ABN is on file using a GA modifier. If a center knows that a procedure should not be covered, then a CPT code should be used to describe the procedure and the billing condition code should reflect that the claim is issued in order to obtain a denial.

Medicare Coverage Decisions Pending

On an ongoing basis, CMS reviews petitions for coverage of additional clinical indications. CMS will initiate a review for a national coverage decision when issues are identified internally with CMS or when a formal request to review an issue is received. These formal requests can be made by individuals (patients, physicians or others) or by groups, such as professional societies. A formal request must be in writing and contain the following components [FR 64(80)]:

- Statement that the document is a "formal request for a national coverage decision.
- Supporting documentation that includes at a minimum:
  - A complete description of the service and the benefit category or categories of the Medicare program to which it applies.
  - A compilation of the medical and scientific information supporting the service, including any clinical trials underway that may impact the decision.
- In the case of a drug or device (or a service using a drug or device subject to regulation by the FDA), the status of FDA approval.

Currently, for PET, CMS is considering requests for expanded coverage of PET for additional indications. To support their decision, the CMS may request a formal technology evaluation, refer the decision to a Medicare Coverage Advisory Committee, or internally make the decision based on the evidence provided and in the public domain [FR 64(80)]. Once a "Decision Memorandum" is published, CMS provides instructions to the Medicare Contractors to begin payment for the services at some future date. In the past, once a decision is made by CMS, it is at least 6 months before coverage is in place for patients. CMS provides the public with updated information on the web regarding the status of current and past coverage decisions at http://cms.hhs.gov/ncdr/ncdr_index.asp.

Conclusion

PET scanning with FDG has become an important tool in the clinical management of patients, with a significant number of peer-reviewed publications supporting its value. Translating the published "value of PET" into insurance coverage requires concerted effort at the local and national levels.

Obtaining appropriate reimbursement for PET services means developing an understanding of the coverage criteria for Medicare patients and identifying coverage guidelines for the private sector in the local region. Once these are known, proper screening of patients to make sure they qualify under coverage rules, accurate coding and billing for the test, along with regular review of payments received, are critical to obtaining the correct reimbursement for the services offered.

References

Cardiac Rehabilitation Programs. In: *Medicare coverage issues manual*, sec. 35–25, rev. 41, 08/89. Washington, DC: Health and Human Services Department, Center for Medicare and Medicaid Services 2004 http://www.cms.hhs.gov/manuals/06_cim/ci50.asp. Accessed June 11, 2004.

Coleman RE, Hoffman JM, Hanson MW, et al. (1991) Clinical application of PET for the evaluation of brain tumors. J Nuc Med 326:616–622.

Conti PS. (1995a) Introduction to imaging brain tumor metabolism with positron emissiom tomography (PET). Cancer Invest 13, 244–259.

Conti PS. Brain and spinal cord tumors. In: Principles of Nuclear Medicine. (Wagner, H.N., Jr., ed.; second edition), Saunders, Philadelphia, Chapter 46, Section 1, 1995b, pp. 1041–1054.

Conti PS, Lilien DL, Grafton ST, Bading JR, Keppler J, and Hawley K. (1996) PET and [18F]-FDG: A clinical update. Nucl Med Biol 23:717–735.

Dehn T. (2003) A Parallax View of Diagnostic Imaging. Imaging Economics.

Determining Liability for Claims for Physician and Supplier Services. In: *Medicare Carriers Manual Part*, Chapter 30: Section 50 Rev 1; 2003. http://www.cms.hhs.gov/medicare/bni/ Accessed June 11, 2004.

DiChiro G. (1986) Positron emission tomography using [18F]fluorodeoxyglucose in brain tumors: A powerful diagnostic and prognostic tool. Invest Radiol 22, 360–371.

Gambhir SS, Czernin J, Schwimmer J, Silverman DHS, Coleman RE, and Phelps ME. (2001) A Tabulated Summary of the FDG PET Literature. J Nucl Med 42:1S-93S.

Gould LK, Goldstein RA, Mullani NA, Kirkeeide RL, Wong WH, Tewson TJ, Berridge MS, Bolomey LA, Hartz RK, Smalling RW, Fuentes F, and Nishikawa A. (1986) Noninvasive assessment of coronary stenoses by myocardial perfusion imaging during pharmacologic coronary vasodilation. Clinical feasibility of positron cardiac imaging without a cyclotron using generator-produced rubidium-82. J Am Coll Cardiol 7:775–89.

Magnetic Resonance Angiography. In: *Medicare coverage issues manual*, sec. 50–14, rev. 170, 05/03. Washington, DC: Health and Human Services Department, Center for Medicare and Medicaid Services 2004 Available at: http://www.cms.hhs.gov/manuals/06_cim/ci50.asp#_50_14. Accessed June 11, 2004.

Medicare Program; Procedures for Making National Coverage Decisions (April 27, 1999) Federal Register 64(80):22619–22625.

Patronas NJ, DiChiro G, Brooks RA, et al. (1982) [18F]-Fluorodeoxyglucose and positron emission tomography in evaluation of radiation necrosis of the brain. Radiology 144, 885–889.

Patronas NJ, DiChiro G, Kufta C, et al. (1985) Prediction of survival in glioma patients by means of positron emission tomography. Neurosurg 62, 816–822.

Positron Emission Tomography Drug Products; Safety and Effectiveness of Certain PET Drugs for Specific Indications. (March 10, 2000) Federal Register 65(48):12999–13010.

Positron emission tomography (PET) scans. In: *Medicare coverage issues manual*, sec. 50–36, rev. 171, 06/03. Washington, DC: Health and Human Services Department, Center for Medicare and Medicaid Services 2004 Available at: http://www.cms.hhs.gov/manuals/06_cim/ci50.asp#_50_36 . Accessed June 11, 2004.

Schelbert HR, Wisenberg G, Phelps ME, Gould KL, Henze E, Hoffman EJ, Gomes A, and Kuhl DE. (1982) Noninvasive assessment of coronary stenoses by myocardial imaging during pharmacologic coronary vasodilation. Am J Cardiol. 49:1197–1207.

Schöder H, Campisi R, Ohtake T, et al. (1999) Blood flow-metabolism imaging with positron emission tomography in patients with diabetes mellitus for the assessment of reversible left ventricular contractile dysfunction. J Am Coll Cardiol. 33:1328–1337.

Tillisch J, Brunken R, Marshall R. (1986) Reversibility of cardiac wall motion abnormalities predicted by positron tomography. New Engl J Med. 314:884–888.

II PET-CT Techniques Applied in Case Studies

James Bading and Peter Shomphe

Studies included in this atlas were acquired with a Biograph LSO PET/CT scanner (Siemens/CPS, Knoxville, TN). The system comprises a dual-slice, spiral CT (Siemens Somatom Emotion) in tandem with an ACCEL PET scanner. The system is optimized for use in whole-body oncology. Intrinsic spatial resolution is 6 mm to 7 mm in the transaxial plane and 5 mm to 7 mm in the axial dimension. Data are acquired strictly in 3D mode (no interring septa), and the design relies on a proprietary calculated correction to remove scatter noise. Standard techniques are used to correct for detector non-uniformity, dead time and randoms noise. Attenuation correction is calculated from coregistered, segmented CT images. PET-CT alignment is ensured via a measurement-based software correction. The system provides 47 transaxial slices and a 15.5 cm axial field of view.

Studies begin with a 2D X-ray topogram, on which the bed position locations for the study are defined. The CT scan is then acquired, followed by the PET scan. When the patient enters the scanner head first, the CT scan is acquired in the superior to inferior aspect, while the PET scan begins at the inferiormost bed position, a sequence defined to minimize bladder activity in the PET scan. The computer system is Windows NT-based with a Siemens/Syngo user interface. It includes of four separate PCs, one each for data acquisition and reconstruction for CT and PET.

The standard scanning protocol for studies presented here arms raised above the head and normal breathing during the CT portion of the CT-PET sequence. All PET images presented in the atlas were reconstructed with either of two manufacturer-recommended ordered subsets estimation maximization (OSEM) techniques: body images—2 iterations, 8 subsets, 5 mm Gaussian postsmoothing; brain images—6 iterations, 16 subsets, 5 mm Gaussian postsmoothing. For whole body exams the CT slice thickness was 5 mm and 4 mm collimation, using 90 to 70 mAs, 130 kVp, and pitch (feed/rotation) of 7.6 mm to 16 mm. Breath-hold chest studies were performed with 5 mm slice thickness and 4 mm collimation, using 80 mAs, 130 kVp and pitch of 12 mm to 16 mm.

Index